Volume 21 • TOPICS IN GEOBIOLOGY • Series Editors: Neil H. Landman and Peter J. Harries

High-Resolution Approaches in Stratigraphic Paleontology

Edited by

Peter J. Harries

Springer

High-Resolution Approaches in Stratigraphic Paleontology

TOPICS IN GEOBIOLOGY

P.J. Harries
Editor

High-Resolution Approaches in Stratigraphic Paleontology

Springer

Editor
P.J. Harries
Department of Geology
University of South Florida
Tampa, USA

ISBN: 978-1-4020-1443-7 e-ISBN: 978-1-4020-9053-0

Library of Congress Control Number: 2008931214

Cover Illustration: The Cenomanian-Turonian stratotype within the Bridge Creek Limestone Member of the Greenhorn Formation, Rock Canyon Anticline, Pueblo, Colorado, United States. Photograph by P.J. Harries, Department of Geology, University of South Florida.

Printed on acid-free paper

9 8 7 6 5 4 3 2 1

springer.com

Contributors

Thomas J. Algeo Department of Geology, University of Cincinnati, Cincinnati, Ohio 45221-0013

Richard K. Bambach Department of Geological Sciences, Virginia Polytechnic Institute and State University, Blacksburg, VA 24060

Carlton E. Brett Department of Geology, University of Cincinnati, Cincinnati, Ohio 45221-0013

Kenneth Carpenter Department of Earth and Space Sciences, Denver Museum of Natural History, 2001 Colorado Blvd., Denver, CO 80205

Roger A Cooper Institute of Geological and Nuclear Sciences Limited, Lower Hutt, New Zealand

Jeffrey G. Eaton Department of Geosciences, Weber State University, Ogden, Utah 84408-2507

Edward Fowler Agua Dulce, California, 91350

Peter J. Harries Dept. of Geology, Univ. of South Florida, 4202 E. Fowler Ave., SCA 528, Tampa, FL 33617-5201

James I. Kirkland Utah Geological Survey, P.O. Box 146100, Salt Lake City, Utah 84114-6100

Susan M. Klofak American Museum of Natural History, 79th Street and Central Park West, New York, NY 10024-5192 and Department of Biology, City College of the City University of New York, Convent Avenue and 138th Street, New York, NY 10031

Marilyn A. Kooser Department of Earth Sciences, University of California, Riverside, California 92521

Michał Kowalewski Department of Geological Sciences, Virginia Polytechnic Institute and State University, Blacksburg, VA 24060

Neil H. Landman American Museum of Natural History, 79th Street and Central Park West, New York, NY 10024-5192

Patrick I. McLaughlin Department of Geology, University of Cincinnati, Cincinnati, Ohio 45221-0013

Jared R. Morrow Department of Earth Sciences, University of Northern Colorado, Greeley, CO 80639

Peter M. Sadler Department of Earth Sciences, University of California, Riverside, Riverside, CA 92521

Charles A. Sandberg United States Geological Survey, Box 25046, MS 939, Federal Center, Denver, CO 80225-0046

Kathleen B. Sarg American Museum of Natural History, 79th Street and Central Park West, New York, NY 10024-5192

Charles E. Savrda Department of Geology and Geography, 210 Petrie Hall, Auburn University, Auburn, Alabama 36849-5305

Mark Webster Department of Earth Sciences, University of California, Riverside, California 92521

Margaret M. Yacobucci Bowling Green State University, Department of Geology, 190 Overman Hall, Bowling Green, OH 43403-0218

Preface

Since at least the Renaissance, as exemplified by Steno's contributions, there has been the recognition that Earth history can be interpreted from the analysis of the geologic record. The primary aim of most geologic studies has been and continues to be the reconstruction of that history, so that theoretically the dynamics of the Earth's systems and the interactions between those systems can be reconstructed along time slices. High-resolution stratigraphic analysis was developed, as the name implies, to glean data from the record at increased levels of temporal and spatial resolution to accomplish that aim. The application of the technique initially focused largely on lithologic and paleontologic indicators and their variability that can be employed to improve resolution and erect frameworks for various intervals in the geologic column.

During the past few decades, especially as paleontology has become a tool used to address an increasing range of geologic, evolutionary and environmental questions, high-resolution approaches have become an integral component of numerous studies. To a certain degree this represents an increased and more detailed analysis of the fossil record, but, to a greater degree, this reflects the need for both temporally and geographically refined paleontologic data to tackle the broad spectrum of questions currently being investigated. Paleontology has undergone a rapid maturation during the past 50 years and one of the important elements of this process has been the realization that to effectively delve into the details of evolutionary and paleoecologic questions, fine temporal resolution is a necessity. However, there are limits to the resolution that can be achieved due to such controls as the rate of rock accumulation, taphonomic overprinting, as well as a wide range of other factors that obscure the record. Furthermore, to a certain degree 'high resolution' is in the eye of the beholder. Because of the vagaries of preservation and due to the ever-changing environments that

were inhabited by organisms of the past, the resolution that can be achieved differs substantially between depositional settings, taxonomic group, and also can be, at least in part, related to the nature of the questions being asked.

The overarching aim of this volume is to look at state-of-the-art approaches currently being used and to show how integrating a variety of these approaches is a necessity to producing and analyzing robust datasets and to delve into some of the limitations inherent in the analysis of paleontologic data. The success of high-resolution paleontologic approaches has been largely triggered by the integration of numerous approaches that have been applied in concert to investigating the geologic record. These approaches come from a wide range of disciplines and integrate lithologic, paleontologic, geochemical, and geophysical data, among others, that have increased the stratigraphic refinement. Although elements of these various approaches are inherent in this book's contributions, the theme of the book is concentrated on paleobiologic approaches to spatial and temporal resolution as well as how refined high-resolution frameworks can be employed to investigate environmental, ecologic, and evolutionary changes and patterns.

This volume loosely covers a spectrum of topics following a progression from more theoretical to more applied contributions. In the theoretical arena, there are a number of critical constraints and concepts that are addressed. One of the over-arching questions in high-resolution paleontology revolves around the rock record itself and how much temporal precision can be teased from it. The contributions in this volume (see Chapters 1 and 4) offer to different perspectives and scales related to the issue and point to the limitations as well as the strengths of the fossil record. In addition, more rigorous application of quantitiative techniques has become an integral part of the geosciences, and their application to various paleontologic problems, including high-resolution problems, is no exception approaches (see Chapters 2, 3, as well as the accompanying CD and Chapter 13).

As all the chapters attest, there is more to high-resolution approaches than simply the ability to document the paleotnologic record at increasingly finer levels of resolution. Data critical to the analysis of a host of evolutionary, ecologic, environmental questions can be generated at sufficient temporal and geographic resolution so that detailed responses to environmental changes and variability can be analyzed. Although the general field is certainly not limited to these topics, this volume focuses on evolutionary and environmental issues (Chapters 5-8) that can only be effectively addressed once a high-resolution database exists. The final set of chapters (9-12) focus on different methodologies that can be employed to produce high-resolution frameworks.

The thirteen chapters that comprise this volume offer a broad perspective on both theoretical and practical issues related to high-resolution paleontologic studies. They not only point to approaches that have been successfully employed to investigate a range of paleobiologic issues, but also

suggest directions for further study and new techniques that can potentially continue to decrease the temporal intervals inherent in our understanding of 'high resolution'. So, break out your hammers, fire up your computers, there's work to be done!

Peter J. Harries
Tampa, Florida

Contents

Chapter 1

The Limits of Paleontological Resolution

MICHAŁ KOWALEWSKI and RICHARD K. BAMBACH

MICHAŁ KOWALEWSKI and RICHARD K. BAMBACH • Department of Geological Sciences, Virginia Polytechnic Institute and State University, Blacksburg, VA 24061.

P.J. Harries (ed.), *High-Resolution Approaches in Stratigraphic Paleontology.*

1. INTRODUCTION

When used by stratigraphers and paleontologists, the term "resolution" typically denotes *stratigraphic resolution* as determined by the finest-scale units or surfaces that can be recognized vertically, traced laterally, and correlated using approaches such as biostratigraphy or sequence stratigraphy. However, the term "resolution" can also denote *depositional resolution* of the physical records (e.g., fossils, grains, diagenetic precipitates, etc.) contained within individual strata. Due to temporal (e.g., Walker and Bambach, 1971; Kidwell and Bosence, 1991) and spatial mixing (e.g., Flessa, 1998), depositional resolution of records contained within individual strata may be much coarser than the stratigraphic resolution of depositional events that produced those strata. Moreover, an individual stratum is made predominately of fossils and sedimentary grains that predate its deposition, but may also include fossils, sedimentary structures, and diagenetic overprints that post-date its deposition. There are two distinct resolution concepts: *stratigraphic resolution* among strata and within-stratum *depositional resolution*.

The relevance of the two concepts depends on the goals of a study. If the task is to correlate units, reconstruct depositional histories of sedimentary basins, or develop a sequence-stratigraphic framework, we are concerned primarily with the stratigraphic resolution determined by the spacing of correlative depositional events and the duration of diastems separating those events (Fig. 1). In some cases, very fine levels of stratigraphic resolution can be achieved laterally by correlating highly resolved records such as varves (e.g., Nederbragt and Thurow, 2001), tree rings (e.g., Lageard *et al*., 1999), or trace-fossil horizons (e.g., Kowalewski and Demko, 1997). A comparably high resolution can be achieved vertically, within single sections, by time-series analyses of continuous cyclic deposits such as tidal deposits (e.g., Miller and Eriksson, 1997).

However, potentially high stratigraphic resolution *among* strata does not

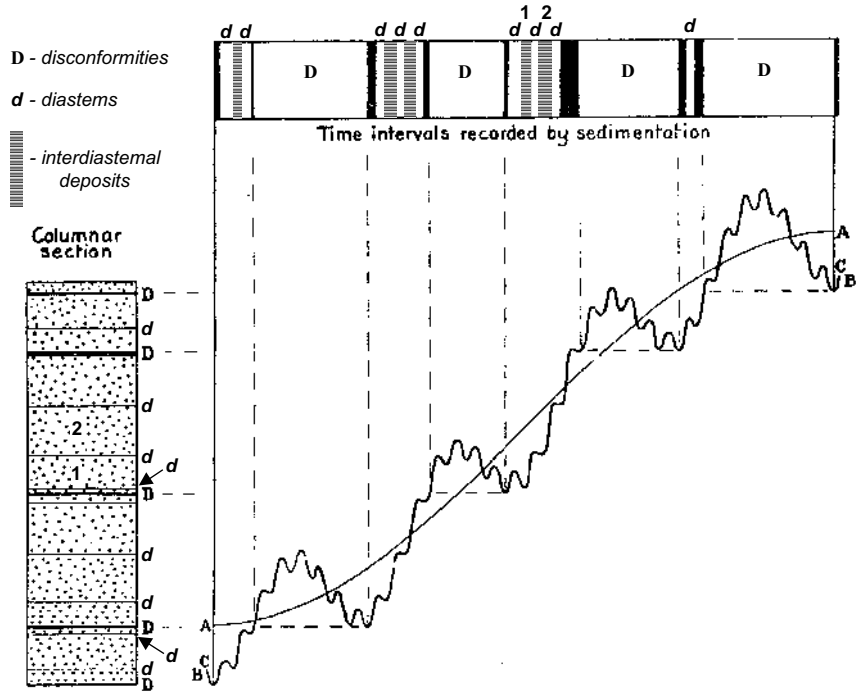

Figure 1. Joseph Barrell's (1917) model for the temporal dynamics of the sedimentary record. Depositional events are separated by diastems (d). Sets of events form higher-order packages bounded by disconformities (D) and controlled by diastrophic oscillations. Conceptually, the model is strikingly close to the approach of sequence stratigraphy developed many decades later (Vail and Mitchum, 1977; Vail *et al*., 1977; Mitchum and Vail, 1977). Strata 1-2 represent interdiastemal deposits and correspond to strata 1 and 2 shown on Figure 2. Unlike the intervals suggested by Barrell's figure, typical diastems represent much longer time intervals than the depositional events they separate. Modified after Barrell (1917, fig. 5).

necessarily imply a comparably high depositional resolution *within* strata. In an example shown here (Fig. 2), the time span of paleontological records contained in Stratum 2 exceeds the duration of the diastems that separate neighboring strata. A fossil from Stratum 2 is not necessarily younger than Stratum 1: the stratigraphic resolution of depositional events can be finer than the resolution of the physical records contained within strata. Thus, if the research objectives involve integrating paleontological data, analyzing isotope ratios, or measuring any parameter from physical materials extracted from within strata, depositional resolution of records needs to be evaluated. Such evaluation will be particularly fruitful when done in the context of theduration of diastems separating that stratum from adjacent units.

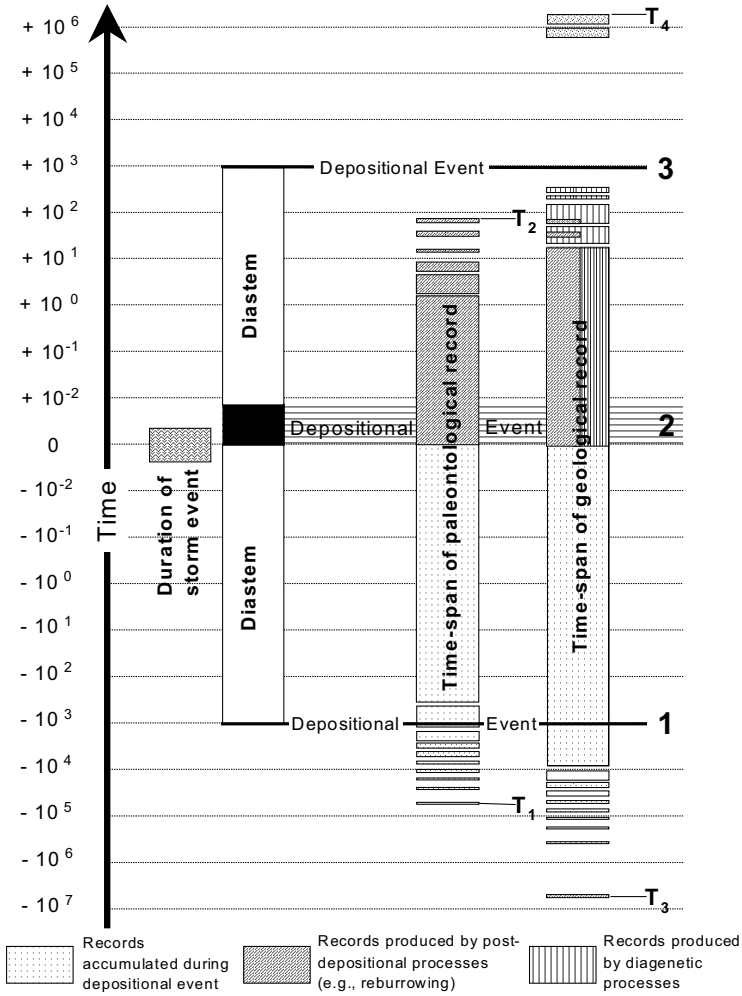

Figure 2. Depositional resolution of a single event (stratum "2" on Figure 1) exemplified by a storm bed. In this hypothetical example, both the paleontological and geological records have time-spans that exceed the duration of the diastems (marked as "d" on Figure 1) separating stratum 2 from the two neighboring depositional events. Thus, depositional resolution of a stratum is much poorer than the stratigraphic resolution of the same sedimentary record. Single depositional events correspond to interdiastemal deposits on Figure 1. Because the time is presented on a logarithmic scale, the lines representing events 1 and 3 are not to scale.

The studies compiled in this volume deal primarily with the stratigraphic resolution and illustrate powerful approaches used to improve the precision and accuracy of stratigraphic correlation. The aim of such studies (e.g., Kauffman *et al*., 1991; Sageman *et al*., 1997) is to maximize resolution of stratigraphic correlation by careful integration of paleontological and stratigraphic data. In contrast, our paper deals with the finest stratigraphic

scale: the internal resolution of single depositional events and their adjacent diastems. Using data amassed in recent years, primarily from modern depositional environments, we examine both depositional resolution of paleontological records contained within single strata as well as temporalcharacteristics of diastems that separate consecutive depositional events. The comparison of temporal characteristics of diastems with the depositional resolution of paleontological records allows us to integrate knowledge about both stratigraphic and depositional resolution into a single analysis. The two metrics of resolution considered jointly provide a useful conceptual insight into the temporal limits of paleontological and geological data.

We focus here on data and interpretations from marine nearshore and shelf environments where relatively frequent disturbance events (hurricanes, storms, pulses of sediment input from coastal settings, etc.) create the conditions that produce distinct bedding, providing the potential for recognizing and interpreting numerous short-term events. As noted by Miall (1990, p. 9): "...such events are typically responsible for deposition of disproportionally large volumes of sediment in sedimentary basins". In North America, for example, they comprise most of the marine Paleozoic sections in the Appalachians and on the craton, large amounts of Mesozoic age marine deposits of the Cordillera, much of the nearshore marine Mesozoic of the craton, and all of the Cretaceous and Cenozoic sedimentation of the Atlantic and Gulf Coastal Plain. Most paleontological studies of benthic faunas derive from deposits representing such settings.

Although basinal settings with less episodic sediment accumulation are not rare, rates of sediment accumulation in basins are commonly relatively low. In such cases, bioturbation processes mix sediment particles (including fossils) of different ages. Thus, the sediment, although possibly accumulated relatively continuously, will no longer preserve the exact superposed position of every grain. This post-depositional mixing makes any bioturbated sediment sample temporally mixed, just as if it had been reworked and redeposited in a short-term event. Martin (1999, Chapters 4, 5) discusses at length the features of “biodiffusion” and “stratigraphic disorder” produced by bioturbation. *Only* laminated basinal sediments can carry a reliable record of depositional resolution at the finest scale, and these settings are relatively uncommon, being generally restricted to anoxic basins. In some settings, such anoxic basins may undergo repeated colonization by benthic fauna (e.g., Röhl *et al*., 2001; Harries, pers. comm., 2001) and may provide higher resolution than what we consider here to be the typical marine fossil record. Barring such exceptions, the concepts discussed below relate to the most common and frequently studied stratigraphic records.

2. DEPOSITIONAL RESOLUTION OF PALEONTOLOGICAL RECORDS

2.1 Time Averaging and Temporal Mixing

It has long been recognized (e.g., Schäfer, 1956; Walker and Bambach, 1971) that fossils may both pre-date (via reworking and bioturbation) and post-date (via post-depositional reburrowing) the stratum that contains them (Fig. 2). Thus, unlike live-collected organisms, fossils found together within a single stratum need not be contemporaneous with one another, but may typically represent mixed remains of organisms that lived at different times and never interacted with one another. That is, paleontological records tend to undergo temporal mixing (e.g., Walker and Bambach, 1971; Peterson, 1977; Wilson, 1988; Goodfriend, 1989; Kidwell and Bosence, 1991; Behrensmeyer, 1991; Flessa, 1993; Kidwell and Behrensmeyer, 1993; Martin, 1993, 1999; Martin *et al*., 1995, 1996; Wehmiller *et al*., 1995; Kowalewski, 1996a; Kidwell, 1998).

Kidwell and Bosence (1991; see also Kidwell and Flessa, 1996) classified paleontological records into four overlapping classes of temporal mixing: ecological census, within-habitat time averaging, environmental condensation, and biostratigraphic condensation. This classification reflects a prevailing point of view (e.g., Kidwell and Bosence, 1991; Kowalewski, 1996a; Martin, 1999) that paleontological records vary along a continuum of time averaging from days to millions of years. It also implies that all records are time-averaged -- indeed, all records must be mixed at some scale as perfect synchronicity is infinitely unlikely (Kowalewski, 1996a). However, from the perspective of depositional and stratigraphic resolution, it seems useful to distinguish "ordinary" (time-averaged) records that dominate sedimentary strata from unusual and easily discernible extremes of snapshots, condensation, and *remanié*. Such "ordinary" strata do not contain any obvious relic fossils and occur within successions of beds separated by regular diastems rather than disconformities. That is, the term time averaging denotes here ubiquitous records that contain no obvious warning signs of mixing or condensation, but still may have a relatively low depositional resolution. Thus, our definition differs from that of many recent studies (e.g., Kidwell and Bosence, 1991; Kowalewski, 1996a; Kidwell and Flessa, 1996; Kidwell, 1998) in that we restrict the concept of time averaging to interdiastemal units and exclude the extreme cases of condensation and *remanié*. We use the term "temporal mixing" to denote all types of records and understand time averaging as a special (inter-diastemal) case of temporal mixing.

Our definition returns to the original definition of time averaging of

Walker and Bambach (1971) who proposed the term to denote subtle mixing that affect unsuspicious-looking deposits, and not obvious cases of culling such as dinosaur teeth in Tertiary river beds (e.g., Argast *et al*., 1987). Thus, time averaging is a subtle temporal mixing. Accordingly, paleontological records are categorized here into three major classes of resolution: (1) snapshots ("ecological census" of Kidwell and Bosence, 1991) that contain fossils that are all contemporaneous with one another; (2) time-averaged records ("within-habitat time averaging") that contain fossils mixed over time intervals notably exceeding the life span of organisms, typically hundreds to thousands of years (see below), but include no signs of substantial temporal mixing associated with condensation or reworking of much older fossils into much younger deposits; and (3) condensed records and *remanié* ("environmental condensation" and "biostratigraphic condensation" *sensu* Kidwell and Bosence, 1991) that include mixtures of fossils culled over longer time scales, typically tens of thousands to millions of years. For more details see Section 2.3 below.

Three aspects of temporal mixing need to be considered when evaluating temporal depositional resolution of a stratum: (1) the duration of temporal mixing (Section 2.2); (2) the internal temporal structure (Section 2.3); and (3) the completeness of the temporally mixed deposit (Section 2.4).

2.2 Duration of Temporal Mixing

The duration of temporal mixing (i.e., the time span represented by fossils contained in a single sample) is the key determinant of depositional resolution of paleontological records contained within individual strata. The shorter the time span of temporal mixing of a given stratum, the finer the depositional resolution of that stratum.

The most common way to measure time averaging is the age range between the youngest and oldest fossil sampled from a stratum (e.g., Flessa and Kowalewski, 1994). The shell half-life (amount of time it takes to destroy 50% of shells; e.g., Meldahl *et al*., 1997) and the standard deviation of dated specimens (Kowalewski *et al*., 1998) have also been used. Regardless of the metric used, temporal mixing can be assessed from various data including actuopaleontological, paleontological, and computer-based approaches. The current estimates come primarily from research in modern and subfossil depositional systems where direct quantitative estimates can be obtained by absolute dating of individual shells. The indirect methods based on faunal differences, shell survival experiments, or resampling methods have also been employed but are much less reliable (see Flessa, 1993) and vary much more in their estimates of temporal mixing (Peterson, 1976; Cadée, 1984; Carthew and Bosence, 1986; Staff *et al*., 1986; West *et al*.,

1990; Kidwell and Bosence, 1991; see Flessa, 1993). Consequently, we focus our discussion here primarily on estimates derived by direct dating of individual specimens and use other lines of evidence only as supplemental sources.

The dating projects conducted to estimate temporal mixing in marine bioclastic deposits (Table 1) are all restricted by the range of radiocarbon dating (the last 40,000 years or so) and necessarily target the youngest fossil record (the latest Pleistocene and Holocene). Except for foraminifers, the estimates in Table 1 were derived by dating individual specimens collected, in most cases, from single sites or single strata. These specimens were collected either from active depositional surfaces with live fauna (mixing estimated by the oldest dated individual) or from single subfossil beds (mixing estimated by the age range between oldest and youngest fossil). Both approaches yield estimates of incipient mixing, prior to any serious temporal culling. They are, therefore, expected to be a good analogue for interdiastemal time averaging, and not condensed records or *remanié*.

The estimates show that regardless of the type of depositional environment (supratidal, intertidal, nearshore subtidal, or offshore shelf) or analyzed taxa (mollusks, brachiopods, or foraminifers), temporal mixing is always present. The variation among the estimates barely exceeds one order of magnitude, with values ranging from a few hundred to several thousand years, suggesting that time averaging of marine shelly fauna varies in a narrow range relative to the overall range that is possible for temporal mixing of fossils (Fig. 3). It is also noteworthy that dating of terrestrial and lacustrine gastropod accumulations yielded strikingly comparable estimates of temporal mixing: hundreds to thousands of years (Cohen, 1989; Goodfriend, 1987, 1989; Goodfriend and Gould, 1996; Goodfriend and Ellis, 2000).

In addition, many studies with other research goals (not included in Table 1) provided multiple dated specimens from single marine sites or surfaces (e.g., Bjorlykke *et al*., 1978; Wilson, 1979, 1988; MacIntyre *et al*., 1978; Nelson *et al*., 1988). These studies yielded comparable estimates (see Flessa, 1993), but were generally on the higher end, reaching as much as 30,000 years. This is at least partly because many of those studies deliberately targeted older materials (for example, MacIntyre *et al*., 1978, specifically dated relic oysters). Higher estimates were also obtained for bivalve shells collected from modern beaches of the eastern United States (Wehmiller *et al*., 1995). In essentially all sites analyzed by Wehmiller *et al*., temporal mixing exceeded 10,000 years: about 60% of shells dated by Wehmiller and his colleagues were Pleistocene in age and some were perhaps as old as 500 to 700 kyr. These shells were derived from

Table 1. Estimates of the duration of temporal mixing in marine bioclastic accumulations in Late Quaternary deposits and/or present-day depositional environments.

Reference	Type of study[1]	Environment /Deposit	Organisms	Temporal mixing[2]	(n)	Age structure
Flessa *et al*.,	Radiocarbon	Tidal flats	Bivalves	3200[3]	(17)	Right-skew
1993	Radiocarbon	Tidal flats	Bivalves	1500[3]	(13)	Right-skew
Flessa and	Literature	Nearshore	Mollusks	1200[3,4]	(63)	Right-skew
Kowalewski,	Literature	Shelf	Mollusks	9200[3,4]	(129)	Right-skew
1994	Literature	Fossil beds	Mollusks	800[3,4]	(35)	Right-skew
	Literature	Beach ridge	Mollusks	1400[3,4]	(49)	Right-skew
Martin *et al*.,	Radiocarbon	Tidal flats	Bivalves	1700[3]	(2)	Not known
1996	Radiocarbon	Tidal flats	Bivalves	2100[3]	(4)	Not known
	Radiocarbon	Tidal flats	Bivalves	800[3]	(2)	Not known
	Radiocarbon	Tidal flats	Forams	2000[3,5]	(1)	Not known
	Radiocarbon	Tidal flats	Forams	1300[3,5]	(1)	Not known
Meldahl *et*	Radiocarbon	Fan delta	Bivalves	1000[3]	(24)	Right-skew
al., 1997	Radiocarbon	Fan delta	Bivalves	1100[3]	(24)	Right-skew
	Radiocarbon	Pocket bay	Bivalves	500[3,6]	(24)	Right-skew
Kowalewski	Amino acids	Beach ridge	Bivalves	300[3.6]	(20)	Uniform
et al., 1998	Amino acids	Beach ridge	Bivalves	200[3,6]	(20)	Uniform
	Amino acids	Beach ridge	Bivalves	1100[3,6]	(20)	Right-skew
	Amino acids	Beach ridge	Bivalves	800[3,6]	(18)	Uniform
	Amino acids	Beach ridge	Bivalves	800[3,6]	(21)	Uniform
	Amino acids	Beach ridge	Bivalves	800[3,6]	(19)	Uniform
	Amino acids	Beach ridge	Bivalves	600[3,6]	(7)	Not known
	Amino acids	Beach ridge	Bivalves	1200[3,6]	(19)	Uniform
	Amino acids	Beach ridge	Bivalves	600[3,6]	(19)	Uniform
Carroll *et*	Amino acids	Inner shelf	Brachiopods	400[3,6]	(19)	Uniform
al., 2000	Amino acids	Inner shelf	Brachiopods	530[3,6]	(20)	Uniform
	Amino acids	Inner shelf	Brachiopods	2000[3,6]	(21)	Right-skew
	Amino acids	Inner shelf	Brachiopods	3100[3,6]	(22)	Right-skew

[1]Studies based on uncalibrated or partly calibrated amino-acid methods (e.g., Powell and Davies, 1990; Wehmiller *et al*., 1995) are not included here because they do not provide estimates that can be expressed in years. Nevertheless, these studies also suggest the levels of temporal mixing on the scale of hundreds to thousands of years.

[2]All estimates in years rounded to the nearest 100. Number of dated specimens provided in parenthesis.

[3]Temporal mixing measured as the age range defined by the difference in age between the youngest and oldest dated specimens in a sample. For active depositional settings that included living fauna, the range was estimated by the oldest dated specimen.

[4]Median values of temporal mixing[3] for sites compiled from the radiocarbon literature estimates (see Flessa and Kowalewski, 1994, for details).

[5]Estimates based on ^{14}C dates of multiple tests of foraminifers (see Martin *et al*., 1995, 1996).

[6]Estimates exclude shells that are outside of the calibration range (i.e., values underestimate the amount of temporal mixing).

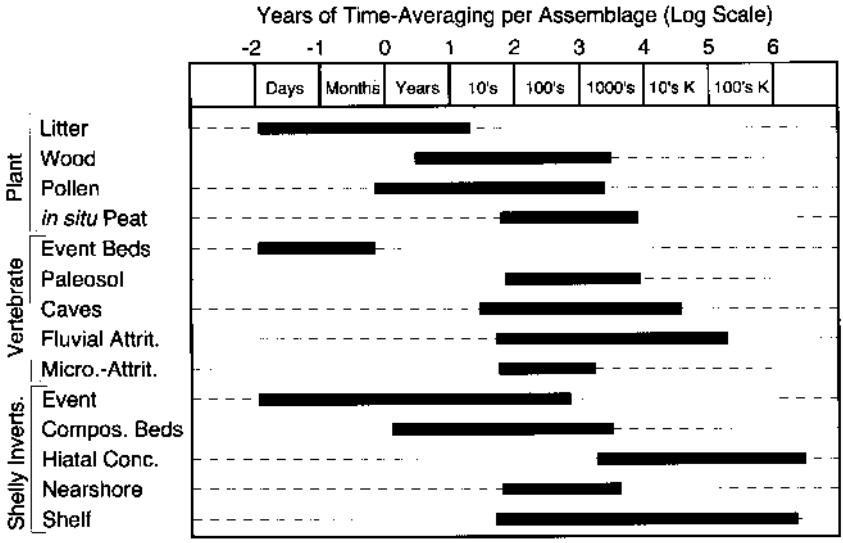

Figure 3. Estimates of temporal mixing for modern and fossil assemblages from terrestrial and marine depositional systems. Reproduced from Behrensmeyer *et al*. (2000, fig. 3) with the permission of the Paleontological Society.

Pleistocene sediments that commonly crop out in the shoreface and inner shelf of the region. This exceptionally high mixing is due to the combination of the rapid, post-glacial sea-level rise and the fact that Holocene sediment cover is thin in the region. Thus, the study provides an analogy for *remanié* rather than interdiastemal time averaging.

Admittedly, considerable risks are involved in extrapolating modern rate estimates into the older record (e.g., Gould, 1965, 1987). However, it should be stressed that the resolution of subfossil and modern accumulations cannot be improved, but only worsened by subsequent geological processes. Diagenetic processes, erosional unroofing, and other processes that may affect surficial deposits before they become fossiliferous strata cannot unmix already mixed bioclasts. They can only mix them further. The more serious problem is that many modern depositional surfaces represent settings where sediment supply is still limited following the end-glaciation sea-level rise. Such settings characterized by unusually low sedimentation rates may be more prone to temporal mixing than typical records. However, studies that targeted areas with high sedimentation rates (e.g., Meldahl *et al*., 1997) -- providing the best analog for interdiastemal deposits -- yielded estimates comparable with those obtained in other studies. This reinforces the validity of the actuopaleontological estimates of temporal mixing.

Mixing can also be inferred using taphonomic, sedimentological and

stratigraphic evidence (e.g., Brett and Baird, 1993; Johnson, 1993; Kidwell, 1993b; Rogers, 1993). Such approaches cannot employ direct dating methods and therefore provide much less precise estimates of temporal mixing. Nevertheless, these studies in the older fossil record suggest scales of temporal mixing (see Kidwell and Behrensmeyer, 1993; Behrensmeyer and Kidwell, 1993; Fig. 3) comparable to those implied by dating projects in the Holocene. Computer models of taphonomic processes (Cutler and Flessa, 1991; Miller and Cummins, 1990, 1993; Powell, 1992; Kowalewski and Misniakiewicz, 1993; Behrensmeyer and Chapman, 1993; Cutler, 1993; Sadler, 1993; Cutler and Behrensmeyer, 1996; Olszewski, 1999) provide supplementary insights that seem consistent with the estimates of Table 1.

A summary of estimates of depositional resolution was provided by Behrensmeyer and Kidwell (1993; see also Martin, 1999) who compiled actualistic, paleontological, and computer-based studies and showed that temporal mixing (including snapshots, time-averaged records, and condensed records and *remanié*) ranges over at least 9 orders of magnitude of time (Fig. 3): from days (10^{-2} years) to millions of years (10^{6} years). If one includes rare cases of early Paleozoic fossils reworked into modern sediments, the range of temporal mixing could be extended up to 10^{8} years. Because well-biomineralized fossils such as mollusks or foraminifers are ubiquitous in the fossil record and very useful in stratigraphy, the resolution suggested by dating projects using bioclastic materials (Table 1) provides a highly relevant estimate of the duration of interdiastemal time averaging. The recent study of Carroll *et al*. (2000) (Table 1) that provides first estimates of temporal mixing for brachiopods reinforces the general validity of estimates obtained for mollusks and foraminifers and suggests that brachiopod-derived bioclasts may undergo as much age mixing as do mollusks.

Despite all caveats and uncertainties, the evidence is strong that, although temporal mixing can vary over 9 orders of magnitude, interdiastemal depositional resolution ranges typically from 100's to 1000's of years.

2.3 Internal Structure of Temporally-Mixed Strata

Temporal aspects of depositional resolution encompass not only the duration of a temporally-mixed record, but also the internal temporal structure of that record. A storm bed that mixes fossils from two short time-intervals separated by a 1000-year gap and a storm bed that mixes fossils representing a continuous 1000-year record are comparable in terms of the duration of temporal mixing, but differ dramatically in their internal temporal structure and completeness.

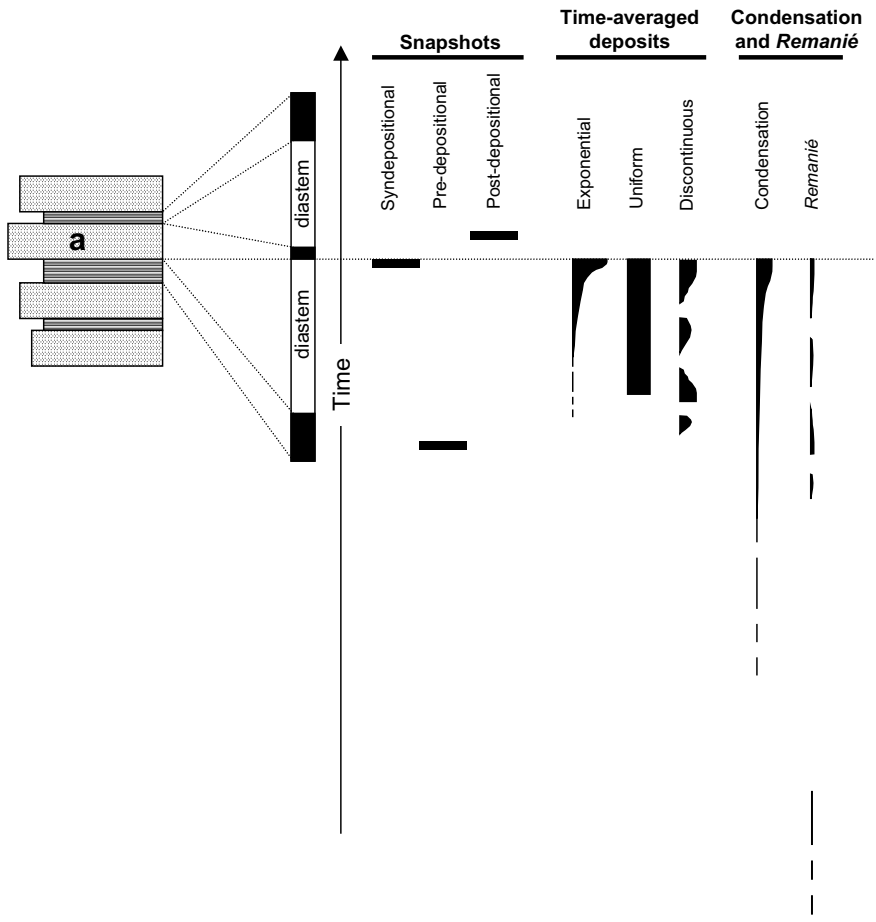

Figure 4. Temporal structure of paleontological records. Depositional resolution of records contained within a single stratum (exemplified by Bed "a") can vary greatly in terms of temporal structure. Solid shapes represent eight hypothetical examples of age structures of fossils that can be preserved in a bed. They illustrate the end-member classes of temporal mixing predicted for marine, bedded deposits. Note that even though the duration of temporal mixing in the three time-averaged records is comparable, they vary in their age structure (the depositional resolution of those records differs subtly despite the same duration of mixing,).

Eight end-member types of records are expected to occur in the fossil record (Fig. 4): three types of snapshots (pre-, syn-, and post-depositional), three types of time-averaged records (exponential, uniform, and discontinuous), condensation, and *remanié*. These types of records are not hypothetical, as most of them have been already illustrated empirically.

2.3.1 Syndepositional Snapshots

These are associated with mass-mortality events, where a bed is dominated by remains of organisms killed during the single depositional event by which the bed formed. Boyajian and Thayer (1995) described a beach deposit on the New Jersey shore that consisted almost exclusively of shells of the bivalve *Spisula* killed during a 1992 winter storm. Fenton (1966) observed similar syndepositional snapshot made of shells of *Lingula* in the Philippines. Ediacaran fossil assemblages are a likely fossil example of syndepositional snapshots (Seilacher, pers. comm. 1992; see also Seilacher, 1989). On the other hand, an obrutionary deposit of shelly organisms need not represent a snapshot because biomineralized fossils are likely to include specimens that predate notably an obrutionary event (e.g., Simões *et al*., 1999). Syndepositional snapshots may be also occasionally observed among trace fossil assemblages made in soft substrates (e.g., Kotake, 1994; Kowalewski and Demko, 1997).

2.3.2 Pre-Depositional Snapshots

Beds where fossil assemblages pre-date the depositional events, have not yet been documented but could be formed by reworking of older snapshots during subsequent depositional events. Such temporal structures are probably rare because they can form only in areas devoid of bioclasts younger than the reworked snapshot materials ("virgin areas" *sensu* Craig and Oertel, 1966).

2.3.3 Post-Depositional Snapshots

These occur whenever colonization events post-date depositional events. Burrowing organisms can attempt to colonize substrate after its deposition and fail to do so. This is documented in the fossil record by unsuccessful attempts of colonization recorded by short-term trace fossil assemblages on top of turbidite-generated sediments (e.g., Föllmi and Grimm, 1990; Grimm and Föllmi, 1994). Body fossil assemblages incorporated after depositional events are also documented (e.g., Richard, 1972; Richards and Bambach, 1975). Such snapshots are probably much less common than syndepositional snapshots.

2.3.4 Exponential Time Averaging

This depositional mode is well documented by dating projects, which show that age-frequency distributions of dated fossils tend to be strongly

right-skewed (Table 1), approximating exponential curves (Flessa *et al*., 1993; Flessa and Kowalewski, 1994; Martin *et al*., 1996; Meldahl *et al*., 1997; Olszewski, 1999; Kowalewski *et al*., 2000). This pattern, somewhat analogous to that resulting from the decay of a radioactive isotope, reflects an exponential loss of older shells through destruction by taphonomic processes (Flessa *et al*., 1993; Flessa and Kowalewski, 1994; Meldahl *et al*., 1997; Martin, 1999). As suggested by dating, exponential time averaging is probably the most common type of time averaging in the marine fossil record in the nearshore and shelfal settings (Table 1).

2.3.5 Uniform Time Averaging

This style of age mixing has been documented recently in a project involving extensive amino-acid racemization dating of shells of the bivalve *Chione fluctifraga* from the Colorado River Delta (Kowalewski *et al*., 1998). For seven out of nine samples of dated shells, age distributions were statistically indistinguishable from a uniform distribution (Table 1). Thus, some shell beds may record the optimal type of time averaging, where paleobiological data are a time-weighted average of the faunal composition from the spectrum of environments that existed during the entire interval of time. When the data from individual samples are pooled, however, the resulting structure of time averaging becomes exponential (Kowalewski *et al*., 2000, fig. 2 therein), suggesting that the structure of time averaging may be partly dependent on sampling and analytical resolutions (see also Fürsich and Aberhan, 1990; Behrensmeyer and Hook, 1992) with exponential time averaging becoming increasingly common at coarser scales of observation.

2.3.6 Discontinuous Time Averaging

This concept was proposed by Fürsich and Aberhan (1990) who pointed out that time averaging can be either continuous with all time-averaged time intervals represented in an assemblage or discontinuous with some of the time intervals missing (see also Fig. 6 later in the text and Kidwell, 1998). The extreme case one could imagine is a deposit made by mixing two syndepositional snapshots that differ notably in age. Obviously, the continuity (i.e., completeness) of a time-averaged record is scale-dependent and therefore the same record may be continuous or discontinuous depending on the level of resolution chosen for analysis.

2.3.7 Condensation

Condensation typically occurs when sedimentation rate is so low as to

allow for a substantial temporal culling of fossils. These types of records are most often associated with major sequence boundaries and maximum flooding surfaces (see below) and include environmental and biostratigraphic condensation. The environmental condensation involves mixing of remains of organisms that lived in different environments (Fürsich, 1978). The co-occurrence of oyster shells with deeper-water faunas condensed together on present-day, sediment-starved shelves (e.g., MacIntyre *et al*., 1978) offers an excellent modern analog of environmental condensation. In the most extreme cases stratigraphic condensation may result, as revealed by co-occurrence within single strata of index fossils from different biostratigraphic zones (e.g., Wendt, 1970; Jenkyns, 1971; Machalski and Walaszczyk, 1987; see Kidwell and Bosence, 1991, p. 181 for more details and references).

2.3.8 Remanié

Remanié (*sensu* Craig, 1966) are extreme cases of temporal mixing via reworking or unroofing with fossils culled over time scales often exceeding millions of years. *Remanié* can result from both abiotic and biotic mechanisms. Abiotic reworking is probably a dominant causal factor. For example, coastal exposures of the fossiliferous Miocene of Maryland contribute 6 to 17 million year old shells to the nearshore deposits forming today (Flessa, 1993). Also, biological *remanié* can form as a result of biological recycling of fossils by hermit crabs (Walker, 1994), but it is difficult to evaluate the frequency and severity of this mechanism.

2.3.9 Summary

The eight types of record can be viewed as end-members along a spectrum of possible records. Intermediates between the types as well as mixtures likely occur even within single-event fossil concentrations (*sensu* Kidwell, 1991a). For example, Simões and Kowalewski (1998) documented that even a deposit that was believed to represent a single storm bed may represent a complex mixture of snapshots and time-averaged records.

An important question is: how common are snapshots, condensation, and *remanié* relative to time-averaged records? Frequency of snapshots is difficult to evaluate for the older record where direct, high-resolution dating of the material is not possible. However, *all* dating studies in modern depositional systems (primarily from nearshore to shelfal environments) reveal substantial time averaging (Table 1) and suggest that snapshots are neither present in subfossil deposits nor are they being formed in modern depositional settings. Because old shells are always present on or just below

modern surfaces (e.g., Flessa and Kowalewski, 1994; Wehmiller *et al*., 1995; Kowalewski *et al*., 1998), and temporal mixing is a function of the availability of old shells in the depositional system, even catastrophic deposits (mass-mortality bone beds, storm shell beds, etc.) will typically contain notable admixtures of older materials (see Brett and Baird, 1993; Kowalewski *et al*., 1998; Simões and Kowalewski, 1998). Thus, if a major storm hit an inner shelf, the resulting deposit, even though formed in several hours, would be made of shells that vary in age by hundreds of years. Only when mass-mortality events occur out of the natural habitat ("virgin area" *sensu* Craig and Oertel, 1966), or when standing populations are abundant enough to overwhelm older bioclastic materials (e.g., Boyajian and Thayer, 1995), depositional snapshots can occur. The frequency of snapshots may be higher in basinal settings when intermittent colonization events may punctuate anoxic conditions, but bedded, nearshore and shelfal successions of strata and bioturbated non-laminated deposits are unlikely to contain snapshot records.

In contrast to snapshots, condensed records may be relatively common in marine sedimentary successions, as indicated by the literature compilation of Kidwell (1991a). The distribution of condensed records within stratigraphic sequences is not uniform, varying depending on subsidence rates and position in the sequence. Condensed shell beds are particularly common in association with maximum flooding surfaces, onlap, and 2nd and 3rd order sequence boundaries (see Carter *et al*., 1991; Kidwell, 1991a, b, 1993a; Holland, 1995; Kondo *et al*., 1998). The condensed nature of records can often be inferred from sedimentary and taphonomic features (phosphorite steinkerns, abundant shark teeth, variable preservation of fossils) (Kidwell, 1991a; Brett and Baird, 1993; Kidwell and Bosence, 1991). Condensation may also be identified by anachronous or ecologically-incompatible fossils (e.g., Fürsich, 1978). *Remanié* are temporally anomalous deposits that should be easy to recognize, with the possible exception of temporal anomalies generated by biological agents (Walker, 1994). No data exist to evaluate the frequency of *remanié* through the Phanerozoic.

In summary, (1) time-averaged records (primarily of exponential type) are the most common types of interdiastemal records from nearshore and shelfal settings, (2) snapshots are rare, (3) condensation may be common around some types of sequence boundaries (but rarely in interdiastemal beds), and (4) *Remanié* are easy to recognize but their frequency in the record is not known. Table 1 provides what we believe to be a picture of typical temporal mixing within bedded successions of strata. Interdiastemal deposits are expected to be characterized by exponential time averaging on the scale of 100's to 1000's years.

2.4 Depositional Completeness

The internal structure of temporally mixed deposits determines *depositional completeness* of records provided by samples taken from those deposits. How continuous or discontinuous is temporal mixing? How temporally complete are records extracted from individual paleontological samples? Those questions cannot be answered for the older fossil record, but some insight can be gained (again) by dating the most recent materials and exploring them in a fashion analogous to estimating paleontological or stratigraphic completeness (e.g., Sadler, 1981; Allmon, 1989; Sadler and Strauss, 1990). Kowalewski *et al*. (1998) defined the temporal completeness of a sample as the percent of time-intervals, within the time-span of a sample, that are represented by the paleontological record (a definition analogous to that for temporal paleontological completeness of Allmon (1989) and McKinney (1991)). For example, at the resolution of 50 years, the completeness of a sample from Beach Ridge 2 (illustrated later in the text; Fig. 6a) is 41%. Nine out of the 22 50-year intervals separating the oldest from the youngest shell in the sample contain records.

Kowalewski *et al*. (1998) found that, at the dating resolution of 50 years, the temporal completeness of the record provided by mollusk samples collected from the beach ridges of the Colorado Delta varied from 41 to 100% and averaged 63.6%. That is, for an average sample, a time series of individually dated shells provided records for over a half of the 50-year time intervals encompassed by that time series. Almost all gaps can be attributed to small sample sizes. The observed completeness of 63.6% was very close to the highest possible completeness value that would be expected for sample sizes available in that study (~20 specimens per sample). That is, if we draw random samples of ~20 shells from a 100%-complete, uniform time-series, the expected completeness is 67.3%. Thus, the samples, when analyzed at this rather high 50-year resolution level, appear to have a continuous (= complete), temporal structure. No other analyses of this sort have been conducted to date, so we have no way of evaluating how common (or rare) continuous and discontinuous age structures are.

2.5 Spatial Resolution

Depositional resolution can also be lowered by lateral transport of fossils. Such transport may not only mix specimens from different regions, thus confusing paleoenvironmental interpretations, but may also enhance temporal mixing by contributing specimens derived from two or more source areas that differ in the age structure of bioclasts. As is the case for temporal mixing, the scale of spatial mixing is not only a function of environmental

setting but also may vary among different types of fossils depending on their size and skeletal durability. Skeletal durability and small weight both may enhance the scale and significance of pre-burial transport (Kowalewski, 1997). Numerous studies suggest, however, that marine macrofossils are typically preserved in their habitats and only a small fraction is transported any substantial distance (see Johnson, 1965; Kidwell and Bosence, 1991; Kidwell and Flessa, 1996; Anderson *et al*., 1997; Behrensmeyer *et al*., 2000). Even in the extreme case of high-energy, shallow-water deposits forming in transgressive settings, only a small fraction of fossils undergoes any substantial transport (Flessa, 1998). Thus, for the dominant type of marine fossiliferous deposits such as shell beds, substantial lateral mixing is probably limited (see also Martin, 1999; Behrensmeyer *et al*., 2000). Moreover, even in the case of some durable microfossils such as foraminifers – which, intuitively, may appear particularly prone to spatial mixing – substantial transport is not very common, especially below wave base (see Bé and Hutson, 1977; Martin, 1999; but see Anderson *et al*., 1987).

Of course, spatial mixing may be substantial in bioclastic concentrations formed at major disconformities, sequence boundaries and maximum flooding surfaces, where temporal mixing is more severe and depositional history of individual fossil concentrations tends to be more complex (e.g., Kidwell, 1991a). However, these generally belong to what we call condensed records and notable spatial mixing is, most likely, negligible in the case of interdiastemal, time-averaged records.

2.6 Factors Controlling Depositional Resolution

Numerous factors can affect the scale of temporal mixing (Kidwell and Bosence, 1991; Flessa and Kowalewski, 1994; Kowalewski, 1996a; Kidwell, 1998). They include (1) intrinsic factors that characterize organisms; (2) direct extrinsic factors of depositional environments; and (3) indirect extrinsic factors.

Intrinsic factors, in particular the type of skeletal material, are important because temporal mixing is largely dependent on the skeletal durability of remains that are being mixed (Kowalewski, 1997). Durable hard parts can survive multiple reworking events and a long residence time near depositional surfaces and, consequently, may undergo temporal mixing on a scale of hundreds to thousands of years (e.g., Behrensmeyer, 1991; Flessa *et al*., 1993). In contrast, fragile remains such as leaves (e.g., Burnham, 1993; Greenwood, 1991; Wing and DiMichelle, 1995) or lingulid brachiopods (e.g., Kowalewski, 1996b) do not last very long on active depositional surfaces. Thus, they are much less prone to temporal mixing and more likely to provide records with a temporal resolution of months or single years. In

fact, we can view the resolution of the fossil record as a reciprocal function of durability of fossils (Fig. 5), as determined by their morphology, mineralogy, and microstructure. The decrease in depositional resolution that typifies durable fossils is compensated by the corresponding increase in the stratigraphic and depositional completeness of their records (Fig. 5). Other intrinsic factors including population density, geographic range, and life habitat can also play an important role. For example, abundant and widespread populations of planktonic foraminifers that provide a lot of material for mixing are more prone to temporal mixing than a single endemic cohort of a deep-infaunal clam, which is less likely to be transported after death and provide few specimens for mixing in the first place.

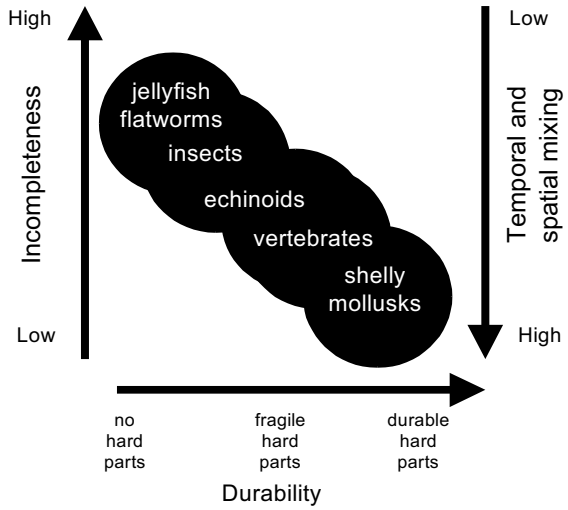

Figure 5. The Reciprocal Taphonomic Model. Increased skeletal durability (X - axis) improves the completeness of the fossil record (left Y-axis). But, organisms with durable skeletons are more prone to post-mortem temporal and spatial mixing (right Y-axis). The black circles represent typical members of a given group of organisms, and not all possible cases of skeletal durability within that group. Modified after Kowalewski, 1997, fig. 1.

Direct extrinsic factors that are important include sedimentation rate, bioturbation, and biotic and abiotic taphonomic agents. Sedimentation rate controls the potential residence time for skeletal remains present around depositional surfaces (see also Kidwell, 1991a, 1998). Decrease in net sedimentation rate correlates with increase in temporal mixing and ultimately can lead to stratigraphic condensation. Meldahl *et al*. (1997) confirmed that pattern by showing that samples of mollusks collected from modern nearshore seafloors vary in duration of temporal mixing as a

function of the local short-term accumulation rates. Bioturbation also plays an important role by mixing shells in surficial sediments and by sheltering bioclasts from harsh surficial taphonomic processes via temporary burial (e.g., Rhoads and Stanley, 1965; Clifton, 1971; Aller, 1982; Meldahl, 1987; Flessa *et al*., 1993; Martin *et al*., 1996; Bradshaw and Scoffin, 2001). Although bioturbation may increase degradation of bioclasts (e.g., Aller, 1982; Davies *et al*., 1989; Walker and Goldstein, 1999), the studies of Flessa *et al*. (1993) and Bradshaw and Scoffin (2001) suggest that the positive role of bioturbators outweighs their negative effects. Taphonomic processes such as chemical dissolution, mechanical fragmentation, bioerosion, and durophagous predation control the rate of destruction of hard parts and may shorten the half-life of bioclasts. A special case is represented by hermit crabs that recycle gastropod shells and can enhance temporal mixing by preventing their final burial (see Walker, 1994).

Indirect extrinsic factors of temporal mixing include: (1) subsidence rate and tectonic setting that control direct extrinsic factors and (2) historical contingencies imposed by sea-level changes. The tectonic setting affects subsidence rate, which in turn influences accommodation space and net-accumulation rates. Tectonic setting can also affect the nature and intensity of taphonomic processes affecting skeletal remains (e.g., Kidwell, 1988; Meldahl and Cutler, 1992). Sea-level changes can also play a fundamental role by creating environments in "virigin areas" that are not contaminated by older fossils. Shells found in nearshore environments today are dominated by specimens from the last 2-3 thousand years (Flessa and Kowalewski, 1994; but see Wehmiller *et al*., 1995) and the lack of older shells reflects the fact that, in most regions, the Holocene transgression did not reach current nearshore habitats before that time. In contrast, early Holocene or even Late Pleistocene shells are quite common in more offshore habitats. Thus, the recent sea-level changes of a given area often set limits on potential temporal mixing (see Flessa and Kowalewski, 1994 for more details).

2.7 Trends through the Phanerozoic

Because many factors controlling temporal mixing show secular trends through time, the depositional resolution of paleontological records is likely to have changed notably through the Phanerozoic. Kidwell and Brenchley (1994, 1996; see also Li and Droser, 1999; Simões *et al*., 2000) documented an increase in thickness and taphonomic complexity of marine skeletal accumulations through the Phanerozoic. Such increase implies a parallel increase in temporal mixing (Kidwell and Brenchley, 1996; Kidwell, 1998). In addition, the increase in rates and depth of bioturbation observed through the Phanerozoic (Thayer, 1983; Ausich and Bottjer, 1982; Droser and

Bottjer, 1989, 1993; Sepkoski *et al*., 1991) may have played an important role in increasing temporal mixing -- not only directly by enhancing temporal mixing of bioclasts (Section 2.6), but also indirectly by decreasing the frequency of *recorded* storms (Brandt and Elias, 1989; Sepkoski *et al*., 1991) and increasing the length of diastems (see Section 3.5 below).

Support for the Phanerozoic increase in temporal mixing was provided by Kidwell (1990), who contrasted the relatively fresh appearance of brachiopods found in Early Paleozoic deposits (indicative of a limited temporal mixing) with the highly variable taphonomic signature of Neogene bivalves (indicative of a poor depositional resolution).

2.8 Inorganic versus Organic Records

Whereas we focus on biological records, the concept of depositional resolution is applicable to many physical records contained in the geological record. Temporal mixing affects sedimentary grains, diagenetic precipitates, silicates forming in magma chambers, and so on. In many cases, inorganic records are time-averaged over much longer time scales than biological records. This is largely due to the fact that silicate minerals are less prone to destruction than carbonate or organic fossils (see Kowalewski and Rimstidt, in press). Also, abiotic grains are not limited to the last half a billion years of the Earth's history and occur over a much larger spectrum of source areas than biological remains. Finally, fossils that are too fragmented or altered have lower informative value, and, thus, have not been evaluated for temporal mixing with such scrutiny as larger, more complete specimens. Because smaller grains tend to last longer, the temporal mixing of biocarbonates may be underestimated relative to detrital zircon or apatite, often dated in studies of provenance (e.g., Ross and Gehrels, 1998; Gehrels *et al*., 1999). This pragmatic bias reflects the real differences between the depositional resolution of *useful* inorganic records and *useful* organic records.

The difference in the resolution between inorganic and organic records, illustrated on our conceptual diagram (Fig. 2), can be demonstrated by comparing age distributions of bioclasts and detrital inorganic grains. The best-documented examples of inorganic mixing is provided by detrital zircon grains (e.g., Ross and Gehrels, 1998; Gehrels *et al*., 1999), for which temporal mixing commonly exceeds a billion years. The comparison of age-distributions derived for bioclasts (Fig. 6a) and zircon grains (Fig. 6b) reveals also intriguing similarities and suggests that a single observational pattern (*sensu* Rogers, 1989) underlies a temporal structure of grains contained in samples extracted from sedimentary rocks (see also

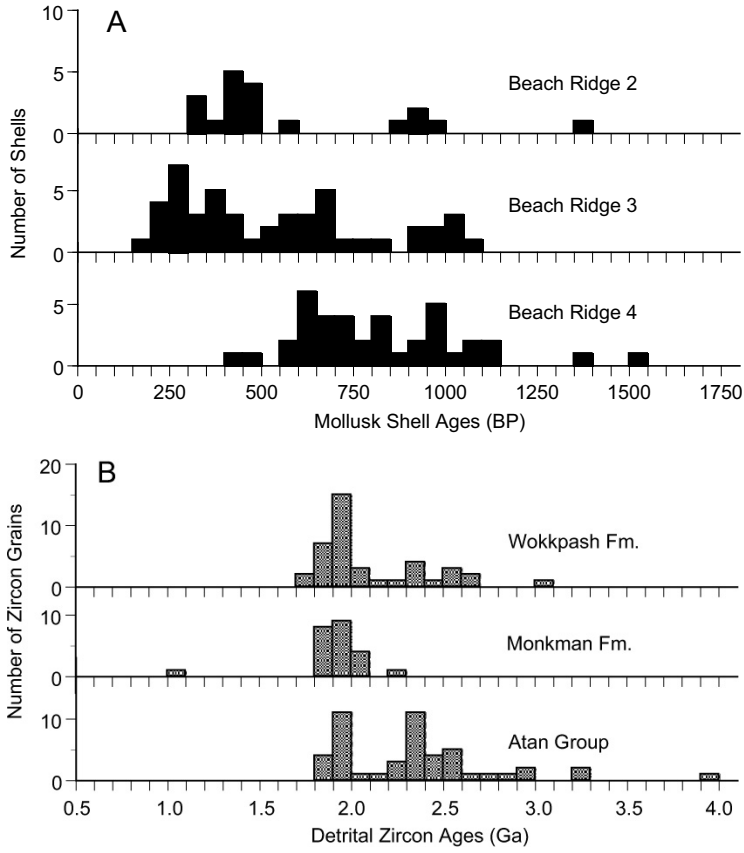

Figure 6. Similarities in age distributions of shells and detrital zircon grains. A. Ages of mollusk shells (*Chione fluctrifaga*) from the Colorado River Delta (Baja California) dated using ^{14}C-calibrated amino-acid racemization methods (data from Kowalewski *et al*., 1998). B. Ages of individual grains of detrital zircon extracted from Paleozoic sandstone samples from British Columbia and dated using U-Pb methods (data from Ross and Gehrels, 1998).

Kowalewski and Rimstidt, in press). Despite extreme difference in the time scale (billions versus hundreds of years) and in the type of grains ($ZrSiO_4$ vs.$CaCO_3$), the temporal age distributions of those two types both display (1) time lags; (2) right skewness; and (3) multimodality. Respectively, these patterns are explainable by scale-independent and grain-independent tendencies for (1) sedimentary grains to predate depositional events; (2) older grains to be more likely to have been destroyed and/or less likely to be at the surface; and (3) source area of grains to have a high stratigraphic heterogeneity. Whereas the processes and temporal scales of the compared systems are obviously very different, the nature of the resulting records is quite comparable.

2.9 Depositional Resolution: A Summary

The previous sections can be summarized in terms of general statements regarding the depositional resolution of the paleontological record. The statements are most applicable to common marine macrofossils and to deposits separated by small-scale diastems and as such are useful in formulating generalizations regarding the limits of depositional resolution for typical fossil records found within bedded successions. The statements should not be, however, extrapolated to less common fossil groups, to extraordinary fossil deposits (*Lagerstätten*), to offshore basinal setting, or to laminated deposits.

1. Depositional resolution of fossils taken from sedimentary rocks is expected to range typically from 100's to 1000's of years.
2. Condensation, resulting in more extensive temporal mixing, should be rare in interdiastemal beds, but may be common around major disconformities, sequence boundaries, or maximum flooding surfaces.
3. Instantaneous snapshots and long-term *remanié* are both possible, but are expected to be much less common than, or easier to distinguish from, time-averaged deposits.
4. The internal structure of time averaging tends to be exponential, reflecting a cumulative loss of older shells to taphonomic processes. To some extent, however, the structure of time averaging is a function of sampling and analytical resolution.
5. Depositional completeness can be high, but data are insufficient at this point to evaluate what is the finest resolution level at which typical samples from the fossil record are complete (continuous).
6. Spatial mixing by lateral post-mortem transport may occur, but is not substantial for common marine benthic macrofossils and even microfossils such as foraminifers appear to have good spatial fidelity.
7. Factors controlling depositional resolution include intrinsic characteristics of organisms (type of skeleton, abundance, habitat, biogeography), direct extrinsic factors of depositional environments (sedimentation rates, bioturbation intensity, and abiotic and biotic taphonomic agents), and indirect taphonomic agents (subsidence rate/tectonic setting, sea-level history).
8. Secular trends in the major factors controlling depositional resolution (in particular factors such as skeletal durability and bioturbation rates) suggest that temporal mixing increased through the Phanerozoic.
9. Given similarities in temporal mixing between zircon grains and bioclasts, many statements regarding depositional resolution of paleontological records may also be applicable to abiotic records.

3. DIASTEMS AND STRATIGRAPHIC RESOLUTION

3.1 Distinguishing Diastems from Disconformities

Diastems are the separations (bedding planes) between depositional units, i.e., beds (Figs 1, 2). Diastems form when sediment accumulation is markedly episodic and intervals of non-deposition or erosion occur between intervals of sediment accumulation. Diastems are very small unconformities, not simply the pauses in sediment accumulation that make the breaks between laminae within beds.

In coining the term diastem, Joseph Barrell (1917, p. 748) made the following distinction: "Numerous breaks are now known to exist in which the beds above and below lie parallel, and, except for some change in fauna or flora, give little or no indication of the great lapse of time which occurred between their deposition. Such breaks are known as disconformities. The present argument enlarges on this conception, holding that the breaks of smaller time interval are still more numerous and may add up to equally large measures of time unrecorded by sedimentation. Such breaks have generally been too brief to give a clue by means of a faunal or floral change, but must be recognized through the physical features of the beds, often most readily because of a sudden change at the break in the character of the rhythms expressed in sedimentation. It is proposed to recognize the aggregate importance of such minor breaks by giving them a special name – 'diastem'.'

After noting that Grabau had coined the term disconformity (Grabau, 1913, p. 821–826), Barrell (1917, p. 794-5) discussed the differences between disconformities (as they are commonly recognized) and the breaks in the record he was calling diastems: "a diastem is a break represented in other regions, often within the same formation, by a bed or series of beds. A disconformity is theoretically traceable over a broad area....the two classes of breaks, although typically distinct, must grade into each other. The assignment of a break to one or the other category must not depend on a doubtfully assigned cause, but must rest on the observable field evidence. Therefore the discrimination should rest for disconformities on breadth of occurrence and faunal or floral change, for diastems on breaks in continuity of lesser areal importance, of greater number, and not characterized by permanent faunal or floral change. The presence of diastems makes for a slow rate of accumulation of a formation, associated with a more rapid rate of accumulation of the individual beds."

3.2 Nature of Diastems

We use the term diastem for the breaks in the continuity of sedimentation that produce bedding as seen in the field. Note that we are not discussing lamination although the breaks between individual laminae are, technically, also small diastems. Nor are we discussing diagenetic fissility in shales. For all practical purposes, the spacing between the disturbance events, which create bedding, records the finest-scale stratigraphic resolution that can be obtained in a section. We treat that spacing as the length of diastems because finer resolution is not generally possible.

Many events which generate stratification are high-energy events such as storms. The bulk of material deposited by storms in shelf settings is usually locally reworked rather than entirely new material eroded from the shoreline and transported onto the shelf (Morton, 1988). Therefore, the diastem under a storm bed represents the time for the original deposition of the sediment now reworked into the new storm-generated bed, as well as the time during which the eroding phase of the storm took place. Thus much of the time represented by a diastem may have geological representation in the depositional temporal mixing of the overlying bed (see Section 2 above).

Some features of the stratigraphic record represent at least part of the time interval (diastem) between bed-forming events. Mudstone caps on storm deposits represent whatever deposition may have occurred in the "fair weather" interval between storms as well as deposition during the interval of waning energy after the high-energy phase of the storm that formed the bulk of the bed. However, it is often difficult to separate the later "fair weather" phase from the waning energy phase in mudstone caps on most storm beds, especially if bioturbation has occurred during the “fair-weather” interval. Bioturbation during the interstorm interval can homogenize the slowly accumulating sediment — as well as the top of the underlying tempestite — so any remaining interstorm stratification and the boundary with the underlying tempestite are destroyed. This is true of most post-Early Ordovician sections (Droser and Bottjer, 1989; Sepkoski *et al*., 1991; Droser and Bottjer, 1993). The impossibility of differentiating post-storm deposition from the fine-grained deposition of storm-resuspended sediment in bioturbated strata is clearly illustrated by Raup and Stanley (1971, fig. 11.1, p. 320 with diagram on p. 321).

Also, some scouring is usually present at most sharp bedding plane surfaces, indicating that some of the record has been eroded. If the top surface of a bed is scoured by a later event, the scouring will erode some sediment that had accumulated as part of the bed, thus "erasing" some preserved record (Goldring and Aigner, 1982). The scoured surface thus represents the time during which the now eroded material was originally

deposited and any interval of time after that deposition was complete, including the brief interval during which the scouring and erosion occurred. In fact, many somewhat smaller events may have occurred and been erased by larger, later events, before, by chance, one is left undisturbed to enter the geological record (Fig. 1; see also Sadler, 1993). The "time gap" at the scoured bedding surface represents all the time since the underlying uneroded material was deposited, including the multiple intervals of deposition and reworking that may have occurred prior to the preserved diastem and deposition of the succeeding bed (see also Seilacher, 1985).

Therefore, it is useful to think of a diastem (physically the sharp bedding plane itself) as representing all the time between bed-forming events, even though some of the preserved sediment in the finer-grained stratum in between the coarser-grained parts of two beds may have accumulated during that interval. In this instance, paleontologists need to realize that fossils found in the finer-grained deposits in between storm-generated, time-averaged shell beds lived during the diastem interval and will be more closely allied in time with the older fraction of reworked and redeposited fossils in the capping shell bed, rather than the younger fraction in the underlying shell bed (see also Sections 2.2 and 4.2).

3.3 Duration of Diastems

Although depositional events can occur in quick succession (as in tidalites – Miller and Eriksson, 1997), the depositional events recorded by most sedimentary bedding are usually separated by longer intervals. For example, the bedding planes (diastems) in a series of stacked storm deposits represent most of the time contained in the section because each depositional event (storm) was of short duration (days).

How long are the intervals in between the short intervals of deposition represented by preserved beds? Intuitively, such intervals may be expected to be brief (even several major storms can occur at one location in one season). However, it typically takes decades to centuries before storms large enough to deposit notable amounts of sediment revisit the same location (Table 2). Thorne *et al*. (1991) calculated that storms capable of depositing 10 cm thick beds occur with a frequency of approximately 200 years in areas with shelf water depths of 20 m and 2000 years for areas with 30 m water depths. This is consistent with applying the probabilistic estimates of Gretener (1967) to the data from Abbott (1996): the largest hurricane events (i.e., events expected to be more commonly preserved, in part because they rework evidence of smaller events) can only be expected to recur with high

Table 2. Estimates on spacing between preservable disturbance events and duration of diastems. All estimates expressed in years.

Type of Estimate	Min (yrs)	Mean spacing (years)	Max (yrs)	References
Recent preservable disturbance events				
10 cm beds in 20 m of water	N/A	200	N/A	Thorne *et al*., 1991
10 cm beds in 30 m of water	N/A	2000	N/A	Thorne *et al*., 1991
98% chance of 2 hurricanes crossing 80 km stretch of coast[1]	25	60	400	Gretener, 1967; Abbott, 1996
98% chance of 2 major hurricanes crossing 80 km stretch of coast[1]	57	268	4000	Gretener, 1967; Abbott, 1996
Temporal spacing of strom washovers				
Low marsh (calibr. accumul.)	N/A	153	N/A	Hippensteel and Martin, 1999
Low/high marsh (calibr. accum.)	N/A	316	N/A	Hippensteel and Martin, 1999
High marsh (no bioturbation)	37	102[2]	167	Hippensteel and Martin, 1999
Low marsh (notable bioturbation)	89	245[2]	445	Hippensteel and Martin, 1999
Paleozoic diastems (intervals between bed forming events)				
Cambrian	100	150[2]	200	Koerschner and Read, 1989
Ordovician (Martinsburg Fm.)	130	1715[2]	3300	Kreisa, 1980, 1981
L. Ordovician (Cincinnatian)	91	215	667	Holland *et al*., 1997
Silurian	163	894[2]	1625	Bambach, 1969 (1/4 of time)

[1] Based on the mean likelihood of 6.7% (range from 1% to 16%) of a hurricane impinging on any 80 km segment of the eastern coast of the United States in any one year. For the largest hurricanes (magnitude IV and V, with winds exceeding 208 km/hr) the mean is only 1.5% (range 0.1 % to 7%) (Abbott, 1996). The interval of near certainty of recurrence (a necessary condition if a succession of strata are to be formed by such events) can be calculated by converting the probability of occurrence to the fractional annual likelihood. Gretener (1967) argued that a rare event with a probablity 1/x has a 98% probablility of occurring after four times x. Thus, it appears that hurricanes will occur within 60 years (4x15), but the largest events, which would be expected to be more commonly preserved, can only be expected to have recurred with high probability on a scale of 268 years (with a range of 60 to 4000 years, depending on the regional frequency of such events).

[2] Estimated as a midpoint of the range defined by the minimum and maximum estimates.

probability on a scale of 268 years (with a range of 60 to 4000 years, depending on the regional frequency of such events) (see Table 2 for details). These theoretical estimates match well with direct assessment of storm washover deposits in marshes along the South Carolina coast (Hippensteel and Martin, 1999). The spacing of storm washover events marked by oceanic foraminifers injected into salt marsh deposits is, on average, 153 years in a core from low marsh deposits calibrated by radiocarbon for overall sediment accumulation rate and 316 years in a

low/high marsh boundary core that also had a calibrated accumulation rate (Table 2). Two other cores, for which sediment accumulation rates were only estimated from other studies in South Carolina, had average washover spacing of 102 and 245 years (mid-points of ranges — see Table 2).

Because increased rates and depths of bioturbation may have decreased the degree of stratigraphic resolution in more recent geologic time (see Section 3.5 below and Kidwell, 1998), we compare the probable spacing between storm beds in the early and mid Paleozoic (when they should have been more frequently preserved) with the intervals between major disturbance events observed today. Numerous sections characterized by storm induced stratification are present in Lower and Mid Paleozoic rocks (Marsaglia and Klein, 1983). Several from eastern North America are well enough known to warrent estimating the average spacing of bed formation.

In southwestern Virginia the Late Ordovician age Martinsburg Formation is a 300-meter thick set of storm-generated beds (Kreisa, 1981) that more closely resembles the facies of the Reedsville Formation of west-central Pennsylvania than the flysch-like lithology of the Martinsburg in its type area. These tempestites are mostly autochthonous sediments resuspended and redeposited by large storms, as indicated by intraclasts of the underlying lithology and the similarity of the fauna in the reworked shell beds when compared to the interbedded shales (Kreisa and Bambach, 1982, Table 1).

Estimates of the time represented by the Martinsburg Formation range from 2 million to 5 million years. The section was measured in large increments (1 to 10 meter subdivisions) with centimeter-scale bed counts only done occasionally to characterize the larger subdivisions of the formation. For this reason we cannot give an exact figure for the number of individual beds in the complete formation. However, the average thickness of the beds in the formation is between 2 and 20 cm, so there are somewhere between 1,500 and 15,000 beds in the formation. Since each bed represents a storm event that lasted no more than a week, the total depositional time represented in the tempestites that comprise virtually the entire section is infinitesimally short: between 30 and 300 years. The bulk of the rest of the time is in the diastems (as well as being represented within the beds by temporal mixing of fossils and reworked sediment). Assuming no major unconformities (and none were detected in Kreisa's [1980, 1981] detailed study of the section), the median spacing of the beds must be somewhere between 130 and 3,300 years (2,000,000/15,000 to 5,000,000/1,500).

The Martinsburg example above and the example from the Silurian that follows use estimates made for the entire sections and do not account for fluctuations in spacing, or variation in completeness of the section that may be associated with fourth (and higher) order sea-level fluctuations. Those effects will be noted when smaller-scale cycling is discussed below.

Calculations similar to those made on the Martinsburg Formation can be made for the 1,200 m thick Silurian section at Arisaig, Nova Scotia. In that section the bedding is also predominantly storm deposition (Bambach, 1969, 1998; Cant, 1980). The age of the Arisaig section extends from early in the Early Silurian continuously into the Early Devonian, an interval of approximately 26 Ma. Although environments vary from deep water to non-marine, there are no marked unconformities and no significant intervals of condensed or omitted section (Bambach, 1998). Bedding ranges from 3 to 30 cm in thickness (with only a few beds ranging up to a meter thick). Individual beds were not counted through the entire section, but counts of parts of the section made from detailed photographs, with scale present in each, document the range of bedding patterns in the whole section. As for the Martinsburg example above, the calculations can only be done as a range encompassing the extremes. The section contains between 4,000 and 40,000 beds. If the section represents 26 Ma, the mean spacing between bed-forming events, then, is between 650 and 6500 years. If we make a more conservative estimate that deposited sediments represent only 25% of the time -- because of possible variation in completeness of parts of the section -- then the average spacing is between 163 and 1625 years. We chose a value of 25%, which is at the higher end of the range of completeness values predicted by Wilkinson *et al*. (1991; see below), because the Arisaig section accumulated in a tectonically active, subsiding area.

Although the Cambrian was a warm interval, Milankovitch-style eustatic sea-level fluctuations can be generated under "greenhouse" conditions by a variety of forcing factors. For example, Jacobs and Sahagian (1993) calculated that several meters of sea-level change would occur just by filling known enclosed basins. Koerschner and Read (1989) document numerous 20 to 100 kyr (Milankovitch) sedimentary cycles in Upper Cambrian rocks in southwestern Virginia. These cycles average 1 to 7 m in thickness, and are recognized by coarse to fine sets of strata representing shallow-subtidal to intertidal shoaling successions. Bedding within the cycles is on the order of one to ten cm in thickness. Recent inspection of the bedding in the cycles indicates that each small cycle has 10 to 20 beds preserved. Wilkinson *et al*. (1991) argue that only 3% to 30% of the time in such meter-scale cratonic cycles is preserved by sedimentation (the rest is included in the cycle-bounding unconformity). If we assume only 10% of the time was recorded by the Cambrian cycles described by Koerschner and Read (1989), then the average temporal spacing of the beds would be 100 to 200 years if they are 20 kyr cycles, the most likely periodicity, twice that if they are 40 kyr cycles, or 500–1,000 years if they are 100 kyr cycles. Koerschner and Read discuss the variability of these cycles at length, pointing out that they are thicker and contain more elements in some settings (both relative to shoreline and

relative to third order transgressive/regressive cycles), so this bed spacing is a very generalized average.

Holland *et al*. (1997) describe bedding patterns in the storm-dominated sediments of the cratonic Upper Ordovician Kope Formation of the type Cincinnatian and present a measured section divided into 40 small-scale cycles. The cycles average about 1.5 meters in thickness and contain a mean of 9.3 beds per cycle (range 3–22 beds). If one assumes only 10% completeness (again on the low side of the Wilkinson *et al.'s*, 1991, range of 3-30%) for the cycles, and if one also assumes that these cycles were produced by Milankovitch-style oscillations of sea-level with a 20 kyr periodicity (as seems likely from many evaluations of "meter-scale" cycles), then the preserved record of storm reworking had an average spacing of 215 years (range from 91 to 667, depending on the number of preserved storm-induced beds and assuming an invariant length for the cycles). Longer periodicities would increase the temporal spacing of preserved storm beds.

The above data are summarized in Table 2. It is interesting that the spacing between bed-forming events in the four Paleozoic examples all fall within the same range of temporal spacing as major bed-forming events observed today. The implication is that diastems, while highly variable in length, have a general likelihood of several centuries to as much as a few thousand years in average duration. The somewhat shorter intervals for data from the Recent and for the Cambrian example, the somewhat longer Ordovician range, and the longer Silurian range may reflect the pattern of incorporation of longer gaps in longer time intervals as originally suggested by Sadler (1981), but some of the differences are probably related to other factors that control duration of diastems themselves (see section 3.4 below).

3.4 Factors Controlling Duration of Diastems

The duration of diastems is influenced by the rate at which accommodation space develops, the frequency of major depositional events, and other factors, including water depth and position in the cycle of sea-level fluctuation.

The rate of development of accommodation space will be significant in determining the duration of diastems between discrete beds. Because the rate at which accommodation space is generated is controlled by slow-rate processes (sea-level rises and subsidence), it is highly unlikely that adequate accommodation space could develop in a matter of decades to centuries to permit closely spaced events to be preserved as discrete beds in the record. The exceptions are tectonically active settings, where subsidence can be rapid (but which seldom produces more than a meter or so of subsidence in any one event) and shoaling parasequences when considerable

accommodation space exists because sea-level rise exceeded sediment accumulation, a common short-term feature following the transgressive phase of Milankovitch-type sea-level cycles when coastal flooding traps sediment up-dip and reduces sediment supply to the shelf.

In addition, through reworking of material that was also likely to have been reworked previously in earlier small events, closely spaced large disturbance events are more likely to simply erase the record of all but the last event of a series rather than leave a stacked set of discrete beds. If relatively closely spaced disturbance events are recorded, they will usually appear as amalgamated beds, preserving a "hierarchy" of partial remnants of a series of storm events. In this instance, the largest event will be the oldest one preserved (the basal part of the amalgamated bed) and each succeeding amalgamated unit represents a later (and somewhat less deeply eroding, and so probably smaller) event. Hence diastems in sections where accommodation space was available to form discrete beds almost certainly represent considerable intervals, not simply successive storm events. This is probably why the spacing between beds in the Ordovician and Silurian examples (Section 3.3) are higher than spacing expected for the successive recurrence of major disturbance events, as observed in the Recent (Table 2). Therefore, most diastems between discrete beds deposited in shelf environments represent time intervals of greater magnitude than intervals between successive disturbance events. This suggests that the common length for many diastems is more than just a few centuries.

Climatic variability related to geographic position also can influence duration of diastems. The range of intervals between repeated storms noted in Table 2 is actually the variation observed at different locations from subtropical to cool temperate latitudes along the Gulf and Atlantic coasts of North America (Abbott, 1996). The one to two orders of magnitude difference between the most frequent and least frequent likelihood of recurrence of hurricanes suggests that a similar variability in duration of diastems could be associated with geographic setting as well. The correspondence of the theoretical spacing of major storm events with the frequency of preserved washovers in South Carolina indicates that this frequency range is a reasonable general picture. As one goes northward, the hurricane danger is replaced by severe winter storms ("nor'easters"), but very large events that will enter the geological record are still going to be less frequent events. Marsaglia and Klein (1983) have illustrated latitudinal variation in storm influence in the geological record.

Water depth is important in controlling the effect of disturbance events on the bottom. There is an order of magnitude difference in the likelihood of events capable of forming a 10 cm thick event bed between settings that differ in water depth by only 10 m (Table 2). Diastems in deeper water

settings may represent longer intervals than those in shallow-water deposits. Although the calculations would be difficult to do for an example from the remote past, the Silurian section noted above (Section 3.3) incorporates a variety of sea-level changes and environments from deep basin to shallow subtidal (Bambach, 1998). Whereas the average durations of diastems calculated for that section average all the environmental variability together, diastem spacing probably is shorter in the shallower water portions of the section and longer in the deeper water portions.

The shorter intervals for diastems calculated for the Cambrian example in Section 3.3 and Table 2 are for sediment cycles influenced by Milankovitch-style eustatic sea-level fluctuations. In this case, the spacing of diastems may be more related to the rate of sediment supply and frequency of bed-forming events rather than development of accommodation space. This is because most beds formed in the shoaling phase of each cycle, probably during and after sea level had risen and produced adequate accommodation space.

3.5 Trends through the Phanerozoic

Plate tectonics has caused geography to change over time and climates and sea level have fluctuated, but most of these changes have produced stochastic variation, not secular trends, in the sedimentary record. However, changes produced by the evolution of life may have produced some secular trends. For example, there may have been some effect on the rate of clastic sediment supply when rooted land plants became widespread in the Devonian (Algeo and Scheckler, 1998; Bambach, 1999) and a second alteration in rate of denudation may have taken place with the rise of extensive grasslands in the mid-Cenozoic (Potts and Behrensmeyer, 1992). Also, Thayer (1983) argued persuasively that the depth and rate of bioturbation has increased markedly over time. Sepkoski *et al*. (1991) showed that this caused change in the preserved style of stratification. This trend has probably influenced the magnitude of preserved diastems by systematically homogenizing the smaller units into the thicker bioturbated beds common in the later Mesozoic and Cenozoic (Kidwell, 1998).

The beds described by Koerschner and Read (1989) include both hardgrounds and “flat-pebble conglomerates”, as is common in Cambrian rocks (Sepkoski, 1982; Sepkoski *et al*., 1991). In the Cambrian, rapid submarine cementation was possible because the sediments were little bioturbated and overlying seawater was not flushed into and through the sediments. Therefore, when chemical conditions in the sediment were right, cement could precipitate close to the sediment-water interface, as it now does only below the taphonomically active zone (Sepkoski, 1982). The thin

bedding in many Cambrian rocks represents resuspended and redeposited material from small storms (Sepkoski, 1982).

Later in the Paleozoic bioturbation commonly was deep enough to homogenize the laminations from small-scale storm disturbance, "erasing" most of those smaller events (Sepkoski *et al*., 1991). But the larger storm events did form discrete beds, commonly on a decimeter, rather than centimeter, scale (as noted above for the Ordovician and Silurian examples). Although the difference in estimated bed spacing in the Cambrian example and the later Paleozoic examples noted above could be related to differences of environment, or even of stratigraphic thickness over which the analyses are conducted, the decades to centuries Cambrian average and the centuries to millennia average for the later Paleozoic may be a function of difference in frequency of preservation of depositional units, too.

Bioturbation to meter-scale depths became widespread in the later Mesozoic and Cenozoic (Thayer, 1983). Shelf sediments of Cretaceous and Cenozoic age are often fully homogenized, with bedding only apparent as storm-concentrated shell beds (Sepkoski *et al*., 1991). In locations such as the Atlantic Coastal Plain, distinct bedding planes are generally restricted to small unconformities in the sections. It is apparent, however, from the "ghosts" of coarse storm concentrations, that sedimentation was just as discontinuous as in the Paleozoic. Yet Paleozoic-style diastems are not commonly preserved as discrete bedding planes because of deep bioturbation. But the same temporal scale for sediment accumulation remains. The Cenozoic beds have simply lost the stratigraphic resolution present in earlier times, as suggested by Kidwell (1998).

3.6 Stratigraphic Resolution: A Summary

The previous sections can be summarized in terms of general statements regarding the stratigraphic resolution of the sedimentary record. These statements are most applicable to marine sedimentary successions separated by small-scale diastems. They should not be extrapolated to offshore basinal settings or more unusual settings, such as lacustrine varves or tidal rythmites, where process systems operate at different temporal scales.

1. At the finest scale (bedding within a section), stratigraphic resolution is dependent on the length of time represented by diastems between beds.
2. Intervals between events that cause stratification vary widely, but several lines of evidence converge on the sense that in shelf settings diastems generally represent a few centuries to a few thousand years.
3. The general age range for the spacing between major storm events occurring at a single spot in the Recent is several centuries to a few thousand years.

4. The age range calculated for the temporal spacing between beds in the early to mid Paleozoic is generally a few centuries to a few thousand years.
5. The rate of formation of accommodation space, geographic setting in relation to climate pattern, and water depth are factors that influence the duration of diastems. When accommodation space is already present (such as after sea-level rise that "outruns" sediment accumulation, as in the transgressive phases of Milankovitch cycles) sedimentation rates and frequency of bed-forming events, rather than rates of formation of accommodation space, dominate in determining the duration of diastems.
6. Because geologic factors, such as the rate at which accommodation space forms, are critical in controlling the accumulation of sets of discrete beds, diastems are likely to be a few millennia in duration, and not just the few centuries that characterize the spacing between bed-forming events.
7. Because we can interpret the depositional mechanics of most beds, and they appear commonly to be deposited in a matter of hours to days, it is clear that the geologic record forms very episodically. Only a small fraction of geologic time is actually represented by the accumulation of sediment as it is preserved in any section. Because of diastems, at the scale of “ecological time” the geological record is lace-like, mostly gaps (diastems) with a scattered set of beds of sediment that accumulated in very short intervals of time (Barrell, 1917; Ager, 1973, 1981, 1993; Sadler, 1981; Sadler and Strauss, 1990; Anders *et al*., 1987).

4. PALEONTOLOGICAL RESOLUTION

4.1 Limits of paleontological resolution

Our view of paleontological resolution is summarized on a schematic diagram that shows a distribution of paleontological records in the bivariate space defined by axes of depositional and stratigraphic resolution (Fig. 7). Given the compiled data (Tables 1 and 2), we argue that the overwhelming majority of records (bedded nearhsore and shelfal deposits) should be characterized by the stratigraphic and depositional resolution in a 10^2-10^4 years range. Because the two resolutions are partly dependent, the records are expected to cluster along the thick diagonal line (Fig. 7). This makes intuitive sense. For example, fossil concentrations at major sequence boundaries and maximum flooding surfaces, where stratigraphic gaps are large, are likely to contain records with high levels of temporal mixing, but snapshots are unlikely to form in such settings. Conversely, fossil

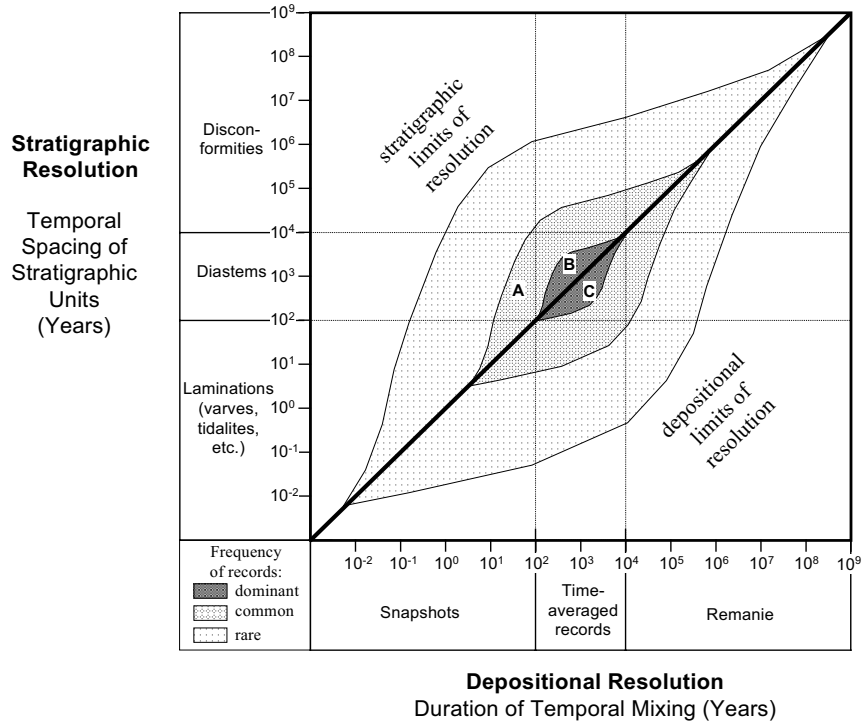

Figure 7. Temporal resolution of paleontological records. Distribution of the records is defined by their depositional resolution (x-axis) and stratigraphic resolution (y-axis). The suggested distribution of records is a rough prediction based on the data reviewed in this paper (see text and Tables 1 - 2). Letters A, B, and C mark three hypothetical examples of paleontological records.

concentrations that formed in settings typified by high-subsidence and sedimentation rates, where stratigraphic successions can be resolved at finer temporal scales, are unlikely to experience extensive temporal mixing, and snapshots are more likely to be preserved there. At the same time, the two resolutions are partly independent. For example, even within the same units, temporal mixing may vary among different types of fossils ("disharmonious time averaging" *sensu* Kowalewski, 1996a) because of intrinsic differences among organisms (e.g., differences in durability). Thus, we expect records to show some divergence from the diagonal line (Fig. 7). This spread should be highest in the region where, for both resolution types, records are common: the temporal ranges of 10^2 to 10^4 years (Tables 1-2).

We trust the diagram as a qualitative generalization, but it should not be used as a reliable quantitative estimate of the actual distribution of paleontological records in terms of their stratigraphic and depositional resolution. At this point we have limited empirical data on each type of

resolution exist (Tables 1-2). Moreover, no bivariate estimates – with both resolutions estimated concomitantly for the same records – are available.

Regardless of all uncertainties, two important generalizations can be made. First, whereas both depositional and stratigraphic resolution may potentially vary over a wide range of temporal scales, the typical (i.e., interdiastemal or within-sequence) records vary over a much narrower range, with both depositional and stratigraphic resolution ranging from hundreds to thousands of years. This means that, typically, the two types of resolution are comparable in their temporal scale and, therefore, both must be considered in determining the resolution of paleontological data. If we ignore one of the resolution types, we may misjudge the actual resolution of our data. This is illustrated on our conceptual diagram (Fig. 7), which shows that any records located to the left of, or above, the diagonal line have their resolution limit imposed by their stratigraphic resolution, whereas any records located to the right of, or below, the diagonal line are limited by their depositional resolution. Second, because some of the variables controlling depositional and stratigraphic resolution are unique (e.g., intrinsic factors of depositional resolution), the two types of resolution need not be fully dependent. In other words, a high depositional resolution of a given record does not have to imply a comparably high stratigraphic resolution, and *vice versa*. The paleontological data extracted from tidal rhythmites need not have daily resolution and correlative successions of storm beds dominated by snapshots cannot be correlated at the resolution of years, even though the records contained in individual snapshots may provide a resolution at such a fine time scale.

4.2 Paleontological Data as Records of Diastems

An important corollary of temporal mixing is that a majority of paleontological data comes from the times corresponding to stratigraphic gaps: bioclasts record organisms that lived during diastems and not during the time when the beds in which they are found were formed (Fig. 8). The extensive temporal mixing documented directly by dating (Table 1) indicates that bioclasts do not just *occasionally* predate depositional events and are not just *slightly* older, but they *often* predate depositional events and are *notably* older, lagging behind by hundreds or thousands of years (Table 1). These are the time scales that correspond to time spans of typical diastems (Table 2). Consequently, paleontological data may often provide a relatively complete record of organisms that lived during time intervals apparently missing from the stratigraphic record. In other words, *beds record depositional events, but their fossils record the preceding diastems!*

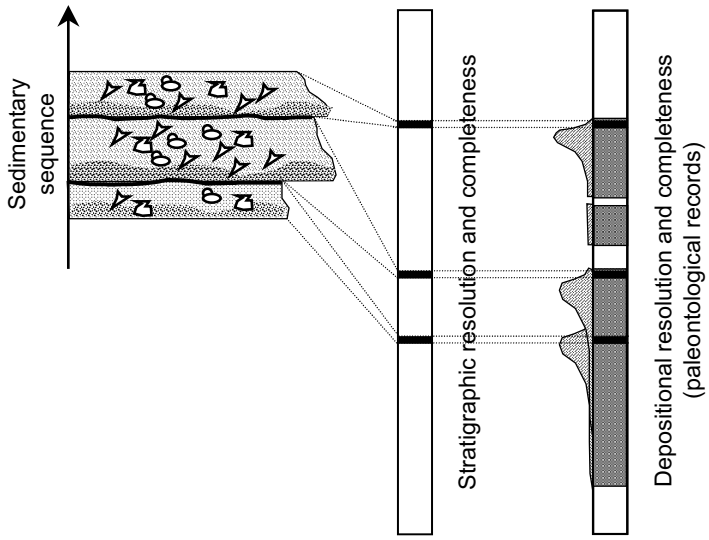

Figure 8. Temporal relationship between the timing of diastems that defined stratigraphic resolution and completeness of a succession and the timing of paleontological records that defines the depositional resolution and completeness of that record. Paleontological records lag behind depositional events and are dominated by records of organisms that lived in the time that is "missing" from the stratigraphic record. The lagging worsens temporal resolution of paleontological records, but improves their completeness.

This is good news indicating that paleontological data provide samples that are much more temporally complete and representative than is suggested by the notoriously high stratigraphic incompleteness of sedimentary successions. And although temporal mixing prevents us from making sequential reconstructions of the paleontological records (with the exception of Late Quaternary records, where high-resolution dating is possible), the average estimates of parameters obtained from fossils are probably much more representative of their true, long-term, average values than is suggested by the sporadic nature of depositional events.

4.3 Stratigraphic and Depositional Completeness

As stressed here, the term completeness, when applied to successions of fossiliferous rocks, cannot only denote stratigraphic completeness (the dominant usage of the term), but also depositional completeness. *Stratigraphic completeness* can be defined as the proportion of the total amount of time represented by a stratigraphic section that is recorded by depositional events, whereas *depositional completeness* can be defined as the proportion of the total amount of time represented by a stratigraphic section that is recorded by physical records such as fossils (see Section 2.4 above).

As argued in section 4.2, due to temporal mixing, fossils record diastems and provide a much more complete record than the stratigraphic units in which they are preserved. Depositional completeness of paleontological records may be much higher than the stratigraphic completeness of the successions that contain these records. For example, Behrensmeyer (1982) postulated a credible hypothetical alluvial succession with 53% depositional paleontological completeness, but only 27% sedimentary completeness. Mixing processes can even lead to overcompleteness with fossils documenting more time-intervals than fall into the time span of a stratigraphic section. Overcompleteness is primarily a microstratigraphic phenomenon observed at very fine resolution levels (Kowalewski, 1996a).

As with stratigraphic completeness (Sadler, 1981), depositional completeness depends on the scale of observation and becomes increasingly incomplete over longer time intervals. Also, longer stratigraphic sections, are likely to include substantial intervals barren of fossils, and consequently, one may expect that, at coarser time scales, stratigraphic completeness should improve relative to depositional completeness.

4.4 Trends through the Phanerozoic

As discussed in sections 2.7 and 3.5, both depositional and stratigraphic resolution may have changed notably through time. The two secular trends have not been controlled by exactly the same suite of factors and, thus, need not have varied necessarily in perfect concert. Nevertheless, the existing data suggest that the duration of diastems and the scale of temporal mixing both have increased through the Phanerozoic. Paleontological resolution, both in its depositional and stratigraphic aspects, has decreased through time.

5. CONCLUSIONS

Numerous researchers have reviewed both temporal mixing (depositional resolution) of fossiliferous deposits (e.g., Wilson, 1988; Kidwell and Bosence, 1991; Kowalewski, 1996a; Kidwell, 1998; Martin, 1999), as well as stratigraphic resolution of sedimentary successions (e.g., Sadler, 1981; Schindel, 1982; Martin, 1999). However, to our knowledge, no explicit attempt to combine these two concepts of paleontological resolution into a single analysis has been made previously. The joint consideration of the two aspects of resolution presented here suggests the following generalizations:

1. Depositional and stratigraphic resolution may both potentially vary over a wide range of temporal scales, but the typical, interdiastemal records vary in a much narrower range from hundreds to thousands of years.

Thus, the two types of resolution are comparable in scale and must be considered jointly when evaluating the resolution of a given fossil record.

2. Depositional and stratigraphic resolution are partly dependent (as they share some controlling factors), and thus, are expected to often correlate with one another: records poorly resolved stratigraphically (separated by long diastems) tend to display high levels of temporal mixing. However, this covariation is not total: depositional and stratigraphic resolutions are partly independent (i.e., some controlling factors are unique) and both may place limits on the resolution of paleontological data.
3. Because bioclasts often predate depositional events by hundreds or thousands of years (i.e., over time scales comparable to those that typify diastems), paleontological data may often provide complete paleontological records for time intervals apparently missing from the record (i.e., beds record depositional events, but their fossils record the preceding diastems). Consequently, paleontological completeness often may be higher than stratigraphic completeness, and the average estimates of parameters obtained from fossils may be more representative of their true long-term, average values than is suggested by the sporadic nature of depositional events.
4. Despite some differences in underlying secular factors, the existing data suggest that depositional and stratigraphic resolution both have decreased through the Phaneorozoic.

We hope that our preliminary generalizations regarding the combined limits of depositional and stratigraphic resolution, the causative factors underlying these limits, and their secular trends, will offer useful guidelines for all those geoscientists that use data from the fossil record in their research. It is clear to us that a twofold consideration of both aspects of paleontological resolution should provide a better conceptual tool for evaluating resolution limits inherent to the fossil record, and consequently, should yield a more realistic picture of the temporal nature of paleontological data.

ACKNOWLEDGMENTS

We thank Peter Harries for inviting us to contribute this chapter. Ron Martin, Steve Holland, and Peter Harries provided numerous useful comments that greatly improved this manuscript. All remaining errors and all arguable semantics are entirely ours.

REFERENCES

Abbott, P. L., 1996, *Natural Disasters*, Brown, Dubuque, Iowa.

Ager, D., 1973, 1981, 1993, *The Nature of the Stratigraphical Record*, 1st, 2nd, and 3rd Eds., MacMillan, London.

Algeo, T. J., and Scheckler, S. E., 1998, Terrestrial-marine teleconnections in the Devonian; links between the evolution of land plants, weathering processes, and marine anoxic events, *Phil. Trans. R. Soc. London, Biol. Sci.* **353**:113-130.

Aller, R. C., 1982, Carbonate dissolution in nearshore terrigenous muds: the role of physical and biological reworking, *J. Geol.* **90**:79-95.

Allmon, W. D., 1989, Paleontological completeness of the record of lower Tertiary mollusks, U.S. Gulf and Atlantic Coastal Plains: Implications for phylogenetic studies, *Hist. Biol.* **3**:141-158.

Anders, M. H., Krueger, S. W., and Sadler, P. M., 1987, A new look at sedimentation rates and the completeness of the stratigraphic record, *J. Geol.* **95**:1–14.

Anderson, L. C., Gupta, B. K., and Byrnes, M. R., 1997, Reduced seasonality of Holocene climate and pervasive mixing of Holocene marine section: Northeastern Gulf of Mexico shelf, *Geology* **25**:127-130.

Argast, S., Farlow, J. O., Gabet, R. M., and Brinkman, D. L., 1987, Transport-induced abrasion of fossil reptilian teeth: implications for the existence of Tertiary dinosaurs in Hell Creek Formation, Montana, *Geology* **15**:927-930.

Ausich, W. I., and Bottjer, D. J., 1982, Tiering in suspension-feeding communities on soft substrata throughout the Phanerozoic, *Science* **216**:173-174.

Bambach, R. K., 1969, *Bivalvia of the Siluro-Devonian Arisaig Group, Nova Scotia*, Unpubl. Ph. D. Dissertation, Yale University, New Haven.

Bambach, R. K., 1998, Silurian sea-level change at Arisaig, Nova Scotia: Comparison with the standard eustatic pattern, in: *Silurian Cycles: Linkages of Dynamic Stratigraphy with Atmospheric, Oceanic, and Tectonic Changes* (E. Landing and M. Johnson, eds.), *New York State Mus. Bull.* **491**:27-37.

Bambach, R. K., 1999, Energetics in the global marine fauna: A connection between terrestrial diversification and change in the marine biosphere, *Geobios* **32**:131-144.

Barrell, J., 1917, Rhythms and the measurements of geologic time, *Geol. Soc. Amer. Bull.* **28**:745–904.

Bé, A. W. H., and Hutson, W. H., 1977, Ecology of planktonic foraminifera and biogeographic pattern of life and fossil assemblages in the Indian Ocean, *Micropaleont.* **23**:369-414.

Behrensmeyer, A. K., 1982, Time resolution in fluvial vertebrate assemblages, *Paleobio.* **8**:211-227.

Behrensmeyer, A. K., 1991, Terrestrial vertebrate accumulations, in: *Taphonomy:Releasing Data Locked in the Fossil Record* (P. A. Allison and D. E. G. Briggs, eds.), *Topics in Geobiology Series 9*, Plenum, New York, pp. 291-335.

Behrensmeyer, A. K., and Chapman, R. E., 1993, Models and simulations of time-averaging in terrestrial vertebrate accumulations, in: *Taphonomic Approaches to Time Resolution in Fossil Assemblages* (S. M. Kidwell and A. K. Behrensmeyer, eds.), *Short Courses in Paleontology 6,* Paleontological Society, Knoxville, pp. 125-149.

Behrensmeyer, A. K., and Hook, R. W., 1992, Paleoenvironmental contexts and taphonomic modes, in: *Terrestrial Ecosystems Through Time* (A. K. Behrensmeyer, J. D. Damuth, W. A. DiMichele, R. Potts, H. D. Sues, and S. L. Wing, eds.), University of Chicago, Chicago, pp. 15-136.

Behrensmeyer, A. K., and Kidwell, S. M., 1993, Summary: Estimates of time-averaging, in:

Taphonomic Approaches to Time Resolution in Fossil Assemblages (S. M., Kidwell and A. K. Behrensmeyer, eds.), *Short Courses in Paleontology 6*, Paleontological Society, Knoxville, pp. 301-302.

Behrensmeyer, A. K., Kidwell, S. M., and Gastaldo, R. A., 2000, Taphonomy and paleobiology, *Paleobio.* (suppl.) **26**:103-147.

Bjorlykke, K., Bue, B., and Elverhoi, A., 1978, Quaternary sediments in the western part of the northwestern Barents Sea and their relation to the underlying Mesozoic bedrock, *Sedimentol*. **25**:227-246.

Boyajian, G. E., and Thayer, C. W., 1995, Clam calamity: A recent supratidal storm-deposit as an analog for fossil shell beds, *Palaios* **10**:484-489.

Bradshaw, C., and Scoffin, T. P., 2001, Differential preservation of gravel-sized grains in Alpheid- versus Callianassid-bioturbated muddy reefal sediments, *Palaios* **16**:185-191.

Brandt, D. S., and Elias, R. J., 1989, Temporal variation in tempestite thickness may be a geological record of atmospheric CO_2, *Geology* **17**:951-952.

Brett, C. E., and Baird, G. C., 1993, Taphonomic approaches to temporal resolution in stratigraphy: examples from Paleozoic marine mudrocks, in: *Taphonomic Approaches to Time Resolution in Fossil Assemblages* (S. M. Kidwell and A. K. Behrensmeyer, eds.), *Short Courses in Paleontology 6*, Paleontological Society, Knoxville, pp. 250-274.

Burnham, R. J., 1993, Time resolution in terrestrial macrofloras: Guidelines from modern accumulations, in: *Taphonomic Approaches to Time Resolution in Fossil Assemblages* (S. M. Kidwell and A. K. Behrensmeyer, eds.), *Short Courses in Paleontology 6*, Paleontological Society, Knoxville, pp. 57-78.

Cadée, G. C., 1984, Macrobenthos and macrobenthic remains on the Oyster ground, North Sea, *Neth. J. Sea Res.* **10**:440-460.

Cant, D. J., 1980, Storm-dominated shallow marine sediments of the Arisaig Group (Silurian-Devonian) of Nova Scotia, *Can. J. Earth Sci.* **17**:120–131.

Carroll, M., Kowalewski, M., Simões, M. G., Goodfriend, G. A., 2000, Quantitative estimates of time-averaging in articulate brachiopod accumulations from a Holocene tropical shelf (Southern Brazil), *Geol. Soc. Amer. Abstr. Progr.* **32**:A13-A14.

Carter, R. M., Abbott, S. T., Fulthorpe, T., Craig, S., Haywick, D. W., and Henderson, R. A., 1991, Application of global sea-level and sequence-stratigraphic models in Southern Hemisphere Neogene strata from New Zealand, in: *Sedimentation, Tectonics and Eustasy; Sea-Level Changes at Active Margins* (D. I. M. Macdonald, ed.), *Inter. Assoc. Sedimentol. Spec. Pub. 12*, Blackwell, Oxford, pp. 41-65.

Carthew, R., and Bosence, D. W. J., 1986, Community preservation in recent shell-gravels, English Channel, *Palaeont.* **29**:243-268.

Clifton, H. E., 1971, Orientation of empty pelecypod shells and shell fragments in quiet water, *J. Sed. Pet.* **41**:671–682.

Cohen, A. S., 1989, The taphonomy of gastropod shell accumulations in large lakes: An example from Lake Tanganyika, Africa, *Paleobio.* **15**:26-44.

Craig, G. Y., 1966, Concepts in palaeoecology, *Earth-Science Rev.* **2**:127-155.

Craig, G. Y., and Oertel, G., 1966, Deterministic models of living and fossil populations of animals, *Quart. J. Geol. Soc. London* **122**:315-355.

Cutler, A. H., 1993, Mathematical models of temporal mixing in the fossil record, in: *Taphonomic Approaches to Time Resolution in Fossil Assemblages* (S. M., Kidwell and A. K. Behrensmeyer, eds.), *Short Courses in Paleontology 6*, Paleontological Society, Knoxville, pp. 169-187.

Cutler, A. H., and Behrensmeyer, A. K., 1996, Models of vertebrate mass mortality events at the K/T boundary, in: *The Cretaceous-Tertiary Event and Other Catastrophes in Earth History* (G. Ryder, D. Fastovsky, and S. Gartner, eds.), *Geol. Soc. Amer. Sp. Pap.*

307:375-379.
Cutler, A. H., and Flessa, K. W., 1990, Fossils out of sequence: computer simulations and strategies for dealing with stratigraphic disorder, *Palaios* **5**:227-235.
Davies, D. J., Powell, E. N., and Stanton, R. J., 1989, Relative rates of dissolution and net sediment accumulation - A commentary: Can shell beds form by the gradual accumulation of biogenic debris on the sea floor? *Lethaia* **22**:207-212.
Droser, M. L., and Bottjer, D. J., 1989, Ordovician increase in extent and depth of bioturbation; implications for understanding early Paleozoic ecospace utilization, *Geology* **17**:850-852.
Droser, M. L., and Bottjer, D. J., 1993, Trends and patterns of Phanerozoic ichnofabrics, *Ann. Rev. Earth Planet. Sci.* **21**:205-225.
Fenton, C. L., 1966, *The Tales Told by Fossils*, Doubleday, Garden City.
Flessa, K. W., 1993, Time-averaging and temporal resolution in Recent marine shelly faunas, in: *Taphonomic Approaches to Time Resolution in Fossil Assemblages* (S. M. Kidwell and A. K. Behrensmeyer, eds.), *Short Courses in Paleontology 6*, Paleontological Society, Knoxville, pp. 9-33.
Flessa, K. W., 1998, Well-traveled cockles: Shell transport during the Holocene transgression of the southern North Sea, *Geology* **26**:187-190.
Flessa, K. W., and Kowalewski, M., 1994, Shell survival and time-averaging in nearshore and shelf environments: estimates from the radiocarbon literature, *Lethaia* **27**:153-165.
Flessa, K. W., Cutler., A. H., and Meldahl, K. H., 1993, Time and taphonomy: Quantitative estimates of time-averaging and stratigraphic disorder in a shallow marine habitat, *Paleobio.* **19**:266-286.
Föllmi, K. B., and Grimm, K. A., 1990, Doomed pioneers; gravity-flow deposition and bioturbation in marine oxygen-deficient environments, *Geology* **18**:1069-1072.
Fürsich, F. T., 1978, The influence of faunal condensation and mixing on the preservation of fossil benthic communities, *Lethaia* **11**:243-250.
Fürsich, F. T., and Aberhan, M., 1990, Significance of time-averaging for paleocommunity analysis, *Lethaia* **23**:143-152.
Gehrels, G. E., Johnsson, M. J., and Howell, D. G., 1999, Detrital zircon geochronology of the Adams Argillite and Nation River Formation, east-central Alaska, USA, *J. Sed. Res.* **A69**:135-144.
Goldring, R., and Aigner, T., 1982, Scour and fill: The significance of event separation, in: *Cyclic and Event Stratification* (G. Einsele and A. Seilacher, eds.), Springer-Verlag, Berlin, pp. 354–362.
Goodfriend, G. A., 1987, Chronostratigraphic studies of sediments in the Negev Desert, using amino acid epimerization analysis of land snail shells, *Quat. Res.* **28**:374-392.
Goodfriend, G. A., 1989, Complementary use of amino-acid epimerization and radiocarbon analysis for dating of mixed-age fossil assemblages, *Radiocarbon* **31**:1041-1047.
Goodfriend, G. A., and Ellis, G. L., 2000, Stable carbon isotope record of middle to late Holocene climate changes from land snail shells at Hinds Cave, Texas, *Quat. Inter.* **67**:47-60.
Goodfriend, G. A., and Gould, S. J., 1996, Paleontology and chronology of two evolutionary transitions by hybridization in the Bahamian land snail *Cerion, Science* **274**:1894-1897.
Gould, S. J., 1965, Is uniformitarianism necessary? *Amer. J. Sci.* **263**:223-228.
Gould, S. J., 1987, *Time's Arrow Time's Cycle*, Penguin Books, London.
Grabau, A. W., 1913, *Principles of Stratigraphy*, Seiler, New York.
Greenwood, D. R., 1991, The taphonomy of plant macrofossils, in: *The Processes of Fossilization* (S. K. Donovan, ed.), Columbia, New York, pp. 141-169.
Gretener, P. E., 1967, Significance of the rare event in geology, *AAPG Bull.* **51**:2197–2206.

Grimm, K. A., and Föllmi, K. B., 1994, Doomed pioneers; allochthonous crustacean tracemakers in anaerobic basinal strata, Oligo-Miocene San Gregorio Formation, Baja California Sur, Mexico, *Palaios* **9**:313-334.

Hippensteel, S. P., and Martin, R. E., 1999, Foraminifera as an indicator of overwash deposits, barrier island sediment supply, and barrier island evolution: Folly Island, South Carolina, *Palaeogeogr. Palaeoclim. Palaeoecol.* **149**:115-125.

Holland, S. M., 1995, The stratigraphic distribution of fossils, *Paleobio.* **21**:92-109.

Holland, S. M., Miller, A. I., Dattilo, B. F., Meyer, D. L., and Diekmeyer, S. L., 1997, Cycle anatomy and variability in the storm-dominated type Cincinnatian (Upper Ordovician): Coming to grips with cycle delineation and genesis, *J. Geol.* **105**:135–182.

Jacobs, D. K., and Sahagian, D. L., 1993, Climate-induced fluctuations in sea level during non-glacial times, *Nature* **361**:710-712.

Jenkyns, H. C., 1971, The genesis of condensed sequences in the Tethyan Jurassic, *Lethaia* **4**:327-352.

Johnson, R. G., 1965, Pelecypod death assemblages in Tomales Bay, California, *J. Paleont.* **39**:80-85.

Johnson, K. R., 1993, Time resolution and the study of Late Cretaceous and Early Tertiary megafloras, in: *Taphonomic Approaches to Time Resolution in Fossil Assemblages* (S. M. Kidwell and A. K. Behrensmeyer, eds.), *Short Courses in Paleontology 6*, Paleontological Society, Knoxville, pp. 210-227.

Kauffman, E. G., Elder, W. P., and Sageman, B. B., 1991, High-resolution correlation; a new tool in chronostratigraphy, in: *Cycles and Events in Stratigraphy* (G. Einsele, W. Ricken, and A. Seilacher, eds.), Springer Verlag, Berlin, pp. 795-819.

Kidwell, S. M., 1988, Taphonomic comparison of passive and active continental margins: Neogene shell beds of the Atlantic coastal plain and northern Gulf of California, *Palaeogeogr. Palaeoclim. Palaeoecol.* **63**:201-223.

Kidwell, S. M., 1989, Stratigraphic condensation of marine transgressive records. Origin of major shell deposits in the Miocene of Maryland, *J. Geol.* **97**:1-24.

Kidwell, S. M., 1990, Phanerozoic evolution of macroinvertebrate shell accumulations; preliminary data from the Jurassic of Britain, in: *Paleocommunity Temporal Dynamics; Patterns and Processes of Long-Term Community Development* (W. Miller, III, ed.), *Paleontological Society Special Publication 5*, Paleontological Society, Knoxville, pp.309-327.

Kidwell, S. M., 1991a, The stratigraphy of shell concentrations, in: *Taphonomy: Releasing Data Locked in the Fossil Record* (P. A. Allison and D. E. G. Briggs, eds.), *Topics in Geobiology Series 9*, Plenum, New York, pp. 211-290.

Kidwell, S. M., 1991b, Condensed deposits in siliciclastic sequences: expected and observed features, in: *Cycles and Events in Stratigraphy* (G. Einsele, W. Ricken, and A. Seilacher, eds.), Springer, Berlin, pp. 682-695.

Kidwell, S. M., 1993a, Taphonomic expressions of sedimentary hiatus: field observations on bioclastic concentrations and sequence anatomy in low, moderate and high subsidence settings, *Geol. Rundsch.* **82**:189-202.

Kidwell, S. M., 1993b, Patterns of time-averaging in the shallow marine fossil record, in: *Taphonomic Approaches to Time Resolution in Fossil Assemblages* (S. M. Kidwell and A. K. Behrensmeyer, eds.), *Short Courses in Paleontology 6,* Paleontological Society, Knoxville, pp. 275-300.

Kidwell, S. M., 1998, Time-averaging in the marine fossil record: Overview of strategies and uncertainties, *Geobios* **30**:977-995.

Kidwell, S. M., and Behrensmeyer, A. K., (eds.), 1993, *Taphonomic Approaches to Time Resolution in Fossil Assemblages*, *Short Courses in Paleontology 6*, Paleontological

Society, Knoxville.
Kidwell, S. M., and Bosence, D. W. J., 1991, Taphonomy and time-averaging of marine shelly faunas, in: *Taphonomy: Releasing Data Locked in the Fossil Record* (P. A. Allison and D. E. G. Briggs, eds.), *Topics in Geobiology Series 9*, Plenum, New York, pp. 115-209.
Kidwell, S. M., and Brenchley, P. J., 1994, Patterns in bioclastic accumulations through the Phanerozoic: Changes in input or in destruction? *Geology* **22**:1139-1143.
Kidwell, S. M., and Brenchley, P. J., 1996, Evolution of the fossil record: thickness trends in marine skeletal accumulations and their implications, in: *Evolutionary Paleobiology* (Jablonski, D., D. H. Erwin, and J. H. Lipps, eds.), University of Chicago, Chicago, pp. 290-336.
Kidwell, S. M., and Flessa, K. W., 1996, The quality of the fossil record; populations, species, and communities, *Ann. Rev. Earth Planet. Sci.* **24**:433-464.
Koerschner, W. F., III, and Read, J. F., 1989, Field and modeling studies of Cambrian carbonate cycles, Virginia Appalachians, *J. Sed. Pet.* **39**:654–687.
Kondo, Y., Abbott, S. T., Kitamura, A., Kamp, P. J., Naish, T. R., Kamataki, T., and Saul, G. S., 1998, The relationship between shellbed type and sequence architecture; examples from Japan and New Zealand, *Sedim. Geol.* **122**:109-127.
Kotake, N., 1994, Population paleoecology of the *Zoophycus*-producing organism, *Palaios* **9**:84-91.
Kowalewski, M., 1996a, Time-averaging, overcompleteness, and the geological record, *J. Geol.* **104**:317-326.
Kowalewski, M., 1996b, Taphonomy of a living fossil: the lingulide brachiopod *Glottidia palmeri* Dall from Baja California, Mexico, *Palaios* **11**:244-265.
Kowalewski, M., 1997, The reciprocal taphonomic model, *Lethaia* **30**:86-88.
Kowalewski, M., and Demko, T. M., 1997, Trace fossils and population paleoecology: comparative analysis of size-frequency distributions derived from burrows, *Lethaia* **29**:113-124.
Kowalewski, M., and Misniakiewicz, W., 1993, Reliability of quantitative data on fossil assemblages: a model, a simulation, and an example, *N. Jahrb. Geol. Paläont., Abh.* **187**:243-260.
Kowalewski, M., and Rimstidt, J. D., in press, Lifetime and age spectra of detrital grains: Toward a unifying theory of sedimentary particles. *J. Geol.* **111**.
Kowalewski, M., Goodfriend, G. A., and Flessa, K. W., 1998, The high-resolution estimates of temporal mixing in shell beds: the evils and virtues of time-averaging, *Paleobio.* **24**:287-304.
Kowalewski, M., Avila Serrano, G. E., Flessa, K. W., and Goodfriend, G. A., 2000, Dead delta's former productivity: Two trillion shells at the mouth of the Colorado River, *Geology* **28**:1059-1062.
Kreisa, R. D., 1980, *The Martinsburg Formation (Middle and Upper Ordovician) and Related Facies, Southwestern Virginia*, Unpubl. Ph. D. dissertation, Virginia Polytechnic Institute and State University, Blacksburg.
Kreisa, R. D., 1981, Storm-generated sedimentary structures in subtidal marine facies with examples from the Middle and Upper Ordovician of southwest Virginia, *J. Sed. Pet.* **51**:823–848.
Kreisa, R. D., and Bambach, R. K., 1982, The role of storm processes in generating shell beds in Paleozoic shelf environments, in: *Cyclic and Event Stratification* (G. Einsele and A. Seilacher, eds.), Springer-Verlag, Berlin, pp. 200-207.
Lageard, J. G. A., Chambers, F. M., and Thomas, P. A., 1999, Climatic significance of the marginalization of Scots pine (*Pinus sylvestris* L.) c. 2500 BC at White Moss, south

Cheshire, UK, *Holocene* **9**:321-331.
Li, X., and Droser, M. L., 1999, Lower and Middle Ordovician shell beds from the Basin and Range Province of the Western United States (California, Nevada, and Utah), *Palaios* **14**:215-233.
Machalski, M., and Walaszczyk, I., 1987, Faunal condensation and mixing in the uppermost Maastrichtian /Danian greensand (middle Vistula Valley, central Poland), *Acta Geol. Pol.* **37**:74-91.
MacIntyre, I. G., Pilkey, O. H., and Stuckenrath, R., 1978, Relict oysters on the United States Atlantic coastal shelf: A reconsideration of their usefulness in understanding late Quaternary sea-level history, *Geol. Soc. Amer. Bull.* **89**:277-282.
Marsaglia, K. M., and Klein, G. D., 1983, The paleogeography of Paleozoic and Mesozoic storm depostional systems, *J. Geol.* **91**:117–142.
Martin, R.E., 1993, Time and taphonomy: Actualistic evidence for time-averaging of benthic formaniferal assemblages, in: *Taphonomic Approaches to Time Resolution in Fossil Assemblages* (S. M. Kidwell and A. K. Behrensmeyer, eds.), *Short Courses in Paleontology 6,* Paleontological Society, Knoxville, pp. 34-56.
Martin, R. E., 1999, *Taphonomy: A Process Approach*, Cambridge University, Cambridge.
Martin, R. E., Harris, M. S., and Liddell, W. D., 1995, Taphonomy and time-averaging of foraminiferal assemblages in Holocene tidal flat sediments, Bahia la Choya, Sonora, Mexico (northern Gulf of California), *Mar. Micropaleont.* **26**:187-206.
Martin, R. J., Wehmiller, J. F., Harris, M. S., and Liddell, W. D., 1996, Comparative taphonomy of bivalves and foraminifera from Holocene tidal flat sediments, Bahia la Choya, Sonora, Mexico (northern Gulf of California): taphonomic grades and temporal resolution, *Paleobio.* **22**:80-90.
McKinney, M. L., 1991, Completeness of the fossil record: an overview, in: *The Processes of Fossilization* (S. K. Donovan, ed.), Columbia, New York, pp. 66-83.
Meldahl, K. H., 1987, Sedimentologic and taphonomic implications of biogenic stratification, *Palaios* **2**:350-358.
Meldahl, K. H., and Cutler, A. H., 1992, Neotectonics and taphonomy: Pleistocene molluscan shell accumulations in the northern Gulf of California, *Palaios* **7**:187-197.
Meldahl, K. H., Flessa, K. W., and Cutler, A. H., 1997, Time-averaging and postmortem skeletal survival in benthic fossil assemblages: quantitative comparisons among Holocene environments, *Paleobio.* **23**:207-229.
Miall, A. D., 1990, *Principles of Sedimentary Basin Analysis,* Springer, New York.
Miller, A. I., and Cummins, H., 1990, A numerical model for formation of fossil assemblages: Estimating the amount of post-mortem transport along environmental gradients, *Palaios* **5**:303-316.
Miller, A. I., and Cummins, H., 1993, Using numerical models to evaluate the consequences of time-averaging in marine fossil assemblages, in: *Taphonomic Approaches to Time Resolution in Fossil Assemblages* (S. M. Kidwell and A. K. Behrensmeyer, eds.), *Short Courses in Paleontology 6,* Paleontological Society, Knoxville, pp. 150-168.
Miller, D. J., and Eriksson, K. A., 1997, Late Mississippian prodeltaic rhythmites in the Appalachian Basin: a hierarchical record of tidal and climatic periodicities, *J. Sed. Res.* **B67**:653-660.
Mitchum, R. M., Jr., Vail, P. R., and Thompson, S., III, 1977, Seismic stratigraphy and global changes of sea level; Part 2, The depositional sequence as a basic unit for stratigraphic analysis, *AAPG Memoir* **26**:53-62.
Morton, R. A., 1988, Nearshore responses to great storms, *Geol. Soc. Amer. Sp. Pap.* **229**:7–22.
Nederbragt, A. J., and Thurow, J. W., 2001, A 6000 yr varve record of Holocene climate in

Saanich Inlet, British Columbia; from digital sediment colour analysis of ODP Leg 169S cores, *Mar. Geol.* **174**:95-110.

Nelson, C. S., Keane, S. L., and Head, P. S., 1988, Non-tropical carbonate deposits on the modern New Zealand shelf, *Sedim. Geol.* **60**:71-94.

Olszewski, T., 1999, Taking advantage of time-averaging, *Paleobio.* **25**:226-238.

Peterson, C. H., 1976, Relative abundance of living and dead molluscs in two California lagoons, *Lethaia* **9**:137-148.

Peterson, C. H., 1977, The paleontological significance of undetected short-term temporal variability, *J. Paleont.* **51**:976-981.

Potts, R., and Behrensmeyer, A. K., 1992, Late Cenozoic terrestrial ecosystems, in: *Terrestrial Ecosystems Through Time* (Behrensmeyer, A. K., J. D. Damuth, W. A. DiMichele, R. Potts, H. D. Sues, and S. L. Wing, eds.), University of Chicago, Chicago, pp. 419-541.

Powell, E. N., 1992, A model for assemblage death formation: Can sediment shelliness be explained? *J. Mar. Res.* **50**:229-265.

Powell, E. N., and Davies, D., 1990, When is an "old" shell really old?, *J. Geol.* **98**:823-844.

Raup, D. M., and Stanley, S. M., 1971, *Principles of Paleontology,* Freeman, San Francisco.

Rhoads, D. C., and Stanley, D. J., 1965, Biogenic graded bedding, *J. Sed. Pet.* **35**:956-963.

Richards, R. P., 1972, Autecology of Richmondian brachiopods (late Ordovician of Indiana and Ohio), *J. Paleont.* **46**:386-405.

Richards, R. P., and Bambach, R K., 1975, Population dynamics of some Paleozoic brachiopods and their paleoecological significance, *J. Paleont.* **49**:775-798.

Rogers, R. D., 1989, Use of observational patterns in geology, *Geology* **17**:131-134.

Rogers, R. R., 1993, Systematic patterns of time-averaging in the terrestrial vertebrate record: A Cretaceous case study, in: *Taphonomic Approaches to Time Resolution in Fossil Assemblages* (S. M. Kidwell, and A. K. Behrensmeyer, eds.), *Short Courses in Paleontology 6,* Paleontological Society, Knoxville, pp. 228-249.

Röhl, H. J., Schmid-Röhl, A., Oschmann, W., Frimmel, A., and Schwark, L., 2001, The *Posidonia* Shale (lower Toarcian) of SW-Germany; an oxygen-depleted ecosystem controlled by sea level and palaeoclimate, *Palaeogeogr. Palaeoclim. Palaeoecol.* **165**:27-52.

Ross, G. M., and Gehrels, G. E., 1998, Detrital zircon geochronology of Neoproterozoic to Permian miogeoclinal strata in British Columbia and Alberta, *Can. J. Earth Sci.* **35**:1380-1401.

Sadler, P. M., 1981, Sediment accumulation rates and the completeness of stratigraphic sections, *J. Geol.* **89**:569–584.

Sadler, P. M., 1993, Models of time-averaging as a maturation process: How soon do sedimentary sections escape reworking? in: *Taphonomic Approaches to Time Resolution in Fossil Assemblages* (S. M. Kidwell and A. K. Behrensmeyer, eds.), *Short Courses in Paleontology 6,* Paleontological Society, Knoxville, pp. 188–209.

Sadler, P. M., and Strauss, D. J., 1990, Estimation of completeness of stratigraphical sections using empirical methods and theoretical models, *J. Geol. Soc. London* **147**:471–485.

Sageman, B. B., Kauffman, E. G., Harries, P. J., and Elder, W. P., 1997, Cenomanian/Turonian bioevents and ecostratigraphy in the Western Interior Basin; contrasting scales of local, regional, and global events, in: *Paleontological Events; Stratigraphic, Ecological, and Evolutionary Implications* (C. E. Brett and G. C. Baird, eds.), Columbia University, New York, pp. 520-570.

Schäfer, W., 1956, *Ecology and Paleoecology of Marine Environments*, (English ed., 1972), University of Chicago, Chicago.

Schindel, D. E., 1982, Resolution analysis: a new approach to the gaps in the fossil record,

Paleobio. **6**:340-353.

Seilacher, A., 1985, The Jeram model: event condensation in a modern intertidal environment, in: *Sedimentary and Evolutionary Cycles* (G. M. Friedmann, ed.), Springer-Verlag, New York, pp. 336-342.

Seilacher, A., 1989, Vendozoa; organismic construction in the Proterozoic biosphere, *Lethaia* **22**:229-239.

Sepkoski, J. J., Jr., 1982, Flat-pebble conglomerates, storm deposits, and the Cambrian bottom fauna, in: *Cyclic and Event Stratification* (Einsele, G., and A. Seilacher, eds.), Springer-Verlag, Berlin, pp. 371–385.

Sepkoski, J. J., Jr., Bambach, R. K., and Droser, M. L., 1991, Secular changes in Phanerozoic event bedding and the biological overprint, in: *Cycles and Events in Stratigraphy* (G. Einsele, W. Ricken, and A. Seilacher, eds.), Springer Verlag, Berlin, pp. 298–312.

Simões, M. G., and Kowalewski, M., 1998, Shell beds as paleoecological puzzles: a case study from the Upper Permian of the Parana Basin, Brazil, *Facies* **38**:175-196.

Simões, M. G., Kowalewski, M., Torello, F. F., and Ghilardi, R. P., 1999, Devonian and Permian benthic marine invertebrates preserved in life position: Taphonomic feedback in a Paleozoic epeiric sea, *XVI Congresso Brasileiro de Paleontologia, Boletim de Resumos,* Crato, CE, Brazil, pp. 109-110.

Simões, M. G., Kowalewski, M., Torello, F. F., Ghilardi, R. P., and Mello, L. H. C., 2000, Early onset of modern-style shell beds in the Permian sequences of the Parana Basin: Implications for the Phanerozoic trend in bioclastic accumulations, *Rev. Brasil. Geosci.* **30**:495-499.

Staff, G. M., Stanton, R. J., Jr., Powell, E. N., and Cummins, H., 1986, Time-averaging, taphonomy, and their impact on paleocommunity reconstruction: Death assemblages in Texas bays, *Geol. Soc. Amer. Bull.* **97**:428-443.

Thayer, C. W., 1983, Sediment-mediated biological disturbance and the evolution of the marine benthos, in: *Biotic Interactions in Recent and Fossil Benthic Communities* (Tevesz, M. J. S., and P. L. McCall, eds.), Plenum Press, New York, pp. 480–625.

Thorne, J. A., Grace, E., Swift, D. J. P., and Niedoroda, A., 1991, Sedimentation on continental margins, III: the depositional fabric — an analytical approach to stratification and facies identification, in: *Shelf Sand and Sandstone Bodies* (D. J. P. Swift, G. F. Oertel, R. W. Tillman, and J. A. Thorne, eds.), *Inter. Assoc. Sedim. Spec. Pub.* **14**: 59–87.

Vail, P. R., and Mitchum, R. M., Jr., 1977, Seismic stratigraphy and global changes of sea level; Part 1, Overview, *AAPG Memoir* **26**:51-52.

Vail, P. R., Mitchum, R. M., Jr., and Thompson, S., III, 1977, Seismic stratigraphy and global changes of sea level; Part 3, Relative changes of sea level from coastal onlap, *AAPG Memoir* **26**:63-81.

Walker, K. R., and Bambach, R. K., 1971, The significance of fossil assemblages from fine-grained sediments: time-averaged communities, *Geol. Soc. Amer. Abstr. Progr.* **3**:783-784.

Walker, S. E., 1994, Biological remanié: gastropod fossils used by the living terrestrial hermit crab, *Coenobita clypeatus*, on Bermuda, *Palaios* **9**:403-412.

Walker, S. E., and Goldstein, S. T., 1999, Taphonomic tiering; experimental field taphonomy of molluscs and Foraminifera above and below the sediment-water interface, *Palaeogeogr. Palaeoclim. Palaeoecol.* **149**:227-244.

Wehmiller, J. F., York, L. L., and Bart, M. L., 1995, Amino-acid racemization geochronology of reworked Quaternary mollusks on U.S. Atlantic coast beaches: implications for chronostratigraphy, taphonomy, and coastal sediment transport, *Mar. Geol.* **124**:303-337.

Wendt, J., 1970, Fossil-Lagerstätten, Nr. 9; Stratigraphische Kondensation in triadischen und jurassischen Cephalopodenkalken der Tethys, *N. Jahrb. Geol. Paläont., Mon.* **7**:433-448.

West, R. R., Rollins, H. B., and Busch, R. M., 1990, Taphonomy and an intertidal palimpset

surface; implications for the fossil record, in: *Paleocommunity Temporal Dynamics; Patterns and Processes of Long-Term Community Development* (W. Miller, III, ed.), *Paleontological Society Special Publication 5*, Paleontological Society, Knoxville, pp. 351-369.

Wilkinson, B. H., Opdyke, B. N., and Algeo, T. J., 1991, Time partitioning in cratonic carbonate rocks, *Geology* **19**:1093–1096.

Wilson, M. V. H., 1988, Taphonomic processes: Information loss and information gain, *Geosci. Can.* **15**:131-148.

Wilson, J. B., 1979, Biogenic carbonate sediments on the Scottish continental shelf and on Rockall Bank, *Mar. Geol.* **33**:85-93.

Wilson, J. B., 1988, A model for temporal changes in the faunal composition of shell gravels during a transgression on the continental shelf around the British Isles, *Sedim. Geol.* **60**:95-105.

Wing, S. L., and DiMichelle, W. A., 1995, Conflict between local and global changes in plant diversity through geological time, *Palaios* **10**:551-564.

Chapter 2

Best-Fit Intervals and Consensus Sequences

Comparison of the Resolving Power of Traditional Biostratigraphy and Computer-Assisted Correlation

PETER M. SADLER and ROGER A. COOPER

PETER M. SADLER • Department of Earth Sciences, University of California, Riverside, Riverside, CA 92521. ROGER A COOPER • Institute of Geological and Nuclear Sciences Limited, Lower Hutt, New Zealand.

P.J. Harries (ed.), *High-Resolution Approaches in Stratigraphic Paleontology.*

1. THE BIOSTRATIGRAPHIC SEQUENCING PROBLEM

Biostratigraphers subdivide geologic time using the sequence of first and last appearances of only a small fraction of the available fossil taxa. Thus, there appears to be considerable scope for improving biostratigraphic resolution simply by incorporating more first and last appearance events. The problem, of course, is that the correct sequence becomes more difficult to determine as the number of events rises. Figure 1 illustrates how a mild example of the problem can be visualized in the form of a tangled fence diagram. It is constructed from the observed ranges of trilobites collected by Palmer (1954) from the Cambrian Riley Formation of Texas. The seven fence posts represent seven different stratigraphic sections. Each wire line connects the horizons of the lowest or highest find of a taxon that has been recovered from adjacent sections. The wire lines cross wherever a pair of events have been preserved in contradictory order in adjacent sections. These Riley data are a classic example of a relatively internally consistent set of range charts. They have become a benchmark for testing and illustrating new quantitative methods: graphic correlation (Shaw, 1964); unitary associations (Guex, 1991); and constrained optimization (Kemple *et al.*, 1995). Nevertheless, 253 of all the possible pairs of first and last appearance events in this data set have been observed in contradictory order. For another 543 pairs, at least one section is equivocal, in the sense that the events are preserved at the same stratigraphic level – a condition that is consistent with either order. Traditionally, the Riley ranges are used to separate only six or seven zones.

In effect, traditional biostratigraphy restores the fence to an untangled appearance by selective removal of lines until those that remain do not cross one-another. But it is likely that many of the lines meet many of the posts at the wrong levels; the highest and lowest finds in these sections are not at the horizons which correspond in age with the true first and last appearances of the taxon. This chapter presents the case for *adjusting all* the fence lines rather than *eliminating most* of them. The resulting fence will have much higher resolution because it retains many more lines. The “best-fit intervals”

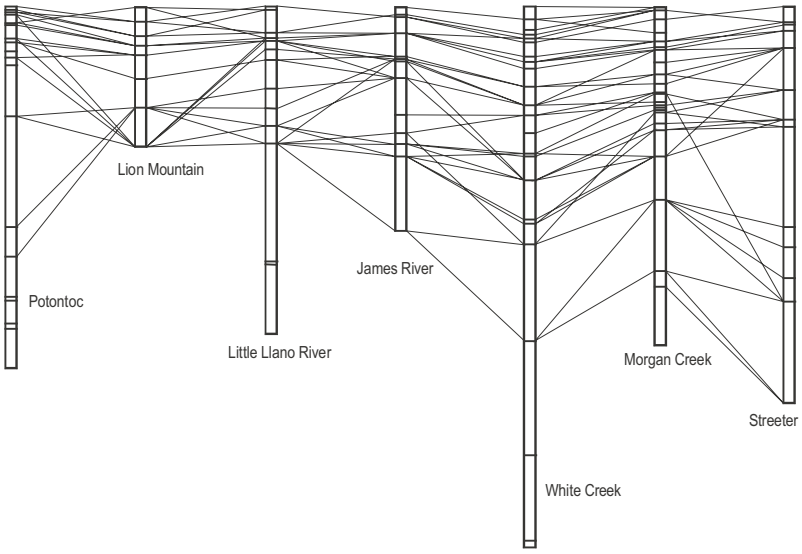

Figure 1. Tangled-fence diagram of the observed contradictions between 7 sections that preserve 62 taxa of the Cambrian Riley Formation of Texas (data from Palmer, 1954; Shaw, 1964). Note that fence lines are drawn only for taxa found in both of the adjacent sections; in order to illustrate the full extent of the tangle we would need to plot every section next to every other (for 7 sections that requires 3 more fences with the posts in a different order). Fossiliferous horizons are marked by horizontal bars in the columnar sections.

mentioned in the title will be shown to express the relative resolving power of the adjusted lines – the range of positions they may occupy in different but equally good solutions to the problem of untangling the fence. The "consensus sequence" will be the largest set of lines that are internally robust in the sense that none of their best-fit intervals overlap.

A few straightforward rules govern the adjustment of the fence lines. They are simpler than the rules for Shaw's (1964) graphic correlation. Nevertheless, the approach requires computer assistance to select the minimum sufficient adjustments from an overwhelming number of options. The results are reproducible and uncertainties in the placement of events can be fully quantified in terms of the fit between the model sequences and the observed local ranges.

Tangled-fence diagrams expose very good reasons why traditional methods use only a fraction of the available first and last appearance events. The task of untangling the fence rapidly becomes totally bewildering as the number of fence posts and the number of wire lines increases. First, in each section there is a possibility that random factors in preservation and collection will cause some pairs of events to be preserved in the wrong order. Thus, the number of pairs of events that are found in contradictory order must be expected to increase with the number of stratigraphic sections

in which both events have been found. This expectation will be confirmed below, using empirical data. Second, the number of possible sequences that can be built from the observed disorder of events grows with the number of taxa. This result will be derived from a consideration of permutations.

The increase in the number of possible solutions with the number of taxa is extremely pernicious. The growth rate is worse than exponential. Familiar problems that encounter the same difficulty include the search for the most parsimonious cladogram and the inversion of geophysical data. Fortunately, this difficulty arises in a large class of very practical commercial problems (termed "non-polynomial complete," Dell *et al.*, 1992), like the routing of delivery vehicles. As a result, the discipline of operations research has focused considerable effort on developing efficient computer algorithms that can solve these tough problems. It is not our purpose to criticize traditional biostratigraphy. Knowing that non-polynomial complete problems have been dubbed "the Mt. Everest of computer science" (Anderson, 2001), it is evident that the traditional culling of events was an intelligent and entirely justified strategy for solving the stratigraphic correlation problem, prior to the availability of computer methods.

Before examining the adaptation of these computer methods to biostratigraphy, we must explore three aspects of the biostratigraphic sequencing problem: 1) the contradictions within the field data that lie at the core of the problem; 2) the rules for resolving them; and 3) the size of the set of feasible sequences that could resolve the contradictions. At the end of the chapter, we discuss selected aspects of four case histories to illustrate the types of results that can be expected: 1) a classic data set for which the results have been compared with a manual solution; 2) a controversial data set for which the differences between two published interpretations can be quantified; 3) a time-scale and biodiversity project that avoids the limitations which traditional zones and stages impose upon resolution; and 4) a set of exploratory wells in which borehole caving compromises the first-appearance data and for which the results have been compared with seismic correlation.

1.1 Contradictions

Inconsistencies in the order of first and last appearances, as recovered from different stratigraphic sections, can be expressed as a contradiction ratio: that proportion of the evidently contradictable pairs of events (A and B) for which the two possible sequences (A-below-B and B-below-A) have each been found in at least one section. Some pairs of events cannot be preserved in contradictory order because the ranges of the corresponding

taxa do not overlap. The "evidently contradictable" pairs are those whose ranges have been observed to overlap. For them, every additional section that is examined means another chance to discover a contradiction.

The causes of contradiction are well known. The distribution of living organisms is patchy. Few individual organisms become fossils and few of these fossils are recovered in identifiable condition. As a result, the stratigraphic ranges of fossil taxa tend to be too short; they underestimate the range of the living organisms. Lowest finds tend to be too late and highest finds too early at any one stratigraphic section when compared with the regional or global range ends that would be the basis of a time scale. The discrepancies are inevitable; they vary from place to place and from taxon to taxon. Thus, contradictions must be expected between the sequences of range-end events preserved in different sections.

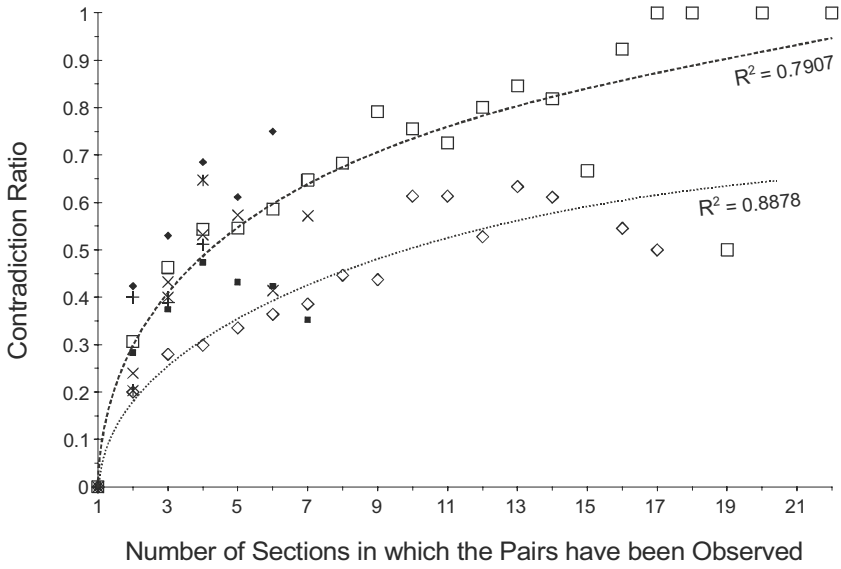

Figure 2. Increase in the pairwise contradiction ratio with increase in the number of sections in which the pairs of taxa are observed. Large open squares and coarsely dashed logarithmic regression: Ordovician through early Devonian graptolites (Sadler and Cooper, unpubl.). Large open diamonds and finely dashed logarithmic regression: Late Miocene to Recent foraminifera and radiolaria from North Atlantic ODP sites. Other data, for which the number of sections is too limited to justify regressions: trilobites of the Cambrian Riley Formation (Palmer, 1954); graptolites of the Mohawk Valley (Goldman *et al.*, 1994); Maastrichtian ammonites of Seymour Island, Antarctica (Macellari, 1984, 1986) and the Bay of Biscay (Ward and Kennedy, 1993).

Empirical evidence (Fig. 2) confirms that contradiction ratios generally increase with the number of sections from which a pair of events has been recovered. The rate of discovery of new contradictions slows as more

sections are added because the odds of contradiction operate on the dwindling population of pairs that still appeared to be consistent after the previous section was examined. But the rate slows faster than would be predicted if the odds of contradiction were constant for every pair of events. Better models for the shape of the regressions in Figure 2 allow the odds of contradiction to vary from pair to pair. Then, the pairs of events with long odds of contradiction are likely to appear consistent until very large numbers of sections have been examined.

It is reasonable to suppose that the properties of pairs of events render some pairs harder than others to preserve in contradictory order. The section of this chapter that deals with traditional zonation explains some of the variation in terms of range lengths and the time separation between events. Other factors probably relate to ecology and preservation. It will require much more data, however, to tease such effects apart on diagrams such as Figure 2.

Of course, failures of preservation and collection alone do not account for all the contradictions. Some reflect genuine differences in the timing of local appearances and disappearances, such as result from slow migrations. Nevertheless, a time scale that is based upon first and last appearances needs the proper order of the regional extreme events - the oldest of the local first appearances and the youngest of the local last appearances. Shaw (1964) established this principle in graphic correlation. The size of the region will be determined by the geographic scope of the correlation problem.

As in graphic correlation (Shaw, 1964), resolving the contradictions requires adjustment of the locally observed range ends until all localities fit one regional sequence of events. An acceptably parsimonious procedure must minimize the sum of all these adjustments. We will demonstrate the natural logic of such a procedure by first considering a trivial correlation problem and then enlarging it to a realistic size. The rules for untangling fence diagrams emerge in the process.

1.2 Rules for Resolving Contradictions

Figure 3 extracts from Shaw's (1964) Riley data an elementary contradiction that involves only two trilobite taxa and two local stratigraphic sections (White Creek and Potontoc). Assuming that the observed ranges are either correct or underestimate the regional range, we can resolve this contradiction without difficulty. (This assumption would be less straightforward for microfossils that are susceptible to benthic mixing; the thickness of the mixing layer then leads to a natural limit for meaningful precision in the measurement and adjustment of ranges.)

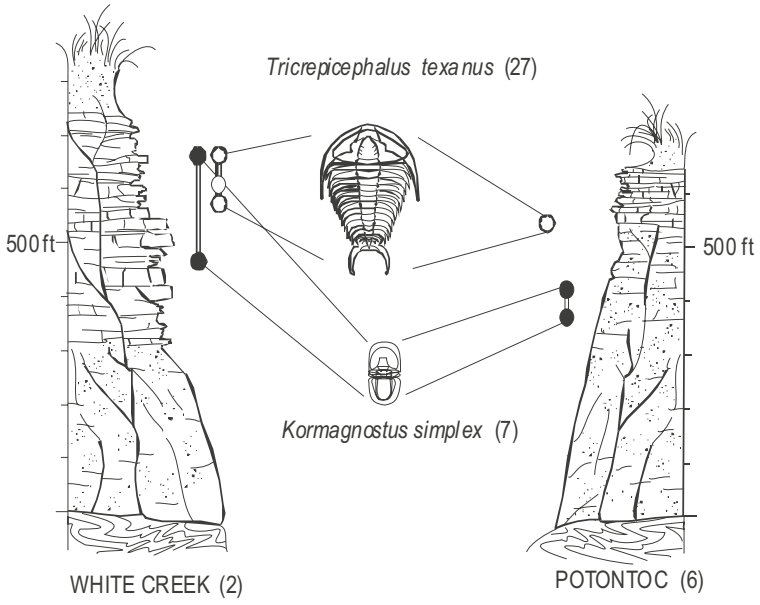

Figure 3. Contradictory ranges of two trilobite taxa from two measured stratigraphic sections in the Upper Cambrian Riley Formation of Texas (Palmer, 1954; Shaw, 1964). The Riley data are presented in feet rather than meters because they are a classic comparative benchmark that has always been analyzed in the original thickness scale (Shaw, 1964; Guex, 1991; Kemple *et al.*, 1995).

The White Creek section proves that the two ranges did overlap in time; the two trilobite taxa must have coexisted. The Potontoc section cannot be read literally as the correct sequence of events, because it fails to record the proven coexistence. So, for a sequence of events that can form the basis of a time scale we choose the sequence of first and last appearance events as preserved at White Creek. Any other sequence for these four events would be less parsimonious, in the sense that it implies either a greater failure of preservation and collection, or a more complex pattern of migration. Thus, very straightforward logic has resolved this elementary contradiction. It is only the huge number of pairs of events in a real data set that overwhelms such mental reasoning. In order to develop a rigorous method that will untangle large data sets, let us pursue this trivial example farther by considering all the possible histories for the two taxa.

Two taxa generate four events: two first appearances and two last appearances. The number of biologically feasible sequences is constrained to be less than the total number of permutations of four events because each first appearance must precede the last appearance of the same taxon. In general, two taxa present six possible sequences of events (Fig. 4). The number six arises as follows: there are two possible choices for the oldest

first appearance and then three options each for the subsequent history. The second taxon might not appear until the first has already disappeared (sequences 1 and 6 in Figure 4); the second taxon might appear within the time span of the first and then outlive it (sequences 2 and 5), or the range of the second taxon might be relatively short and fall entirely with the range of the first (sequences 3 and 4).

Before trying to choose which of these six options best fits the field observations, notice that they exclude the possibility that two events are exactly simultaneous. That possibility raises questions about meaningful and practical limits to the measurement of time that do not yield simple

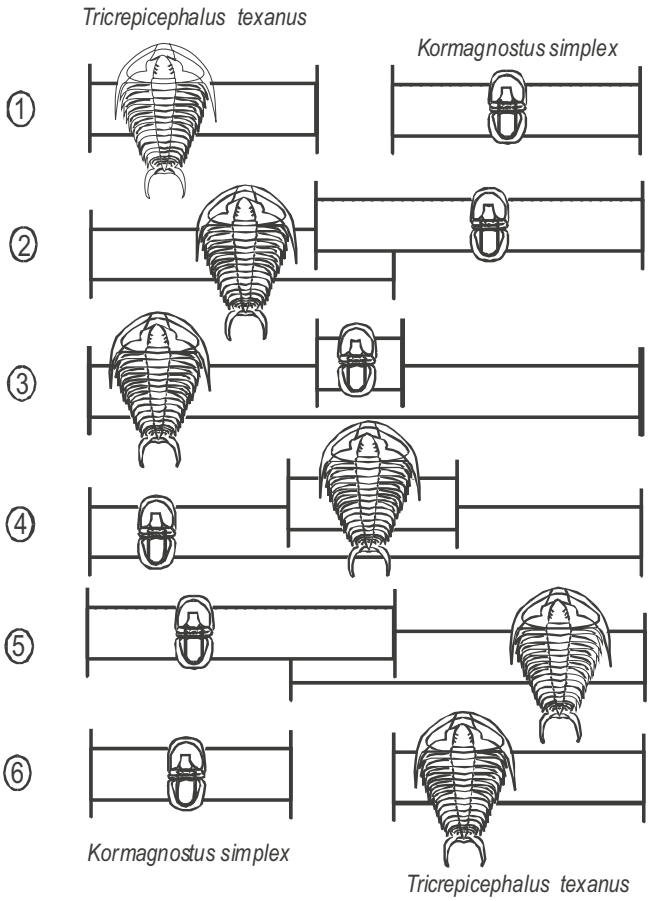

Figure 4. Six feasible sequences for the first and last appearance events of two taxa. Time progresses from left to right. For each case, the ruled and the white rectangles represent the two taxon ranges, first appearance on the left, last appearance on the right.

answers. Accordingly, the possibility of simultaneous events is deliberately reserved for the task of scaling the time intervals between events in the best sequence. Separating questions of sequence and spacing brings several advantages (Kemple *et al.*, 1995). It means that, although the choice of best sequence does not allow ties, the resolvable interval between events may later be assigned a practical value of zero. Zero spacing would be permitted where no section can resolve a stratigraphic separation between adjacent events, either because they occur at the same level or because the separation between them is smaller than the thickness of the benthic mixing layer.

Of course, if pairs of events can have zero spacing, they can generate sequences that are practically indistinguishable. The sequences would differ only in the order of pairs of adjacent events. They would be one case of different sequences that fit the field data equally well. The concept of equally well-fit sequences is central to the development of best-fit intervals and consensus sequences.

Another critical concept is constraint. The stratigraphic observation that two taxa must coexist provides a constraint on the number of *geologically* feasible sequences. In our elementary example, this constraint eliminates two of the six sequences (1 and 6) because the two taxon ranges overlap at White Creek. In order to choose the best of the remaining four sequences (2, 3, 4, and 5), determine the minimum net adjustment that would be necessary to make both stratigraphic sections fit each sequence. The best, or most parsimonious, sequence would then be the one that requires the least adjustment of the observed ranges. Thus, the problem naturally takes the form of a constrained optimization (Kemple *et al.*, 1989) with two fundamental rules. First, eliminate sequences that fail to honor observed coexistences; then search among the remainder for the one that best fits the field observations in the sense that it minimizes the implied failings of the preservation and collection process. The magnitude of the misfit is the sum of all the necessary *ad hoc* range adjustments (Table 1). It can be measured in a variety of ways (Kemple *et al.*, 1995). The raw total length of all the range adjustments, expressed as stratigraphic thickness, will suffice to apply the rules of optimization to Figure 3. Table 1 summarizes the results.

Table 1. Misfit between field observations and the six model sequences in Figure 4. ("INFINITE!" misfit indicates that the sequence fails to meet the coexistence constraints)

Model Sequence:	1	2	3	4	5	6
Misfit with observations:	INFINITE!	390 ft	270 ft	120 ft	120 ft	INFINITE!

Remember that the adjustments may only lengthen the observed ranges, not shorten them. Also, where two events are preserved at the same stratigraphic horizon either of them may be interpreted to have occurred

before the other, because we can assume that sediment accumulated too slowly (or with too much mixing) to resolve the true separation. Operationally, this leads to two more rules: a single configuration of observed ranges may be compatible with more than one sequence of events; and range extensions do not alter the observed sequence of events unless they extend an observed range to an horizon where another event has been observed.

Sequences 4 and 5 in Figure 4 both resemble the field observations, to the extent that taxon *Kormagnostus simplex* appears before *Tricrepicephalus texanus*. These two sequences share the same minimal misfit (120 ft) because they require only that the top of the range of *K simplex* at Potontoc be extended up to the horizon of the last appearance of *T. texanus*. Fitting the observed ranges to sequences 2 or 3 requires substantially more adjustment because the range of *T. texanus* must be extended downward in both sections. The field observations do not fit sequence 2 unless all three of the extensions are adopted from Figure 5, giving a total misfit of 390 ft. Sequence 2 has the worst fit.

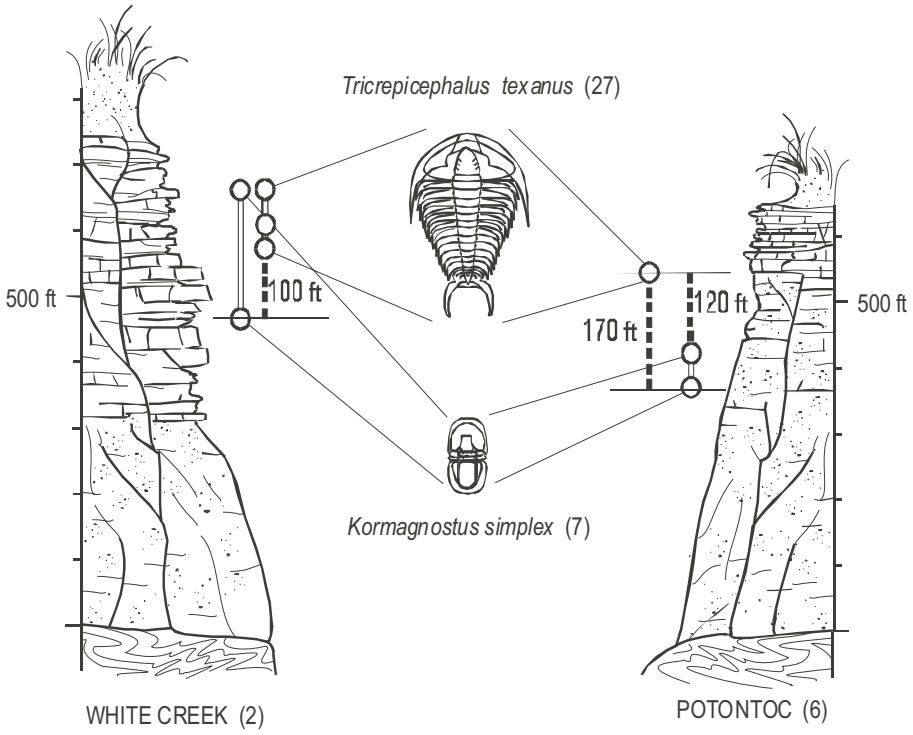

Figure 5. The set of minimum range extensions that, in different combinations, can adapt the observed ranges in each section to fit any feasible sequence of events (Fig. 4).

Together, sequences 4 and 5 are the set of most parsimonious solutions for this elementary problem in the sense that they imply the minimum failing of the fossil record *in these two sections*. After more sections and taxa are added, this element of the solution might need to change in order to minimize extensions to other observed ranges. Therefore, the optimization of larger data sets cannot readily be constructed piecemeal from a set of two-by-two elements, with each element remaining as simple as our example. Rather, the necessary adjustments must be considered for whole sequences. The addition of more taxa improves the potential resolution. In general, it is to be hoped that the inclusion of more sections improves the quality of the solution. Additional sections improve the chances of finding the earliest and latest occurrences and of observing all pairs of events in the correct order.

1.3 The Number of Possible Sequences

The rules for resolving contradictions do not alter when the number of taxa and sections increases. An increase in the number of sections simply lengthens the computation time required to find and sum all the appropriate range extensions for any one sequence. But increasing the number of taxa has an alarming effect on the number of feasible sequences that must be evaluated. Consider adding just one more taxon to the previous example.

The third taxon (Fig. 6) adds a fifth and sixth event to the model sequences. The first two taxa have filled four of the six positions (large open circles in Fig. 6) and they can do so in six different ways. For the two new events, imagine a pair of possible place-holders (small filled circles in Fig. 6) at the beginning of the line, at the end of the line, and between each pair of the four filled positions. The place-holders are paired to admit the possibility that the new first appearance and last appearance events will occupy adjacent positions.

Now consider *all* the ways to insert the two new events, proceeding systematically, as follows. Place the first appearance of the new taxon in the earliest placeholder and count the number of possible younger positions for the last appearance (only one in each pair of small filled circles except that shared with the first appearance). Move the first appearance to the next oldest pair and repeat the process. Total the options for the two new events (5+4+3+2+1 = 15) and multiply by the permutations of the previous four events (15 x 6 = 90) to discover that there are ninety sequences of events for three taxa. Some of these may fail to satisfy coexistence criteria; the remainder will all be compatible with the observed ranges plus various combinations of range extensions.

Figure 7 adds a fourth taxon and repeats the previous calculations, but with more placeholders for the new events. The previous three taxa filled

six positions in ninety possible ways. The two new events have twenty-eight (7+6+5+4+3+2+1) different possible options for their insertion into the sequence and the number of possible sequences has jumped to 2,520 with only four taxa. The number of possible ways to consider untangling a four-taxon fence diagram would be daunting. The whole Riley data set (Fig. 1) has 62 taxa!

Figures 6 and 7 have revealed the rules for biostratigraphic permutations in a form that allows the total to be calculated for any larger number of taxa. Each additional taxon causes the previous size of the problem to be multiplied by the factor:

$$(2n\text{-}1) + (2n\text{-}2) + (2n\text{-}3) + \ . \ . \ . \ + 2 + 1$$

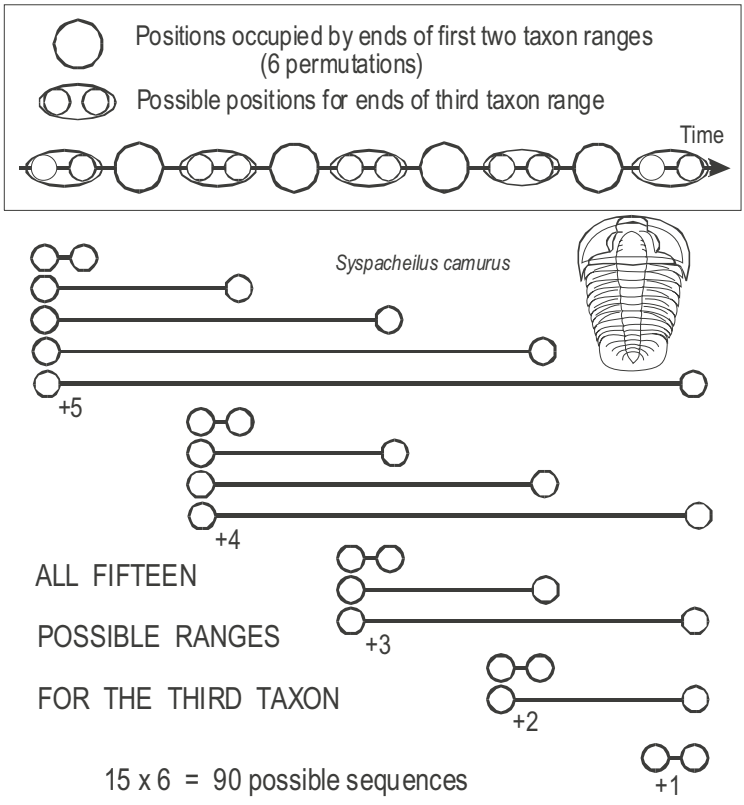

Figure 6. Calculation of the number of biologically feasible sequences of first and last events after the addition of a third taxon to the problem in Figure 3. New positions in the sequence (ruled circles) disappear unless occupied. The new positions are shown in pairs with vertical ruling for first appearance (FAD) and horizontal ruling for the last appearance (LAD). The distinction between the two positions in the paired ruled circles disappears unless the FAD and LAD of *S. camurus* occupy adjacent positions. Further explanation in text.

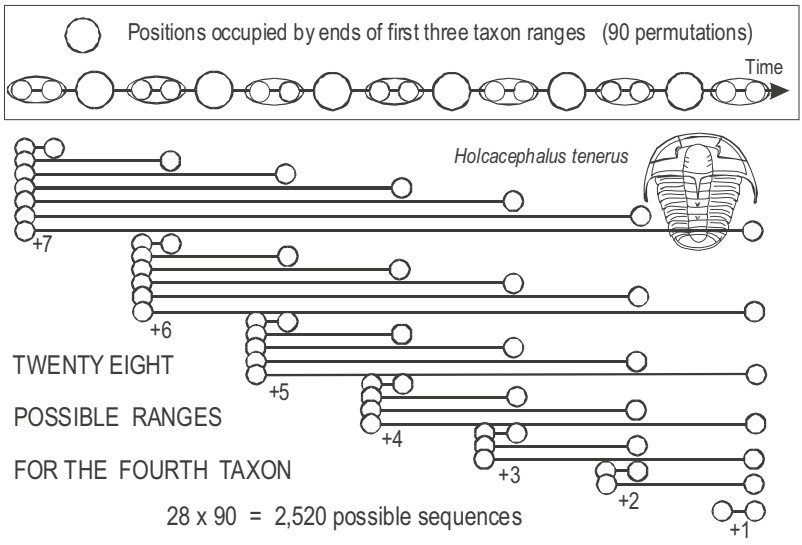

Figure 7. Calculation of the number of biologically feasible sequences of first and last events after the addition of a fourth taxon to the sequencing problem posed by Figure 3. Symbols as in Figure 6.

where *n* is the new total number of taxa and 2n the total number of events. Table 2 depicts how the number of feasible sequences grows to much more than half a billion for only seven taxa.

Although observed coexistences reduce the number of feasible sequences, even the most extreme constraint - requiring that every taxon must coexist with all others - still leaves over twenty-five million possible histories for just seven taxa. Calculating the number of possible sequences with this maximum coexistence constraint for *n* taxa is relatively straightforward. The *n* first occurrences must all lie in the first half of the sequence because no taxon disappears until all have appeared. So, there are *n* factorial ways to arrange all the first occurrences. This number must be multiplied by another *n* factorial, which is the number of ways to arrange the *n* last occurrences in the second half of the sequence.

Figure 8 plots the further increase in the number of permutations up to 100 taxa. Notice that the number of feasible sequences grows to exceed 10^{300}, a colossal number. For the 62 taxa in the Riley data set, the number of feasible sequences surely exceeds 10^{150} regardless of the number of coexistence constraints. To appreciate just how daunting the problem has become, imagine that it takes only one nanosecond to evaluate each sequence in terms of its fit with the field observations in the seven sections in the Riley problem. All of geological time amounts to far less than

Table 2. The growth of the number of biologically feasible sequences with the number of taxa

Number of taxa:	1	2	3	4	5	6	7
Feasible sequences - with no coexistence constraints	1	6	90	2,520	113,400	7,484,400	681,080,400
- with the maximum set of coexistence constraints	1	4	36	576	14,400	518,400	25,401,600

10^{30}nanoseconds. It is clearly beyond the scope of simple mental arithmetic to untangle (optimally) all the contradictions among the 62 taxa and seven sections in Figure 1. Furthermore, even a computer will need an intelligent algorithm that can find the best-fit sequence without conducting an exhaustive search of all possible sequences.

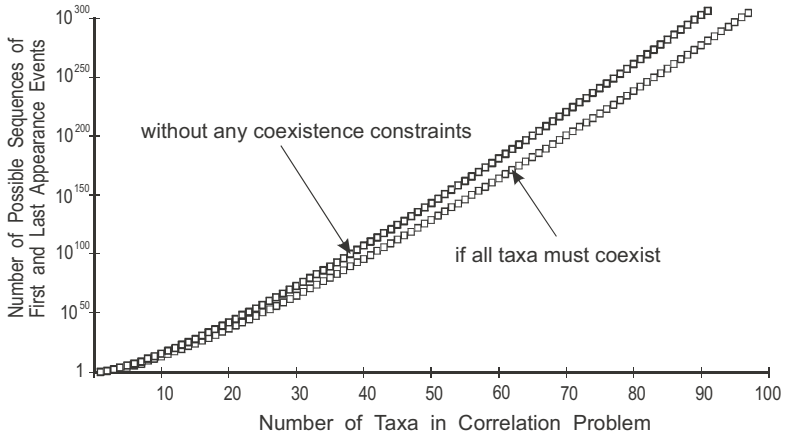

Figure 8. The increase in the number of feasible sequences of first and last appearance events as the number of taxa increases. Realistic levels of coexistence constraint lie between the two curves. The upper curve includes no coexistence constraints; it requires only that each taxon must appear before it can go extinct. The lower curve represents the most constrained case - one in which all taxa are known to coexist with all others.

Correlation problems may include non-biostratigraphic events. These are unpaired events, such as ash falls, for which there is no *a priori* constraint equivalent to the sequencing of first and last appearances of the same taxon. Assuming such event beds are distinctive and positively identified, however, their position in a stratigraphic section cannot be moved up or down like a taxon range-end to fit the section to a particular sequence of events. Thus, these events are constrained to remain in the order of their appearance in stratigraphic sections. First appearances of taxa that lie stratigraphically below an ash bed must be earlier in sequence, because first

appearances may not be adjusted upward. Similarly, a last occurrence is certainly younger than any ash bed that lies below it in a single stratigraphic section. In this way, ash beds that can be matched across several sections serve to constrain the number of feasible sequences to be lower than the totals shown in Figure 8 for biostratigraphic events alone. Ash beds whose relative age has been established by radiometric dating can serve a similar purpose even if they are not known from the same stratigraphic sections.

2. TRADITIONAL BIOSTRATIGRAPHIC INTERVAL ZONES

Traditional zonal biostratigraphy justifiably avoids the nightmares inherent in Figures 1 and 8 by selecting a relatively small number of first and last appearances to define the boundaries of interval zones. Of course, the price for simplifying the problem by culling events is likely to be a loss of resolution. The data set for the Riley Formation includes 124 range-end events; yet only six or seven biozones were traditionally used to subdivide this stratigraphic interval. Although it may be unrealistic to expect all 124 events to be practically applicable to time correlation, Shaw's (1964) graphic correlation showed that reducing them to six was far too conservative. If the exercise is to determine the history of standing diversity, however, then the proper permutation is needed for all 124 events - including the first and last appearances of taxa that are known from only one section.

For very practical reasons, the traditional selection of range ends favors abundant, distinctive, and cosmopolitan taxa. But the most critical requirement is to limit the selection to those events that are almost always found in the same order. Consider how this requirement inevitably leads to the culling-out of long-ranged taxa and closely-spaced events. The longer the taxon range, the greater will be the maximum possible discrepancy between the real and observed range ends - the observed ends might fall anywhere within the real range. The smaller the interval between a pair of events, the smaller will be the discrepancy (in one range or both) that is sufficient to reverse their preserved order.

If few index taxa are chosen and they are relatively short ranged and their range-end events are sufficiently widely separated from those of other chosen taxa, then their order of preservation will inevitably appear relatively stable. There may be equally good events that must be excluded from the index set because they are too close to a selected event or two. Nevertheless, exceptions to the most frequently observed order of selected events do occasionally emerge. These anomalies are corrected on an ad hoc basis and comfortably explained by appeal to one or other of the processes that cause

ranges to be under-represented. Although the same biases affect all observed range ends, no attempt is made to correct the others.

Traditional correlation uses the observed range ends, not adjusted range ends. When comparing the sparse tie lines of a traditional fence diagram with a full set of adjusted tie-lines drawn by a computer, it is natural to ask whether the impression of increased temporal resolution might be partly illusory. Remember, however, that the traditional lines cannot be assumed to be precisely located, simply because they do not cross. The precision may be partly illusory in both cases. Computer-assisted correlation addresses this question of reliability internally by analyzing the full set of equally best-fit solutions. Traditional biostratigraphy uses independent tests, such as chemostratigraphic markers and paleomagnetic reversals, to test for diachronism in zone boundaries. In this way, many traditional zones have been shown to be remarkably reliable. Computer-assisted correlation can easily and more effectively incorporate this same strategy. As explained above, marker beds and age constraints should be added to the list of events for which the computer algorithms seek an optimal sequence. Such fixed markers serve to direct the range adjustments to the more diachronous range ends.

2.1 Assemblage Zones

A significantly different method of building a time scale from biostratigraphic information also deserves attention. Rather than observed range ends, it exploits only the more trustworthy observations of overlapping ranges. These overlaps record the coexistence of taxa. The method groups coexisting taxa into assemblages and then orders these assemblages, from oldest to youngest, as criteria for determining relative age in a succession of coarse assemblage zones. The Wood Committee (Wood *et al.*, 1941) built the sequence of North American Land Mammal Ages this way. The approach has been quantified and automated by Guex (Guex and Davaud, 1984; Guex, 1991) under the term "unitary associations." Alroy (1992) used essentially the same quantitative approach, developed independently, to improve upon the resolution achieved by the Wood Committee.

This seriation of faunal assemblages does not always produce a dramatic increase in resolution relative to the traditional event-based zones. Guex (1991) extracted eight assemblages for the Riley data set, for example. Nevertheless, his unitary association method is a very powerful approach to correlation problems in which direct evidence of superposition is rather sparse; this problem may arise because the faunas are isolated, or the fossiliferous sections span very short stratigraphic intervals, or the fossil-bearing strata are highly deformed. Radiolarian faunas from cherts at convergent plate boundaries frequently fall into the last category. For an

example of isolated faunas, see the chapter by Webster *et al.* in this volume.

The method of unitary associations is more conservative than our treatment of the Riley example, but it suggests a means to augment our measure of misfit. Unitary associations do not consider range extensions at all; instead they exploit coexistence as the means of both constraint and optimization. Hypothetical sequences of first and last occurrences tend to imply more coexistences than are actually observed. An optimal sequence would minimize the number of coexistences ("conjunctions" in Alroy's terms) that are implied but not observed in any of the faunas. This "excess coexistence" factor can easily be added onto the measure of misfit derived from range extensions. The additional penalty proves to be essential for correlation problems that span a time interval which is much longer than the individual stratigraphic sections (e.g., the graptolite case study, below).

Readers who are wary of relative stratigraphic thickness as a proxy for time may have been uncomfortable with its use as a measure of misfit in our trivial example from the Riley Formation. Unitary associations then seem very attractive because they avoid connections between rock thickness and time. In the next section we explain how constrained optimization can measure misfit without reference to stratigraphic thickness.

3. COMPUTER-ASSISTED CORRELATION

Although the biostratigraphic sequencing problem is substantial, our analysis of a small part of the Riley data set has shown that it should be tractable. For all 124 range-end events, the number of possible sequences becomes dauntingly large, but the rules for selecting the best sequences were found to be few and simple. Iterative application of simple rules is a task well-suited to computers. Kemple *et al.* (1989, 1995) have formalized the rules as a constrained optimization. The CONOP9 software for Windows 95/98/NT platforms (see Chapter 13 and accompanying CD; Sadler, 2000) implements this method and has been used for the remainder of this chapter. There are alternative automated approaches and, to some extent, CONOP9 can mimic them. The method of unitary association (Guex 1991; Alroy, 1992) has already been mentioned. The RASC software (Agterberg and Nel, 1982a,b; Agterberg and Gradstein, 1996, 1999) builds sequences from the most commonly observed pairwise ordering of preserved events. It must exclude events that are observed in very few sections, but is significantly faster than CONOP9 as a result. A comparable approach appears in CONOP9 as an alternative measure of misfit (see below).

3.1 Constrained Optimization

As in our trivial example of two trilobites in two stratigraphic sections, constrained optimization eliminates sequences that fail to reproduce all observed coexistences (constraint) and then searches among the remainder for those that best-fit the field data (optimization). The choice of constraints is obvious, but two critical procedural choices must be made in order to implement an optimization by computer: 1) select a measure of the misfit between possible sequences and the field observations – the best-fit sequence is likely to vary with this choice; and 2) select a search procedure that chooses the sequence with the best fit – this decision should determine the efficiency of the search, but not the outcome.

3.2 Measures of Misfit

Several options are available for measuring the misfit between the observed ranges and a hypothetical possible sequence of events. Our trivial example used an interval measure, formulated from the length of the adjustments needed to make observed ranges fit the proposed sequence. Some other measures are ordinal and based upon the number of locally observed pairwise sequences of events that are contradicted by the proposed sequence (comparable with the ranking and scaling method, Agterberg and Gradstein, 1996). A third class of measures uses the implied but unobserved coexistences (comparable with the unitary association method; Guex, 1991). Compound measures may be produced by summing two or more of these three types of measure. The more complex the measure, however, the more difficult it becomes to interpret the outcome of the optimization.

The best-fit solution is likely to vary with the measure of misfit. Therefore, the choice should be guided by purpose. For interval measures a critical decision concerns whether the size of the range adjustments will be measured in raw stratigraphic thickness or in numbers of event horizons. The former (penalty = ‘interval’ in CONOP9 syntax) favors the sequences preserved in relatively thick sections; its use is justified where the sedimentary facies are uniform or thicker sections are thought to provide better resolution. The latter (penalty = ‘level’ or penalty = ‘eventual’ in CONOP9 syntax) favors sequences preserved in the most fossiliferous sections; it is generally preferable and certainly advisable when the sedimentary facies and the rate of accumulation are known to vary significantly from section to section. By measuring range adjustments as the number of local events or event horizons that must be “leapfrogged,” it avoids using relative thickness as a proxy for duration and shares some of the conservatism inherent in the unitary associations. method

Ordinal measures of misfit (penalty = 'ordinal' or penalty = 'rascal' in CONOP9 syntax) favor the most frequently observed order of events. They may be minimized faster than interval measures because they make local range adjustments only once, after the best-fit sequence has been found. A solution that minimizes ordinal misfit predicts the most likely sequence of events at a single locality, such as the next well drilled in a program of petroleum exploration (Cooper *et al.*, 2001). It might handle the problems of reworking better than other measures. A solution that minimizes interval misfit estimates the regional sequence of origination and extinction events; it is therefore likely to be better suited to building time scales and solving paleobiological sequencing problems.

3.3 Search Heuristics

The size of a correlation problem is given by the number of events to be placed in sequence and the number of stratigraphic sections in which they have been observed. Figure 8 shows that the size of the stratigraphic correlation problem, as measured by the number of solutions to consider, grows at a faster than exponential rate as the number of taxa increases. The number of events and the number of sections together determine the number of operations required to evaluate the misfit for any one of the model sequences. In practice, the best estimator of total computation time is the number of locally observed range ends. Every case of a taxon that is not found in a particular local section reduces the computation time because it reduces by two the number of locally observed range ends that are candidates for adjustment.

All the efficient options for this optimization search by trial and error, iteratively improving their trial solutions until finding the best fit without the hopeless task of examining all possible sequences. It is hard to find any satisfactory means of implementing the most popular forms of genetic algorithm that involve both mutation and hybridization. Because each event in a biostratigraphic sequence may appear only once, the task of making a viable hybrid from two or more model sequences appears to be less efficient than simply continuing the trial and error process for one sequence. So far, search algorithms that iteratively mutate a single sequence reach the solution fastest. Kemple *et al.* (1995) discuss several options and give a detailed account of "simulated annealing" (Kirkpatrick *et al*., 1983), the search heuristic which CONOP9 uses most extensively.

For this chapter, we briefly outline the progress of a typical search by simulated annealing. It has three basic requirements: 1) an initial guess, which may be any feasible trial sequence of events; 2) a means of mutating one trial to generate new trial sequences; and 3) rules for deciding whether to

accept the new sequence or return to the previous one and make a different modification. Simulated annealing always uses the same standard rules for accepting or rejecting each trial. But the means of mutating one trial sequence to generate the next must be suited to biostratigraphic sequences if simulated annealing is to converge efficiently on the best fit.

The most efficient means of mutating a sequence selects one event at random from the previous sequence and moves it to a random new position. Sadler (2000) explains other options and their uses. For the early trials, the simulated annealing algorithm accepts quite "bad" mutations that significantly increase the misfit. Bad mutations may lead to a better fit in subsequent trials. More importantly, they prevent the search from becoming trapped at a sub-optimal solution. Throughout the search, however, the rate of acceptance of bad mutations diminishes as the algorithm progressively lowers the maximum size of the temporarily acceptable deteriorations in fit. In effect, this allows an initially rather coarse search strategy to become progressively finer and "home in" effectively on the best-fit solution. The strategy of accepting some bad mutations allows simulated annealing to proceed without hybridization; it is one end-member in the range of evolutionary algorithms.

While searching, CONOP9 displays each trial sequence as one frame in an animated and rather stylized range chart (Figs. 9-inset, 10-inset; if the number of taxa exceeds the number of lines on the screen, a standing diversity curve can be animated instead). At first, the range chart shows that most ranges are long, and all taxa coexist in the middle of the sequence. For its initial guess, CONOP9 has placed all the first occurrences in random order in the first half of the sequence and all last occurrences, independently randomized, into the last half. This simple ploy satisfies all possible coexistence constraints. Of course, such an initial guess fits the empirical data very poorly; and early mutations of the sequence rapidly reduce the misfit (Fig. 9). The progressive reduction of both the acceptance threshold for bad mutations and the misfit between the trials and the field observations are plotted on top of the animated range chart. Ideally, both curves fall smoothly and exponentially from a steep initial descent in the upper left of the graph to a horizontal finish in the lower right (Fig. 10). The initial value of the acceptance threshold and its exponential reduction must be programmed in advance; they correspond to the initial temperature and the slow cooling schedule of the annealing analogue (Kemple *et al.* 1995). In contrast, the smoothly diminishing returns in the improvement of fit emerge at run-time, but only if the annealing schedule was set appropriately for the size and complexity of the problem. The number of sequences examined in a successful simulated annealing may reach many tens of millions for very

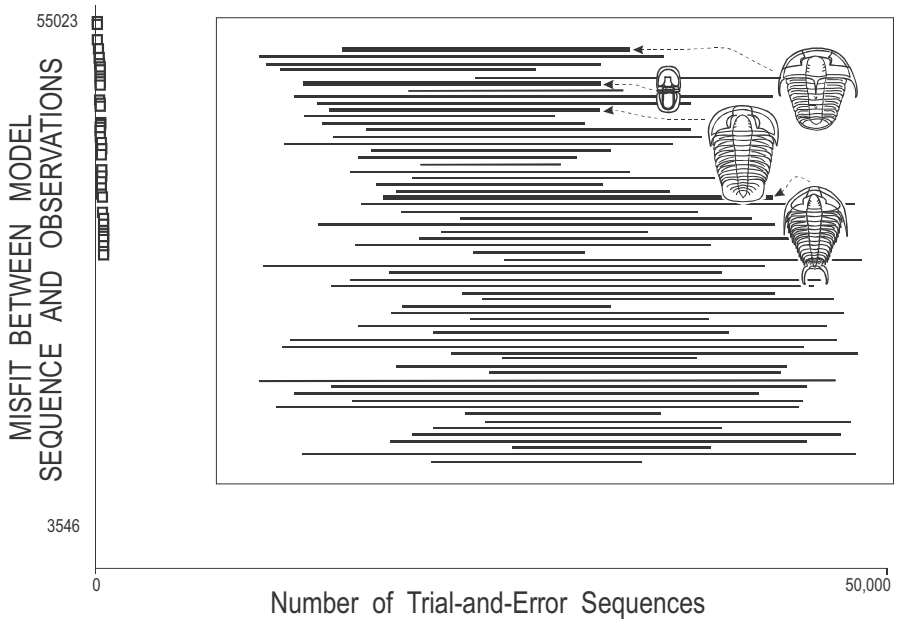

Figure 9. Rapidly improved fit after about one thousand trials in a CONOP9 search for the best-fit solution to the Riley correlation problem, from a random initial guess. This is modified from a snapshot of the computer screen during a CONOP9 search. Two diagrams that are superimposed on the screen have been separated here for clarity. 1) Main graph: open squares in the upper left plot the falling misfit, from top to bottom, as the number of trials increases, from left to right. 2) Inset box: the horizontal lines are relative ranges for the 62 trilobite taxa, first appearance to the left, last appearance to the right. This snapshot shows the ranges corresponding to the latest trial sequence; during a search, they become an "animated range chart" in which range ends continually adjust to depict the current trial. Illustrations of trilobites have been added to locate the four taxa used in Figures 5-7; they would not appear on the screen during an actual CONOP9 run.

large data sets, but is far fewer than the totals charted in Figure 8. The heuristic rapidly finds optimal solutions for moderately large instances (up to 100 taxa) and very good solutions for extremely large instances (in excess of 500 taxa). For the latter, it is possible to improve the solution by re-running the search, but starting from the previous best sequence and with a low rate of acceptance for bad mutations.

4. BEST-FIT INTERVALS

The best-fit sequence found by constrained optimization is seldom a unique solution for a biostratigraphic sequencing problem; several slightly

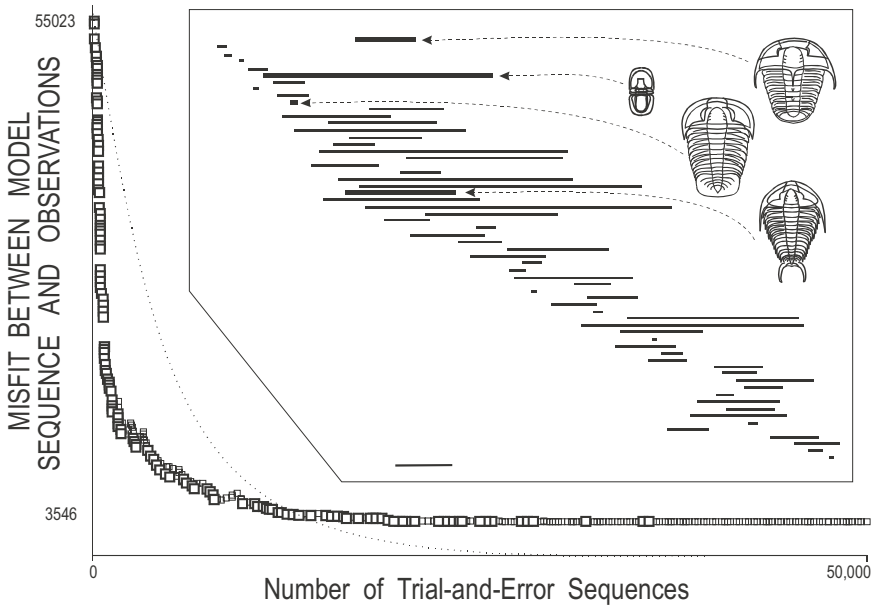

Figure 10. Snapshot of the final trial in a CONOP9 search for the best-fit solution to the Riley data set. Large open squares plot the reduction of misfit with the field observations through a search of 50,000 trial sequences. Small squares indicate that a trial mutation was accepted even though it did not immediately reduce the misfit. At the end of a well-tuned search by simulated annealing, the rate of discovery of better solutions has slowed exponentially leading to a run of unsuccessful trials. The dotted line charts the falling probability of accepting "bad" mutations (increases in misfit; see text). Inset box: taxon ranges in the best-fit solution; compare Figure 9; the diagonal arrangement of the best-fit ranges is an artifact of Shaw's (1964) numbering of taxa that generally proceeded up-section.

different sequences of events typically fit the field observations equally well. Some events may have a constant position throughout this set of equally best-fit sequences; others will be less tightly constrained. The best-fit interval for an event is the range of positions that it takes in the whole set of equally best-fit sequences. The best-fit interval is the flat base of a "relaxed-fit" curve that plots the smallest known misfit as a function of the position of one event across all positions in the overall sequence (Fig. 11).

The operational challenge in mapping out the best-fit intervals, is to find the full set of equally best-fit sequences. Given any one of the best-fit sequences it is straightforward to begin to explore the extent of each best-fit interval; while keeping the remainder of the events in the same relative position, move one event up and down the sequence, recalculating the misfit each step of the way. This strategy can be rapidly completed after a single search, but may not establish the full limits of the best-fit interval. For that, all other events should be allowed to reoptimize around the moving event when it appears to have stepped beyond its best-fit interval.

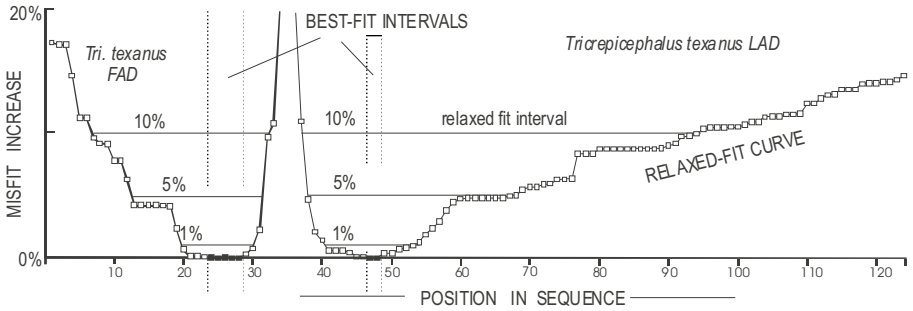

Figure 11. Best-fit intervals and relaxed fit curves for the range ends of *Tricrepicephalus texanus* in the Riley data set. The curves plot the best-known fit as a function of the position of one event in the sequence. Relaxed fit is expressed as a percentage increase in misfit relative to the fit of the optimal sequences. The best fit for the LAD is tighter than for the FAD; but the LAD interval expands faster when the fit is relaxed. Because the FAD constrains the lowest possible position of the corresponding LAD, and vice versa, both curves are asymmetric; the steeper limbs of the relaxed fit curves mark the younger end of the FAD curve and the older end of the LAD curve.

For every event and each of its possible relative positions in the sequence of all events, there will be one or several arrangements of all other events that minimize the misfit. It would not be feasible to complete all these minimizations except for small data sets. An exahustive mapping of the best-fit intevals faces the unmanageably huge numbers of possible sequences predicted by Figure 8. Fortunately, a large majority of the overwhelming number of possible sequences lie far from the best-fit intervals (Fig. 12). It is feasible to reduce the efficiency of the simulated annealing heuristic so that the search deliberately dawdles among the near-optimal and optimal sequences close to the region of best fit. Figure 11 was prepared in this fashion: sub-optimal searches were allowed to loop for days, visiting many millions of near-optimal sequences in order to reduce the risk of underestimating the width of the best-fit intervals.

The average size of the best-fit intervals for all the events measures the resolving power of the whole set of N events. The best-constrained events occupy the same position in all best-fit sequences; their best-fit intervals have size 1 because they span only one position in sequence. Totally unconstrained events fit equally well in all N positions; their best-fit interval would have size N. Therefore the mean best-fit interval for all events ranges from 1.0, for the best possible resolution, to N for a completely unconstrained set of events. For the Riley data set, the mean best-fit interval is 3.2 positions wide. The reciprocal of the average best-fit interval might be a more intuitive measure; it decreases below 1 as resolution deteriorates. But the minimum value would vary from problem to problem, unless the total number of events is rescaled to a constant value based upon 1/N.

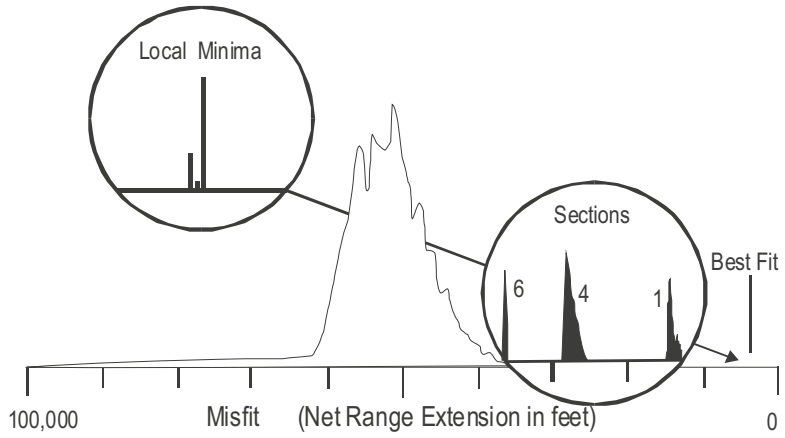

Figure 12. Vertical ruled curve: misfit frequency distribution for a million random sequences fit to the Riley data set (62 taxa; 7 sections). The best-fit sequence, local minima, and sequences that would be generated from local sections are not visible at the scale of the ruled curve – they are typically not discovered in one million random mutations. Inset circles greatly exaggerate vertical scale, showing what might become visible in the tail of the distribution after trillions of trials; they are accurate representations, constructed by long sequences of non-random trials that target the tail. Black histograms: misfit frequencies for sequences developed from a single section, with missing taxa inserted at random. Section 1 (Morgan Creek) is superior to sections 4 (Little Llano River) and 6 (Potontoc). Local Minima: frequency distribution outcomes of a separate set of searches designed to stop at any local minimum encountered in the misfit landscape. In this instance, the tallest of the local minima is the best fit; it captures more of the random searches than the sub-optimal minima.

4.1 Consensus Sequences

The best-fit intervals for a set of events typically overlap with one another to some degree. A sub-set of the events can be selected, on the mcondition that their best-fit intervals do not overlap, to form a consensus sequence in the sense that they have the same positions, relative to one another, in all the equally best-fit sequences. Although maximum consensus sequences contain less than the full set of available events, they often exceed the traditional biostratigraphic resolution by an order of magnitude (Table 3). Sets of events with the same best-fit intervals are alternates for one-another in the consensus sequence. Subsets of events with substantial overlap in their best-fit intervals, but no overlap with other subsets, might be used as the basis for defining the limits of assemblage zones. Thus, best-fit intervals and consensus sequences can place traditional zonation methods on a rigorous footing. Algorithms in CONOP9 rapidly extract consensus sequences once the best-fit intervals have been determined.

4.2 Relaxed-Fit Intervals

Some of the precision of the best-fit measures is likely illusory. This becomes most evident when different measures of misfit generate small differences in the set of best-fit sequences. The best-fit intervals can often be reduced in length simply by combining two measures of misfit into a single optimization criterion. Thus, for any one measure, solutions that almost match the best-known fit might, for practical purposes, be regarded as equally good. Similarly, knowledge of the thickness of the benthic mixing zone, for example, could be used to place limits on the meaningful differences in fit, when these are measured in stratigraphic thicknesses.

Relaxing the best-fit criterion to include all sequences within 0.01% or 0.05% of the best fit would be a conservative approach to the sequencing problem. This allows the intervals to include sequences that are best fit by other measures of misfit. The curves of Figure 11 define all possible relaxed-fit intervals for a pair of events. If these relaxed-fit curves are regarded as cross-sections of a bathtub, then progressive relaxation corresponds to filling the bath and monitoring relaxed-fit intervals by the increasing width of the water surface.

As the relaxation progresses, and larger differences of fit are ignored, the number of non-overlapping best-fit intervals decreases, and the resolving power of the consensus sequence deteriorates. In order to lower the resolution to the level of traditional biostratigraphic zonation, the best fit criterion must be relaxed as much as 20% in some case studies and as little as 0.2% in others (Table 3). This percentage relaxation varies with the number of events and sections in the problem. The size of the total misfit, and any percentage of it, tend to grow with the number of locally observed range ends. Thus, relaxation by a fixed percentage of the best-fit permits the greatest relaxation in instances of the problem with the most sections and taxa. When the purpose is to compare data sets of different size, relaxation should be expressed as a multiple of the average misfit for a single event in the best-fit sequence of each data set. Unlike the more familiar percentage, this *ad hoc* average measure corrects for raw differences in the total number of locally observed events and in the degree of internal contradiction.

4.3 Rating Stratigraphic Sections

Best-fit intervals can measure the resolving power of individual stratigraphic events and, if averaged, the resolving power of whole sets of events. They cannot measure the quality of single sections because best-fit intervals only emerge after the sections have been composited into a single sequence. Raw measures of misfit offer two possibilities to rate stratigraphic

sections. First, individual range extensions may be summed across all ranges observed in a section. This effectively measures the departure of the section from the composite sequence, but must be treated carefully as a measure of the relative quality of different sections. As mentioned above, the total misfit tends to increase with the number of taxa that a section preserves. Every observed taxon adds two range-ends that might need adjustment. Calculating the average extension per taxon can compensate for the correlation between net adjustment and the number of observed taxa.

A better measure would not simply correct for taxonomic richness, however; it would include taxon richness as a positive attribute of a section. The second possible use of raw misfit values achieves this goal by generating a set of sequences of events from the range chart of a single section. Taxa missing from that section are added in random positions, constrained only by the coexistences observed elsewhere. Each sequence in the set can then be assigned a misfit value which is the total range adjustment needed to fit all other sections to this sequence. The whole set produces a frequency distribution of misfit values that is characteristic for the section from which the set was generated (black histograms in Fig. 12). High values of misfit result naturally from two attributes of poor sections: missing taxa and poorly recovered taxa. Sequences generated from poor sections fail to place many of either kind of taxa within their best-fit intervals, the missing taxa, because they are inserted at random into the sequence, and the poorly recovered taxa because their observed ranges are too short, whether as a result of poor preservation or sparse sampling.

5. CASE STUDIES

We illustrate the benefits of computer-assisted correlation by reference to selected features of the four case studies listed in Table 3. The data sets vary considerably in size and complexity, presenting different challenges for the search heuristic. The best-fit solutions for the Riley and Mohawk problems have both been reproduced by numerous relatively short searches. Because the graptolite clade and Taranaki basin problems include much larger numbers of taxa, very long searches have identified several near-optimal solutions that vary in detail but might not include very best solution.

Table 3 reports the length of the searches as a number of trials, because running time varies with the hardware used. Representative running times with 400-600 MHz Pentium III processors and 64-128Mb of RAM are as follows (hardware and solution times have improved considerably since this table was written). The best-known solution for the Riley data set emerges in less than 30 seconds. A fairly good solution for the graptolite clade

Table 3. Statistical Summary of the Selected Case Studies

Case Study	Riley Formation	Mohawk Valley	Graptolite Clade	Taranaki Basin (3 studies)
Location	Texas	New York	World-wide	New Zealand
Problem	correlation	correlation	seriation	correlation with range tops*
Age	Late Cambrian	Late Middle Ordovician	Cambrian - Devonian	Paleocene - Miocene
Duration	~ 10 Ma	< 10 Ma	~ 100 Ma	~ 45 Ma
Traditional resolution	6-7 zones	3-4 zones	52-78 zones	16 stages
Number of sections	7 sections	6 sections	169 sections	8 wells
Clade	trilobites	graptolites	graptolites	microfossils
Number of taxa	62	21	570	87 – 178
Observed local ranges	201	58	2997	508 – 1054
Number of taxa observed to coexist	348 pairs	74 pairs	6881 pairs	1,035 – 5,905 pairs
Rate of pairwise contradiction	18%	23%	24%	58 – 61% (tops and bases)
Number of tuff beds	0	5	22	0
Number of trials in search	40 - 50,000	50 - 100,000	>25 million	1 - 2 million
Minimum misfit	3546 feet	461 meters	7632 levels	23,383 – 68,541 meters
Average misfit per range end	8.8 feet	3.97 meters	1.27 levels (7.6 meters)	48.2 – 34.8 meters
Additional implied coexistences	64 pairs	10 pairs	5295 pairs	1,593 – 6,302 pairs
Conjunction index (Alroy, 1992)	0.84	0.97	0.57	0.39 – 0.48
Consensus sequence	50-60 events	31-40 events	>1000 events	>50 events*
Resolution increase relative to traditional	7 - 10 fold	7 – 10 fold	> 10 fold	> 9 fold
Relaxed consensus that matches traditional resolution	6 - 10% relaxation	25 - 40% relaxation	0.2 - 0.5% relaxation	n.a.*
References and sources	Palmer, 1954; Shaw, 1964; Kemple *et al.*, 1995.	Cisne *et al.*, 1982; Goldman *et al.*, 1994; Sadler and Kemple, 1995.	Sadler and Cooper, in prep.	Cooper *et al.* 2000; Cooper et al, 2001; Sadler, unpubl.

*borehole caving compromises first appearances and the consensus sequence algorithms

emerges in less than two days, but the search may continue to find small improvements for another 10-15 days. To map out the best-fit intervals for the Riley problem, such hardware should be left to loop through suboptimal

searches for 2-3 days. For a data set as large as the graptolite clade, the mapping of best-fit intervals should be run continuously as a background task for a month or more.

5.1 Riley Formation, Texas: A Classic Correlation Problem

Trilobite faunas collected by Palmer (1954) from the Upper Cambrian Riley Formation of Texas became a classic data set when Shaw (1964) used the range charts to demonstrate his graphic correlation method. Kemple *et al.* (1995) used Shaw's data in order to test constrained optimization against Shaw's best graphical solution. Shaw's method has the appearance of considerable subjectivity because of his *ad hoc* justification of more and less reliable range ends. Kemple *et al.* achieved considerable agreement with Shaw's result, without recourse to CONOP9's ability to weight individually every observed range end in every section. They weighted all events equally.

Shaw's graphic method built the solution piecemeal, one section at a time. Several reiterations were needed to converge on a stable solution and Shaw wrote many pages of *ad hoc* justification concerning the local observations that he considered most reliable. Because Kemple *et al.* (1995) reached essentially the same solution without using differential weighting, they argue that Shaw's evaluation of the relative reliability of different events was not really subjective. Rather, it was Shaw's only means to incorporate objective information from the whole data set while evaluating one or two sections at a time. Of course, the computer-assisted optimization uses all the information throughout. Its optimization criteria are explicit in advance and require less than one minute to generate a best-fit solution that unscrambles the fence diagram (compare Figs. 1 and 13).

Shaw used 62 taxa from seven sections, which all span approximately the same interval. Thus, one measure of the size of the problem is 868, the number of local range ends that must ultimately be located. In fact, no section yielded all taxa. Only 402 range ends were actually observed. This smaller number, is a better guide to the time required to compute the misfit for any one geologically feasible sequence of events. Of the observed range ends, only 325 can be usefully adjusted in the course of constrained optimization. Some of the remaining range ends cannot be meaningfully extended because they already lie at the top or bottom of the investigated stratigraphic section. For others, no contradictions arise concerning their placement in sequence because the taxon was found in only one section.

The best-fit sequences for the Riley Formation require the adjustment of

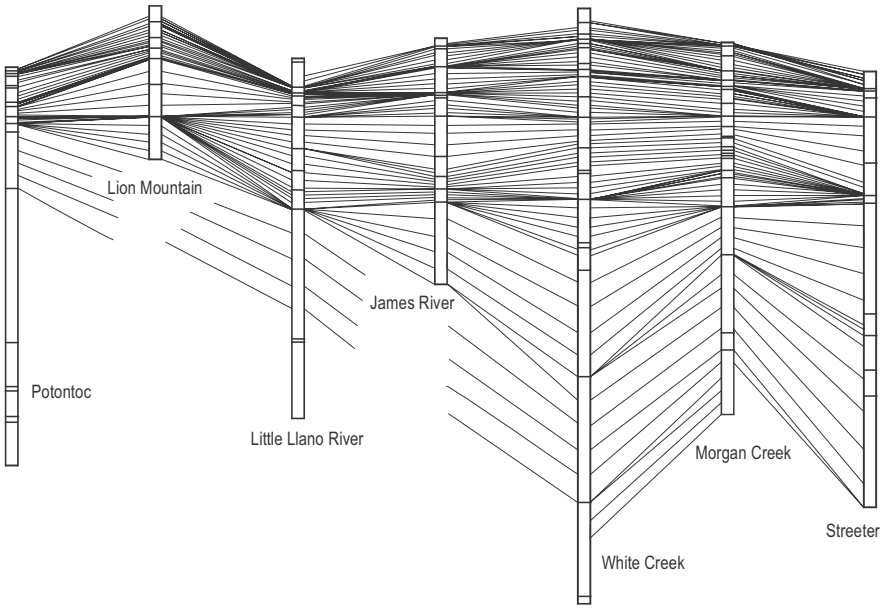

Figure 13. Best-fit fence diagram for the Riley data set. The best-fit solutions place tie lines only at observed event horizons, shown by horizontal bars that divide the section columns. For this figure, the placed levels were subjected to a 5-level moving average that reduces the number of spurious convergences and highlights more robust evidence for condensed levels.

117 of the observed range ends for a total misfit of 3546 feet. Because two thirds of the improvable range ends required no adjustment, the average extension is less than ten feet per event. This compares favorably with the average 21-foot spacing between observed event horizons. The extended ranges imply only 71 more coexisting pairs of taxa than the 348 actually observed coexistences that served to constrain the solution.

How real is the fine resolution implied by all the adjusted tie-lines in Figure 13? Figure 14 summarizes the best-fit intervals for all 124 events. Clearly, a few events may occupy ten or more positions without impacting the best-known fit. For many others, the best fit is achieved in a unique position. In the best resolved portions of the sequence, the best-fit intervals of adjacent events do not overlap. Five such intervals, spanning two to eleven positions in sequence, can be subdivided by using all the first and last appearance events within them. They separate six portions of the sequence in which many larger best-fit intervals overlap with one another. In some ways, these six portions resemble assemblage zones that might be defined on the basis of a suite of events. The number of these gross subdivisions of the sequence resembles the number of traditional zones, suggesting that the traditional resolution is entirely reasonable, given the lack of computer assistance to resolve contradictions.

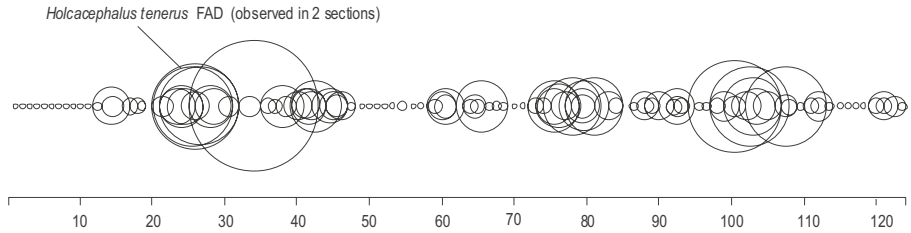

Figure 14. Best-fit intervals for all 124 events in the Riley data set, plotted against an ordinal time-scale with 124 divisions that young from left to right. Each circle represents the range of positions that an event occupies in the set of all equally best-fit sequences. One circle (ruled) is labeled to identify the event. There is a circle for every event, but some coincide exactly.

Figure 15 illustrates a maximum-consensus sequence – the largest number of non-overlapping circles that can be extracted from Figure 14. For the Riley Formation, these maximum consensus sequences include 50-60 events, depending on the measure of misfit. This amounts to a seven- to nine-fold increase in resolution relative to traditional zonation. To reduce the consensus sequence to only 6 or 7 events, a resolution comparable with traditional zonations, we must relax the fit criteria to accept all sequences within 6 – 10% of the best fit.

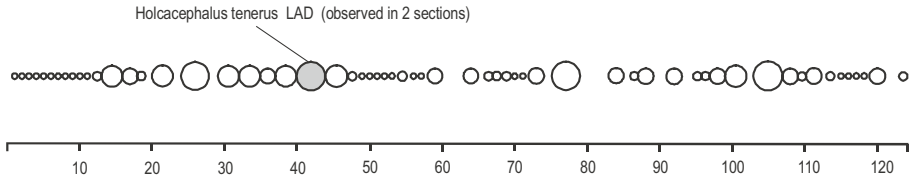

Figure 15. A maximum-consensus sequence for the Riley data set. This figure is developed automatically from Figure 14 by selecting the largest number of non-overlapping circles. Each circle represents one event; one is labeled as an example.

5.2 The Ordovician of the Mohawk Valley: Quantifying Alternate Correlation Models

The late Ordovician graptolite-, conodont-, and K-bentonite-bearing sequences of the Mohawk Valley in New York State alternate between limestone facies (Trenton, Dolgeville, etc.) and shale facies (Utica). The facies boundaries are diachronous. The preferential recovery of graptolites from the shales and conodonts from the limestones leads to severe contradictions between the sequences of first and last appearance events preserved in the local sections.

Not surprisingly, two quite different model correlations have been proposed for these rocks. One relies primarily on matching K-bentonite

beds from locality to locality (Cisne and Rabe, 1978; Cisne *et al.*, 1982a,b); the other places more reliance on the observed ranges of graptolites (Goldman *et al.*, 1994). The differences are significant because they substantially alter the interpretation of the off-shelf Dolgeville limestone facies: in one it is a long-lived shelf-fringing facies and in the other it is a short-lived pulse, perhaps indicative of a sea-level excursion. In the former interpretation, all sections overlap considerably in time; in the latter, two sections, Dolgeville Dam and Nowadaga Creek, are significantly younger than the others (Fig. 16; Sadler and Kemple, 1995).

Sadler and Kemple (1995) showed how constrained optimization can be used to quantify and thus compare the fit of the rival solutions to the field data. They examined 15 graptolite taxa from 6 sections. Here, we present the results for a slightly larger data set with the same six sections but using all 21 graptolite taxa from Goldman *et al.* (1994) and five distinctive clusters of K-bentonites. The six additional graptolite taxa occur in only one section and do not alter the solution. The K-bentonite clusters fall outside the controversial intervals.

The model sequence with the best fit to the observed data from the six Mohawk sections has a net misfit of only 461 m. It closely resembles the solution published by Goldman *et al.* (1994). One may visualize this value as the lowest point in a "landscape" of misfit values. Different latitude and longitude coordinates in this analogy refer to different sequences of events. Elevation increases with misfit. Sequences that resemble the solution preferred by Cisne *et al.* (1982a,b) would come from the bottoms of a cluster of closed depressions in such a landscape. The floors of these depressions have misfit values of 595-610 m, about a one third deterioration in fit, relative to the best-fit sequence. Figure 17 indicates that these closed depressions have a large catchment area; they trap a much larger proportion of optimization runs than the true minimum. As a result, the best-fit sequence is extraordinarily difficult to find for this data set.

Compared with this Mohawk example, most correlation problems have less severe internal contradictions. Typical instances of the biostratigraphic sequencing problem correspond to misfit landscapes with fewer and smaller local minima. These minima are closer to the global minimum and they trap fewer runs.

The relaxed-fit curves for the graptolite events (e.g., Figs. 18-19) reflect the high rate of internal contradiction and the existence of the cluster of local minima. Rather than the usual progressive deterioration of fit away from the best-fit interval, the curves for several species (e.g., *Dicranograptus nicholsoni* and *Orthograptus pageanus*) show secondary minima or a pronounced shelf at about a 30% relaxation of fit.

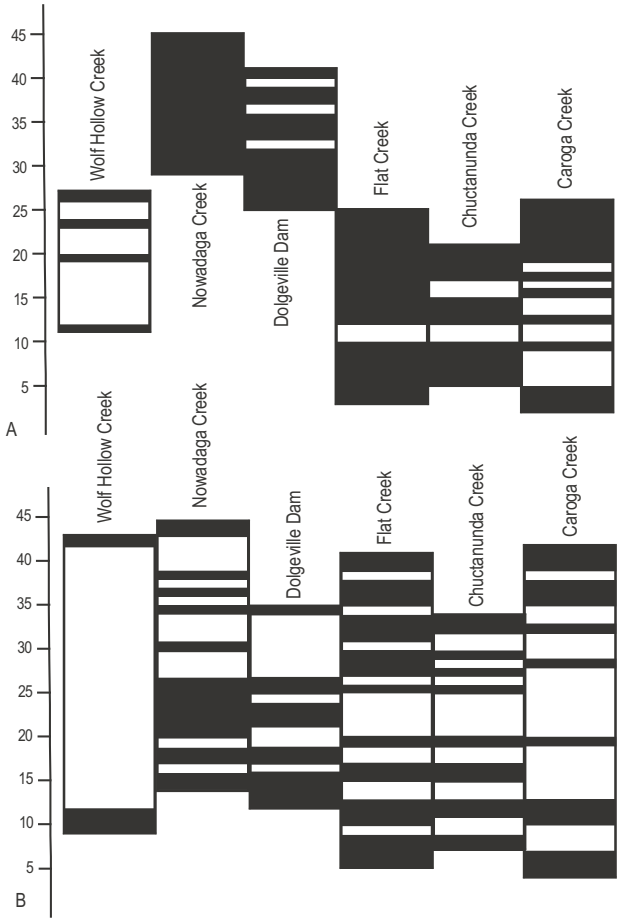

Figure 16. Two correlations of the six Mohawk sections. Vertical "time" axis is the ordinal sequence of events. Black bars indicate range-end events actually observed in the section. Events adjusted to the section top or base are not counted into the range of the section in this plot. Correlation A uses the best-fit sequence with a misfit of 461 meters; it resembles the one proposed by Goldman *et al.* (1994) in its placement of the Dolgeville section. Correlation B is one example of correlations generated by non-optimal misfits in the range 595-610 meters that resemble the placement of the Dolgeville section by Cisne *et al.* (1982).

In addition, there are events with very shallow relaxed-fit curves, indicating that their position in sequence is entirely poorly constrained. The last appearance of *Corynoides calicularis* (Fig. 19) is weakly constrained by field observations. The species was found in only one of the six sections and at only one level; it has no observed coexistences. Although such unique finds have no local resolving power for correlation, they should not automatically be thrown out of the analysis. First, the best-fit interval

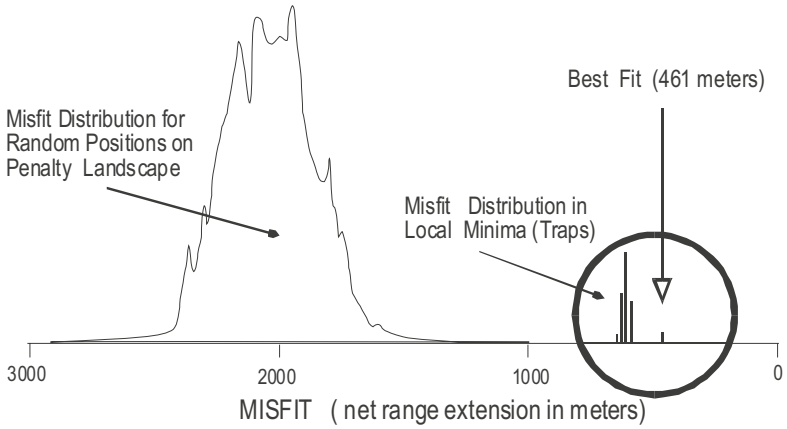

Figure 17. Frequency distribution of misfit for all feasible sequences of the 47 events in the Mohawk data set. Ruled curve: misfit distribution for one million random feasible sequences. Five vertical bars in circle with great vertical exaggeration: frequency distribution of local minima found by one thousand runs from random starting positions by greedy algorithms that cannot exit local minima. On the scale used for the ruled curve, these misfit values are so rare as to be indistinguishable above the axis of the plot.

provides a measure of the low resolving power that may be preferable to a probabilistic confidence interval. Second, the unique events may deserve inclusion in an accompanying analysis of standing diversity. Third, a rare or unique find may be a key index fossil for zones established in a neighboring faunal province.

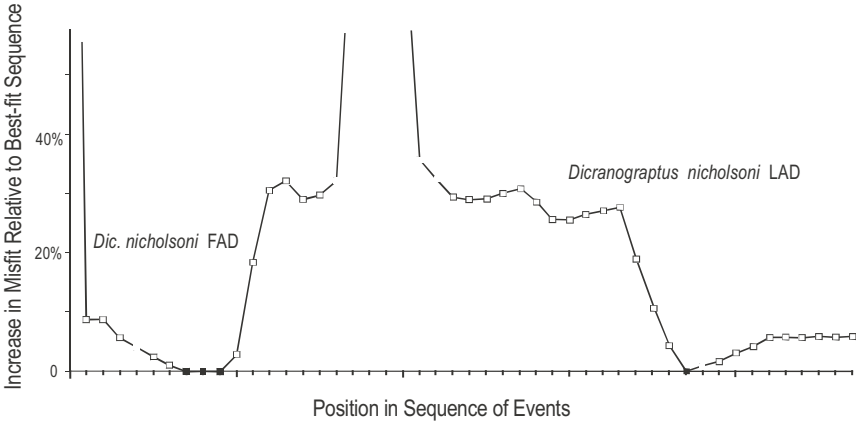

Figure 18. Relaxed-fit curves for the first- and last appearance events of *Dicranograptus nicholsoni*, found in four of the six sections in the Mohawk Valley data set. Note the secondary minima at about a 30% misfit increase, which compares with the suboptimal sequences that generate solutions of the kind favored by Cisne *et al.* (1982a, b).

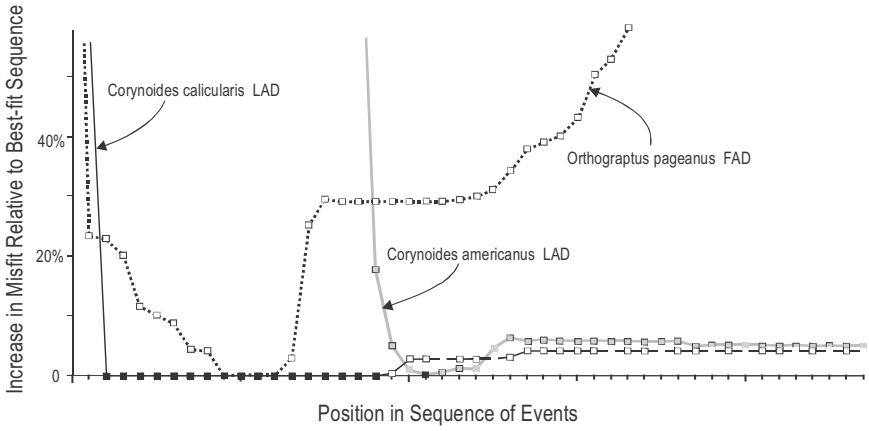

Figure 19. Additional representative examples of relaxed-fit curves for selected graptolite first- and last-appearance events in the Mohawk Valley data set. (Explanation in text.)

Although *Corynoides americanus* is observed in three of the six Mohawk sections, the relaxed-fit curve for its last appearance is still very shallow. This event is preserved in rather inconsistent positions relative to other taxa, but the maximum possible range extension is limited because the highest finds of *C. americanus* are close to the top of the sections in which the species is found. Because observed fossil ranges almost always contain gaps, ranges that end near the limits of measured sections are traditionally considered unsuitable for correlation; another find may lie just beyond the collected interval. The relaxed-fit curves confirm that the constrained optimization automatically incorporates this stratigraphic wisdom.

Measures of misfit can be designed which will continue to increase when ranges are extended beyond the limits of a section to higher or lower positions in the regional sequence of events. When added to the primary measure of misfit, these secondary measures tighten the relaxed fit curves. Such secondary measures are justified when the individual sections are so short, relative to the time interval represented across all sections, that some pairs of sections do not overlap in time. Whether or not the Mohawk data fit this criterion depends upon the preferred correlation model. The best-fit sequence (Fig. 16A) indicates that a secondary measure would be justified.

Several different formulations are possible for a misfit measure that discourages the extension of ranges beyond the measured section. The simplest of them minimizes the net length of all the ranges, as measured by their span of positions in the model sequence; it favors hypothetical sequences with short-lived taxa, but does necessarily improve the fit with the field observations.

A better option borrows from Guex' (1991) and Alroy's (1992) use of

coexistences. As a taxon range is progressively extended, it is likely to overlap with an increasing number of other taxon ranges. Thus, the extended ranges tend to imply a greater number of pairs of coexisting taxa than have actually been observed. The number of implied coexistences minus the number of observed coexistences is another measure of misfit between the field observations and a hypothetical sequence of range-end events. Such a measure of misfit manages to limit the growth of poorly constrained ranges beyond the local stratigraphic sections and, at the same time, reinforces the fit with observed coexistences. For the Mohawk problem, addition of such an auxiliary measure of misfit to the primary measure favors solutions of the kind advocated by Goldman *et al.* (1994). It alters the misfit landscape in such a way that the best-fit solution is found more readily. But some searches still tend to get stuck in the local sub-optimal minima in the penalty landscape, which represent solutions like the ones proposed by Cisne *et al.* (1982a, b). These "traps" persist until the auxiliary measure, based on coexistences, is assigned more than twice the weight of the interval measure of misfit.

The full set of best-fit intervals for the Mohawk problem (Fig. 20) reveals that the interval of poorest resolution lies at the beginning of the sequence. The top of the sequence may be only marginally better constrained. As the fit is relaxed, several best-fit intervals near the top of the sequence expand very rapidly. A 5% relaxation of fit would be excessive for well constrained biostratigraphic data sets of this size. For the Mohawk Valley, however, we have seen that the published alternative interpretation corresponds to about a 30% relaxation.

Solutions for many instances of the correlation problem can be improved by adding more fossil clades. Again, the Mohawk problem proves to be more difficult than usual. The addition of the conodont taxa to this correlation problem does not improve the solution (Sadler and Kemple, 1995). The conodont taxa appear to be longer ranging than both the measured sections and the graptolite taxa. Because the conodonts are restricted to the limestone facies, many different limestone intervals appear to record the same suite of ranges. Accordingly, when conodonts are included the CONOP9 algorithms tend to produce a correlation of the limestones that resembles a simplistic lithostratigraphic correlation. Evidently the addition of more taxa does not necessarily improve the resolution unless the taxa are short-lived relative to the measured sections and any facies that preferentially preserves them. Better solutions to the Mohawk correlation problem are emerging from improved correlation of K-bentonite beds. C. E. Mitchell and his colleagues (pers. comm.) have considerably increased the number of K-bentonites that can be traced in the field and matched from section to section by chemical fingerprinting.

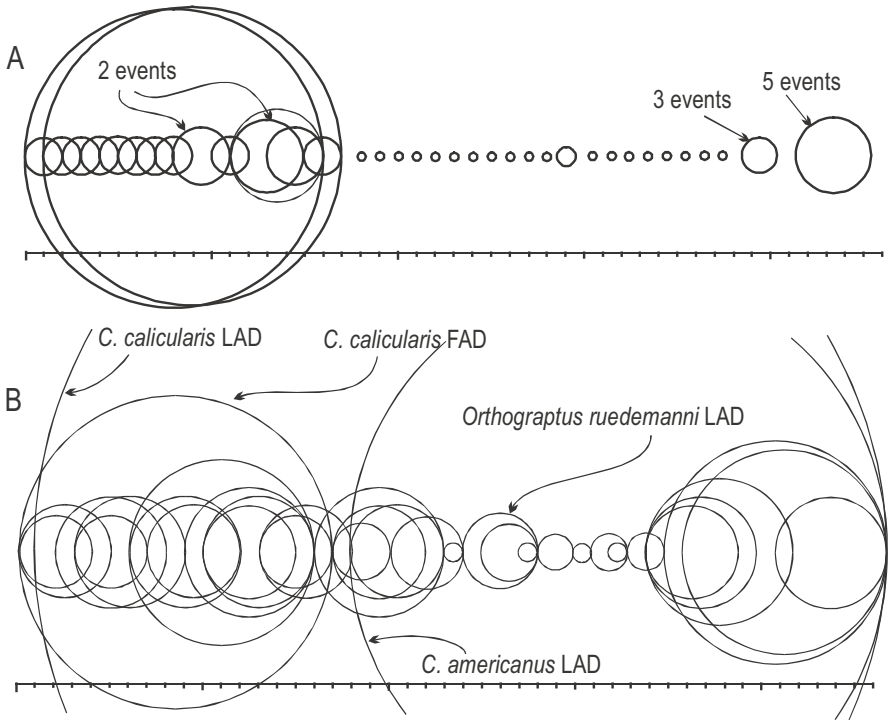

Figure 20. Best-fit intervals (A) and 5% relaxed fit intervals (B) for the Mohawk events plotted as a sequence of overlapping circles. Each event is represented by a circle that extends from the earliest to the latest position that it occupies in the set of best-fit sequences (A) or the larger set with misfit values up to 5% higher than the best-known fit (B). The horizontal scale is the ordinal sequence of events, from the oldest at the left end. A is labeled to show positions in the sequence where two or more circles are exactly coincident.

5.3 The Graptolite Clade: High-Resolution Time Scales and Diversity Curves

This is the largest of the selected case histories. The original purpose was to build an end-Cambrian through early Devonian time scale upon the ranges of 570 graptolite taxa from 169 sections globally. Twenty-two dated K-bentonites provide absolute age control. The search algorithm incorporated these K-bentonites into all the trial sequences according to their associated faunas. The faunas may be preserved within, above, or below the dated beds; any of these situations allows the dated bed and the faunas to be entered as a short stratigraphic section. It did not matter that the dated beds were very rarely found in long stratigraphic sections with good range charts. Associated conodont faunas could be used as proxies for graptolites if other

published sections identified which graptolite taxa could overlap with these conodont ranges. CONOP9 offers several options for building composite sections that scale the intervals between events by reference to the local stratigraphic thicknesses. With radiometric dates included in the best-fit sequence it is possible to identify which of these composites is an acceptable approximation for a time scale.

For this chapter, the case history serves to explain the special problems associated with seriation. Because the individual sections span only a fraction of the total time interval from Cambrian to Devonian, most pairs of sections share no taxa and do not overlap at all in time; they must be stacked in series. A typical correlation problem produces a parallel arrangement of sections with considerable overlap. The term "seriation" better describes the graptolite clade problem. It requires the secondary measure of misfit provided by the number of coexistences that are implied by a trial sequence but represent an excess over those coexistences actually observed in the field.

Good solutions emerge for correlation problems when using only the positive evidence; i.e., misfit is measured solely in terms of the extension of observed local ranges. No additional misfit accrues for inserting a taxon that is completely missing from a given section. This negative evidence becomes necessary in seriation. To understand why, imagine an extreme situation in which this case history includes Ordovician and Devonian sections, but omits the intervening Silurian. Without the Silurian sections, the constrained optimization would still find the best-fit sequences within the Ordovician taxa and within the Devonian taxa. But it would arbitrarily interleave the two solutions into a single sequence that is stratigraphically ridiculous. A stratigrapher would instinctively avoid this error by using the negative evidence that the Ordovician sections and the Devonian sections have no taxa in common. Even with the Silurian included, some arbitrary interleaving is still likely to occur, because the Ordovician taxa are relatively provincial and the available sections are unevenly distributed through the time interval. For example, too many of the measured sections terminate at the Ordovician-Silurian boundary.

Augmenting the interval measure of misfit in proportion to the excess coexistences removes the arbitrary interleaving. Even if the interleaving would eventually be removed by a constrained optimization of positive evidence alone, the augmented measure rids the search of this problem much sooner, making the optimization far more efficient and less liable to terminate in a local sub-optimal minimum.

There remains only the question of how heavily the auxiliary measure should be weighted. For this seriation problem, one tenth to one-hundredth of the number of implied additional coexistences proved to be a sufficient

weight for the negative evidence. If the weight is too high, it tends to force apart sequences of taxa from genuinely coeval geographic provinces. The coeval provinces are held together in the trial sequences by a few shared taxa and by those rare sections that are long enough to extend through changes in provinciality. Therefore, it is essential that the misfit due to coexistences not outweigh the misfit due to range extensions of the cosmopolitan taxa; otherwise, coeval provinces can be teased apart. CONOP9 does not yet have a means to consider geographic proximity and facies similarity; these legitimate aspects of stratigraphers' expertise can be captured only by running subsets of the sections to generate composite sequences for individual provinces and facies. To minimize such problems in this instance, the graptolite seriation was restricted to off-shelf sections in slates and shales.

When augmented by a small fraction of the coexistence excess, the total misfit measure gains in precision and discriminating power. This tends to reduce the width of the best-fit intervals and steepen the relaxed-fit curves (at least the portions close to the best-fit interval). As a result, the consensus sequence for the graptolite clade includes over 1000 events whose best-fit intervals do not overlap. A slightly relaxed fit interval (0.01 - 0.05%) might be more realistic in this case. But graptolites do offer uncommonly high resolving power, even with traditional biostratigraphic interval zones.

For building time scales and for questions of the history of global biodiversity, the computer-assistance brings a significant advantage. Most traditional approaches to these problems are forced to operate at the resolution of zones and stages. For diversity studies, binning the counts by zones may generate spurious peaks and troughs because range ends do not correspond to the zone boundaries and the zones have unequal length. For time scales, radiometric dates are often interpolated at the scale of stages. The computer-assisted process avoids the limitations of zones and stages by operating at the scale of individual events. This is closest to the scale of the raw field observations and removes one level of subjectivity and possible error.

The graptolite case study now includes over 1100 taxa and more than 200 stratigraphic sections. The results are too voluminous to present in detail here. Figure 21 serves as an example. It displays an interpretation of the history of graptolite biodiversity that follows directly from a best-fit sequence. Biodiversity is incremented by one for every first-appearance event and decremented by one for every last appearance to produce a continuous, high resolution, interval free curve. The time scale for Figure 21 is generated by averaging the stratigraphic separations of the events, across all sections, after the ranges have all been adjusted to fit the best sequence

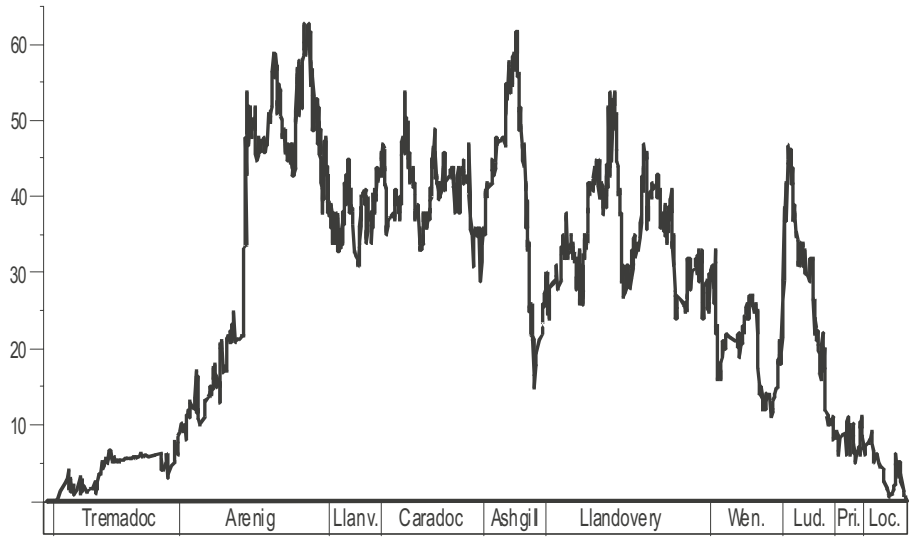

Figure 21. Diversity history of the graptolite clade according to one best-fit sequence for the data set described in Table 3, augmented by all the graptolite taxa found at only one locality. The total taxon count in this diagram is 1136 graptolite species and subspecies. A running total of first appearances minus last appearances determines the standing diversity (vertical axis). The horizontal time axis is a scaled composite section, based on average stratigraphic separations, which gives a good linear regression when the best-fit positions of dated K-bentonites are plotted against a time scale. Stage boundaries were placed according to the position, in this scaled best-fit composite sequence, of the traditional index fossils.

and the section thicknesses have been rescaled to reflect their range of events in the best-fit sequence. This is one of ten scaling options in CONOP9; it produces the best linear correlation with the 22 radiometric dates in this instance.

Traditional binning of diversity data into zones generates discontinuous histograms and introduces severe bias (Foote, 2001). The bias can be eliminated by counting taxa that cross zonal boundaries, but the results remain discontinuous and their reliability difficult to quantify. The "continuous" diversity curves described here inherit measures of their quality and reliability directly from the misfit values attached to the sequences from which they were generated. By superimposing diversity curves from all the best-fit sequences, it is possible to generate a reliability interval for diversity curve. By examining the results of progressively relaxed fit, it is possible to quantify the relative reliability of different peaks and trough in the curve according to the level of relaxation at which they disappear. CONOP9 offers the option to examine the progress of the diversity curve during the search for the best-fit sequence. In this "animated diversity curve" the most robust features emerge at high values of misfit; the

least robust features remain volatile to the end of the search for the best-fit sequence. The diversity curve for the graptolite clade is initially unimodal, with a single maximum. The next feature to emerge in most runs is the late Ordovician extinction event.

5.4 The Taranaki Basin: Integration with Seismic Stratigraphy

Eight wells from the Taranaki Basin, off the west coast of North Island New Zealand, were initially correlated to compare three different automated procedures for biostratigraphic correlation – RASC/CASC, CONOP, and GRAPHCOR (Cooper *et al.*, 2001). A line of three of the wells was used to compare the results from CONOP9 with seismic cross-sections (Cooper *et al.*, 2000). The published studies used only 87 of 573 microfossil ranges available for the eight wells. The severe cull was necessary to ensure that all events were found in at least four wells, a precaution to ensure robust results from the RASC program. For this chapter we repeated the optimization with a larger data set that included the 178 most reliable taxa. Table 3 summarizes results for both data sets.

Unlike the stratigraphic sections in the three case histories discussed above, the Taranaki wells do not necessarily record the bases of ranges properly. The taxa are microfossils and some may have been recovered from sediment that fell to anomalously low levels in the well bore during drilling. Accordingly, Cooper *et al.* (2001) omitted the first appearance events from their analysis. Because the CONOP9 algorithms then required that all ranges have two ends, the bases were assigned zero weights so that they would not influence the solution.

Fortunately, some coexistence constraint can be applied without recourse to the first-appearance events. If a pair of last appearances is observed in the opposite order in two different wells, then it follows that the corresponding ranges must overlap. Nevertheless, the unconstrained bases reduce the number of coexistences that can be proven. They also complicate the construction of best-fit curves for the last appearances. The first appearance events do not appear randomly in the best-fit sequences but tend to dominate the lower portions of the sequence, where they bloat the best-fit intervals of other events. Accordingly, this case study has focused on the use of the untangled fence diagrams, in which the tie lines for first appearances are simply omitted.

The constrained optimization adjusts range ends and inserts missing events. The resulting fence diagrams not only untangle the observed tie lines, they also contain tie-lines that were previously missing. As a result of the increased number of ties generated by CONOP9, as compared with

traditional New Zealand stage boundaries, the convergence and divergence of tie lines in the fence diagrams reveal patterns that resemble the condensed sections, lapouts, and sequence boundaries in seismic sections (Fig. 22).

The mathematically smallest misfit with the field observations is never achieved by placing tie lines in the fence diagrams at intermediate positions between observed first- and last-appearance horizons. For more insightful comparison with sequence-stratigraphic correlations and seismic lines, however, Cooper *et al.* (2000) found it useful to adjust the positions of tie-lines in the fence diagrams by smoothing the distances between adjacent lines. Moving average windows have been used that encompass groups of three, five, or seven adjacent tie lines. The smoothing does not alter the sequence of tie lines and the corresponding events; it adjusts only the stratigraphic distances between them. Smoothing has two useful effects for the visual inspection of possible sequence boundaries; it eliminates convergences that give the appearance of hiatuses where support is poor (few tie lines) and it separates coincident tie lines to sharpen the appearance of hiatuses and condensation where support is strong.

The term "support" refers to the number of adjusted range ends that are placed at the same level. In order to fit observed ranges to the model sequences with minimum adjustments, we have seen that computer algorithms extend ranges only to stratigraphic horizons at which other events have been observed. This exaggerates the number of convergences of tie lines in sections where the sampled horizons are sparse. The local stratigraphic distances between adjacent samples may be regarded as uncertainty intervals on the observed range ends in individual sections - additional collecting horizons might have extended the range ends into these intervals. The best-fit sequence can improve substantially upon these uncertainty intervals by compositing information from all sections; but the unsmoothed fence diagram exposes the limitations of individual sections. In effect, smoothing makes a somewhat arbitrary, but more realistic, placement of the tie lines by moving them into the uncertainty intervals, while retaining their order in the best-fit sequence.

Where fossiliferous horizons are wide-spaced and diversity is low, evidence of real convergence must be weak. By spreading tie lines into the uncertainty intervals between collecting horizons, the smoothing effectively eliminates convergences that are supported small numbers of lines and likely to be artificial; e.g., lower parts of the fences in Figure 22. Convergences of more than three, five, or seven tie lines remain evident after three-, five-, and seven-point smoothing, respectively.

Where the faunas are rich and collecting horizons are closely spaced, the unsmoothed fence diagrams have a different problem: many tie-lines may lie

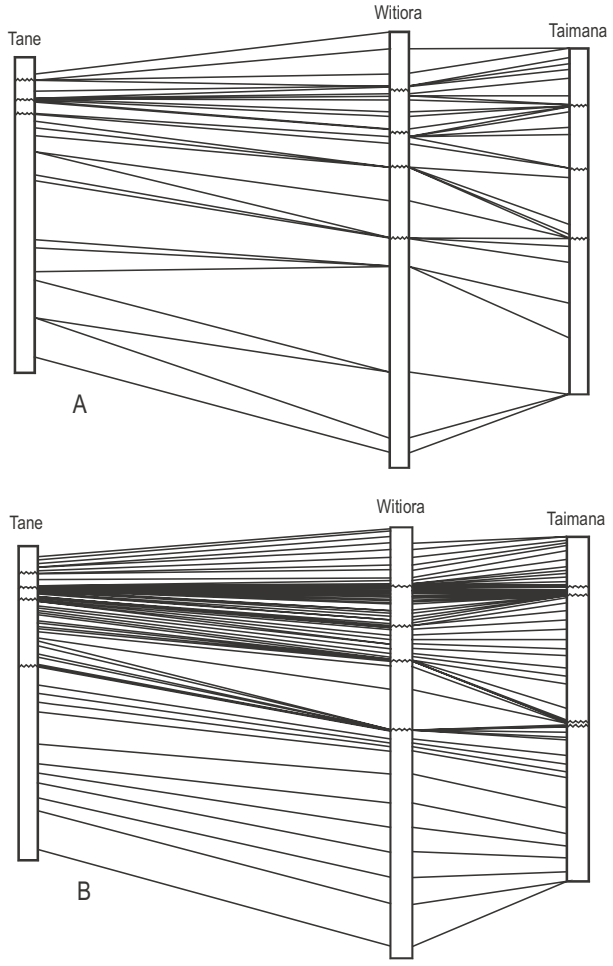

Figure 22. Unscrambled fence diagram of three wells from the Taranaki Basin without (A) and with (B) 7-point smoothing of the elevations of event horizons. The unsmoothed diagram places tie-lines to minimize range extensions; it does not reveal where many lines coincide. The smoothed diagram allows tie-lines to move into intervals between collecting horizons; it eliminates weak convergences and reveals the levels of strong condensation and convergence.

hidden, directly beneath other lines that connect the same horizons. Smoothing causes some of the hidden lines to separate and diverge, but the closely spaced event horizons prevent them from separating very far. Not all the coincident lines are separated; their number is still limited by the number of points in the moving average. Thus, the smoothed diagrams retain the patterns of condensation and convergence that point to the best-supported and most likely horizons of hiatus or sequence boundaries. Cooper *et al.* (2000) had considerable success matching these convergences with the lapout patterns of seismic reflectors and the lithostratigraphic evidence of

hiatus. Indeed, the fit with the high-quality portion of their seismic data was so good that they were emboldened to use the biostratigraphic fence diagram to correct their initial interpretations where the seismic quality was poor and faults complicated the seismic images.

6. CONCLUSIONS

Computer-assisted biostratigraphy may increase resolution by an order of magnitude relative to traditional biostratigraphic interval zones and assemblage zones (Fig. 23) because it solves for the sequence of so many more first- and last-appearance events. The preferred solution is a sequence of events that is characterized by the minimum misfit when compared with all the locally observed taxon ranges. After each measured section has been adjusted to match the solution, the misfit may be summarized by three conceptually different measures. Each totals up a different aspect of the minimum necessary adjustments: 1) the extensions of the local taxon ranges; 2) the locally observed pairs of events whose order is reversed; or 3) the number of additional coexistences that are generated by the range adjustments. A weighted sum of the first and third options can solve seriation problems in which the individual measured sections are much shorter than the total time interval under investigation. The coexistence term should be weighted less than the interval term.

Very simple rules govern computer-assisted searches for an optimal sequence of first and last appearance events that minimizes misfit with the observed fossil ranges. The computer algorithms invert the problem and search through possible solutions by trial and error, using the same few rules that guide manual comparison of alternative sequences. Computer memories allow bewilderingly large data sets to be analyzed. Efficient heuristic search procedures find the best of all possible solutions even when these solutions are far too numerous for an exhaustive examination.

The misfit assigned to the best-fit sequence may be apportioned by event and/or section to reveal the sources of discrepancy with the field observations. Misfit measures may also be used to compare the quality of individual sections in a way that balances the number and fidelity of the preserved taxon ranges.

Because they use available taxon range-ends, including those whose relative age is rather poorly constrained, the computer-assisted solutions are, of course, not unique. The same observed ranges may allow a substantial set of equally well-fit solutions. Best-fit intervals map the range of positions

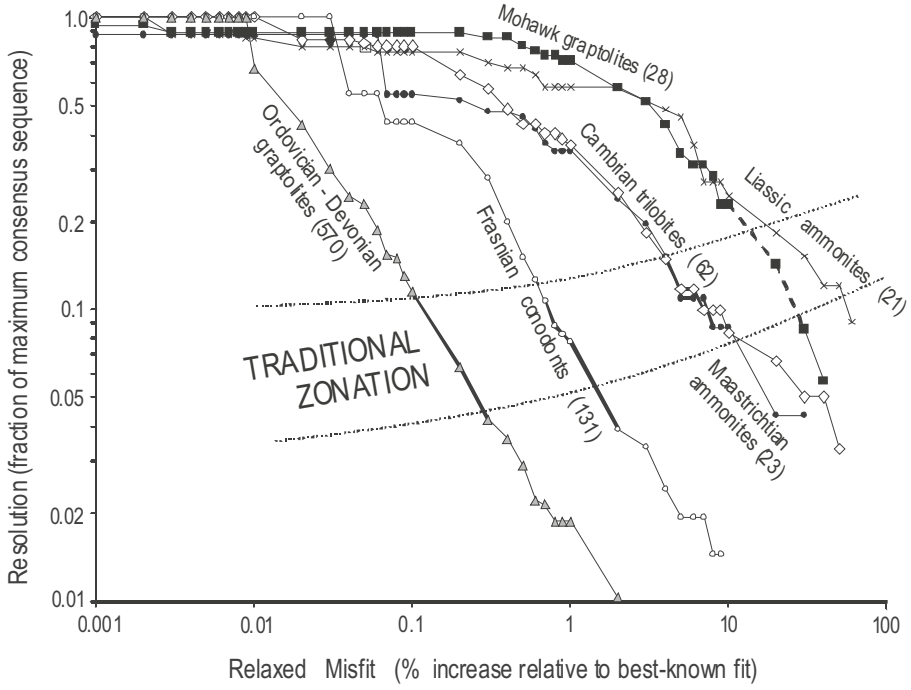

Figure 23. Comparison of the resolution achieved by traditional and computer-assisted biostratigraphy. Computer-generated sequences are charted as the loss of resolution, in terms of the fraction of events that remain in the consensus sequences (vertical axis), as the misfit is progressively relaxed relative to the best-known fit (horizontal axis). Heavy portions of the curves indicate where the numbers of events in the consensus sequence correspond to the numbers of traditional subdivisions. In addition to case histories discussed above, curves are shown for Frasnian conodonts (Klapper, *et al.* 1995 and additional written communications), Upper Liassic ammonite genera (Arkell, 1933, and references therein), and Maastrichtian ammonite species (Macellari, 1984, 1986; Ward and Kennedy, 1993). Numbers in parentheses indicate how many taxa were included in each optimization. The band between dotted lines attempts to generalize the resolution achieved by traditional zonation.

that a single event may occupy in the set of equally best fit sequences. After all the best-fit intervals are reduced to a consensus sequence, which retains only the non-overlapping intervals, an order of magnitude more events may remain than in a traditional biostratigraphic zonation. The resulting fence diagrams have far more detail than traditional correlations. Contradictions in the field observations have been resolved by a conservative adjustment of all the tie lines in the fence, rather than mere culling of lines.

By retaining so many more tie lines, computer-assisted fence diagrams, facilitate comparison with sequence-stratigraphic models and seismic lines. By working at the level of individual observed events, computer-assisted time scales and diversity curves remove the biases otherwise imposed by

arbitrary stages and zones. The most significant advantage, however, may be the ability of computer-assisted methods to provide reproducible results and quantify many aspects of the solutions to correlation and seriation problems. The best-fit intervals, for example, provide a natural, but previously unattainable, means to quantify the resolving power of all the individual first and last appearance events.

ACKNOWLEDG MENTS

Development of the CONOP software is currently supported by NSF grant EAR9980372 to Sadler. Two of our case studies were facilitated by the generous support for visiting scientists provided by the New Zealand Crown Research Institute for Geological and Nuclear Sciences. Peter Harries, Gilbert Klapper and Charles Marshall provided valuable assistance by drawing our attention to passages in the manuscript that were in need of more lucid explanation.

REFERENCES

Agterberg, F. P., and Gradstein, F. M., 1996, *RASC and CASC: Biostratigraphic Zonation and Correlation Software, Version 15*.

Agterberg, F. P., and Gradstein, F. M., 1999, The RASC method for ranking and scaling of biostratigraphic events, *Ear. Sci. Rev*. **46**:1-25.

Agterberg, F. P. and Nel, L. D., 1982a, Algorithms for the ranking of stratigraphic events. *Comp. Geosci*. **8**:69-90.

Agterberg, F. P. and Nel, L. D., 1982b, Algorithms for the scaling of stratigraphic events. *Comp. Geosci*. **8**:163-189.

Alroy, J., 1992, Conjunction among taxonomic distributions and the Miocene mammalian biochronology of the Great Plains, *Paleobio*., **18**:326-343.

Anderson, M. K., 2001, Quantum computing: Souped-up software gets a virtual test, *Science* **292**:419

Arkell, W. J., 1933, *The Jurassic System in Great Britain*, Oxford University Press.

Cisne, J. L., and Rabe, B. D., 1978, Coenocorrelation: gradient analysis of fossil communities and its applications in stratigraphy, *Lethaia* **11**:341-364.

Cisne, J. L., Karig, D. E., Rabe, B. D., and Hay, B. J., 1982a, Topography and tectonics of the Taconic outer trench slope as revealed through gradient analysis of fossil assemblages, *Lethaia* **15**:229-246.

Cisne, J. L., Chandlee, G. O., Rabe, B. D., and Cohen, J. A., 1982b, Clinal variation, episodic extinction, and possible parapatric speciation: The trilobite *Flexycalymene seneria* along an Ordovician depth gradient, *Lethaia* **15**:325-341.

Cooper, R. A., Crampton, J. S., Raine, J. I., Gradstein, F. M., Morgans, H. E. G., Sadler, P. M., Strong, C. P., Waghorn, D., and Wilson, G. J., 2001, Quantitative biostratigraphy of the Taranaki Basin, New Zealand - a deterministic and probabilistic approach, *AAPG Bull*.

Cooper, R.A., Crampton, J.S., Uruski, C.I., 2000. The time-calibrated composite - a powerful

tool in basin exploration, in: *Proceedings of the 2000 New Zealand Petroleum Conference, Christchurch, New Zealand*, Ministry of Commerce, Wellington, pp. 346-354.

Dell, R., Kemple, W. K., and Tovey, P., 1992, Heuristically solving the stratigraphic correlation problem, in: *Proceedings of the Institute of Industrial Engineers First Industrial Engineering Research Conference*, pp. 293-297.

Goldman, D., Mitchell, C. E., Bergstrom, S. G., Delano, J. W., and Tice, S. T., 1994, K-bentonites and graptolite stratigraphy in the Middle Ordovician of New York State and Quebec: A new chronostratigraphic model, *Palaios* **9**:124-143.

Guex, J., 1991, *Biochronological Correlations*, Springer Verlag, Berlin.

Guex, J., and Davaud, E., 1984, Unitary associations method: Use of graph theory and computer algorithms, Comp. Geosci. **10**:69-96.

Kemple, W. G., Sadler, P. M., and Strauss, D. J., 1989, A prototype constrained optimization solution to the time correlation problem, Geol. Surv. Can. Pap. **89-9**:417-425.

Kemple, W. G., Sadler, P. M., and Strauss, D. J., 1995, Extending graphic correlation to N dimensions: The stratigraphic correlation problem as constrained optimization, in: *Graphic Correlation* (K. O. Mann and H. R. Lane, eds.), SEPM Sp. Pap. **53**:65–82.

Kirkpatrick, S., Gelatt, C. D., and Vecchi, M. P., 1983, Optimization by simulated annealing, *Science* **220**:671-680.

Klapper, G., Kirchgasser, W, T., and Baeseman, J. F., 1995, Graphic correlation of a Frasnian (Upper Devonian) composite standard, in: *Graphic Correlation* (K. O. Mann and H. R. Lane, eds.), *SEPM Sp. Pap*. **53**:177–184.

Macellari, C. E., 1984, Late Cretaceous stratigraphy, sedimentology, and macropaleontology of Seymour Island, Antarctic Peninsula, Unpubl. Ph. D. dissertation, The Ohio State University.

Macellari, C. E., 1986, Late Campanian-Maastrichtian ammonite fauna from Seymour Island (Antarctic Peninsula), *Paleont. Soc. Mem.* **18**:1-55

Palmer, A. R., 1954, The faunas of the Riley Formation in Central Texas, *J. Paleont*. **28**:709-786.

Sadler, P. M., 2000*, Constrained Optimization Approaches to the Paleobiologic Correlation and Seriation Problems: A Users' Guide and Reference Manual to the CONOP Program Family, Version 6.5*, University of California, Riverside.

Sadler P. M. and Kemple, W. G., 1995, Using rapid, multidimensional, graphic correlation to evaluate chronostratigraphic models for the Mid-Ordovician of the Mohawk Valley, New York, in: *Ordovician Odyssey: Short Papers for the Seventh International Symposium on the Ordovician System.* (J. D. Cooper, M. L. Droser and S. C. Finney, eds.), *SEPM Pac. Sect. Book* **77**:257-260.

Shaw, A. B., 1964, Time in Stratigraphy, McGraw-Hill, New York.

Ward, P. D., and W. J. Kennedy, 1993, Maastrichtian ammonites from the Biscay region (France, Spain), *Paleont. Soc. Mem.* **34**:58 p.

Wood, H. E., Chaney R. W., Clark, J., Colbert E. H., Jepsen, G. L., Reeside, J. B., and Stock, C., 1941, Nomenclature and correlation of the North American continental Tertiary, *Geol. Soc. Am. Bull.* **52**:1-48.

Chapter 3

Combining Stratigraphic Sections and Museum Collections to Increase Biostratigraphic Resolution

Application to Lower Cambrian Trilobites from Southern California

MARK WEBSTER, PETER M. SADLER, MARILYN A. KOOSER, and EDWARD FOWLER

MARK WEBSTER, PETER M. SADLER, and MARILYN A. KOOSER • Department of Earth Sciences, University of California, Riverside, California 92521. EDWARD FOWLER • Agua Dulce, California, 91350.

P.J. Harries (ed.), *High-Resolution Approaches in Stratigraphic Paleontology.*

1. QUESTIONS OF PRECISION AND THOROUGHNESS

Range charts are the critical limiting factor for biostratigraphic resolution. High-resolution biostratigraphy requires detailed local range charts that resolve the first and last appearances of numerous fossil species with centimeter precision. Unless the fossil collecting is also extraordinarily thorough, range charts underestimate the full length of taxon ranges and miss rare taxa altogether. High precision involves collecting fossils from thin rock intervals and recording precisely the stratigraphic separation of these intervals. Thoroughness has two components: 1) collecting at many stratigraphic levels; and 2) processing enough rock at each level to find the local highest and lowest occurrences of both the abundant taxa and the rare taxa.

Field projects with realistic deadlines achieve precision more easily than thoroughness, especially in the collection of macrofossils. It may be feasible to excavate clean, continuous exposures and carefully measure the position of each sampled interval. Time will likely be inadequate, however, to examine as much rock as one would wish. Museum collections appear to offer an easy means to increase the thoroughness of a measured section. They often house rich faunas that combine decades of collecting by many individuals. Although museums might not retain all the mediocre specimens of common taxa, their selectivity may be expected to include several kinds of specimen that are important for range charts: rare taxa not seen in all measured sections; individual finds that extend the known taxon range; and fossils from nearly barren rock intervals. Unfortunately, the attractive taxonomic richness in museum collections is likely to be offset by accompanying records that are of variable quality and typically lack detail concerning the precise provenance of the specimens.

This chapter explores options for using rich, but loosely documented, museum collections to test and augment range charts from more precisely measured stratigraphic sections. After reviewing the types of essential information that range charts contain, we categorize museum specimens according to the aspects of this information that they can augment. Then we turn to computer-assisted methods of combining the information from museum collections and measured sections.

At each step, we illustrate the dilemma of precision and thoroughness with the real example of olenelloid trilobites from Lower Cambrian outcrops in two neighboring mountain ranges in the eastern Mojave Desert of southern California (Fig. 1), and from the reference collections of the Geology Museum at the University of California, Riverside (UCR). We

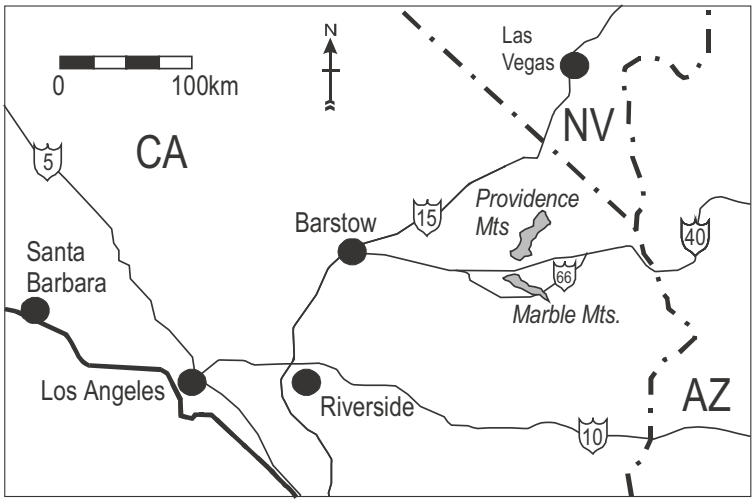

Figure 1. Location of the Marble Mountains and Providence Mountains.

combine the insights of a systematist (M.W.), a stratigrapher (P.M.S.), a museum curator (M.A.K.) and a fossil collector (E.F.), all intimately familiar with these outcrops and collections.

2. THE CRUCIAL CONTENTS OF RANGE CHARTS

Local range charts (e.g., Figs. 2, 3) depict the observed durations of fossil taxa against a scale of stratigraphic distance in a measured section of rock strata. The sequence and spacing of the stratigraphically lowest and highest finds of all taxa are sufficient primary information in the sense that nothing more is required to establish all the ranges; a taxon range connects the lowest and the highest finds. Nevertheless, any suite of ranges contains secondary pattern elements that, while not necessary to construct a range chart from a measured section, may be recognized in museum collections. A good range chart will also include ancillary information from the measured section that has bearing on the reliability of the observed range ends.

The pattern of a suite of ranges reveals the overlap of taxa. This secondary information can be tested and improved by the contents of museum collections, whether or not the museum specimens are accompanied by locality information that is precise enough to insert a specimen directly into the series of faunas from the measured section. In particular, consider whether two taxa can be shown to have coexisted and, if not, which is the younger:

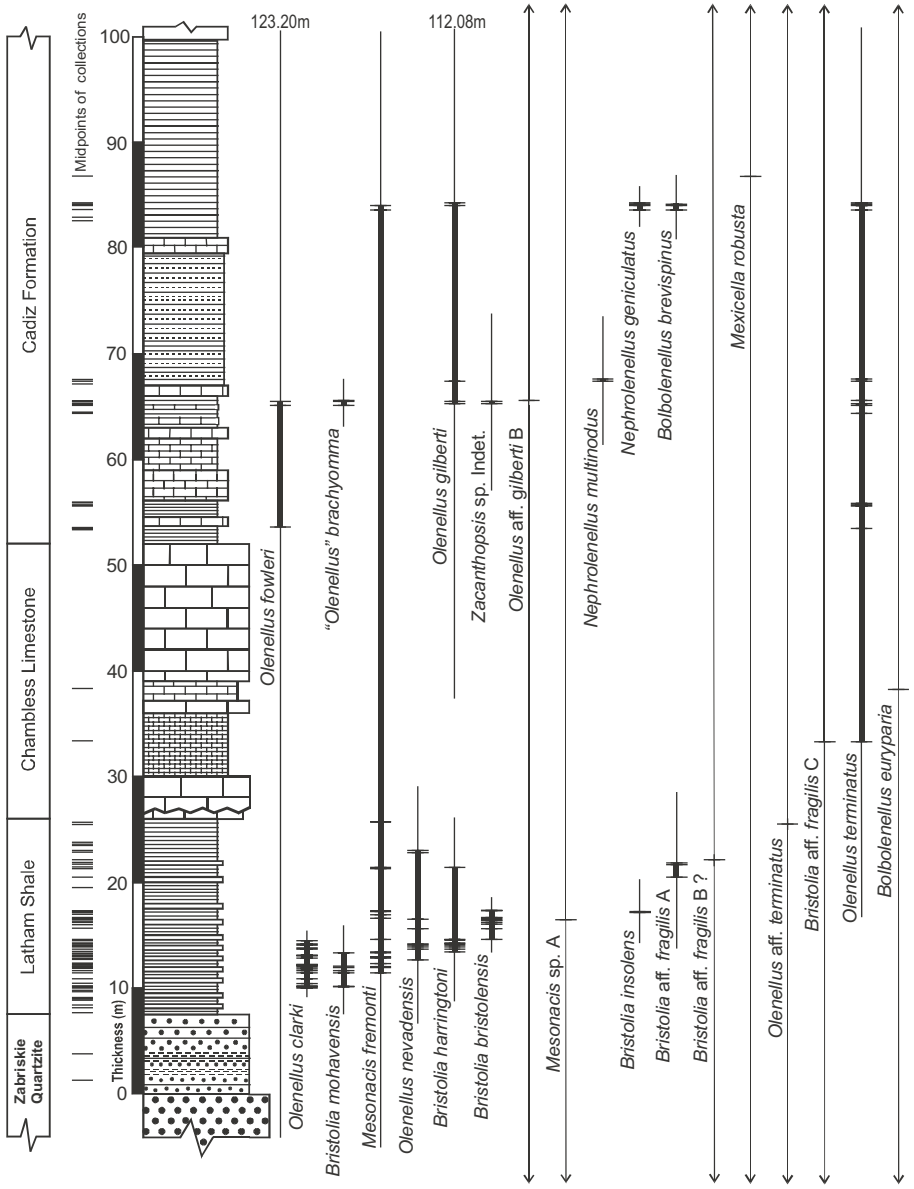

Figure 2. Range chart for trilobite-bearing Lower Cambrian and lowest Middle Cambrian strata of the southernmost Marble Mountains. Collections (second column from left) indicate fossiliferous levels whether or not the materials include identifiable trilobite species. The Latham Shale and Cadiz Formations were examined continuously. Thick vertical lines are observed species ranges drawn through all identifiable finds (horizontal cross bars). Thin vertical lines are 95% confidence intervals based on the number of finds in the range (two parameter case from Strauss and Sadler, 1989, Table 1). Infinite range extensions, which result from a single find, are terminated with arrowheads. Values in meters indicate the position of the ends of long finite extensions that lie beyond the figure.

a) The *overlap* or conjunction (*sensu* Alroy, 1992) of locally observed ranges shows that the taxa coexisted at that location. Because the observation of a co-occurrence is positive evidence and independent of the sampling technique, this information is particularly worth seeking in museum collections. We refer here to physical co-occurrences at the same place, not the mere temporal overlap of ranges. The latter emerges when range charts from separate localities are correlated into one composite range chart. Physical co-occurrence data can be sufficient information to establish a temporal sequence of faunal assemblages (Guex and Davaud, 1984; Guex, 1991, Alroy, 1992). Such data alone do not indicate, however, which end of the sequence is youngest (polarity).
b) The existence and duration of gaps between non-overlapping pairs of ranges (*disjunctions*, *sensu* Alroy, 1992) cannot be proved with complete certainty. They are likely to be exaggerated if the collecting was not thorough. Furthermore, they may be disproved by one isolated collection that demonstrates a co-occurrence.
c) The *polarity* or superposition of two disjunct ranges indicates which taxon of a disjunct pair is the younger. If the ranges are truly disjunct, then two isolated faunas, each containing one of the pair, can be arranged in the correct order. Note that for taxa with overlapping ranges, the evidence of polarity rests in the sequence of their first- and last-appearance events and requires thorough collecting. We refer here to indications of polarity that might be gleaned from isolated finds of two taxa that are not sufficient to identify their range ends.

   Because polarity depends upon the negative evidence of disjunction, however, false polarities may be indicated if collecting has not been thorough. The disjunctions that are least likely to be negated by new finds are those between pairs of abundant taxa that are routinely separated by gaps longer than the combined lengths of their observed ranges. Museum specimens that are merely referred to different lithostratigraphic formations may suffice to prove superpositional relationships for short-lived taxa with disjunct ranges.
d) The *duration* of a taxon range is liable to underestimation. More thorough collection tends to lengthen the known ranges. Because longer ranges generate more overlaps, the duration of ranges will likely be related to the number of co-occurrences (Fig. 4).

Total observed ranges, from the lowest to the highest local find of a taxon, often pass through fossiliferous levels and barren strata. The interval of uncertainty between the highest find and the real range end is potentially as large as, or even larger than, the thickest barren interval within the range.

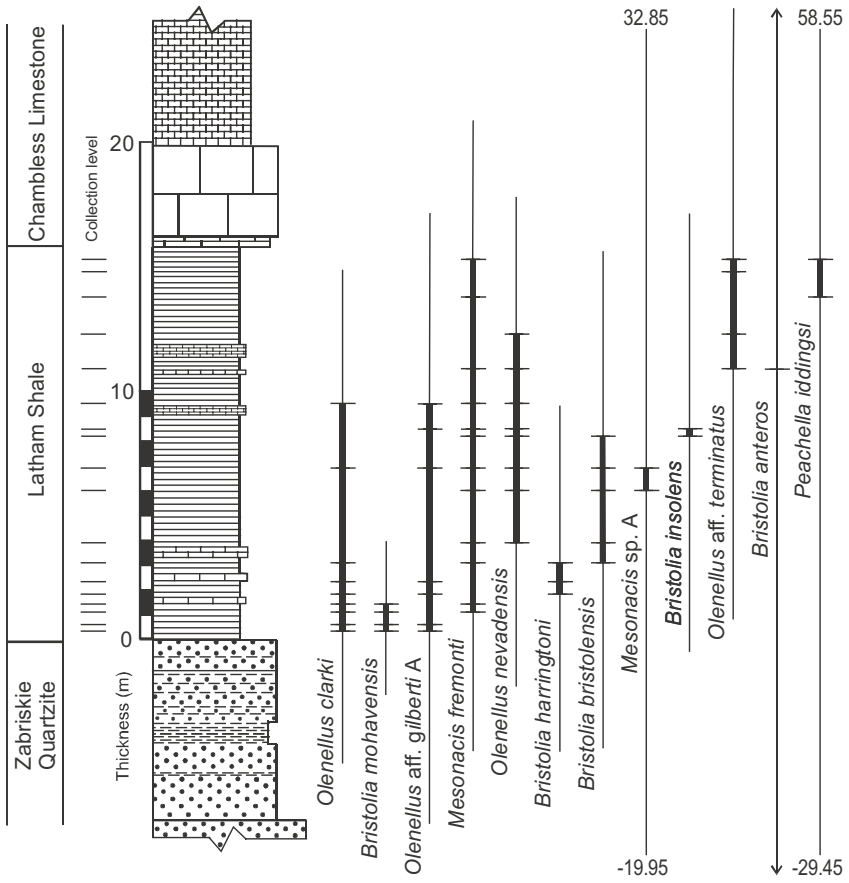

Figure 3. Range chart for olenelloid trilobites in the Latham Shale of the Summit Springs section in the Providence Mountains. Symbols as in Fig. 2. Collection was limited to excavations at the levels shown.

Museum collections have some potential to augment several kinds of information from observed ranges that provide better estimates the reliability of range ends.

a) The number and position of *finds* between the lowest and the highest may be used to place statistical confidence intervals upon the range ends (e.g., Paul, 1982; Strauss and Sadler, 1989; Marshall, 1990, 1994). Even if the formula for a confidence interval requires only the number of finds, the distribution of spaces between the finds will likely need to meet some preconditions. Confidence intervals spanning large stratigraphic distances indicate where collecting might not have been thorough enough (Figs. 2, 3).
b) The stratigraphic position of all samples or *collecting levels* helps distinguish between gaps in a taxon range that result from "not-

looking" and those caused by "not-finding" the taxon. Figure 3 indicates the position of discrete sampling horizons; intervening levels were not searched. Figure 2 is based upon continuous searching in the shales; it indicates every level at which any fossil material was found.

c) Sedimentary *facies changes* indicate levels at which the ends of observed ranges might result from changes in the habitat-related abundance of living individuals. The preservational mode of fossilized individuals, or the difficulty of collecting identifiable fossil specimens (e.g., top of the Latham Shale in Fig. 2).
d) The *abundance* of taxa at each level indicates whether gaps and range ends are associated with intervals of low abundance. Relative abundance in measured sections and museum collections is a guide to the relative thoroughness of the collecting.

2.1 Observed Olenelloid Taxon Ranges

The collecting of Cambrian trilobites from the Marble Mountains began nearly a century ago (Darton, 1907; Clark, 1921; Resser, 1928; Hazzard, 1933; Crickmay, 1933; Mason, 1935; Hazzard and Mason, 1936; Riccio, 1952; Mount, 1974, 1976). The thoroughness with which these macrofossils can be collected varies with sedimentary facies. The following brief review of the mode of occurrence and our collecting strategies will provide essential preliminary insights into the distribution of gaps and fossiliferous horizons in the range charts (Figs. 2, 3).

The richest olenelloid faunas are preserved in the Latham Shale, a formation named by Hazzard (1954) for a topographically recessive unit of approximately 15 m of fine-grained, gray-green shale that is often obscured by large, fallen blocks of the overlying cliff-forming limestone. We prepared clean, continuous exposures by digging trenches between the fallen blocks. The individual trenches do not span the entire thickness of the Latham Shale; overlapping trenches were combined into a complete section by tracing thin marker beds of cross-laminated sandstone and limestone. In fewer than 12 months, natural movement of the shale talus significantly refills the trenches, reducing them to subtle swales. Detailed trench locality maps and logs are kept with our collections at the UCR Geology Museum. Most of the Latham Shale yields disarticulated trilobite remains. At rare horizons, however, the majority of specimens are partly articulated.

Lithologically indistinguishable Latham Shale crops out in the nearby Providence Mountains where one of us (E.F.) collected systematically in 1994. The UCR museum houses collections from both localities. The measured section from the Providence Mountains (Fig. 3) tests and amplifies

our attempt to add museum collections to the measured section from the Marble Mountains. Although collecting strategies in both mountain ranges processed unprecedented volumes of Latham Shale, they emphasize different aspects of thoroughness. Collecting in the long trenches in the Marble Mountains strove for stratigraphic continuity, trying to examine every parting; it generated relatively small, closely spaced faunas. In the Providence Mountains, the collecting effort concentrated upon large volumes of rock at discrete levels approximately 1 m apart. Sampled horizons in the Providence Mountains have produced 9 to 110 identifiable specimens each at 18 levels (chosen in advance), as contrasted with 1 to 41 identifiable specimens each at 54 levels (determined by the position of finds) from trenches in the Latham Shale of the Marble Mountains.

The Latham Shale overlies coarse, cross-bedded, trace-fossil-bearing quartz arenites of the Zabriskie Quartzite (Hazzard 1937) via a thin transitional interval of interbedded sandstones and shales that we interpret as a record of increasing depth of deposition. Although trilobites have not been recovered from the Zabriskie Quartzite, the olenelloids were likely extant at this locality before the quartz sands were deposited. Siltstones and quartz arenites of the underlying Wood Canyon Formation (Nolan, 1929) preserve rare *Cruziana* traces and have yielded a single poorly preserved specimen that Mount (1976) referred to the genus *Olenellus*.

Above the Latham Shale lies the distinctive, cliff-forming, oncolitic Chambless Limestone (Hazzard, 1954). The transition does not record a simple upward shallowing from the shale to the top of the limestone, as might be expected for a classic shale-limestone cyclothem. Rather, the shallowest conditions occur at the base of the oncolitic facies. The close of Latham Shale accumulation was marked by the deposition of less than 1 m of non-oncolitic, coarse, cross-bedded, bioclastic packstones which we interpret to have been deposited at a time of rapid shallowing. The upper surface of the cross-bedded packstone unit is a microkarstic erosion surface with up to 10 cm of steep castellated relief that records the maximum exposure. Subsequent drowning of this surface abruptly introduced coarse packstones, which are dominated by large, exquisitely detailed oncoliths and were once quarried from the Marble Mountains as an ornamental building stone. Smaller, less-well-preserved oncoliths, occur in the wackestones and mudstones that dominate most of the succeeding Chambless Limestone.

Both fresh and weathered surfaces of the Chambless Limestone reveal numerous disarticulated trilobite fragments in cross section. For most of these limestones, however, we have found no way to crack the rocks that separates the surfaces of the trilobite fragments from the matrix to reveal diagnostic features. Identifiable specimens have been recovered only from two non-oncolitic intervals in the Chambless Limestone. Both occur in the

lower half of the formation -- an interval of silty, calcareous, minimally fissile mudstones and a black oncolith-free interval of rubbly-weathering, dark, micritic, platy wackestones (Fig. 2). The former is well exposed only after rock-falls and yields sparse trilobite impressions when split. The latter reveals a few identifiable trilobites on weathered surfaces and the matrix breaks away from others when the mudstones are hammered perpendicular to bedding.

Recoverable olenelloids become more abundant again in the overlying Cadiz Formation (Hazzard and Mason, 1936), a heterogeneous succession of micaceous shales, siltstones and sandstones with subordinate limestone beds. The upward transition from the Chambless Limestone occupies several meters of irregular and nodular beds of calcareous mudstones and wackestones, intercalated with siliciclastic mudstones. The trilobite-bearing shales of the Cadiz Formation are generally coarser and more micaceous than the Latham Shale. They likely represent shallower marine deposits. The Middle Cambrian portion of the Cadiz Formation begins near the top of our range chart (Fig. 2), with the appearance of *Mexicella robusta*. It includes distinctive oolitic limestone beds and brightly colored red, green and purple shales.

Our range chart for the Latham Shale and lower Cadiz Formation (Fig. 2) is the product of two years collecting through continuous artificial exposures in a suite of trenches dug into the shales. Near the surface, the shales disintegrate to splintery fragments, smaller than many of the trilobite cephala. Our shallow excavations reached down to intact material that was split and searched layer by layer. Limestone and sandstone facies have been examined in natural outcrops between the trenches.

The trenching and bed-by-bed searching that led to Figure 2 are far more stratigraphically continuous and precise than any previous collecting in these formations. They have produced at least eight trilobite species from the Cadiz Formation and high in the Latham Shale that are not found in previous collections from the same area, now housed in the UCR Geology Museum. Nevertheless, the museum collections, which represent 55 years of relatively unsystematic collecting by many individuals, contain four species that we had not yet found in the trenches -- *Peachella iddingsi*, *Olenellus* aff. *gilberti* A and *Bristolia anteros* from the Latham Shale, as well as *O. puertoblancoensis* from the Chambless Limestone. It is these “missing” species that we particularly wish to incorporate into the range chart for the Marble Mountains.

The differences between our new collections and the museum holdings have quite straightforward origins. Material from a few pits in the Latham Shale, which are continually enlarged by amateur collectors and geology classes, dominate the museum collections. Our trenches tap into intervals

that are otherwise generally inaccessible. But the trenches typically excavate a swath less than 1 m wide; at no level does the volume of material we processed compare with that taken from corresponding intervals in the pits. Near the top of the Latham Shale, we had a single trench with relatively few fossiliferous levels. (The postscript summarizes results from an overlapping trench opened while this chapter was in review.) The less fossiliferous Cadiz Formation has attracted few casual collectors, especially in its Lower Cambrian portion. Museums hold correspondingly few Lower Cambrian fossils from the Cadiz Formation and our trenching there qualifies as the most successful collecting to date.

2.2 Internal Evidence of Shortfall in the Observed Taxon Ranges

Three lines of evidence indicate that some observed taxon ranges in the measured section from the Marble Mountains potentially fall short of the true local ranges; 1) the length of ranges relative to the nearby Providence Mountains section for the same stratigraphic interval; 2) the number of observed co-occurrences relative to the number of overlapping ranges; and 3) the size of gaps within the observed ranges. All three justify the appeal to museum collections to fill gaps in the coverage of the measured section.

Comparison of the two measured sections for the Latham Shale immediately reveals some shortcomings of thoroughness in collecting from the Marble Mountains. The relatively large volumes of rock processed at the fossiliferous levels in the Providence Mountains have yielded three species not yet found in the trenches in the Marble Mountains. *Bristolia anteros* and *Peachella iddingsi* are rare and probably short-ranged species. *Olenellus* aff. *gilberti* A is a long-ranged but even rarer species whose presence is recorded by only one individual in most samples. It would be possible to argue that the "missing" species reflect real discontinuities in the original geographic ranges, were it not for the fact that all three occur in the UCR museum collections from the Marble Mountains. This permits us to use the Providence Mountains to test the methods of incorporating museum collections into the measured section. Also, the trenches did yield one questionable specimen of *O.* aff. *gilberti* A.

Although greater ambiguity arises concerning differences in the lengths of ranges in the two sections, the much longer range for *Olenellus clarki* in the Providence Mountains is clearly also based upon recovering rare individuals. The species is 3 to 30 times more abundant in the lowest one-third of its range in the Providence Mountains than in the upper two-thirds. The length, position, and richness of co-occurring taxa for the lowest one-third seems to match the total observed range for the taxon in the trenches at

the Marble Mountains. It is reasonable to surmise that something resembling the sparsely populated upper two-thirds of the range also occurs in the Marble Mountains but was missed by the trenching strategy (see postscript). The pattern of abundance in some other taxon ranges supports this interpretation.

In spite of the disadvantages of sample size, the trenches in the Marble Mountains have yielded a single specimen of *Bristolia harringtoni* much higher in the Latham Shale than the apparent top of its range in the Providence Mountains. The ranges observed by continuous sampling in the Marble Mountains reveal a pattern of lower occurrence rates toward the top of observed ranges for *B. harringtoni*, *Olenellus nevadensis*, and *Mesonacis fremonti*. This is more than an artifact of sample spacing. It is reflected in failed co-occurrences -- within the gaps in these ranges are levels that yield other taxa. The sample spacing in the Providence Mountains is less likely to reveal such traits. Evidently, collections based upon large samples can usefully be incorporated into measured sections with relatively continuous sampling but smaller samples.

The observed taxon ranges in the measured sections fulfill the simple prediction that the number of overlapping ranges will increase with the length of the observed range (Fig. 4). Zero range length in Figure 4 means that the taxon was found at only one level. Any reasonable regression through the number of overlapping ranges intercepts zero range length at 3 to 5 overlaps because there are three to five long-ranging taxa at every level and even the shortest-ranged taxa must overlap with them. The large open symbols in Figure 4, which support such regressions, describe the properties of whole observed ranges as drawn through gaps in the ranges. The asterisks plot the significantly smaller numbers of overlapping ranges that can be shown by actual co-occurrences of fossil taxa at the individual collection levels. Most collection intervals have not yet yielded all the taxa that are known to range through them. Because the higher recovery rates are all from the Providence Mountains, we reasonably conclude that the pattern is an artifact of gaps caused by sample size, and does not record the genuinely patchy distribution of living taxa at the scale of tens of kilometers (see postscript for evidence of patchiness at the scale of hundreds of meters).

The gaps within a taxon range result from the same types of failures in fossil preservation and collection that explain the shortfall between the observed range and true range ends. Accordingly, the size distribution of these gaps have been used to construct 95% confidence intervals for the position of true range ends in Figures 2 and 3. The intervals are based on the average length of gaps within the observed range, using the formulae provided by Strauss and Sadler (1989). The total length of the observed

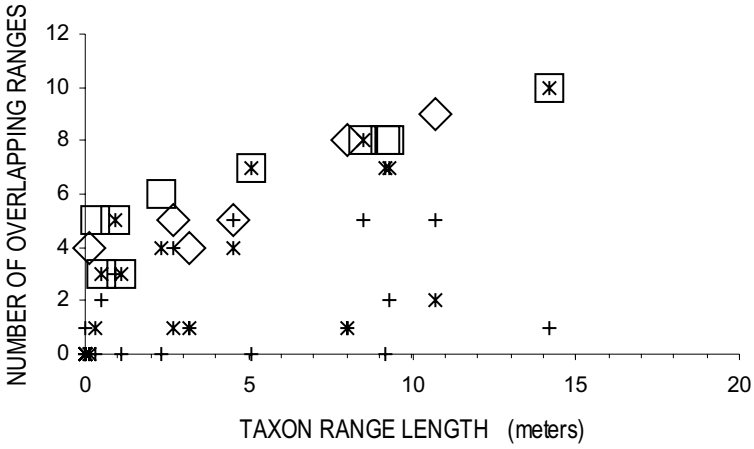

Figure 4. Number of overlapping ranges as a function of range length in the measured sections of Latham Shale in the Marble Mountains (diamonds) and the Providence Mountains (squares). The number of overlaps are underestimated by the actual co-occurrences at single levels in the measured sections (asterisks) and on slab-samples in the museum collections (crosses). Asterisks and crosses combine information from both localities.

range and the number of levels at which the taxon is found determine the average gap length; they are therefore the critical variables for length of the confidence intervals. Ranges based on a single find, for example, lead to infinitely long confidence intervals because they contain no information about average gap length.

As the number of finds increases, the confidence intervals shorten relative to the observed range length. For a range based on fewer than six finds, the combined length of the upper and lower confidence intervals exceeds the length of the observed range. For most taxa, the 95% confidence extensions on the observed ranges in the Marble Mountains are longer than the distance to the next closest range end (Fig. 2). *Olenellus clarki* appears to be an exception; but our previous comparison with the Providence Mountains indicates how badly misleading the confidence intervals become when critical assumptions are not satisfied.

The confidence intervals assume that the likelihood of finding a taxon is uniform within its range. As judged by the abrupt change in its abundance in the Providence Mountains, *O. clarki* violates this assumption. The tight confidence intervals on the range ends of *O. clarki* in the Marble Mountains result from many fossiliferous horizons which, as discussed above, may be restricted to the lowest one-third of the true range. Marshall (1994) explained how to relax the assumption that finds are equally likely at all

levels. His method depends upon approximating the tails of the real frequency distribution of gap sizes and assumes that gap size is not correlated with position in the range. Again, *O. clarki* violates the crucial assumption; significantly larger gaps characterize the upper two thirds of the range.

For the Latham Shale, comparison with independent collections allows the reliability of range ends to be assessed without making severe assumptions about randomness or estimating statistical parameters from the frequency distributions for the gaps in the observed range. The local shortfalls in range ends lead to contradictions between different sections. Resolving the differences compensates directly for shortfall. Rather than attempting to place a confidence interval on each local range, we seek the highest of the local last appearances and the lowest of the first appearances. We will show how museum holdings allow this strategy to be pursued further than measured sections alone would permit. As preparation, let us review the nature of museum holdings.

3. THE DOCUMENTATION AVAILABLE FOR MUSEUM COLLECTIONS

Museum collections consist of the specimens themselves, plus supporting documents concerning their taxonomic assignment, collecting locality, and other information related to their acquisition. The specimens can be re-examined and their taxonomy updated, if necessary. The geographic and stratigraphic descriptions of the collection locality cause far more difficulties than the original taxonomic identifications, because they can so rarely be improved.

Supporting documents do not often supply the precision that is needed to place a museum fauna into a more recently measured section. In a more likely best-case situation, the museum houses a series of faunas which are precisely stratigraphically located in an accompanying description of a different measured section. Computer algorithms can generate a composite of two or more sections, even if their individual sampled intervals cannot be manually interleaved into one section. Different problems arise where the documents describe a more restricted collection interval (a small excavation or a very short measured section), but leave the stratigraphic position lamentably loosely identified. Not all compositing algorithms can make good use of a “section” with only one collection level. In the worst instances, one locality number covers a blend of isolated material that was picked up across a wide stratigraphic interval. This creates a false impression of co-occurrences. Strong incentives to work with such

imprecisely documented parts of museum collections arise from the fact that they are numerous and may involve large and diverse faunas that include the rare taxa we wish to add to the range charts.

In order to examine the potential uses for faunas from the whole array of situations presented by museum documents, we must first distinguish geographic and stratigraphic aspects of precision. Geographic precision varies from coarse identifiers such as a county, a mountain range, or a nearby town, to precise map coordinates or marked maps and photographs. For the present purposes we consider only those museum materials that can be confidently placed within one kilometer of our measured section at the southernmost edge of the Marble Mountains.

Stratigraphic resolution entails questions of interval and position. The first question asks simply: how thick was the sampled interval? It is useful to distinguish four levels of decreasing resolution in the thickness of the sampled interval.

a) A single bedding *surface*, interpreted with care, might provide reasonable indications of contemporaneous co-occurring individuals. Many shell pavements, however, almost certainly "time-average" (Walker and Bambach, 1971) individuals from a living community over a time interval longer than one generation. A few simple shell pavements occur within the Latham Shale. We accept their contents as evidence of co-occurring taxa, but not necessarily co-occurring individuals.
b) A single depositional *bed*, properly interpreted, might reveal coexisting taxa for biostratigraphic purposes. For example, particular care is needed to tease apart the depositional history of shell beds (Kidwell, 1991) because they may contain significant condensation, mixing and hiatus surfaces. Turbidites exemplify short-lived deposits that can mix indigenous and transported trilobites (e.g., Babcock, 1994a,b). The Latham Shale, however, contains neither shell beds nor coarse turbidites capable of reworking fragments of trilobite large enough for olenelloid species to be identified.
c) A measured *interval* that encompasses many beds is unlikely to be useful unless the information concerning position allows it to be associated confidently with a single sample in the measured section or positioned within a barren portion between samples.
d) A wide collecting *area* and collections that include loose material from talus (or "float") serve only to fill out faunal lists for whole formations and members.

The question about position asks: can the sampled interval be positioned relative to unambiguous lithostratigraphic coordinates that are recognizable

in the measured section? Consider three possibilities:

a) Measured distances above or below a lithostratigraphic boundary may serve to place collections in stratigraphic order. But we note that some measurements made by different collectors or on different dates can be incompatible. In extreme cases, we have found reported distances above the base of a stratigraphic unit that exceed our estimates of the total thickness of that unit. Ranges of distances reported for two collections may overlap, leaving relative age unresolved.
b) An assignment that only identifies the lithostratigraphic unit provides enough information to position the faunal list relative to those from underlying and overlying formations. The range chart for the Marble Mountains spans three lithologically distinct fossiliferous formations.
c) A distinctive lithology may allow a museum specimen to be examined and assigned to a particular bed or member, in spite of less informative documentation. For example, the UCR collection contains *Olenellus puertoblancoensis* within a distinctive minimally fissile calcareous shale facies that is known only from one interval, low in the Chambless Limestone of the southern Marble Mountains.

Considering all of the preceding discussion, the following (italicized) categories of useful types of museum materials emerge. In the definitions, "specimens" are individual fossils. *Slab samples* present one or more rock surfaces that preserve specimens of two or more taxa on the same surface and (absent reworking) demonstrate their coexistence for biostratigraphic purposes. *Spot collections* consist of all the specimens from a single stratigraphic interval that is at least as finely resolved as those in the measured section. The necessary resolution for this category therefore varies from project to project. *Blended collections* mix all the materials from a wider interval, possibly including loose surficial "float," and assign them all to one formation and location number. Within the blended-collections and spot-collections there may be slab-samples.

Collection series are suites of any of the previous categories that can be placed confidently in correct stratigraphic order. The best examples would be a series of spot-collections whose spacing is recorded in descriptions of a previous measured section. Some useful information may be extracted from much looser series, such as a suite of blended-collections, one from each of the successive stratigraphic formations, especially if they contain rare taxa not recovered from the measured section. For all the taxa contained in the faunal list for one unit, the sequence of first and last occurrences remains unknown. Nonetheless, a subset of taxa from the whole suite of blended-collections, one taxon for each lithostratigraphic unit, may be placed in true

stratigraphic order to build a *pseudosection* that summarizes the reliable information about sequence.

A pseudosection retains the sequence properties of a real stratigraphic section, but not the true interval spacing. The samples in a pseudosection are not necessarily from one single line of collections but they do still share geographic proximity. Where the unit thicknesses are known, it is possible to give the pseudosection some vertical scaling by placing faunas at the midpoints of their respective units -- this ploy increases the range of numerical methods that can be used to combine the pseudosections with real measured sections. Collection series that are built from the documentation of real museum holdings usually contain a mixture of spot collections and slab samples, in addition to blended collections. For them, the pseudosections gain significant detail because an ordered series of taxa or coexisting sets of taxa may be incorporated for a single stratigraphic unit.

The number of taxa in a single pseudosection is most severely limited by the constraint that it must not imply any unproven coexistences. Although each pseudosection contains few taxa relative to a real measured section, many different subsets of taxa may be extracted from one collection-series to build several pseudosections. The purpose is to combine all the rare taxa with others that are better represented in the measured sections.

With slab samples and spot collections from museums to demonstrate the coexistences and pseudosections to provide sequence information, it is possible to insert missing taxa into measured sections and to adjust the ranges of under-represented taxa. Of course, the insertion and adjustment process should apply the minimum changes necessary to bring the measured section into agreement with information gleaned from the museum collections. It should also provide rigorous quantification of the precision or confidence levels for the results. Automated numerical methods achieve these goals and allow large sets of data to be combined. Before turning to the numerical methods, however, it is worthwhile to question whether any information may be gleaned from the relative frequency of slabs that preserve different pairs of taxa. Are the most frequently encountered pairs those with the stratigraphically longest overlap between their ranges?

3.1 The Frequency Distribution of Slab-Samples

In UCR collections from the Latham Shale, some of the shale “slabs” that preserve identifiable parts of two different taxa are only a few square centimeters in area. In the field, the size of shale pieces appears to be determined primarily by depth of excavation below the weathered surface, rather than any stratigraphically distributed differences in shale lithology.

Accordingly, the frequency of different taxon pairs in slab-samples should relate to the patterns of overlap in the range chart, not variations in preservation. We compared the frequency of slab-samples in the museum collection with the range chart drawn independently from the measured section alone.

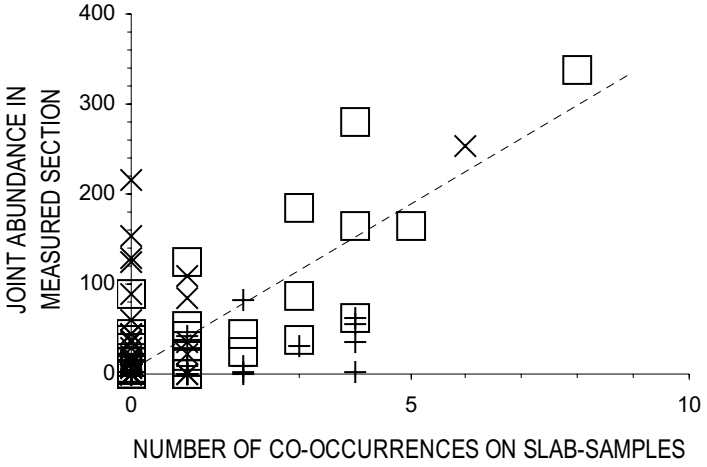

Figure 5. The frequency of coexisting taxon pairs, as proved by slab-samples from the Latham Shale in the Marble and Providence Mountains. Open squares and regression line: both localities. The regression has a correlation coefficient of 0.73. Crosses; values from the Marble Mountains only. X's: values from the Providence Mountains only.

Only one convincing empirical correlation emerges. It is the logical one between the frequency of museum slabs and the joint abundance of the two taxa at those levels in the section where both occur (Fig. 5); i.e., the product of the length of overlap of the two ranges and the average combined abundance of the two taxa at horizons in the overlap interval. Correlation coefficients are very weak between the frequency of museum slab-samples and all the simpler attributes of the range charts: the stratigraphic thickness of the interval in which the two taxon ranges overlap; the number of collection levels in the section that contain both taxa; and the abundance of the two taxa as estimated from their entire range (not just the interval of overlap). Therefore, museum slab samples alone do not provide a direct, reliable guide to the length of the overlap interval between taxon ranges. They need an independent measure of joint abundance in that interval. Spot collections would provide this measure and thereby the promise of reconstructing more of the pattern of ranges from isolated samples. Unfortunately, there are not enough spot collections in the UCR museum

holdings to permit reliable estimates of joint abundance of overlapping taxa.

Note that the relationship in Figure 5 weakens dramatically when the two Latham Shale localities are considered separately. For the Providence Mountains alone, there appear to be too few slab samples in the museum collections. For the Marble Mountains alone, there is a richer set of slab samples but, perhaps, some range lengths are underestimated in the measured sections and would benefit from augmentation by the museum collections. Which ranges should be adjusted and by how much? The most parsimonious solution would be the minimum set of range extensions necessary to satisfy all the additional coexistences demonstrated by museum slabs and observed in the Providence Mountains. Computer algorithms can find such solutions.

4. COMBINING INFORMATION

Museum collections provide two types of information that deserve to be combined with measured sections: 1) coexistences, as indicated by slab samples and spot collections; and 2) superposition, as indicated by partial sections and pseudosections reconstructed from collection-series. Two conceptually different tasks are involved: seriation and time correlation. Seriation places isolated samples into chronological order; e.g., ordering a suite of slabs. Time correlation matches levels of the same age between the parts of two or more sections or series that span the same time interval; e.g., combining the two range charts for the Latham Shale, one from the Marble Mountains and one from the Providence Mountains. Many practical problems are a combination of stratigraphic correlation and seriation in the sense that some pairs of the fragmentary sections do not overlap with one another; e.g., combining measured sections, partial sections, pseudosections, and spot collections. Pure seriation problems lack polarity -- seriation routines alone cannot determine which end of the series is younger. Adding a correlative section or pseudosection provides polarity. For both stratigraphic correlation and seriation there exist numerical methods that provide a reproducible objective basis and a means to automate the treatment of large data sets.

4.1 Seriating Isolated Slabs and Spot-Collections

Guex (1991), Guex and Davaud (1984), and Alroy (1992) have described numerical methods that seriate isolated faunas. Guex treated small data sets by manipulating the rows and columns in a coexistence matrix (Fig. 6). Because every taxon is assigned one row and one column, any pair of

taxa corresponds to two cells in the matrix that may be marked to indicate whether the two taxa coexist. Black and gray cells in Figure 6 tabulate coexistences proven by museum slab samples from the Marble Mountains. Of course, cells along the major diagonal of the matrix compare each taxon with itself; each half of the matrix on either side of this diagonal duplicates the information in the other half. For large data sets, Guex analyzed a coexistence map according to graph theory. Figure 7 illustrates the simple map that corresponds with the data in the matrix in Figure 6. For a full account of the graph theory, the reader is referred to Guex (1991). We will briefly describe his use of the coexistence matrix.

For the initial coexistence matrix, any sequence of taxa may be selected for the row labels; the columns must always be labeled in the same sequence as the rows. Subsequently the rows and columns in the matrix are rearranged so that cells which correspond to coexisting taxa become concentrated close to the diagonal of the matrix. The logic behind algorithms that can rearrange the matrix need not concern us here. It is sufficient to imagine a manual trial-and-error process. Figure 6 shows one possible solution for slab samples from the Marble Mountains. Some other arrangements are equally good. Notice, for example, that the first four row and column labels may be placed in any internal order without compromising the concentration of coexistences along the diagonal. Neither would it matter if they were moved, as a group, to the opposite end of the sequence. The slab samples tell us only that all four taxa coexist with one another and with no other taxa in the list.

Ideally, when the rearrangement is complete, no disjunct pairs (white cells in Figure 6) should remain embedded within the diagonal zone of dark cells that record coexistences. These embedded white cells are coexistences that are implied to exist but have not been observed. In analogous fashion, the ranges of two taxa may overlap when a range chart is drawn through all finds, even though the two taxa were never observed at the same level. If the slab-samples and the coexistence matrix drawn from them include no evidence of relative age or stratigraphic superposition, then the most parsimonious sequence must merely minimize the number of embedded white cells.

Once a parsimonious diagonal arrangement is achieved, each partial-row in the right-hand half of the symmetrical matrix (black cell rows in Figure 6) corresponds to a mutually coexistent set of taxa. Not every row is a biostratigraphically useful assemblage. We have already noted, for example, that the top four rows may be placed in any order and still represent the same single assemblage. Thus, the second, third, and fourth rows are merely subsets of the assemblage in the first row and do not represent “maximal

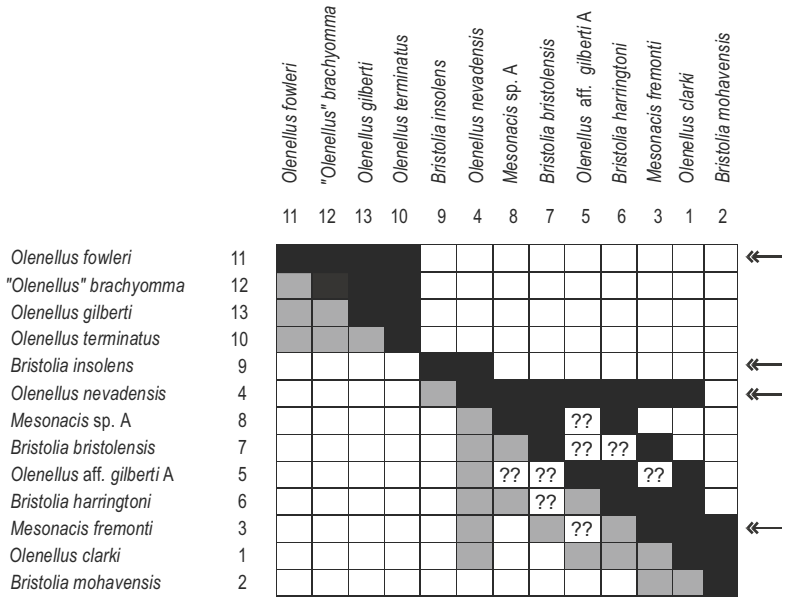

Figure 6. Coexistence matrix for olenelloid species on slab-samples and in spot-collections from the Marble Mountains in the UCR museum. Taxon numbers as in Figure 7 and Table 1. Black cells and gray cells indicate observed coexistences. The order of the rows and columns has been permuted according to the results of one 20-step reciprocal averaging run that led to the scores in Table 1. Question marks in embedded white cells indicate unsampled coexistences. Arrows locate biostratigraphically useful assemblages ("maximal unitary associations" of Guex, 1991). The gray cells lie in the redundant half of the matrix that is to be ignored when reading the assemblages by row. During the permutation process, however, cells may switch from the one half of the matrix to the other, and both cells need to be marked for each known coexistence of two different taxa.

unitary associations" (Guex, 1991). The Guex method eliminates all partial rows that contain only a subset of the coexistences in the half rows above, to leave a series of "unitary associations" that effectively provide a suite of assemblage zones in stratigraphic order.

For the Marble Mountains matrix in Figure 6, four assemblages remain: (10,11,12,13), (9,4), (4,8,7,5,6,3,1), and (3,1,2) in order from youngest to oldest. The matrix alone does not establish the polarity of the series. We chose Figure 6 rather than some other equally parsimonious arrangements by applying two additional pieces of information. The first is legitimately derived from the museum collections; museum labels indicate that taxa 10 to 13 occur in spot-collections from the Cadiz Formation whereas the coexistences for taxa 1 to 9 are established by slabs from the older Latham Shale.

Manipulation of the matrix soon shows that taxon 9 is best placed before

or after taxa 1 to 8, because the slab samples prove only a single coexistence involving this taxon and the other eight from the Latham Shale. Similarly, taxa 9 and 2 are best placed at opposite ends of the Latham Shale group, because they share no coexistent taxa. But the museum information is inadequate to choose between the two options. Figure 6 also used the information that in measured sections taxon 9 has been found only in the upper half of the Latham Shale.

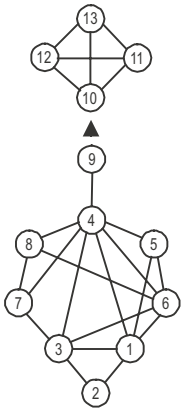

Figure 7. The matrix from Figure 6 recast as a semi-oriented coexistence graph in the sense of Guex (1991). Circled numbers at the vertices correspond to the taxa in Table 1 and Figure 6. Tie lines that connect vertices are edges that indicate observed coexistences in slab-samples and spot collections from the Marble Mountains. The arrow indicates stratigraphic superposition of four taxa from spot-collections in the Cadiz Formation (10-13) above nine taxa from slab samples in the Latham Shales (1-9). The arrow does not physically link vertices 9 and 10 because the corresponding taxa were not observed to coexist. The graph does not, therefore, indicate which taxa in the two clusters should be closest. The clusters are free to rotate relative to one another.

One semi-directional coexistence graph (Fig. 7) combines all the coexistence and superposition information from UCR's museum slabs and spot collections from the Marble Mountains. Figure 6 is one of several equally parsimonious permutations of the coexistence matrix. All include some embedded white cells that suggest unsampled coexistences. The coexistence graph in Figure 7 is more informative because it captures all the potential coexistence anomalies in one diagram. Any subset of four vertices, for example, with the property that they can be arranged into a quadrilateral that lacks diagonal connections, represents an impossible combination of coexistences for a range chart (Guex, 1991). Either the missing diagonals represent a real coexistence that has been missed (very likely in our slab samples), or a pair of the quadrilateral edges are false coexistences, resulting from reworking or misidentification.

The quadrilateral formed by the taxa 6, 3, 8, and 7 is a good example. It is missing both diagonals. A trivial exercise confirms that no reasonable range chart can be drawn to reproduce this situation. Imagine any arbitrary range chart in which taxa 8 and 3 do not overlap with one another. Then add a range for taxon 6 that overlaps with both taxa 8 and 3; it must span the gap between them. Now it is clearly impossible to draw an uninterrupted range for taxon 7 such that it overlaps with taxa 3 and 8, but not taxon 6. Compare the matrix representation in Figure 6. Notice that the missing diagonal coexistence 6-7 corresponds to an embedded white cell. The 3-8 cell interrupts a row, but is not fully embedded in this matrix; alternative, equally parsimonious permutations do embed the 3-8 cell. Thus, Figures 6 and 7 demonstrate that the slab samples and spot collections do not represent all the real coexistences. The diagrams do not, however, indicate unambiguously which coexistences are really missing.

Guex's (1991) book provides an excellent account of the different combinations of coexistence and superposition relationships, together with the parts of graph theory used to solve large instances of the seriation problem. For the handful of slab samples in the Latham Shale, the full Guex programs are not necessary. Alroy (1992) describes a simple iterative "reciprocal-averaging" method that solves the matrix permutation part of the problem numerically. Alroy's formulae are easily implemented on a spreadsheet. They generate numerical scores for each row that range from one to zero. After enough iterations, the scores converge on stable values that indicate a parsimonious order for the rows and columns of taxa.

Table 1 presents a typical set of results of reciprocal averaging that emerge, after 20 iterations, for the museum collections from the Latham Shale and the Cadiz Formation. The scores stabilize to four or more decimal places, but tend to converge on only two values; in the particular run summarized in Table 1, these values are exactly 0.0 for all the Cadiz taxa and approach 1.0 for the Latham taxa. Some runs stabilize with the scores for the Cadiz taxa at 1.0, because no polarity information is included. Because the calculations are very fast, it was a simple matter to wait for a solution that honored the polarity information used in Figures 6 and 7.

The tabulated scores for the Cadiz taxa indicate no preferred order, as is fitting for taxa all found in the same spot-collections. The numerical differences between the Latham taxa are vanishingly small and vary from run to run. No confident sequencing of these events is possible, except to note that *Bristolia mohavensis* and *B. insolens* likely appear towards the opposite ends of the sequence of Latham Shale taxa. As already noted, no evidence of the correct polarity within the Latham sequence has been found in the museum collections.

Table 1. One set of the typical results after 20 iterations of reciprocal averaging scores for olenelloid taxa in slab samples from the Marble Mountains (taxa numbered as in Figs. 6, 7)

TAXON NAME	TAXON NUMBER	RESCALED RECIPROCAL AVERAGE SCORE
Olenellus fowleri	11	0.00000
"Olenellus" brachyomma	12	0.00000
Olenellus gilberti	13	0.00000
Olenellus terminatus	10	0.00000
Bristolia insolens	9	0.99993
Olenellus nevadensis	4	0.99997
Mesonacis sp. A	8	0.99997
Bristolia bristolensis	7	0.99997
Olenellus aff. *gilberti* A	5	0.99998
Bristolia harringtoni	6	0.99998
Mesonacis fremonti	3	0.99998
Olenellus clarki	1	0.99999
Bristolia mohavensis	2	1.00000

Alroy (1992) does not extract assemblage zones from the optimized coexistence matrix. Where longer time spans and greater faunal diversity lead to numerical scores that are better differentiated than in our rather trivial example, he proceeds to use the individual taxon scores to rank the real faunal lists and from them generate range charts which predict the sequence of first and last occurrences. In other data sets, therefore, the process may have considerable potential for generating pseudosections from isolated spot collections.

Unfortunately, reciprocal averaging achieves little more for the museum collections in the Marble Mountains problem than to confirm the formation-level faunal lists and indicate that the slab samples fail to capture all the coexistences. It does not enable us to build detailed pseudosections. Two factors that frustrate our attempt might not arise in other instances: 1) the separations of olenelloid first and last events are small compared with the lengths of the taxon ranges; and 2) there are too few spot collections that might provide more complete lists of conjunct ranges and constrain the number of range charts that can be built from a parsimonious co-occurrence matrix. Notice that the Marble Mountains reveal a general potential weakness of this use of slab samples and seriation; the Cadiz and Latham taxa are preserved in different sedimentary facies. If a section exposes an alternation of two facies that preserve different taxa, then there will be pairs of taxa, one from each facies, which cannot be found on slab samples whether or not their ranges overlap.

We could eliminate these frustrations by incorporating all the spot collections from the trenches. But reliance upon coexistence is then very conservative. Both the Guex (1991) and Alroy (1992) approaches to seriation would tend to waste some of the precise information about

sequence that is contained in the measured section. This information is better exploited by numerical *correlation* methods that can incorporate the isolated samples together with measured sections.

4.2 Correlating Museum Collections and Pseudosections

Correlation uses locally observed sequences of first and last appearance events as the primary information. The individual local sequences are provided by different stratigraphic sections. It is usually evident that they cannot all be entirely reliable indicators of the global sequence of events because they contradict one another in detail concerning the sequence of some of the first and last appearances. Good correlation algorithms resolve the contradictions to generate a more reliable composite sequence. They vary in their choice of models and assumptions. The RASC program (Agterberg and Gradstein, 1996), for example, assumes that errors in the stratigraphic position of observed events are normally distributed. Accordingly, its algorithms search for the most commonly preserved sequences of events. By contrast, graphic correlation (Shaw, 1964) assumes that reworking and caving problems can be identified in advance, leaving the true ranges systematically underestimated by observed ranges. Accordingly, its algorithms seek the earliest of the first events and the latest of the last events. For our macrofossil ranges, the assumptions of graphic correlation are preferable because reworking is highly unlikely. The observed taxon ranges will not overestimate true ranges unless fossils are misidentified.

Contradictory indications of the sequence of first and last appearance events are resolved by constrained optimization algorithms in the CONOP9 program (Kemple *et al.*, 1989, 1995; Sadler and Kemple, 1995; Sadler, 2000; Sadler and Cooper, this volume). The constraints require that any feasible sequence must contain all the observed overlaps between taxon ranges. Thus, this program has the advantage that it can seamlessly incorporate slab samples which are, in effect, one-level stratigraphic sections that record co-occurrences but do not reveal sequence. The optimal feasible sequence is one to which all the locally observed sequences can be fit with the minimum net extension of observed ranges. Kemple *et al.* (1995) explain in detail how the algorithms find an optimal sequence. The result is a parsimonious interpretation of the fossil record in the sense that it minimizes the failings in the collection process implied by the ad-hoc adjustments of observed ranges. The range extensions may be measured in different ways; the choice influences the outcome and should be based upon the nature of the stratigraphic sections. For the Marble Mountains problem, there are no lateral variations in lithology and the range extensions may safely be measured in rock thicknesses. When correlating sections from

contrasting facies it would be better to measure range extensions by the number of fossiliferous horizons or range-ends that must be crossed; this favors the sequences preserved in the more fossiliferous or intensely sampled sections.

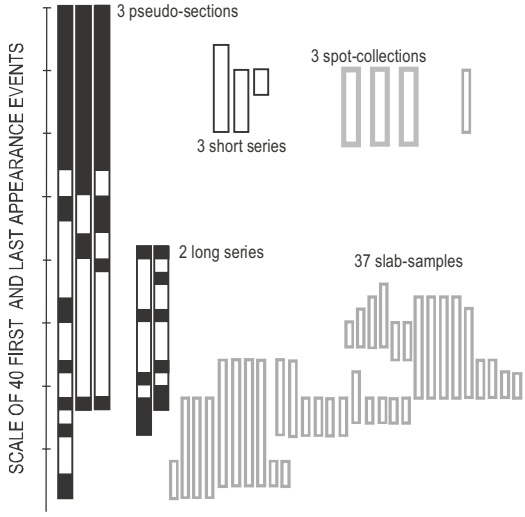

Figure 8. Seriation/correlation of slab-samples, spot-collections, pseudosections and collection series from the UCR museum holdings for the Latham Shale in the Marble Mountains. The vertical scale is derived from the optimal ordinal arrangement of all the included first and last occurrence events. Further explanation in the text.

Figure 8 summarizes how constrained optimization has fit all the UCR museum information from the Marble Mountains to a single ordinal time scale, with one unit for each first and last appearance in the data set. The ordinal scale is derived from pseudosections and collection series, with adjustments to ensure that it honors all additional co-occurrences preserved on the slabs. For pseudosections and long collection series with more than three levels, the rectangles in Figure 8 indicate the minimum span of contained events. Each solid black interval indicates a first or last appearance event that is observed in the series and not extended beyond the ends of the section by the constrained optimization. Blank intervals indicate that the series is lacking an intervening event that is known from other samples in the set. Shorter series have, at most, one collection level that is not terminal, so it is likely that all adjusted ranges will be extended to the limits of the series, leaving no black intervals. For spot collections and slab samples, the gray rectangles in Figure 8 indicate the maximum span of possible positions in the sequence that the fauna may occupy. The length of the gray rectangles varies with the length of the overlap between the ranges

of the preserved taxa, as implied by the optimal sequence.

CONOP9 can be made to optimize a set of slab samples and spot collections alone; simply set the optimization to find a sequence of events that minimizes the number of implied coexistences that have not been observed. Inclusion of the three pseudosections and the five collection series provides polarity for the optimization. Without them, the seriation of the slab samples would provide many more equally well-fit solutions. Of course, the vertical scale in Figure 8 contains sufficient information to construct a range chart. Rather than pausing now to examine the order of events in this intermediate sequence derived from the museum collections alone, let us move on to add these results into the measured section and then construct the corresponding range chart.

4.3 Compositing Museum Collections and Measured Sections

Figure 9 displays the results of using CONOP9 to incorporate the museum collections into the measured section from the Marble Mountains. It uses the scale of stratigraphic thickness from the trenches. The extended ranges honor the additional proven coexistences. Several missing taxa have been inserted according to their coexistences and their position in pseudosections or collection series. Distinctive rock matrix on one museum specimen allowed *Olenellus puertoblancoensis* to be placed in a narrow interval in the Chambless Limestone. This was achieved by including an inferred co-occurrence with *Bristolia* aff. *fragilis* C and *O. terminatus*, recovered from that interval in the measured section.

The range for *Olenellus* aff. *gilberti* A serves as an informative example for the entire optimization. Slab samples prove that the taxon coexists with *O. clarki*, *O. nevadensis*, and *Bristolia harringtoni*. Therefore, the algorithm inserted a short range that satisfies these three overlaps. Because *O.* aff. *gilberti* A is known only as a single questionable specimen in the trenches at the Marble Mountains it does not appear in the original range chart (Fig. 2). But the questionable specimen was found very close to the insertion level; therefore, Figure 9 was amended to show a find and a very short extension. The range of *B. insolens* was extended downward in order to fit with all the known coexistences at this level. These particular ranges change again with the inclusion of evidence from the Providence Mountains.

Figure 10 redraws taxon ranges in the Latham Shale after further adjustment by CONOP9 to accommodate the additional information in the measured section and museum specimens from the Providence Mountains. Notice, for example, that the last appearance of *Olenellus clarki* is extended

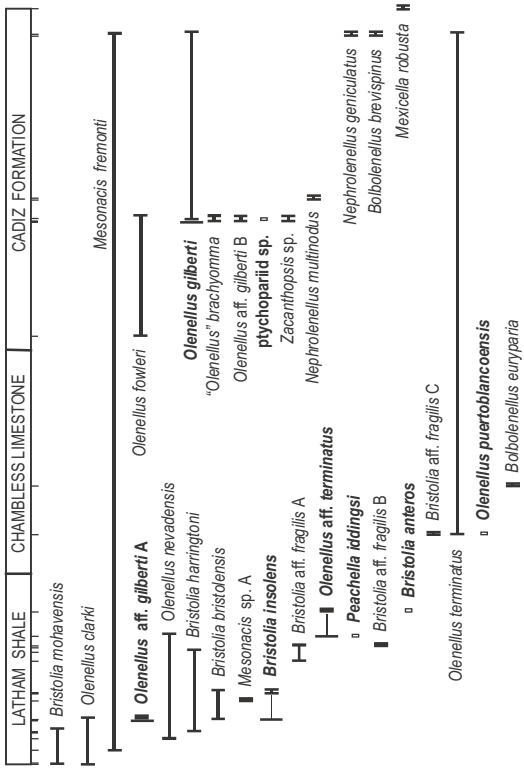

Figure 9. Range chart for the measured section in the Marble Mountains, after compositing with museum collections for the same locality. Vertical lines with short terminal bars = observed ranges. Bold taxon names indicate improvements to measured section. Vertical lines with long terminal bars = range extensions. Open rectangles = insertion of missing species.

significantly higher because, as previously noted, the large sample sizes in the Providence Mountains have captured late appearances of the taxon where its abundance is presumably low enough to be missed in the trench samples.

The adjusted position of the last appearance of *Olenellus clarki* is not determined directly by the stratigraphic thickness of its range in the Providence Mountains, or by reference to the lithostratigraphic boundaries that occur in both measured sections. Biostratigraphic evidence drives the constrained optimization and the algorithm extends the range to honor those additional coexistences that are known from the Providence Mountains. Furthermore, the algorithm extended the range of *O. clarki* upward instead of using the less parsimonious alternative that would have extended the ranges of several coexisting taxa downward. The alternative would have required a greater net adjustment to the range chart. Thus, the treatment of

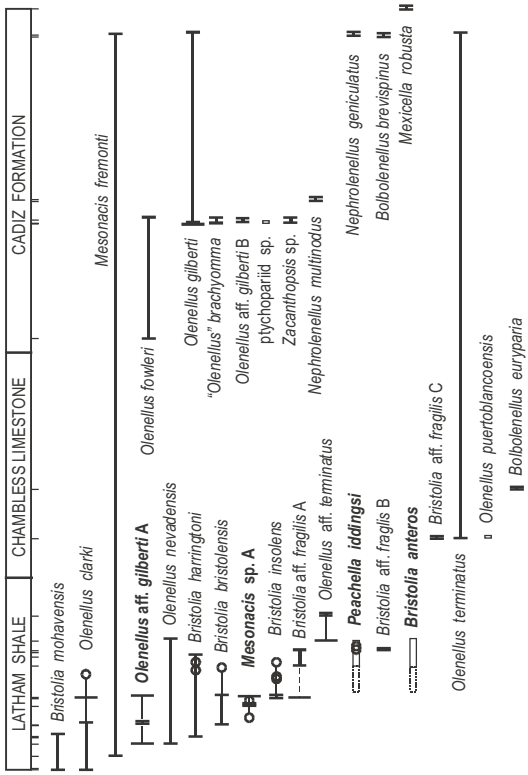

Figure 10. Range chart for the measured section in the Marble Mountains, after compositing with the section from the Providence Mountains and museum collections from both locations. Boldface indicates taxon ranges improved relative to Figure 9. Vertical lines with short terminal bars (that merge for short ranges): ranges based on information from the Marble Mountains. Lighter lines and longer terminal bars; range extensions fit by CONOP9. Open rectangles: taxon ranges inserted by CONOP9, dashed where shrunk by later finds (see postscript). Open circles; critical finds from most recent trenches in the Marble Mountains (see postscript).

this one range end illustrates both constraint (honors observed coexistences) and optimization (minimizes the required adjustments).

Notice also that the ranges do not simply lengthen from Figure 9 to Figure 10; some shorten. Even a single item of significant new information can change multiple components of the previously most parsimonious set of adjustments. For example, the upward extension of *O clarki* and *O.* aff. *gilberti* A allows the previous downward extension of *Bristolia insolens* to be retracted; it now satisfies all proven coexistences without any extensions on the observed range. This is just one of the many interactions between the different sources of information that are best handled automatically rather

than juggled mentally. Besides guaranteeing to consider an immense number of possible arrangements, the benefits of automation include speed and reproducibility.

Figure 10 completes the process of combining all the information contained in specimens for which we have checked the taxonomic assignments. It might be improved by further trenching (see postscript), or recourse to more localities and museums. The next closest Lower Cambrian sections that we have measured reveal different sedimentary facies. Range charts for these sections need to be augmented separately with corresponding museum collections and then compared with the Latham Shale in order to reveal possible facies constraints on the paleogeographic distribution of taxa. There are other smaller, but relevant, museum collections, at the Los Angeles County Museum for example. It is an advantage of the automated compositing process that the range charts may be re-optimized and updated in a matter of minutes once the taxonomy of these other collections has been checked.

5. CONCLUSIONS

Composite sections that combine information from museum collections with range charts from measured sections yield encouraging improvements in resolving power. The composite sections can take advantage of decades of previous collecting without placing very exacting demands on museum documentation of the stratigraphic position of collecting sites. Our case history indicates that this extra effort can be worthwhile even for measured sections in which macrofossils have been collected with unusual thoroughness.

Even though the trilobite collecting associated with our two measured sections for the Latham Shale surely ranks among the most thorough for Lower Cambrian sections in the southwestern United States, the inadequacies of the individual sections are quite evident. Effort devoted to continuous sampling reduced the recovery of rare taxa at some levels. Apportioning more time for processing large volumes of rock at discrete sampling levels improves the recovery of rare taxa, but the reduced number of sampled intervals compromises the resolution of range ends for more abundant taxa.

It is obviously worthwhile to supplement continuous sampling by processing larger volumes of rock from the more richly fossiliferous intervals. Effective supplementary sampling, which recovers rare taxa and increases the number of proven co-occurrences, can be achieved by incorporating information from museum collections. Increasing the number

of known coexistences improves the results of correlation by constrained optimization. Although the optimization operates primarily on the observed sequences of first and last occurrence events, observed coexistences constrain the number of feasible sequences. Thus, observed ranges may be extended to accommodate additional coexistences.

Slab samples and spot collections that prove co-occurrences are the most reliable and readily exploitable of the isolated collections held in museums. Slab samples must be individually sought out to establish that a single piece of rock bears more than one taxon, but they place almost no demands on the stratigraphic precision of the museum locality records – geographic position may suffice. For spot collections, the locality records must confirm that all listed taxa were recovered from a narrow stratigraphic interval. Spot collections and single taxa from coarsely blended collections (one from each successive lithostratigraphic formation), may be combined into pseudosections. Thus, rare taxa that were not found in a measured section may be provided with sufficient coexistence and sequence information that a computer algorithm can insert them reliably into the composite section.

The notion of incorporating museum finds into range charts is not new. The keys to our successful compositing of these different types of data are two attributes of the computer algorithms. First, they can optimize large volumes of information with inter-relationships that are too complex for mental arithmetic (Sadler and Cooper, this volume); with their assistance it is feasible to add numerous separate items of information from museum collections. Second, the algorithms place stratigraphic correlation and seriation on an objective, reproducible basis; their rules for the compositing process are explicit and their results are reproducible and quantified. Comparable computer-assisted methods are already routine for related paleobiological tasks. The stratigraphic correlation and seriation algorithms in CONOP9 apply the rules of parsimony in a manner analogous to automated searches for most parsimonious cladograms. (Copies of the programs and sample data sets are available from P.M.S. on request.)

6. POSTSCRIPT

This chapter illustrated its methods using the current results of an ongoing investigation. While the manuscript was in review, we intensified the search for fossils in the upper portion of the Latham Shale in the Marble Mountains where the composite section indicates that additional taxa should be present. Targeting the level in existing trenches where *Peachella iddingsi* was predicted, we eventually found one individual of this taxon. A new set of trenches through the upper Latham Shale, opened 100 m away along

strike, revealed many richly fossiliferous horizons (LaGrange, 2002). The stark contrast with the earlier, less fossiliferous trench at this level reveals a small-scale patchiness in the distribution of trilobites within these shales. The new trenching confirms several predictions of the compositing exercise and adds new features to the range chart. Critical new finds are indicated by circles in Figure 10. Two fossiliferous levels, 1 m apart, establish the expected short range for *P. iddingsi* high in the Latham Shale. Finds of *Mesonacis* sp. A confirm the upward range extension indicated for that species.

Two rare occurrences of *Olenellus clarki* in the new trenches vindicate the upward range extension suggested by the composite section. The observed range now extends considerably beyond the abundant interval previously established lower in the formation (and beyond the range extension in the composite section). The range of *Bristolia bristolensis* is similarly extended upward by new finds. Sparse occurrences high in the range of these two olenelloids invalidate the short confidence intervals calculated for the previously-known ranges (Fig. 2) but match the pattern of finds of *O. clarki* in the Providence Mountains (Fig. 3).

Five new finds of *B. insolens* within an interval of 4 m extend the earlier solitary find from the Marble Mountains trenches into a range slightly longer than that in the Providence Mountains. New finds of *B. harringtoni* confirm the earlier observation that there are late occurrences of the species in the Marble Mountains significantly above the top of the range established in the Providence Mountains. The new trench adds five finds in an interval of approximately 1 m at a level where a single late occurrence previously established the top of the range. The new trench provides no mid-range finds, however, thus introducing the possibility that *B. harringtoni* is a Lazarus taxon with two disjunct ranges.

Even before *Bristolia anteros* was found in the new trenches, the other new finds permitted the projected positions of *B. anteros* to be more narrowly constrained. The observation of younger occurrences of *O. clarki* and *B. bristolensis* changes the impact of the known coexistences, allowing the lower half of the projected range of positions for *B. anteros* to be eliminated (dashed rectangle in Figure 10). After it was too late to redraw figure 10, specimens of *B. anteros* were recovered from the predicted interval (LaGrange, 2002). The previously suggested range extension for *B.* aff. *fragilis* A may also be removed. The ranges of *O. clarki* and *B. bristolensis* in the Marble Mountains had appeared to be reliable, because they were established on numerous closely-spaced finds with coexistences comparable to those in the Providence Mountains. The new finds indicate that these ranges should have been given more freedom to adjust during the compositing process.

The lesson from this postscript will be familiar to many; the goal of finishing a range chart is unreachable. Additional collecting may eliminate some gaps and discrepancies. But the same extra effort reveals new features in existing ranges and uncovers rarer taxa whose ranges remain poorly established, thus, inviting more collecting expeditions and repeating the cycle. Our own additions to the museum materials confirm that the augmented range chart from the Marble Mountains is still not exhaustive. Although specimens collected from talus in the Latham Shale include *Anomalocaris*, the genus has not yet been recovered *in situ* from any of our trenches.

ACKNOWLEDGEMENTS

This project is partially funded by NSF grant EAR-9980372 to P.M.S. Leslie Knox (now Mrs. Webster), Jennifer LaGrange, Jennifer Jones, Brenda Hunda, Sinnie Chen, Min-Hyoung Kim, and Jason Odell assisted in the collection of fossils from the trenches. Pete Palmer and Fred Sundberg identified Middle Cambrian trilobite material for us. Linda and Mike McCollum shared their measured sections and fossil locality information. Christian Gronau sent pictures of his collections from the Chambless Limestone. Art and Rosemond Riggle generously donated their trilobite collections from the Latham Shale in the Marble Mountains. Loren Babcock, Tim White, and Peter Harries helped us tighten the manuscript in many critical places.

REFERENCES

Agterberg, F. P., and Gradstein, F. M., 1996, *RASC and CASC: Biostratigraphic Zonation and Correlation Software, version 15*.

Alroy, J., 1992, Conjunction among taxonomic distributions and the Miocene mammalian biochronology of the Great Plains, *Paleobio*. **18**:326-343.

Babcock, L. E., 1994a, Systematics and phylogenetics of polymeroid trilobites from the Henson Gletscher and Kap Stanton Formations (Middle Cambrian), North Greenland, *Grøn. Geol. Under. Bull.* **169**:79-127.

Babcock, L. E., 1994b, Biogeography and biofacies patterns of Middle Cambrian polymeroid trilobites from North Greenland: Palaeogeographic and palaeo-oceanographic implications, *Grøn. Geol. Under. Bull.* **169**:129-147.

Clark, C. W., 1921, Lower and middle Cambrian formations of the Mohave Desert, *Univ. Calif. Pub. Geol. Sci. Bull.* **13**:1-7.

Crickmay, C. H., 1933, Paleontology, in: Hazzard, J. C., Note on the Cambrian rocks of the eastern Mohave Desert Mohave Desert, California, with a paleontology report by Colin H. Crickmay, *Calif. Pub. Geol. Sci. Bull.* **23**:71-80.

Darton, N. H., 1907, Discovery of Cambrian rocks in southeastern California, *J. Geol.*

15:470-475.

Guex, J., 1991, *Biochronological Correlations*, Springer Verlag, Berlin.

Guex, J., and Davaud, E., 1984, Unitary associations method: Use of graph theory and computer algorithms, *Comp. Geosci*. **10**:69-96.

Hazzard, J. C., 1933, Note on the Cambrian rocks of the eastern Mohave Desert Mohave Desert, California, with a paleontological report by Colin H. Crickmay, *Calif. Pub. Geol. Sci. Bull.* **23**:57-80.

Hazzard, J. C., 1937, Paleozoic section in the Nopah and Resting Springs Mountains, Inyo County, California, *Calif. J. Mines Geol*. **33**:273-339

Hazzard, J. C., 1954, Rocks and structure of the northern Providence Mountains, San Bernardino County, California*, Calif. Div. Mines Bull*., **170**:27-35.

Hazzard, J. C., and Mason, J. F., 1936, Middle Cambrian formations of the Providence and Marble Mountains, California, *Geol. Soc. Am. Bull.* **47**:229-240.

Kemple, W. G., Sadler, P. M., and Strauss, D. J., 1989, A prototype constrained optimization solution to the time correlation problem*, Geol. Surv. Can. Pap.* **89-9**:417-425.

Kemple, W. G., Sadler, P. M., and Strauss, D. J., 1995, Extending graphic correlation to N dimensions: The stratigraphic correlation problem as constrained optimization, in: *Graphic Correlation* (K. O. Mann and H. R Lane., eds.), *SEPM Sp. Pap*. **53**:65–82.

Kidwell, S. M., 1991, The stratigraphy of shell concentrations, in: *Taphonomy; Releasing Data Locked in the Fossil Record* (P. A. Allison and D. E. G. Briggs, eds.), Plenum Press, New York, pp. 211-290.

LaGrange, J. E.. 2002, Biostratigraphy of Olenelloid Trilobites from the Lower Cambrian of the Southeastern Marble Mountains: Pushing the Limits of the Resolution of the Fossil Record, unpublished senior thesis, University of California, Riverside, Geology Museum, 44 p., 5 appendices.

Marshall, C. R., 1990, Confidence intervals upon stratigraphic ranges, *Paleobio*. **16**:1-10.

Marshall, C. R., 1994, Confidence intervals on stratigraphic ranges: Partial relaxation of the assumption of randomly distributed fossil horizons, *Paleobio* **20**:459-469.

Mason, J. F., 1935, Fauna of the Cambrian Cadiz Formation, Marble Mountains, California, *S. Calif. Acad. Sci. Bull.* **34**:97-119.

Mount, J. D., 1974, Early Cambrian faunas from the Marble and Providence Mountains, San Bernardino County, California, *Bull. S. Calif. Paleont. Soc*. **6**:1-5.

Mount, J. D., 1976, Early Cambrian faunas from Eastern San Bernardino County, California, *Bull. S. Calif. Paleont. Soc*. **8**:173-182.

Nolan, T. B., 1929, Notes on the stratigraphy and structure of the northwest portion of Spring Mountain, Nevada, *Am. J. Sci*. **17**:461-472.

Paul, C. R. C., 1982, The adequacy of the fossil record, in: *Problems of Phylogenetic Reconstruction* (K. A. Joysey and A. E. Friday eds.), *System. Assoc. Sp. Vol.* **21**:75-117.

Resser, C. E., 1928, Cambrian fossils from the Mohave Desert, *Smith. Misc. Coll*. **81**:1-14.

Riccio, J. F., 1952, The lower Cambrian Olenellidae of the southern Marble Mountains, *S. Calif. Acad. Sci. Bull*. **51**:25-49.

Sadler, P. M., 2000, *Constrained Optimization Approaches to the Paleobiologic Correlation and Seriation Problems: A Users' Guide and Reference Manual to the CONOP Program Family, Version 6.5*, University of California, Riverside.

Sadler, P. M., and Cooper, R. A., this volume, Best-fit intervals and consensus sequences; comparison of the resolving power of traditional biostratigraphy and computer-assisted correlation.

Sadler P. M., and Kemple, W. G., 1995, Using rapid, multidimensional, graphic correlation to evaluate chronostratigraphic models for the Mid-Ordovician of the Mohawk Valley, New York, in: *Ordovician Odyssey: Short Papers for the Seventh International Symposium on*

the Ordovician System (J. D. Cooper, M. L. Droser and S. C. Finney, eds*.), SEPM Pac. Sec. Book* **77**:257-260.

Shaw, A. B., 1964, *Time in Stratigraphy*, McGraw-Hill, New York.

Strauss, D., and Sadler, P. M., 1989, Classical confidence intervals and Bayesian probability estimates for ends of local taxon ranges, *Math. Geol*. **21**:411- 427.

Walker, K. R., and Bambach, R. K., 1971, The significance of fossil assemblages from fine-grained sediments: Time-averaged communities, *Geol. Soc. Am. Abstr. Prog*. **3**:783-784.

Chapter 4

Zoophycos, Systematic Stratigraphic Leaking, and Lamella Stratigraphy

Do Some Spreiten Contain a Unique Record of High-Frequency Depositional Dynamics?

CHARLES E. SAVRDA

1. ICHNOLOGY'S ROLE IN STRATIGRAPHY

Stratigraphy is defined very broadly as the "science of rock

CHARLES E. SAVRDA • Department of Geology and Geography, 210 Petrie Hall, Auburn University, Auburn, Alabama 36849-5305.

P.J. Harries (ed.), *High-Resolution Approaches in Stratigraphic Paleontology.*

strata....concerned not only with the original succession and age relations of rock strata but also...with all characters and attributes of rock strata...and their interpretation in terms of environment or mode of origin, and geologic history" (Bates and Jackson, 1987, p. 649). Ichnology, the study of "post-depositional biological effects on sedimentary deposits" (Ekdale *et al.*, 1984a, p. 4) manifest in distinct trace fossils and/or bioturbate textures, provides important tools for stratigraphic studies. Indeed, an accounting of previous and potential stratigraphic applications of ichnology would require nearly as much page space as would an inclusive summary of the myriad components of stratigraphy itself. Stratigraphic applications of ichnology include trace-fossil biostratigraphy of the Neoproterozoic-Cambrian transition (e.g., see MacNaughton and Narbonne, 1999; and references therein) and use of ichnofacies and ichnofabrics for depositional facies analyses (e.g., see Pemberton, 1992; and references therein), delineation of sequence stratigraphic packages and bounding surfaces (e.g., MacEachern *et al.*, 1992; Savrda, 1995; Savrda *et al.*, 2001; and references therein), and interpretation of Milankovitch-type depositional cycles (cyclostratigraphy; e.g., Savrda, 1995; Locklair and Savrda, 1998a; and references therein).

Whether these and related stratigraphic applications are regarded as high-resolution depends on the perceptions of the investigator and the problems they seek to address. In many applications (e.g., cyclostratigraphy), ichnology helps decipher processes that operate at time scales on the order of 10^4 to 10^5 yrs and, hence, in the context of geologic time can be considered a high-resolution tool. In the body fossil realm, examples abound of even higher resolution; for example, lamina-scale analyses of microfossil constituents (Chang *et al.*, 1998) and sclerochronologic studies of individual skeletons (e.g., Kirby *et al.*, 1998; Fatherree *et al.*, 1998) have provided records of paleoenvironmental change metered on scales of days to decades. Can trace fossils be employed in a similar manner? Most stratigraphers likely would suggest not, citing the well-known fact that, at these temporal scales, bioturbation is responsible for the *reduction* of stratigraphic resolution. Nonetheless, certain trace fossils that reflect a particular behavior, namely non-selective reverse conveyor feeding, may preserve a record of marine depositional processes and events that otherwise is destroyed by intense bioturbation. This contribution explores this hypothesis, with emphasis on the depositional records potentially preserved in *Zoophycos* spreiten and their promise for cyclostratigraphic and other investigations.

2. BIOTURBATION AND LOSS OF STRATIGRAPHIC RESOLUTION

In oxygen-deficient settings where benthos are limited or excluded, accumulating muds are characterized by fine laminae that reflect slow, often seasonally variable hemipelagic sedimentation (linked to seasonal variations in productivity, clastic runoff, etc.), but also may include thin beds that reflect rapid depositional events of variable frequency associated with storms, mass-movement events, or other unusual oceanographic perturbations (e.g., see Soutar *et al.*, 1981; Thornton, 1984; Wetzel, 1991a; Fig. 1A). However, most Phanerozoic marine mudrocks, particularly those deposited in low-energy, oxygenated settings, are thoroughly bioturbated and, hence, lack a record of high-frequency cycles and events (e.g., Fig. 1B). In general, for oxygenated settings, only rapid, high-magnitude depositional events that result in the accumulation of relatively thick layers survive the onslaught of persistent bioturbation.

The blurring of the depositional record and consequent time averaging by bioturbation is related to both diffusive biogenic mixing and vertical advection of sedimentary particles through the sediment column (Guinasso and Schink, 1975; Robbins *et al.*, 1979). The upward and downward advection of sedimentary grains by biogenic activity results in stratigraphic reworking and stratigraphic leaking, respectively.

These processes are best viewed in the context of burrow stratigraphy or substrate tiering. Modern marine hemipelagic/pelagic substrates generally can be divided into two main layers – the surface-mixed and transition layers – on the basis of the character and extent of active bioturbation (Berger *et al.*, 1979; Ekdale *et al.*, 1984b). The surface-mixed layer, typically 8 to 10 cm thick (range = 3 to 15 cm; Ekdale *et al.*, 1984a), is a relatively fluid zone of rapid and continuous homogenization by epibenthic and shallow endobenthic animals (Berger and Johnson, 1978; Berger *et al.*, 1979; Ekdale *et al.*, 1984b). Stirring in the mixed layer may be facilitated by the dominance in its lower parts of conveyor processors – organisms that advect sediment upwards (Bromley, 1996) and thereby induce stratigraphic reworking.

Vertical advective processes continue in the underlying transition layer, a zone of heterogeneous mixing by organisms that live or feed at greater depths in the substrate. These organisms produce both open burrows and actively filled traces that can include spreite structures. The transition layer itself also may exhibit tiering; that is, trace-producing organisms preferentially occupy different levels beneath the mixed layer (Wetzel, 1983, 1991b; Ekdale, 1985). Deeper tiers, which may extend 1 m or more below

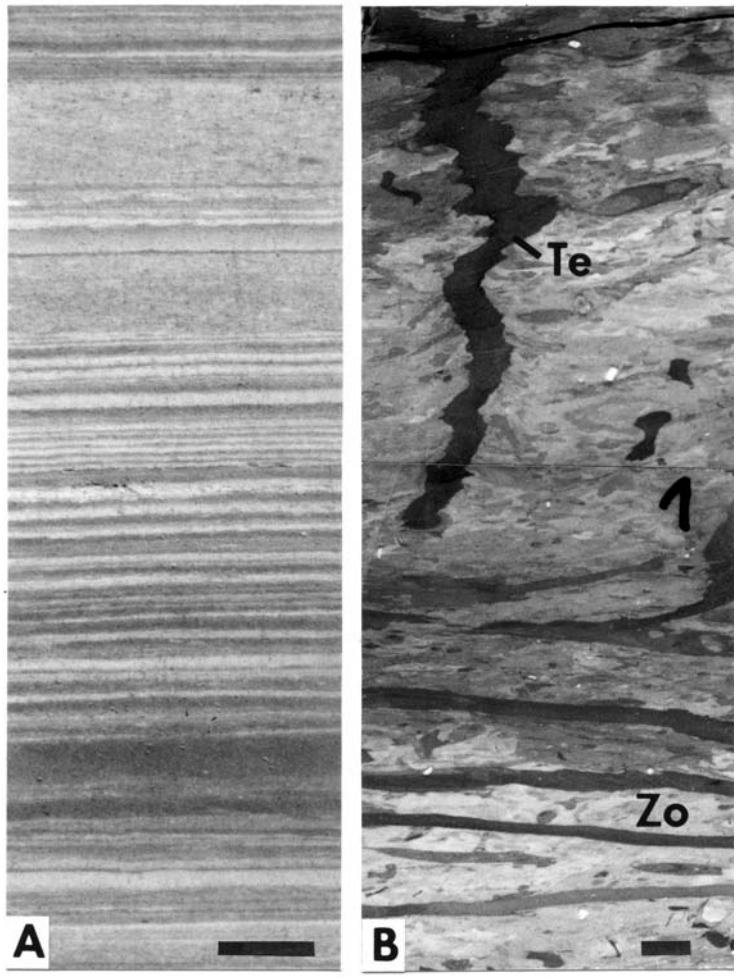

Figure 1. Fabrics in unbioturbated (A) and bioturbated (B) pelagic/hemipelagic mudrock sequences. Laminae and thin beds in A (diatomite, Miocene Monterey Formation, California) provide a high-resolution record of depositional dynamics. Fabrics in B (marlstone, Cretaceous Niobrara Formation, Colorado), produced during passage through the surface mixed layer (diffusely burrowed background fabrics) and transition layer (distinct trace fossils), are time-averaged and hence provide lower resolution. Transition-layer trace fossils in B include *Teichnichnus* (Te; dark, vertical structure) and *Zoophycos* (Zo; section through multiwhorled form), both of which appear to contain darker sediments from above (black mark at right center is a core marker). Scale bars are 1 cm long.

the sediment-water interface, often are occupied by reverse conveyor feeders that displace sediments downward (Bromley, 1996). This activity, along with the passive filling of open burrows, results in stratigraphic leaking.

The extent of time averaging that results from bioturbation primarily depends on mixed-layer thickness and sedimentation rate (Guinasso and

Schink, 1975) but typically is substantial for most pelagic and hemipelagic sequences. As an example, consider a 10-cm sequence of mudrock deposited at rates of 5 to 50 cm/ky. In the absence of bioturbation, this sequence may preserve a detailed record of paleoenvironmental dynamics operating over periods as short as a day to several hundred years (Figs. 1A and 2A; Wetzel, 1991a). However, the addition of mixed-layer bioturbation alone would convert that same interval to a seemingly uniform sequence representing the time-averaged product of 200 to 2000 yr of sedimentation (assuming a mixed-layer thickness of ~10 cm). As long as mixed-layer bioturbation persists, and as long as sedimentation is slow (cm or dm/ky) and continuous, only the lower-frequency changes (those occurring over periods of 10^4 yr or longer) that impact a depositional regime are manifested in the stratigraphic record (Fig. 2B). Of course, vertical transport of sediment (whether upward reworking, downward leaking, or both) by transition-layer burrowers may blur the record further.

Given the effects outlined above, it is not surprising that bioturbation is widely perceived as detrimental to high-resolution stratigraphic studies. However, it is possible that the producers of some deep transition-layer trace fossils, through a process of *systematic leaking*, actually may preserve partial records of short-term depositional processes that otherwise are eradicated completely by mixed-layer bioturbation. The potential of deciphering such a record from individual trace fossils is revealed in the spreiten of *Zoophycos*.

3. *ZOOPHYCOS* AND SYSTEMATIC STRATIGRAPHIC LEAKING

3.1 Trace Morphology

Zoophycos is a complex burrow system that generally consists of three basic parts: (1) lamellae (major and minor), that comprise (2) helically coiled, sheet-like spreite or lamina, and (3) a cylindrical tunnel or tube with axial and marginal components (Fig. 3; Simpson, 1970; Hantzschel, 1975). Various morphotypes of *Zoophycos* are recognized based on the arrangement of laminae around the structure's central axis and the tube's shape and disposition (e.g., Wetzel and Werner, 1981; Bromley, 1991; Ekdale, 1992). These structures also differ with respect to source and recognized degree of pelletization of sediments in the lamellae. The latter parameters play a paramount role in the behavioral analysis of the tracemaker.

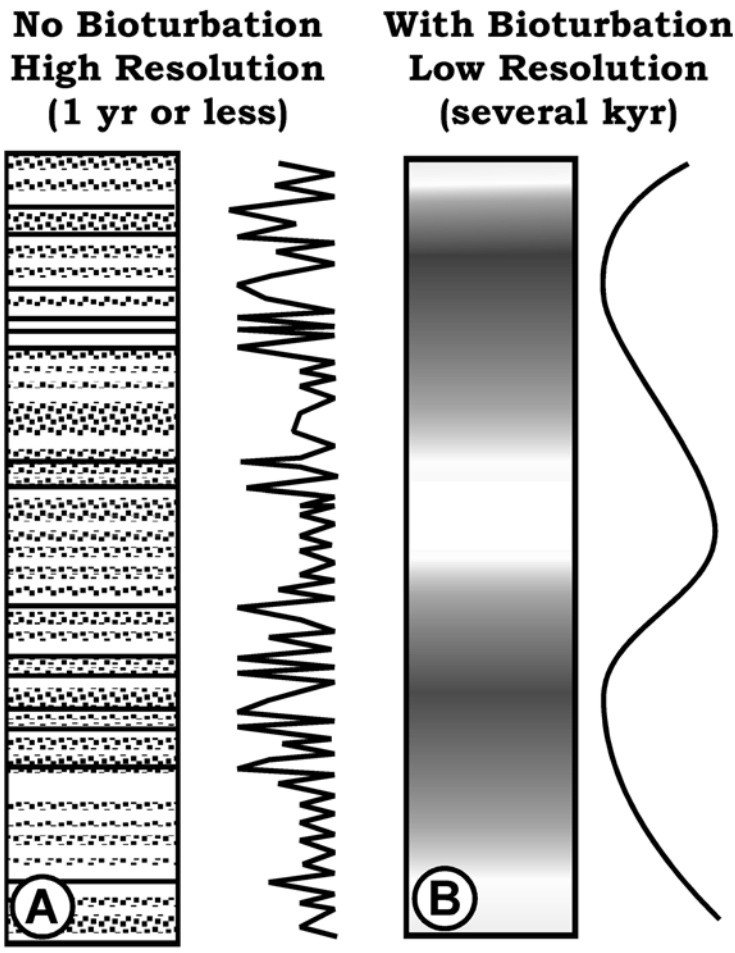

Figure 2. Schematic representation of temporal resolution and time averaging manifested in unbioturbated and bioturbated pelagic/hemipelagic sequences. Unbioturbated sequences (A) may contain a record of short-term dynamics, including pulsed depositional events. With the occurrence of bioturbation (B), the same primary record would be blurred significantly and only longer-term, lower-frequency trends are preserved.

3.2 Behavioral Interpretation

It is recognized widely that the broad morphological range of *Zoophycos* indicates that structures collectively assigned to this ichnotaxon were produced by a variety of animals with different behavioral routines (e.g., Bromley, 1991; Miller, 1991; Ekdale, 1992; Fu and Werner, 1995; Olivero and Gaillard, 1996). However, the extent of behavioral differences only recently has been appreciated. Traditionally, *Zoophycos* has been considered

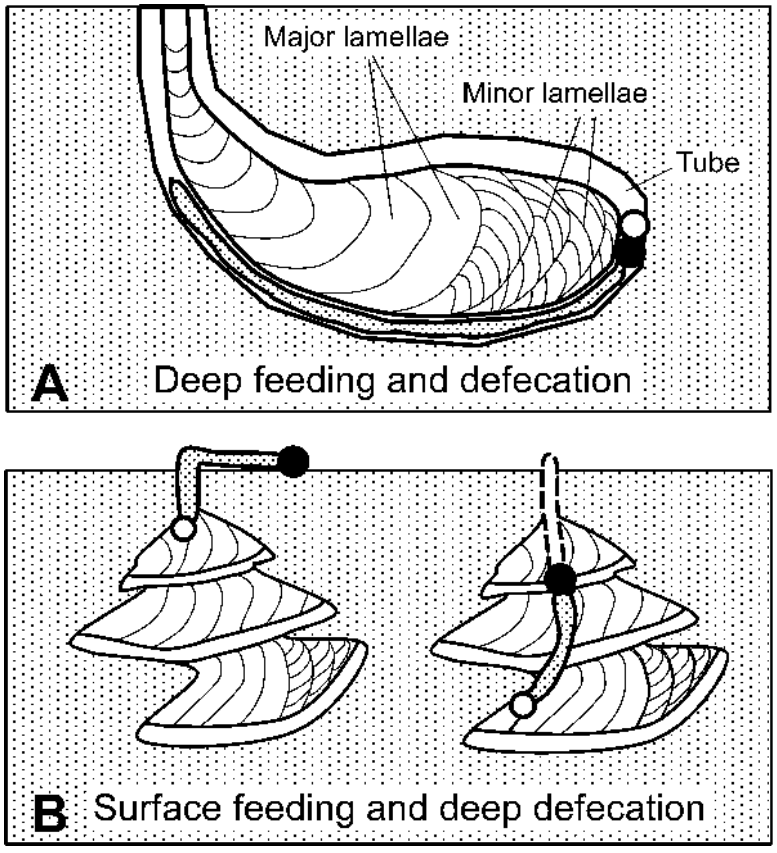

Figure 3. Morphologic features and generalized behavioral models for *Zoophycos* (for simplicity, minor lamellae are shown only in a portion of spreiten). (A) Basic *Zoophycos* morphology and traditional interpretation as the trace of deep, deposit-feeding worms. (B) Interpretation as a deep waste repository of a surface detritus feeder (after Kotake, 1989). In both A and B, feeding and defecating ends of tracemakers are indicated by filled (black) and open circles, respectively. Interpretation in A requires an animal with a u-shaped digestive tract. In B, the activities of the tracemaker result in systematic stratigraphic leaking.

as a systematic feeding structure produced by sessile, deep, deposit-feeding worms (e.g., Seilacher, 1967; Simpson, 1970; Wetzel and Werner, 1981; Ekdale, 1985; Ekdale and Lewis, 1991; Fig. 3A). This interpretation largely was based on the highly organized pattern of construction, which seemingly bespeaks a systematic strip-mining operation, the typical pelletization of parts of the lamellae, and the fact that *Zoophycos* represents a deep-tier, transition-layer trace fossil.

Although the tracemakers undoubtedly did occupy deep tiers (Ekdale and Bromley, 1991; Savrda, 1992; Kotake, 1993), the conviction that these organisms uniformly were deep deposit feeders was severely challenged by

Kotake's (1989) study of *Zoophycos* in Pliocene ash-bearing deposits of Japan. Based on stratigraphic leaking of volcanic ash, Kotake (1989, 1991) clearly demonstrated that pelleted fills in *Zoophycos* spreiten were derived from overlying horizons near the tops of axial tunnels. He used this evidence to propose that these *Zoophycos* were deep waste repositories produced by sessile organisms feeding non-selectively on detritus at the sediment-water interface (Fig. 3B). Although some subsequent studies lend support to the traditional deep-deposit-feeder model for certain *Zoophycos* morphotypes (e.g., Olivero and Gaillard, 1996), other studies support Kotake's (1989) paradigm in that they indicate downward transport of pelleted sediments in *Zoophycos* lamellae (e.g., Ekdale and Bromley, 1991; Miller, 1991; Fu and Werner, 1995; Locklair and Savrda, 1998a).

What does the downward transport of surficial sediments indicate about animal behavior? Kotake (1989, 1991, 1992) suggested that *Zoophycos* signifies a deep waste repository of surface detritus feeders, possibly echiurian worms. Unwillingly to accept the intricately methodical fabrication of *Zoophycos* as a mere "cess-pit," Bromley (1991) proposed that systematic downward transport of pelleted sediment may reflect other activities, including food caching (*sensu* Jumars *et al.*, 1990) and microbial gardening. These trophic models certainly warrant further exploration. However, whatever the purpose of downward advection, the *Zoophycos* tracemakers operated as reverse conveyors by non-selectively removing and methodically redepositing surface sediments to substrate depths that were immune to the random stirring of the mixed layer. It is this systematic leaking that may provide an exploitable record of short-term depositional dynamics.

3.3 Lamella Stratigraphy

The basic precept forwarded here is that lamellae of *Zoophycos* spreiten may be employed in much the same way that growth intervals are employed in sclerochronologic studies of body fossils (Fig. 4), an approach referred to herein as *lamella stratigraphy*. In relatively complete and adequately preserved specimens of *Zoophycos*, a growth vector is easily recognized; that is, the relative order of production of minor and major lamellae can be determined and, hence, successive growth stages of the spreite can be identified (e.g., Kotake, 1989). Each growth stage corresponds to a distinct phase of non-selective feeding by the organism at the seafloor, and the major lamellae likely correspond to individual feeding episodes (Kotake, 1991). Theoretically then, examination of successively younger pelleted parts of the spreite could provide a sequential record of the types of sediment available at the sediment-water interface (Fig. 4).

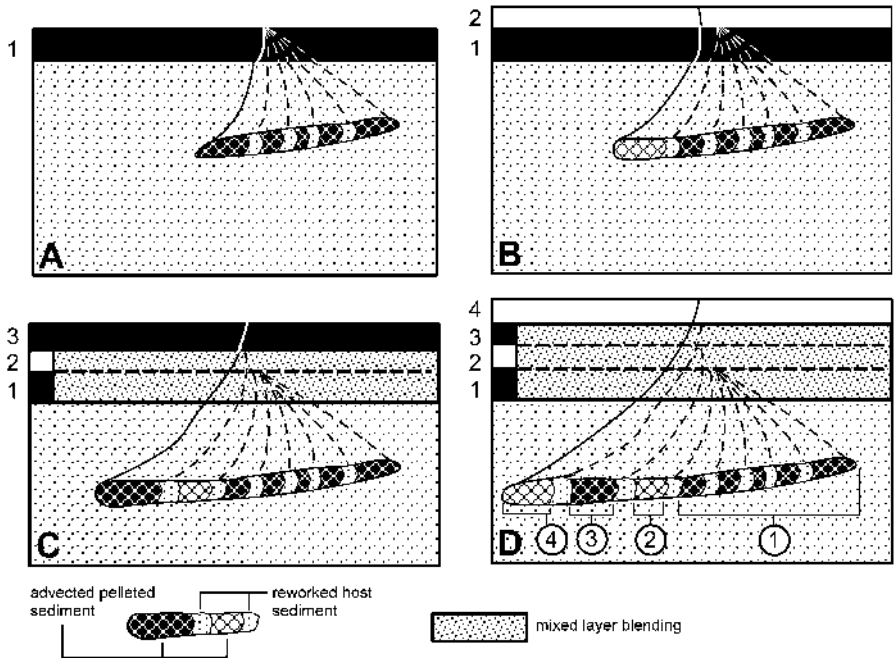

Figure 4. Highly schematic representation (in vertical section) of *Zoophycos* lamella stratigraphy and its potential record of short-term depositional dynamics. Solid lines extending from the sediment-water interface approximate the position of the migrating tube (not shown). Light and dark pelleted lamellae, which reflect stratigraphic leaking of surface sediments of variable character, are separated by host sediments reworked by the tracemaker (major and minor lamellae are not differentiated in this cartoon). In D, sequentially formed, pelleted lamellae (1, 2, 3, and 4) in the spreite record hypothetical depositional events 1 through 4 (e.g., pulsed delivery episodes), which are otherwise destroyed by mixed-layer bioturbation.

If the character of sediment available at the seafloor remains constant during the life span of a *Zoophycos* tracemaker, sediment composing the pelleted lamellae should be uniform throughout the spreite. However, in response to productivity events, storms, and other processes, pulsed fluxes of organic matter (see Jumars *et al.*, 1990; Smith, 1994), clastic sediments, and/or biogenic constituents could occur during a tracemaker's life time. Although evidence for this pulsed delivery in the form of laminae or beds eventually will be obliterated by mixed-layer bioturbation, a record of such short-term depositional events may be sequestered in the *Zoophycos* spreite in the form of sedimentologic, geochemical, and/or micropaleontologic variations among pelleted lamellae (Fig. 4). Kotake's (1989) observations of ash-dominated pelleted lamellae within otherwise mud-dominated *Zoophycos* spreiten, and observations by the author (see below) lend credence to this conjecture.

Can *Zoophycos*-bearing deposits yield a continuous record of depositional dynamics such as that in unbioturbated strata? Certainly not. Owing to patchy distributions and complexities of population dynamics for *Zoophycos* producers (see Wetzel and Werner, 1981; Kotake, 1994), it is likely that *Zoophycos* spreiten available for study in any sequence collectively would provide an incomplete temporal record, even for highly ichnofossil-rich exposures. Moreover, determination of relative ages of spreiten, or of lamellae within different spreiten, would be difficult at best. Additional problems are predicted in the analyses of individual spreiten. Given the uncertainties regarding the longevity of individual tracemakers (presumably a few years to tens of years?), the period of deposition represented by pelleted lamellae in a spreite is not known. Furthermore, the fidelity of any lamella stratigraphy as a true depositional time series likely would be impacted variably by the interplay of physical and biological factors. The former include erosional events, sedimentation rates, and the frequency and magnitude of pulsed depositional events, while the latter include the actual depth and frequency of surface feeding by the tracemaker and the rate at and extent to which mixed-layer bioturbators modify pulse-delivered sediments.

Nonetheless, if preserved, a partial record of depositional dynamics is better than no record at all and may have implications for broader stratigraphic studies. The potential application of lamella stratigraphy is exemplified below via consideration of *Zoophycos* in the Upper Cretaceous Demopolis Chalk.

4. DEMOPOLIS CHALK - POTENTIAL CASE STUDY

4.1 General Stratigraphic Framework

The Campanian Demopolis Chalk is exposed in an arcuate belt extending through three eastern Gulf coastal plain states (Alabama, Mississippi, and Tennessee). The bulk of the Demopolis was deposited during a major transgression in a passive-margin shelf setting and, like many Cretaceous chalk sequences, is dominated by decimeter-scale rhythmic alternation of light-gray to white, organic-poor chalks (up to 95% $CaCO_3$, as low as 0.4% organic C) and darker (medium to light gray) organic-rich marls ($CaCO_3$ as low as 53%, up to 1.2% organic C). Spectral analyses of carbonate and grayscale time series by Warren and Savrda (1998) indicate that carbonate rhythms were controlled by Milankovitch orbital parameters. Net sediment-

accumulation rate for the interval studied averaged ~3.0 to 3.5 cm/ka, but it apparently varied from 1 to 12 cm/ka in response to climate-induced dilution cycles.

4.2 General Ichnology

Chalks and marls in the Demopolis are completely bioturbated. Ichnofabrics are typical of pelagic deposits; diffusely burrow-mottled background fabrics that reflect passage through the surface mixed layer are overprinted by distinct ichnofossils emplaced during subsequent passage through the transition layer (Figs. 5 and 6). Ichnofossil assemblages in the chalk and marl units are virtually identical. Both are dominated by *Phycosiphon*, *Chondrites*, *Planolites*, *Taenidium*, *Teichichnus*, *Thalassinoides*, and *Zoophycos*, and they indicate deposition in a quiet, consistently well-oxygenated, outer-shelf setting (Locklair and Savrda, 1998a).

Contrast between distinct burrows and host sediments is greatest at bed transitions (Savrda, 1992; Locklair and Savrda, 1998a). Upper parts of light-colored chalk units are overprinted by well-defined dark ichnofossils that pipe downward from and were emplaced during deposition of overlying marls. Similarly, the tops of darker marl units are overprinted by well-defined lighter traces piped downward from overlying chalks (Figs. 5 and 6). These intervals are referred to as dark-on-light (DOL) and light-on-dark (LOD) piped zones, respectively. Comparative analysis of *Zoophycos* in LOD and DOL piped zones provided both a test of behavioral models and the seed for the lamella-stratigraphy concept.

4.3 Zoophycos

Observations of *Zoophycos* in Demopolis Chalk are limited mainly to vertical core and outcrop faces. Planar to helicoidal *Zoophycos* spreiten range from 0.2 to 2.0 cm thick and up to 1 m wide (e.g., Fig. 5). Where observed, marginal tubes range from 4 to 7 mm in diameter (Locklair and Savrda, 1998a). Piped-zone penetration depths for *Zoophycos* average 20 cm but may range up to 50 cm, indicating that the tracemakers occupied substrate depths of at least that much below the mixed layer (Locklair and Savrda, 1998b).

In cross-sectional view, lamellae show alternating light and dark sediment packages of variable width. Generally, in LOD piped zones, lighter-colored components of lamellae are dominant (wider), contain small (~1 x 0.5 mm) ovate pellets, and can be linked to immediately overlying chalk beds, while

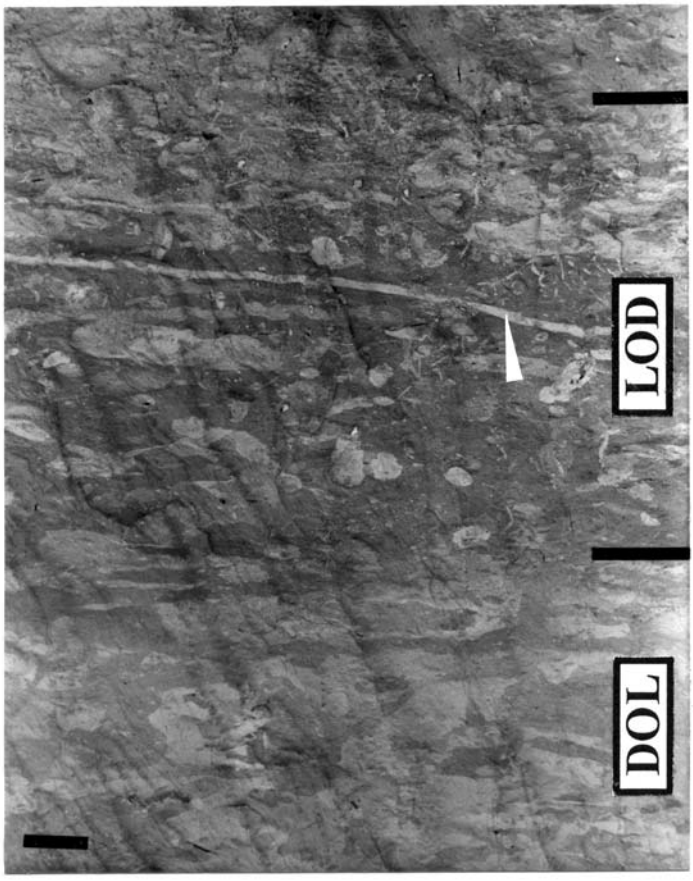

Figure 5. Well-defined burrows within light-on-dark (LOD) and dark-on-light (DOL) piped zones at marl-chalk and chalk-marl transitions, respectively, in Cretaceous Demopolis Chalk. Narrow light band (arrow head) across central part of LOD is a planar *Zoophycos* spreite. Scale bar is 5 cm long (modified from Savrda and Locklair, 1998a).

darker components are subordinate, unpelleted, and virtually identical to surrounding sediments (Figs. 6, 7A). The reverse generally is true for DOL piped zones; the dominant, pelleted parts of lamellae are characterized by dark-colored sediments that match the overlying marls, whereas subordinate, unpelleted components of lamellae have affinities to the lighter chalks of the background (Figs. 6, 7B). These observations clearly indicate a systematic downward transport of sediment to form the pelleted lamellae, and they are consistent with Kotake's (1989, 1991) behavorial interpretation for *Zoophycos* as the trace of surface-feeding, deep-defecating organisms.

The generalities described above provide an adequate test of behavioral

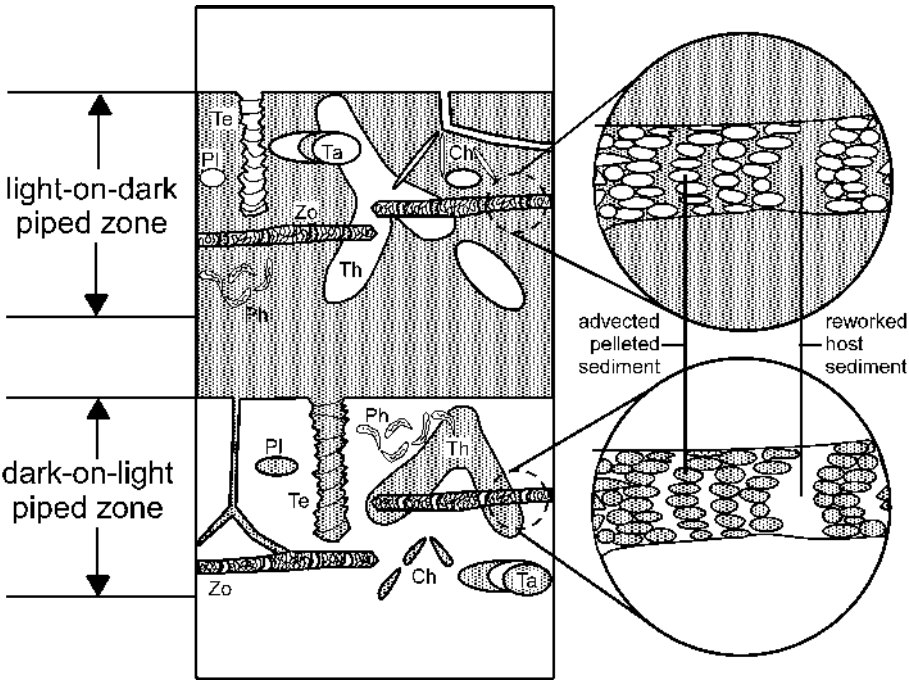

Figure 6. Schematic representation of *Zoophycos* (Zo) spreiten and other recurring ichnofossils in piped zones in the Demopolis Chalk (Ph = *Phycosiphon*, Pl = *Planolites*, Te = *Teichichnus*, Ta = *Taenidium*, Th = *Thalassinoides*, and Ch = *Chondrites*). In both LOD and DOL piped zones, *Zoophycos* spreiten are dominated by pelleted lamellae that can be linked, based on color and composition, to overlying source beds.

models. Nonetheless, some exceptions to these trends in spreite organization have been observed. Locklair and Savrda (1998a) noted the apparent absence of pellets in some lamellae containing vertically advected sediment. More significant, the author has noted in several spreiten the presence of lamellar components that resemble neither the surrounding sediment nor the overlying source bed. As an example, a *Zoophycos* spreite within a LOD piped zone was observed to contain a ~4-cm-wide lamella consisting of very dark gray to black, apparently organic-rich, carbonate-poor clay. Such deviations from the normal spreite organization originally confounded behavioral interpretation but ultimately provided the inspiration for hypothesized lamella stratigraphy. The clay-dominated sediment in the dark lamella likely reflects surface feeding shortly after a pulsed flux of clastic sediment to a carbonate-dominated shelf, presumably related to a storm event that is not recorded in the now homogeneous chalk above.

The dark, clay-rich lamella apparently manifests a short-term change in sediment delivery to the seafloor. Do *Zoophycos* spreiten contain records of

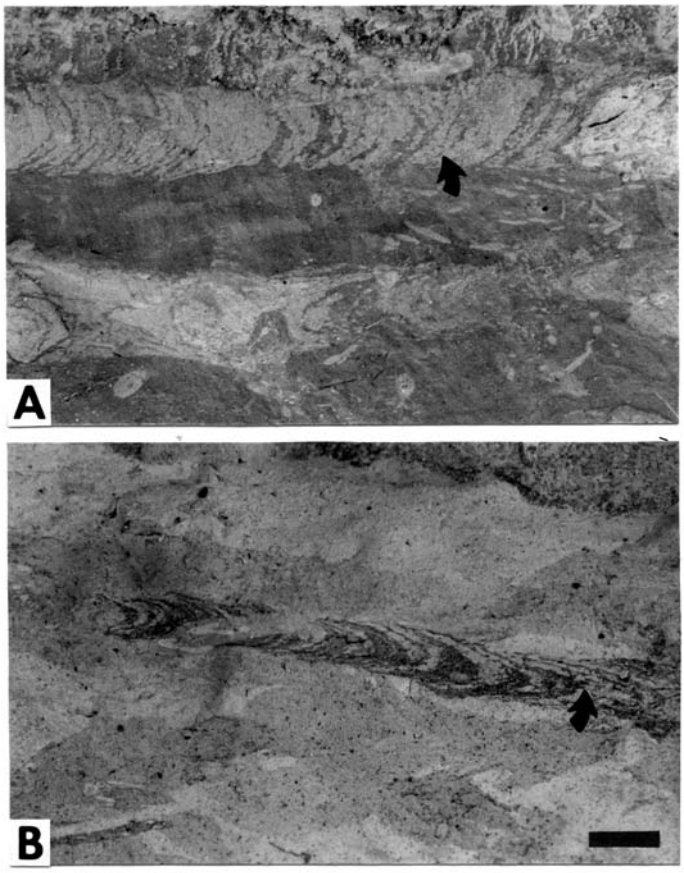

Figure 7. *Zoophycos* in LOD (A) and DOL (B) piped zones of Demopolis Chalk. Note pelletization of lighter sediments in spreite in A (e.g., at arrow). Although more obscure, pelletization of darker parts of spreite is apparent on the right end of the spreite in B (arrow). Scales for both photos are the same (scale bar = 1 cm long).

other less conspicuous variations in depositional regime that were otherwise erased by mixed-layer bioturbation? Do pelleted lamellae preserve a record of more subtle short-term changes in the relative fluxes of carbonate and clastics? Do they contain a record of variation in microfossil constituents that might reflect high-frequency variations in productivity? Do lamellae preserve an account of stable isotopic shifts that reflect paleoceanographic perturbations? Answers to these and related questions may be gleaned from careful study of *Zoophycos* lamellae in deposits like the Demopolis Chalk. Anticipating that the answer to some of these queries is at least a qualified "yes," it is worth considering some potential applications, including the study of depositional cyclicity.

5. POTENTIAL APPLICATION IN CYCLOSTRATIGRAPHY

Decimeter-scale bedding rhythms common in pelagic carbonate sequences, particularly those of Cretaceous age, have been linked to changes in the climate-ocean system driven by Milankovitch orbital cycles (e.g., Fischer, 1991; Schwarzacher, 1993; de Boer and Smith, 1994; and references therein). The sedimentologic response in marine settings to orbitally-induced climate changes is variable. Carbonate rhythms have been attributed to one or a combination of paleoceanographic

s, the most important of which in shallower-water sequences are variations in the production of biogenic carbonate (productivity cycles) and the influx of clastic sediments (dilution cycles; Arthur *et al.*, 1986).

Although sometimes vexing (see Arthur *et al.*, 1984), the discrimination between productivity and dilution cycles can be made for particular rhythmite sequences. The chalk-marl rhythms of the Demopolis Chalk, for example, are believed to be related primarily to dilution cycles; i.e., marls represent periods of increased flux of clastic muds (Warren and Savrda, 1998; Locklair and Savrda, 1998a). But, how did this dilution mechanism operate? Carbonate time series for the Demopolis Chalk (Warren and Savrda, 1998) exhibit high-amplitude cycles through which carbonate content appears to change more or less gradually (Fig. 8A). This could imply that changes in clastic flux occurred slowly over the course of each cycle, perhaps reflecting gradual changes in precipitation and runoff (Fig. 8B). However, there are other tenable, seemingly more credible explanations. Perhaps a steady background level of clastic input was maintained and, instead, deposition was controlled by long-term, climate-induced changes in the frequency and/or magnitude of short-term, pulsed clastic sedimentation episodes (Fig. 8C, D) associated, perhaps, with storm events. In this case, although the long-term cycle is preserved, the record of the higher-frequency events does not withstand the time-averaging effects of continuous bioturbation.

These and other potential explanations cannot be assessed effectively for bioturbated pelagic sequences using traditional sedimentologic or stratigraphic approaches. However, lamella stratigraphy of *Zoophycos* potentially can help address these types of problems. For example, comparative studies of spreiten in LOD and DOL piped zones might reveal recognizable differences in the frequency (and perhaps magnitude) of pulsed clastic depositional events between chalk and marl phases. In a similar way, geochemical and microfossil analyses of *Zoophycos* spreiten might reveal other types of short-term changes that can be applied towards a better

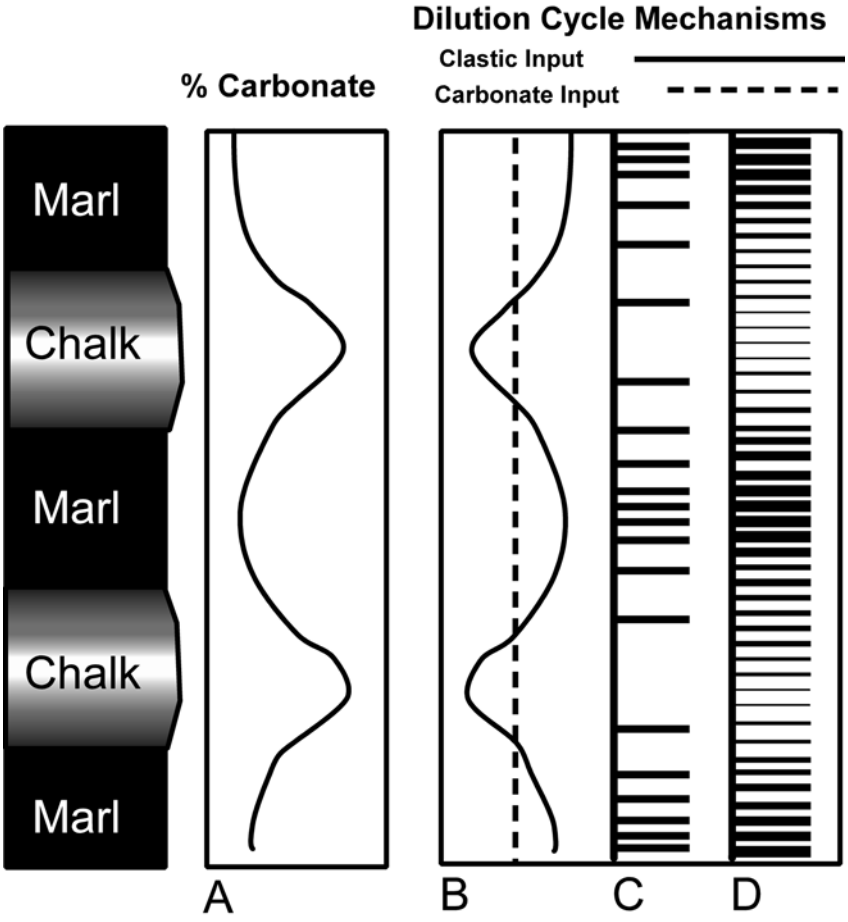

Figure 8. Schematic representation of potential mechanisms responsible for dilution cycles manifested in bioturbated chalk-mark sequences. Due to time-averaging, it normally is not possible to determine if apparently gradual, decimeter-scale changes in carbonate content (A) are the product of gradual changes in the background flux of clastic sediment (B) or of changes in the frequency (C) and/or magnitude (D) of pulsed clastic delivery events. Lamella stratigraphy of associated *Zoophycos* spreiten potentially can assist in evaluating depositional mechanisms.

understanding of cyclic and event processes and responses in pertinent depositional systems.

6. SUMMARY

Ichnology has been employed in various stratigraphic applications to decipher processes that operated over periods as short as 10^4 to 10^5 years.

For pelagic/hemipelagic strata, applications requiring even higher resolution are generally thwarted by the bioturbation process itself, because random mixing and preferential vertical advection of sediments by burrowers result in significant time averaging. Nonetheless, trace fossils produced by certain organisms – those that non-selectively feed at the seafloor and then convey their waste products to substrate depths that are less vulnerable to intense biogenic mixing – may preserve records of depositional processes and pulsed delivery events that otherwise are erased by bioturbation at shallower substrate levels. Although other ichnotaxa also may warrant consideration (e.g., *Phymatoderma*; see Miller and Aalto, 1998), *Zoophycos* spreiten that reflect the pertinent behavioral routine present a prime opportunity to evaluate this hypothesis. These structures, which are relatively common in pelagic/hemipelagic deposits, were produced by deep-tier, presumably long-lived, sessile, reverse conveyor feeders that sequentially added new lamellae composed of seafloor-derived sediments.

The extent to which meaningful *Zoophycos* lamella stratigraphies can be constructed and then applied towards an understanding of cyclic sedimentation and event processes hidden in bioturbated, time-averaged sequences has not yet been gauged. Determining whether the approach is whimsical or worthwhile will require a closer look at sedimentologic, geochemical, and micropaleontologic variability within *Zoophycos* spreiten. Further studies of these ichnofossils preserved at bed transitions within the Demopolis Chalk are planned.

ACKNOWLEDGMENTS

The author is grateful to the volume editor for encouraging the contribution of this paper, and to Mary L. Droser and an anonymous reviewer for critiques of an earlier version of this manuscript.

REFERENCES

Arthur, M. A., Dean, W. E., Bottjer, D. J., and Scholle, *P.* A., 1984, Rhythmic bedding in Mesozoic-Cenozoic pelagic carbonate sequences: The primary and diagenetic origin of Milankovitch-like cycles: in: *Milankovitch and Climate, Part I* (A. L. Berger *et al.*, eds.), D. Reidel Publishing Co., Dordrecht, p*p.* 191-222.

Arthur, M. A., Bottjer, D. J., Dean, W. E., Fischer, A. G., Hattin, D. E., Kauffman, E. G., Pratt, L. M., and Scholle, *P.* A., 1986, Rhythmic bedding in Upper Cretaceous pelagic carbonate sequences: Varying sedimentary response to climatic forcing, *Geology* **14**:153-156.

Bates, R. L., and Jackson, J. A., 1987, *Glossary of Geology, Third Edition*, American Geological Institute, Alexandria.

Berger, W. H., and Johnson, R. F., 1978, On the thickness and ^{14}C age of the mixed layer in deep-sea carbonates, *Ear. Planet. Sci. Let*. **41**:223-227.

Berger, W. H., Ekdale, A. A., and Bryant, *P.* F., 1979, Selective preservation of burrows in deep-sea carbonates, *Mar. Geol*. **32**:205-230.

Bromley, R. G., 1991, *Zoophycos*: Strip mine, refuse dump, cache, or sewage farm?, *Lethaia* **24**:460-462.

Bromley, R. G., 1996, *Trace Fossils – Biology, Taphonomy, and Applications*, Chapman and Hall, London.

Chang, A. S., Grimm, K. A., and White, L. D., 1998, Diatomaceous sediments from the Miocene Monterey Formation, California: A lamina-scale investigation of biological, ecological, and sedimentary processes, *Palaios* **13**:439-458.

de Boer, *P.* L., and Smith, D. G., 1994, Orbital forcing and cyclic sequences, in: *Orbital Forcing and Cyclic Sequences* (*P.* L. de Boer and D. G. Smith, eds.), *Int. Assoc. Sed. Sp. Pub*. **19**:1-14

Ekdale, A. A., 1985, Paleoecology of the marine endobenthos, *Palaeogeo. Palaeoclim, Palaeoeco.* **50**:63-81.

Ekdale, A. A., 1992, Muckraking and mudslinging: The joys of deposit-feeding, in: *Trace Fossils* (C. G. Maples and R. R. West, eds.), *Paleont. Soc. Short Course* **5**:145-171.

Ekdale, A .A., and Bromley, R. G., 1991, Analysis of composite ichnofabrics: An example in uppermost Cretaceous chalk of Denmark, *Palaios* **6**:232-249.

Ekdale, A. A., and Lewis, D. W., 1991, The New Zealand *Zoophycos* revisited: Morphology, ethology, and paleoecology, *Ichnos* **1**:183-194.

Ekdale, A. A., Bromley, R. G., and Pemberton, S. G., 1984a, Ichnology- Trace fossils in sedimentology and stratigraphy, *SEPM Short Course* **15**:317 p.

Ekdale, A. A., Muller, L. N., and Novak, M. T., 1984b, Quantitative ichnology of modern pelagic deposits in the abyssal Pacific, *Palaeogeo. Palaeoclim. Palaeoeco.* **45**:189-223.

Fatherree, J. W., Harries, *P.* J., and Quinn, T. M., 1998, Oxygen and carbon isotopic "dissection" of *Baculites compressus* (Mollusca: Cephalopoda) from the Pierre Shale (Upper Campanian) of South Dakota: Implication for paleoenvironmental reconstructions, *Palaios* **13**:376-385.

Fischer, A. G., 1991, Orbital cyclicity in Mesozoic strata, *Ann. Rev. Ear. Planet. Sci*. **14**:335-376.

Fu, S., and Werner, F., 1995, Is *Zoophycos* a feeding trace?, *N. Jahrb. Geol. Paläont. Abh.* **195**:37-47.

Guinasso, N. L., and Schink, D. R., 1975, Quantitative estimates of biological mixing in abyssal sediments: *J. Geophys. Res*. **80**:3032-3043.

Hantzschel, W., 1975, Trace fossils and problematica: in: *Treatise on Invertebrate Paleontology, Part W, Miscellaneous, Supplement 1, 2nd Edition* (Teichert, C., ed.), Geological Society of America and Kansas University Press, Boulder, and Lawrence.

Jumars, *P.* A., Mayer, L. M., Deming, J. W., Baross, J. A., and Wheatcroft, R. A., 1990, Deep-sea deposit-feeding strategies suggested by environmental and feeding constraints, *Phil. Trans. R. Soc. Lond.* **A331**:85-101.

Kirby, M. X., Soniat, T. M., and Spero, H. J., 1998, Stable siotope sclerochronology of Pleistocene and Recent oyster shells (*Crassostrea virginica*), *Palaios* **13**:560-569.

Kotake, N., 1989, Paleoecology of the *Zoophycos* producers, *Lethaia* **22**:379-385.

Kotake, N., 1991, Non-selective surface deposit feeding by the *Zoophycos* producers, *Lethaia* **24**:379-385.

Kotake, N., 1992, Deep-sea echiurians: Possible producers of *Zoophycos*, *Lethaia* **25**:311-316.

Kotake, N., 1993, Tiering of trace fossil assemblages in Plio-Pleistocene bathyal deposits of

Boso Peninsula, Japan, *Palaios* **8**:544-553.

Kotake, N., 1994, Population paleoecology of the *Zoophycos*-producing animal, *Palaios* **9**:84-91.

Locklair, R. E., and Savrda, C. E., 1998a, Ichnology of rhythmically bedded Demopolis Chalk (Upper Cretaceous, Alabama): Implications for paleoenvironment, depositional cycle origins, and tracemaker behavior, *Palaios* **13**:423-438.

Locklair, R. E., and Savrda, C. E., 1998b, Ichnofossil tiering analysis of a rhythmically bedded chalk-marl sequence in the Upper Cretaceous of Alabama, *Lethaia* **31**:311-322.

MacEachern, J. A., Raychaudhuri, I., and Pemberton, S .G., 1992, Stratigraphic application of the *Glossifungites* ichnofacies: Delineating discontinuities in the rock record, in: *Application of Ichnology to Petroleum Exploration* (S. G. Pemberton, ed.), *SEPM Core Workshop* **17**:169-198.

MacNaughton, R. B., and Narbonne, G. M., 1999, Evolution and ecology of Neoproterozoic-Lower Cambrian trace fossils, NW Canada, *Palaios* **14**:97-115.

Miller, M. F., 1991, Morphology and paleoenvironmental distribution of Paleozoic *Spirophyton* and *Zoophycos*: Implications for the *Zoophycos* ichnofacies, *Palaios* **6**:410-425.

Miller, W., III, and Aalto, K. R., 1998, Anatomy of a complex trace fossil: *Phymatoderma* from Pliocene bathyal mudstone, northwestern Ecuador, *Paleont. Res*. **2**:266-274.

Olivero, D., and Gaillard, C., 1996, Paleoecology of Jurassic *Zoophycos* from south-eastern France, *Ichnos* **4**:249-260.

Pemberton, S. G., ed., 1992, *Application of Ichnology to Petroleum Exploration*, *SEPM Core Workshop* **17**:429 *p.*

Robbins, J. A., McCall, *P.* L., Fisher, J. B., and Krezoski, J. R., 1979, Effect of deposit feeders on migration of ^{137}Cs in lake sediments, *Ear. Planet. Sci. Let*. **42**:277-287.

Savrda, C. E., 1992, Trace fossils and benthic oxygenation, in: *Trace Fossils* (C. G. Maples and R. R. West, eds.), *Paleont. Soc. Short Course* **5**:172-196.

Savrda, C. E., 1995, Ichnologic applications in paleoceanographic, paleoclimatic, and sea-level studies, *Palaios* **10**:565-577.

Savrda, C. E., Browning, J. V., Krawinkel, H., and Hesselbo, S. P., 2001, Firmground ichnofabrics in deep-water sequence stratigraphy, Tertiary clinoform-toe deposits, New Jersey slope, *Palaios* **16**:294-305.

Schwarzacher, W., 1993, *Cyclostratigraphy and Milankovitch Theory*, Elsevier, Amsterdam, *Devel. Sed*. **52**:225 p.

Seilacher, A., 1967, Fossil behaviour, *Sci. Am*. **217**:72-80.

Simpson, S., 1970, Notes on *Zoophycos* and *Spirophyton*, in: *Trace Fossils* (T. *P.* Crimes and J. C. Harper, eds.), *Geol. J. Sp. Iss*. **3**:505-514.

Smith, C. R., 1994, Tempo and mode in deep-sea benthic ecology: Punctuated equilibrium revisited, *Palaios* **9**:3-13.

Soutar, A., Johnson, S. R., and Baumgartner, T. R., 1981, In search of modern analogs to the Monterey Formation, in: *The Monterey Formation and Related Siliceous Rocks of California*, *SEPM Pac. Sec. Sp. Pub*. **15**:123-147.

Thornton, S. E., 1984, Basin model for hemipelagic sedimentation in a tectonically active continental margin: Santa Barbara Basin, California continental borderland, in: *Fine-Grained Sediments: Deep-Water Processes and Facies* (D. A. V. Stow and D. J. W. Piper, eds.), *Geol. Soc. Lond. Sp. Pub*. **15**:377-394.

Warren, J. D., and Savrda, C. E., 1998, Carbonate cycles in Upper Cretaceous (Campanian) Demopolis Chalk, west-central Alabama, *Gulf Coast Assoc. Geol. Soc. Trans*. **48**:487-497.

Wetzel, A., 1983, Biogenic sedimentary structures in a modern upwelling regime: Northwest Africa, in: *Coastal Upwelling and its Sedimentary Record, Part B, Sedimentary Records of*

Ancient Coastal Upwelling (J. Thiede and E. Suess, eds.), Plenum, New York, p*p.* 123-144.

Wetzel, A., 1991a, Stratification in black shales: Depositional models and timing- an overview: in: *Cycles and Events in Stratigraphy* (G. Einsele, W. Ricken, and A. Seilacher, eds.), Springer Verlag, Berlin, p*p.* 508-523.

Wetzel, A., 1991b, Ecologic interpretation of deep-sea trace fossil communities, *Palaeogeo. Palaeoclim. Palaeoeco*. **85**:47-69.

Wetzel, A., and Werner, F., 1981, Morphology and ecological significance of *Zoophycos* in deep-sea sediments, *Palaeogeo. Palaeoclim. Palaeoeco*. **32**:185-212.

Chapter 5

Variation in Adult Size of Scaphitid Ammonites from the Upper Cretaceous Pierre Shale and Fox Hills Formation

NEIL H. LANDMAN, SUSAN M. KLOFAK, and KATHLEEN B. SARG

NEIL H. LANDMAN • American Museum of Natural History, 79th Street and Central Park West, New York, NY 10024-5192. SUSAN M. KLOFAK • American Museum of Natural History, 79th Street and Central Park West, New York, NY 10024-5192 and Department of Biology, City College of the City University of New York, Convent Avenue and 138th Street, New York, NY 10031. KATHLEEN B. SARG • American Museum of Natural History, 79th Street and Central Park West, New York, NY 10024-5192.

P.J. Harries (ed.), *High-Resolution Approaches in Stratigraphic Paleontology.*

1. INTRODUCTION

The rich fossil record of ammonites provides an opportunity to investigate the size variation of an individual ammonite species over its geographic and temporal range. However, the requirements for such studies are daunting: a sufficiently large sample for statistical analysis, a series of closely spaced geographic localities with detailed stratigraphic data about the distribution of specimens at each locality, a means of precisely correlating from one stratigraphic section to another, a knowledge of the taxonomy of the species that takes into account the possibility of sexual dimorphism, and, finally, an understanding of the ontogeny of the species to facilitate comparisons of specimens at the same ontogenetic stage.

The ammonites in the Upper Cretaceous Western Interior Seaway satisfy many of these requirements. These ammonites are abundant, widely distributed, and occur in a well-documented lithostratigraphic and biostratigraphic sequence (see, for example, the numerous papers by W. A. Cobban and W. J. Kennedy). Among the ammonites from the Western Interior, none surpasses the scaphites in affording excellent material for study. They combine superb preservation, easily identifiable growth stages, and clearly defined dimorphs (Cobban, 1969). As in other ammonites (Calloman, 1981; Davis et al., 1996), the dimorphs are referred to as macroconchs (presumed to be the females) and microconchs (presumed to be the males).

This paper concentrates on a single scaphite species, *Hoploscaphites nicolletii* (Morton, 1842), that is endemic to North and South Dakota. It occurs in the Upper Cretaceous (Maastrichtian) Pierre Shale and Fox Hills Formation. The stratigraphy and paleoenvironments of the Fox Hills Formation have been documented by Waage (1968), and the scaphites from this formation have been monographed by Landman and Waage (1993). In this paper, we examine the variation in the size at maturity of this species both stratigraphically and geographically. Most of this study concerns the

macroconchs because they constitute the bulk of the sample. There are three closely related sets of questions:

1) What is the geographic variation in adult size of the macroconchs in one time interval? Are there differences in size related to differences in the environment? The geographic area over which this species occurs ranges from several 100 to approximately 3000 km^2 depending on the time interval considered. Present-day cephalopods commonly show a variety of distributional patterns related to distance from shore (see Boyle, 1983). Are any patterns discernible in this species at the level of time resolution available?

2) What is the stratigraphic (= temporal) variation in adult size of this species? Is there a unidirectional trend? How does such a trend relate to changes in the environment? The time period over which this species lived is approximately 0.75 Ma (based on an interpolation of the age estimates given in Kauffman et al., 1993). If there is stratigraphic variation in adult size, do both dimorphs show the same pattern?

3) Is there any evidence of more than one size class in the macroconchs of this species? Several studies of scaphites have documented wide variation in the size at maturity within a single dimorph (Cobban, 1969; Kennedy, 1986a, b). Size-frequency histograms of some of the scaphite species from the Fox Hills Formation have suggested the possibility of two macroconch size classes per species (Landman and Waage, 1993, figs. 57, 58, 75, 89, 112, and 134). In a provocative study on Jurassic ammonites, Matyja (1986, 1994) identified as many as three morphs per species. He argued that such morphs represented individuals that matured at different sizes due to differences in rate of growth and age at maturity and called this phenomenon "developmental polymorphism" (but see Callomon, 1988, for a counter-argument). In support of this interpretation, he cited several studies of present-day cephalopods in which different populations, sometimes belonging to the same sex, reached maturity at different sizes.

The macroconchs of *Hoploscaphites nicolletii* all basically exhibit the same shape and ornament and presumably represent the same sex (female). However, as Matyja (1994) has argued, different populations of the same sex can mature at different ages and, therefore, can appear as different size classes. Our goal is to determine, given a large enough sample, whether there is, in fact, any evidence for more than one size class in these macroconchs.

2. GEOGRAPHIC AND STRATIGRAPHIC SETTING

The specimens used in this study were obtained from the lower part of

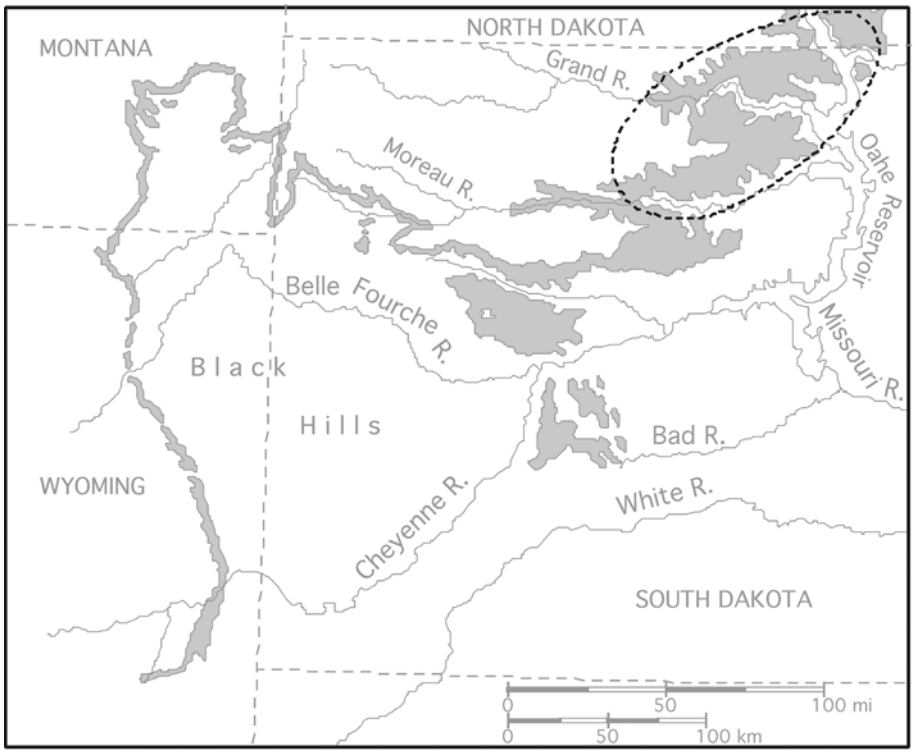

Figure 1. Map of the Fox Hills Formation outcrop (shaded area) showing the study area (dashed line).

the Fox Hills Formation in north-central South Dakota (referred to as the type area, Waage, 1968) and south-central North Dakota and from the upper part of the underlying Pierre Shale in north-central South Dakota (Fig. 1). These areas lie in portions of Corson, Ziebach, and Dewey counties, South Dakota, and in Emmons County, North Dakota.

In the Pierre Shale, *Hoploscaphites nicolletii* occurs at only one locality in the Elk Butte Member, just below the base of the Fox Hills Formation (Fig. 2). This member consists of silty clays with occasional sideritic and limestone concretions and contains few macrofossils, although small linguloid brachiopods are locally common (Waage, 1968).

In the Fox Hills Formation, *Hoploscaphites nicolletii* ranges through the lowermost 15 m of the Trail City Member (Waage, 1968). This member is divisible into two laterally intergrading lithofacies, the Little Eagle and Irish Creek lithofacies (Fig. 2). The Little Eagle lithofacies occurs in the eastern two-thirds of the type area of the Fox Hills Formation. It consists of bioturbated clayey silts and contains numerous layers of concretions, many

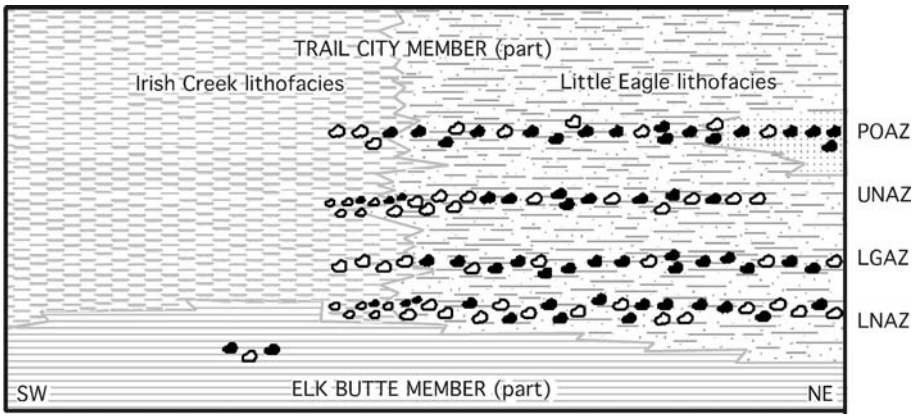

Figure 2. Simplified stratigraphic section of portions of the Elk Butte Member of the Pierre Shale and of the Trail City Member of the Fox Hills Formation in north-central South Dakota. *Hoploscaphites nicolletii* occurs in the upper part of the Elk Butte Member and in each of the assemblage zones in the lower Trail City Member (LNAZ = Lower *nicolletii* Assemblage Zone; LGAZ = *Limopsis-Gervillia* Assemblage Zone; UNAZ = Upper *nicolletii* Assemblage Zone; POAZ = *Protocardia-Oxytoma* Assemblage Zone). The Elk Butte Member is a thinly laminated silty shale. The Trail City Member consists of two facies, the Irish Creek lithofacies in the west, a sequence of thinly interbedded siltstone and shale, and the Little Eagle lithofacies in the east, a bioturbated clayey siltstone with numerous layers of fossiliferous concretions. There is an influx of sand in POAZ. Closed symbols represent fossiliferous concretions; open symbols, unfossiliferous.

of which are abundantly fossiliferous and furnish most of the material for this study. This lithofacies becomes increasingly sandy upward and grades into the overlying Timber Lake Member. The Irish Creek lithofacies occurs in the western third of the type area and consists of thinly interbedded clays and silts with few macrofossils.

3. DISTRIBUTION OF *HOPLOSCAPHITES NICOLLETII* IN THE TRAIL CITY MEMBER

Hoploscaphites nicolletii occurs in four assemblage zones in the Trail City Member (Fig. 2; Waage, 1964, 1968). Each zone consists of one or more concretionary layers and is characterized by a distinctive assemblage of fossils including ammonites, gastropods, and bivalves. The zones are described below in stratigraphic order from oldest to youngest.

3.1 Lower *nicolletii* Assemblage Zone (LNAZ)

This zone covers the broadest geographic area of the four assemblage

zones, approximately 3,000 km^2 in South Dakota; it is also present in Emmons County, North Dakota (Waage, 1968, fig. 16). In South Dakota, this zone forms a lobate pattern extending from the Grand to the Moreau rivers. Macroconchs of *Hoploscaphites nicolletii* are very abundant in this zone and have been estimated to number in the hundreds of millions (Waage, 1964, 1968). This zone consists of a northeastern and a southwestern phase of fossil distribution (Waage, 1968, p. 64, fig. 16 where the boundary between these two phases is indicated by the dashed line demarcating the "limit of large concretions with abundant *S. (H.) nicolleti*"). The change from one phase to the other is gradual and occurs in the southwestern portion of the Little Eagle lithofacies several kilometers east of the transition to the Irish Creek lithofacies. The northeastern phase is characterized by several layers of large concretions (up to 0.5 m diameter; Waage, 1968, pl. 2A, B), many of which contain numerous macroconchs of *H. nicolletii*. The southwestern phase is characterized by smaller concretions (up to 0.1 m diameter; Waage, 1968, pl. 2C) scattered among occasional larger ones. The macroconchs of *H. nicolletii* in this area tend to occur in the small concretions as single specimens. These small concretions occupy approximately the same stratigraphic position as the larger concretions to the northeast and are presumably co-eval.

3.2 *Limopsis-Gervillia* Assemblage Zone (LGAZ)

This zone covers nearly the same geographic area as LNAZ (approximately 2,500 km^2 in South Dakota) and is also present in North Dakota (Waage, 1968, fig 17). The concretions in this zone are richly fossiliferous but have fewer macroconchs of *Hoploscaphites nicolletii* both in terms of absolute numbers and as a percentage of the total fauna than those in LNAZ. In addition, there is no transition from large fossiliferous concretions in the northeast to smaller, less fossiliferous concretions in the southwest.

3.3 Upper *nicolletii* Assemblage Zone (UNAZ)

This zone covers the smallest geographic area of any zone (approximately 900 km^2) and is limited to a narrow band extending from the Grand to Moreau rivers (Waage, 1968, fig. 18). UNAZ, like LNAZ, shows two phases, a northeastern phase of large fossiliferous concretions and a southwestern phase of smaller, more sparsely fossiliferous concretions (Waage, 1968, p. 65, 66, fig. 18 where the boundary between these two phases is indicated by the dashed line demarcating the "area of concretions with abundant *nicolleti*"). The change from one phase to the other occurs in

the southwestern portion of the Little Eagle lithofacies near the start of the transition to the Irish Creek lithofacies. (Note that the actual geographic position of this boundary is different from that in LNAZ.) The small concretions have been referred to as *Actinosepia* concretions by Waage (1965, 1968, p. 67, 68), because some of them contain specimens of the coleoid *Actinosepia canadensis* Whiteaves. Scaphites also occur in these small concretions as single specimens. These small concretions occupy approximately the same stratigraphic position as the larger, more fossiliferous concretions to the northeast and are presumably co-eval.

3.4 *Protocardia-Oxytoma* Assemblage Zone (POAZ)

This zone covers approximately 2,300 km^2 in South Dakota but does not extend into North Dakota (Waage, 1968, fig. 18). The concretions in this zone gradually become unfossiliferous toward the western edge of the Little Eagle lithofacies but do not show two phases of fossil distribution. This zone also differs from LNAZ and UNAZ in having fewer macroconchs of *Hoploscaphites nicolletii* in terms of both absolute numbers and as a percentage of the total fauna.

4. PALEOENVIRONMENTAL RECONSTRUCTION

Both the Elk Butte and Trail City members represent subtidal environments seaward of an advancing delta in the west (see Cobban et al. 1994, for the position of the western shoreline in the slightly older zone of *Baculites clinolobatus*). The Elk Butte Member was deposited in an offshore environment below wave base (Rhoads et al., 1972). The Trail City Member was deposited in a subtidal environment on and around a submarine sand body that prograded into the type area of the Fox Hills Formation from the northeast (Waage, 1968). The well-mixed sediments of the Little Eagle lithofacies indicate the existence of a more favorable environment for infaunal organisms than do the relatively undisturbed sediments of the Irish Creek lithofacies.

According to Waage (1968), the four assemblage zones in the Trail City Member represent periodic slack periods in the growth of the submarine sand body and the consequent re-establishment of hospitable living conditions, probably associated with a southwest flowing current. The major environmental change in the Trail City Member occurred during POAZ at which time there was an increase in the amount of sand, indicating an advance of the submarine sand bar into the study area.

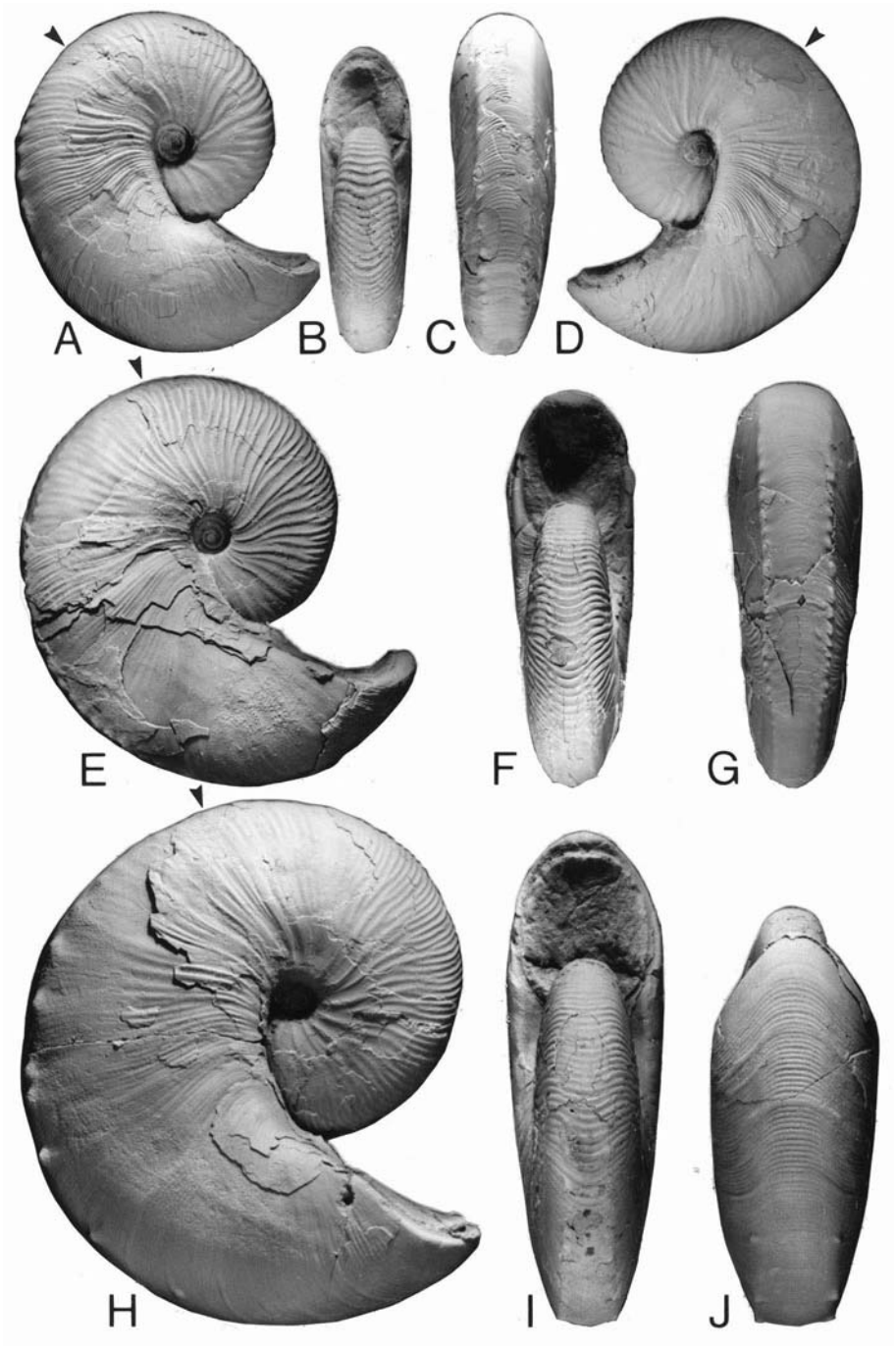
A
B
C
D
E
F
G
H
I
J

The fossil accumulations in the Trail City Member probably represent mass mortalities without much subsequent transport (Waage, 1964; 1968, p. 554). The cause of this mortality is unknown, but it may be related to perturbations in the environment (e.g., a sudden influx of freshwater into the area or a rapid depletion of oxygen) or incidents in the life history of the animals themselves (e.g., mass mortality of the scaphite macroconchs following spawning). Whatever the event, it seems to have occurred nearlysimultaneously over a broad geographic area; this is indicated by the fact that the fossil accumulations are widely distributed and are homogeneous in faunal composition and mode of occurrence throughout most of their extent. The common occurrence of jaws inside scaphite body chambers attests to rapid burial with little subsequent transport. Thus, these accumulations probably reflect the original geographic distribution of the animals involved, an essential prerequisite for this study.

5. DESCRIPTION *OF HOPLOSCAPHITES NICOLLETII*

All of the specimens in this study belong to *Hoploscaphites nicolletii*. The morphology of this species has been described in detail by Landman and Waage (1993), and only a brief summary is presented here. This species is easily differentiated into dimorphs, which are distinguished mainly by morphology, not size.

The adult macroconch is moderately large, compressed, and tightly coiled (Figs. 3, 4). It is subcircular in overall outline. The shaft of the body chamber is short. As in other scaphitid macroconchs, the umbilical shoulder of the shaft is straight in lateral view. However, there is some variation with respect to size. In very large specimens, a dorsal swelling sometimes appears on the umbilical shoulder. In very small specimens, the umbilical shoulder is slightly concave rather than straight. There is only a small gap or none at all between the phragmocone and hook. The anterior portion of the body chamber is covered by fine, closely spaced ribs. Ventrolateral tubercles occur on the adapical portion of the body chamber and are generally closely spaced. They attain their maximum size at mid-shaft

Figure 3. Hoploscaphites nicolletii (Morton, 1842), macroconchs, Trail City Member, Fox Hills Formation. A-D. Small adult (LMAX = 46.5 mm), hypotype, YPM 27224, loc. 44, LNAZ, North Dakota. A, Right lateral; B, apertural; C, ventral; D, left lateral. E-G. Average size adult (LMAX = 57.0 mm), neotype, YPM 27222, loc. 54, LNAZ, South Dakota. E, Right lateral; F, apertural; G, ventral. H-J. Large adult (LMAX = 71.2 mm), hypotype, YPM 27247, loc. 62, POAZ, South Dakota. H, Right lateral; I, apertural; J, ventral hook. The arrows mark the base of the body chamber. All natural size.

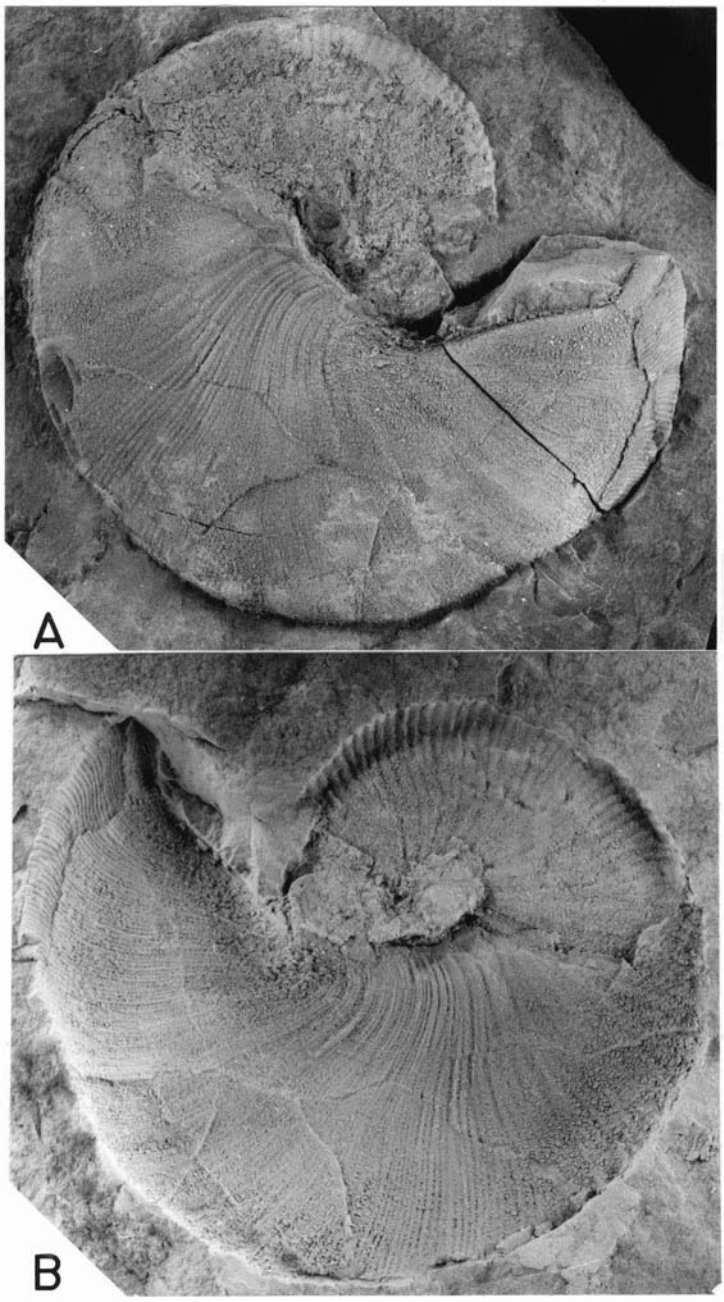

Figure 4. Hoploscaphites nicolletii (Morton, 1842), large macroconch (LMAX = 89.0 mm) in sideritic concretion, hypotype, YPM 27227, loc. 307, uppermost Elk Butte Member, Pierre Shale, South Dakota. A, Right lateral; B, mold in concretion. Both natural size.

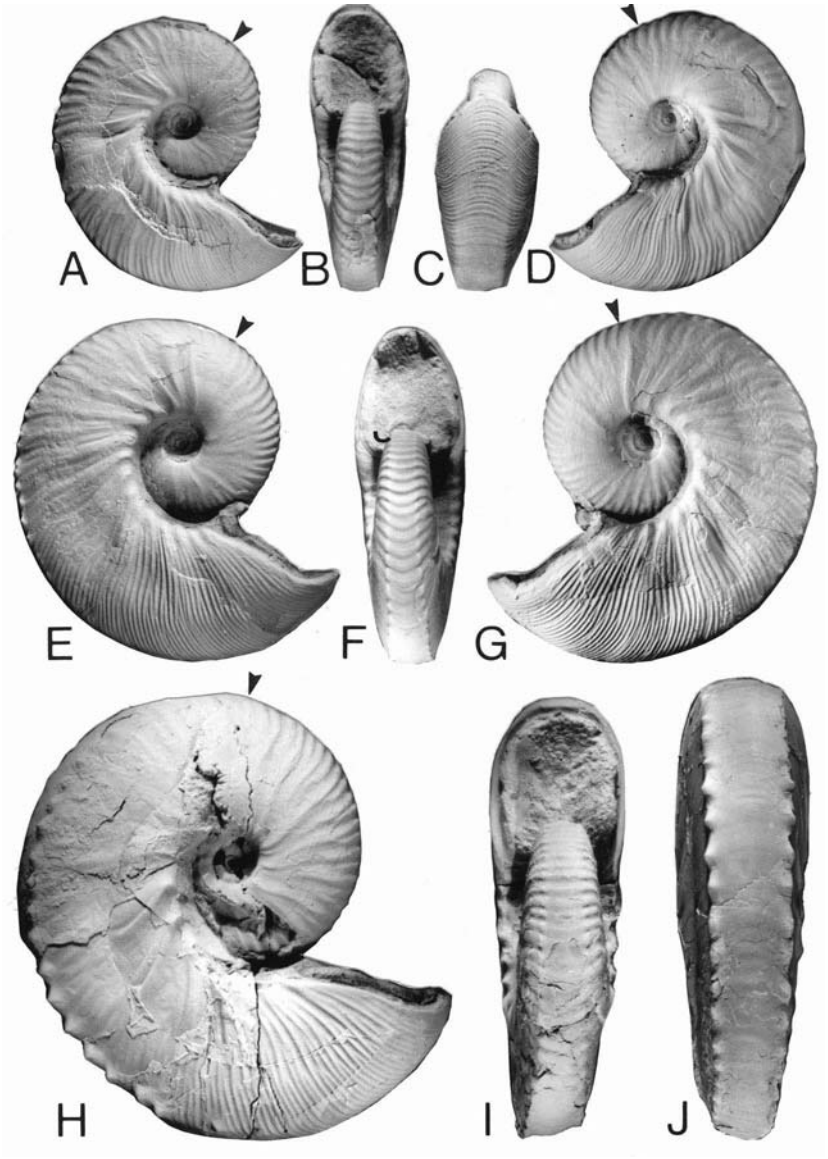

Figure 5. *Hoploscaphites nicolletii* (Morton, 1842), microconchs, Fox Hills Formation, South Dakota. A-D. Small adult (LMAX = 38.0 mm), hypotype, YPM 23707, loc. 52, UNAZ. A, Right lateral; B, apertural; C, ventral hook; D, left lateral. E-G. Average size adult (LMAX = 48.2 mm), hypotype, YPM 27236, loc. 17, UNAZ. E, Right lateral; F, apertural; G, left lateral. H-J. Large adult (LMAX = 62.2 mm), hypotype, YPM 27238, loc. 85, POAZ. H, Right lateral; I, apertural; J, ventral. The arrows mark the base of the body chamber. All natural size.

where they develop a clavate appearance.

The adult microconch is generally smaller than the macroconch but the two dimorphs overlap for part of their size range (Fig. 5). The umbilical shoulder of the shaft in microconchs parallels the curve of the venter, forming a flat, broad dorsal shelf that slopes gently outward at a right or obtuse angle to the flanks. In larger specimens, there is a gap between the phragmocone and hook. The shell is strongly compressed with nearly flattened flanks. Ribs are broad on the exposed phragmocone but become finer and more closely spaced on the adoral portion of the body chamber. Umbilicolateral bullae are usually present on the shaft and hook. Ventrolateral tubercles occur on the adapical portion of the body chamber, and, in some specimens, on the phragmocone.

6. MATERIAL

Most of our sample consists of macroconchs. The overwhelming abundance of macroconchs versus microconchs in the Fox Hills Formation was noted by Landman and Waage (1993) and probably reflects a taphonomic bias (? mass mortality of macroconchs following spawning, segregation of sexes, etc.). There are 1,279 macroconchs and 28 microconchs in our sample. The number of specimens in the Elk Butte Member and in each of the zones in the Trail City Member is given in Table 1. The specimens in the Trail City Member occur in concretions and are generally undeformed. The specimens in the Elk Butte Member also occur in concretions but are crushed laterally; however, they are well enough preserved to measure.

Table 1. Description of *Hoploscaphites nicolletii* samples.*

	Number of Specimens		Number of Localities	
	m	**M**	**m**	**M**
Trail City Member (total)	28	1279	22	92
POAZ	7	128	6	37
UNAZ	7	147	5	22
LGAZ	3	52	3	31
LNAZ	7	851	5	57
Elk Butte	-	21	-	1

*Note that the sum of the specimens for each of the zones in the Trail City Member is less than the total number of specimens for the Trail City Member because this total also includes specimens whose zone is unknown or in question. In contrast, the sum of the localities for each of the zones in the Trail City Member is more than the total number of localities for the Trail City Member because this total counts each locality only once even though it may appear in more than one zone. M = macroconch; m = microconch; zonal abbreviations are given in Fig. 2.

The vast majority of the specimens used in this study are housed in the Division of Invertebrate Paleontology (IP) at the Yale Peabody Museum (YPM). (The only exceptions are a few specimens from the Elk Butte Member that are housed in the American Museum of Natural History or in the private collection of Helen Ross (Timber Lake, South Dakota)). All of the YPM specimens were collected by Karl Waage and his students between 1956 and 1985. Data records for these specimens are stored in YPM's computerized catalog system Argus. Each specimen bears a YPM specimen number (e.g., 27224) and is identified by taxon and dimorph. Specimen numbers are linked to YPM-IP locality numbers that include information about stratigraphy (e.g., formation, member, zone, facies), geography (e.g., state, county, township, range), collector, and date of collection. YPM-IP locality numbers are in turn tied into Karl Waage's informal field numbers, which include only geographic information (YPM-IP locality numbers begin with a letter, e.g., A221, C382; Waage's informal field numbers do not). Each locality number (loc.), either in the YPM-IP series or in Waage's informal field number series, corresponds to a unique combination of latitude and longitude (the latter is given a negative sign in this study to indicate values west of the Greenwich Meridian). Because every specimen in the YPM database is cross-referenced by stratigraphy and geography, it is possible to generate lists of specimens for any zone, facies, and geographic area desired, thus making the present study possible.

There are a total of 92 localities for the macroconchs and a total of 22 localities for the microconchs (Table 1). These localities occur in exposures along the Grand River in Corson County and along the Moreau River in Dewey and Ziebach counties, South Dakota. There is also one locality (loc. 44) in Emmons County, North Dakota. The distribution of these localities does not fit any preconceived grid pattern but simply reflects where exposures are available and where specimens occur.

7. METHODOLOGY

The maximum size (LMAX) of each specimen was measured (Fig. 6). This is the standard measurement for size in scaphites as employed by Riccardi (1983, fig. 1) and Landman and Waage (1993, fig. 9). Two measurements were taken for each specimen using a digital caliper and the result was averaged to the nearest 0.1 mm.

To analyze the size variation of a sample, the mean ($\bar{x}$), standard deviation (SD), and skewness (Sk) were calculated, and size-frequency histograms were prepared using JMP version 3.2.1 for Apple Macintosh.

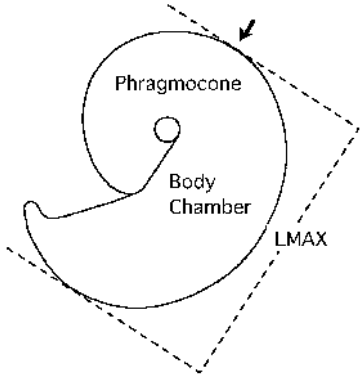

Figure 6. Diagram of a macroconch of *Hoploscaphites nicolletii* showing the measurement of maximum size (LMAX) used in this study. The arrow indicates the base of the body chamber.

The histograms were constructed using 5 mm-size intervals. Each size interval was defined so that LMAX was greater than or equal to a but less than b. For example, the 50-55 mm-size interval represents values of LMAX greater than or equal to 50 mm and less than 55 mm (in effect, less than or equal to 54.9 mm).

Starting with the macroconchs, a size-frequency histogram was prepared for each member. Next, the sample was analyzed by assemblage zone. The mean and standard deviation of the samples at each locality within a zone were calculated. The pool of locality means was subdivided into size groups of 5 mm each (e.g., means greater than or equal to 60 mm and less than 65 mm), and a different symbol was assigned to each size group. These symbols were plotted on a map of each assemblage zone according to locality.

The geographic pattern of size variation was examined within each assemblage zone. The locality means were regressed separately against latitude and longitude (based on current positions, not paleoreconstructions). We used a regression program that weighted each locality by its sample size (SAS version 6.12 for PC computers). In addition, samples from localities from different geographic areas were compared as follows: 1) samples from along the Grand River versus those from along the Moreau River simply because these two areas represent northern and southern populations without any samples in between and 2) samples from the northeastern phase versus those from the southwestern phase of fossil distribution in LNAZ and UNAZ.

To explore further size variation at specific sites and investigate the possible existence of multiple size classes at maturity, size-frequency histograms were prepared for individual localities with large sample sizes.

Size-frequency histograms of samples from individual concretions at these sites also were prepared because such concretions probably formed rapidly, preserving specimens that lived at nearly the same time (Waage, 1964).

Because the sample size of the microconchs is much smaller than that of the macroconchs, size-frequency histograms of the microconchs were prepared only for the Trail City Member and for each assemblage zone.

In evaluating results, student's t-tests (two-tailed) were used to compare sample means and to determine the departure of slopes from zero in regression analyses. Differences at the 0.05 level were considered statistically significant unless otherwise indicated. In multiple pairwise comparisons, the overall level of significance was further divided by the number of pairwise comparisons present to calculate a more conservative level of significance.

8. VARIATION IN ADULT SIZE OF *HOPLOSCAPHITES NICOLLETII* MACROCONCHS

8.1 Elk Butte Member

The size-frequency histogram of the macroconchs from the Elk Butte Member is shown in Figure 7. The sample consists of only 21 specimens. The distribution is nearly flat for most of its range. LMAX ranges from 73.0 mm to 101.6 mm with a mean of 86.6 mm. This mean is significantly higher (at the 0.001 level) than that of any assemblage zone from the Trail City

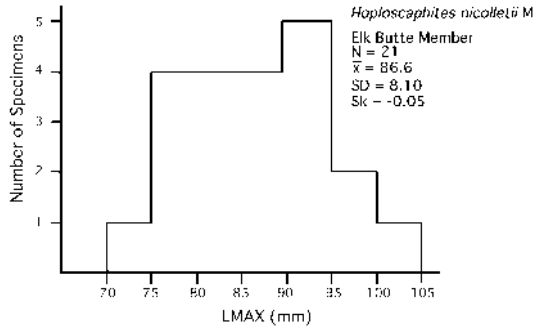

Figure 7. Size-frequency histogram of *Hoploscaphites nicolletii* macroconchs from the Elk Butte Member. Abbreviations: N = number of specimens; $\bar{x}$ = mean; SD = standard deviation; Sk = skewness.

Member. The ratio of the largest specimen to that of the smallest is 1.39.

8.2 Trail City Member

The size-frequency histogram of the macroconchs from the Trail City Member is shown in Figure 8. The size of the sample (N = 1,279) is much larger than that reported in Landman and Waage (1993, p. 85, fig. 57, N = 345) and includes approximately 600 additional specimens from LNAZ. The distribution is slightly asymmetric with a small right-hand tail. There is a single mode in the 55-60 mm-size interval. LMAX ranges from 42.7 mm to 92.3 mm with a mean of 59.7 mm. The ratio of the size of the largest specimen to that of the smallest is 2.16.

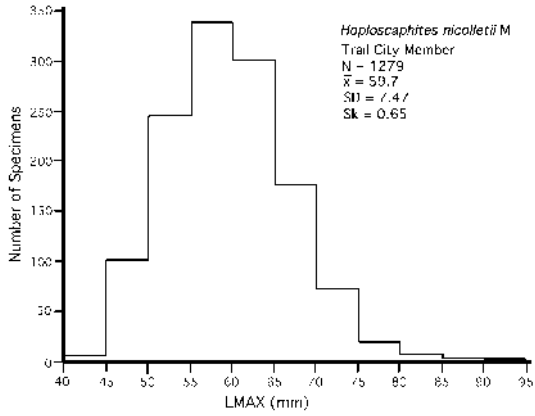

Figure 8. Size-frequency histogram of *Hoploscaphites nicolletii* macroconchs from the Trail City Member. This sample includes specimens from each of the assemblage zones as well as 101 specimens whose assemblage zone is unknown or in question. Abbreviations as in Fig. 7.

8.2.1 Lower *nicolletii* Assemblage Zone (LNAZ)

There are 851 specimens in the sample from this zone (Fig. 9; compare with Landman and Waage, 1993, table 7, fig. 58, N = 210). The size distribution is nearly symmetric with a small right hand tail and is similar in shape to the distribution for the entire Trail City Member. There is a single peak in the 55-60 mm-size interval. LMAX ranges from 42.7 mm to 92.3 mm, with a mean of 58.4 mm. The ratio of the size of the largest specimen to that of the smallest is 2.16.

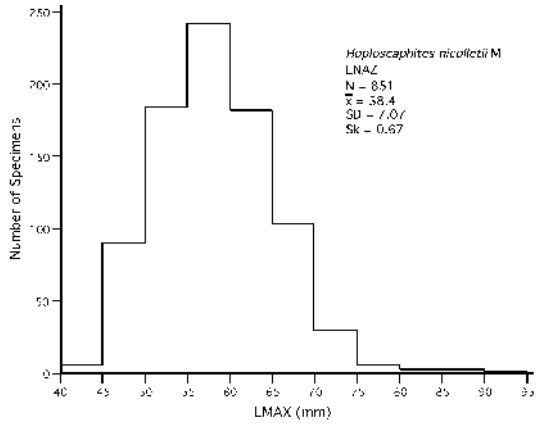

Figure 9. Size-frequency histogram of *Hoploscaphites nicolletii* macroconchs from LNAZ. This sample includes eight specimens whose localities are unknown. Abbreviations as in Fig. 7.

Table 2 presents a statistical analysis of the samples at 57 localities in North and South Dakota. Sample sizes vary widely from 1 to 105 specimens, but most localities are represented by more than 8 specimens. The locality means were analyzed as described in the methodology section. The results are presented in Figure 10.

Table 2. Adult size (LMAX) of *Hoploscaphites nicolletii* macroconchs at 57 localities in LNAZ.*

LOC	N	x	SD	MIN	MAX
1	12	57.4	5.03	51.0	64.9
6	12	60.4	7.69	49.2	73.3
8	9	55.8	6.46	46.5	65.8
10	2	51.2	2.69	49.3	53.1
17	2	59.3	7.21	54.2	64.4
18	15	56.8	7.43	45.7	67.3
20	24	57.8	6.14	48.5	67.7
21	87	58.2	6.70	42.7	74.7
25	1	58.6	-	-	-
34	1	53.0	-	-	-
44	105	58.1	7.94	43.2	89.8
46	13	54.7	4.88	47.3	62.5
47	13	57.7	5.63	49.0	71.0
50	70	57.6	6.40	44.9	73.8
51	5	61.2	4.90	55.1	66.5
52	10	67.8	9.51	57.1	92.3
53	50	56.0	5.86	46.9	70.6
54	67	56.7	5.42	47.0	69.7
55	19	56.7	5.30	46.9	68.0
63	22	61.3	6.46	45.4	70.5

Table 2. Continued.

64	9	60.0	6.29	50.9	73.2
66	22	58.9	7.17	44.7	74.5
69	1	75.7	-	-	-
70	2	57.9	11.63	49.7	66.2
79	13	60.2	9.05	48.7	77.1
88	5	66.1	3.40	61.3	69.8
89	2	61.0	0.11	61.0	61.1
95	4	59.3	10.5	49.9	73.9
99	14	60.1	5.80	49.8	70.0
104	15	57.7	6.38	49.4	69.7
116	2	60.6	1.66	59.4	61.8
118	1	47.7	-	-	-
120	9	58.4	6.82	46.8	66.4
177	38	58.2	6.52	46.0	73.5
191	2	60.0	1.24	59.2	60.9
193	3	63.8	2.98	60.8	66.8
204	3	65.0	6.35	57.8	69.8
206	4	57.0	7.14	49.6	64.8
208	22	56.9	6.59	48.2	67.9
209	45	58.8	8.32	44.7	86.7
216	13	61.1	9.06	45.6	77.0
218	3	59.3	11.19	47.5	69.7
219	12	62.5	7.67	55.6	83.2
229	2	62.7	5.87	58.5	66.8
231	2	76.8	13.93	66.9	86.6
234	1	65.9	-	-	-
236	2	53.1	5.44	49.3	57.0
237	1	72.6	-	-	-
238	7	59.6	3.90	53.9	64.4
240	1	56.0	-	-	-
242	5	61.8	6.06	55.9	71.1
243	7	65.8	8.51	58.3	81.6
246	2	65.0	5.48	61.1	68.8
249	15	60.6	5.69	50.4	71.0
256	1	70.7	-	-	-
303	12	56.3	4.83	51.4	68.6
C382	2	58.1	2.51	56.4	59.9

*LOC = locality number (= Karl Waage field number or YPM-IP locality number); x = mean (mm); SD = standard deviation; MIN = locality minimum (mm); MAX = locality maximum (mm).

The locality means were regressed separately against latitude and longitude, using a regression program that weighted each locality by its sample size. The analysis revealed a statistically significant relationship, with larger specimens in the southwest (at the 0.0001 level for both latitude and longitude). The analysis was rerun excluding the single locality in North

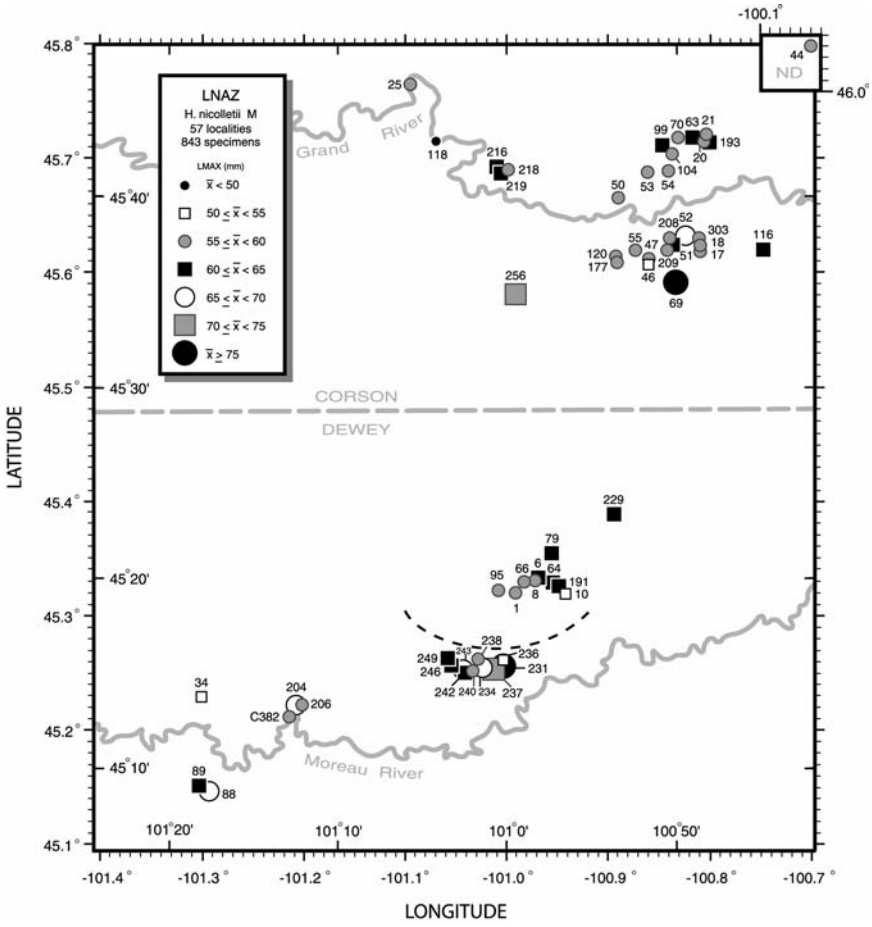

Figure 10. Map showing the mean size of the samples of *Hoploscaphites nicolletii* macroconchs at each of the localities in LNAZ. $\bar{x}$ = locality mean. Symbols represent 5 mm size classes. The locality number appears next to the symbol. The dashed line represents the approximate boundary between the northeastern and southwestern phases of fossil distribution (see Waage, 1968, pp. 64, 65, fig. 16).

Dakota because it was considered a geographic outlier; the relationship was unaffected.

To explore further the geographic pattern of size variation, specimens at localities along the Grand River (Corson County) were compared to those along the Moreau River (Dewey County) (Fig. 11A). The size-frequency histograms for these two samples are similar in shape, with a single mode in each sample in the 55-60 mm-size interval, although the mode is better defined in the Grand River sample. The range in both samples is nearly identical (42.7 mm - 92.3 mm in Corson County versus 44.7 mm - 86.6 mm

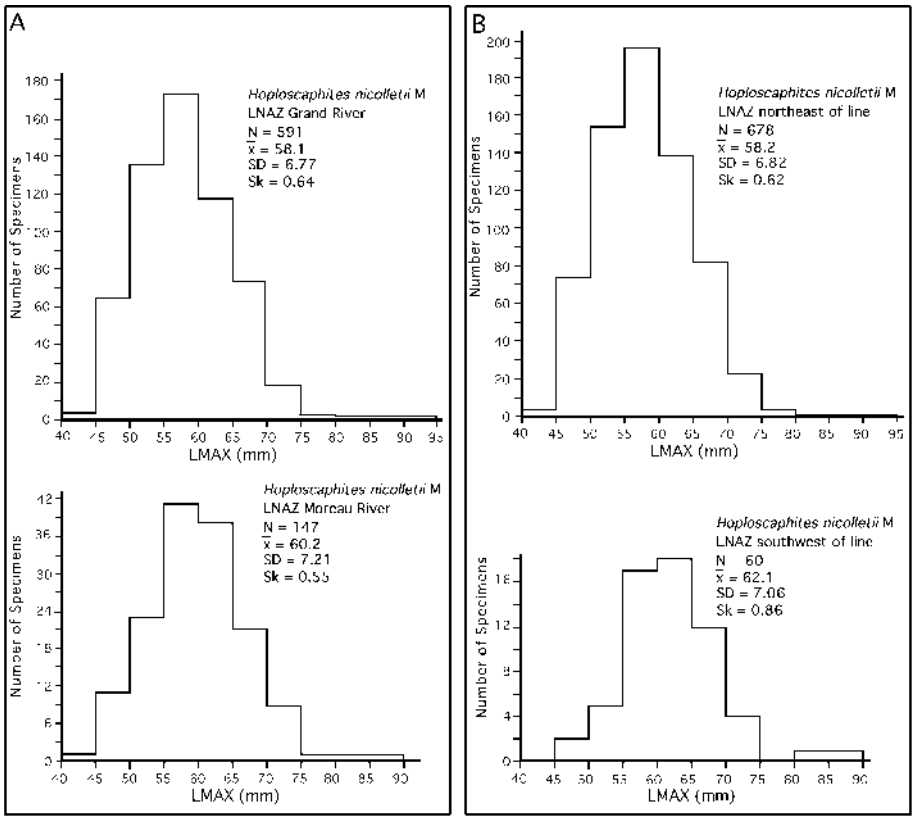

Figure 11. Size-frequency histograms of *Hoploscaphites nicolletii* macroconchs from LNAZ. A. Comparison of samples from exposures along the Grand River (Corson County) versus those along the Moreau River (Dewey County). B. Comparison of samples from southwest versus northeast of the dashed line in Fig. 10. Note that the vertical axes are not identical. Abbreviations as in Fig. 7.

in Dewey County). However, there is a statistically significant difference in the means of the two samples at the 0.005 level (58.1 mm in Corson County versus 60.2 mm in Dewey County).

Specimens at localities northeast and southwest of the dashed line in Figure 10 (the approximate boundary between the northwestern and southeastern phases of fossil distribution) (excluding loc. 44 in North Dakota) were also compared (Fig. 11B). A comparison of the size-

Figure 12. Size-frequency histograms of *Hoploscaphites nicolletii* macroconchs from selected localities in LNAZ. Samples are arranged by locality number. Locs. 21, 44, 50, 53, and 54 are northeast of the dashed line in Fig. 10; locs. 238, 243, and 249 are southwest of this line. Note that the vertical axes are not identical. Abbreviations as in Fig. 7; see Fig. 10 for locality map.

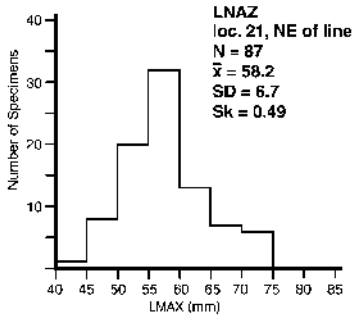
LNAZ
loc. 21, NE of line
N = 87
x̄ = 58.2
SD = 6.7
Sk = 0.49
Number of Specimens
LMAX (mm)

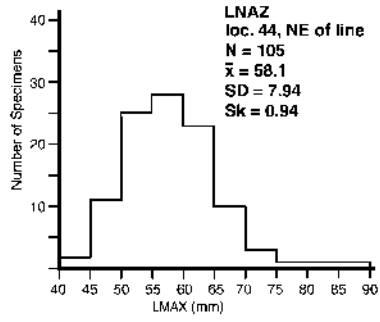
LNAZ
loc. 44, NE of line
N = 105
x̄ = 58.1
SD = 7.94
Sk = 0.94
Number of Specimens
LMAX (mm)

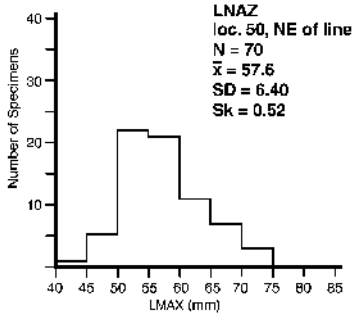
LNAZ
loc. 50, NE of line
N = 70
x̄ = 57.6
SD = 6.40
Sk = 0.52
Number of Specimens
LMAX (mm)

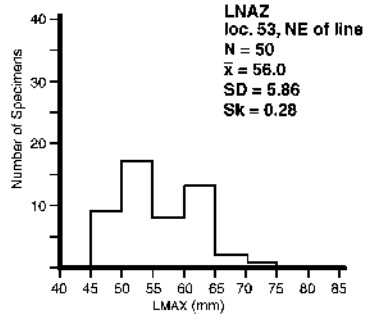
LNAZ
loc. 53, NE of line
N = 50
x̄ = 56.0
SD = 5.86
Sk = 0.28
Number of Specimens
LMAX (mm)

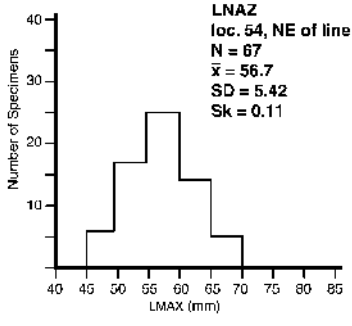
LNAZ
loc. 54, NE of line
N = 67
x̄ = 56.7
SD = 5.42
Sk = 0.11
Number of Specimens
LMAX (mm)

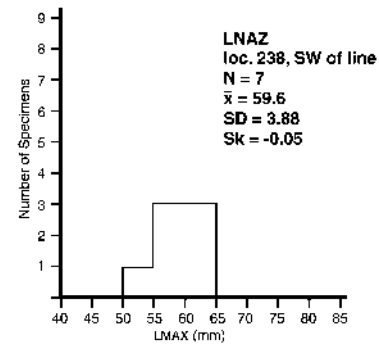
LNAZ
loc. 238, SW of line
N = 7
x̄ = 59.6
SD = 3.88
Sk = -0.05
Number of Specimens
LMAX (mm)

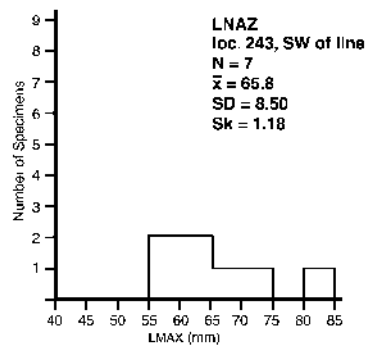
LNAZ
loc. 243, SW of line
N = 7
x̄ = 65.8
SD = 8.50
Sk = 1.18
Number of Specimens
LMAX (mm)

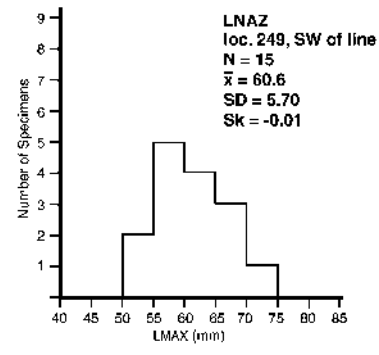
LNAZ
loc. 249, SW of line
N = 15
x̄ = 60.6
SD = 5.70
Sk = -0.01
Number of Specimens
LMAX (mm)

frequency histograms of the samples from these two areas reveals a single mode in both histograms. It occurs in the 55-60 mm-size interval in the northeastern sample and in the 55-65 mm-size interval in the southwestern sample. Not unexpectedly, there is a statistically significant difference in the means between the two samples at the 0.001 level (58.2 mm in the northeastern sample versus 62.1 mm in the southwestern sample).

To investigate the variation in size at specific sites, size-frequency histograms were prepared for eight localities, five northeast of the dashed line with 50 to 105 specimens each, and three southwest of the dashed line with only 7 to 15 specimens each (Fig. 12).

One of the five localities northeast of the line is located in North Dakota (loc. 44) and the others are along the Grand River (locs. 21, 50, 53, and 54). The means of these samples range from 56.7 mm to 58.2 mm. The samples from locs. 21, 44, and 54 each have a single mode in the 55-60 mm-size interval. The sample from loc. 50 has a broad mode in the 50-60 mm-size interval. In contrast, the sample from loc. 53 has two modes, a primary mode in the 50-55 mm-size interval and a secondary mode in the 60-65 mm-size interval. However, the difference between these two modes is only three specimens.

The means of the samples from the three southwestern localities (locs. 238, 243, and 249) range from 59.6 mm to 65.8 mm. These means are higher than those in the samples from the northeastern localities. The smallest specimens in the southwestern localities are in the 50-55 mm-size interval, whereas the smallest specimens in the northeastern localities are in the 40-45 mm-size interval.

There are 33 concretions in our sample that contain large accumulations (more than 5 specimens each) of *Hoploscaphites nicolletii* (Table 3). We confine our discussion to concretions with 10 or more specimens (15 concretions). All but three of these concretions (A221, A353, A354) are from exposures along the Grand River. Several of the concretions are from the same locality. The size-frequency histograms of these samples are presented in Figure 13. Most concretions have 10-15 specimens. The size distributions are generally right skewed. In most concretions, the smallest specimens are in the 45-50 mm-size interval, and the largest specimens are in the 65-75 mm-size interval. When a peak is present, it occurs in the 50-60 mm-size interval. The only exception is A547 (loc. 63) in which the peak occurs in the 65-70 mm-size interval.

Samples from concretions from the same locality show similar size distributions. For example, samples from the three concretions at loc. 50 each have a single mode in the 50-55 mm-size interval. Samples from the two concretions at loc. 21 each have a single mode in the 55-60 mm-size

Table 3. Adult size (LMAX) of *Hoploscaphites nicolletii* macroconchs in 33 concretions in LNAZ.*

LOC.	CONC	N	x	SD	MIN	MAX
6	A221	12	56.8	5.55	49.2	66.6
8	A232	6	55.3	7.90	46.5	65.8
18	A259	12	55.6	7.44	45.7	67.3
20	A266	6	56.4	7.23	49.1	65.3
20	A4659	13	57.7	5.92	48.5	67.7
21	A270	28	56.8	5.46	48.0	69.1
21	A272	10	56.0	6.02	42.7	67.7
44	A352	6	55.9	6.37	47.4	63.4
44	A353	20	57.5	7.38	41.4	70.0
44	A354	31	54.4	5.71	45.4	72.5
44	A358	5	56.4	3.68	52.6	61.9
46	A362	8	53.5	4.99	47.3	62.5
46	A363	5	56.8	4.37	49.3	60.2
47	A366	7	56.9	4.21	49.0	61.1
50	A386	6	57.4	6.21	50.2	67.7
50	A387	10	57.5	7.73	49.2	71.2
50	A388	14	54.2	7.00	44.9	73.8
50	A390	5	57.2	5.75	48.0	63.3
50	A391	10	57.0	6.12	48.3	70.6
54	A432	8	56.6	4.43	52.4	64.6
55	A437	12	55.5	5.00	46.9	62.4
63	A547	22	61.3	6.46	45.4	70.5
66	A620	7	59.8	7.44	44.7	67.4
66	A621	7	56.0	6.84	48.2	69.5
66	A623	7	59.7	7.36	52.5	74.5
79	A713	6	61.3	10.37	49.1	77.1
79	A714	5	56.6	8.49	48.7	66.4
99	A956	5	61.8	5.75	56.3	70.0
104	A959	13	57.9	6.75	49.5	69.7
177	A1305	20	57.3	7.14	46.0	70.5
177	A1310	8	61.9	6.89	53.5	73.5
243	A1072	5	68.5	8.78	58.6	81.6
303	A4705	11	56.3	5.06	51.4	68.6

*See Table 2 for an explanation of abbreviations. CONC = a single concretion specified by a YPM-IP A number.

interval. The distribution of the smaller sample (A272) fits into that of the larger sample (A270). The samples from the two concretions at loc. 44 each have a single mode in the 55-60 mm-size interval, but the mode is better defined in A353.

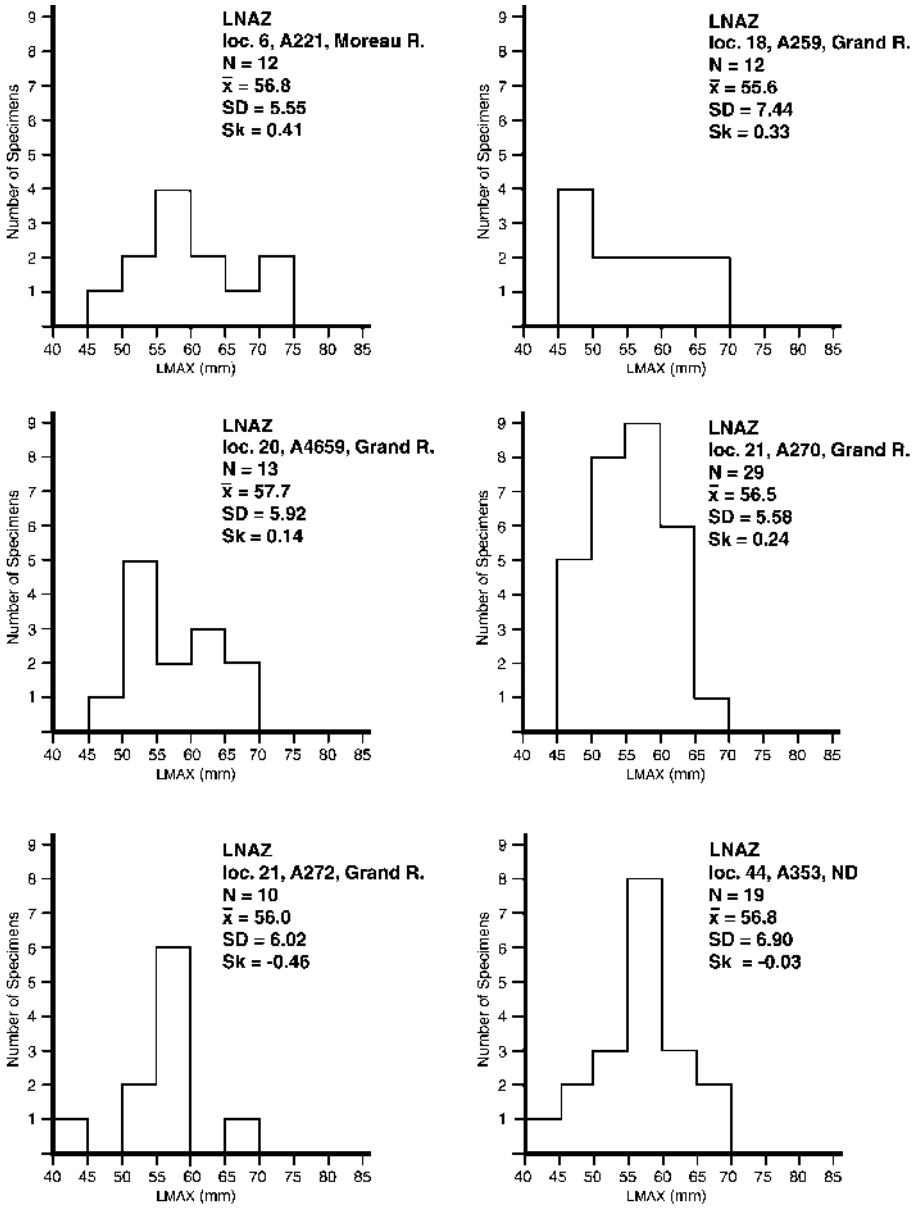

Figure 13. Size-frequency histograms of *Hoploscaphites nicolletii* macroconchs from individual concretions with 10 or more specimens in LNAZ and UNAZ. Samples are arranged by locality number except for the sample from UNAZ. All concretions are from exposures along the Grand River except those from locs. 6 (Moreau River, northeast of the dashed line in Fig. 10) and 44 (North Dakota). Abbreviations as in Fig. 7; see Fig. 10 for locality map.

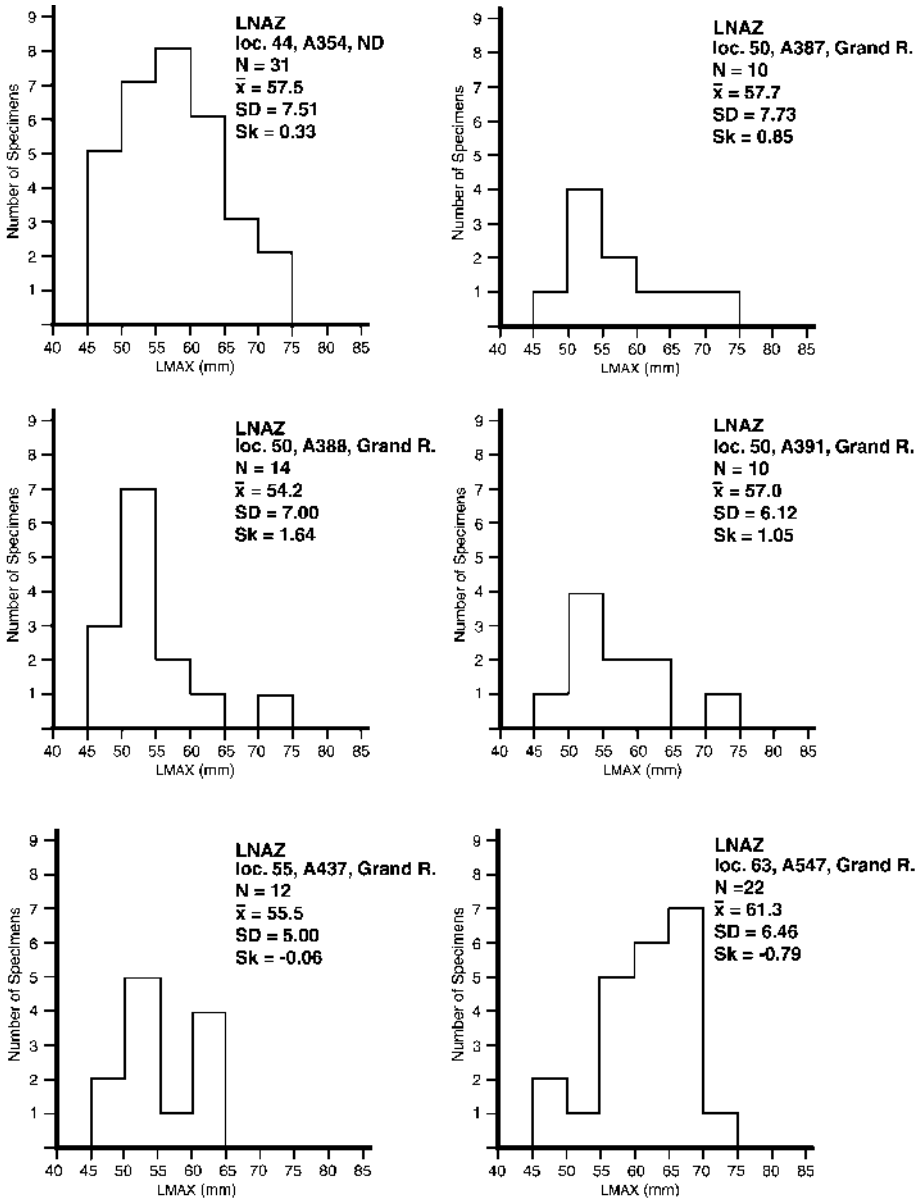

Figure 13. Continued.

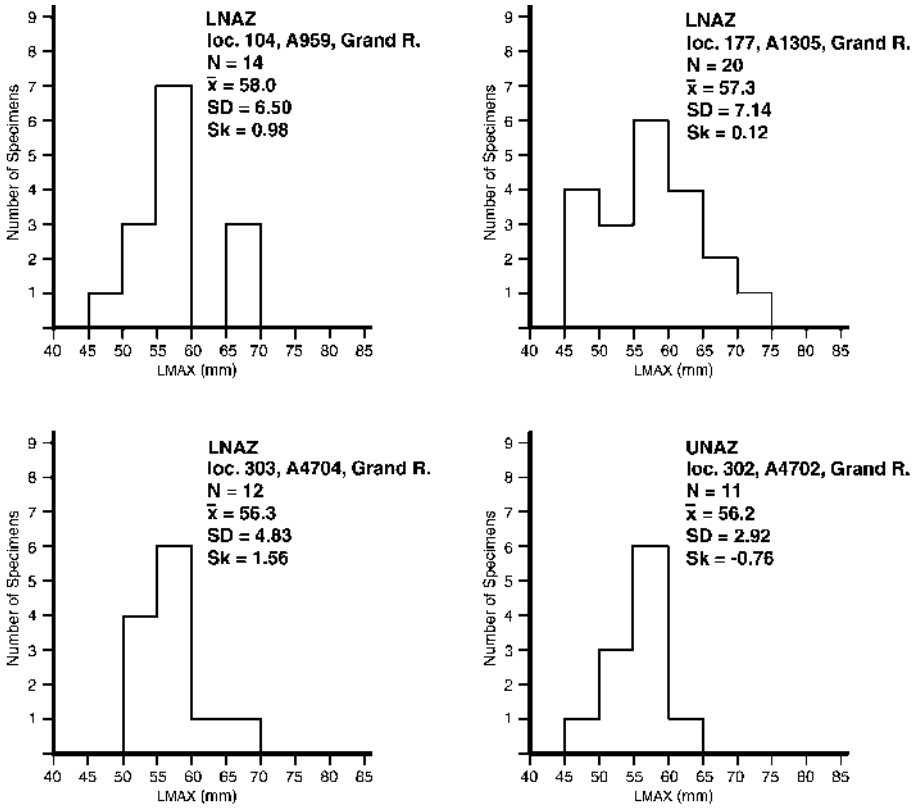

Figure 13. Continued.

8.2.2 *Limopsis-Gervillia* Assemblage Zone (LGAZ)

There are 52 specimens in the sample from this zone (compare with Landman and Waage, 1993, table 7, fig. 58, N = 29). The size distribution is right skewed with a broad peak in the 55-65 mm-size interval (Fig. 14). The mean is 61.4 mm, which is significantly larger than that in LNAZ (58.4 mm) at the 0.005 level. LMAX ranges from 49.3 mm to 79.5 mm. The ratio of the size of the largest specimen to that of the smallest is 1.61.

The statistical analysis of the samples at 31 localities is given in Table 4. There are few specimens per locality, with most localities represented by only one or two specimens. The maximum number of specimens at any one locality is seven. Locality means were analyzed as described in the methodology section. The results are presented in Figure 15.

A regression analysis of locality means against latitude and longitude, weighted by sample size, did not reveal any statistically significant relationship, suggesting that the geographic distribution of size is fairly uniform in this zone.

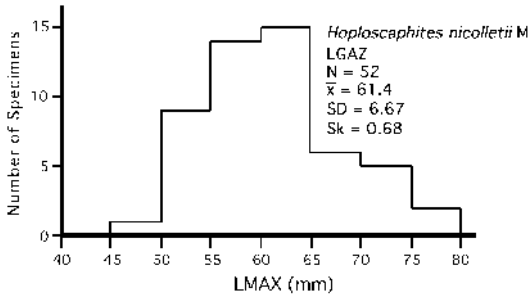

Figure 14. Size-frequency histogram of *Hoploscaphites nicolletii* macroconchs from LGAZ. Abbreviations as in Fig. 7.

Table 4. Adult size (LMAX) of *Hoploscaphites nicolletii* macroconchs at 31 localities in LGAZ.*

LOC	N	x	SD	MIN	MAX
1	1	74.8	-	-	-
3	1	57.8	-	-	-
6	1	57.1	-	-	-
8	3	61.2	6.29	54.0	65.6
17	1	64.6	-	-	-
21	1	60.5	-	-	-
25	3	60.0	10.00	49.1	68.8
26	1	59.7	-	-	-
46	1	61.6	-	-	-
47	2	58.7	4.21	55.8	61.7
50	1	65.0	-	-	-
51	1	72.2	-	-	-
52	1	53.1	-	-	-
53	1	67.4	-	-	-
54	4	62.0	6.25	56.5	71.0
62	1	62.1	-	-	-
64	1	79.5	-	-	-
66	1	62.7	-	-	-
69	1	66.5	-	-	-
86	1	73.4	-	-	-
104	2	54.2	0.04	54.2	54.3
108	1	57.7	-	-	-
115	5	59.2	4.73	54.3	67.1
119	1	52.6	-	-	-
177	7	57.7	4.23	51.2	62.4
234	1	56.8	-	-	-
236	1	62.3	-	-	-
242	1	54.8	-	-	-
248	1	58.6	-	-	-
303	1	70.8	-	-	-
C412	3	67.1	7.13	62.9	75.4

*See Table 2 for an explanation of abbreviations.

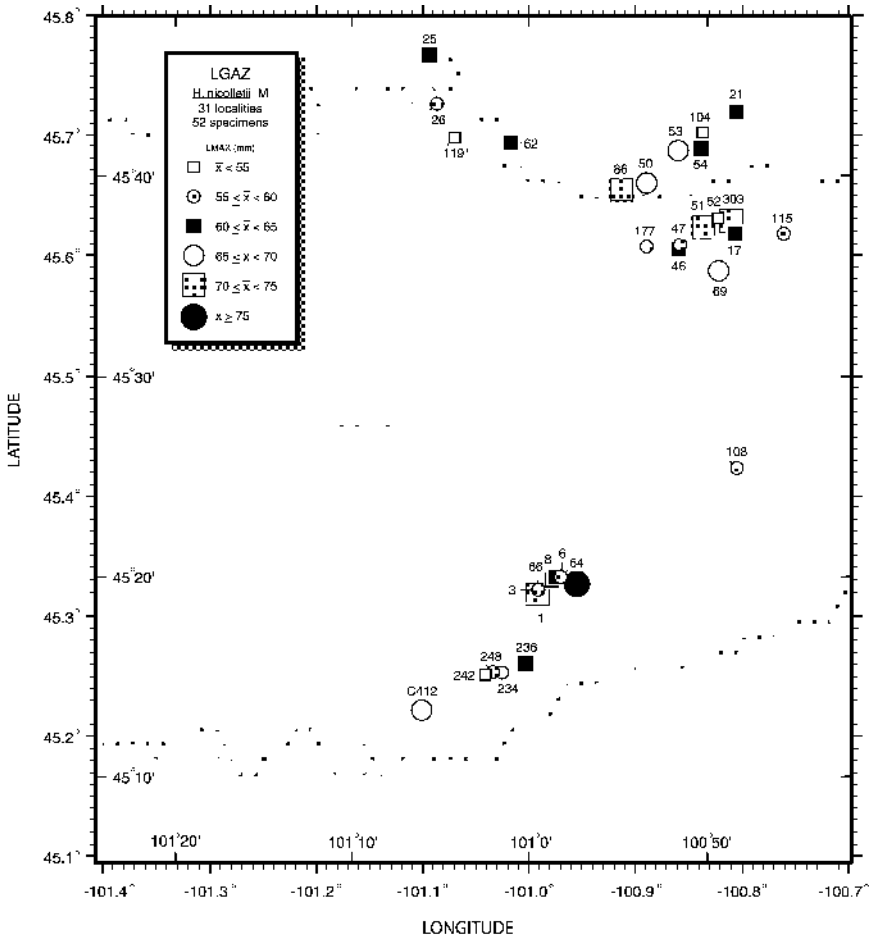

Figure 15. Map showing the mean size of the samples of *Hoploscaphites nicolletii* macroconchs at each of the localities in LGAZ. $\bar{x}$ = locality mean. Symbols represent 5 mm size groups. The locality number appears next to the symbol.

The samples at localities along the Grand River (Corson County) were compared with those along the Moreau River (Dewey County) (Fig. 16). There is a poorly defined mode in the 60-65 mm-size interval in the Grand River sample and a broad, better-defined mode in the 55-65 mm-size interval in the Moreau River sample. The means are 60.7 mm and 63.0 mm, respectively, and the difference is not statistically significant.

8.2.3 Upper *nicolletii* Assemblage Zone (UNAZ)

The specimens from UNAZ comprise the second largest sample (N =

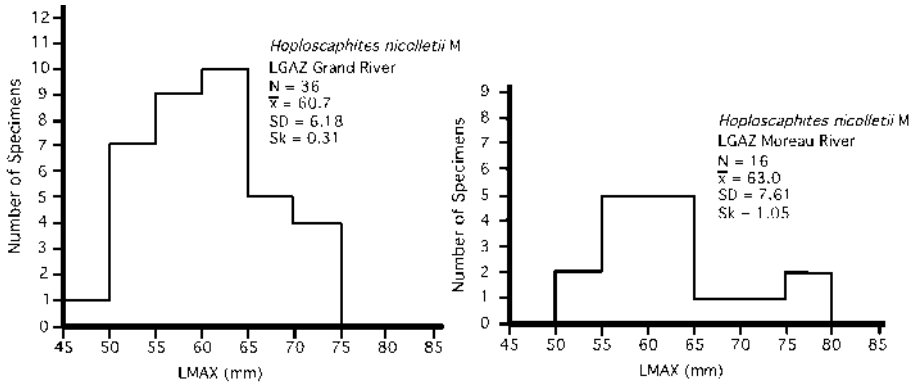

Figure 16. Size-frequency histograms of *Hoploscaphites nicolletii* macroconchs from LGAZ. Comparison of samples from exposures along the Grand River (Corson County) versus those along the Moreau River (Dewey County). Abbreviations as in Fig. 7.

147). The size distribution is slightly right skewed (Fig. 17; compare with Landman and Waage, 1993, table 7, fig. 58, N = 53). There is a single mode in the 55-60 mm-size interval with a mean of 60.8 mm. This mean is not significantly different from that in LGAZ (61.4 mm), but it is significantly larger than that in LNAZ (58.4 mm) at the 0.001 level. LMAX ranges from 45.4 mm to 88.3 mm. The ratio of the size of the largest specimen to that of the smallest is 1.94.

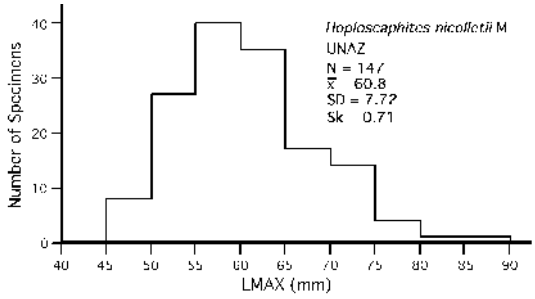

Figure 17. Size-frequency histogram of *Hoploscaphites nicolletii* macroconchs from UNAZ. Abbreviations as in Fig. 7.

The statistical analysis of the samples at 22 localities is given in Table 5. The number of specimens per locality varies widely with almost half of the localities represented by 7 or more specimens. Locality means were analyzed as described in the methodology section. The results are presented in Figure 18.

The regression analysis of locality means against latitude and longitude,

Table 5. Adult size (LMAX) of *Hoploscaphites nicolletii* macroconchs at 22 localities in UNAZ.*

LOC	N	x	SD	MIN	MAX
3	4	59.9	14.60	45.4	74.4
8	11	57.5	5.65	50.8	70.9
17	13	59.9	4.90	52.4	70.4
30	1	77.5	-	-	-
51	15	57.5	6.97	47.4	69.4
52	18	57.8	5.26	48.3	71.0
53	5	62.4	8.83	53.6	72.5
54	9	58.6	6.61	52.9	69.9
69	7	59.7	4.61	52.8	66.2
77	14	69.4	6.94	61.5	88.3
78	3	61.1	3.22	58.7	64.8
82	16	57.3	5.39	48.0	64.1
95	3	70.9	2.89	68.7	74.2
191	3	69.1	6.67	62.0	75.3
198	1	69.0	-	-	-
199	1	58.9	-	-	-
200	1	78.7	-	-	-
201	2	66.0	1.41	65.0	67.0
209	3	57.5	5.53	51.1	61.7
213	3	72.1	1.86	70.8	74.3
301	2	64.5	1.38	63.5	65.5
302	12	56.2	2.79	49.9	60.3

*See Table 2 for an explanation of abbreviations.

weighted by sample size, shows a significant correlation at the 0.0001 level for both latitude and longitude. As in LNAZ, larger specimens occur in the southwestern portion of the fossil distribution.

We also compared the samples of specimens in exposures along the Grand River (Corson County) versus those along the Moreau River (Dewey County) (Fig. 19A). The means of the samples from these two areas are 58.3 mm and 66.1 mm, respectively - the difference is statistically significant at the 0.001 level. The smallest specimens are in the 45-50 mm-size interval in both areas, but the largest specimens in Corson County are in the 70-75 mm-size interval, whereas the largest specimen in Dewey County is in the 85-90 mm-size interval.

We further compared the samples of specimens at localities northeast and southwest of the dashed line in Figure 18 (the approximate boundary between the two phases of fossil distribution). The mean of the sample southwest of the dashed line (69.4 mm) is significantly larger than that of the sample northeast of the dashed line (59.4 mm) at the 0.001 level (Fig. 19B). There is also a difference in the modal size class: 65-70 mm southwest of the

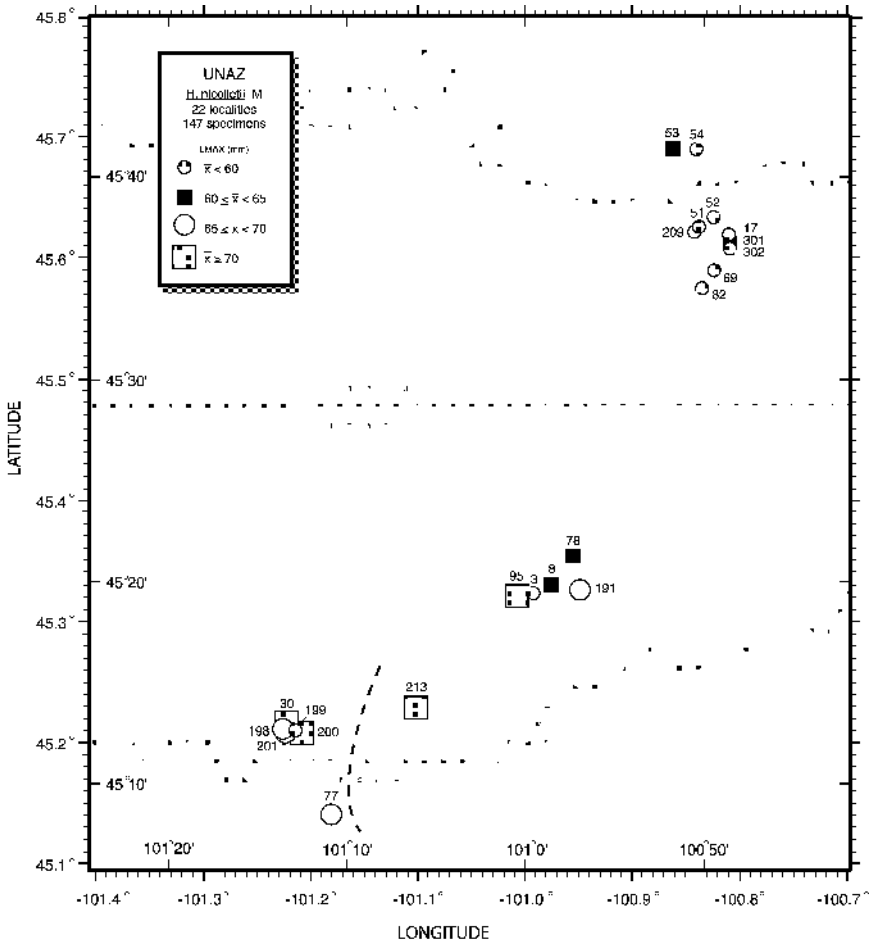

Figure 18. Map showing the mean size of the samples of *Hoploscaphites nicolletii* macroconchs at each of the localities in UNAZ. $\bar{x}$ = locality mean. Symbols represent 5 mm size groups. The locality number appears next to the symbol. The dashed line represents the approximate boundary between the northeastern and southwestern phases of fossil distribution (see Waage, 1968, pp. 67, 68, fig. 18).

line versus 55-60 mm northeast of the line. In addition, the range in size of the southwestern sample (58.9-88.3 mm) is truncated relative to that of the northeastern sample (45.4- 84.5 mm).

To explore the pattern of size variation at specific sites, we examined the samples at six localities (Fig. 20). All localities have relatively few specimens. Two of the localities are from along the Moreau River (locs. 8 and 77), one of which lies southwest of the dashed line (loc. 77), and four localities are from along the Grand River (locs. 17, 51, 52, and 82). The

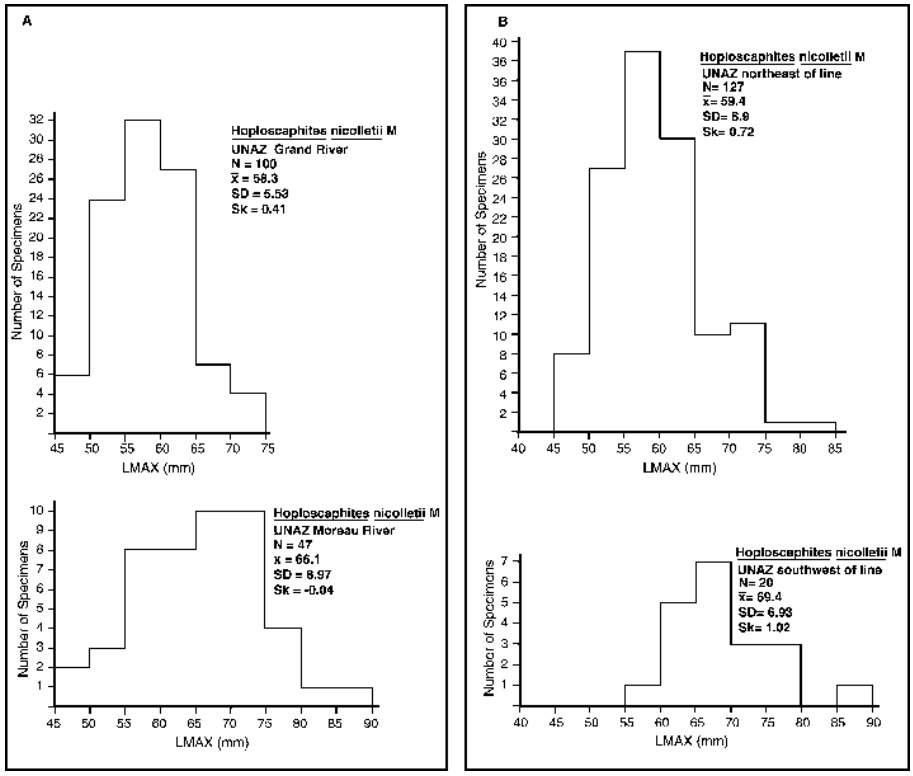

Figure 19. Size-frequency histograms of *Hoploscaphites nicolletii* macroconchs from UNAZ. A. Comparison of samples from exposures along the Grand River (Corson County) versus those along the Moreau River (Dewey County). B. Comparison of samples from southwest versus northeast of the dashed line in Fig. 18. Note that the vertical axes are not identical. Abbreviations as in Fig. 7.

mean at loc. 77 (69.4 mm) is significantly higher than the means at the five other localities (at the 0.01 level with respect to loc. 8; at the 0.001 level with respect to the other four localities).

There is only one concretion in UNAZ that contains a large accumulation of macroconchs (Fig. 13). This sample has a mode in the 55-60 mm-size interval with a mean of 56.2 mm.

8.2.4 *Protocardia-Oxytoma* Assemblage Zone (POAZ)

The size-frequency histogram of the specimens from POAZ (N = 128) is shown in Figure 21. The distribution is slightly right skewed with a broad mode in the 60-70 mm-size interval (compare with Landman and Waage, 1993, table 7, fig. 58, N = 53). The mean is 65.6 mm, which is significantly

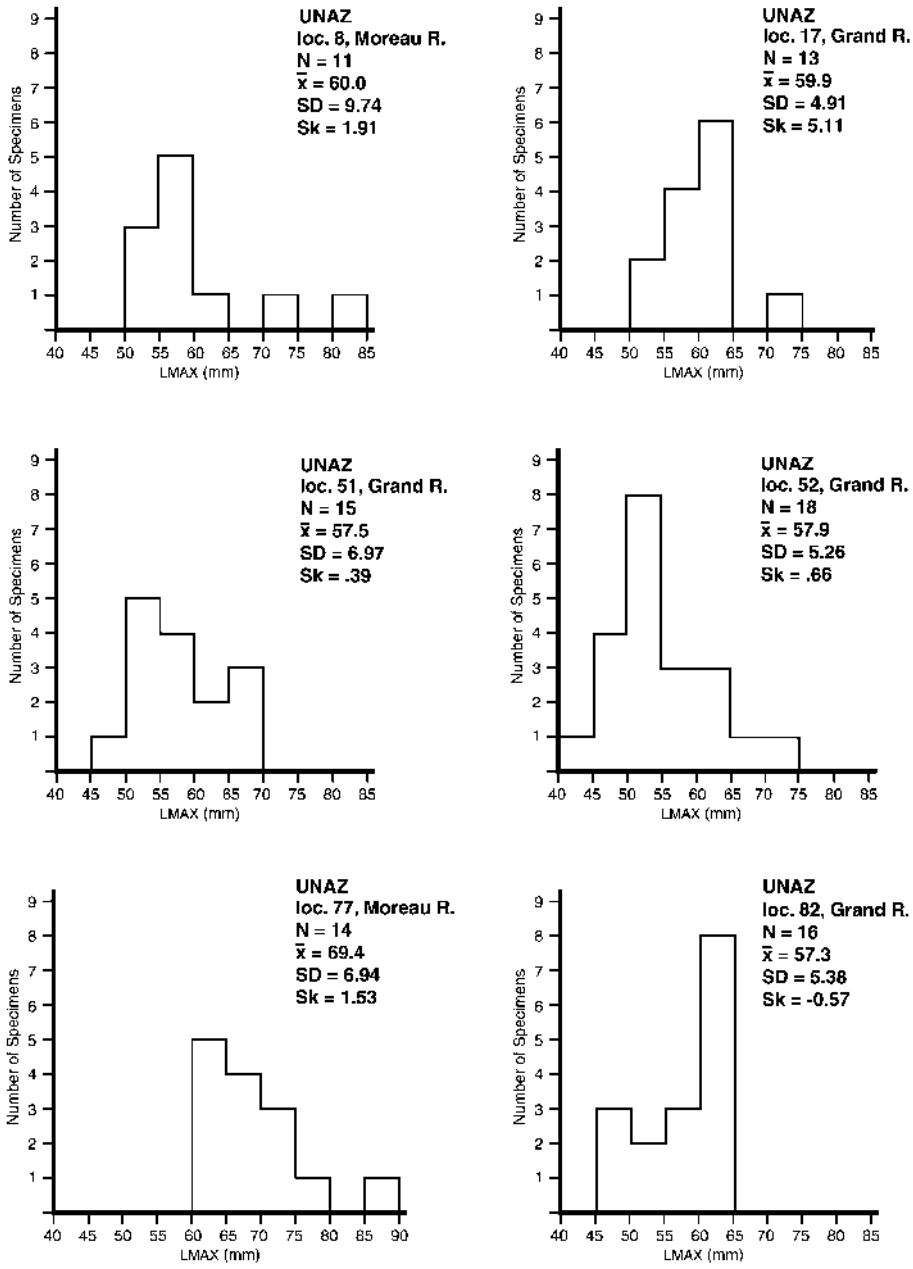

Figure 20. Size-frequency histograms of *Hoploscaphites nicolletii* macroconchs from selected localities in UNAZ. Samples are arranged by locality number. Locs. 8 and 77 are from the Moreau River, northeast and southwest of the dashed line in Fig. 18, respectively; locs. 17, 51, 52, and 82 are from the Grand River. Abbreviations as in Fig. 7; see Fig. 18 for locality map.

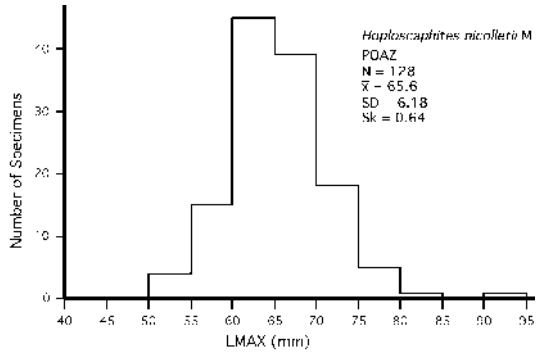

Figure 21. Size-frequency histogram of *Hoploscaphites nicolletii* macroconchs from POAZ. Abbreviations as in Fig. 7.

larger (at the 0.001 level) than that in any other assemblage zone. The size of the smallest specimen (51.0 mm) is larger than that of the smallest specimen in any other assemblage zone. The size of the largest specimen (91.7 mm) is comparable to that of the largest specimen in LNAZ (92.3 mm). The ratio of the size of the largest specimen in POAZ to that of the smallest is 1.80.

The statistical analysis of the samples at 37 localities is given in Table 6. The number of specimens per locality varies widely with most localities represented by only one to five specimens. Locality means were analyzed as described in the methodology section. The results are presented in Figure 22. A regression analysis of the locality means against latitude and longitude, weighted by sample size, revealed no trend.

We also compared the samples along the Grand River versus those along the Moreau River (Fig. 23). The means are the same in both samples (65.4 mm). The size distribution of the Grand River sample is left skewed with a mode in the 65-70 mm-size interval. The size distribution of the Moreau River sample is more symmetrical with a mode in the 60-65 mm-size interval.

The size-frequency histograms of the samples from the four most fossiliferous localities are shown in Figure 24. Loc. 25 is from the Grand River (N = 13), and the remaining samples (locs. 191, 214, and 236) are from along the Moreau River (N = 8-12). The means range from 61.3 mm to 67.8 mm.

Table 6. Adult size (LMAX) of *Hoploscaphites nicolletii* macroconchs at 37 localities in POAZ.*

LOC	N	x	SD	MIN	MAX
3	3	67.2	5.22	61.7	72.0
6	4	68.2	2.93	64.9	71.0
8	3	67.3	7.60	62.6	76.1
10	3	64.3	8.59	56.6	73.6
13	3	70.3	8.55	62.7	79.6
17	4	70.1	16.40	52.0	91.7
25	13	66.3	4.14	59.9	72.8
52	1	56.2	-	-	-
57	6	64.3	3.94	60.4	70.2
62	1	74.1	-	-	-
66	6	67.0	7.48	61.2	81.2
69	1	57.4	-	-	-
79	2	69.3	6.68	64.6	74.1
89	2	60.0	4.03	57.2	62.9
95	3	64.4	9.46	54.8	73.7
106	1	69.3	-	-	-
108	1	63.8	-	-	-
115	1	52.2	-	-	-
142	1	61.7	-	-	-
150	2	59.8	3.68	57.2	62.4
191	9	65.5	6.54	57.7	79.4
199	2	68.0	0.11	67.9	68.1
204	1	68.4	-	-	-
213	4	67.3	4.05	62.6	72.5
214	8	67.8	5.59	58.1	75.6
231	2	57.1	8.63	51.0	63.2
232	1	74.8	-	-	-
233	6	67.4	3.45	64.8	74.0
236	12	61.2	4.29	56.5	68.7
237	5	63.6	3.26	60.1	67.4
238	1	64.2	-	-	-
246	6	65.2	4.06	60.5	71.4
247	3	67.3	2.33	64.7	69.1
248	1	65.8	-	-	-
249	2	65.1	1.24	64.2	66.0
301	1	57.5	-	-	-
C410	2	65.3	4.91	61.8	68.8

*See Table 2 for an explanation of abbreviations.

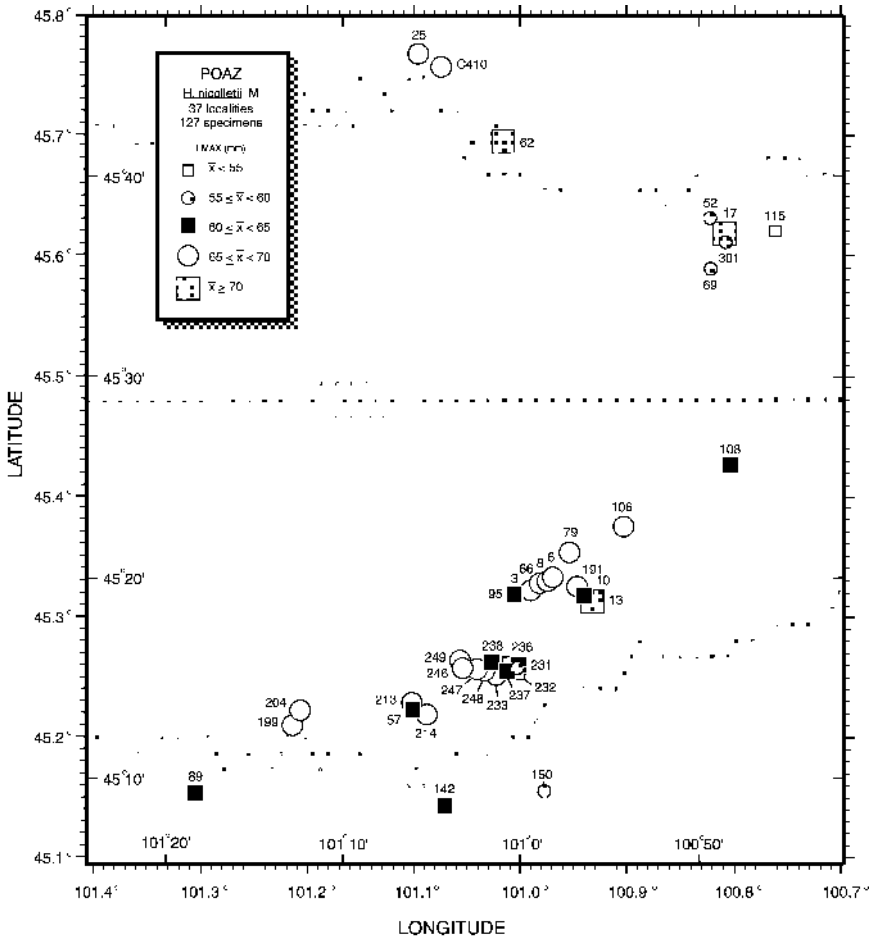

Figure 22. Map showing the mean size of the samples of *Hoploscaphites nicolletii* macroconchs at each of the localities in POAZ. $\bar{x}$ = locality mean. Symbols represent 5 mm size groups. The locality number appears next to the symbol.

9. ADULT-SIZE VARIATION IN *HOPLOSCAPHITES NICOLLETII* MICROCONCHS

The sample of *Hoploscaphites nicolletii* microconchs from the Trail City Member is small (N = 28), but larger than that reported in Landman and Waage (1993, p. 81, N = 13). The size-frequency distribution shows three modes with the most prominent mode in the 60-65 mm-size class (Fig. 25).

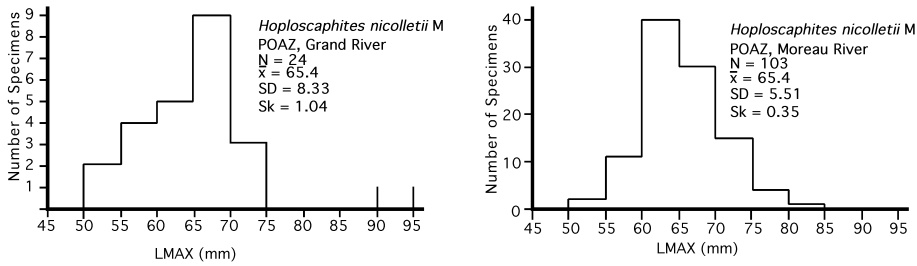

Figure 23. Size-frequency histograms of Hoploscaphites nicolletii macroconchs from POAZ. Comparison of samples from exposures along the Grand River (Corson County) versus those along the Moreau River (Dewey County). Note that the vertical axes are not identical. Abbreviations as in Fig. 7.

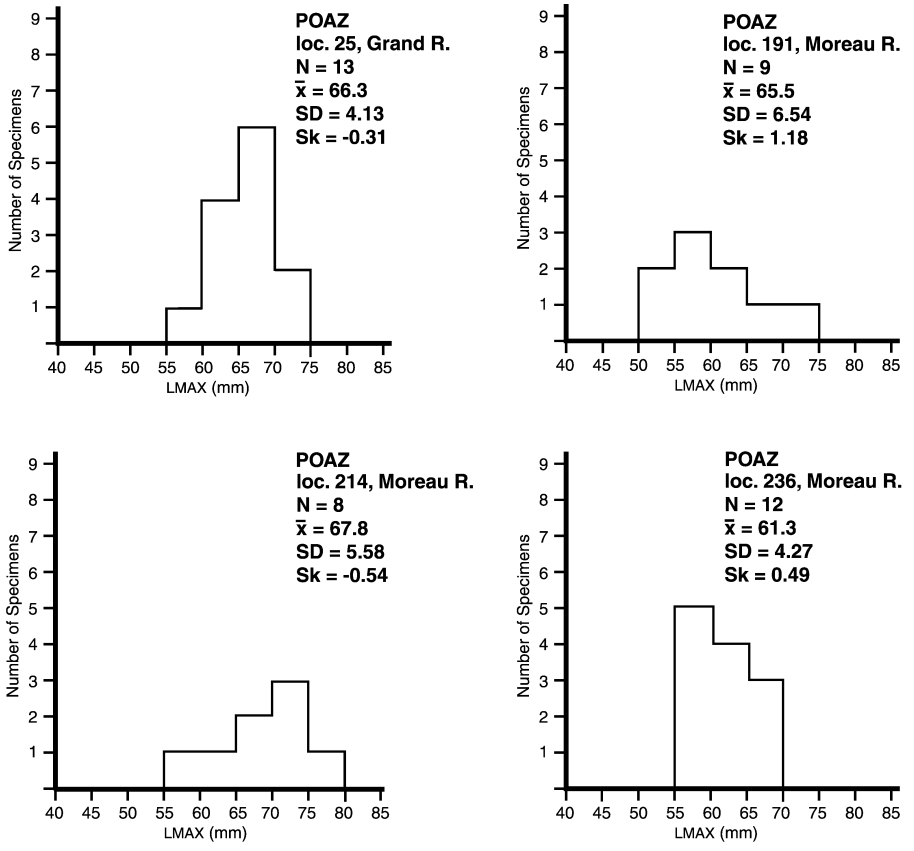

Figure 24. Size-frequency histograms of *Hoploscaphites nicolletii* macroconchs from selected localities in POAZ. Abbreviations as in Fig. 7; see Fig. 22 for locality map.

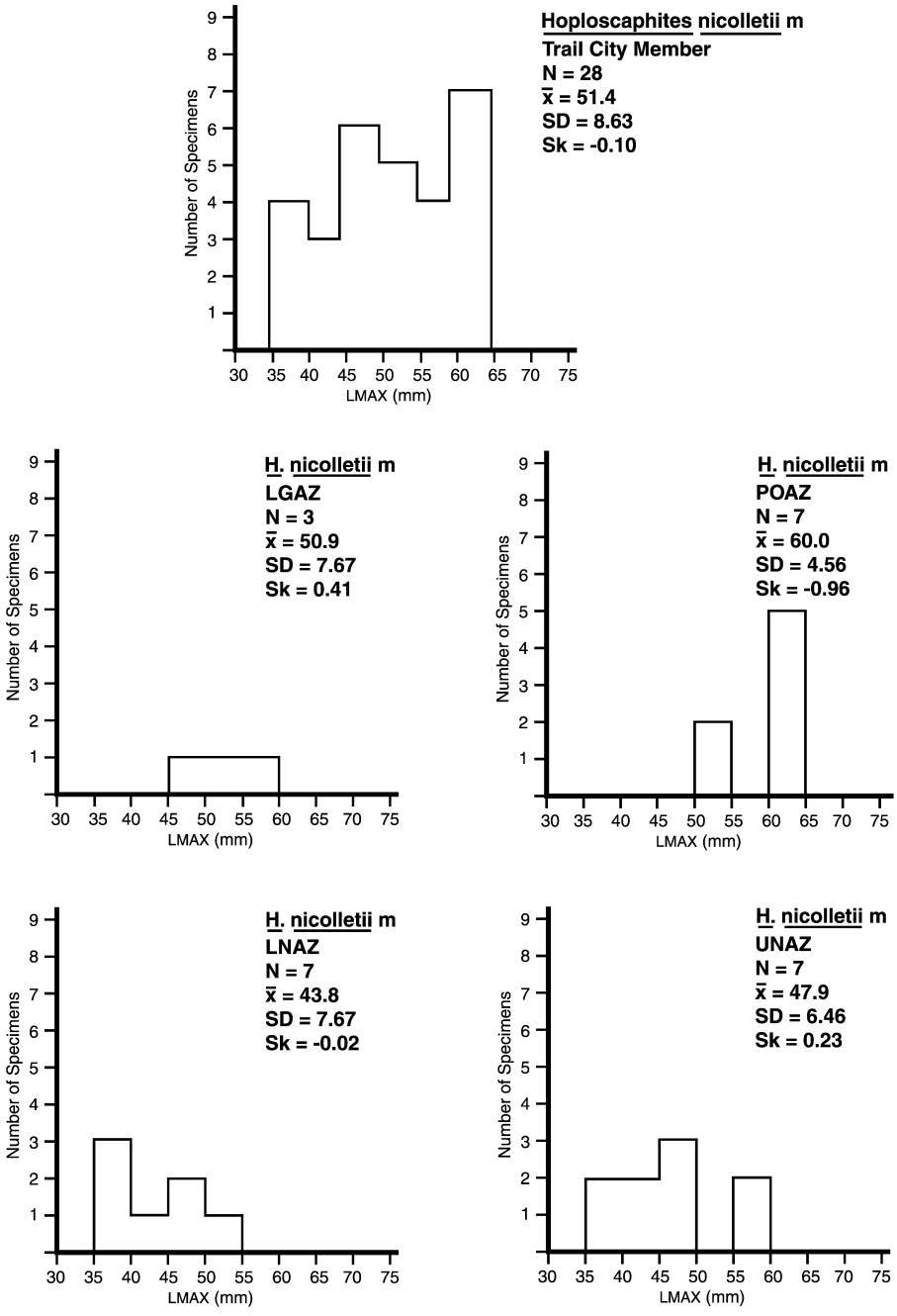

Figure 25. Size-frequency histograms of *Hoploscaphites nicolletii* microconchs from the Trail City Member and from each of its assemblage zones. Abbreviations as in Fig. 7.

The mean of the sample is 51.4 mm. The mean size of the microconchs is approximately 85% that of the co-occurring macroconchs. The dimorphs overlap for approximately 55% of their total combined size range.

Size-frequency histograms were prepared for the sample of microconchs from each assemblage zone (Fig. 25). Because there are so few specimens in each sample, it is difficult to draw any conclusions about the modal size class and the shape of each distribution. However, the stratigraphic pattern of size variation of the microconchs is similar to that of the co-occurring macroconchs. The mean size of the microconchs is 43.8 mm in LNAZ, 50.9 mm in LGAZ, 47.9 mm in UNAZ, and 60.0 mm in POAZ.

10. DISCUSSION

10.1 Geographic pattern of size variation

Two assemblage zones (LNAZ and UNAZ) show a geographic pattern of size variation. In both zones, larger macroconchs of *Hoploscaphites nicolletii* occur in the southwestern portion, and smaller macroconchs occur in the northeastern portion, of the species distribution. That these two zones show similar patterns in size variation is not surprising, given the fact that both zones contain an abundance of *H. nicolletii* macroconchs and exhibit two nearly identical phases of fossil distribution.

The difference in adult size within each of these zones is probably an ecophenotypic response to differences in the environment. The southwestern area near the transition to the Irish Creek lithofacies may have represented a quiet lagoonal or estuarine environment seaward of the delta on the distal end of the southwest flowing current (Fig. 26). The fauna in this area was relatively depauperate (that is, few species and individuals). This environment did not support large populations of scaphites, perhaps due to low oxygen levels or less than normal marine salinities. In contrast, the northeastern area in the middle of the Little Eagle lithofacies may have represented a better oxygenated, higher energy environment, with a more normal marine salinity, immediately down current of the submarine sand bar (Fig. 26). The scaphites in this area were very abundant and were accompanied by a diverse fauna, including both nektic and benthic organisms.

The precise environmental conditions responsible for the differences in adult size are unknown. However, a correlation between adult size and environment has been reported in many other ammonites (Hewitt and Hurst,

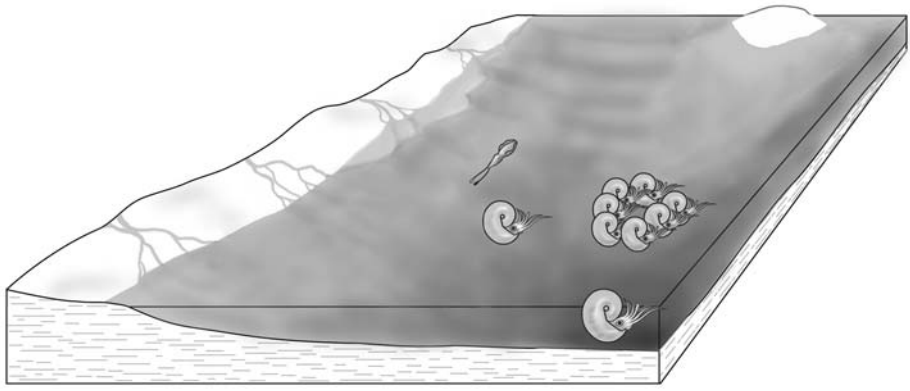

Figure 26. Reconstruction of the paleoenvironments represented by the upper part of the Elk Butte Member and the lower part of the Trail City Member in north-central South Dakota. This reconstruction is a time composite and is therefore generalized. The western margin of the study area (left side of the diagram) was bounded by a delta and its associated drainage system. During Elk Butte time, a small population of very large individuals of *Hoploscaphites nicolletii* inhabited an offshore environment below wave base (foreground). During Trail City time, a submarine sand bar (background) grew into the area from the northeast in association with a southwest flowing current. The position of this sand bar was relatively stable except for a pulse of growth during POAZ. Large populations of *H. nicolletii* periodically inhabited the subtidal environment on the downcurrent end of this sand bar (middle, right). However, in LNAZ, and again in UNAZ, two populations lived side by side: a very large population of average size individuals on the downcurrent end of the bar (middle, right) and another, much smaller population of larger individuals to the southwest (middle, left). In UNAZ, this area also was inhabited by the coleoid *Actinosepia canadensis* (middle, far left). (Scaphite symbols represent macroconchs of *H. nicolletii*) (After Rhoads et al., 1972).

1977; Mancini, 1978; Elmi and Benshili, 1987; Kemper and Wiedenroth, 1987; Stevens, 1988; Mignot et al., 1993, Matyja and Wierzbowski, 2000; Reboulet, 2001). In present-day cephalopods, the size at maturity is known to depend on a variety of factors including nutrient supply, light intensity, temperature, dissolved oxygen, and depth (Bucher et al., 1996). Many of these same factors must have played a role in determining the size at maturity of these scaphites although which of these factors was most important is unclear.

Unlike LNAZ and UNAZ, there are no statistically significant correlations between adult size and latitude and longitude in the samples from LGAZ and POAZ. It is possible that the data in these two zones are not sufficiently powerful to detect trends even if they existed. However, both zones differ from LNAZ and UNAZ in having fewer macroconchs of *Hoploscaphites nicolletii* and in exhibiting only one phase of fossil distribution.

10.2 Stratigraphic pattern of size variation

Figure 27 shows the stratigraphic pattern of size variation in both dimorphs of *Hoploscaphites nicolletii* in the Pierre Shale and Fox Hills Formation. The mean size fluctuates with no unidirectional change upsection. The pattern is identical in both dimorphs although the microconchs are represented by very few specimens. As a result, most of our discussion is confined to the macroconchs.

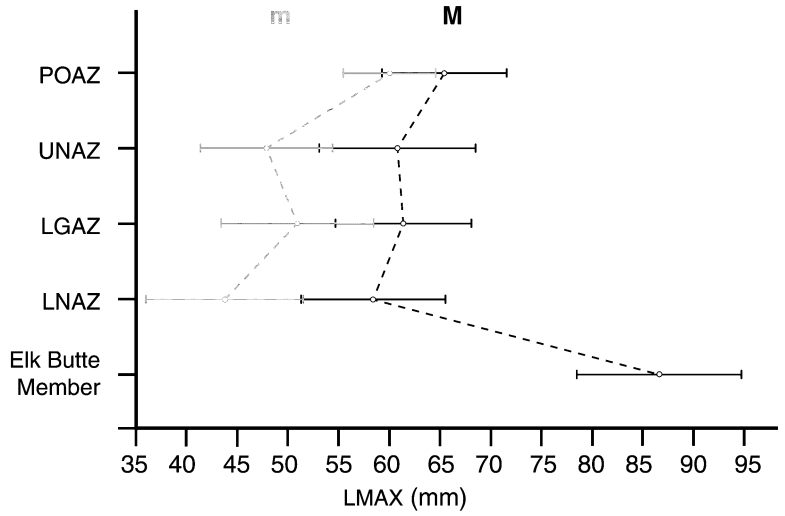

Figure 27. The stratigraphic pattern of size variation in the samples of microconchs (m) and macroconchs (M) of *Hoploscaphites nicolletii* from the upper part of the Elk Butte Member and the lower part of the Trail City Member. The means are plotted ±1σ. Abbreviations as in Fig. 7.

The fluctuations in mean size can be correlated with changes in the environment. The largest mean size occurs in the Elk Butte Member (86.6 mm), which probably represented a subtidal environment below wave base (Fig. 26). The general paucity of macrofossils throughout most of this member suggests fairly inhospitable living conditions or at least unfavorable conditions for fossil preservation. The environment represented by the upper part of the member, the source of our sample, must have been unusual in some way because other organisms that occur there are also gigantic, including other species of scaphites and bivalves. The factors responsible for this gigantism are unknown.

In the Trail City Member, the mean size in the lower three zones is nearly constant with only minor fluctuations. The mean size is 58.4 mm in LNAZ, 61.4 mm in LGAZ, and 60.2 mm in UNAZ. In each of these time intervals,

the animals lived in a similar environment downcurrent of the submarine sand bar (Fig. 26). The most notable change in mean size occurs in POAZ ($\bar{x}$ = 65.6 mm). This change correlates with a marked change in the paleoenvironmental regime. There is a sudden increase in the percentage of sand at this time, which is related to the advance of the submarine sand body into the area. The continued growth of this submarine sand body coincided with the disappearance (= extinction) of *Hoploscaphites nicolletii* and the appearance of the closely related species *Hoploscaphites comprimus* (Owen, 1852). This species inhabited the shallow subtidal environment on the margins of the sand body.

Thus, the macroconchs of *Hoploscaphites nicolletii* show fluctuations in mean size with no unidirectional change upsection. The mean size at the first appearance of the species in the Elk Butte Member is significantly larger than that at its last appearance in POAZ. However, for most of its stratigraphic range in the Trail City Member, the mean size remains relatively stable.

This pattern of relative stability over 0.75 Ma is indicative of stasis during the evolutionary history of this species (see Eldredge and Gould, 1972; Eldredge, 1989; Gould and Eldredge, 1977; Williamson, 1981). Similar patterns of stasis have been reported in other taxa. For example, Raup and Crick (1981, fig. 3) documented a pattern of random fluctuations in the size of a Jurassic ammonite from England. Lieberman et al. (1994, 1995) documented a similar pattern of random fluctuations in the morphology of two Devonian species of brachiopods over approximately 5 Ma. In contrast, Hallam (1978) documented a gradual increase in size in several species of Jurassic bivalves (see Hallam, 1998, for a recent review of punctuated equilbria versus phyletic gradualism).

10.3 Multiple size classes at maturity

The modal size class of *Hoploscaphites nicolletii* macroconchs differs between the Elk Butte and Trail City members. In the Elk Butte Member, the size distribution is nearly flat with a broad mode in the 75-95 mm-size interval. In the Trail City Member, the size distribution is unimodal with a well-defined mode in the 55-60 mm-size interval. The shape of this distribution contrasts with that published in Landman and Waage (1993, fig. 57), which showed two modes, a primary mode in the 55-60 mm-size interval and a secondary mode in the 70-75 mm-size interval. However, the sample in our study is much larger and includes approximately 600 additional specimens.

Within the Trail City Member, the size distribution in each assemblage zone is unimodal (compare with Landman and Waage, 1993, fig. 58).

However, the modal size class varies among zones: 55-60 mm in LNAZ and UNAZ, 55-65 mm in LGAZ, and 60-70 mm in POAZ. In addition, in two of the assemblage zones (LNAZ and UNAZ) there are significant differences in mean size between samples from different geographic areas.

Samples from individual localities offer an approximation of the size variation at a single time and place. It is important to note, however, that except for five localities from LNAZ with 50 or more specimens, most localities discussed here have fewer than 20 specimens. Nevertheless, in all localities examined, with only one exception, the size distribution is unimodal. In the one exception (loc. 53), the distribution is bimodal, but the difference in the modes is only three specimens.

Samples from individual concretions offer the best approximation of the size variation at a single time and place because these concretions probably preserve animals that lived at the same time. The 15 concretions in LNAZ with 10 or more specimens each constitute the largest samples. There is no evidence for bimodality in any of these samples. Samples from concretions from the same locality show the same modal size class.

Thus, there is no indication of the existence of more than one adult size class of macroconchs at any one time and place. However, there are significant differences in mean size between populations from different time intervals and from different geographic areas within the same time interval. Such differences in mean size may have been associated with changes in the rate of growth or timing of maturation, as suggested by the theory of developmental polymorphism (Matyja, 1986).

11. CONCLUSIONS

1) In two of the assemblage zones, LNAZ and UNAZ, macroconchs of *Hoploscaphites nicolletii* show a geographic pattern of size variation with larger specimens in the southwestern portion and smaller specimens in the northeastern portion of the species distribution. This size difference is attributed to differences in the environment between these two areas. No such size differences occur in LGAZ and POAZ, suggesting the existence at these times of a more uniform environment throughout the area of species distribution.

2) The adult size of *Hoploscaphites nicolletii* fluctuated over geologic time (approximately 0.75 Ma) with no undirectional change. Such fluctuations corresponded with changes in the environment and appear to have been ecophenotypic. This pattern of stratigraphic variation suggests stasis during the evolutionary history of this species.

3) Samples of macroconchs of *Hoploscaphites nicolletii* from a single

time and place show only a single size mode. However, there are significant differences in adult size between samples from different time intervals and from different geographic areas within the same time interval.

4) Populations of *Hoploscaphites nicolletii* are dimorphic consisting of macroconchs and microconchs. There is no evidence of polymorphism.

ACKNOWLEDGMENTS

We thank the late Karl M. Waage, Tim White, and Cope MacClintock (all Yale University) for their enormous help in this project, the late Les Marcus (AMNH) for his invaluable assistance in the statistical analysis of the data, and Bruce Lieberman (University of Kansas), Richard A. Davis (College of Mount St. Joseph), Peter Harries (University of South Florida) and Neal Larson (Black Hills Museum of Natural History) for reviewing an early draft of this manuscript and making many helpful suggestions. In addition, we thank Bushra Hussaini (AMNH) who measured specimens and converted the locality data into latitude and longitude; Marie Lawrence (AMNH) who organized the data in the departmental computer; Portia Rollings (AMNH) who carefully prepared all the figures; and Stephanie Crooms (AMNH) who word processed the manuscript.

REFERENCES

Boyle, P. R. (ed.), 1983, *Cephalopod Life Cycles*, Vol. 1, Academic Press, New York.

Bucher, H., Landman, N. H., Klofak, S. M., and Guex, J., 1996, Mode and rate of growth in ammonoids, in: *Ammonoid Paleobiology* (N. H. Landman, K. Tanabe, and R. A. Davis, eds.), Plenum Press, New York, pp. 407-461.

Callomon, J. H., 1981, Dimorphism in ammonoids, in: *The Ammonoidea* (House, M. R. and Senior, J. R., eds.), *Syst. Ass. Sp. Vol*. **18**:257-273.

Callomon, J. H., 1988, [Review of] Matyja, B. A., 1986, Developmental polymorphism in Oxfordian ammonites, *Acta Geol. Pol*. **36**:37-68, *Cephalopod Newsl*. **9**:14-16.

Cobban, W. A., Merewether, E. A., Fouch, T. D., and Obradovich, J. D., 1994, Some Cretaceous shorelines in the Western Interior of the United States, in: *Mesozoic Systems of the Rocky Mountain Region, USA* (M. V. Caputo, J. A. Peterson, and K. Franczyk, eds.), SEPM Rocky Mountain Section, Denver, pp. 393-413.

Cobban, W. A., 1969, The Late Cretaceous ammonites *Scaphites leei* Reeside and *Scaphites hippocrepis* (DeKay) in the Western Interior of the United States, *U. S. Geol. Surv. Prof. Pap.* **619**:29 p.

Davis, R. A., Landman, N. H., Dommergues, J.-L., Marchand, D., and Bucher, H., 1996, Mature modifications and dimorphism in ammonoid cephalopods, in: *Ammonoid Paleobiology* (N. H. Landman, K. Tanabe, and R. A. Davis, eds.), Plenum Press, New York, pp. 463-539.

Eldredge, N., 1989, *Macroevolutionary Dynamics*, McGraw Hill, New York.

Eldredge, N., and Gould, S. J., 1972, Punctuated equilibria: An alternative to phyletic gradualism, in: *Models in Paleobiology* (T. J. Schopf, ed.), Freeman, Cooper, San Francisco, pp. 82-115.

Elmi, S., and Benshili, K. 1987, Relation entre la structuration tectonique, la composition des peuplements et l'évolution: exemple du Toarcien du Moyen-Atlas méridional (Maroc), *Boll. Soc. Paleontol. Ital.* **26**:47-62.

Gould, S. J., and Eldredge, N., 1977, Punctuated equilibria: the tempo and mode of evolution reconsidered, *Paleobio.* **3**:115-151.

Hallam, A., 1978, How rare is phyletic gradualism and what is its evolutionary significance? Evidence from Jurassic bivalves, *Paleobio.* **4**:16-25.

Hallam, A., 1998, Speciation patterns and trends in the fossil record, *Geobios* 30:921-930.

Hewitt, R. A., and Hurst, J. M., 1977, Size changes in Jurassic liparoceratid ammonites and their stratigraphic and ecological significance, *Lethaia* **10**:287-301.

Kauffman, E. G., Sageman, B. B., Kirkland, J. I, Elder, W. P., Harries, P. J., and Villamil, T. 1993, Molluscan biostratigraphy of the Cretaceous Western Interior Basin, North America, in: *Evolution of the Western Interior Basin* (W. G. E. Caldwell and E. G. Kauffman, eds.), *Geol. Assoc. Can. Sp. Pap*. **39**:397-434.

Kemper, E., and Wiedenroth, K. 1987, Klima und Tier-Migrationen am Beispiel der früh-kretazischen Ammoniten Nordwestdeutschlands, *Geol. Jahr*. **A96**:315-363.

Kennedy, W. J., 1986a, The ammonite fauna of the Calcaire à *Baculites* (Upper Maastrichtian) of the Cotentin Peninsula (Manche, France), *Palaeont.* **29**:25-83.

Kennedy, W. J., 1986b, The ammonite fauna of the type Maastrichtian with a revision of *Ammonites colligatus* Binkhorst, 1861, *Bull. Inst. R. Sci. Nat. Belg.* **56**:151-267.

Landman, N. H., and Waage, K. M., 1993, Scaphitid ammonites of the Upper Cretaceous (Maastrichtian) Fox Hills Formation in South Dakota and Wyoming, *Bull. Am. Mus. Nat. Hist.* **215**:1-257.

Lieberman, B. S., Brett, C. E., and Eldredge, N., 1994, Patterns and processes of stasis in two species lineages of brachiopods from the Middle Devonian of New York State, *Amer. Mus. Novitates* **3114**:1-23.

Lieberman, B. S., Brett, C. E., and Eldredge, N., 1995, A study of stasis and change in two species lineages from the Middle Devonian of New York State, *Paleobio.* **21**:15-27.

Mancini, E. A., 1978, Origin of micromorph faunas in the geologic record, *J. Paleontol*. **52**:311-322.

Matyja, B. A., 1986, Developmental polymorphism in Oxfordian ammonites, *Acta Geol. Pol*. **36**:37-68.

Matyja, B. A., 1994, Developmental polymorphism in the Oxfordian ammonite subfamily Peltoceratinae, *Palaeopelagos Special Publication 1, Proceedings of the 3rd Pergola International Symposium, Rome*, pp. 277-286.

Matyja, B. A., and Wierzbowski, A. 2000. Biological response of ammonites to changing environmental conditions: An example of Boreal *Amoeboceras* invasions into Submediterranean Province during Late Oxfordian, *Acta Geol. Pol.* **50**:45-54.

Mignot, Y., Elmi, S., and Dommergues, J.-L, 1993, Croissance et miniaturisation de quelques *Hildoceras* (Cephalopoda) en liasion avec des environnements contraignant de la Tethys toarcienne, *Geobios. Mem. Spec*. **15**:305-312.

Morton, S. G., 1842, Description of some new species of organic remains of the Cretaceous Group of the United States with a tabular view of the fossils hitherto discovered in this formation, *J. Acad. Nat. Sci. Phil.* **8**:207-227.

Owen, D. D., 1852, Description of new and imperfectly known genera and species of organic remains, collected during the geological surveys of Wisconsin, Iowa, and Minnesota, in: *Report of a Geological Survey of Wisconsin, Iowa, and Minnesota; and Incidentally of a*

Portion of Nebraska Territory, Lippincott, Philadelphia, pp. 573-587.

Raup, D. M., and Crick, R. E., 1981, Evolution of single characters in the Jurassic ammonite *Kosmoceras*, *Paleobio.* **7**:200-215.

Reboulet, S. 2001. Limiting factors on shell growth, mode of life and segregation of Valanginian ammonoid populations: evidence from adult-size variations, *Geobios* **34**:423-435.

Rhoads, D. C., Speden, I. G., and Waage, K. M., 1972, Trophic group analysis of Upper Cretaceous (Maastrichtian) bivalve assemblages from South Dakota, *AAPG Bull.* **56**:1100-1113.

Riccardi, A. C., 1983, Scaphitids from the Upper Campanian-Lower Maastrichtian Bearpaw Formation of the Western Interior of Canada, *Geol. Surv. Can. Bull.* **354**:1-51.

Stevens, G. R., 1988, Giant ammonites: A review, in: *Cephalopods - Present and Past* (J. Wiedmann and J. Kullmann, eds.) Schweizerbart'sche Verlagsbuchhandlungs, Stuttgart, pp. 141-166.

Waage, K. M., 1964, Origin of repeated fossiliferous concretion layers in the Fox Hills Formation, *Kansas Geol. Surv. Bull*. **169**:541-563.

Waage, K. M., 1965, The Late Cretaceous coleoid cephalopod *Actinosepia canadensis* Whiteaves, *Peabody Mus. Nat. Hist. Yale Univ. Postilla* **94**:1-33.

Waage, K. M., 1968, The type Fox Hills Formation, Cretaceous (Maastrichtian), South Dakota, Part 1, stratigraphy and paleoenvironments, *Peabody Mus. Nat. Hist. Yale Univ. Bull*. **27**:1-175.

Williamson, P. G., 1981, Paleontological documentation of speciation in Cenozoic molluscs from Turkana Basin, *Nature* **293**:437-443.

Chapter 6

Controls on Shell Shape in Acanthoceratid Ammonites from the Cenomanian-Turonian Western Interior Seaway

MARGARET M. YACOBUCCI

1. INTRODUCTION

Epeiric seas have often played host to the rapid evolutionary radiations of ammonoid groups. The Cretaceous Western Interior Seaway was no

MARGARET M. YACOBUCCI • Bowling Green State University, Department of Geology, 190 Overman Hall, Bowling Green, OH 43403-0218.

P.J. Harries (ed.), *High-Resolution Approaches in Stratigraphic Paleontology.*

exception. Members of the ornamented ammonite family Acanthoceratidae migrated into and radiated within the newly formed Western Interior Seaway during the Cenomanian. Due to the intensive work on constructing a high-resolution stratigraphic framework for the Western Interior (see Kauffman, 1986; Kauffman *et al.,* 1987, 1993; Kauffman and Caldwell, 1993 for overviews), this radiation of ammonites is extremely well-constrained stratigraphically, geographically, and temporally. The well-defined and limited nature of the acanthoceratid diversification makes the event a natural experiment for exploring patterns and processes associated with rapid endemic radiations.

1.1 Ammonoid Shell Shape

One pattern that certainly requires exploration is the increased variation in shell shape often seen in epeiric sea ammonites (Haas, 1946; Reeside and Cobban, 1960; Reyment, 1975, 1988; Crick, 1978; Callomon, 1985; Reyment and Kennedy, 1991; Dagys and Weitschat, 1993; Jacobs *et al.,* 1993, 1994; Checa *et al.,* 1997). The evolutionary significance of such variability has not been fully appreciated. Theoretically, morphological variation may promote the origination of new taxa (West-Eberhard, 1989; McCune, 1990; Lloyd and Gould 1993) as well as provide a taxon with protection from extinction (Sheldon, 1993). Many ammonoid groups underwent rapid evolutionary radiations within epeiric seaways; these radiations may be associated with enhanced morphological variability. However, before we can formulate hypotheses about the role that morphological variability may play in the production of new diversity, we must demonstrate that these variable morphologies are not themselves merely an ecophenotypic response to varying environments. If we cannot rule out ecophenotypy, the patterns in shell morphology we observe may be telling us more about environmental shifts than evolutionary processes.

The crucial question is whether shell morphology is more a function of the environment in which an ammonite found itself, or of the ammonite's genetic-developmental program (or, more broadly, phylogenetic relationships). Of course, these are not mutually exclusive categories – natural selection ensures a relationship between genetically determined morphologies and the environments to which they are adapted. Natural selection can also act upon the type and extent of ecophenotypic response to the environment (Williams, 1966; West-Eberhard, 1989). However, ammonoid workers frequently relate shell shape strictly to environmental influences; fossil taxa that show an array of forms are often assumed *a priori* to be ecophenotypically plastic (e.g., Crick, 1978; Reyment and Kennedy, 1991). In some cases, specific relationships between morphology and

environment can be demonstrated. For instance, in *Scaphites whitfieldi* from the Turonian of the Western Interior, Jacobs *et al.* (1993, 1994) found that the width of the whorl section correlates with facies distribution, so that compressed shells with lower drag coefficients appear in higher current energy environments. These results suggest that an ammonite's morphology may be more a response to the environment than a reflection of phylogenetic constraints. They also suggest that morphological variability within an ammonoid species strongly reflects environmental, rather than genetic, variation.

On the other hand, the notion of internal controls on shell form has also been suggested. Callomon (1985), for instance, noted that a high range of morphological variation in the Jurassic cardioceratids persisted for several million years despite migrations and changes in habitat, suggesting that shell morphology is not strictly tied to particular environmental conditions. Reyment (1988) attributed the pronounced variability of Cretaceous vascoceratids from West Africa to genetically based, multiple niche polymorphism, which is common in modern gastropods (Goodfriend, 1986).

Of course, even if a relationship between shell morphology and an environmental factor can be shown, such a link does not by itself prove that morphology is controlled by that factor. For example, given a correlation between shell shape and facies, the underlying *cause* of the differing shell shapes may not be facies *per se,* but rather some related factor, such as the geographical region, time interval, or stage of a sea-level cycle in which the ammonoids lived. Alternatively, it is possible that more complex, higher level processes were operating. For instance, suppose we find that more rounded shell shapes are associated with a time of peak transgression. This pattern could result from the high sea-level stand promoting the diversification of clades characterized by more rounded shells. Thus taxon sorting results, with an environmental factor causing a proliferation of a particular shell shape, even though the shell shape itself is phylogenetically constrained.

1.2 Previous Work

The distribution of ammonite morphotypes in the Cenomanian-Turonian Western Interior Seaway has been previously investigated. In a series of papers, Batt (1989, 1991, 1993) related ammonite shell forms to environmental factors within the seaway. He examined more than 7,000 specimens of all ammonites known from the seaway and grouped them into morphotypes based on the degree of shell involution, the shell width, the whorl section, and ornamentation. He distinguished 18 morphotype groups, whose geographic distributions he then plotted onto facies maps constructed

for each ammonite zone. From these maps, it was apparent that most ammonites were not restricted to particular depths or facies, although very heavily ornamented forms (including many acanthoceratids) and compressed discoidal forms tended to occur in areas where water depth was less than 50 or 100 meters. Batt inferred mode of life from both shell shape and the relative height of suture elements, as expressed by the Sutural Amplitude Index (SAI) (defined as ten times the ratio of maximum suture element height to suture length). From these, he argued that forms like adult acanthoceratids, with heavy ornament and relatively low SAIs (despite their sutures' high general complexity) were likely to be restricted to shallow nektobenthic habitats, while taxa with higher SAIs (even if ornamented, like the Turonian acanthoceratid *Mammites)* could be found in deeper water.

Batt's work has been invaluable for documenting broad patterns of morphotype distribution, but cannot answer several important questions on what controls ammonoid morphology. Because his primary interest was in using ammonite distributions to infer paleoenvironments, he intentionally avoided considering individual taxa within each morphotype group. He argued that taxonomy was not a good environmental indicator, since individual species tended to be widespread throughout the seaway. Hence, his work cannot address phylogenetic aspects of shell shape. Nor did he address temporal or regional differences within the seaway. Also, the use of suture morphology as a measure of depth tolerance may not be reliable (Saunders, 1995, Saunders and Work, 1996; Daniel *et al.,* 1997; but see also Hewitt and Westermann, 1997).

To properly understand controls on ammonite shell shape, we need to look at the detailed regional, temporal, and environmental patterns of shell shape distribution within several lineages of a well-defined clade. The radiation of acanthoceratid ammonites during the Cenomanian-Turonian Greenhorn Cyclothem provides an opportunity to rigorously test which of a host of factors may control ammonoid shell shape. We can determine how shell shape relates to the facies, the region of the seaway, and the time interval in which individuals are found; and we may contrast these patterns to phylogenetic groupings of individuals. If it is found that shell shape and morphological variability do not correlate with major environmental changes, but rather have strong heritable components, the validity of evolutionary studies of ammonoid shell shape will be supported.

2. METHODOLOGY

Many groups of ammonites show a strong correlation among basic shell

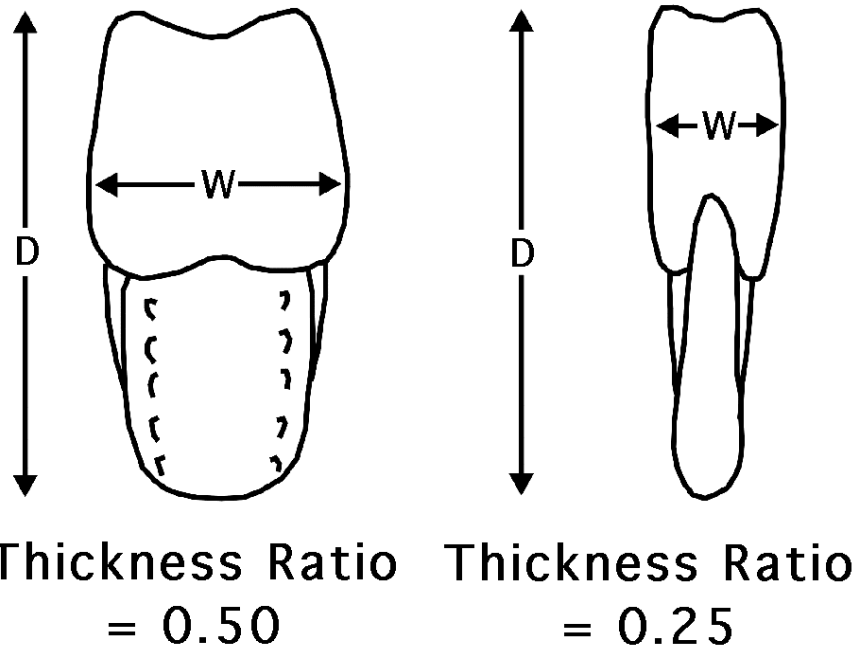

Figure 1. The thickness ratio is the whorl width (W) divided by the shell diameter (D). Ammonites with thickness ratios greater than 0.50 are considered depressed; those with thickness ratios less than 0.30 are considered compressed.

shape parameters. Individuals tend to have either narrow, tall whorl sections and narrow umbilici, or wide, short whorl sections and wide umbilici. This association is so common it has been named Buckman's Law of Covariation (Westermann, 1966). Because of this correlation, a single metric can provide a useful shorthand to capture most of the characteristic shell shape for each specimen. One commonly used metric is the ratio of whorl width to shell diameter, the *thickness ratio* (Fig. 1). Ammonites with thickness ratios below 0.30 are generally considered compressed while those with thickness ratios above 0.50 are considered depressed (Fig. 2). Thickness ratios have been used to relate ammonite shell shape to environmental parameters (Jacobs *et al.,* 1993, 1994).

I calculated thickness ratios from measured widths and diameters of 346 specimens; these represent 16 Late Albian, Cenomanian, and Turonian ammonite genera from the Western Interior and Texas. In addition to fourteen acanthoceratid genera, the purported ancestor to the first acanthoceratids (*Stoliczkaia*) and the mortoniceratid *Mortoniceras*, which is abundant in the Late Albian of Texas, were included for comparison. Both adults and juveniles were considered together, as a way of increasing sample

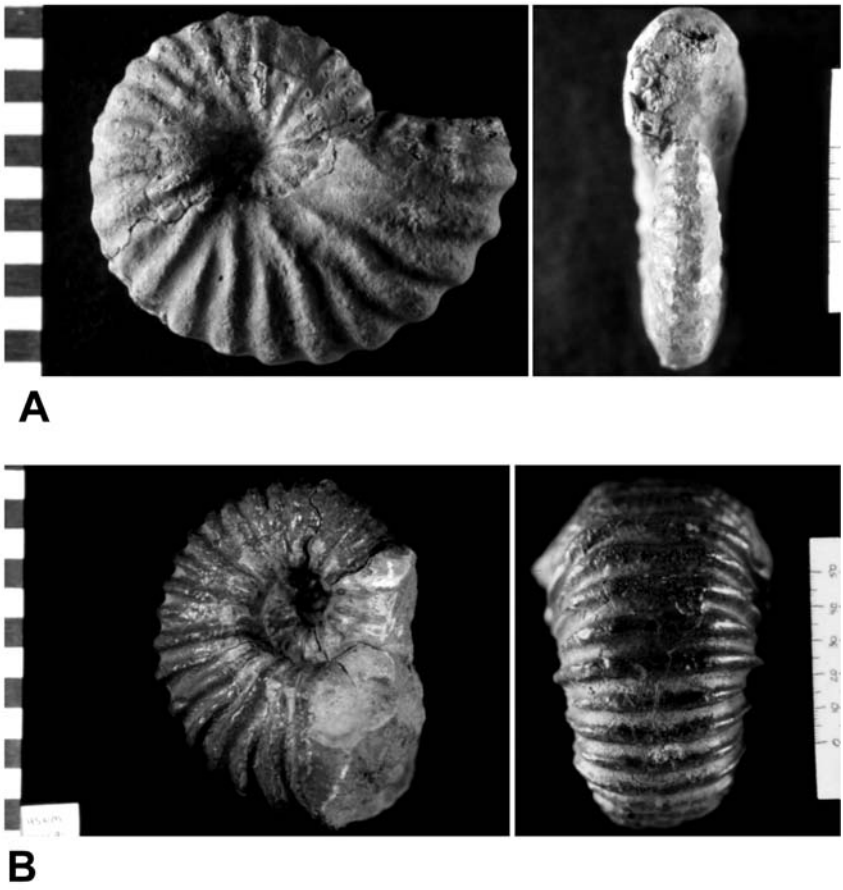

Figure 2. The thickness ratio is the whorl width (W) divided by the shell diameter (D). Ammonites with thickness ratios greater than 0.50 are considered depressed; those with thickness ratios less than 0.30 are considered compressed. A. Two views of *Metoicoceras mosbyense* (USNM 427949), Mosby Sandstone Member, Belle Fourche Shale, Petroleum Co., Montana. Thickness ratio = 0.30. B. Two views of *Calycoceras canitaurinum* (USNM 422696), Frontier Formation, Bighorn Co., Wyoming. Thickness ratio = 0.59. Scale bars in cm.

sizes. Sexual dimorphism has been proposed for a few of the acanthoceratid taxa, but is relatively minor and difficult to discern (Wright and Kennedy, 1981, 1984, 1987; Cobban, 1987; Kennedy, 1988; Cobban and Kennedy, 1991); hence, no dimorphs were distinguished. I used only specimens that had adequate locality information for determining from which ammonite zone the specimen derived, and whether the specimen came from a muddy, silty, or sandy facies. Facies were defined solely by grain sizes (so, for instance, both carbonate and siliciclastic muds were considered “muddy”), as

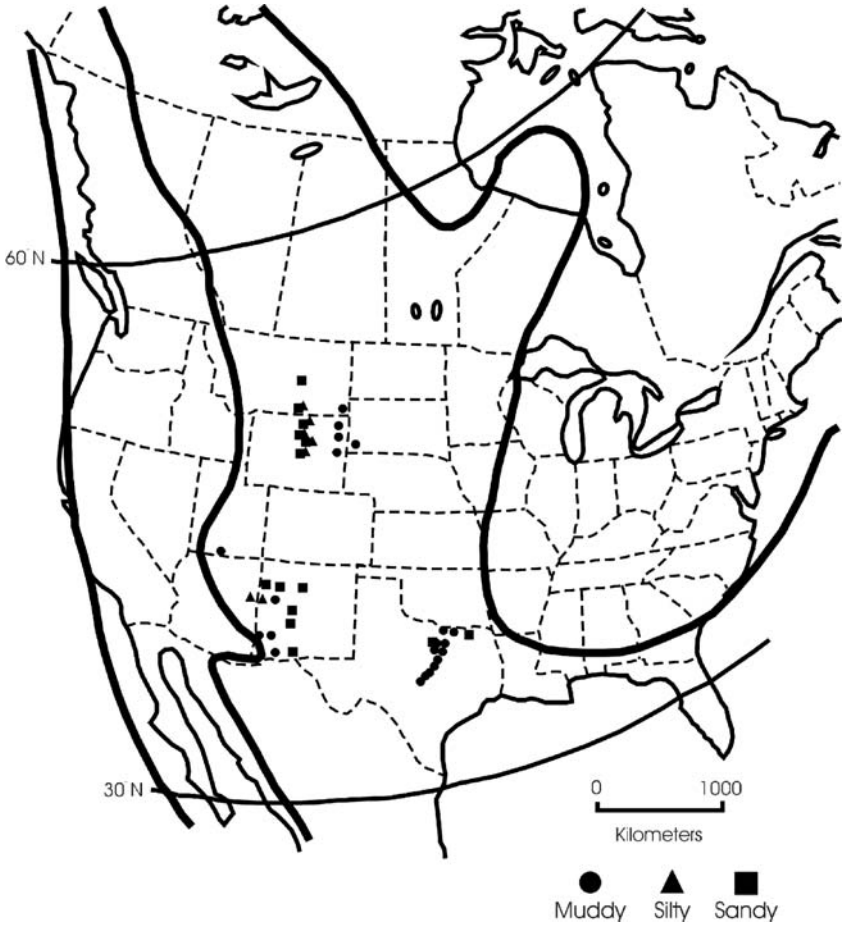

Figure 3. Locality map. Localities are grouped by county, with facies indicated by symbols. Paleoshoreline is from Batt (1989) and Roberts and Kirschbaum (1995). Approximate paleolatitudes are from Smith *et al.* (1994).

the hydrodynamic conditions at the time of deposition are the parameter of interest. I also divided the data into three distinct regions — the Northern Western Interior (Montana, Wyoming, South Dakota), Southern Western Interior (New Mexico, Arizona, Southern Utah), and Texas — that capture both latitudinal and onshore-offshore differences.

The map in Figure 3 shows the ammonite localities used (grouped by county). Facies are indicated by symbols. The paleo-shoreline is based on reconstructions by Batt (1989) and Roberts and Kirschbaum (1995); approximate paleolatitudes are from Smith *et al.* (1994). Figure 4 provides a time scale with radiometric dates and recognized Western Interior and Texas ammonite zones for the Late Albian through mid-Turonian.

Absolute Age	Stage	Ammonite Zone		
90.51±0.45 Ma →	Middle Turonian	23	*P. hyatti*	
		22	*P. percarinatus*	
		21	*C. woollgari*	
	Lower Turonian	20	*M. nodosoides*	
		19	*V. birchbyi*	
93.25±0.55 Ma →		18	*P. flexuosum*	
	Upper Cenomanian	17	*N. scotti*	
93.59±0.58 Ma →		16	*N. juddii*	
		15	*V. cauvini*	
93.49±0.89 Ma →		14	*S. gracile*	
		13	*M. mosbyense*	*D. conditum*
		12		*D. albertense*
		11	*D. problematicum*	
94.63±0.61 Ma →		10	*D. pondi*	
	Middle Cenomanian	9	*P. wyomingense*	
94.93±0.53 Ma →		8	*A. amphibolum*	
		7	*A. bellense*	
		6	*P. muldoonense*	
		5	*A. granerosense*	
95.78±0.61 Ma →		4	*C. tarrantense*	
	Lower Cenomanian	3	*F. brundrettei*	
		2	*A. inconstans*	
98.5±0.5 Ma →		1	*M. mantelli*	
	Upper Albian	0	Unzoned	

Figure 4. Ammonite zones and absolute ages for the Late Albian through Middle Turonian Western Interior and Texas. Radiometric dates are from Obradovich (1993); ammonite zones are based on Cobban (1988, 1990) and Hancock *et al.* (1993).

To test for controls on thickness ratio, I ran the analysis as follows. Each specimen was assigned to categories based on the facies, region, and ammonite zone in which it occurred, and to which taxon it belonged. Two levels of comparison were performed, one comparing different genera and one comparing species within the genus *Metoicoceras* (the genus for which I had the most specimens). Distributions of thickness ratio were plotted and summary statistics calculated for each grouping. I then tested for significant effects of these factors on thickness ratio, by performing statistical tests comparing the central tendencies of these distributions. Ordinarily, an

analysis of variance would be the appropriate statistical technique, but many of the distributions violated one or both of two key assumptions of ANOVAs: normality and equal variances. In the case of non-normal distributions, a nonparametric Kruskal-Wallis test that compares the medians of the distributions was performed, and significantly different pairs were determined from Bonferroni post-hoc hypothesis tests (the Bonferroni test multiples p-values by the total number of tests performed, because when testing the significance of multiple pairs, the possibility of finding one significant difference purely by chance increases with the number of pairs tested). In cases where the variances were unequal, an unplanned comparisons test among pairs of means using the Games and Howell method was used (Sokal and Rohlf, 1981). All calculations were done using Microsoft Excel for Windows 95 v. 7.0 and SYSTAT for Windows v. 6.0.

3. RESULTS

3.1 Comparing Genera

Histograms showing the distribution of thickness ratios within each *facies* are shown in Figure 5. Summary statistics for these distributions are shown in Table 1. Considerably more specimens are found in muddy facies than in silty or sandy facies, and the distribution of thickness ratios in muddy facies is significantly right-skewed ($p = 0.006$). The higher number of individuals in muddy facies seems to reflect a preference for these facies.

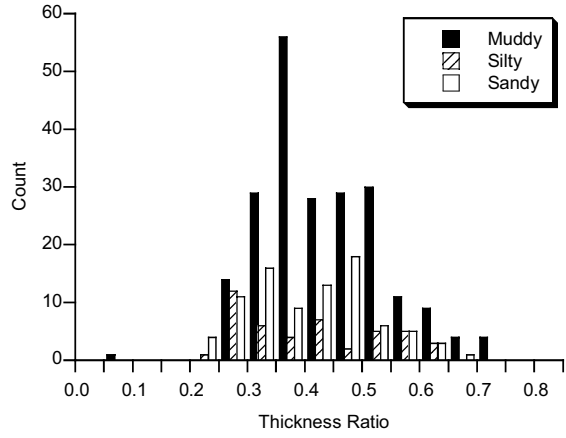

Figure 5. Distributions of thickness ratios for all genera grouped by facies.

Table 1. Summary statistics for thickness ratios grouped by facies.

FACIES	Mean	Median	SD	n
Muddy	0.429	0.407	0.106	215
Silty	0.402	0.387	0.116	45
Sandy	0.403	0.409	0.108	86

No evidence exists for extensive post-mortem transport of these specimens. Also, the acanthoceratid genera considered here are all found in muddy facies and seven are found *only* in muddy facies (the single measured specimen of *Conlinoceras* is from a sandy unit, but the genus is also known from muddy facies). A Kruskal-Wallis test shows no significant differences in median thickness ratio among the three facies ($p = 0.075$).

The distributions of thickness ratio within the three *regions* are shown in Figure 6; summary statistics in Table 2. The distribution of thickness ratios for specimens from the northern Western Interior is distinctly bimodal – a possible explanation for this will be discussed below. Due to inequal variances, tests for significantly different pairs of means were conducted using the Games and Howell method. There were no significant differences at the $p = 0.05$ level.

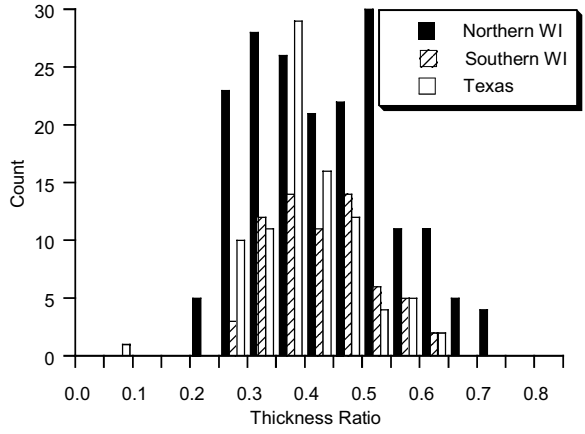

Figure 6. Distributions of thickness ratios for all genera grouped by region.

Table 2. Summary statistics for thickness ratios grouped by region.

REGION	Mean	Median	SD	n
Northern WI	0.430	0.422	0.121	186
Southern WI	0.421	0.422	0.088	67
Texas	0.397	0.386	0.092	90

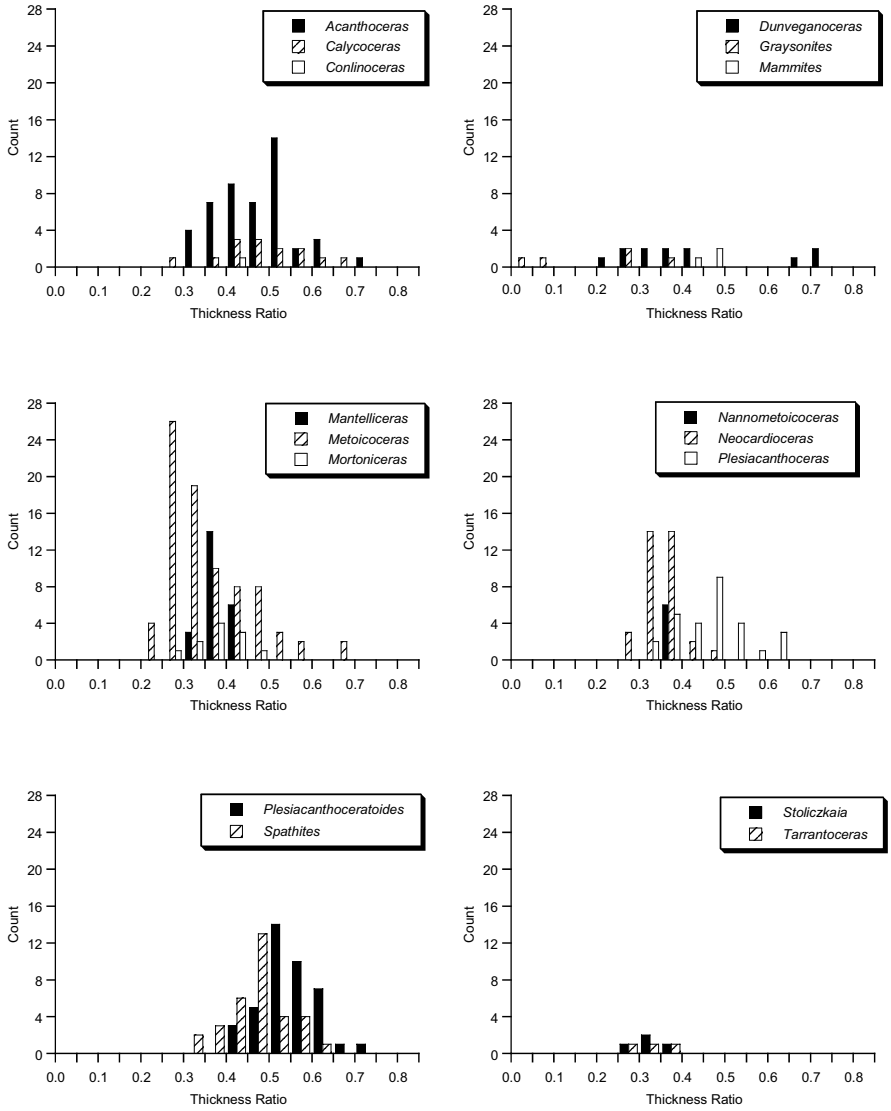

Figure 7. Distributions of thickness ratios for all genera grouped by genus.

Thickness ratio distributions for each *genus* are shown in Figure 7; summary statistics in Table 3. *Metoicoceras* and *Neocardioceras* show significant right skew (p = 0.000 and 0.004). Again, due to inequal variances, significantly different pairs of means were determined using the Games and Howell method. Results of these tests are given in Table 4. The general pattern shows that the genera *Mantelliceras*, *Metoicoceras*, *Nannometoicoceras*, and *Neocardioceras* have relatively low mean thickness ratios, whereas *Acanthoceras*, *Plesiacanthoceras*, *Plesiacanthoceratoides*,

and *Spathites* have relatively high mean thickness ratios. These results show a mixed phylogenetic response. The two progenic dwarf offshoot taxa, *Nannometoicoceras* and *Plesiacanthoceratoides*, retain similar thickness ratios to their parent taxa, *Metoicoceras* and *Plesiacanthoceras*. However, the significantly compressed genus *Metoicoceras* is the ancestor of the depressed *Spathites* (Kennedy *et al*., 1980; Wright and Kennedy, 1981). The two non-acanthoceratid genera included for comparison, *Stoliczkaia* and *Mortoniceras*, are not significantly different from the acanthoceratids.

Table 3. Summary statistics for thickness ratios grouped by genus.

GENUS	Mean	Median	SD	n
Acanthoceras	0.467	0.457	0.091	47
Calycoceras	0.486	0.472	0.105	14
Conlinoceras	(0.404)	(0.404)	-----	1
Dunveganoceras	0.429	0.383	0.178	12
Graysonites	0.255	0.276	0.121	4
Mammites	0.444	0.445	0.040	3
Mantelliceras	0.378	0.369	0.030	23
Metoicoceras	0.353	0.317	0.099	82
Mortoniceras	0.373	0.372	0.049	11
Nannometoicoceras	0.366	0.363	0.018	6
Neocardioceras	0.345	0.343	0.040	34
Plesiacanthoceras	0.458	0.466	0.081	28
Plesiacanthoceratoides	0.545	0.543	0.062	41
Spathites	0.466	0.463	0.068	33
Stoliczkaia	0.312	0.312	0.053	4
Tarrantoceras	0.315	0.322	0.042	3

Finally, thickness ratios for all specimens found in each ammonite *zone* are plotted in Figure 8; summary statistics for these distributions are in Table 5. These distributions are considerably more distinct from one another than are those of the other factors. Unplanned comparisons using the Games and Howell method were calculated for all pairs of distributions. Results of these tests are given in Table 6. A conspicuous temporal pattern to these mean thickness ratios can be seen – Upper Cenomanian zones are significantly lower than Middle Cenomanian and Turonian zones. This difference accounts for the bimodality of the distribution of thickness ratios for specimens from the Northern Western Interior – Middle and Upper Cenomanian specimens are pooled, each with its own unimodal distribution (Fig. 9). While this temporal pattern is intriguing, it is difficult to separate these differences from those for genera. Three of the four genera with the highest mean thickness ratios are Middle Cenomanian (the other is Turonian), and three of the four genera with the lowest mean thickness ratios

Table 4. Pairs of genera with significantly different mean thickness ratios.[a]

GENUS	Aca	Cal	Con	Dun	Gra	Mam	Man	Met	Mor	Nan	Neo	Ple	Poi	Spa	Sto	Tar
Aca	-----	-----	-----	-----	-----	-----	-----	-----	-----	-----	-----	-----	-----	-----	-----	-----
Cal																
Con																
Dun																
Gra																
Mam																
Man	●															
Met	●															
Mor																
Nan	●															
Neo	●															
Ple								●		●						
Poi							●	●	●	●	●					
Spa							●	●		●	●					
Sto													●			
Tar													●			

[a]Bullets indicate pairs significantly different with $p<0.05$. In general, *Mantelliceras*, *Metoicoceras*, *Nannometoicoceras*, and *Neocardioceras* have low mean thickness ratios, while *Acanthoceras*, *Plesiacanthoceras*, *Plesiacanthoceratoides*, and *Spathites* have high mean thickness ratios.

are Upper Cenomanian (the other is Lower Cenomanian). Hence, it is unclear whether the temporal pattern actually reflects a purely phylogenetic phenomenon, or whether something about these time periods promoted the occurrence of taxa with higher or lower thickness ratios.

In sum, comparisons among genera show that the thickness ratio of these acanthoceratid ammonites is not related to the facies or to the region in

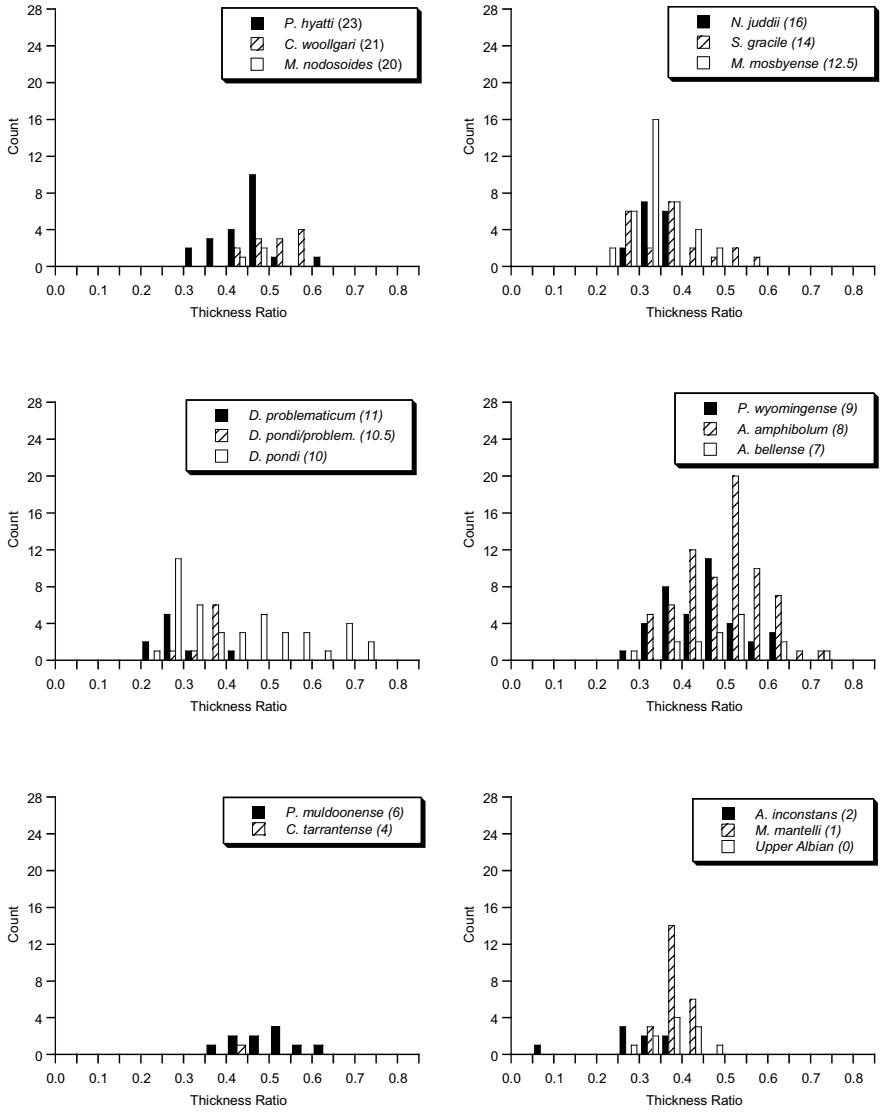

Figure 8. Distributions of thickness ratios for all genera grouped by ammonite zone.

which they are found. Some genera do have significantly higher or lower mean thickness ratios than others. Upper Cenomanian acanthoceratids seem to have a lower mean thickness ratio than those that preceded or followed them.

Table 5. Summary statistics for thickness ratios grouped by zone.

ZONE	Mean	Median	SD	n
***Prionocyclus hyatti* (23)**	0.443	0.453	0.065	21
***Collignoniceras woollgari* (21)**	0.507	0.512	0.052	12
***Mammites nodosoides* (20)**	0.444	0.445	0.040	3
***Neocardioceras juddii* (16)**	0.330	0.326	0.025	15
***Sciponoceras gracile* (14)**	0.370	0.360	0.091	21
***Metoicoceras mosbyense* (12.5)**	0.335	0.329	0.065	37
***Dunveganoceras. problematicum* (11)**	0.285	0.271	0.063	9
***Dun. pondi/Dun. problematicum* (10.5)**	0.343	0.360	0.036	8
***Dunveganoceras pondi* (10)**	0.429	0.403	0.147	42
***Plesiacanthoceras wyomingense* (9)**	0.443	0.456	0.089	38
***Acanthoceras amphibolum* (8)**	0.492	0.505	0.091	71
***Acanthoceras bellense* (7)**	0.487	0.484	0.106	16
***Plesiacanthoceras muldoonense* (6)**	0.488	0.498	0.073	10
***Conlinoceras tarrantense* (4)**	(0.404)	(0.404)	-----	1
***Acompsoceras inconstans* (2)**	0.284	0.290	0.092	8
***Mantelliceras mantelli* (1)**	0.378	0.369	0.030	23
Late Albian (0)	0.373	0.372	0.049	11

3.2 Comparing Species of *Metoicoceras*

Moving down a taxonomic level to look at patterns among the eight species within the genus *Metoicoceras*, we find some intriguing differences from the generic-level comparisons. Histograms showing the distribution of thickness ratio for specimens of *Metoicoceras* for the three *facies* are plotted in Figure 10; summary statistics are given in Table 7. The distribution for those specimens found in muddy facies is considerably broader than those for silty and sandy facies. An unplanned comparison test shows that the mean thickness ratio for the muddy facies specimens is significantly higher than those for the silty or sandy facies ($p < 0.05$). Hence, for individuals *within* a genus, facies *does* seem to correlate with shell shape, even though it was not important when multiple genera were pooled together.

The same may be true for regional differences. Histograms for *Metoicoceras* individuals from the three *regions* are plotted in Figure 11; summary statistics are given in Table 8. A Kruskal-Wallis test on the medians gives a p-value very close to significant ($p = 0.064$). The median thickness ratio for the specimens from the southern Western Interior is somewhat higher than that for the northern Western Interior, though this is significant only at the $p = 0.10$ level. The southern distribution is also not right-skewed, as the distributions for specimens from the northern Western Interior and from Texas are.

Table 6. Pairs of ammonite zones with significantly different mean thickness ratios.[b]

	LAl.	E.Cenom.		Middle Cenomanian					Late Cenomanian						E.-Mid Turonian		
ZONE	**0**	**1**	**2**	**4**	**6**	**7**	**8**	**9**	**10**	**11**	**11**	**13**	**14**	**16**	**20**	**21**	**23**
0	-----																
1		-----															
2			-----														
4				-----													
6					-----												
7						-----											
8							-----										
9								-----									
10									-----								
11							●	●		-----							
11					●	●	●	●			-----						
13					●		●	●				-----					
14							●						-----				
16					●	●	●	●						-----			
20															-----		
21		●	●							●	●	●	●	●		-----	
23										●	●	●		●			-----

[b]Bullets indicate pairs significantly different at $p<0.05$.

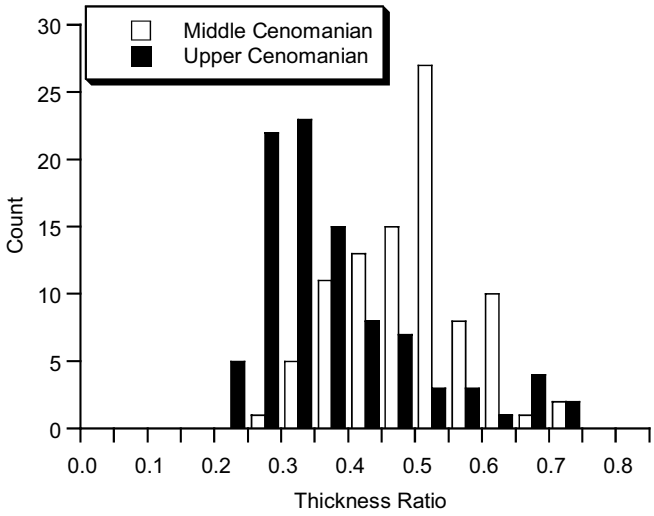

Figure 9. Distributions of thickness ratios for all genera from the Northern Western Interior. Open bars are for Middle Cenomanian specimens; shaded bars are for Upper Cenomanian specimens. Note that combining specimens from these two time periods results in a bimodal distribution overall.

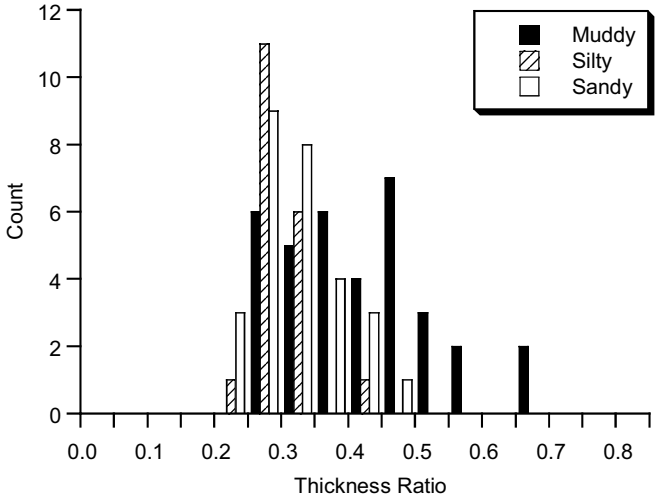

Figure 10. Distributions of thickness ratios for *Metoicoceras* grouped by facies.

The distributions of thickness ratios for *species* of *Metoicoceras* are plotted in Figure 12; summary statistics are listed in Table 9. A Kruskal-Wallis test shows a significant difference in median thickness ratio among these species ($p = 0.0002$). Bonferroni post-hoc comparisons show that this

Table 7. Summary statistics for Metoicoceras thickness ratios grouped by facies.

FACIES	Mean	Median	SD	n
Muddy	0.415	0.409	0.108	35
Silty	0.298	0.283	0.041	19
Sandy	0.314	0.301	0.067	28

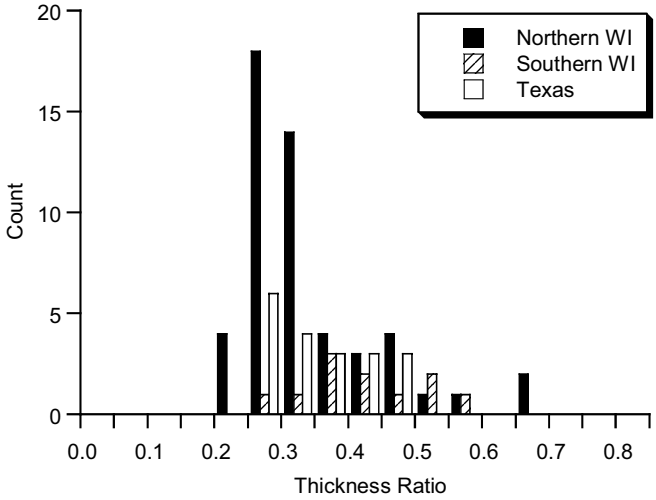

Figure 11. Distributions of thickness ratios for *Metoicoceras* grouped by region.

Table 8. Summary statistics for *Metoicoceras* thickness ratios grouped by region.

REGION	Mean	Median	SD	n
Northern WI	0.341	0.310	0.103	51
Southern WI	0.408	0.395	0.098	11
Texas	0.352	0.323	0.080	19

difference is due to the high median thickness ratios for *M. sp. A* and *M. latoventer*. Other species are not significantly different from each other.

These differences may be related to differences in thickness ratio among the five ammonite zones in which *Metoicoceras* occurs. Histograms for each of these *zones* are plotted in Figure 13; summary statistics are given in Table 10. A Kruskal-Wallis test shows significantly different median thickness ratios among these five zones ($p = 0.028$). The oldest *Metoicoceras* species, from the latest Middle Cenomanian *P. wyomingense* Zone, have a higher median thickness ratio than those from the Late Cenomanian *D. problematicum* and *M. mosbyense* Zones. This pattern is likely due to the presence of *M. latoventer* in the *P. wyomingense* Zone — this species has a significantly higher thickness ratio than most other *Metoicoceras* species.

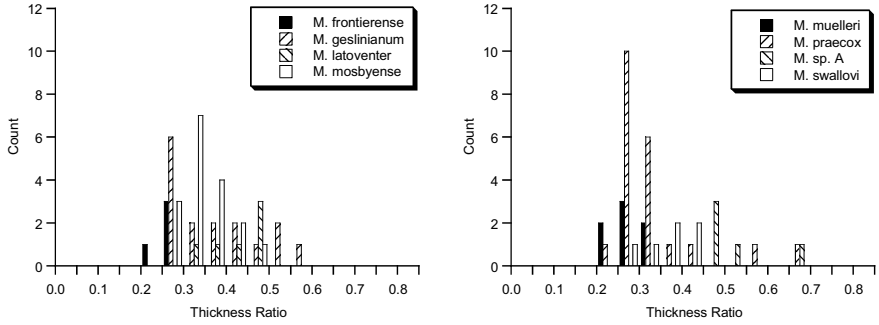

Figure 12. Distributions of thickness ratios for *Metoicoceras* grouped by species.

Table 9. Summary statistics for *Metoicoceras* species thickness ratios grouped by species.

M. frontierense	0.263	0.275	0.034	4
M. geslinianum	0.369	0.330	0.104	16
M. latoventer	0.427	0.452	0.076	6
M. mosbyense	0.343	0.317	0.065	17
M. muelleri	0.266	0.258	0.042	7
M. praecox	0.332	0.290	0.100	21
M. **sp. A**	0.524	0.490	0.073	5
M. swallovi	0.359	0.370	0.055	6

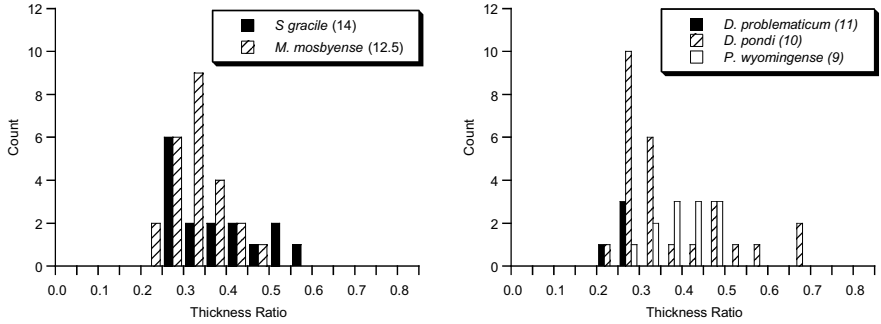

Figure 13. Distributions of thickness ratios for *Metoicoceras* grouped by ammonite zone.

Table 10. Summary statistics for *Metoicoceras* species thickness ratios grouped by zone.

ZONE	Mean	Median	SD	n
***Plesiacanthoceras wyomingense* (9)**	0.393	0.395	0.072	12
***Dunveganoceras pondi* (10)**	0.369	0.318	0.122	26
***D. problematicum* (11)**	0.263	0.275	0.034	4
***Metoicoceras mosbyense* (12.5)**	0.320	0.309	0.068	24
***Sciponoceras gracile* (14)**	0.369	0.330	0.104	16

In sum, specimens of *Metoicoceras* from muddy facies have a higher mean thickness ratio than those from silty or sandy facies. Specimens from the southern Western Interior have somewhat higher thickness ratios than those from the northern Western Interior or Texas. The species *M.* sp. A and *M. latoventer*, and specimens from the Middle Cenomanian seem to have higher thickness ratios.

4. DISCUSSION

4.1 A Complicating Factor – Size

Before interpreting these results, we should note that the thickness ratio is in part a function of the size of the ammonite, as can be seen from a plot of whorl width versus shell diameter (Fig. 14). The slope of the plot is width/diameter = thickness ratio, so changes in slope show changes in thickness ratio. A break in slope occurs at approximately 50 mm in diameter, indicating that small and/or juvenile ammonites are necessarily more rounded than larger and/or adult ammonites (a fitted regression line for specimens less than 50 mm in diameter shows a significantly higher slope than that for larger specimens; Fig. 14). This is consistent with hydrodynamic studies, which have found that at Reynolds numbers less than about 5×10^3, which corresponds to diameters less than 50 mm assuming reasonable swimming or current velocities, more rounded shells actually have less drag than more "streamlined" forms, and would therefore be preferred hydrodynamically (Jacobs, 1992).

Given this inherent relationship between thickness ratio and size, the possibility that differences in thickness ratio are actually solely reflecting size differences should be considered. For instance, if we look at the distributions of diameters for specimens of *Metoicoceras* grouped by facies, there is a large peak of small specimens from muddy facies (Fig. 15). This may be due to the larger sample size for muddy facies, a preservational or sampling bias, or may reflect an actual size segregation, with smaller and/or juvenile ammonites preferring deeper water. The significantly higher mean thickness ratio for *Metoicoceras* specimens from muddy facies, then, may simply reflect this size difference. One might infer from this that juvenile or small individuals prefer quieter and/or deeper water; however, the complete range of diameters can be found in both muddy and sandy facies – there appears to be no *limitation* of size in a particular facies. Also, when all *genera* are compared, no significant differences in thickness ratio among

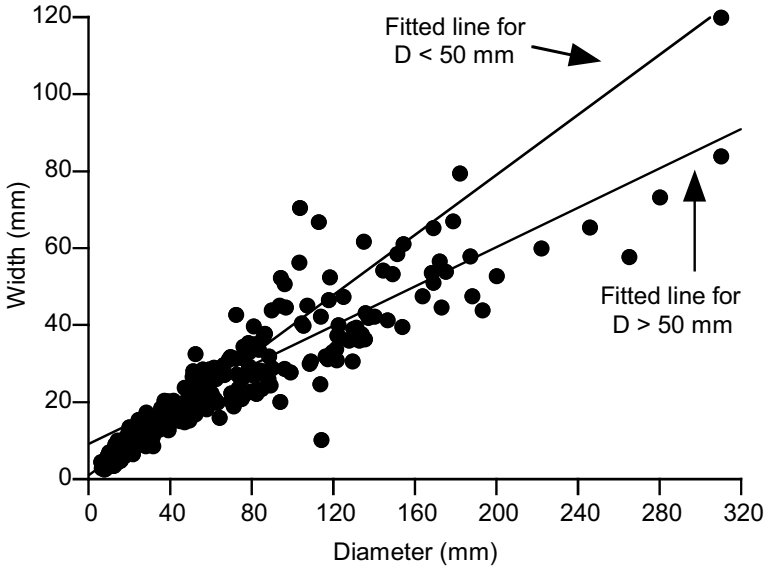

Figure 14. Plot of whorl width versus shell diameter for all specimens. Fitted lines are superimposed for diameters smaller than and larger than 50 mm. The slope represents the thickness ratio; note the significantly lower slope for diameters larger than 50 mm.

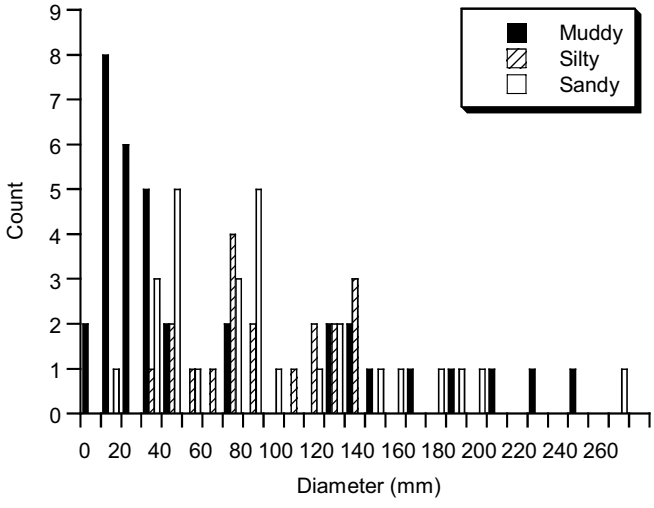

Figure 15. Distributions of shell diameters for *Metoicoceras* grouped by facies.

facies are apparent, despite the significantly lower ($p<0.05$) mean diameter of specimens from muddy facies compared to sandy facies. Therefore, while the concentration of smaller specimens in muddy facies may explain the difference in mean thickness ratio among facies for *Metoicoceras*, it has no

effect on the distribution of thickness ratios when all taxa are considered.

Size may also explain some of the significant differences found among regions and species for *Metoicoceras*. Specimens from the southern Western Interior are on average smaller than those from the northern Western Interior or Texas, and the species with the highest mean thickness ratio, *M. sp. A*, is known only from juvenile specimens (Cobban and Kennedy, 1991). This explanation, however, does not hold for *M. latoventer*; it is similar in size to *M. swallovi* and *M. mosbyense*, but has a significantly higher thickness ratio.

Size does *not* explain the significant differences in shell shape among genera of acanthoceratids or among specimens from different time intervals. For instance, the dwarf genus *Nannometoicoceras* has a relatively low thickness ratio despite having a mean adult diameter of only 21.8 mm, while the genus *Spathites*, with a mean diameter (68.9 mm) slightly higher than the overall average, has a particularly high mean thickness ratio. No significant correlation between mean diameter and mean thickness ratio exists for specimens from each zone ($r^2 = 0.11$), nor is there a correlation of mean diameter with zone ($r^2 = 0.06$). Hence the temporal pattern of high to low to high thickness ratios from the Middle Cenomanian through the Middle Turonian seems to be a real phenomenon that bears further investigation.

4.2 Temporal Trends in Acanthoceratid Shell Shape

To understand possible causes of this temporal pattern in thickness ratios, we should consider several environmental events that occurred within the seaway (summarized in Figure 16). First, there is the Greenhorn transgression itself. Sea level began to rise in the Lower and Middle Cenomanian; mid transgression occurred in the *C. canitaurinum* and *M. mosbyense* Zones of the Upper Cenomanian; late transgression occurred through the *S. gracile* and *N. juddii* Zones of the Upper Cenomanian; and peak transgression was reached in the Lower Turonian *W. coloradoense* and *M. nodosoides* Zones. Regression was underway by the Middle Turonian (Batt, 1989). This general trend of sea-level rise was possibly punctuated by three short-term lowstands during the *M. mosbyense* Zone (Sageman, 1996).

Another factor to consider is, of course, the Cenomanian-Turonian mass extinction event. This event resulted in the extinction of 35% of ammonoid genera in the Western Interior (Elder, 1989). Recent intensive work within the Western Interior Seaway has clarified the timing of Late Cenomanian-Early Turonian extinctions (Elder, 1989; Kauffman, 1995). Within the Western Interior Seaway, five stepped molluscan extinctions have been identified in the Late Cenomanian, beginning approximately 520 kyr (lower

Absolute Age (Ma)	Substage	Ammonite Zone		Greenhorn Transgression	C-T Extinctions	Acanthoceratid Shell Shape
90.51±0.45 →	Middle Turonian	23 P. hyatti		Regression		Depressed
		22 P. percarinatus				
		21 C. woollgari				
	Lower Turonian	20 M. nodosoides		Peak	Last step in WIS	
		19 V. birchbyi				
93.25±0.55 →		18 P. flexuosum				
	Upper Cenomanian	17 N. scotti		Late		Compressed
93.59±0.58 →		16 N. juddii				
		15 V. cauvini				
93.49±0.89 →		14 S. gracile			First step in WIS	
		13 M. mosbyense	D. conditum	Middle		
		12	D. albertense			
		11 D. problematicum				
94.63±0.61 →		10 D. pondi				Both
	Middle Cenomanian	9 P. wyomingense		Early		Depressed
94.93±0.53 →		8 A. amphibolum				
		7 A. bellense				
		6 P. muldoonense				
		5 A. granerosense				
95.78±0.61 →		4 C. tarrantense				
	Lower Cenoman.	3 F. brundrettei				Compressed
		2 A. inconstans				
98.50±0.50 →		1 M. mantelli				
	Upper Albian	0				

Figure 16. Chart showing key events within the Western Interior Seaway in relation to changes in shell shape. Radiometric dates are from Obradovich (1993); ammonite zones are based on Cobban (1988b, 1990) and Hancock *et al.* (1993); C-T extinction steps are from Elder (1989).

S. gracile Zone) prior to the Cenomanian-Turonian boundary. Three lesser extinctions or turnovers occurred in the 230 to 940 kyr after the boundary. Hence, the C-T extinction event was over by the middle of the *M. nodosoides* Zone. Acanthoceratid ammonites were especially hard-hit at the second extinction step, which occurred between the *S. gracile* and *N. juddii* Zones (Elder, 1989).

How do these events relate to the documented changes in thickness ratio over time? First, consider the shift from more depressed to more compressed shell forms. This shift had occurred by the early Late Cenomanian (*D. problematicum* Zone), *before* the Cenomanian-Turonian extinction events begin, so it is unlikely to be due to deteriorating environmental conditions (expansion of oxygen minimum zones, temperature and/or salinity fluctuations, etc.). Nor do the C-T events seem to affect acanthoceratid shell form once they occur. As for sea level, the change in average thickness ratio occurs by the time of mid-transgression, so while it could be a response to deepening or to lateral expansion of the seaway (increasing the extent of both deep-water and shallow-coastal habitats), there is no further change as transgression reaches its peak. The rapid lowstands during the *M. mosbyense* Zone documented by Sageman (1996) appear to have no effect on acanthoceratid thickness ratios, as the distribution of thickness ratios from this time period is unimodal with a relatively low mean (Fig. 8).

We must also consider the reversion to more rounded shell shapes in the Turonian. As this shift involves only two taxa, it could simply be due to chance; the two Turonian acanthoceratids included here, *Mammites* and *Spathites*, may have just happened to both have higher thickness ratios (recall that *Spathites* was initially derived from *Metoicoceras*, an Upper Cenomanian compressed form). The shift cannot be related to the C-T extinction because it occurs before the return of more stable environmental conditions. Neither can the reversion be explained as a response to a return to shallower water conditions, because we are still at peak transgression when *Spathites* and *Mammites* make their appearance.

The two most conspicuous environmental events of the Cenomanian-Turonian, then, cannot be related to the temporal pattern in acanthoceratid shell shape. Especially surprising is the lack of any clear relationship between shell form and sea-level change, given the strong emphasis that paleontologists usually place on sea level as a controlling factor of ammonoid form and diversity. It is worth considering, then, how the pattern documented above contrasts with that found for other groups.

Several papers published in *Sedimentary and Evolutionary Cycles* (Bayer and Seilacher, eds., 1985) addressed the phenomenon of iterative evolution of ammonoid shell form. This repetition of shell forms through time in

unrelated groups has been recognized as a common feature among ammonoids for over a century. As Haas (1942, p. 644) stated: "By sifting [through] some of the ammonitological monographs of the last six decades or so I have arrived at the conviction that such examples of homeomorphies might be increased almost *ad infinitum*." Paleontologists realized at an early stage that these repeated forms do not reflect phylogenetic relationships. Such iteration may be simply a product of ammonoids having to "choose" from a limited number of available morphologies, but many authors have found a direct relationship between these morphological cycles and cycles of sea level.

Bayer and McGhee (1984, 1985) documented repeated patterns of morphological change in three ammonite families during three transgressive-regressive cycles in the Aalenian-Bajocian of southern Germany. Members of the Graphoceratidae, Hammoceratidae, and Sonniniidae all show the same increase in degree of involution, decrease in whorl breadth, decrease in ornamentation, and decrease in sutural complexity through a cycle. This iterative evolution among unrelated taxa would suggest that the change in sea level, or something directly correlated with it, is driving the changes in morphology. In the same volume, Donovan (1985) examined trends in shell shape during the Early Jurassic transgression in southern England. He found no correlation of shell form with facies, but did find a sequence of evolute unkeeled forms leading to involute keeled forms as transgression progressed, with the extremely compressed and involute shallow water oxycones appearing during times of regression. What this sequence might mean, Donovan declined to speculate: "In view of our lack of knowledge of ammonite mode of life, we may hardly expect to find satisfactory explanations of any correlations that may be observed" (p. 56).

As previously discussed, Jacobs *et al.* (1994) were able to suggest a specific mechanism for an association between more compressed shells and shallower water in *Scaphites whitfieldi* from the Upper Turonian of the Western Interior Seaway. They found a correlation between thickness ratio and facies, with more compressed forms associated with coarser grained facies. Because compressed forms are more hydrodynamically efficient at higher swimming or current speeds, they argued that compressed ammonites would be preferred in shallower, higher energy environments.

On the other hand, Korn (1995) documented a pattern that may provide a different explanation for a relationship between sea level and morphological change. In a study of Late Devonian goniatite and clymeniid ammonoids from Germany, he found an association between paedomorphosis (a heterochronic pattern where adult descendants resemble juvenile ancestors) and a regressive trend; presumably the regression produced more unstable conditions, which allowed ammonoid groups whose individuals had earlier

individual maturation times to be more successful. Many ammonoids show a trend during ontogeny towards becoming more compressed. Paedomorphosis, then, would result in more rounded descendants. Hence, we have one explanation, hydrodynamic efficiency, to explain a trend to more compressed forms with a drop in sea level, and another, paedomorphosis, to explain a trend to more depressed forms with a drop in sea level.

However, other authors have documented a much more complex relationship between sea level and shell form than a simple "shallow equals compressed and deep equals depressed" equation. This complexity is especially conspicuous in the latest Cenomanian-Turonian Trans-Saharan Seaway, which intermittently connected the Gulf of Guinea and the Tethyan proto-Mediterranean across North and West Africa. In detailed biostratigraphic studies of the Ashaka section in northeast Nigeria, Courville (1992) and Courville and Thierry (1993) document a complicated sequence of morphologies among vascoceratid and pseudotissotiid ammonites. The initial transgressive interval in northeast Nigeria was marked by rounder ammonites that became more compressed and involute as conditions deepened. Then, with the initial formation of the connection with the Tethyan arm of the seaway, more evolute and depressed forms made their appearance; these were still presumably in relatively shallow water. As conditions deepened further, a very evolute but compressed group gave rise to an involute and depressed group of ammonites. Then at peak transgression, more compressed forms once again became predominant, and persisted as shallowing proceeded. So here, as in my acanthoceratid example, no simple relationship exists between sea level and ammonite morphology.

But why not? First of all, we encounter several problems with any attempt at correlating changing ammonoid form with changes in sea level. Obviously, correlation does not necessitate cause. The causal factor may not be sea level, but something related to it, or some complex interaction among several factors. Or the correlation may simply be a spurious match, signifying nothing. Most workers investigating sea level as a controlling factor assume that environment *drives* evolution – that if one sees a correlation, the physical environment must be controlling the passively responding biota. Rarely is any attempt made to justify such an assumption.

Of course, another explanation for the temporal pattern in thickness ratios exists, one that almost certainly explains the complexities of the Nigerian record: the morphological trends are really phylogenetic trends, reflecting the differential persistence of either more or less compressed *taxa*, rather than individuals. This may seem to be saying the same thing, but keep in mind how variable the individual acanthoceratid taxa are. If environmental

pressure (either selective or ecophenotypic) for individual ammonites to be more compressed were the only operative factor, we would expect a contraction of variability *within* a taxon and a trend *within* a taxon to lower thickness ratios (Fig. 17). We do not see this. Instead, we see a shift from Middle Cenomanian taxa, which are on average more depressed (though variable), to Upper Cenomanian taxa, which are on average more compressed (though variable), then back to more depressed forms in the Turonian.

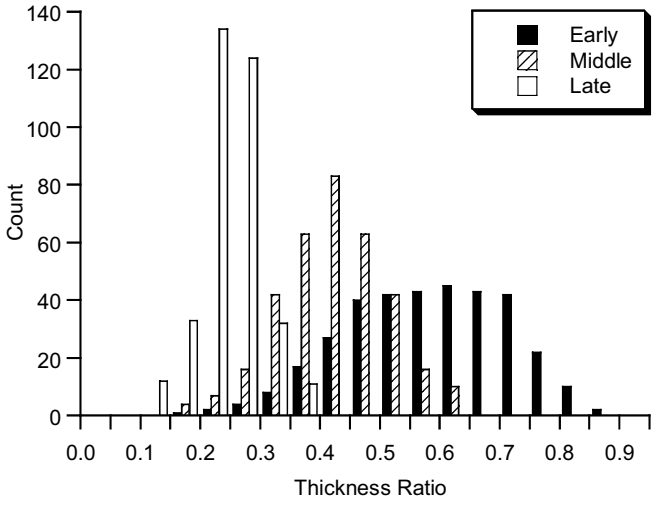

Figure 17. Hypothetical case of lower thickness ratios over time. In this case, environmental pressure favoring individuals with lower thickness ratios results in a reduction of intra-taxic variability through time.

Hence, changing shell form through time may be explainable not as a passive response of individuals to environmental pressures, but rather as due to the preponderance of more compressed taxa during the Upper Cenomanian (or more depressed taxa during the Middle Cenomanian and Turonian). But now we must ask why this preponderance occurred. Is the pattern merely a coincidence – there just happened to be more compressed genera in the Upper Cenomanian – or were Upper Cenomanian compressed taxa promoted in some way? I doubt the temporal pattern observed was due only to chance. Five of six genera measured from the Upper Cenomanian have median thickness ratios less than 0.4, while five of seven and two of two genera, respectively, from the Middle Cenomanian and Turonian have median thickness ratios greater than 0.4. The phenomenon of narrowing shell shape in the Upper Cenomanian relative to periods before and after seems too pervasive to be a chance occurrence.

Heterochrony provides another possible explanation for the temporal trend in shell shape. As I have already noted, many ammonites, including these acanthoceratids, show a trend toward more compressed shells through ontogeny. If some external environmental factor favored peramorphosis during the Upper Cenomanian, we would see a preponderance of more "adult" looking, compressed ammonites across several taxa. However peramorphosis is usually favored in stable environments (Gould, 1977; McKinney, 1986; McNamara, 1988), and it is clear that, for at least part of the Upper Cenomanian, the conditions in the Western Interior Seaway were anything but stable (Kauffman, 1995).

A third potential explanation cites a process that I have already mentioned – taxon sorting. If some factor preferentially promoted the production or persistence of taxa with compressed shells during the Upper Cenomanian (or depressed shells during the Middle Cenomanian and Turonian), we would see the pattern that we do. But does such sorting make sense in this particular case? In principle, several possible mechanisms can achieve such sorting. For instance, if shell shape is biased or irreversible (*i.e.,* if depressed forms can give rise to compressed forms, but not vice versa), we might expect to see an accumulation of compressed forms over time. But clearly this is not the case here, since shell shape reverts back in the Turonian to depressed forms from compressed ancestors. Obvious environmental changes that might affect speciation potential, such as sea level changes that would affect habitat area, cannot be related to the changes in shell shape. The lack of a relationship between shell shape and region of the seaway rules out preferential geographic range restriction. Species sorting, then, may explain the trend, but the cause of the sorting is unclear.

5. CONCLUSIONS

To summarize the main findings of this work, neither facies nor regional differences affect the average thickness ratio of Western Interior acanthoceratid genera. However, such differences do affect the shell shape of species in the genus *Metoicoceras*; this relationship could be due to the correlation of shell size and thickness ratio. The genera *Acanthoceras*, *Plesiacanthoceras*, *Plesiacanthoceratoides*, and *Spathites* and the species *Metoicoceras* sp. *A* and *M. latoventer* have significantly higher thickness ratios, while the genera *Mantelliceras*, *Metoicoceras*, *Nannometoicoceras*, and *Neocardioceras* have significantly lower thickness ratios. Genera and species of *Metoicoceras* tend to have lower thickness ratios during the Late Cenomanian compared to the Middle Cenomanian or Lower Turonian.

These findings substantiate the claim that ammonoid shell shape did not

merely respond passively to environmental changes. Major environmental events had no appreciable effect on shell shape. Average thickness ratios did not fluctuate with the environment and variability in shell shape remained high regardless of environmental changes. These observations validate the evolutionary study of ammonoid shell shape, by implying that strong heritable components exist for ammonoid morphology. However, the scale of analysis matters. For instance, species of *Metoicoceras* show a relationship with facies that is not found when comparing genera. Certainly no one "rule" exists for how ammonoid morphology relates to the environment. We are beyond the point where merely noting a correlation between, say, sea level changes and morphological changes is a sufficient explanation of the cause of those morphological changes. It is apparent from this study and from others (e.g., Courville (1992) and Courville and Thierry (1993)) that ammonoid morphology reflects a complex interaction of environmental, developmental, and genetic factors – not an outrageous claim, to be sure, but one that is seldom taken fully to heart.

ACKNOWLEDGMENTS

I wish to thank David K. Jacobs, Neil H. Landman, and Peter J. Harries for their helpful comments and suggestions to improve this chapter, and Jann Thompson and Mark Florence for providing access to specimens at the U. S. National Museum of Natural History, Washington, D.C.

REFERENCES

Batt, R. J., 1989, Ammonite shell morphospace distribution in the Western Interior Greenhorn Sea and some paleoecological implications, *Palaios* **4**:32-43.

Batt, R. J., 1991, Sutural amplitude of ammonite shells as a paleoenvironmental indicator, *Lethaia* **24**:219-255.

Batt, R. J., 1993, Ammonite morphotypes as indicators of oxygenation in a Cretaceous epicontinental sea, *Lethaia* **26**: 49-63.

Bayer, U., and McGhee, G. R., Jr., 1984, Iterative evolution of Middle Jurassic ammonite faunas, *Lethaia* **17**:1-16.

Bayer, U., and McGhee, G. R., Jr., 1985, Evolution in marginal epicontinental basins: The role of phylogenetic and ecological factors, in: *Sedimentary and Evolutionary Cycles*, (U. Bayer and A. Seilacher, eds.), Springer Verlag, Berlin,:164-220.

Bayer, U., and Seilacher, A. (eds.), 1985, *Sedimentary and Evolutionary Cycles*, Springer Verlag, Berlin, *Lect. Notes Ear. Sci.* **1**.

Becker, R. T., 1993, Anoxia, eustatic changes, and Upper Devonian to lowermost Carboniferous global ammonoid diversity, in: *The Ammonoidea: Environment, Ecology, and Evolutionary Change* (M. R. House, ed.), *Syst. Assoc. Sp. Vol.* **47**:115-163.

Callomon, J. H., 1985, The evolution of the Jurassic ammonite family Cardioceratidae, *Sp.*

Pap. Palaeont. **33**:49-90.
Checa, A., Company, M., Sandoval, J., and Weitschat, W., 1997, Covariation of morphological characters in the Triassic ammonoid *Czekanowskites rieberi*, *Lethaia* **29**:225-235.
Cobban, W. A., 1987, Some Middle Cenomanian (Upper Cretaceous) Acanthoceratid Ammonites from the Western Interior of the United States, *U. S. Geol. Surv. Bull.* **1445**.
Cobban, W. A., 1988, Some Acanthoceratid Ammonites from Upper Cenomanian (Upper Cretaceous) Rocks of Wyoming, *U. S. Geol. Surv. Bull.* **1353**.
Cobban, W. A., 1990, Ammonites and some characteristic bivalves from the Upper Cretaceous Frontier Formation, Natrona County, Wyoming, *U. S. Geol. Surv. Bull.* **1917-B**.
Cobban, W. A., and Kennedy, W. J., 1991, Evolution and biogeography of the Cenomanian (Upper Cretaceous) ammonite *Metoicoceras* Hyatt, 1903, with a revision of *Metoicoceras praecox* Haas, 1949, *U. S. Geol. Surv. Bull.* **1934**.
Courville, P., 1992, Les Vascoceratinae et les Pseudotissotiinae (Ammonitina) d'Ashaka (NE Nigeria): Relations avec leur environnement biosédimentaire, *Bull. Centres Rech. Explor.-Prod. Elf Aquitaine* **16**:407-457.
Courville, P., and Thierry, J., 1993, Nouvelles données biostratigraphiques sur les dépots cénomano-turoniens de Nord-Est du fossé de la Bénoué (Nigéria), *Cret. Res.* **14**:385-396.
Crick, R. E., 1978, Morphological variations in the ammonite *Scaphites* of the Blue Hill Member, Carlile Shale, Upper Cretaceous, Kansas, *Univ. Kans. Paleont. Cont.* **88**.
Dagys, A. S., and Wietschat, W., 1993, Extensive intraspecific variation in a Triassic ammonoid from Siberia, *Lethaia* **26**:113-121.
Daniel, T. L., Helmuth, B. S., Saunders, W. B., and Ward, P. D., 1997, Septal complexity in ammonoid cephalopods increased mechanical risk and limited depth, *Paleobio.* **23**:470-481.
Donovan, D. T., 1985, Ammonite shell form and transgression in the British Lower Jurassic, in: *Sedimentary and Evolutionary Cycles* (U. Bayer and A. Seilacher, eds.), Springer-Verlag, Berlin *Lect. Notes Ear. Sci.* **1:**48-57.
Elder, W. P., 1989, Molluscan extinction patterns across the Cenomanian-Turonian Stage boundary in the western interior of the United States, *Paleobio.* **15**: 299-320.
Goodfriend, G. A., 1986, Variation in land-snail shell form and size and its causes: A review, *Syst. Zool.* **35**: 204-223.
Gould, S. J., 1977, *Ontogeny and Phylogeny*, Harvard University Press, Cambridge.
Haas, O., 1942, Recurrence of morphological types and evolutionary cycles in Mesozoic ammonites, *J. Paleont.* **16**: 643-650.
Haas, O., 1946, Intraspecific variation in, and ontogeny of, *Prionotropis woollgari* and *Prionocyclus wyomingense*, *Bull. Am. Mus. Nat. Hist.* **86**:.
Hancock, J. M., Kennedy, W. J., and Cobban, W. A., 1993, A correlation of the Upper Albian to basal Coniacian sequences of northwest Europe, Texas and the United States Western Interior, in: *Evolution of the Western Interior Basin* (W. G. E. Caldwell and E. G. Kauffman, eds.), *Geol. Assoc. Can. Sp. Pap*. **39**:453-476.
Hewitt, R. A., and Westermann, G. E. G., 1997, Mechanical significance of ammonoid septa with complex sutures, *Lethaia* **30**:205-212.
Jacobs, D. K., 1992, Shape, drag, and power in ammonoid swimming, *Paleobio.* **18**:203-220.
Jacobs, D. K., Landman, N. H., and Chamberlain, J. A., Jr., 1993, Intraspecific variation in shell shape, hydrodynamics, and facies relationships in *Scaphites whitfieldi*, an Upper Cretaceous ammonoid from the Carlile Shale, *Geol. Assoc. Am. Abs. Prog.* **25**:A51.
Jacobs, D. K., Landman, N. H., and Chamberlain, J. A., Jr., 1994, Ammonite shell shape covaries with facies and hydrodynamics: Iterative evolution as a response to changes in

basinal environment, *Geology* **22**:905-908.
Kauffman, E. G., 1986, High-resolution event stratigraphy: Regional and global Cretaceous bio-events, in: *Global Bio-events: A Critical Approach*, (Otto H. Walliser, ed.), Springer Verlag, Berlin, *Lect. Notes Ear. Sci.* **8**:279-335.
Kauffman, E. G., 1995, Global change leading to biodiversity crisis in a greenhouse world: The Cenomanian-Turonian (Cretaceous) mass extinction, in: *Effects of Past Global Change on Life*, National Research Council, National Academy Press, Washington, D. C., pp. 47-71.
Kauffman, E. G., and Caldwell, W. G. E., 1993, The Western Interior Basin in Space and Time, in: *Evolution of the Western Interior Basin* (W. G. E. Caldwell and E. G. Kauffman, eds.), *Geol. Assoc. Can. Sp. Pap*. **39**:1-30.
Kauffman, E. G., Sageman, B. B., Elder, W. P., and E. R. Gustason, E. R., 1987, *High-resolution event stratigraphy, Greenhorn Cyclothem (Cretaceous: Cenomanian-Turonian), Western Interior Basin of Colorado and Utah*, Geological Society of America, Rocky Mountain Section Meeting, Field Guide, Boulder.
Kauffman, E. G., Sageman, B. B., Kirkland, J. I., Elder, W. P., Harries, P. J., and Villamil, T., 1993, Molluscan biostratigraphy of the Western Interior Cretaceous Basin, in: *Evolution of the Western Interior Basin* (W. G. E. Caldwell and E. G. Kauffman, eds.), *Geol. Assoc. Can. Sp. Pap*. **39**:397-434.
Kennedy, W. J., 1971, Cenomanian ammonites from southern England, *Palaeont. Assoc*., *Sp. Pap. Palaeont.* **8**.
Kennedy, W. J., 1988, Late Cenomanian and Turonian ammonite faunas from north-east and central Texas, *Sp. Pap. Palaeont.* **39**.
Kennedy, W. J., Wright, C. W., and Hancock, J. M., 1980, Origin, evolution, and systematics of the Cretaceous ammonoid *Spathites*, *Palaeont.* **23**:821-837.
Korn, D., 1995, Paedomorphosis of ammonoids as a result of sealevel fluctuations in the Late Devonian *Wocklumeria* Stufe, *Lethaia* **28**:155-165.
Lloyd, E. A, and Gould, S. J., 1993, Species selection on variability, *Proc. Nat. Acad. Sci.* **90**:595-599.
McCune, A. R., 1990, Evolutionary novelty and atavism in the *Semionotus* Complex: Relaxed selection during colonization of an expanding lake, *Evol.* **44**:71-85.
McKinney, M. L., 1986, Ecological causation of heterochrony: test and implications for evolutionary theory, *Paleobio.* **12**:282-289.
McNamara, K. J., 1988, The abundance of heterochrony in the fossil record, in: *Heterochrony in Evolution* (M. L. McKinney, ed.), Plenum Press, New York, pp. 287-325.
Obradovich, J. D., 1993, A Cretaceous Time Scale, in: *Evolution of the Western Interior Basin*, (W. G. E. Caldwell and E. G. Kauffman, eds.), *Geol. Assoc. Can. Sp. Pap*. **39**:379-396.
Reeside, J. B., Jr., and Cobban, W. A., 1960, Studies of the Mowry Shale (Cretaceous) and contemporary formations in the United States and Canada, *U. S. Geol. Surv. Prof. Pap.* **355**.
Reyment, R. A., 1975, Analysis of a generic level transition in Cretaceous ammonites, *Evolution* **28**:665-676.
Reyment, R. A., 1988, Does sexual dimorphism occur in Upper Cretaceous ammonites?, *Senck. Leth.* **69**:109-119.
Reyment, R. A., and Kennedy, W. J., 1991, Phenotypic plasticity in a Cretaceous ammonite analyzed by multivariate statistical methods, *Evol. Biol.* **25**:411-426.
Roberts, L. N. R., and Kirschbaum, M. A., 1995, Paleogeography of the Late Cretaceous of the Western Interior of Middle North America – Coal distribution and sediment accumulation, *U. S. Geol. Surv. Prof. Pap.* **1561**.

Sageman, B. B., 1996, Lowstand tempestites: Depositional model for Cretaceous skeletal limestones, Western Interior basin, *Geology* **24**:888-892.

Saunders, W. B., 1995, The ammonoid suture problem: relationships between shell and septum thickness and suture complexity in Paleozoic ammonoids, *Paleobio.* **21**:343-355.

Saunders, W. B., and Work, D. M., 1996, Shell morphology and suture complexity in Upper Carboniferous ammonoids, *Paleobio.* **22**:189-218.

Sheldon, P. R., 1993, Making sense of microevolutionary patterns, in: *Evolutionary Patterns and Processes* (D. R. Lees and D. Edwards, eds.), *Linnean Soc. Sym. Vol.* **14**:19-31.

Smith, A. G., Smith, D. G., and Funnell, B. M., 1994, *Atlas of Mesozoic and Cenozoic Coastlines*, Cambridge University Press, Cambridge.

Sokal, R. R., and Rohlf, F. J., 1981, *Biometry: The Principles and Practice of Statistics in Biological Research*, W. H. Freeman and Company, New York.

West-Eberhard, M. J., 1989, Phenotypic plasticity and the origins of diversity, *Ann. Rev. Ecol. Syst.* **20**:249-278.

Westermann, G. E. G., 1966, Covariation and taxonomy of the Jurassic ammonite *Sonninia adicra* (Waagen), *N. Jahrb. Geol. Paläont., Abh.* **124**:289-312.

Williams, G. C., 1966, *Adaptation and Natural Selection*, Princeton, Princeton University Press.

Wright, C. W., and Kennedy, W. J., 1981, *The Ammonoidea of the Plenus Marls and the Middle Chalk*, Monograph of the Palaeontological Society, London.

Wright, C. W., and Kennedy, W. J., 1984, *The Ammonoidea of the Lower Chalk, Part 1*, Monograph of the Palaeontological Society, London, pp. 1-126.

Wright, C. W., and Kennedy, W. J., 1987, *The Ammonoidea of the Lower Chalk, Part 2*, Monograph of the Palaeontological Society, London, pp. 127-218.

Yacobucci, M. M., 1999, Plasticity of developmental timing as the underlying cause of high speciation rates in ammonoids: An example from the Cenomanian Western Interior Seaway of North America. In: *Advancing Research in Living and Fossil Cephalopods*, *Proceedings, IV International Symposium Cephalopods – Present and Past, Granada, Spain, July 15-17, 1996* (F. Olóriz and F. J. Rodríguez-Tovar, eds.), Plenum Press, New York, pp. 59-76.

Chapter 7

A Reappraisal of the Relationship between Sea Level and Species Richness

PETER J. HARRIES

1. INTRODUCTION

The relationship between area and species richness was documented as early as the mid-17th century (see discussion in Rosenzweig, 1995), but it was not until the publication of MacArthur and Wilson's (1967) *The Theory of Island Biogeography* that the hypothesis became ingrained in ecological

PETER J. HARRIES • Department of Geology, University of South Florida, 4202 E. Fowler Ave., SCA 528, Tampa, FL 33620-5201.

P.J. Harries (ed.), *High-Resolution Approaches in Stratigraphic Paleontology.*

theory. Their work forcefully presented substantial empirical evidence that explained the nature of, and possibly the controls of, diversity, at least on oceanic islands. Their hypothesis that species-level diversity is dependent upon area raised the hopes of paleontologists that this relationship could readily be applied to the fossil record of marine organisms and hence to the history of life. The paleontologic application of this concept was founded on the belief that the species-area relationship should hold for benthic marine organisms responding to changes in shelf areas primarily affected by sea-level fluctuations. Therefore, diversity increases and declines chronicled in the fossil record would largely represent transgressions and regressions, respectively, as far as benthic organisms are concerned. These patterns are overprinted by plate tectonic, evolutionary, and mass-extinction events, but nevertheless sea-level changes should be a dominant control.

A number of early studies pointed to the potential applicability of the species-area effect for various intervals of geologic time (e.g., Johnson, 1974; Schopf, 1974; Simberloff, 1974). In addition, building on earlier work by Newell (1967), there were attempts to relate Phanerozoic compilations of species-level diversity, such as that by Raup (1976a), to sea-level fluctuations (e.g., (Sepkoski, 1976); but see reinterpretation by (Flessa and Sepkoski, 1978). The species diversity reflected in these compilations were largely controlled by sampling vagaries, especially controlled by outcrop area and rock volume available for study (Raup, 1976b), and certain groups, intervals, and regions were and continue to be better studied than others. Furthermore, the fauna was treated *in toto*, rather than focusing on individual groups has been the case in neontologic work. More recent work focused on specific taxonomic groups and geologic intervals, however, has suggested otherwise. Valentine and Jablonski's (1991) study of Pleistocene and Holocene sea-level fluctuations suggests that the rapid and substantial sea-level changes over the past 1 Myr had no effect upon diversity – the existing data show virtually no faunal differences between these sea-level highstands. McGhee (1991, 1992), based on species richness as well as evolutionary rates in Devonian brachiopod species as a response to sea-level change, concluded that sea level, as well as the rate of sea-level change, showed virtually no correlation with either variable. This pointed to a minimal control by sea level, hence changes in shelf area, in regulating benthic organisms and suggested that patterns documented in modern oceans may be a very recent phenomenon or simply fortuitous.

2. APPROACH

This study aims to use the methodology employed by McGhee (1991) to

investigate the relationship between sea level and inoceramid bivalve species richness from the Cretaceous Western Interior Seaway of North America (WIS) to further elucidate the relationship between species richness and sea level in the paleontologic record. Although McRoberts and Aberhan (1997) have suggested an alternative method for approaching the problem, that methodology was not employed herein primarily because the approach in its reliance on smoothing out sea-level fluctuations and also in its use of various ranking and scaling techniques to 'bin' diversity and sea level unnecessarily removes detailed information critical to the type of analysis undertaken here.

The neontologic basis for this approach is rooted in a variety of studies that have empirically derived an equation that encapsulates this modern relationship (see summaries in MacArthur and Wilson, 1967, and Rosenzweig, 1995). The equation – termed the "Arrhenius equation" after the Swedish ecologist who first formulated it – that has been employed to quantify the species-area relationship is:

$$S = cA^z \quad (1)$$

Where S is the number of species, A represents the area, and c and z are constants that determine the slope of a curve constructed with the data (see Rosenzweig, 1995, for a more complete treatment of this topic). When dealing with the geologic record, however, the ability to accurately reconstruct the area of past epicontinental seaways is difficult due to the erosion or lack of exposure of the sedimentary record in some regions and the difficulties of reconstructing paleotopography. Therefore, rather than attempting to reconstruct the changing marine-shelf area through the interval studied, sea level is used here as a proxy for area (discussed in more detail below). Although the exact relationship between the two is difficult, if not impossible, to determine, a range of sea-level curves exist for the interval which can be used as proxies for shelf area.

2.1 Cretaceous Inoceramid Data

Traditionally, the bulk of neontologic data used in support of the species-area hypothesis has been collected from various islands (e.g., data summarized in MacArthur and Wilson, 1967, and Rosenzweig, 1995). This study, however, will examine one very common biotic component – the inoceramid bivalves – collected from an epicontinental seaway. These seaways are viewed as "inverse islands" inasmuch as they are surrounded by land and their area waxed and waned as sea level rose and fell. The origin of the inoceramids lie in the (Browne and Newell, 1966; Waterhouse, 1970), and they became at least locally abundant during various intervals in the

Jurassic (e.g., Komatsu *et al.*, 2001). However, it was not until the Cretaceous, especially from the Albian through the Maastrichtian, that they achieved their acme in species richness and abundance. During the Late Cretaceous, they dominated many level-bottom communities, thriving in a wide range of environments spanning a spectrum from basinal limestones to deep-water black shales, indicative of oxygen-depleted conditions, to shoreface sandstones (e.g., Kauffman and Harries, 1996). This environmental tolerance was combined with very wide biogeographic distribution for many inoceramid species probably reflecting the presence of long-lived planktotrophic larvae (Kauffman, 1975).

This study will focus on the Late Albian through the latest Cretaceous inoceramids from the WIS. The data employed in this study are derived from Kauffman *et al.*'s (1993) compilation of molluscan species ranges spanning the Albian through Maastrichtian. These data comprise the only continuous compilation of inoceramid data through the study interval, and represent the efforts of a single working group using consistent collection techniques and taxonomic designations. Although the WIS inoceramid faunas of several of the intervals have been investigated more recently by other authors (i.e., the Cenomanian-Turonian interval by Kennedy *et al.* (Kennedy *et al.*, 2000); the Late Turonian-Coniacian interval by Collom (1991; 1998) and Walaszczyk and Cobban (2000), and the Campanian-Maastrichtian by Walaszczyk *et al.* (2001), to maintain consistency in approach and taxonomic designation, the results of these studies were not incorporated into the data used here. This was also done because in a number of the studies mentioned above the samples employed were amassed largely for ammonite studies, thus the inoceramid faunas may not have been completely sampled. Finally, the generic designations of Kauffman *et al.* (1993) have been maintained to avoid complications in discerning how the data was derived. However, more recent work suggests that a number of the taxa should be assigned to different genera.

Initially, inoceramid species richness was determined for the study interval and calibrated to at the ammonite biozone level. The temporal resolution afforded by this ammonite biostratigraphic scheme averages 0.46 ± 0.28 Myr throughout the entire interval based on the chronology erected by Kauffman *et al.* (1993). The longest biozone is 1.54 Myr and delineates an unzoned portion of the Albian where no known inoceramid fauna has been documented, whereas the shortest biozone encompasses the Late Cenomanian *Neocardioceras* biozone with a duration of only 0.05 Myr (see Appendix A). In cases where numerical ages were designated for mid points of the ammonite biozones on the original plots (see figs. 7 through 12 in Kauffman *et al.*, 1993), ages for the beginning and end of these zones had to be extrapolated. In such cases, the time between the age designations were

evenly divided between the biozones. The species compilation itself was erected by plotting the entire range of all the species identified (Fig. 1); the subspecies designations employed in Kauffman *et al.* (1993) were only used to determine the maximum stratigraphic range for their respective species.

2.2 Cretaceous Sea Level

Utilizing the plethora of well-exposed Cretaceous outcrops globally as well as the thick sequences of Late Cretaceous sequences known from subsurface data, a number of sea-level curves have been generated for this period. In this study, three of these Cretaceous sea-level curves are compared (Fig. 2): 1) Kauffman and Caldwell's (1993) sea-level compilation for the WIS; 2) Hancock's (1989) curve based on the English chalk sequences; and 3) Haq *et al.*'s (1989) eustatic curve derived from the interpretation of the seismic stratigraphy of passive margins. As shown in Figure 2, the three curves have some similarities, but a considerable amount of variation. This variability is interpreted to reflect a number of differences in the manner in which the data were collected and interpreted, problems in comparing the various chrononlogic correlations, the lithologies studied, and, in the case of the Haq *et al.* (1989) curve, the seismic data employed to construct their curve. One of the primary sources to explain the vagaries between the sea-level curves is that both Hancock's (1989) as well as Kauffman and Caldwell's (1993) curve reflect the interplay of relative and eustatic sea-level changes. On the other hand, Haq *et al.*'s (1989) curve apparently represents eustatic fluctuations with a minimal, if any, signature of relative changes. Therefore, the dominance of relative changes may not only account for the numerous small-scale differences between curves, but also some of the broader differences, such as the relative lack of significant regression from the Coniacian through the Maastrichtian portrayed in the Hancock curve.

Although it may be tempting to match potential correlative peaks between the various curves (i.e., "tune" the curves), the validity of such correlations is suspect and more akin to matching (Miall, 1992). Some of the differences in timing are, at least in part, due to the different biostratigraphic systems employed as well as their temporal resolving power. The WIS and the Anglo-Paris Basin have extremely refined, integrated macro- and micropaleontologic biostratigraphies (e.g., Kauffman *et al.*, 1993) allowing more refined temporal resolution than the zonation used by Haq *et al.* (1989). Such differences in temporal resolution and precision may account for some offsets in position of various points, such as peak transgression and regression, comprising the curves. The two most similar curves are those of

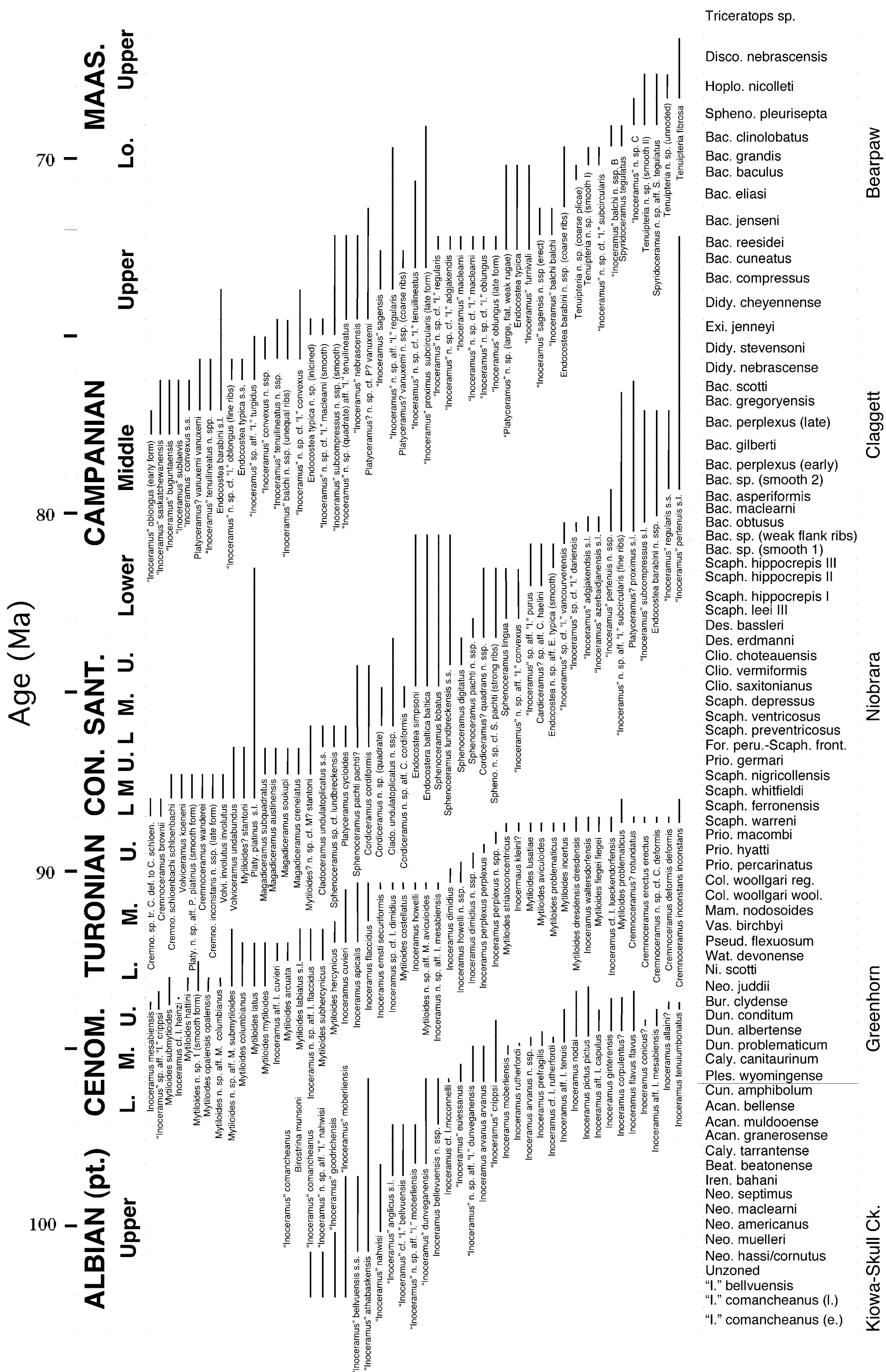

Age (Ma)
100
90
80
70
ALBIAN (pt.)
Upper
CENOM.
L. M. U.
TURONIAN
L. M. U.
CON.
L M U.
SANT.
L M. U.
CAMPANIAN
Lower
Middle
Upper
MAAS.
Lo.
Upper
Kiowa-Skull Ck.
Greenhorn
Niobrara
Claggett
Bearpaw

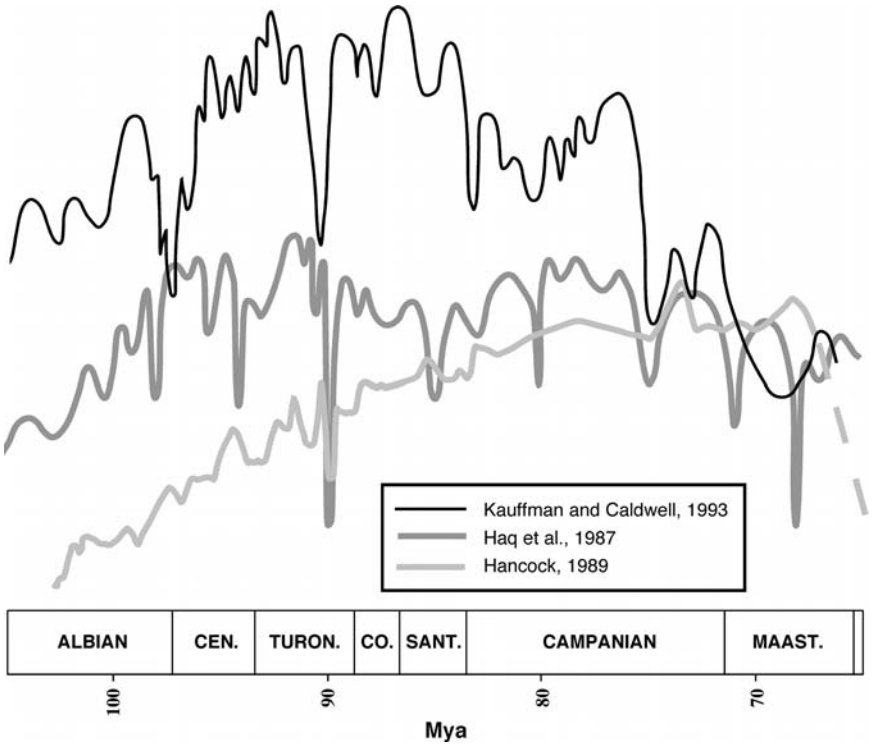

Figure 2. A comparison of Kauffman and Caldwell's (1993), Hancock's (1989), and Haq et al.'s (1989) sea-level curves established for the WIS, the Anglo-Paris Basin, and global eustasy, respectively.

Haq *et al.* (1989) and Kauffman and Caldwell (1993) (Fig. 3), although there still are considerable differences not only in the magnitude of change, but also in the timing of peaks (Fig. 2). Overall, the Hancock (1989) curve negatively correlates with that of Kauffman and Caldwell (1993), but as discussed in Hancock and Kauffman (1979), this is not surprising given the lack of significant regressions recorded in the Santonian through Maastrichtian carbonate-dominated interval in the Anglo-Paris Basin.

Figure 1. Compilation of range data for WIS inoceramid species from Kauffman et al. (1993). The ranges of the subspecies depicted in the range plots in Kauffman et al. (1993) have been included with their respective species. The chronology as well as the position of stage and substage boundaries from Kauffman et al. (1993). The boundaries of the various cyclothems based on sea-level lowstands from Kauffman and Caldwell's (1993) sea-level curve. The species shown with ranges in gray at the bottom of the diagram represent ranges of taxa from the northern arm of the WIS prior to the flooding of the entire basin in Late Albian. It should be noted that the generic concepts of the Kauffman et al. (1993) are maintained for consistency with the initial work, although a number of the taxa should be assigned to other genera based on more recent work.

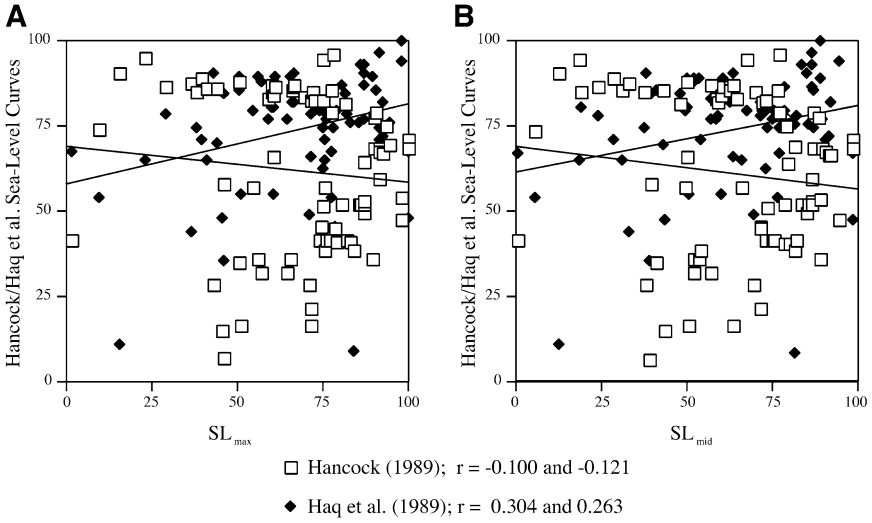

Figure 3. Plots depicting the degree of similarity between SL_{max} and SL_{mid} (see text for explanation) from Kauffman and Caldwell's (1993), respectively, and Hancock's (1989) and Haq et al.'s (1989) sea level curves. The r-values are listed in order for A and B, respectively.

Another aspect of sea level is that it is composed of a hierarchy of numerous different cycles with varying durations (e.g., see discussion in Miall, 1997). Traditionally, sedimentation within the Cretaceous WIS marine record has been subdivided into nine transgressive-regressive (T-R) cycles. The first four of these – Beattie Peaks, Mount Goodenough, and Clearwater cyclothems – are solely recorded from the northern part of the basin and are not considered in this study due to the lack of highly refined inoceramid range data. Incursions from Tethys during these cyclothems were blocked by the Ouachita and central Texas uplifts as well as relatively low eustatic sea level (Kauffman and Caldwell, 1993). This paper focuses on the next five cyclothems: the Kiowa-Skull Creek (108-97 Ma), the Greenhorn (97-90 Ma), the Niobrara (90-81 Ma), the Claggett (81-74 Ma), and the Bearpaw (74-67 Ma) T-R cycles. These T-R cycles had a profound affect on the nature of the WIS. Not only did they modify the area of shallow-marine habitats available, but they also determined the distribution of sedimentary environments and, thus, the paleoenvironments which existed within the epicontinental seaway (Kauffman, 1977b).

In this study, a relative scale for water depth is used that ranges from 0 to 100, because the absolute range of sea-level variation is rarely given for most reconstructions (with the exception of the Haq *et al.* (1987) approach is an exception). Values of 0 and 100 were assigned to the lowest and highest sea-level position during the study interval for each of the three curves, and all other-values were designated based on the position of sea level relative to

that scale. None of the sea-level curves were "tuned" to the diversity data (i.e., peaks and troughs in the two data sets were not aligned) as is commonly done, for instance, in paleoclimatic studies. Although this certainly would have improved the correlation and may be justified to a degree given the biostratigraphic error associated with erecting the curves themselves, the potential for circularity in the approach outweighed the potential for improved correlation. For the Kauffman and Caldwell (1993) curve, values were determined for both maximum sea level during an ammonite biozone (SL_{max}) and also at the mid-point of the biozone (SL_{mid}), whereas for the Hancock (1987) and Haq *et al.* (1989) curves only SL_{mid} values were used.

3. TRENDS IN SPECIES RICHNESS

The compilation of WIS inoceramid species (n = 179) reveals 11 species richness peaks that occur in the following levels: Upper Albian, Middle Cenomanian, Upper Cenomanian, spanning the Lower-Middle Turonian boundary, across the Middle-Upper Turonian boundary, across the Lower-Middle Coniacian boundary, Upper Coniacian, Lower Campanian, lower Middle Campanian, upper Middle Campanian, and latest Upper Campanian (Fig. 4). Most of these peaks represent relatively short periods of increased species richness, except for the broader peak in the Late Albian that indicates a lengthier plateau. With the exceptions of the smaller Albian plateau and the larger Late Campanian peak, the overall level of diversity achieved is quite similar between the various peaks. There are also 11 lows in species richness. These occur in the Early Cenomanian, Middle Cenomanian, at the Cenomanian-Turonian boundary, in the late Early and Middle Turonian, Upper Turonian, Middle Coniacian, Middle Santonian, at the Lower-Middle Campanian boundary, in the Middle Campanian, Upper Campanian and in the Upper Maastrichtian, where the inoceramids went extinct. In contrast to the species richness peaks, the species richness lows tend to last somewhat longer temporally and more variable in terms of the levels obtain.

Figure 4 portrays the two components controlling inoceramid diversity through the interval: origination and extinction. Given the virtual cosmopolitan distribution of the Inoceramidae, even at the species level, at first consideration the terms first and last appearances may be more appropriate than origination and extinction. However, because inoceramids appear to have had long-lived planktotrophic larvae (Kauffman, 1975) and occur virtually simultaneously throughout their paleogeographic range

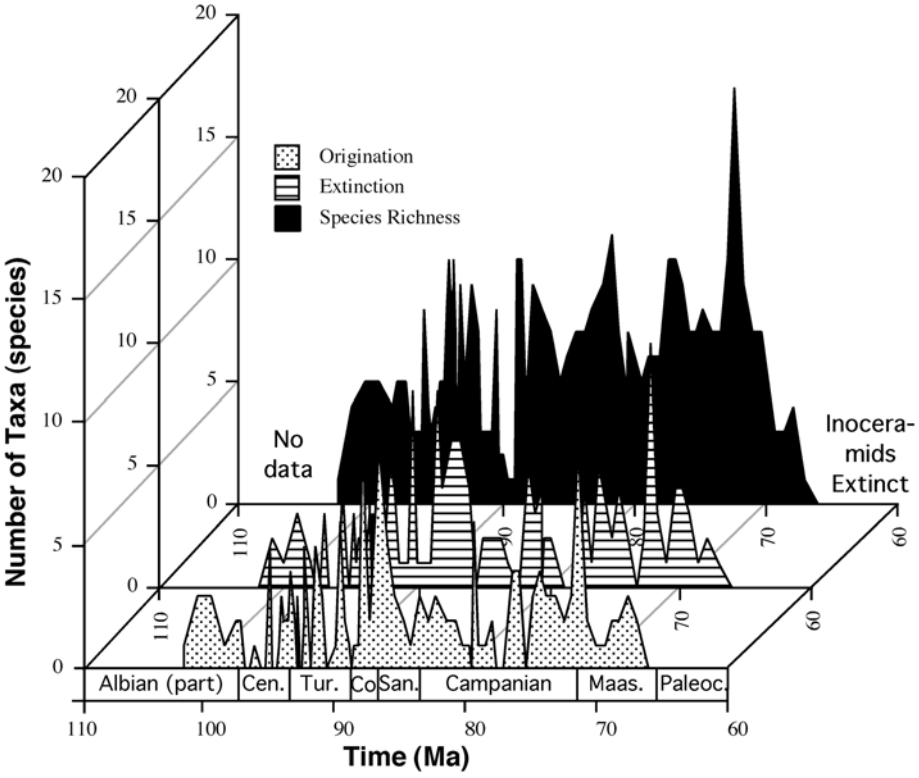

Figure 4. Diagram showing the relationships between WIS inoceramid species richness, origination and extinction through the study interval.

(Kauffman, 1977a; Seibertz, 1979; Harries, 1993; Harries *et al.*, 1996), it is here assumed that for the WIS origination/first appearance as well as extinction/last appearance are temporally equivalent. These data are considerably more variable than those for diversity. This suggests that there is a substantial amount of evolution occurring within this group and that species richness reflects the complicated interplay between origination and extinction; neither variable considered in isolation is the most-prominent driving mechanism to explain the observed changes. However, because there is a reasonable amount of correlation (r = 0.635) between number of species origins and extinctions (Fig. 5), the diversity curve does not reflect all the volatility seen in origination and extinction, and a portion of the curve simply portrays faunal turnover. In many cases the two processes acting in opposition serve to dampen the amount of variability displayed in diversity. In addition, although one might expect there to be an offset between the extinction and origination of taxa provided that vacated ecospace is required for speciation, but this does not appear to hold for the WIS inoceramids at

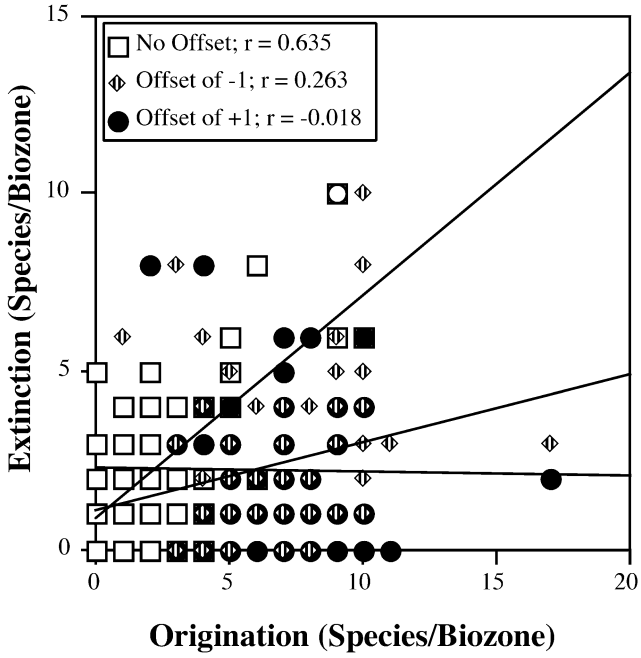

Figure 5. Cross plot showing the relationship between the number of WIS inoceramid originations (or first appearances) and extinctions (or last appearances) per ammonite biozone. The data were also offset relative to each other by one biozone (-1 and +1) to test whether there is a lag time between the two components of species richness. Both offsets showed a pronounced decrease in r-values.

the level of temporal resolution used here. Based on the decreasing degree of correlation, r = 0.263 and –0.018 for a negative and positive offset of one ammonite biozone for the extinction data relative to the origination, respectively (Fig. 5), offset does not enhance the correlation and suggests that the two variables are dominantly in phase; e.g., extinction tends to be high when origination is high and vice versa. This suggests that much of the inoceramid turnover reflects pseudoextinction, although the timing of these speciation events

Another manner in which to approach the data is through an examination of origination and extinction rates. For this approach, rates were calculated based on the temporal lengths of the ammonite biozones. Therefore, several of the pronounced origination and extinction peaks (see Fig. 6) may be artifacts of the shorter lengths of some ammonite biozones. Assuming evenly spaced extinction or origination events and a constant resulting overall rate, if the duration of the sample interval (or ammonite biozone as in this case) fluctuates, the rate would also appear to fluctuate. The strongest

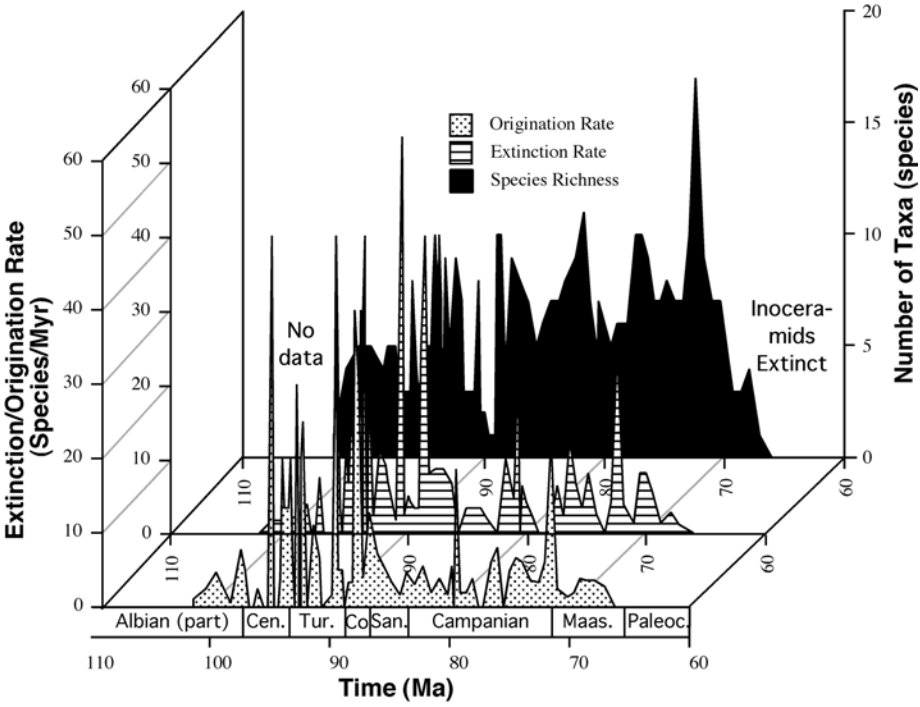

Figure 6. Diagram showing the relationships between WIS inoceramid species richness as well as origination and extinction rates through the study interval.

correlations between origination and extinction rates exist for data from the same biozones with an r-value of 0.594. When the data were offset by a biozone in either direction, r-values ranged from 0.184 to 0.002 for offsets of +1 and –1, respectively (see Fig. 7). As is the case with the diversity data, offset does not enhance the correlation, further emphasizing that these processes often acted in tandem.

4. RESULTS

4.1 Comparison with Cretaceous Sea-Level Curves

Both the Kauffman and Caldwell (1993) sea-level curve and the inoceramid data are from the same basin, but for comparison the inoceramid species richness is also compared to the Hancock (1987) and Haq *et al.* (1989) curves. Following the approach of McGhee (1991), initially all data

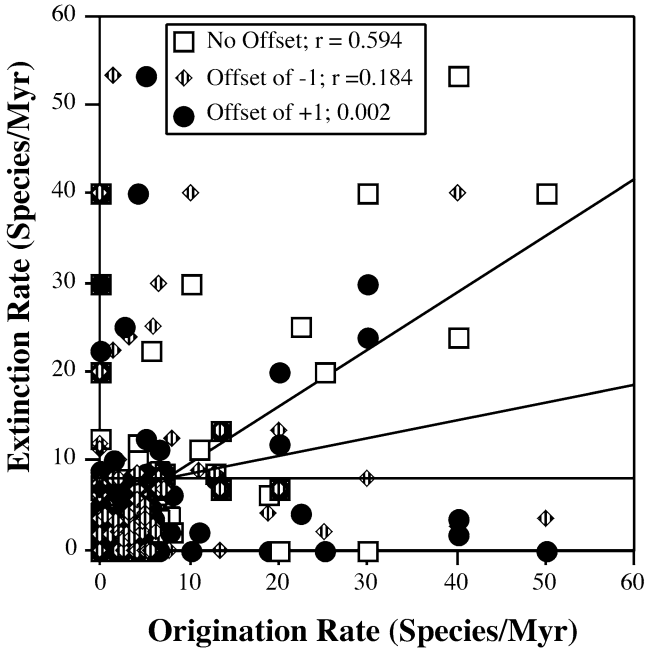

Figure 7. Cross plot showing the relationship between the number of WIS inoceramid origination (or first appearance) and extinction (or last appearance) rates per ammonite biozone. The data were also offset relative to each other by one biozone (-1 and +1) to test whether there is a lag time between the two components of species richness. Both offsets showed a pronounced decrease in r-values.

points were compiled and compared to their relative sea level. As depicted in Figure 8 and Table 1, this shows a fairly weak correlation for all sea-level curves with r-values ranging from a maximum of 0.328 for the Hancock curve to a minimum of 0.015 for the Haq *et al.* curve. Overall, the broad scatter of the data as well as a relative weakness in their correlation suggests a small role of sea level in regulating inoceramid diversity. This impression is very similar to the conclusion of McGhee (1991), who, based on an even weaker correlation (r = 0.007) in Devonian brachiopods from New York State, suggested that sea level played an extremely limited, if any, role in controlling or regulating brachiopod biodiversity.

4.2 Comparison at the Cyclothem Level

Traditionally, the notion has been that the level of species richness obtained is independent of time; if there is a given area available for colonization, then the number of species inhabiting that given area should be

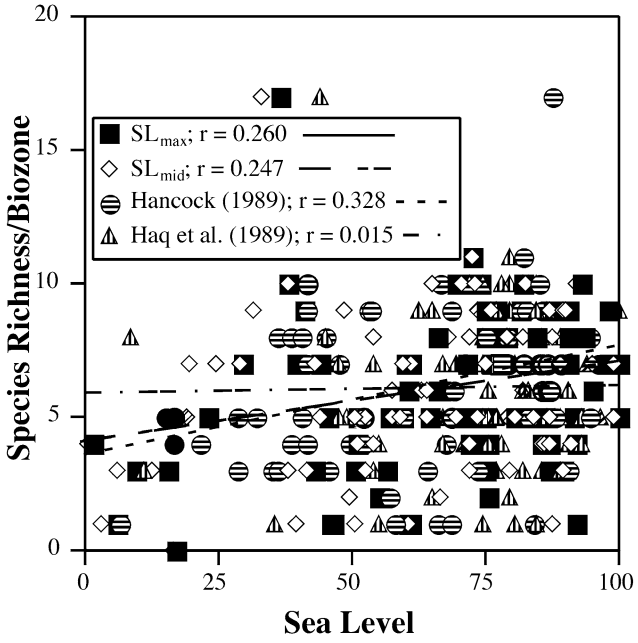

Figure 8. Cross plot of the relationships between WIS inoceramid species richness and the sea-level curves of Kauffman and Caldwell (1993), Hancock (1989), and Haq et al. (1989). SL_{max} and SL_{min} refer to the values for the Kauffman and Caldwell (1993) sea-level curve measured at the highest stand of sea level and at the sea-level position at the midpoint of the ammonite biozones, respectively.

Table 1. Summary of the r-values for the entire data set and for the individual cyclothems.

	r-Values for Sea-Level Curves			
	K & C - max	K & C - mid	Hancock	Haq et al.
All data	0.260	0.247	0.328	0.015
Cyclothem				
Kiowa-Skull Creek	0.533	0.562	0.548	0.309
Greenhorn	0.295	0.325	-0.259	-0.143
Niobrara	0.391	0.319	0.554	0.010
Claggett	0.559	0.237	0.039	0.262
Bearpaw	0.700	0.697	0.287	0.111

equivalent irrespective of any temporal differences. There is, however, no basis for this assumption other than a firm belief in uniformitarianism, and the data presented here challenge the validity of this paradigm. If, however, the data are viewed from a different perspective, they offer intriguing insights into the relationship between sea level and inoceramid species richness and point to the importance of temporal differences. The method used here is to parse the data into subgroups defined by boundaries between individual cyclothems recorded within the WIS. Using the large-scale

temporal and spatial distribution of Cretaceous sedimentary rocks, Kauffman (1977) subdivided marine and marginal marine rocks of the southern WIS into nine cyclothems. Each cyclothem represents a major transgression and regression that is equivalent to the 2nd-order cycles defined by Vail *et al.* (1977) and last approximately 5 to 10 Ma. Although for the most part this study follows the cyclothems as delineated by Kauffman (1977), there are two notable exceptions. First, due to the condensed nature of the earliest sequences as well as the limited temporal biostratigraphic resolution during the interval, the Kiowa and Skull Creek cyclothems are combined into a single one. Second, the Bearpaw and Fox Hills cyclothems have been combined into a single unit based on the diachroneity of the contact between the units representing the two cyclothems as well as biostratigraphic evidence that indicates the Fox Hills Sandstone represents the nearshore environment during the Bearpaw Sea regression. This suggests that typical Fox Hills ammonites were also found in sediments synchronous with Bearpaw deposition (Kennedy *et al.*, 1998).

Figure 9A-E and Table 1 depict the correlation between inoceramid species richness and sea level for individual cyclothems for the various sea-level curves used in this study (see above for discussion). For all but the Claggett Cyclothem, the weakest correlation is between species richness and the Haq *et al.* (1989) curve. The Hancock (1987) curve, on the other hand, shows relatively strong correlations with inoceramid species richness for the Kiowa-Skull Creek and Niobrara cyclothems, but much weaker correlations with the other three. Finally, the Kauffman and Caldwell curve displays relatively strong correlations with the Kiowa-Skull Creek, Claggett, and Bearpaw cyclothems. For SL_{max}, all r-values are greater than those when the entire dataset is considered.

5. DISCUSSION

One of the intriguing aspects of the distribution of organisms today is the relative consistency in diversity trends related to both spatial and latitudinal gradients. As documented by numerous neontologists working on a broad spectrum of taxonomic groups (see Rosenzweig, 1995 for an excellent summary), there is a very strong, positive correlation between area and diversity. In the vast majority of cases when the log of area is compared to the log of the number of species, it yields a strongly linear correlation. What controls these consistent patterns, however, has been the source of considerable debate among ecologists, especially those concerned with conservation issues (see discussion in Hill *et al.*, 1994).

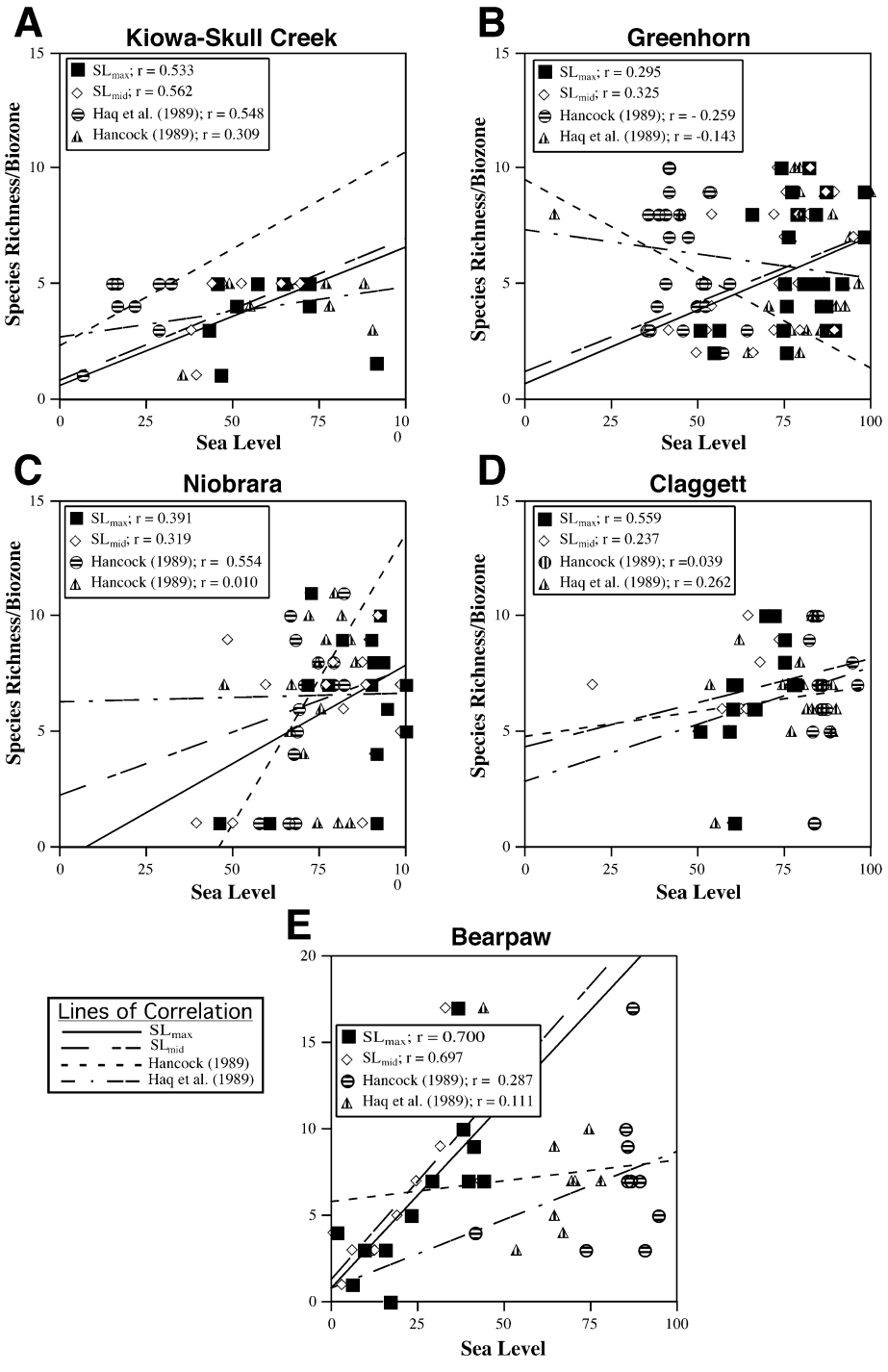
A
Kiowa-Skull Creek
SLmax; r = 0.533
SLmid; r = 0.562
Haq et al. (1989); r = 0.548
Hancock (1989); r = 0.309
Species Richness/Biozone
Sea Level
B
Greenhorn
SLmax; r = 0.295
SLmid; r = 0.325
Hancock (1989); r = - 0.259
Haq et al. (1989); r = -0.143
Species Richness/Biozone
Sea Level
C
Niobrara
SLmax; r = 0.391
SLmid; r = 0.319
Hancock (1989); r = 0.554
Hancock (1989); r = 0.010
Species Richness/Biozone
Sea Level
D
Claggett
SLmax; r = 0.559
SLmid; r = 0.237
Hancock (1989); r =0.039
Haq et al. (1989); r = 0.262
Species Richness/Biozone
Sea Level
E
Bearpaw
SLmax; r = 0.700
SLmid; r = 0.697
Hancock (1989); r = 0.287
Haq et al. (1989); r = 0.111
Sea Level
Lines of Correlation
SLmax
SLmid
Hancock (1989)
Haq et al. (1989)

Despite the ubiquity of the species-area pattern in neontological data, when tested against paleontologic data, results have been far less obvious, consistent, or meaningful. One of the problems in applying the technique to the geologic record is that it is very difficult not only to sample species richness in the fossil record as thoroughly as can readily be accomplished in the modern but also to determine the areal extent of past habitats. This is largely due to the taphonomic and sampling biases inherent in the fossil record. In the marine realm, the best proxy for area that can be employed to interpret the fossil record is sea level. Given the interest in sea-level fluctuation, because of the dominant role it plays in regulating diverse processes ranging from sedimentation to evolution, detailed sea-level curves have been constructed both at regional – depicting the interplay of eustatic and relative fluctuations – and global scales. Because it is very difficult, if not impossible, to reconstruct the detailed topography of the shelf and basins in the geologic past, an exact measure of area flooded or exposed as sea level drops and falls cannot be obtained. This problem is lessened considerably because slopes in intracontinental basins and especially on passive margin shelves are negligible and laterally consistent. The slopes within the WIS were probably almost horizontal, especially the along the eastern portion of the basin, the so-called Eastern Platform, which was relatively stable. Therefore, sea level affords a reasonable approximation of the degree of flooding, hence the area of the WIS flooded through the late Early and Late Cretaceous. The facies models for sedimentation within the Western Interior (e.g., Kauffman, 1977) strongly points to the efficacy of the method in that as sea level rises, the number of depositional environments and, concomitantly, habitats increase. The number of habitats present has been deemed the primary control on the positive correlation between diversity and area (e.g., Boecklen and Gotelli, 1984; Buckley, 1985) and therefore sea level is forcing this habitat increase as water depth and flooded area increase.

Another important element related to sea level and inoceramid species richness is the level of correlation from one cyclothem to the next. The results strongly suggest that there is no equilibrium level for diversity throughout time; environmental, ecologic, and evolutionary changes in addition to sea level fluctuations obviously affect existing diversity.

Therefore, data that span significant intervals of geologic time cannot be effectively compared without taking into account the temporal variability in these variables. Some considerations must be made, however, when smaller portions of a larger data set are used. Because only a portion (approximately

Figure 9. Cross plots of the relationships per cyclothem between WIS inoceramid species richness and the sea-level curves of Kauffman and Caldwell (1993), Hancock (1989), and Haq et al. (1989). See Figure 8 for the definitions of SL_{max} and SL_{mid}.

20%) of the data set is being considered for each cyclothem, there is the potential that this will produce increased r-values as a statistical artifact. Table 2 lists changes in r-values calculated simply as a function of decreasing amount of the data. In this case, every other data point was successively removed until only 1/16 of the data remained; the r-values systematically increase as incrementally smaller subsets of the original data are plotted.

Table 2. Summary of the change in r-values as a progressively smaller portion of the data set is used.

	All	**1/2**	**1/4**	**1/8**	**1/16**
r-value	0.260	0.386	0.436	0.471	0.595

To test whether a similar relationship exists for the data analyzed herein, r-values were calculated with the sea level and species richness data displaced relative to each other, so that sea level was compared to species richness offset by from one to three ammonite biozone towards both younger and older biozones. With the exception of data from the Bearpaw cyclothem that show high r-values throughout, maximum r-values are obtained where there is either no offset or where the offset is either one biozone in either direction (Fig. 10). It should be noted that the sea-level and species richness curves were not tuned to each other, so it is likely that the actual relationship could be displaced by a biozone. The fact that the r-values are highest where the data have not been offset or only at an offset of single biozone combined with the reduction of r-values to with greater offsets, however, allows greater confidence that the increased r-values seen for individual cyclothems are not a statistical artifact of using a reduced portion of the initial data set.

With respect to correlation (see Table 1), the variation in r-value shows a consistent trend regardless of whether SL_{max}, or SL_{mid} is compared to species richness, with the exception of the r-value for SL_{mid} during the Claggett Cyclothem. Initial r-values are average in the Kiowa-Skull Creek Cyclothem, become substantially lower in the Greenhorn Cyclothem, and then rise through the Niobrara to the Bearpaw cyclothems. This trend may initially appear to represent random changes in diversity, but a closer examination of the data suggests otherwise.

The Kiowa-Skull Creek Cyclothem has a maximum species diversity of five, whereas in all the other cyclothems the maximum is essentially twice as large. Furthermore, this cyclothem represents the initial flooding of the southern arm of the WIS. Therefore, the initial, Albian marine incursion into the WIS may have dampened the evolutionary and ecological response of the inoceramid clade as it radiated to fill these new epicontinental niches resulting in decreased species richness. In addition, immigrants into the

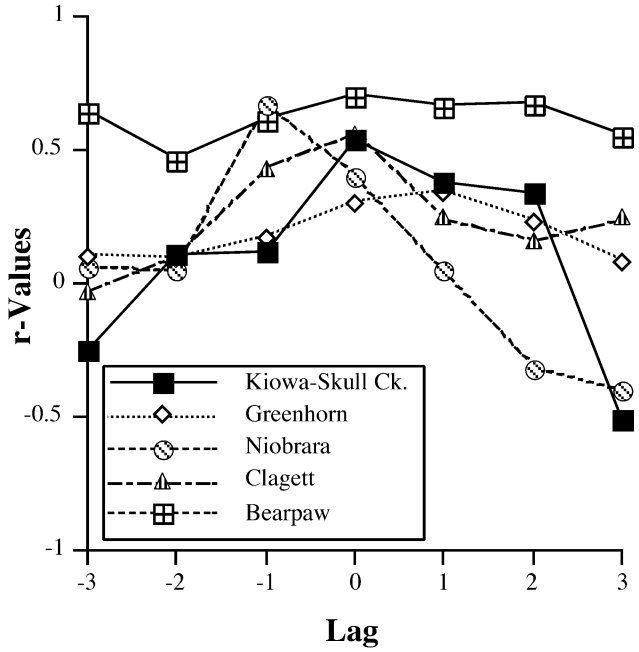

Figure 10. Plot of the r-values as the species richness and SLmax data are offset with respect to on another. In this case, the offset spans from –3 to +3. Except for the Bearpaw cyclothem, the plots show a consistent pattern of decreasing r-values at offsets ≥2. The position of peak r-vales ranging from –1 to 1 probably represents small correlation differences between the chronology used for the inoceramid ranges and the sea level curves.

basin may not have appeared as soon as their habitats became established within the WIS. This may have been especially true if migratory routes, such as the epeiric passage between the seaway and the northern Atlantic that was located through the current Hudson's Bay (White *et al.*, 2000), only were present at higher sea levels. As a result of long-lived planktotrophic larvae (Kauffman, 1975), the widespread distribution of various Cretaceous inoceramid taxa would have facilitated rapid colonization of the WIS provided proper habitats and migratory pathways were available. In addition, the biostratigraphic and inoceramid range data for this interval are coarser than for any other interval considered in this study, and, therefore, diversity estimates for this ≈13 Ma interval may yield a less accurate reflection of true diversity at a given sea level. Finally, the relatively high r-values are heavily influenced by the points at species richness of 1 that are fairly isolated from the bulk of the data. If those points are removed, the r-values are reduced to 0.456, 0.395, 0.001, and –0.427 for SL_{max}, SL_{mid}, Hancock, and Haq *et al.* sea-level curves, respectively. If the potential outliers are removed from other cyclothem datasets, the r-values all increase with the exception of the Greenhorn cyclothem. However, these higher

values were not used herein.

The relatively low r-values in the Greenhorn cyclothem (Fig. 9B), however, are profoundly influenced by a different process: mass extinction. As has been documented by numerous workers (e.g., Elder, 1987b; 1989; Harries, 1999; Jarvis *et al.*, 1988), the Cenomanian-Turonian boundary interval is associated with a step-wise mass extinction. One of the interesting features of this mass extinction is that it occurs very close to maximum flooding, thus there is a substantial amount of biotic overturn, especially among the inoceramids (Elder, 1987a; 1991; Harries *et al.*, 1996; Kauffman and Harries, 1996; Kennedy *et al.*, 2000) during both the extinction and repopulation intervals (*sensu* Harries *et al.*, 1990), respectively, that preceded and succeeded the boundary. This biotic disruption resulted in widely differing values at relatively high sea levels (above a value of ≈70; e.g., Fig. 9B) reflecting the biotic volatility through this crisis, and effectively eliminating any correlation between the two values. This notable disruption of sea-level's role in regulating diversity is a further indication of a similar phenomenon between mass extinction and background levels, initially discussed by Jablonski (1986). However, in this case the difference is related to a diversity control rather than on the nature of biotic selectivity.

Through the Niobrara and Bearpaw cyclothems, the level of correlation between inoceramid species richness and relative sea level progressively increases. During this interval, environmental conditions were relatively stable except near the Turonian-Coniacian boundary. This boundary is characterized by a pronounced change in the inoceramid fauna marked by the first appearance of the distinctive genus *Cremnoceramus*, some biotic turnover (e.g., Collom, 1998; Walaszczyk and Cobban, 2000) and a pronounced global geochemical excursion (e.g., Arthur *et al.*, 1985; Arthur and Sageman, 1994). During the Campanian-Early Maastrichtian interval period of relative environmental stability at shelf depths in mid-latitudes (Barrera and Savin, 1999) – an interval virtually equivalent to the span of the Bearpaw and Claggett cyclothems – represents a period of relatively high species richness in various invertebrate groups, such as rudistids (Johnson and Kauffman, 1990). The slightly lower r-values in the Claggett Cyclothem may be influenced by the disappearance of virtually all inoceramids, with the exception of the enigmatic genus *Tenuipteria*, in the highest Lower Maastrichtian *Baculites clinolobatus* Zone. Because sea level was relatively low (Fig. 2) and the WIS was spatially quite limited during this biozone, the event did not have a profound effect on correlation, although it certainly played a critical role in inoceramid evolution.

Overall, the observed correlation between the different cyclothems (Fig. 9) suggests that sea level played a significant role in regulating inoceramid

diversity, although the importance of the control depends on the relative impact of other forcing mechanisms. For instance, during initial flooding of the WIS, the correlation between the sea level and inoceramid species richness is relatively weak, whereas, once the seaway was established and environmental conditions stabilized, not only was species richness higher, but sea level played a more important role in regulating diversity. The data also clearly reflect a major difference between background intervals and those associated with mass extinction. During the Cenomanian-Turonian event, the correlation is the weakest of any of the cylcothems, which emphasizes the expected influence of large-scale perturbations on biotic groups associated with these biotic crises. Furthermore, the dramatic increase in correlation between the data analyzed at the cyclothem level rather than as a single data set, confirms that there is not a characteristic level of diversity for a given sea level (i.e., the highest sea level does not correlate with the highest inoceramid diversity). Finally, it appears as though there is some "evolutionary memory" from one cyclothem to another. That is, the level of diversity reached in succeeding cyclothems is dependent on what occurred previously. As seen in the interval recorded in the Niobrara and Bearpaw cyclothems, inoceramid species richness and the degree of correlation increase, suggesting a period of prolonged environmental and evolutionary stability when sea-level fluctuations would most profoundly influence species richness.

Because species richness is at least partially a reflection of habitat diversity (e.g., Boecklen, 1984; Buckley, 1985), it is also important to consider how changes in sea level affect the variability in environment present within the WIS. Kauffman's (1977) cyclothem model implies the temporal repetition of facies as similar depositional environments are repeated and hence the repetition of lithology, this is true only at a fairly gross scale of observation. A more-detailed view of the similar units from the various cyclothems points to the distinctiveness of units found in each cyclothem, although it is clear that as sea level rises and floods the basin, the number of lithofacies present within the basin increases. This is to be expected because although similar sea-level positions may be reached in each cyclothem, changing sedimentation, biotic, climatic, and oceanographic conditions between the various cyclothems also heavily influences the sedimentary units deposited.

To test whether this cyclothemic-level of analysis is uniquely applicable to Late Cretaceous inoceramids and, therefore, of limited utility in explaining diversity patterns in the paleontologic record, McGhee's (1991) Late Devonian brachiopod data were reanalyzed in a similar manner to that employed here. His analysis focused on the brachiopods of New York and

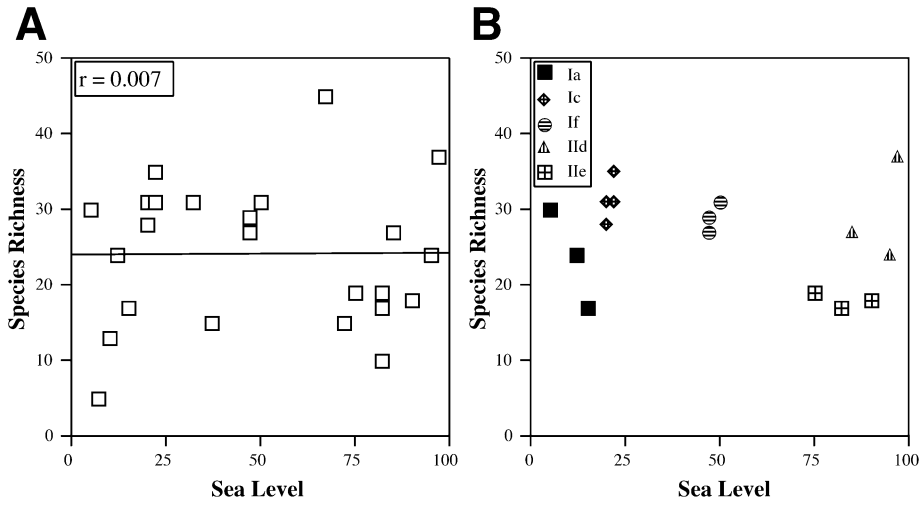

Figure 11. A. Cross plot depicting the relationship between relative sea level and species richness for McGhee's (1991) Devonian brachiopods from New York State. B. Replot of a subset of the data at the cyclothem level. Only those cyclothems that contained at least four data points were included. The paucity of data points, however, makes it impossible to calculate reliable r-values (see text for discussion).

compared sea level and species richness from the Praghian (Early Devonian) through the Fammenian (latest Devonian). Figure 11A depicts the entire McGhee data set plotted *in toto* against sea level. As mirrored in the results of the Cretaceous inoceramids reported above, the correlation is very weak, having an r-value of 0.007. McGhee (1991) used Johnson *et al.*'s (1985) Devonian sea-level curve, and it is subdivided into a 12 smaller-scale cycles (Ia – IIf; 3rd order?), and this allows the data to be analyzed on a per cycle basis. It should also be noted that the Devonian cycles are fairly similar in duration to, although generally somewhat shorter, than the Late Cretaceous cyclothems employed above (3rd order versus 2nd order?). Whereas the average duration of the five Cretaceous transgressive-regressive cycles is 7.3 ± 1.2 Ma, those in the Devonian average 3.6 ± 1.8 Ma. There are some limitations to this reanalysis. First, the brachiopod data are not as temporally refined as the inoceramid data; therefore, the expected level of correlation should be lower than for the latter because of the effects of time averaging through long intervals. Second, although McGhee's data span a total of 12 sea-level cycles, given the relative sparseness of intervals for some cycles, only five cyclothems had three or more data points and thus included in this reanalysis. Unfortunately, data are too sparse for any meaningful analysis similar to that shown here; as noted above, r-values tend to increase when smaller data sets are analyzed. Therefore, given the small number of data points per cyclothem, the chances of having a high r-value is large.

However, Figure 11B shows that the data from cyclothems Ia, Ic, If, IId, and IIe cluster discretely. This suggests that the r-values would be substantially higher for individual cycles if sufficient data were available for a meaningful analysis. As seen in the inoceramid example above, this further promotes the notion that species richness does not achieve a given "equilibrium" that is independent of time.

One of the most intriguing aspects of the two studies is the similar effect of mass extinction on the correlation between sea level and diversity. Despite some difference of opinion on Late Devonian sea level, the bulk of available evidence suggests that the Frasnian-Fammenian (F-F) mass extinction – one of the "big five" (Sepkoski, 1993) – occurred near maximum flooding (see discussion in Morrow and Sandberg, this volume). The admittedly limited data shown in Figure 11B for the Fammenian cycle IIe suggest that there is weaker, negative correlation (the r-value for the three points is –0.466). This resembles the trend seen for the Late Cretaceous inoceramids during the C-T mass extinction close to peak highstand in the Greenhorn Cyclothem. This points to the existence of profound differences between the controls on species richness between background and mass extinction intervals, differences that have also been suggested based on various evolutionary and ecologic characteristics (see Jablonski, 1986). This suggests that when mass extinctions occur near peak highstand, they disrupt the typical positive correlation between species richness and sea level. It would, however, be interesting to examine the effects across a mass extinction event that is associated with lower sea levels, such as the Permo-Triassic (e.g., Erwin, 1993) or the Cretaceous-Tertiary (e.g., Haq *et al.*, 1989).

Valentine and Jablonski (1991) also attempted to evaluate the efficacy of the species-area effect by investigating change in species composition through the Quaternary. They compared molluscan biotas preserved within various Pleistocene terraces along the West Coast of the United States to current biodiversity. Their results indicate that there were few, if any, biotic differences between them. Therefore, they concluded that the link between molluscan diversity and sea level is weak, because the significant changes in sea level during the Quaternary should have resulted in diversity change. There are several reasons, however, why this test of the concept is partially flawed. First, the western margin of North America is active, resulting in a fairly limited shelf as compared to passive margins, and therefore changes in sea level will not be associated with dramatic changes in shelf area with sea level retreat. Furthermore, the shelf area around such features as islands as well as the Baja California, will increase and will offset at least some of the shallow shelf environment lost on the continental margin itself. Secondly and potentially most importantly, the rapidity and magnitude of sea-level

change during the Quaternary is unparalleled in the Cenozoic at least and perhaps throughout Earth history. This rate of change is far greater than evolutionary rates, and therefore how the biota and, more importantly, species richness respond to such rapid changes is unclear. Furthermore, due a lack of low-stand deposits analyzed, there is neither a way of determining if diversity varies at different sea levels nor can it be determined whether present biodiversity represents the lowest or highest sea level. Potentially, the biota present during Quaternary sea-level highstands may be indicative of the species "equilibrium" when the shallow-shelf area was at a minimum, and because the rate of change is so rapid, not only are evolutionary events precluded, but even the effects of potential immigration and emigration are limited.

6. CONCLUSIONS

The cyclothem-level analysis of WIS inoceramid taxa through the Late Cretaceous points to a significant role for sea level, and hence area, in regulating species richness. This contrasts quite markedly with results from other recent studies, this increased correlation largely reflects incorporation of a temporal element. Imbedded in the assumptions of previous studies s the unstated presumption that a given sea level (and hence a given area) should be associated with a given species richness. This approach is based on a strict application of neontological methodology. Because neontological data, by definition, are collected from a single temporal horizon, they ignore the temporal element. The analysis of sea level and inoceramid species richness presented here, however, points to the necessity of considering temporal differences when attempting these types of comparisons. In sum, the manner in which it regulates species richness is time dependent. There is not an "equilibrium value" that is obtained at a given sea level; instead, that value is in part influenced by sea level, but also is a response to various additional ecologic, environmental, and evolutionary factors that also fluctuate through time. To better test the broader utility of the results obtained in this study, the approach employed here needs to be applied to additional data sets spanning different geologic intervals and/or taxonomic groups. Additionally, to better understand species richness and to more effectively model the changes in species richness through time, a wider range of variables (i.e., temperature and its variablity, range of habitats, plate configuration) need to be incorporated into the species-area equation.

ACKNOWLEDGMENTS

I would like to thank Christopher Collom, James Crampton, Erle Kauffman, and Jim Sorauf for their insightful and thoughtful reviews that helped to hone the argument presented here. Furthermore, I am grateful to Erle Kauffman and all of his students that contributed to producing the molluscan database from which this analysis is drawn. Finally, I thank my USF collegues, Chuck Connor and Rick Oches, in steering away from some statistical pitfalls.

REFERENCES

Arthur, M. A., Dean, W. E., Pollastro, R. M., Claypool, G. E. and Scholle, P. A., 1985, Comparative geochemical and mineralogical studies of two cyclic trangressive pelagic limestone units, Cretaceous Western Interior Basin, U. S., in: *Fine-grained Deposits and Biofacies of the Cretaceous Western Interior Seaway: Evidence of Cyclic Sedimentary Processes* (L. M. Pratt, E. G. Kauffman and F. B. Zelt, eds.), SEPM 1985 Midyear Meeting, Golden, CO, Fieldtrip Guidebook, 4I, pp. 16-27.

Arthur, M. A. and Sageman, B. B., 1994, Marine black shales: Depositional mechanisms and environments of ancient deposits, *Ann. Rev. Earth Planet. Sci.*, **22**:499-551.

Barrera, E. and Savin, S. M., 1999, Evolution of late Campanian-Maastrichtian marine climates and oceans, in: *Evolution of the Cretaceous Ocean-Climate System* (E. Barrera and C. C. Johnson, eds.), *Geol. Soc. Am. Sp. Pap.* **332**:245-282.

Boecklen, W. J. and Gotelli, N. J., 1984, Island biogeography theory and conservation practice: species-area or specious-area relationships, *Biol. Cons.* **29**:63-80.

Browne, I. A. and Newell, N. D., 1966, The genus *Aphanaia* Koninck, 1877, Permian representative of the Inoceramidae, *Am. Mus. Nat. Hist. Novitates* **2252**:1-10.

Buckley, R. C., 1985, Distinguishing the effects of area and habitat type on island plant species richness by separating floristic elements and substrate types and controlling for island isolation, *J. Biogeog.* **12**:527-535.

Collom, C. J., 1991, High-resolution stratigraphic and paleoenvironmental analysis of the Turonian-Coniacian stage boundary interval (Late Cretaceous) in the lower Fort Hays Limestone Member, Niobrara Formation, Colorado and New Mexico, Unpubl. MS thesis, Brigham Young University, Provo.

Collom, C. J., 1998, Taxonomy, biostratigraphy, and phylogeny of the Upper Cretaceous bivalve *Cremnoceramus* (Inoceramidae) in the Western Interior of Canada and the United States, in: *Bivalves: An Eon of Evolution -- Paleobiological Studies Honoring Norman D. Newell*, (P.A. Johnson and J.W. Haggart, eds.), University of Calgary Press, Calgary, pp. 119-142.

Elder, W. P., 1987a, The Cenomanian-Turonian (Cretaceous) stage boundary extinctions in the Western Interior of the United States, Unpubl. PhD diss., University of Colorado, Boulder.

Elder, W. P., 1987b, The paleoecology of the Cenomanian-Turonian (Cretaceous) stage boundary extinction at Black Mesa, Arizona, *Palaios* **2**:24-40.

Elder, W. P., 1989, Molluscan extinction patterns across the Cenomanian-Turonian stage boundary in the Western Interior of the United States, *Paleobio.* **15**:299-320.

Elder, W. P., 1991, *Mytiloides hattini* n. sp.: A guide fossil for the base of the Turonian in the

Western Interior of North America, *J. Paleont.* **65**:234-241.

Erwin, D. H., 1993, *The Great Paleozoic Crisis. Life and Death in the Permian*, Columbia University Press, New York

Flessa, K. W. and Sepkoski, J. J., Jr., 1978, On the relationship between diversity and changes in habitable area, *Paleobio.* **4**:359-366.

Hancock, J. M., 1989, Sea-level changes in the British region during the Late Cretaceous, *Proc. Geol. Assoc.* **100**:565-594.

Hancock, J. M. and Kauffman, E. G., 1979, The great transgressions of the Late Cretaceous, *J. Geol. Soc. Lond.* **136**:175-186.

Haq, B. U., Hardenbol, J. and Vail, P. R., 1989, Mesozoic and Cenozoic chronostratigraphy and eustatic cycles, in: *Sea-Level Changes: An Integrated Approach*, (C.K. Wilgus, B. S. Hastings, C. G. St. C. Kendall, H. W. Posamentier, C. A. Ross, and V. C. Van Wagnoner, , eds.), *SEPM Sp. Pub.* **42**:71-108.

Harries, P. J., 1993, Dynamics of survival following the Cenomanian-Turonian (Upper Cretaceous) mas s extinction event, *Cret. Res.* **14**:563-583.

Harries, P. J., 1999, Repopulations from Cretaceous mass extinctions: Enviromental and/or evolutionary controls, in: *Evolution of the Cretaceous Ocean-Climate System*, (E. Barrera and C. C. Johnson, eds.), *Geol. Soc. Am. Sp. Pap.* **332**:345-364.

Harries, P. J. and Kauffman, E.G., 1990, Patterns of survival and recovery following the Cenomanian-Turonian (Late Cretaceous) mass extinction in the Western Interior Basin, United States, in: *Extinction Events in Earth History* (E.G. Kauffman and O.H. Walliser, eds.), *Lect. Notes Earth Hist*. **30**:277-298.

Harries, P. J., Kauffman, E. G., and Crampton, J. S., 1996, Lower Turonian Euramerican Inoceramidae: A morphologic, taxonomic, and biostratigraphic overview, in: *New Developments in Cretaceous Research Topics: Proceedings of the 4th International Cretaceous Symposium*, (C. Spaeth, ed.), *Mitt. Geol.-Paläont. Instit. Univ. Hamburg* **77**:641-671.

Hill, J. L., Curran, P. J. and Foody, G. M., 1994, The effect of sampling on the species-area curve, *Glob. Ecol. Biogeog. Lett.* **4**:97-106.

Jablonski, D., 1986, Background and mass extinctions: The alternation of macroevolutionary regimes, *Science* **231**:129-133.

Jarvis, I., Carson, G. A., Cooper, M. K. E., Hart, M. B., Leary, P. N., Tocher, B. A., Horne, D., and Rosenfeld, A.., 1988, Microfossil assemblages and the Cenomanian-Turonian (Late Cretaceous) Oceanic Anoxic Event, *Cret. Res.* **9**:3-103.

Johnson, C. C. and Kauffman, E. G., 1990, Originations, radiations and extinctions of Cretaceous rudistid bivalve species in the Caribbean Province, in: *Extinction Events in Earth History*, (E. G. Kauffman and O. H. Walliser, eds.), *Lect. Notes Earth Hist*. **30**:305-324.

Johnson, J. G., 1974, Extinction of perched faunas, *Geology* **2**:479-482.

Kauffman, E. G., 1975, Dispersal and biostratigraphic potential of Cretaceous benthonic Bivalvia in the Western Interior, in: *The Cretaceous System in the Western Interior of North America*, (W. G. E. Caldwell, ed.), *Geol. Assoc. Can. Sp. Pap.* **13**:163-194.

Kauffman, E. G., 1977a, Systematic, biostratigraphic, and biogeographic relationships between middle Cretaceous Euramerican and North Pacific Inoceramidae, *Palaeont. Soc. Jap. Sp. Pap.* **21**:169-212.

Kauffman, E. G., 1977b, Upper Cretaceous cyclothems, biotas, and environments, Rock Canyon Anticline, Pueblo, Colorado, in: *Cretaceous Facies, Faunas, and Paleoenvironments across the Western Interior Basin, Field Guide*, (E.G. Kauffman, ed.), *Mount. Geol.* **13**:129-152.

Kauffman, E. G. and Caldwell, W. G. E., 1993, The Western Interior Basin in space and time,

in: *Evolution of the Western Interior Basin*, (W. G. E. Caldwell and E. G. Kauffman, eds.), *Geol. Assoc. Can. Sp. Pap.* **39**:1-30.

Kauffman, E. G. and Harries, P. J., 1996, The importance of crisis progenitors in recovery from mass extinction, in: *Biotic Recovery from Mass Extinction Events*, (M.B. Hart, ed.), *Geol. Soc. Lond. Sp. Pub*. **102**:15-39.

Kauffman, E. G., Sageman, B. B., Kirkland, J. I., Elder, W. P., Harries, P. J., and Villamil, T., 1993, Molluscan biostratigraphy of the Cretaceous Western Interior Basin, North America, in: *Evolution of the Western Interior Basin*, (W. G. E. Caldwell and E. G. Kauffman, eds.), *Geol. Assoc. Can. Sp. Pap.* **39**:397-434.

Kennedy, W. J., Landman, N. H., Christensen, W. K., Cobban, W. A. and Hancock, J. M., 1998, Marine connections in North America during the late Maastrichtian; palaeogeographic and palaeobiogeographic significance of *Jeletzkytes nebrascensis* Zone cephalopod fauna from the Elk Butte Member of the Pierre Shale, SE South Dakota and NE Nebraska, *Cret. Res.* **19**:745-775.

Kennedy, W. J., Walaszczyk, I. and Cobban, W. A., 2000, Pueblo, Colorado, USA, candidate global boundary stratotype section and point for the base of the Turonian Stage of the Cretaceous, and for the base of the middle Turonian Substage, with a revision of the Inoceramidae (Bivalvia), *Acta Geol. Pol.* **50**:295-334.

Komatsu, T., Saito, R. and Fürsich, F. T., 2001, Mode of occurrence and composition of bivalves of the Middle Jurassic Mitarai Formation, Tetori Group, Japan, *Paleont. Res.* **5**:121-129.

MacArthur, R. H. and Wilson, E. O., 1967, *The Theory of Island Biogeography*, Princeton University Press, Princeton.

McGhee, G. R., Jr., 1991, Extinction and diversification in the Devonian Brachiopoda of New York State; no correlation with sea level, *Hist. Biol.* **5**:215-227.

McGhee, G. R., Jr., 1992, Evolutionary biology of the Devonian Brachiopoda of New York State: no correlation with rate of change of sea level?, *Lethaia* **25**:165-172.

McRoberts, C. A. and Aberhan, M., 1997, Marine diversity and sea-level changes: Numerical tests for association using Early Jurassic bivalves, *Geol. Rundsch.* **86**:160-167.

Miall, A. D., 1992, Exxon global cycle chart: An event for every occasion?, *Geology* **20**:787-790.

Miall, A. D., 1997, *The Geology of Stratigraphic Sequences*, Springer-Verlag, Berlin

Newell, N. D., 1967, Revolutions in the history of life, *Geol. Soc. Am. Sp. Pap.* **89**:63-91.

Raup, D. M., 1976a, Species diversity in the Phanerozoic: A tabulation, *Paleobiol.* **2**:279-288.

Raup, D. M., 1976b, Species diversity in the Phanerozoic: An interpretation, *Paleobiol.* **2**:289-297.

Rosenzweig, M. L., 1995, *Species Diversity in Space and Time*, Cambridge University Press, Cambridge.

Schopf, T. J. M., 1974, Permo-Triassic extinctions: Relation to sea-floor spreading, *J. Geol.* **82**:129-143.

Seibertz, E., 1979, Biostratigraphie im Turon des SE-Münsterlandes und Anpassung an die internationale Gliederung aufgrund von Vergliechen mit anderen Oberkreide-Gebieten, *Newsl. Strat.* **8**:111-123.

Sepkoski, J. J., Jr., 1976, Species diversity in the Phanerozoic: Species-area effects, *Paleobiol.* **2**:298-303.

Sepkoski, J. J., Jr., 1993, Ten years in the library: New data confirm paleontological patterns, *Paleobiol.* **19**:43-51.

Simberloff, D., 1974, Permo-Triassic extinctions: Effects of area on biotic equilibrium, *Journal of Geology*, **82**:267-274.

Vail, P. R., Mitchum, R. M., Jr., Todd, R. G., Widmier, J. M., Thompson, S., III, Sangree, J.

B., and Bubb, J. N., 1977, Seismic stratigraphy and global changes in sea level, in: *Seismic Stratigraphy - applications to hydrocarbon exploration*, (C. E. Payton, ed.), *AAPG Mem*. 26:49-212.

Valentine, J. W. and Jablonski, D., 1991, Biotic effects of sea level change; the Pleistocene test, *J. Geophys. Res. B* **96**:6873-6878.

Walaszczyk, I. and Cobban, W. A., 2000, Inoceramid faunas and biostratigraphy of the Upper Turonian-Lower Coniacian of the Western Interior of the United States, *Palaeont. Assoc. Sp. Pap.* **64**:1-118.

Walaszczyk, I., Cobban, W. A. and Harries, P .J., 2001, Inoceramids and inoceramid biostratigraphy of the Campanian and Maastrichtian of the United States Western Interior Basin, *Revue Paléobiol. Genève* **20**:117-234.

Waterhouse, J.B., 1970, Permoceramus, a new inoceramid bivalve from the Permian of eastern, *New Zeal. J. Geol. Geophys.* **13**:760-766.

White, T.S., Witzke, B.J. and Ludvigson, G.A., 2000, Evidence for an Albian Hudson Arm connection between the Cretaceous Western Interior Seaway of North America and the Labrador Sea, *Geol. Soc. Am. Bull.* **112**:1342-1355.

Appendix 1. Age constraints and inoceramid species richness and turnover dynamics (both derived from Kauffman et al., 1993) compiled for each ammonite biozone for the Late Albian through the early Late Maastrichtian. Dur. = duration, Occ. = occurrence, Sp. Rich. = species richness, orig. = origination (or immigration) rate, and ext. = extinction (or emigration) rate. Sea level was determined using a relative scale where the lowest point in a given curve was given a value of 0 and the maximum sea-level highstand was given a value of 100. SL_{max} and SL_{mid} are based on the Kauffman and Caldwell's (1993) curve, and the data for the other two curves are derived from Hancock (1989) and Haq *et al*. (1989).

BIOZONE	TIMING (Mya) Start	Mid-Zone	End	Dur.
Albian				
"Inoceramus" comancheanus (lower)	102.8	102.0	102.0	0.8
"Inoceramus" comancheanus (upper)	102.0	100.8	100.8	1.3
"Inoceramus" bellvuensis	100.8	100.1	100.1	0.7
Unzoned	100.1	98.6	98.6	1.5
Neogastroplites haasi/cornutus	98.6	98.3	98.3	0.3
Neogastroplites muelleri	98.3	97.9	97.9	0.4
Neogastroplites americanus	97.9	97.6	97.6	0.3
Neogastroplites maclearni	97.6	97.2	97.2	0.4
Cenomanian				
Neogastroplites septimus	97.2	96.8	96.8	0.4
Irenicoceras bahani	96.8	96.4	96.4	0.4
Beattonoceras beattonense	96.4	96.0	96.0	0.4
Calycoceras tarrantense	96.0	95.8	95.8	0.1
Acanthoceras granerosense	95.8	95.5	95.5	0.3
Acanthoceras muldoonense	95.5	95.3	95.3	0.3
Acanthoceras bellense	95.3	95.0	95.0	0.3
Cunningtoniceras amphibolum	95.0	94.9	94.9	0.2
Plesiacanthoceras wyomingense	94.9	94.7	94.7	0.1
Calycoceras canitaurinum	94.7	94.6	94.6	0.2
Dunveganoceras problematicum	94.6	94.4	94.4	0.1
Dunveganoceras albertense	94.4	94.2	94.2	0.2
Dunveganoceras conditum	94.2	93.9	93.9	0.3
Vascoceras diartianum	93.9	93.8	93.8	0.1
Euomphaloceras septemsariatum	93.8	93.7	93.7	0.1
Burroceras clydense	93.7	93.6	93.6	0.1
Neocardioceras juddii	93.6	93.6	93.6	0.0
Nigericeras scotti	93.6	93.4	93.4	0.1
Turonian				
Watinoceras devonense	93.4	93.3	93.3	0.1
Pseudaspidoceras flexuosum	93.3	93.1	93.1	0.2
Vascoceras birchbyi	93.1	92.6	92.6	0.5
Mammites nodosoides	92.6	92.1	92.1	0.5
Collignonoceras woollgari woollgari	92.1	91.7	91.7	0.4
Collignonoceras woollgari regulare	91.7	91.5	91.5	0.2
Prionocyclus percarinatus	91.2	90.6	90.6	0.7
Prionocyclus hyatti	90.6	90.4	90.4	0.1
Prionocyclus macombi	90.4	90.0	90.0	0.4
Scaphites warreni	90.0	89.8	89.8	0.2
Scaphites ferronensis	89.8	89.6	89.6	0.3
Scaphites whitfieldi	89.6	89.3	89.3	0.3

Inoceramid Species Richness Dynamics			Evolutionary Rate (sp./My)		Sea Level (relative units)			
1st Occ.	Last Occ.	Sp. Rich.	Orig.	Ext.	SL_{max}	SL_{mid}	Han-cock	Haq et al.
1	0	1	1.3	0	46.2	39.4	6.5	35.4
3	2	4	2.4	2	50.8	50.8	16.2	54.9
3	1	5	4.6	2	45.4	43.8	14.6	47.6
1	3	5	0.6	2	71.7	63.9	16.3	65.9
2	1	4	7.7	4	71.7	71.7	21.1	78.1
2	0	5	5	0	70.9	69.5	28.4	48.8
0	0	5	0	0	64.5	57.2	31.6	76.8
0	3	5	0	8	57.0	52.4	31.7	87.8
1	0	3	2.5	0	43.1	38.1	28.4	90.2
0	0	3	0	0	50.5	41.3	34.9	85.4
0	0	3	0	0	56.2	52.5	35.7	89.0
5	4	8	50	40	65.7	53.8	35.7	89.0
0	1	4	0	3	75.5	54.0	38.2	70.7
0	0	3	0	0	74.7	71.9	45.4	81.7
1	3	4	4	12	86.9	85.5	49.5	90.2
3	1	4	20	7	87.1	86.9	51.9	92.7
2	2	5	13	13	85.9	83.7	51.9	92.7
2	2	5	13	13	80.5	78.9	51.9	86.6
2	1	5	13	7	74.9	73.6	51.1	74.4
4	0	8	20	0	78.3	72.0	44.6	45.1
2	2	10	6.7	7	82.1	82.3	41.4	78.1
0	3	8	0	30	78.9	78.8	40.6	79.3
3	0	9	30	0	77.0	75.7	41.4	79.3
1	3	10	10	30	74.0	73.0	41.4	79.3
0	2	7	0	40	75.9	75.1	41.4	76.8
0	3	5	0	20	82.9	80.5	40.6	75.6
2	0	4	20	0	85.6	86.0	51.9	75.6
5	4	9	25	20	87.1	86.8	52.8	86.6
0	1	5	0	2	91.5	86.7	59.2	96.3
5	5	9	11	11	98.0	89.4	53.6	100.0
3	4	7	6.7	9	98.0	94.9	47.1	93.9
0	1	3	0	7	87.1	79.6	64.1	76.8
1	1	3	1.5	2	89.3	89.3	35.9	89.0
6	8	8	40	53	84.2	81.9	38.3	8.5
2	1	2	5	2	75.4	66.2	56.9	64.6
1	1	2	5	5	54.7	49.5	56.9	79.3
0	1	1	0	4	45.8	39.6	57.7	84.2
1	1	1	3.3	3	60.5	50.1	65.8	80.5

BIOZONE	TIMING (Mya) Start	Mid-Zone	End	Dur.
Scaphites nigricollensis	89.3	89.0	89.0	0.3
Prionocyclus germari	89.0	88.7	88.7	0.3
Scaphites frontierensis - Forresteria peruana	88.7	88.5	88.5	0.2
Coniacian				
Scaphites preventricosus	88.5	88.0	88.0	0.5
Scaphites ventricosus	88.0	87.3	87.3	0.7
Scaphites depressus	87.3	86.6	86.6	0.7
Santonian				
Clioscaphites saxitonianus	86.6	86.0	86.0	0.6
Clioscaphites vermiformis	86.0	85.4	85.4	0.6
Clioscaphites chotauensis	85.4	84.8	84.8	0.6
Desmoscaphites erdmanni	84.8	84.2	84.2	0.6
Desmoscaphites bassleri	84.2	83.5	83.5	0.7
Campanian				
Scaphites leei III	83.5	83.0	83.0	0.5
Scaphites hippocrepis I	83.0	82.0	82.0	1.0
Scaphites hippocrepis II	82.0	81.5	81.5	0.5
Scaphites hippocrepis III	81.5	80.8	80.8	0.7
Baculites sp. (smooth 1)	80.8	80.6	80.6	0.2
Baculites sp. (weak flank ribs)	80.6	80.6	80.6	0.1
Baculites obtusus	80.6	80.3	80.3	0.3
Baculites maclearni	80.3	79.8	79.8	0.5
Baculites asperiformis	79.8	79.3	79.3	0.5
Baculites sp. (smooth 2)	79.3	78.8	78.8	0.5
Baculites perplexus (early)	78.8	78.4	78.4	0.4
Baculites gilberti	78.4	77.8	77.8	0.6
Baculites perplexus (late)	77.8	77.1	77.1	0.7
Baculites gregoryensis	77.1	76.6	76.6	0.5
Baculites scotti	76.6	76.2	76.2	0.4
Didymoceras nebrascense	76.2	75.6	75.6	0.6
Didymoceras stevensoni	75.6	75.0	75.0	0.6
Exiteloceras jenneyi	75.0	74.5	74.5	0.5
Didymoceras cheyennense	74.5	73.7	73.7	0.8
Baculites compressus	73.7	73.1	73.1	0.6
Baculites cuneatus	73.1	72.6	72.6	0.5
Baculites reesidei	72.6	72.2	72.2	0.4
Baculites jenseni	72.2	71.4	71.4	0.8
Maastrichtian				
Baculites eliasi	71.4	70.7	70.7	0.8
Baculites baculus	70.7	70.2	70.2	0.5

Inoceramid Species Richness Dynamics			Evolutionary Rate (sp./My)		Sea Level (relative units)			
1st Occ.	Last Occ.	Sp. Rich.	Orig.	Ext.	SL_{max}	SL_{mid}	Han-cock	Haq et al.
1	1	1	3.3	3	91.7	87.4	68.2	74.4
10	6	10	40	24	92.7	92.4	66.6	81.7
6	8	10	30	40	92.7	91.9	66.6	72.0
2	4	4	4	8	91.7	90.9	67.4	70.7
9	6	9	13	9	90.2	89.7	68.2	76.8
5	6	8	7.1	9	93.5	79.1	74.7	74.4
3	4	7	5	7	99.8	98.7	70.7	47.6
2	0	5	3.3	0	99.8	98.7	68.3	67.1
1	2	6	1.7	3	94.7	81.9	69.1	75.6
3	2	7	4.6	3	77.6	77.1	78.8	67.1
2	2	7	3.1	3	90.2	88.7	77.2	78.1
3	1	8	5.5	2	90.4	87.4	78.8	85.4
2	0	9	2	0	81.4	48.4	81.3	84.2
2	5	11	4	10	72.5	72.3	82.1	79.3
1	3	7	1.5	5	71.3	59.5	82.1	78.1
1	4	5	5.6	22	59.2	58.9	82.9	76.8
0	0	1	0	0	60.7	60.2	83.7	54.9
6	2	7	19	6	61.0	60.7	86.2	89.0
1	2	6	2	4	60.2	57.2	87.0	82.9
1	1	5	2	2	50.6	50.1	87.8	89.0
2	0	6	4	0	66.5	64.0	87.0	90.2
0	0	6	0	0	66.3	62.7	86.2	81.7
0	0	6	0	0	66.0	62.7	85.4	81.7
4	4	10	6.2	6	71.8	70.3	84.6	84.2
4	1	10	8	2	69.5	64.7	83.0	82.9
0	5	9	0	13	75.1	73.3	82.2	62.2
3	4	7	5	7	77.3	76.8	85.5	53.7
4	2	7	6.7	3	78.1	77.3	96.0	74.4
3	4	8	6	8	74.8	67.8	94.4	79.3
3	2	7	3.8	3	60.0	19.4	84.7	80.5
2	0	7	3.3	0	29.2	24.4	86.4	78.1
3	2	10	6	4	38.0	37.8	84.8	74.4
9	10	17	23	25	36.3	33.0	87.2	43.9
2	3	9	2.5	4	40.8	31.5	85.6	64.6
1	1	7	1.3	1	44.1	43.1	85.6	69.5
1	4	7	2	8	39.6	29.0	88.9	70.7

BIOZONE	TIMING (Mya) Start	Mid-Zone	End	Dur.
Baculites grandis	70.2	69.7	69.7	0.5
Baculites clinolobatus	69.7	69.1	69.1	0.6
Sphenodiscus pleurisepta	69.1	68.3	68.3	0.8
Hoploscaphites nicoletti	68.3	67.6	67.6	0.8
Discoscaphites nebrascensis	67.6	66.6	66.6	1.0
Triceratops sp.	66.6	65.4	65.4	1.2

Inoceramid Species Richness Dynamics			Evolutionary Rate (sp./My)		Sea Level (relative units)			
1st Occ.	Last Occ.	Sp. Rich.	Orig.	Ext.	SL_{max}	SL_{mid}	Han-cock	Haq et al.
2	4	5	4	8	22.9	18.9	94.5	64.6
2	3	3	3.6	5	15.4	12.6	90.5	11.0
3	1	3	3.8	1	9.3	5.8	73.6	53.7
2	2	4	2.7	3	1.5	0.5	41.4	67.1
0	1	1	0	1	5.8	2.8		
0	0	0	0	0	16.9	16.4		

Chapter 8

Diversity Patterns of Nonmarine Cretaceous Vertebrates of the Western Interior Basin

JEFFREY G. EATON and JAMES I. KIRKLAND

JEFFREY G. EATON • Department of Geosciences, Weber State University, Ogden, Utah 84408-2507. JAMES I. KIRKLAND • Utah Geological Survey, P.O. Box 146100, Salt Lake City, Utah 84114-6100.

P.J. Harries (ed.), *High-Resolution Approaches in Stratigraphic Paleontology.*

1. INTRODUCTION

Recent studies (e.g., Winkler *et al*., 1995; Archibald, 1996; Eaton *et al*., 1997) have suggested relationships between eustasy during specific intervals within the Cretaceous and early Tertiary (Albian-Aptian, Cenomanian-Turonian, Maastrichtian-Tertiary, respectively) and the evolution of vertebrate faunas. Predictions based on the studies of relatively narrow time intervals (4 million years or less) have not been tested as part of a consistent pattern over long-term eustatic fluctuations.

Considerable attention has been paid to the relationship of Cretaceous eustasy to the evolution of marine invertebrate communities or taxonomic groups within the Western Interior of North America (e.g., Kauffman *et al*., 1993; Harries, this volume), but no similar studies have been undertaken among nonmarine vertebrates. There are good reasons for considering such an attempt to be, at this time, premature (see section entitled "Limitations of the Data" below), but the potential of such an approach is unclear until such an analysis is undertaken.

This paper represents a preliminary attempt at compiling data on the occurrences of nonmarine vertebrates within the Cretaceous Western Interior of North America. The authors have no illusions of this representing a conclusive study of the relationship between vertebrate evolution and eustatic or other environmental change, but rather a starting point. We have attempted to gather a reasonable sample of data regarding the distribution of nonmarine vertebrate orders, families, and genera spanning the Barremian through Maastrichtian stages of the Cretaceous. The Western Interior to date has not yielded any unequivocal records of older Cretaceous vertebrates. Nonetheless, these faunas span the remarkable development and fluctuations of a great epicontinental seaway that divided North America into two subcontinents for a span of almost 45 million years (e.g., Roberts and Kirschbaum, 1995). Such an event must have had enormous effects on the climate, the distribution of organisms, the food chain, and paleogeography. It seems reasonable to suggest that major perturbations of the paleoenvironment should have had some consequences in terms of the evolution of nonmarine communities.

Certainly eustasy can have strong geographic controls on the distribution of faunas. One direct result of eustatic fall is the opening of corridors for dispersal. Connections between Eurasia and North America have been documented both for the Albian-Cenomanian (Cifelli, Kirkland *et al*., 1997;

Kirkland *et al*., 1997, 1999) and near the end of the Cretaceous (Clemens and Kielan-Jaworowska, 1979). Connections with South America have been suggested by the occurrence of titanosaurid sauropods in the latest Cretaceous of North America and hadrosaurs in the latest Cretaceous of South America (Lucas and Hunt, 1989; Brett-Surman, 1979).

During the Cretaceous, the Western Interior's history is further complicated by tectonic activity. The development of the Western Interior depositional basin is intrinsically tied to the genesis of the Sevier Orogenic Belt that may at times overprint eustatic changes (e.g., Eaton *et al*., 1990), and modify both paleogeography and paleoclimate.

2. BASIS FOR TAXONOMIC OCCURRENCES

Data were collected on the occurrences of nonmarine vertebrates in the Cretaceous of the Western Interior of North America (Appendix 1). The term "nonmarine" is used because our faunas include taxa that are purely terrestrial, purely freshwater, or those that inhabit brackish as well as freshwater environments. Marine vertebrates were ignored due to their relatively incomplete record and because they represent a system that is in synchroneity with the expansion and contraction of the seaway. We were specifically interested in how nonmarine vertebrates respond to changes in sea level. Poorly known groups such as birds were also ignored because it was felt the rarity of bird occurrences would do little to elucidate the pattern of nonmarine evolution.

It is difficult to make a clear distinction between freshwater and brackish fish taxa. We attempted to include those fish that may have played a significant role in freshwater settings (e.g., *Hybodus* and *Lepidotes*) and generally follow the listing provided in Russell (1988).

Summary texts were used as available for general information on the Cretaceous faunas of the Western Interior such as Russell (1988) for the fishes, Clemens *et al*. (1979) for mammals, and Kirkland *et al*. (1998) for dinosaurs of the Colorado Plateau. Where higher-level classification was difficult to resolve or in question, Carroll (1988) was used as it represents a standard source for classification. McKenna and Bell (1997) were consulted regarding some problematic areas of mammalian classification. The sources for vertebrate data for each stage are presented below.

2.1 Barremian

The Barremian stage is poorly represented in nonmarine Lower Cretaceous rocks of the Western Interior. The Barremian spans

approximately 6 Ma (Gradstein *et al*., 1994) and is represented by vertebrate faunas from the Yellow Cat Member of the Cedar Mountain Formation of Kirkland *et al*. (1997, 1999) and the Poison Strip Member (Tidwell *et al*., 2001) in east-central Utah and the Lakota Formation of the Black Hills region (Lucas, 1993). The exact position of these faunas within the Barremian is beyond current resolution (it is arbitrarily shown in the tables and Appendix 1 as late Barremian).

2.2 Albian-Aptian

The Aptian through most of the Albian has not yet been faunally distinguished on the basis of nonmarine vertebrates although the interval spans approximately 27.5 Ma (Harland *et al*., 1990). The Cedar Mountain Formation contains the Aptian-Albian Ruby Ranch local fauna (Kirkland *et al*., 1997; Chinnery *et al*., 1998; Tidwell *et al*., 1999; Carpenter *et al*., 2001). Again, refinement within this span of time is not currently possible so this fauna is shown in Appendix 1 as spanning the Aptian-Albian boundary.

The vertebrates from the Comanche Series (including the Trinity Group, and in particular the Paluxy and Antlers formations) of Texas, Arkansas, and Oklahoma probably span the late Aptian and early Albian (Langston, 1974). The sources for these faunas, as presented in Appendix 1, are Langston (1974), Clemens *et al*. (1979), Winkler *et al*. (1990), and Cifelli *et al*., (1997). The Kootenai Formation of Montana (Throckmorton *et al*., 1981) and the Cloverly Formation of Montana and Wyoming also contain vertebrate faunas that span the late Aptian and early Albian. Ostrom (1970), Jenkins and Schaff (1988), and Cifelli (1999) were used as the sources for the Cloverly fauna.

2.3 Latest Albian - Early Cenomanian

The Mussentuchit local fauna of the Cedar Mountain Formation, east-central Utah, is so close to the Albian-Cenomanian boundary (Cifelli *et al*., 1999; Kirkland *et al*., 1997) that we show the taxa from this fauna crossing the Early-Late Cretaceous boundary, placing the age of the fauna at approximately 99 Ma (Gradstein *et al*., 1994). Faunas are based on Carpenter *et al.* (1999), Cifelli and Madsen (1999), Cifelli *et al* (1999), Fiorillo (1999), Kirkland *et al.* (1999), and Nydam (1999).

2.4 Cenomanian

A middle Cenomanian fauna has been recovered from the Woodbine Formation of Texas (Lee, 1995, 1997; Head, 1997). Cenomanian faunas are

described from the Dakota Formation of southern Utah (Eaton 1993, 1995; Eaton *et al*., 1997; Eaton *et al*., 1999a). The close association of the fauna with overlying brackish (uppermost Dakota Formation) and marine rocks (lower part of the Tropic Shale) of late Cenomanian age is the basis for considering it to be late Cenomanian in age (Eaton, 1991, 1993).

2.5 Turonian

Wolfe *et al*. (1997) and Wolfe and Kirkland (1998) have provided a preliminary report on vertebrates from probable mid-Turonian localities in the lower part of the Moreno Hill Formation of west-central New Mexico, and in Kirkland and Wolfe (2001) the oldest North American therizinosaur is described. Faunas of late(?) Turonian age have been recovered from the Smoky Hollow Member of the Straight Cliffs Formation in southwestern Utah (Cifelli, 1990; Eaton, 1995; Eaton *et al*., 1997; Eaton *et al*., 1999a).

2.6 Coniacian

Late(?) Coniacian nonmarine vertebrate localities are known from the Markagunt Plateau of southwestern Utah (Eaton, Diem *et al*., 1999). Although the localities have produced a limited fauna, much potential remains for these localities. At this time a few fish and a single mammalian genus have been identified.

2.7 Santonian

Santonian fossils have been found throughout the John Henry Member of the Straight Cliffs Formation on the Kaiparowits Plateau, southern Utah (Eaton *et al*., 1999a). The John Henry Member spans the Late Coniacian through the Santonian (Eaton, 1991). It is not certain if the Coniacian portion of the member has been sampled for vertebrates. The Coniacian would be restricted to the lowest part of the 250-m-thick member and the lowest well-sampled locality is more than 60 m above the base (Eaton and Cifelli, 1988; Eaton, 1991). For this reason, the material recovered from the John Henry Member is not considered to range back into the Coniacian. The faunas recovered from the Santonian part of the formation show strong brackish influence and are not very diverse in terms of terrestrial vertebrates. No distinct break in the fauna has been observed within the John Henry Member on the Kaiparowits Plateau, so the fauna is estimated to span the Santonian in Appendix 1.

In the Straight Cliffs Formation of the Markagunt Plateau of southwestern Utah, another presumably Santonian fauna has been recovered

from two localities (Eaton *et al*., 1999b). The lower locality (UMNH VP Loc. 10, see Eaton *et al*., 1999b, fig. 2) is about 110 m above an ash bed dated at 86.72±0.58 Ma (Eaton *et al.*, 1999), a date that would place the ash bed in the upper Coniacian (Gradstein *et al*., 1994). The locality is also approximately 140 m above a locality (UMNH VP Loc. 8, see Eaton *et al*., 1999b, fig. 2) that contains abundant brackish-water taxa indicating the Coniacian transgressive event seen at the base of the John Henry Member in the Kaiparowits region. The locality (UMNH VP Loc. 10, *ibid.*) is approximately 270 m below the top of the Cretaceous section on the Markagunt Plateau. The upper locality (UMNH VP Loc. 11, *ibid.*) is within a few meters of the top of the Cretaceous section. Nichols (1997) has bracketed both of these localities as Santonian based on palynomorphs. Material from the lower locality is estimated to be in the early Santonian in Appendix 1. The single unique occurrence from the upper locality (*Iquiladelphis*) is placed in the late Santonian.

The Milk River fauna of Canada has generally been included in the early Campanian (e.g., Fox, 1976a) but re-examination of marine molluscs suggests it may be latest Santonian in age (Braman, pers. comm., 1997). Milk River fauna taxa are included both in the late Santonian and early Campanian in Appendix 1. If this placement is correct, the Aquilan Land Mammal "Age" may range into the Santonian. The fauna is based on lists in Clemens *et al*. (1979), and Clemens and Lillegraven (1986).

Carpenter *et al.* (1995), have reported three dinosaurs from the Niobrara Chalk Formation of Kansas. Two of the taxa are from a section that ranges from Coniacian to Santonian and are indicated here in the early Santonian. The other taxon occurs close to the Santonian-Campanian boundary and is included both in the late Santonian and early Campanian in Appendix 1.

2.8 Campanian

The Campanian encompasses roughly 12 million years and is complex and difficult to divide, in part because of the inadequate stratotype (Harland *et al*., 1990; Gradstein *et al*., 1994). In this study, the fauna from the Wahweap Formation (Eaton *et al*., 1999a) is placed in the Early Campanian, and not in the Santonian. This is based on correlation to laterally equivalent sections to the east in the Henry Basin that are underlain by earliest Campanian marine rocks (based on the occurrence of *Scaphites hippocrepis*, see Eaton, 1990); however, the fauna is very similar to that recovered from the upper part of the Milk River Formation of possible latest Santonian age. Important to the placement of the Santonian-Campanian boundary is the position of the *Scaphites hippocrepis* Dekay (1828) zone which Cobban *et al.* (1994) have maintained is early Campanian in age (and see Kennedy *et*

al., 1997). Leahy and Lerbekmo (1994) suggested, based on the recorrelation of fossil occurrences and paleomagnetic data, that the boundary occurs above the *Scaphites hippocrepis* zone at the base of the *Baculites scotti* Cobban (1958) zone. If Leahy and Lerbekmo are correct, then some, if not all, of the Wahweap fauna could be late Santonian in age.

Faunas considered to represent the Judithian Land-Mammal "Age," which includes the faunas from the Oldman and Dinosaur Park formations of the Judith River Group (southern Alberta), Judith River Formation (Montana), the "Mesaverde" Formation of Wyoming (Lillegraven and McKenna, 1986), the Kaiparowits Formation of southern Utah, the lower part of the Kirtland Formation of New Mexico (following Fassett and Steiner, 1997), and the Aguja Formation of Texas, are placed here in the late Campanian. We are also including the fauna from the Fruitland Formation of New Mexico in the late Campanian following the placement of Hunt and Lucas (1993). Data were taken from Clemens *et al*. (1979), Lillegraven and McKenna (1986), Fiorillo (1989), Archibald and Bryant (1990), Keqin and Fox (1991), Montellano (1992), Rowe *et al*. (1992), Hunt and Lucas (1993), Cifelli (1994), Eberth (1997b), Lehman (1997), McCord (1998), Eaton *et al*. (1999a), Sullivan (1999), Burnham *et al.* (2000), Ford and Kirkland (in press). Wilson *et al*. (1992) provided data on Campanian (and Maastrichtian) pikes (Esocidae).

2.9 Maastrichtian

The Maastrichtian Stage persisted for approximately 6 Ma (Obradovich, 1993; Gradstein *et al*., 1994). The Maastrichtian has only one formal North American Land-Mammal "Age," the Lancian, but another older "Age," which was termed the Edmontonian by Russell (1964, 1975), may be present between the Judithian and the Lancian. The Horseshoe Canyon Formation of south-central Alberta appears to span the latest Campanian at least into the early Maastrichtian (Eberth, 1997a).

We are including faunas from the Lance Formation (Wyoming), the Scollard Formation (south-central Alberta), Frenchman Formation (southwestern Saskatchewan), basal Ravenscrag Formation (southwestern Saskatchewan), the Laramie Formation (northeastern Colorado), the Naashoibito Member of the Kirtland Formation (New Mexico), and the lower part of the North Horn Formation (central Utah) in the Maastrichtian. The Hell Creek Formation (northeastern Montana) also contains Lancian faunas, but reworking in the Paleocene portion of the section (Bug Creek Anthills) has resulted in considerable mixing of faunas. Therefore, we have used Lofgren's (1995; table 11), Bryant's (1989; table 4), and Archibald and Bryant's (1990, table 1) faunal lists that are, with certainty, from the

Cretaceous part of the Hell Creek Formation. Other sources used include Cifelli *et al.* (1999), Cross and Yi (1997), Eberth (1997a), Galton (1995), Krause (1992), Carpenter (1979), Estes and Sanchiz (1982), Storer (1991), and Fox (1976b).

2.10 Limitations of the Data

Appendix 1 must be considered a work in progress and there are undoubtedly both errors and omissions. It was not possible to review the entire Cretaceous literature and in many instances ages or taxonomic occurrences had to be interpreted or inferred. The list is considered to be cuurent to September, 1999, the date the manuscript was submitted. We look forward to improving this list and request that corrections and additions be submitted to the senior author (via e-mail: jeaton@weber.edu). Copies of the database will be made available to all interested researchers.

Anyone who has worked in terrestrial sections knows that there are an enormous number of constraints on the types of data that can be collected and correlations that can be made with terrestrial faunas and stratigraphy. The resolution of stages in the nonmarine of North America is relatively poor both because the stages are defined on marine sections in Europe, and because many of these boundaries are so poorly defined that their precise determination, even in marine sequences, is extremely difficult. Currently, we have the following significant difficulties in age placement of faunas: 1) substage placement of known Barremian faunas is uncertain; 2) Aptian-Albian faunas are often lumped because of the difficulty of recognizing these as distinct stages in terrestrial stratigraphic units; 3) Albian-Cenomanian faunas are lumped together because error ranges in radiometric dates spans the stage boundary (Cifelli *et al*., 1997; Kirkland *et al*., 1997); 4) placement of the Santonian-Campanian boundary is in contention in the Western Interior (Lillegraven, 1991; Leahy and Lerbekmo, 1994) making age determinations for faunas near those boundaries difficult; and 5) placement of the Campanian-Maastrichtian boundary is also controversial (e.g., Eaton, 1987), raising questions about the age of faunas near that boundary. Clearly, better stage and substage resolution is necessary in order to accurately compare faunas to each other and to eustatic curves.

Many of the stages here are represented by relatively few localities of limited geographic extent. Only the Campanian and Maastrichtian are broadly represented from north to south across the Western Interior. Some stages and substages are almost completely unrepresented by faunas anywhere in the Western Interior (e.g., the Coniacian; the early Santonian) and faunas from the eastern shore are very rare. These leave substantial gaps in our record of vertebrate evolution.

Some of the faunas are relatively poorly known (e.g., Barremian) and others are relatively well known (e.g, late Maastrichtian), but even the well-known faunas represent only a fraction of the biodiversity likely to have been present regionally. Also, little is known of many significant components of the terrestrial environments, such as insects.

It is also evident that, in the stratigraphic record, transgressive events leave a poor record and appear to be relatively fast, often leaving a reworked lag deposit marking the event. Marked regressive events will tend to result in upland erosion and the stacking of sands by braided rivers as river gradients readjust to sea level (see Eaton *et al*., 1997). As such, most fossiliferous terrestrial deposits associated with epeiric seaways form during high- or lowstand phases of eustasy. This suggests that in general we will have a poor record of terrestrial diversity during marked regressive or transgressive events leaving brief, but significant, gaps in the record at critical times.

Systematic problems are also difficult to evaluate. Are fish genera equivalent to mammalian genera? Which classification does one choose to use, as this can have a profound effect on the number of taxa counted during a given interval. An example is the bewildering and almost inexplicable family-level classification of turtles, which varies in virtually all examined faunal lists. Choices had to be made by the authors that reflect either our attempts at understanding consensus among many workers, our biases, or arbitrary decisions when we had little basis for making a judgment.

In some reports only orders or families are reported with no reference to lower level taxonomy. In these instances, it was assumed the lower level taxonomic units must be present, and in these cases “family indet.” or "genus indet." appears under the higher level taxonomic name. In some instances we are aware of new genera that are currently being described. If a manuscript name was available, that name is placed in quotes, and if there was as yet no manuscript name, then these taxa are listed as "genera nov." Taxa that have been reported with a questioned or conferred (cf.) identification are indicated with a "?" in Appendix 1. Regardless of the certainty of the identification, these occurrences do imply the presence of another taxon within the fauna.

2.11 Basis for Numerical Counts

Certain assumptions were made in an attempt to take a reasonably meaningful count of the taxa shown in Appendix 1. If gaps between the occurrences of taxa were of a duration of a stage or less and occurred during an interval that is poorly represented by known faunas, it was assumed that the taxon was present throughout that stage. In other instances, when the

gap was greater than a stage, the occurrences are shown as disjunct with gaps occurring in the known range. Not counting taxa within these gaps may result in the under counting of certain taxa, yet care must be taken as these gaps may represent actual local extinctions (e.g., most regard the Cretaceous gap in the occurrence of sauropods to be real although new discoveries in the late Campanian of Arizona and Mexico have raided new doubts, McCord, 1997 and Kirkland, pers. obs.). In order to be consistent, and because there was no meaningful basis to determine which of these gaps were real or not, ranges were not considered to be continuous if a gap of greater than a stage was present. The intent of the data is to record occurrences of taxonomic groups within the strata of the Western Interior, rather than the longevity of individual taxonomic units.

In very rare cases there are reports of taxa that we considered as unlikely to be correct and these are indicated by a "*" in Appendix 1. These occurrences are not counted in the totals. Families that were considered indeterminate were included in the count as many of these may represent new families; however, this may tend to slightly over count families as they may not actually represent families different from those listed.

In separating aquatic from terrestrial taxa, we followed Eaton *et al*. (1997) in counting fish, amphibians, turtles, and crocodilians as aquatic; all other orders were considered to be terrestrial. Although this is probably an oversimplification, it is likely to be more consistent than attempting to assess the habitat preferences of all taxa presented in Appendix 1. Table 1 presents the summary data including the total numbers of orders, families, and genera separated into appropriate substages. Each taxonomic level is further subdivided into totals for aquatic and terrestrial taxa.

2.12 Plotting of Taxonomic Diversity Against Sea-Level Curves

The substage diversity numbers presented in Table 1 were directly plotted using a spread-sheet program. The resulting diversity curves were plotted against the sea-level curve of Kauffman and Caldwell (1993), which was modified to represent the standard substages used in Harland *et al*. (1990) and Gradstein *et al*. (1994), rather than dividing each stage of the Cretaceous into early, middle, and late.

3. RESULTS OF TAXONOMIC DIVERSITY-SEA-LEVEL PLOTS

Figure 1 shows diversity among all orders, aquatic orders, and terrestrial

Table 1. Number of Late Cretaceous nonmarine orders, families, and genera present in substages of the Western Interior of North America.

Stage	Barremian	Aptian		Albian			Cenomanian			Turonian			Coniacian		Santonian		Campanian			Maastrchtian	
Substage	L	E	L	E	M	L	E	M	L	E	M	L	E	L	E	L	E	M	L	E	L
TOTAL ORDERS	17	17	38	39	36	41	41	37	38	31	32	33	30	30	32	38	41	40	46	44	47
Aquatic Orders	6	6	14	15	13	14	14	14	15	11	11	12	11	11	12	14	15	15	16	16	17
Terrestrial Orders	11	11	24	24	23	27	27	23	23	20	21	21	19	19	20	24	26	25	30	28	30
TOTAL FAMILIES	21	20	59	69	60	70	68	57	60	54	59	68	57	57	66	77	78	76	117	103	111
Aquatic Families	6	6	19	24	21	22	22	21	22	18	19	25	21	21	24	26	26	26	37	33	37
Terrestrial Families	15	14	40	45	39	48	46	36	38	36	40	43	36	36	42	51	52	50	80	70	74
TOTAL GENERA	27	18	64	74	61	101	95	63	66	57	64	73	61	59	81	99	103	94	210	159	176
Aquatic Genera	7	5	20	26	21	32	32	23	24	18	19	27	22	22	27	30	30	30	53	49	57
Terrestrial Genera	20	13	44	48	40	69	63	40	42	39	45	46	39	37	54	69	73	64	157	110	119

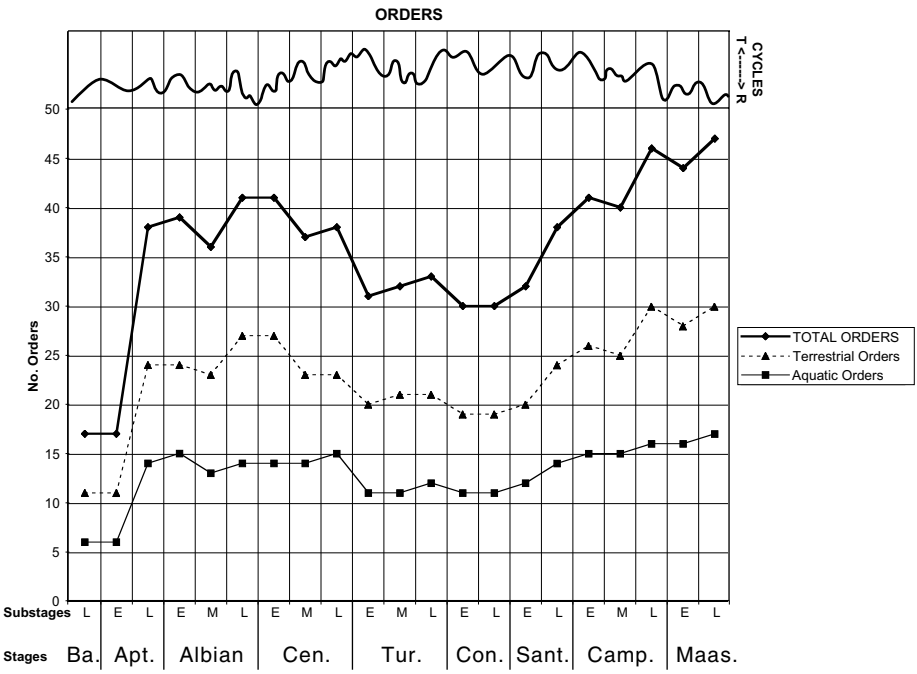

Figure 1. The number of all orders, aquatic orders, and terrestrial orders present in the Western Interior from the Barremian through the Maastrichtian plotted against the modified sea level curve of Kauffman and Caldwell (1993).

orders plotted against the modifed sea-level curves of Kauffman and Caldwell (1993). Following the early Aptian, there is an increase in the number of orders that subsequently declines modestly across the Cenomanian-Turonian boundary, reflecting a global extinction event (Eaton *et al*., 1997). The number of orders remains relatively constant through the Turonian-Coniacian, although this is a relatively poorly sampled interval. Throughout the remainder of the Cretaceous there is an almost continuous increase in the number of both terrestial and aquatic orders. There appears to be a slight drop in diversity during the lower Maastrichtian. Although this appears to correlate to a marked drop in sea level, it more than likely represents a sampling bias as early Maastrichtian faunas are much more poorly known than are those of the later Maastrichtian. By the end of the Maastrichtian, during continued regression, the number of orders is as high as at any time in the Cretaceous. The pattern of increase and decrease in numbers of orders shows no strong correpondence to the sea-level curve. At the end of the Maastrichtian, it is clear that the number of orders is not decreasing, but may in fact be increasing. This may reflect diversification related to an expanded terrestrial environment resulting from the withdrawal of epeiric seaways from much of the region.

The record for families (Fig. 2) shows more distinct, although not entirely synchronous, paralleling of the sea-level curve than did the plots of orders, particularly in the Aptian through the early Coniacian. All families diversify from the early Aptian to early Albian, possibly reflecting the increased wetness following the dry monsoonal patterns that characterized the Late Jurassic and Early Cretaceous through the Barremian (Kirkland *et al*., 1999). The rise of angiosperms may have also played a role in the increased diversity (see Lupia *et al*., in press) as did a possible Asian immigration event (Kirkland, 1996; Kirkland *et al*., 1999). There is a drop in terrestrial family diversity from the early to middle Cenomanian prior to the C-T extinction event. There is a decline in aquatic diversity following the Cenomanian that may reflect the removal of vast areas of floodplain as the epeiric sea approached the base of the Sevier Orogenic Belt (Eaton *et al*., 1997). The aquatic fauna recovers by the end of the Turonian. From the middle Coniacian through the Santonian, familial diversity shows little change, but this is currently the most poorly sampled interval in the Late Cretaceous. There is a sharp rise in the number of both aquatic and terrestrial families from the middle to late Campanian. This increase occurs

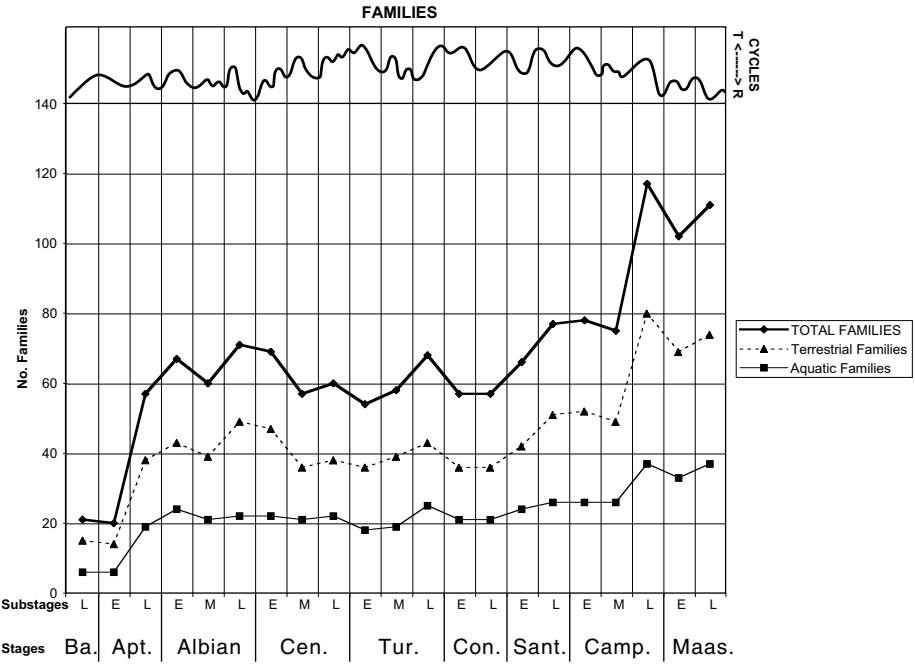

Figure 2. The number of all families, aquatic families, and terrestrial families present in the Western Interior from the Barremian through the Maastrichtian plotted against the modified sea level curve of Kauffman and Caldwell (1993).

during an episode of eustatic rise, but more than likely represents abundant late Campanian localities (e.g., Lehman, 1997**)** that have produced extraordinarily diverse dinosaur faunas. There is a slight decrease in diversity into the Maastrichtian that appears to correspond to a dramatic eustatic fall; however, this again may represent a sampling bias as early Maastrichtian faunas are much more poorly known than are either late Campanian or late Maastrichtian faunas. Family diversity is only slightly lower than the Cretaceous maximum (late Campanian) during the late Maastrichtian.

Figure 3 includes plots of generic diversity against the modified sea level curves of Kauffman and Caldwell (1993). There is a slight decline in terrestrial genera immediately following the Barremian resulting from a decrease in dinosaur diversity (Kirkland *et al*., 1999). Evident in this plot is the relative evenness in numbers of aquatic genera throughout the Cretaceous showing a slight increase in the late Campanian. Also evident is the remarkable increase in the number of terrestrial genera in the late Campanian (possibly coupled with transgression) and a drop in diversity in the beginning of the Maastrichtian (possibly coupled with regression) that rapidly equilibrates and the numbers rise somewhat to the end of the Maastrichtian. The diversity curve for terrestrial genera is much more variable than that for aquatic genera, suggesting some degree of buffering in aquatic environments. There appears to be some parallel oscillation of curves evident, particularly between the diversity curve for terrestrial taxa and eustasy as the seaway withdraws in the later part of the Cretaceous. However, it is unclear if sampling biases or actual correlation between eustasy and diversity are the primary factor.

4. INTERPRETATION OF DIVERSITY-EUSTASY PLOTS

The decline in ordinal diversity across the Cenomanian-Turonian boundary is probably related to the global extinction event and is most marked in aquatic orders. It was suggested in Eaton *et al*. (1997) that this may be related to the elimination of floodplain habitats along the western margin of the epicontinental sea during the maximum flooding event and that transgression might actually result in diversification of terrestrial faunas. As a result of the increased data on Early Cretaceous and early Cenomanian faunas since publication of Eaton *et al.* (1997), it is apparent now that there is no increase in the overall diversity of terrestrial vertebrates at the end of

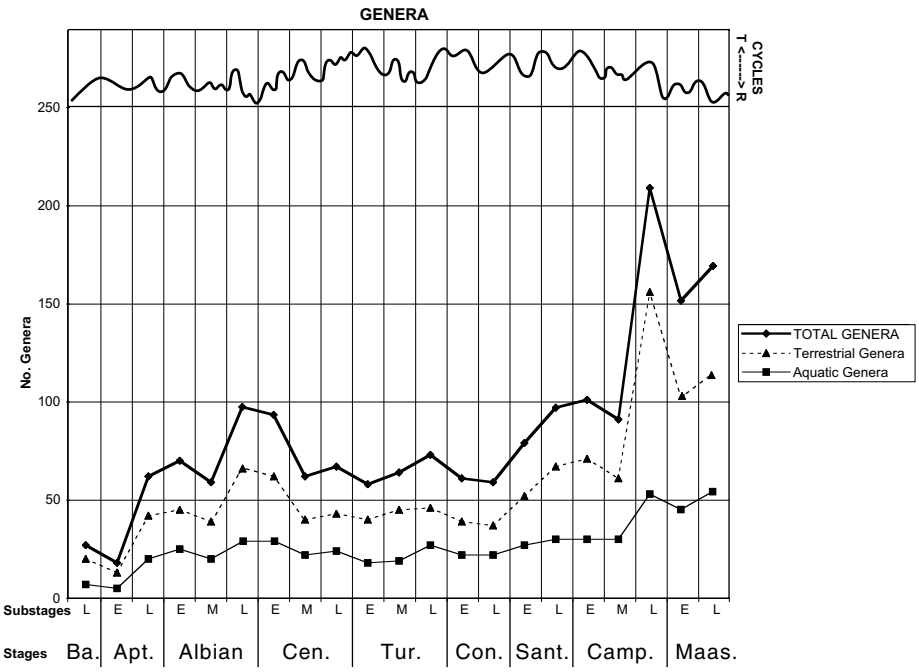

Figure 3. The number of all genera, aquatic genera, and terrestrial genera present in the Western Interior from the Barremian through the Maastrichtian plotted against the modified sea-level curve of Kauffman and Caldwell (1993).

the Cenomanian into the Turonian. The marked increase in terrestrial genera at the end of the Campanian seems to coincide with a transgressive event and the following reduction in diversity appears to be associated with the sea-level fall in the early Maastrichtian. However, it is unknown if any of thesecorrelations represent actual changes in diversity or only sampling biases.

It was suggested by Eaton *et al*. (1997) that episodes of diversification associated with transgression may reflect both an increase in evolutionary pressure as available habitat area diminished, and an increased diversity of food sources as brackish-water taxa invade riverine systems. The data presented here do not support an increase in terrestrial diversity during the Cenomanian-Turonian highstand event, but there is an apparent correlation of that nature in the late Campanian increase in diversity that does correlate to a highstand event. However, this marked increase in diversity is, at least to some degree, a result of sampling bias. It was also suggested in Eaton *et al*. (1997) that during regression the withdrawal of brackish associated faunas (with river incisions at coasts, see fig. 4, Eaton *et al*., 1997) would result in reduced biodiversity in the coastal floodplain environment. This pattern would suggest a brief decline in diversity associated with regression

followed by stabilization. This pattern appears to occur across the Cenomanian-Turonian and Campanian-Maastrichtian boundaries; however, sampling problems abound and during other major regressions (in more poorly sampled intervals) there is no decline in diversity. Also, this pattern does not appear to hold for the Aptian-Albian or Albian-Cenomanian boundaries where there seems to be high generic diversity that is maintained during episodes of lowered sea level. This sustained diversity may be the result of dispersal events during lowstands as has been suggested for these intervals by Winkler *et al*. (1995), Kirkland (1996), Cifelli *et al*. (1997), and Kirkland *et al*. (1999). However, precise correlation of these faunas to the sea-level curve is lacking and unequivocal conclusions are premature. This lack of apparent direct correlation between eustasy and changes in diversity probably suggests that the driving forces of diversity are very complex. Even in cases of extremely well-sampled marine faunas, such as Devonian brachiopods, diversity and sea level show no correlation (McGhee, 1992; but see Harries, this volume, for a different interpretation).

A general observation that can be made is that increased diversity is evident in the number of families and genera through the Cretaceous. This is not as clearly the case in diversity of orders. After the initial rise in diversity during by the Aptian-Albian, the diversity of orders declines into the middle of the Late Cretaceous and then increases to the end of the Cretaceous. It is apparent that the Cenomanian-Turonian extinction event is most pronounced at the ordinal level. The curve also indicates that there was no significant decline in diversity, at least at the substage level, prior to the K-T boundary event. It is tempting to consider the slight decline in families and genera (not reflected in the number of orders) from the late Campanian to late Maastrichtian as a factor that contributed to the sudden extinction of dinosaurs and other taxa at the end of the Cretaceous. This decline in terrestrial genera following the Campanian is largely the result of a decline in dinosaur diversity. There are 48 genera of dinosaurs present in the Late Campanian and only 27 are present by the Late Maastrichtian (about a 44% reduction) which may suggest some factor was preferentially reducing the numbers of dinosaur taxa relative to other groups. Archibald (1996) has suggested that habitat fragmentation that occurred with the withdrawal of the seaway may have strongly impacted dinosaur diversity.

Aquatic taxa demonstrate much less variation in diversity over the Cretaceous than do terrestrial taxa. Eaton *et al*. (1997) had suggested the possibility that transgressive events limited the extent of riverine systems ultimately reducing aquatic diversity. With regression the systems expands allowing an increase in aquatic diversity. The curves in Figure 3 do not bear this out except for the Cenomanian-Turonian event. This may reflect the extent of the Greenhorn transgression which practically reached the base of

the Sevier orogenic belt and virtually restricted riverine systems to the mountain fronts (Eaton *et al.*, 1997). Prior and subsequent transgressive events were never of this extent and therefore may not have had such a pronounced impact upon riverine and floodplain systems. In fact, there appears to be surprisingly little change in the diversity of aquatic genera across the late Campanian transgression and early Maastrichtian regression. Although there is some apparent reduction in diversity across this boundary, this may only represent a sampling bias due to the relatively poorly known early Maastrichtian faunas.

5. COMPARISONS TO PALEOTEMPERATURE CURVES

McKinney and Oyen (1989) have argued that temperature is a more direct control on diversity and extinction than is sea level. With that in mind, we made comparisons of our diversity curves to various stable oxygen isotope and paleobotanically based paleotemperature curves.

The stable oxygen isotope curve shows an overall decrease in surface-water temperatures through the Cretaceous. There is a temperature high across the Albian-Cenomanian boundary, a gradual decline into the Campanian, a middle Campanian increase, and a gradual decline to the end of the Cretaceous (based on curves presented in Frakes *et al*., 1992, chapter 8, fig. 8.3). One of the temperature highs corresponds roughly to the Albian-Cenomanian diversity high, but the late Campanian diversity increase corresponds to an episode of temperature decline that continues into the Maastrichtian.

Perhaps a more direct method of estimating land temperatures can be derived from leaf-margin studies (work of Wolfe and Upchurch, 1987, and summaries in Frakes *et al*., 1992, and Crowley and North, 1991). The general land-temperature pattern shows a gradual increase in temperature from the Albian through the Santonian, a slightly lower and stable temperature through most of the Campanian, dropping to a low in the beginning of the Maastrichtian and rising to a Cretaceous high by the end of the Maastrichtian. This curve has virtually no correlation to the diversity curves except for the slight early Maastrichtian reduction in diversity which probably is a result of sampling biases rather than a real change in diversity.

It may not be surprising that there is not a direct correspondence between paleotemperature and vertebrate diversity. Prothero (1999), in a study of four major climatic events in the Tertiary, found virtually no correspondence between mammalian diversity and paleotemperature. He suggested that controls on mammalian evolution are more complex than previously

supposed, and we would tend to extend that supposition to the entire Vertebrata.

6. COMPARISONS TO ANGIOSPERM DIVERSITY PATTERNS

Lupia *et al*. (in press) have made an assessment of plant diversity through the Cretaceous. They show a marked increase in angiosperm diversity from the Barremian through the Cenomanian that roughly corresponds to the increased diversity seen in terrestrial vertebrates. There is a marked decline of ephedroid (Gentales) as well as *Classopollis* (conifer) pollen, but not angiosperms, around the Cenomanian-Turonian boundary which is significant enough to suggest the influence of external factors. Lupia *et al.* (in press) suggest that climatic cooling is the cause of this reduction. The decline also coincides with the ordinal reduction seen in nonmarine vertebrates. There is a decline in angiosperm genera from the middle Campanian to the early Maastrichtian that is the opposite of the pattern seen in nonmarine vertebrates which increase dramatically in the late Campanian but possibly show a decline in the early Maastrichtian. Angiosperm genera increase in number to the end of the Maastrichtian as do nonmarine vertebrate orders, families, and species. Angiosperm species show a somewhat different pattern. Angiosperm species peak in the Albian and subsequently decline to the Campanian and then increase dramatically from the middle Campanian into the Maastrichtian. This pattern matches that of nonmarine vertebrates. Angiosperm species diversity subsequently declines from the Maastrichtian into the Paleocene, a pattern that differs significantly from that of angiosperm genera and terrestrial taxa. It would be an important next step in the comparison of angiosperm and vertebrate diversity patterns to assess vertebrates at the species level so direct comparisons can be made.

7. CONCLUSIONS

It is clear that the Cretaceous terrestrial record will need to become more robust, better correlated, and more temporally refined before certain conclusions can be made regarding the influence of eustasy or temperature upon nonmarine diversity. Orders demonstrate relatively small changes in diversity during the Late Cretaceous, but more dramatic fluctuations in diversity occur at the familial and generic levels. It is also evident that the aquatic faunas demonstrate a narrower range of fluctuations in diversity

through the Late Cretaceous than do terrestrial faunas. The trends may suggest some influence of eustatic cycles, but more probably indicate that biotic diversity responds to the complex interactions of eustasy, temperature, paleogeography, dispersal events, biotic interactions, and tectonics in such a way that diversity changes during any interval may result from a unique combination of factors.

It is expected that, to some degree, our diversity curves reflect sampling biases rather than actual changes in diversity. When matching them against other kinds of curves to interpret causal relationships, caution must be taken with regards to the almost inevitable certainty that poorly constrained curves are bound to match somewhere and suggest a pattern. Miall (1992) already has made this observation in terms of using eustatic cycles for chronostratigraphic correlation, and the same cautions must be applied to interpreting the causes of changes in biotic diversity.

ACKNOWLEDGMENTS

Drs. Bruce MacFadden and Peter Harries are thanked for their thoughtful reviews of the manuscript.

REFERENCES

Archibald, J. D., 1996, *Dinosaur Extinction and the End of an Era: What the Fossils Say*, Columbia University Press, New York.

Archibald, J. D., and Bryant, L. J., 1990, Differential Cretaceous/Tertiary extinctions of nonmarine vertebrates; evidence from northeastern Montana, in: *Global Catastrophes in Earth History; An Interdisciplinary Conference on Impacts, Volcanism, and Mass Mortality* (V. L. Sharpton and P. D. Ward, eds.), *Geol. Soc. Amer. Spec. Pap.* **247**:549-562.

Brett-Surman, M. K., 1979, Phylogeny and palaeobiogeography of hadrosaurian dinosaurs, *Nature* **277**:560-562.

Bryant, L. J., 1989, Non-dinosaurian lower vertebrates across the Cretaceous-Tertiary boundary in Northeastern Montana, *Univ. Cal. Pub. Geol. Sci.* **134**:1-107.

Burnham, D. A., Derstler, K. L., Currie, P. J., Bakker, R. T., Zhou, Z., and Ostrom, J. H., 2000, Remarkable new bird-like dinosaur (Theropoda: Maniraptora) from the Upper Cretaceous of Montana, *Univ. Kansas Paleon. Contribs*. **13**:1-14.

Carpenter, K., 1979, Vertebrate fauna of the Laramie Formation (Maestrichtian), Weld County, Colorado, *Contribs. Geol. Univ. Wyo*. **17**:37-49.

Carpenter, K., Kirkland, J.I., Burge, D., and Bird, J., 1999, Ankylosaurs (Dinosauria: Ornithischia) of the Cedar Mountain Formation, Utah, and their stratigraphic distribution, in: *Vertebrate Paleontology in Utah* (D. D. Gillette, ed.), *Utah Geol. Surv. Misc. Pub.* **99-1**:243-251.

Carpenter, K., Kirkland, J. I., Burge, D., and Bird, J., 2001, Disarticulated skull of a primitive ankylosaurid from the Lower Cretaceous of eastern Utah, in*: The Armored Dinosaurs* (K.

Carpenter, ed.), Univ. of Indiana Press, Bloomington, p. 211-238. .

Carpenter, K., Dilkes, D., and Weishampel, D. B., 1995, The dinosaurs of the Niobrara Chalk Formation (Upper Cretaceous, Kansas), *J. Vert. Paleo.* **15**:275-297.

Carroll, R. L., 1988, *Vertebrate Paleontology and Evolution*, W.H. Freeman and Company, New York.

Chinnery, B. J., Lipka, T. R., Kirkland, J. I., Parrish, J. M., and Brett-Surman, M. K., 1998, Neoceratopsian teeth from the Lower to Middle Cretaceous of North America, in*: Lower to Middle Cretaceous Non-Marine Faunas* (S. G. Lucas, J. I. Kirkland, and J. W. Estep, eds.), *New Mex. Mus. Nat. Hist. Sci. Bull.* **14**:297-302.

Cifelli, R. L., 1990, Cretaceous mammals of southern Utah. III. Therian mammals from the Turonian (early Late Cretaceous), *J. Vert. Paleo.* **10**:332-345.

Cifelli, R. L., 1994, Therian mammals of the Terlingua local fauna (Judithian), Aguja Formation, Big Bend of the Rio Grande, Texas, *Contrib. Geol. Univ. Wyo.* **30**:117-136.

Cifelli, R. L., 1999, Tribosphenic mammal from the North American Early Cretaceous, *Nature* **401**:363-366.

Cifelli, R. L., Gardner, J. D., Nydam, R. L., and Brinkman, D. L., 1997, Additions to the vertebrate fauna of the Antlers formation (Lower Cretaceous), southeastern Oklahoma, *Okla. Geol. Notes* **54:**124-131.

Cifelli, R. L., and Madsen, S. K., 1999, Spalacotheriid symmetrodonts (Mammalia) from the medial Cretaceous (upper Albian or lower Cenomanian) Mussentuchit local fauna, Cedar Mountain Formation, Utah, USA, *Geodiversitas* **21**:167-214.

Cifelli, R. L., Kirkland, J. I., Weil, A., Deino, A. L., and Kowallis, B. J., 1997, High-precision $^{40}Ar/^{39}Ar$ geochronology and the advent of North America's Late Cretaceous terrestrial fauna, *Proc. Natl. Acad. Sci.* **94**:11163-11167.

Cifelli, R. L., Nydam, R. L., Gardner, J. D., Weil, A., Eaton, J. G., Kirkland, J. I., and Madsen, S. K., 1999, Medial Cretaceous vertebrates from the Cedar Mountain Formation, Emery County: The Mussentuchit Local Fauna, in: *Vertebrate Paleontology in Utah* (D. D. Gillette, ed.), *Utah Geol. Surv. Misc. Pub.* **99-1**:377-388.

Clemens, W. A., and Kielan-Jaworowska, Z., 1979, Multituberculata, in*: Mesozoic Mammals: The First Two-Thirds of Mammalian History* (J. A. Lillegraven, Z. Kielan-Jaworowska, and W. A. Clemens, eds.)*,* University of California Press, Berkeley, pp. 99-149.

Clemens, W. A., and Lillegraven, J. A., 1986, New Late Cretaceous, North American advanced therian mammals that fit neither the marsupial nor eutherian molds*, Contrib. Geol. Univ. Wyo. Spec. Pap*. **3**:55-85.

Clemens, W. A., Lillegraven, J. A., Lindsay, E. H., and Simpson, G. G., 1979, Where, when, and what - a survey of known Mesozoic mammal distribution, in*: Mesozoic Mammals: The First Two-Thirds of Mammalian History* (J. A. Lillegraven, Z. Kielan-Jaworowska, and W. A. Clemens, eds.), University of California Press, Berkeley, pp. 7-58.

Cobban, W. A., Merewether, E. A., Fouch, T. D., and Obradovich, J. D., 1994, Some Cretaceous shorelines in the Western Interior of the United States, in: *Mesozoic Systems of the Rocky Mountain Region, USA* (M. V. Caputo, J. A. Peterson, and K. J. Franszck, eds.), *SEPM Rocky Moun. Sec.*, pp. 393-413.

Cross, A. T., and Yi, M. S., 1997, Palynology and a review of vertebrate faunas of the Late Cretaceous-Paleocene North Horn Formation, Price Canyon, Wasatch Plateau, and environs, Utah, U.S.A., in: *Dinofest International Proceedings* (D. L. Wolberg, E. Stump, and G. D. Rosenberg, eds.), *Acad. Nat. Sci., Phila*., pp. 417-455.

Crowley, T. J., and North, G. R., 1991, *Paleoclimatology*, Oxford University Press, Oxford, *Mono. Geol. Geophys*. **16**:339 p.

Eaton, J. G., 1987, The Campanian-Maastrichtian boundary in the Western Interior of North America, *Newsl. Stratigr*. **18**:31-39.

Eaton, J. G., 1990, Stratigraphic revision of Campanian (Upper Cretaceous) rocks in the Henry Basin, Utah, *Mountain Geol.* **10**:27-38.

Eaton, J. G., 1991, Biostratigraphic framework for the Upper Cretaceous rocks of the Kaiparowits Plateau, southern Utah, in: *Stratigraphy, Depositional Environments, and Sedimentary Tectonics of the Western Margin, Cretaceous Western Interior Seaway* (J. D. Nations and J. G. Eaton, eds.), *Geol. Soc. Amer. Spec. Pap.* **260**:47-63.

Eaton, J. G., 1993, Therian mammals from the Cenomanian (Upper Cretaceous) Dakota Formation, southwestern Utah, *J. Vert. Paleo.* **13**:105-124.

Eaton, J. G., 1995, Cenomanian and Turonian (early Late Cretaceous) multituberculate mammals from southwestern Utah, *J. Vert. Paleo.* **15**:761-784.

Eaton, J. G., and Cifelli, R. L., 1988, Preliminary report on the Late Cretaceous mammals of the Kaiparowits Plateau, southern Utah, *Contrib. Geol. Univ. Wyo.* **26**:45-55.

Eaton, J. G., Cifelli, R. L., Hutchison, J. H., Kirkland, J. I., and Parrish, J. M., 1999a, Cretaceous faunas of the Kaiparowits Plateau, South Central Utah, in*: Vertebrate Paleontology in Utah* (D. D. Gillette, ed.), *Utah Geol. Surv. Misc. Pub.* **99-1**:345-354.

Eaton, J. G., Diem, S., Archibald, J. D., Schierup, C., and Munk, H., 1999b, Vertebrate paleontology of the Upper Cretaceous rocks of the Markagunt Plateau, southwestern Utah, in: *Vertebrate Paleontology in Utah* (D. D. Gillette, ed.), *Utah Geol. Surv. Misc. Pub.* **99-1**:323-334.

Eaton, J. G., Kirkland, J. I., and Kauffman, E. G., 1990, Evidence and dating of mid-Cretaceous tectonic activity in the San Rafael Swell, Emery County, Utah, *Mountain Geol.* **27**:39-45.

Eaton, J. G., Kirkland, J. I., Hutchison, J. H., Denton, R., O'Neill, R. C., and Parrish, J. M., 1997, Nonmarine extinction across the Cenomanian-Turonian boundary, southwestern Utah, with a comparison to the Cretaceous-Tertiary extinction event, *Geol. Soc. Amer. Bull.* **109**:560-567.

Eaton, J. G., Maldonado, F., and MacIntosh, W. C., 1999c, New radiometric dates from Upper Cretaceous rocks of the Markagunt Plateau, southwestern Utah, and their bearing on subsidence histories, *Geol. Soc. Amer. Abs. Prog.* **31**:A-11.

Eberth, D. A., 1997a, Edmonton group, in: *Encyclopedia of Dinosaurs* (K. Padian and P. J. Currie, eds.), Academic Press, pp. 199-204.

Eberth, D. A., 1997b, Judith River wedge, in: *Encyclopedia of Dinosaurs* (K. Padian and P. J. Currie, eds.), Academic Press, pp. 379-385.

Estes, R., and Sanchiz, B., 1982, New discoglossid and palaeobatrachid frogs from the Late Cretaceous of Wyoming and Montana, and a review of other frogs from the Lance and Hell Creek formations, *J. Vert. Paleo.* **2**:9-20.

Fassett, J. E., and Steiner, M. B., 1997, Precise age of C33N-C32R magnetic-polarity reversal, San Juan Basin, New Mexico and Colorado, in: *Mesozoic Geology and Paleontology of the Four Corners Region*, *New Mex. Geol. Soc. Guidebook*, 48th Field Conf., p. 239-247.

Fiorillo, A. R., 1989, The vertebrate fauna from the Judith River Formation (Late Cretaceous) of Wheatland and Golden Valley Counties, Montana, *The Mosasaur, Del. Val. Paleo. Soc.* **4**:127-142.

Fiorillo, A. R., 1999, Non-mammalian microvertebrate remains from the Robison eggshell site, Cedar Mountain Formation (Lower Cretaceous), Emery County, Utah, *in Vertebrate Paleontology in Utah* (D. D. Gillette, ed.), *Utah Geol. Surv. Misc. Pub*. **99-1**:259-268.

Ford, T. L., and Kirkland, J. I., in press, The Carlsbad ankylosaur (Ornithischia, Ankylosauria): an ankylosaurid and not a nodosaurid, in: *The Armored Dinosaurs* (K. Carpenter, ed.), Univ. Indiana Press.

Fox, R. C., 1976a, Additions to the mammalian local fauna from the Upper Milk River

Formation (Upper Cretaceous), Alberta, *Can. J. Earth Sci.* **13**:1105-1118.

Fox, R. C., 1976b, Cretaceous mammals (Meniscoessus intermedius, new species, and Alphadon sp.) from the lowermost Oldman Formation, Alberta, *Can. J. Earth Sci.* **13**:1216-1222.

Frakes, L. A., Francis, J. E., and Syktus, J. L., 1992, *Climate Modes of the Phanerozoic*, Cambridge University Press, Cambridge.

Galton, P. M., 1995, The species of the basal hypsilophodontid dinosaur Thescelosaurus Gilmore (Ornithischia: Ornithopoda) from the Late Cretaceous of North America*, N. Jb. Geol. Palaont. Abh.* **198**:297-311.

Gradstein, F. M., Agterberg, F. P., Ogg, J. G., Hardenbol, J., van Veen, P., Thierry, J., and Huang, Z., 1994, A Mesozoic time scale, *J. Geophys. Res.* **99**:24,051-24,074.

Harland, W. B., Armstrong, R. L., Cox, A. V., Craig, L. E., Smith, A. G., and Smith, D. G., 1990, *A Geologic Time Scale*, Cambridge University Press, Cambridge.

Harries, P. J., this volume, Does sea-level control Late Cretaceous inoceramid diversity?, in: High-Resolution Approaches in Paleontology (P. J. Harries, ed.), Plenum Press, Topics on Geobiology series p. **XX.**

Head, J. J., 1997, A primitive hadrosaurid (Dinosauria, Ornithischia) from the Cretaceous of Texas, Unpubl. M.S. thesis, Southern Methodist University, Dallas.

Hunt, A. P., and Lucas, S. G., 1993, Cretaceous vertebrates of New Mexico, *New Mex. Mus. Nat. Hist. Bull.* **2**:77-91.

Jenkins, F. A., Jr., and Schaff, C. R., 1988, The Early Cretaceous mammal Gobiconodon (Mammalia, Triconodonta) from the Cloverly Formation in Montana, *J. Vert. Paleo.* **8**:1-24.

Kauffman, E. G., and Caldwell, W. G. E., 1993, Overview: Western Interior Basin, in: *Evolution of the Western Interior Basin, North America* (W. G. E. Caldwell and E. G. Kauffman, eds*.), Geol. Assoc. Can. Sp. Pap.* **39**:1-30.

Kauffman, E. G., Sageman, B. B., Kirkland, J. I., Elder, W. P., Harries, P. J., and Villamil, T., 1993, Molluscan biostratigraphy of the Cretaceous Western Interior Basin, North America, in: *Evolution of the Western Interior Basin, North America* (W. G. E. Caldwell and E. G. Kauffman, eds.), *Geol. Assoc. Can. Sp. Pap.* **39**:397-434.

Kennedy, W. J., Cobban, W. A., and Landman, N. H., Campanian ammonites from the Tombigbee Sand Member of the Eutaw Formation, the Mooreville Formation, and the basal part of the Demopolis Formation in Mississippi and Alabama, *Am. Mus. Novitates* **3201**:1-44.

Keqin, G., and Fox, R. C., 1991, New teiid lizards from the Upper Cretaceous Oldman Formation (Judithian) of southeastern Alberta, Canada, with a review of the Cretaceous record of teiids, *Annals Carn. Mus.* **60**:145-162.

Kirkland, J. I., 1996, Biogeography of western North America's mid-Cretaceous dinosaur faunas: Losing European ties and the first great Asian-North American interchange, *J. Vert. Paleo.* **16**:45A.

Kirkland, J. I., Britt, B., Burge, D. L., Carpenter, K., Cifelli, R., Decourten, F., Eaton, J., Hasiotis, S., and Lawton, T., 1997, Lower to middle Cretaceous dinosaur faunas of the central Colorado Plateau: A key to understanding 35 million years of tectonics, sedimentology, evolution, and biogeography, *Brig. Young Univ. Geol. Studies* **42**:69-103.

Kirkland, J. I., Cifelli, R., Britt, B., Burge, D. L., DeCourten, F., Eaton, J. G. and Parrish, M., 1999, Distribution of vertebrate faunas in the Cedar Mountain Formation, east-central Utah, in: *Vertebrate Paleontology of Utah* (D. D. Gillette, ed.), *Utah Geol. Surv. Misc. Pub.* **99-1**:201-218.

Kirkland, J. I. and Wolfe, D.G., 2001, First Definitive Therizinosaurid (Dinosauria, Theropoda) from North America, *J. Vert. Paleont*. **21**:410-414.

Krause, D. W., 1992, *Clemensodon megaloba*, a new genus and species of Multituberculata (Mammalia) from the Upper Cretaceous type Lance Formation, Powder River Basin, Wyoming, *Paleo Bios* **14**:1-8.

Langston, W. Jr., 1974, Nonmammalian Commanchean tetrapods, in*: Aspects of Trinity Division Geology* (B. F. Perkins, ed.), *Geosci. Man* **8**:77-102.

Leahy, G. D., and Lerbekmo, J. F., 1994, Macrofossil magnetobiostratigraphy for the upper Santonian - lower Campanian interval in the Western Interior of North America: comparisons with European stage boundaries and planktonic foraminiferal zonal boundaries, *Can. J. Earth Sci.* **32**:247-260.

Lee, Y., 1995, Mid-Cretaceous archosaur faunal changes in Texas, in*: Sixth Symposium on Mesozoic Terrestrial Ecosystems and Biota, Short Papers* (A. Sun and Y. Wang, eds.), China Ocean Press, Beijing, pp. 143-146.

Lee, Y., 1997, The Archosauria from the Woodbine Formation (Cenomanian) in Texas, J. Paleont. **71**:1147-1156.

Lehman, T. M., 1997, Late Campanian dinosaur biogeography in the Western Interior of North America, in: *Dinofest International Proceedings* (D.L. Wolberg, E. Stump, and G.D. Rosenberg, eds.), The Academy of Natural Science, Philadelphia, pp. 223-240.

Lillegraven, J. A., 1991, Stratigraphic placement of the Santonian-Campanian boundary (Upper Cretaceous) in the North American Gulf Coastal Plain and Western Interior, with implications to global geochronology, *Cret. Res.* **12**:115-136.

Lillegraven, J. A., and McKenna, M. C., 1986, Fossil mammals from the "Mesaverde" Formation (Late Cretaceous, Judithian) of the Bighorn and Wind river Basins, Wyoming, with definitions of Late Cretaceous North American Land-Mammal "Ages", *Amer. Mus. Novitates* **2840**:1-68.

Lofgren, D. L., 1995, The Bug Creek problem and the Cretaceous-Tertiary transition at McQuire Creek, Montana, *Univ. Calif. Pub. Geol. Sci*. **140**:1-185.

Lucas, S. G., 1993, Vertebrate biochronology of the Jurassic-Cretaceous boundary, North America Western Interior, *Mod. Geol*. **18**:371-390.

Lucas, S. G., and Hunt, A. P., 1989, Alamosaurus and the sauropod hiatus in the Cretaceous of the North American Western Interior, *Geol. Soc. Amer. Spec. Pap.* **238**:75-85.

Lupia, R., Crane, P. R., and Lidgard, S., in press, Angiosperm diversification and mid-Cretaceous environmental change, in: *Biotic Responses to Global Change: The Last 145 Million Years*, Cambridge University Press.

McCord, R. D., II, 1997, An Arizona titanosaurid sauropod and revision of the Late Cretaceous Adobe Canyon fauna*, J. Vert. Paleo.* **17**:620-622.

McCord, R. D., II, 1998, A new genus of and species of Cretaceous polyglyphanodontine lizard (Squamata, Teiidae) from the Kaiparowits Plateau, Utah, in: *Advances in Vertebrate Paleontology and Geochronology* (Y. Tomida, L. J. Flynn, and L. L. Jacobs, eds*.), Nat. Sci. Mus. (Tokyo) Monographs* **14**:281-292.

McGhee, G. R., Jr., 1992, Evolutionary biology of the Devonian Brachiopoda of New York State: no correlation with rate of change of sea-level?, *Lethaia* **25**:165-172.

McKenna, M. C., and Bell, S. K., 1997, *Classification of Mammals Above the Species Level*, Columbia University Press, New York.

McKinney, M. L., and Oyen, C. W., 1989, Causation and nonrandomness in biological and geological time series: temperature as a proximal control of extinction and diversity, *Palaios* **4**:3-15.

Miall, A. D., 1992, Exxon global cycle chart: an event for every occasion?, *Geology* **20**:787-790.

Montellano, M., 1992, Mammalian fauna of the Judith River Formation (Late Cretaceous, Judithian), northcentral Montana, *Univ. Calif. Publ. Geol. Sci.* **136**:1-115.

Nichols, D. J., 1997, Palynology and ages of some Upper Cretaceous Formations in the Markagunt and northwestern Kaiparowits Plateaus, southwestern Utah, in: *Geologic Studies in the Basin and Range-Colorado Plateau Transition in Southeastern Nevada, Southwestern Utah, and Northwestern Arizona, 1995* (F. Maldonado and L. D. Nealey, eds.), *U. S. Geol. Surv. Bull.* **2153**:81-95.

Nydam, R. L., 1999, Polyglyphanodontinae (Squamata: Teiidae) from the medial and Late Cretaceous: new taxa from Utah, U.S.A. and Baja California Del Norte, Mexico, in: *Vertebrate Paleontology in Utah* (D. D. Gillette, ed.), *Utah Geol. Surv. Misc. Pub.* **99-1**:303-317.

Obradovich, J. D., 1993, A Cretaceous time scale, in *Evolution of the Western Interior Basin* (W. G. E. Caldwell and E. G. Kauffman, eds.), *Geol. Assoc. Can. Sp. Pap.* **39**:379-396.

Ostrom, J. H., 1970, Stratigraphy and paleontology of the Cloverly Formation (Lower Cretaceous) of the Bighorn Basin area, Wyoming and Montana, *Peabody Mus. Nat. Hist. Bull.* **35**:1-234.

Prothero, D. R., 1999, Does climatic change drive mammalian evolution?, *Geol. Soc. Amer. Today* **9**:1-7.

Roberts, L. N. R., and Kirschbaum, M. A., 1995, Paleogeography of the Late Cretaceous of the Western Interior of middle North America – coal distribution and sediment accumulation, *U. S. Geol. Surv. Prof. Pap.* **1561**:115 p.

Rowe, T., Cifelli, R. L., Lehman, T. M., and Weil, A., 1992, The Campanian Terlingua local fauna, with a summary of other vertebrates from the Aguja Formation, Trans-Pecos Texas, *J. Vert. Paleo.* **12**:472-493.

Russell, L. S., 1964, Cretaceous non-marine faunas of northwestern North America, *Roy. Ontario Mus., Life Sci. Contrib.* **61**:1-24.

Russell, L. S., 1975, Mammalian faunal succession in the Cretaceous system of western North America, in *The Cretaceous System in the Western Interior of North America* (W. G. E. Caldwell, ed.), *Geol. Assoc. Can. Sp. Pap.* **13**:137-161.

Russell, D. A., 1988, A checklist of North American Marine Cretaceous vertebrates including fresh water fishes: *Occas. Pap. Tyrrell Mus. Palaeo.* 4:1-57.

Storer, J. E., 1991, The mammals of the Gryde local fauna, Frenchman Formation (Maastrichtian: Lancian), Saskatchewan, *J. Vert. Paleo.* **11**:350-369.

Sullivan, R. M., 1999, Nodocephalosaurus kirtlandenesis, gen. et sp. nov., a new ankylosaurid dinosaur (Ornithischia: Ankylosauria) from the Upper Cretaceous Kirtland Formation (Upper Campanian), San Juan Basin, New Mexico, *J. Vert. Paleo.* **19**:126-139.

Throckmorton, G. S., Hopson, J. A., and Parks, P., 1981, A redescription of *Toxolophosaurus cloudi* Olsen, a Lower Cretaceous herbivorous sphenodontid reptile, *J. Paleont.* **55**:586-597.

Tidwell, V., Carpenter, K., and Brooks, B., 1999, New sauropod from the Lower Cretaceous of Utah, USA, *Oryctos* **2**:21-37.

Tidwell, V., Carpenter, K., and Meyer, S., 2001, A new titanosauriform (Saurapoda) from the Poison Strip Member of the Cedar Mountain Formation (Lower Cretaceous), Utah, in: *Mesozoic Vertebrate Life* (D. Tanke and K. Carpenter, eds.), Indiana Univ. Press, Bloomington, p. 139-165.

Wilson, M. V. H., Brinkman, D. B., and Neuman, A. G., 1992, Cretaceous Esocoidei (Teleostei): Early radiation of the pikes in North American fresh waters, *J. Paleont.* **66**:839-846.

Winkler, D. A., Jacobs, L. L., Lee, Y., and Murray, P. A., 1995, Sea level fluctuations and terrestrial faunal change in north-central Texas, in: *Sixth Symposium on Mesozoic Terrestrial Ecosystems and Biota, Short Papers* (A. Sun and Y. Wang, eds.), China Ocean Press, Beijing, pp. 175-177.

Winkler, D. A., Murray, P. A., and Jacobs, L. L., 1990, Early Cretaceous (Comanchean) vertebrates of central Texas, *J. Vert. Paleo.* **10**:95-116.

Wolfe, D. G., and Kirkland, J. I., 1998, *Zuniceratops christopheri* n. gen. & n. sp., a ceratopsian dinosaur from the Moreno Hill Formation (Cretaceous, Turonian) of west-central New Mexico, in Lower to Middle Cretaceous Non-marine Faunas, *New Mex. Mus. Nat. Hist. Sci. Bull.* **14**:303-318.

Wolfe, D. G., Kirkland, J. I., Denton, R., and Anderson, B. G., 1997, A new terrestrial vertebrate record from the Moreno Hill Formation (Turonian, Cretaceous), west-central New Mexico, *J. Vert. Paleo.* **17**(suppl. to 3)**:** 85A-86A.

Wolfe, J. A., and Upchurch, G. R., 1987, North American nonmarine climates and vegetation during the Late Cretaceous, *Palaeogeog. Palaeoclimatol. Palaeocol.* **61**:33-77.

Appendix 1. Occurrences of nonmarine vertebrate orders (O), families (F), and genera (G) in the Cretaceous Western Interior Basin. Boldface type indicate a recorded occurrence; regular type indicates inferred occurrence; "a" indicates taxon counted as aquatic; "?" indicates questionable occurrence; "*" indicates an unusual report of a taxon not counted in totals.

	Barremian	Aptian		Albian			Cenomanian		
Taxon	**L**	**E**	**L**	**E**	**M**	**L**	**E**	**M**	**L**
Chondrichthyes									
Hybodontiformes	**Oa**	**Oa**	**Oa**	**Oa**	Oa	**Oa**	**Oa**	**Oa**	**Oa**
Ptychodontidae				**Fa**					
Hylaeobatis				**Ga**?					
Hybodontidae	**Fa**	**Fa**	**Fa**	**Fa**	Fa	**Fa**	**Fa**	Fa	**Fa**
Hybodus	**Ga?**	**Ga**	**Ga**	**Ga**	Ga	Ga	Ga	Ga	**Ga**
Polyacrodontidae			**Fa**	**Fa**	Fa	**Fa**	**Fa**	**Fa**	**Fa**
Polyacrodus						**Ga**	**Ga**	Ga	**Ga**
Lissodus (=*Lonchidion*)			**Ga**	**Ga**	Ga	**Ga**	**Ga**	**Ga**	**Ga**
Orectolobiformes						**Oa**	**Oa**	**Oa**	Oa
Ginglymostomatidae						**Fa**	**Fa**	**Fa**	Fa
Squatirhina						**Ga**	**Ga**?	Ga	Ga
Cantioscyllium						**Ga**	**Ga**	**Ga**	Ga
Cretorectolobus						**Ga**	**Ga**		
Rajiformes			**Oa**	**Oa**	Oa	**Oa**	**Oa**	Oa	**Oa**
Rhinobatidae				**Fa**	Fa	**Fa**	**Fa**	Fa	**Fa**
cf. *Baibisha*						**Ga**	**Ga**		
Rhinobatus				**Ga**	Ga	**Ga**	**Ga**	**Ga**	
Pseudohypolophus						**Ga**	**Ga**		
genera nov.									**Ga**
Myledaphus									
Sclerorhynchidae			**Fa**	**Fa**	Fa	**Fa**	**Fa**	Fa	Fa
genus indet.			**Ga**	**Ga**	Ga				
Ischyrhiza						**Ga**	**Ga**	Ga	Ga
Osteichthyes									
Dipnoi	**Oa**	**Oa**	**Oa**	**Oa**	Oa	**Oa**	**Oa**	**Oa**	**Oa**
Ceratodontidae	**Fa**	**Fa**	**Fa**	**Fa**	Fa	**Fa**	**Fa**	**Fa**	**Fa**
Ceratodus	**Ga**	**Ga**	**Ga**	**Ga**	Ga	**Ga**	**Ga**	**Ga**	**Ga**
Semionotiformes	**Oa**	**Oa**	**Oa**?	**Oa**?	Oa	**Oa**	**Oa**	Oa	**Oa**
Semionotidae	**Fa**	**Fa**	**Fa**?	**Fa**?	Fa	**Fa**	**Fa**	Fa	**Fa**
Semionotus	**Ga**								
Lepidotes	**Ga**	**Ga**	**Ga**	Ga	Ga	**Ga**	**Ga**		
genus indet.				Ga	Ga				
genera nov.						**Ga**	**Ga**	Ga	**Ga**
Dapedius									**Ga**?
Lepisosteiformes			**Oa**	**Oa**	Oa	**Oa**	**Oa**	Oa	Oa

Turonian			Coniacian		Santonian		Campanian			Maastrichtian	
E	**M**	**L**	**E**	**L**	**E**	**L**	**E**	**M**	**L**	**E**	**L**
Oa	Oa	**Oa**	Oa	**Oa**	**Oa**	**Oa**	**Oa**	**Oa**	**Oa**	**Oa**	**Oa**
Fa	Fa	**Fa**	Fa	**Fa**	**Fa**	**Fa**	**Fa**	**Fa**	**Fa**		
Ga	Ga	**Ga**	Ga	**Ga**	**Ga**	**Ga**	**Ga**	**Ga**	**Ga**		
Fa	Fa	**Fa**	Fa	**Fa**	**Fa**	**Fa**	**Fa**	**Fa**	**Fa**	Fa	**Fa**
											Ga
Ga	Ga	**Ga**	Ga	**Ga**	**Ga**	**Ga**	**Ga**	**Ga**	**Ga**	Ga	**Ga**
Oa	Oa	**Oa**	Oa	Oa	**Oa**	**Oa**	**Oa**	**Oa**	**Oa**	**Oa**	**Oa**
Fa	Fa	**Fa**	Fa	Fa	**Fa**	**Fa**	**Fa**	**Fa**	**Fa**	**Fa**	**Fa**
Ga	Ga	**Ga**	Ga	Ga	**Ga**	**Ga**	**Ga**	**Ga**	**Ga**	**Ga**	**Ga**
Ga	Ga	**Ga**	Ga	**Ga**?	**Ga**	**Ga**	**Ga**	**Ga**	**Ga**	**Ga**	**Ga**
Oa	Oa	**Oa**	Oa	**Oa**	**Oa**	**Oa**	**Oa**	**Oa**	**Oa**	**Oa**	**Oa**
Fa	Fa	Fa	Fa	**Fa**	**Fa**	**Fa**	**Fa**	**Fa**	**Fa**	**Fa**	**Fa**
Ga	Ga	**Ga**	Ga	Ga	**Ga**	**Ga**	**Ga**	Ga			
									Ga	**Ga**	**Ga**
Fa	Fa	**Fa**	Fa	Fa	**Fa**	**Fa**	**Fa**	**Fa**	**Fa**	**Fa**	**Fa**
Ga	Ga	**Ga**	Ga	Ga	**Ga**	**Ga**	**Ga**	**Ga**	**Ga**	**Ga**	**Ga**
									*		
Oa	**Oa**	**Oa**	Oa	**Oa**	**Oa**	**Oa**	**Oa**	**Oa**	**Oa**	**Oa**	**Oa**

	Barremian	Aptian		Albian			Cenomanian		
Taxon	**L**	**E**	**L**	**E**	**M**	**L**	**E**	**M**	**L**
Lepisosteidae			**Fa**	**Fa**	Fa	**Fa**	Fa	Fa	Fa
Lepisosteus (Astractosteus)			**Ga**	**Ga**	Ga	**Ga**	Ga	Ga	Ga
Pycnodontiformes			**Oa**	**Oa**	Oa	**Oa**	**Oa**	Oa	**Oa**
Pycnodontidae			**Fa**	**Fa**	Fa	**Fa**	**Fa**	Fa	**Fa**
Palaeobalistum			**Ga**?	**Ga**?					
Gyronchus			**Ga**	**Ga**					
Amiiformes	**Oa**	**Oa**	**Oa**	**Oa**	Oa	Oa	Oa	Oa	**Oa**
Amiidae	**Fa**	**Fa**	**Fa**	**Fa**	Fa	Fa	Fa	Fa	**Fa**
Amia	**Ga**								
genus indet.					Ga	Ga	Ga	Ga	Ga
Melvius			**Ga**?	**Ga**					
Platacodon									
Kindleia									
Aspidorhynchiformes			**Oa**	**Oa**					
Aspidorhynchidae			**Fa**	**Fa**					
Belonostomus			**Ga**	**Ga**					
Palaeonisciformes									
Platysomidae									
Platysomus									
Leptolepiformes			**Oa**	**Oa**					
Leptolepidae			**Fa**	**Fa**					
Clupavus			**Ga**	**Ga**					
Osteoglossiformes									
Ostariostomidae									
Ostariostoma									
Elopiformes			**Oa**	**Oa**	Oa	Oa	Oa	Oa	**Oa**?
family indet.			**Fa**	**Fa**	Fa	Fa	Fa	Fa	**Fa**?
genus indet.			**Ga**	**Ga**	Ga	Ga	Ga	Ga	**Ga**?
Elopidae									
Paratarpon									
Phyllodontidae			**Fa**	**Fa**	Fa	Fa	Fa	Fa	**Fa**?
Casierius			**Ga**	**Ga**					
genus indet.					Ga	Ga	Ga	Ga	**Ga**?
Parabula									
Pseudoegertonia									
Phyllodus									
Albulidae									
Coriops									
Salmoniformes									
Esodidae									
Encodus						**Ga**	**Ga**		

Turonian			Coniacian		Santonian		Campanian			Maastrichtian	
E	**M**	**L**	**E**	**L**	**E**	**L**	**E**	**M**	**L**	**E**	**L**
Fa	**Fa**	**Fa**	Fa	**Fa**	**Fa**	**Fa**	**Fa**	**Fa**	**Fa**	**Fa**	**Fa**
Ga	**Ga**	**Ga**	Ga	**Ga**	**Ga**	**Ga**	**Ga**	**Ga**	**Ga**	**Ga**	**Ga**
Oa	Oa	**Oa**	Oa	Oa	**Oa**	**Oa**	**Oa**	**Oa**	**Oa**	**Oa**	**Oa**
Fa	Fa	**Fa**	Fa	Fa	**Fa**	**Fa**	**Fa**	**Fa**	**Fa**	**Fa**	**Fa**
					Ga	**Ga**	**Ga**	**Ga**	**Ga**	**Ga**	**Ga**
Ga											
	Ga	**Ga**	Ga	Ga	**Ga**	**Ga**	**Ga**	**Ga**	**Ga**	**Ga**	**Ga**
						Ga	**Ga**	**Ga**	**Ga**	**Ga**	**Ga**
									Ga	**Ga**	
						Oa	**Oa**	**Oa**	**Oa**	**Oa**	**Oa**
						Fa	**Fa**	**Fa**	**Fa**	**Fa**	**Fa**
						Ga	**Ga**	**Ga**	**Ga**	**Ga**	**Ga**
		Oa									
		Fa									
		Ga									
									Oa	Oa	**Oa**
									Fa	Fa	**Fa**
									Ga	Ga	**Ga**
Oa	Oa	**Oa**	Oa	Oa	**Oa**	**Oa**	**Oa**	**Oa**	**Oa**	**Oa**	**Oa**
Fa	Fa										
Ga	Ga										
		Fa	Fa	Fa	**Fa**	**Fa**	**Fa**	**Fa**	**Fa**	**Fa**	**Fa**
		Ga	Ga	Ga	**Ga**	**Ga**	**Ga**	**Ga**	**Ga**	**Ga**	**Ga**
Fa	Fa	**Fa**?	Fa	Fa	**Fa**?	**Fa**?	**Fa**?	Fa	**Fa**	Fa	**Fa**
Ga	Ga	**Ga**?	Ga	Ga							
					Ga	**Ga**	**Ga**	**Ga**	**Ga**	**Ga**	**Ga**
									Ga		
											Ga
									Fa	Fa	**Fa**
									Ga	Ga	**Ga**
							Oa	**Oa**	**Oa**	Oa	**Oa**
							Fa	**Fa**	**Fa**	Fa	**Fa**

	Barremian	Aptian		Albian			Cenomanian		
Taxon	**L**	**E**	**L**	**E**	**M**	**L**	**E**	**M**	**L**
Oldmanesox									
Estesesox									
Peridiformes									**Oa**
Colobodontidae									**Fa**
Colobodus									**Ga**?
Perciformes									
Palaeolabridae									
Palaeolabrus									
Acipenseriformes									
Acipenseridae									
Acipenser									
Diphyodus									
Polyodontidae									
Paleopsephurus									
Family indet.									
Protoscaphirhynchus									
Cypriniformes									
Cyprinodae									
genus indet.									
Amphibia									
Allocaudata			**Oa**	**Oa**	Oa	**Oa**	**Oa**	Oa	**Oa**
Albanerpetontidae			**Fa**	**Fa**	Fa	**Fa**	**Fa**	Fa	**Fa**
Albanerpeton			**Ga**?	**Ga**?	Ga	**Ga**?	**Ga**?	Ga	**Ga**?
Urodela			**Oa**	**Oa**	Oa	**Oa**	**Oa**	Oa	Oa
Prosirenidae			**Fa**	**Fa**	Fa	**Fa**	**Fa**		
Prosiren			**Ga**	**Ga**					
genus indet.					Ga	**Ga**	**Ga**		
family indet.								Fa	Fa
genus indet.								Ga	Ga
Batrachosauridae									
Batrachosauroides									
genus indet.									
Prodesmodon									
Opisthotriton									
Scapherpetontidae									
Scapherpeton									
Lisserpeton									
Piceoerpeton									
Sirenidae									
Habrosaurus									
Amphiumidae									

Turonian			Coniacian		Santonian		Campanian			Maastrichtian	
E	**M**	**L**	**E**	**L**	**E**	**L**	**E**	**M**	**L**	**E**	**L**
									Ga		
							Ga	**Ga**	**Ga**	Ga	**Ga**
					Oa	**Oa**	**Oa**	**Oa**	**Oa**	Oa	**Oa**
					Fa	**Fa**	**Fa**	**Fa**	**Fa**	Fa	**Fa**
					Ga	**Ga**	**Ga**	**Ga**	**Ga**	Ga	**Ga**
						Oa	Oa	Oa	**Oa**	**Oa**	**Oa**
						Fa	Fa	Fa	**Fa**	**Fa**	**Fa**
						Ga	Ga	Ga	**Ga**	**Ga**	**Ga**
										Ga	
									Fa	**Fa**	**Fa**
									Ga	**Ga**	**Ga**
											Fa
											Ga
											Oa
											Fa
											Ga
Oa	Oa	**Oa**	Oa	Oa	**Oa**	**Oa**	Oa	Oa	**Oa**	Oa	**Oa**
Fa	Fa	**Fa**	Fa	Fa	**Fa**	**Fa**	Fa	Fa	Fa	Fa	**Fa**
Ga	Ga	**Ga**?	Ga	Ga	**Ga**	**Ga**	Ga	Ga	**Ga**	Ga	**Ga**
Oa	Oa	**Oa**	Oa	Oa	**Oa**	**Oa**	**Oa**	**Oa**	**Oa**	Oa	**Oa**
Fa	Fa										
Ga	Ga										
		Fa	Fa	Fa	**Fa**	Fa	**Fa**	**Fa**	**Fa**	Fa	**Fa**
		Ga?									
			Ga	Ga							
					Ga	Ga	Ga	Ga	**Ga**	Ga	**Ga**
					Ga	Ga	**Ga**	**Ga**	**Ga**	Ga	**Ga**
									Fa	Fa	**Fa**
									Ga	Ga	**Ga**
									Ga	Ga	**Ga**
											Ga?
									Fa	Fa	**Fa**
									Ga	Ga	**Ga**
									Fa	Fa	**Fa**?

	Barremian	Aptian		Albian			Cenomanian		
Taxon	**L**	**E**	**L**	**E**	**M**	**L**	**E**	**M**	**L**
Proamphiuma									
Anura				**Oa**?	Oa	**Oa**	**Oa**	Oa	Oa
family indet.					Fa	Fa	Fa	Fa	Fa
genus indet.					Ga	Ga	Ga	Ga	Ga
Discoglossidae				**Fa**?					
genus indet.				**Ga**?					
Scotiphryne									
Paradiscoglossus									
Pelobatidae									
Eopelobates									
Palaeobatrachidae									
Palaeobatrachus									
Family indet.									
Theatonius									
Reptilia									
Chelonia	**Oa**	**Oa**	**Oa**	**Oa**	Oa	**Oa**	**Oa**	**Oa**	**Oa**
Pleurosternidae	**Fa?**	**Fa**	**Fa**?	**Fa**	Fa	**Fa**	**Fa**	Fa	Fa
Glyptops	**Ga**?	**Ga**	**Ga**?	**Ga**	Ga	**Ga**	**Ga**	Ga	**Ga**
Compsemys									
Family indet.			Fa	Fa	Fa	Fa	Fa	Fa	Fa
Naomichelys			**Ga**	**Ga**	Ga	**Ga**	**Ga**	Ga	**Ga**?
genus indet.									
Hoplochelys									
Baenidae			**Fa**	**Fa**	Fa	**Fa**	**Fa**	Fa	**Fa**?
Trinitichelys			**Ga**	**Ga**					
genus indet.					Ga	Ga	Ga	Ga	
Dinochelys									**Ga**?
Baena									
Boremys									
Thescelus									
Plesiobaena									
Eubaena									
Sygiochelys									
Palatobaena									
Pelomedusidae									
Bothremys									
Adocidae									
genus indet.									
Adocus									
Trionychidae									
genus indet.									

Turonian			Coniacian		Santonian		Campanian			Maastrichtian	
E	**M**	**L**	**E**	**L**	**E**	**L**	**E**	**M**	**L**	**E**	**L**
									Ga	Ga	**Ga**?
Oa	Oa	**Oa**	Oa	Oa	**Oa**	**Oa**	Oa	Oa	**Oa**	Oa	**Oa**
Fa	Fa		Fa	Fa	Fa	Fa	Fa	Fa			
Ga	Ga		Ga	Ga	Ga	Ga	Ga	Ga			
		Fa							**Fa**	Fa	**Fa**
		Ga							**Ga**	Ga	**Ga**
											Ga
		Fa							**Fa**		
		Ga							**Ga**		
									Fa	Fa	**Fa?**
									Ga	Ga	**Ga?**
											Fa
											Ga
Oa	Oa	**Oa**	Oa	**Oa**	**Oa**	**Oa**	**Oa**	**Oa**	**Oa**	**Oa**	**Oa**
Fa	Fa	**Fa**	Fa	Fa	**Fa**	**Fa**	**Fa**	**Fa**	**Fa**	Fa	**Fa**
		Ga	Ga	Ga	**Ga**	**Ga**	**Ga**	**Ga**	**Ga**	Ga	**Ga**
Fa	Fa	Fa	Fa	Fa	Fa	Fa	Fa	Fa	Fa	Fa	Fa
Ga	Ga	**Ga**?	Ga	**Ga**?	**Ga**	**Ga**	**Ga**	**Ga**	**Ga**		
										Ga	
											Ga
Fa	**Fa**	**Fa**	Fa	Fa	**Fa**	**Fa**	**Fa**	**Fa**	**Fa**	Fa	**Fa**
Ga	Ga	Ga	Ga	Ga							
					Ga?	**Ga**?	**Ga**	**Ga**	**Ga**	**Ga**?	**Ga**?
									Ga	**Ga**	
										Ga	**Ga**
									Ga	Ga	**Ga**
											Ga
											Ga
											Ga
		Fa	Fa	Fa	**Fa**	**Fa**	Fa	Fa	**Fa**		
		Ga	Ga	Ga	**Ga**	**Ga**	Ga	Ga	**Ga**		
		Fa?	Fa	Fa	**Fa**	**Fa**	**Fa**	**Fa**	**Fa**	**Fa**	**Fa**
		Ga	Ga	Ga							
					Ga	**Ga**	**Ga**	**Ga**	**Ga**	**Ga**	**Ga**
	Fa	**Fa**	Fa	Fa	**Fa**	**Fa**	Fa	Fa	**Fa**	**Fa**	**Fa**
	Ga	**Ga**	Ga	Ga							

	Barremian	Aptian		Albian			Cenomanian		
Taxon	**L**	**E**	**L**	**E**	**M**	**L**	**E**	**M**	**L**
Aspideretes									
Trionyx									
Plastomenus									
Platypeltis									
Helopanoplia									
Chelydridae									
genus indet.									
Emarginochelys									
Nanhsiungchelyidae									
Basilemys									
Neurankylidae									
Neurankylus									
Macrobaenidae									
"Clemmys"									
Kinosternidae									
genus indet.									
Archosauromorpha									
Champsosauridae									
Champosaurus									
Squamata			**O**	**O**	O	**O**	**O**	O	**O**
Teiidae			**F**?	**F**?	F	**F**	**F**	F	**F**
genus indet.			G	G	G	G	G	G	G
Peneteius						*	*		
Docothodon						**Ga**	**Ga**		
Chamops									
Polyglyphanodon									
Leptochamops									
Meniscognathus									
Sauriscus									
Paraglyphanodon									
Glyptogenys									
Socognathus									
Sphenosiagon									
Gerontoseps									
Manangyasaurus									
Heptosphenus									
Scincidae			**F**?	**F**?	F	F	F	F	**F**
genus indet.			**G**?	**G**?	G	G	G	G	**G**
Contogenys									
Sauriscus									
Cordylidae									**F**

Turonian			Coniacian		Santonian		Campanian			Maastrichtian	
E	**M**	**L**	**E**	**L**	**E**	**L**	**E**	**M**	**L**	**E**	**L**
					Ga	**Ga**	**Ga**?	Ga	**Ga**	**Ga**	**Ga**
									Ga	Ga	**Ga**
									Ga	**Ga**	**Ga**?
										Ga	
											Ga
		Fa							**Fa**	Fa	**Fa**
		Ga							Ga	Ga	
											Ga
					Fa	**Fa**	**Fa**	**Fa**	**Fa**	**Fa**	**Fa**
					Ga	**Ga**	**Ga**	**Ga**	**Ga**	**Ga**	**Ga**
									Fa	**Fa**	**Fa**
									Ga	**Ga**	**Ga**
									Fa	Fa	**Fa**
									Ga	Ga	**Ga**
											Fa
											Ga
									O	**O**	**O**
									F	**F**	**F**
									G	**G**	**G**
O	**O**	**O**	O	**O**	**O**	**O**	**O**	**O**	**O**	O	**O**
F	F	**F**	F	**F**	**F**	**F**	**F**	**F**	**F**	F	**F**
G	G										
											G
		G	G	G	**G**	G	**G**	G	**G**	G	**G**
		G							**G**?	G	**G**
					G	G	G	G	**G**	G	**G**
					G	G	G	G	**G**		
					G						
					G	**G**	G	G	**G**	G	**G**
									G		
									G		
									G		
									G		
								G	**G**		
											G
F	F	**F**	F	F	**F**	F	F	F	**F**	F	**F**
G	G										
		G	G	G	**G**	G	G	G	**G**	G	**G**
									G		

	Barremian	Aptian		Albian			Cenomanian		
Taxon	**L**	**E**	**L**	**E**	**M**	**L**	**E**	**M**	**L**
genus indet.									**G**
Paramacellodidae			**F**?	**F**?	F	F	F	F	**F**
genus indet.			**G**?	**G**?	G	G	G	G	
Saurilodon									**G**?
Anguidae				**F**?	F	F	F	F	**F**
genus indet.				**G**?	G	G	G	G	**G**
Odaxosaurus (Peltosaurus)									
Gerrhonotus									
Proxestops									
Pancelosaurus									
Dorsetisauridae									
Dorsetisaurus									
Necrosauridae									
genus indet.									
Parasaniwa									
Colpodontosaurus									
Varanidae									
genus indet.									
Palaeosaniwa									
Xenosauridae									
Restes									
Exostinus									
Helodermatidae						**F**?	**F**?		
genus indet.						**G**?	**G**?		
Paraderma									
Family incertae sedis									
Litakis									
Serpentes						**O**	**O**		
Aniliidae						**F**	**F**		
Coniophis						**G**	**G**		
Boidae									
genus indet.									
Rhynchocephalia	**O**?	**O**	**O**	**O**					
Spheodontidae	**F**?	**F**	**F**	**F**					
Toxolophosaurus	**G**?	**G**	**G**	**G**					
Crocodylia	**Oa**	**Oa**	**Oa**	**Oa**	Oa	**Oa**	**Oa**	Oa	**Oa**
family indet.	**Fa**	**Fa**							
genus indet.	**Ga**	**Ga**							
Bernissartiidae			**Fa**	**Fa**	Fa	**Fa**	**Fa**	**Fa**?	**Fa**?
Bernissartia			**Ga**	**Ga**	Ga	**Ga**	**Ga**	**Ga**?	Ga
Goniopholidae			**Fa**?	**Fa**	Fa	**Fa**	**Fa**	**Fa**	**Fa**

Turonian			Coniacian		Santonian		Campanian			Maastrichtian	
E	**M**	**L**	**E**	**L**	**E**	**L**	**E**	**M**	**L**	**E**	**L**
F	**F**	**F**	F	F	**F**	**F**	**F**	**F**	**F**	F	**F**
G	**G**										
		G	G	G	**G**	**G**	G	G	**G**	G	**G**
									G?		
									G		
									G		
		F									
		G									
		F	F	F	**F**	F	F	F	**F**	F	**F**
		G	G	G							
					G	G	G	G	**G**	G	**G**
									G	G	**G**
					F	**F**	**F**	**F**	**F**	F	**F**
					G	**G**	**G**	**G**			
					G	**G**	G	G	**G**	G	**G**
									F	F	**F**
									G		
									G	G	**G**
									F	F	**F**
									G	G	**G**
									F	F	**F**
									G	G	**G**
									O	O	**O**
									F	F	**F**
									G	G	**G**
								F	**F**	F	**F**
											G
Oa	Oa	**Oa**	Oa	**Oa**	**Oa**	**Oa**	**Oa**	**Oa**	**Oa**	**Oa**	**Oa**
Fa	Fa	**Fa**	Fa	Fa	**Fa**	**Fa**	**Fa**	**Fa**	**Fa**		
Ga	Ga	**Ga**	Ga	Ga	**Ga**	**Ga**	**Ga**	**Ga**	**Ga**		
Fa	Fa	**Fa**	Fa	Fa	**Fa**	**Fa**	**Fa**	**Fa**	**Fa**	**Fa**	**Fa**

	Barremian	Aptian		Albian			Cenomanian		
Taxon	**L**	**E**	**L**	**E**	**M**	**L**	**E**	**M**	**L**
Dakotasuchus			**Ga**?	**Ga**?	Ga	**Ga**?	**Ga**?		
Polydectes						**Ga**	**Ga**		
Woodbinesuchus								**Ga**	
genus indet.									
Goniopholis						**Ga**	**Ga**	Ga	**Ga**
Atoposauridae				**Fa**?	Fa	**Fa**	**Fa**		
genus indet.				**Ga**?	Ga	**Ga**	**Ga**		
Theriosuchus						**Ga**	**Ga**		
Pholidosauridae				**Fa**?	Fa	**Fa**	**Fa**	Fa	**Fa**
genus indet.				**Ga**?	Ga			Ga	
Machimosaurus						**Ga**	**Ga**		
Teleorhinus									**Ga**
Crocodylidae									
genus indet.									
Deinosuchus									
Leidyosuchus									
Brachychampsa									
Albertochampsa									
Thoracosaurus									
Strangeruchampsa									
Allognathosuchus									
Theropoda	**O**	**O**	**O**	**O**	O	**O**	**O**	**O**	**O**
Dromaeosauridae	**F**	**F**	**F**	**F**	F	**F**	**F**	F	**F**
Utahraptor	**G**								
genus nov.									
genus indet.		G					G	G	G
Deinonychus			**G**	**G**	G	**G**?	**G**?		
Dromaeosaurus									
Saurornitholestes									
Elmisauridae									
Elmisaurus									
Chirostenotes									
Ornithomimidae			**F**	**F**			**F**?		
genus indet.			G	G			**G**?		
Ornithomimus									
Dromiceiomimus									
Struthiomimus									
Oviraptoridae			**F**	**F**					
Microvenator			**G**	**G**					
Caenagnathus									
Macrophalangia									

Turonian			Coniacian		Santonian		Campanian			Maastrichtian	
E	**M**	**L**	**E**	**L**	**E**	**L**	**E**	**M**	**L**	**E**	**L**
Ga	Ga	Ga	Ga	Ga	Ga	Ga	Ga	Ga			
									Ga	**Ga**	**Ga**
					Fa	**Fa**					
					Ga	**Ga**					
Fa	Fa	**Fa**									
Ga	Ga	**Ga**?									
		Fa	Fa	Fa	Fa	**Fa**	**Fa**	**Fa**	**Fa**	**Fa**	**Fa**
			Ga	Ga	Ga	Ga					
									Ga		
		Ga							**Ga**	**Ga**	**Ga**
		Ga					**Ga**	**Ga**	**Ga**	**Ga**	**Ga**
									Ga		
									Ga	**Ga**?	**Ga**
										Ga	
											Ga?
O	O	**O**	O	O	**O**	**O**	**O**	**O**	**O**	**O**	**O**
F	F	**F**	F	F	F	**F**?	**F**	**F**	**F**	**F**	**F**
	G										
G	G	G	G	G	G	G	G	G			
									G	**G**?	
									G	**G**	**G**
									F	F	**F**
									G		
									G	**G**	**G**
						F	F	F	**F**	F	**F**
						G	G	G			
									G	**G**	**G**
									G	**G**	
									G	**G**	**G**
									F	**F**	
									G		
									G		

	Barremian	Aptian		Albian			Cenomanian		
Taxon	**L**	**E**	**L**	**E**	**M**	**L**	**E**	**M**	**L**
genus indet.									
Therizinosauridae								**F**	
Nothronychus								**G**	
Erlickosaurus									
Troodontidae						**F**	**F**	F	**F**
Troodon						**G**?	**G**?	G	**G**?
genus indet.									
Allosauridae			**F**	**F**	F	**F**?			
Acrocanthosaurus			**G**	**G**					
genera nov.			**G**	**G**	G	G			
Tyrannosauridae						**F**	**F**	F	**F**
Alectrosaurus						**G**	**G**		
genus indet.							G	G	G
Aublysodon									
Daspletosaurus									
Albertosaurus									
Gorgosaurus									
Nanotyrannus									
Tyrannosaurus									
Family indet.	**F**	F	F?	F?	F	F?	F?	F	F?
Paronychodon						**G**?	**G**?	G	**G**?
Richardoestesia	**G**?	G	**G**?	**G**?	G	**G**?	**G**?	G	**G**?
"Nedcolbertia"	**G**								
Avisaurus									
Sauropoda	**O**	**O**	**O**	**O**	O	**O**?	**O**?		
Camarasauridae	**F**								
genus indet.	G								
Titanosauridae	**F**	**F**	**F**?	F	F	**F**?			
genus indet.	G	G	G	G	G	G			
Alamosaurus									
Brachiosauridae	**F**	F	**F**	**F**	F	**F**?	**F**?		
genus indet.	**G**	G							
Pleurocoelus (= Astrodon)			**G**	**G**	G	**G**?	**G**?		
Sonorosaurus			**G**	**G**					
Ornithopoda	**O**	**O**	**O**	**O**	O	**O**	**O**	O	**O**
Iquanodontidae	**F**	**F**	**F**	**F**	F	**F**?	**F**?		
Iquanodon	**G**								
Camptosaurus	**G**								
Tenontosaurus			**G**	**G**	G	**G**?	**G**?		
genera nov.	**G**	G					G		G
Hypsilophidontidae	**F**	**F**	**F**	**F**	F	**F**	**F**	F	**F**

Turonian			Coniacian		Santonian		Campanian			Maastrichtian	
E	**M**	**L**	**E**	**L**	**E**	**L**	**E**	**M**	**L**	**E**	**L**
										G	
									G?		
F	F	**F**	F	F	F	**F**	**F**	**F**	**F**	**F**	**F**
							G	**G**	**G**	**G**	**G**
G	G	G	G	G	G	G					
F	F	**F**?	F	F	**F**?	F	**F**	**F**	**F**	**F**	**F**
G	G										
		G?	G	G	**G**?	G	G	G	**G**	**G**	**G**
									G	**G**	
							G?	G	**G**	**G**	**G**?
									G		
											G
											G
F	F	F?							F	F	F
G	G	**G**?							**G**	G	**G**
G	**G**?								**G**		
									G?		
											O
											F
											G
O	O	**O**	O	O	**O**	**O**	**O**	**O**	**O**	**O**	**O**
	G										
F	F	**F**							**F**?	**F**	**F**

	Barremian	Aptian		Albian			Cenomanian		
Taxon	**L**	**E**	**L**	**E**	**M**	**L**	**E**	**M**	**L**
Hypsilophodon	**G**								
genera nov.			**G**						
Zephrosaurus			**G**	G	G	**G**?	**G**?		
genus indet.		**G**					G	G	G
Orodromeus									
Parkosaurus									
Thescelosaurus									
Bugenasaura									
Hadrosauridae						**F**	**F**	**F**	**F**
"Eolambia"							**G**		
Protohadros								**G**	
genus indet.						G			G
Claosaurus									
Maiasaura									
Brachylophosaurus									
Corythosaurus									
Gryposaurus									
Kritosaurus									
Lambeosaurus									
Prosaurolophus									
Brachyceratops									
Parasaurolophus									
Saurolophus									
Hypacrosaurus									
Anasazisaurus									
Naashoibitosaurus									
Edmontosaurus									
Anatotitan									
Fabrosauridae									
genus indet.									
Ankylosauria	**O**	**O**	**O**	**O**	O	**O**	**O**	**O**	**O**
Pinasuchus									
Polacanthidae	**F**								
Gastonia	**G**								
Polacanthus	**G**								
Ankylosauridae						**F**			
cf. Shamosaurus						**G**			
Cedarpelta						**G**			
Euoplocephalus									
Anodontosaurus									
Ankylosaurus									

Turonian			Coniacian		Santonian		Campanian			Maastrichtian	
E	**M**	**L**	**E**	**L**	**E**	**L**	**E**	**M**	**L**	**E**	**L**
G	G	G									
									G		
										G	**G**
									G	G	**G**
											G
F	**F**	**F**	F	F	**F**	**F**	**F**?	F	**F**	**F**	**F**
G	G	G	G	G	G			G			
						G	**G**				
									G		
									G		
									G		
						G	G	G	**G**		
									G		
									G		
									G		
									G	**G**	
									G	**G**	**G**
										G	
									G	**G**	
										G	
											G
									G?	**G**	**G**
											G
					F?	**F**?					
					G?	**G**?					
O	O	**O**	O	O	**O**	**O**	O	O	**O**	**O**	**O**
											G
	F?								**F**	**F**	**F**
									G	**G**	
										G	
											G

	Barremian	Aptian		Albian			Cenomanian		
Taxon	**L**	**E**	**L**	**E**	**M**	**L**	**E**	**M**	**L**
genus indet.									
Nodosauridae	**F**	**F**	**F**	**F**	F	**F**	**F**	**F**	**F**
Gastonia	**G**								
Hoplitosaurus	**G**								
Sauropelta			**G**	**G**	G	**G**?			
Silvisaurus						**G**			
Texasetes						**G**			
genus indet.		**G**			G			G	G
Pawpawsaurus						**G**			
Anamantarx						**G**	**G**		
Nodosaurus						**G**			
Stegopelta						**G**			
Hierosaurus									
Niobrarasaurus									
Panoplosaurus									
Edmontonia									
Pachycephalosauria						**O**	**O**		
family indet.						F	F		
genus indet.						G	G		
Pachycephalosauridae									
Stegoceras									
Gravitholus									
Ornatotholus									
Pachycephalosaurus									
Stygimoloch									
Ceratopsia						**O**	**O**	O	O
family indet.						F	F	F	F
genus indet.						G	G	G	G
Protoceratopsidae			*						
Leptoceratops									
Montanaceratops									
Ceratopsidae			**F**	**F**	F	F	**F**		
genus indet.			**G**	**G**	G	G	**G**		
Zuniceratops									
Pentaceratops									
Anchiceratops									
Centrosaurus									
Chasmosaurus									
Monoclonius									
Styracosaurus									
Avaceratops									

Turonian			Coniacian		Santonian		Campanian			Maastrichtian	
E	**M**	**L**	**E**	**L**	**E**	**L**	**E**	**M**	**L**	**E**	**L**
	G										
F	F	**F**	F	F	**F**	**F**	**F**?	F	**F**	**F**	**F**
G	G	G	G	G		G	G	G			
					G						
					G						
									G	**G**	
									G	**G**	**G**
	O								**O**	**O**	**O**
	F										
	G										
									F	**F**	**F**
									G	**G**	**G**
									G		
									G		
									G	G	**G**
											G
O	O	**O**					**O**	O	**O**	**O**	**O**
F		F					F	F			
G		G					G	G			
						F	F	F	**F**	**F**	**F**
									G?	G	**G**
						G?	G	G	**G**		
	F								**F**	**F**	**F**
	G										
									G	**G**	
									G	**G**	
									G		
									G		
									G	G	**G**
									G		
									G		

	Barremian	Aptian		Albian			Cenomanian		
Taxon	**L**	**E**	**L**	**E**	**M**	**L**	**E**	**M**	**L**
Einiosaurus									
Achelousaurus									
Brachyceratops									
Pachyrhinosaurus									
Arrhinoceratops									
Torosaurus									
Triceratops									
Mammalia									
Triconodonta			**O**	**O**	O	**O**	**O**		
Triconodontidae			**F**	**F**	F	**F**	**F**		
Astroconodon			**G**	**G**	G	**G**	**G**		
Alticonondon									
Gobiconodontidae			**F**	**F**					
Gobiconodon			**G**	**G**					
Multituberculata			**O**	**O**	O	**O**	**O**	O	**O**
Family indet.			F	F	F	F	F	F	F
Paracimexomys			**G**?	**G**?	G	**G**?	**G**?	G	**G**
genus nov. A						**G**	**G**		
genus nov. B						**G**	**G**		
genus nov. C						**G**	**G**		
Dakotamys									**G**
Bryceomys						**G**	**G**	G	G
Cimexomys									
Viridomys									
Essonodon									
Clemensodon									
Cimolodontidae									**F**
genus indet.									**G**
Cimolodon									
Cimolomyidae									
Cimolomys									
Meniscoessus									
Neoplagiaulacidae									
Mesodma									
Neoplagiaulax									
Parectypodus									
Ptilodontidae									
Kimbetohia									
Eucosmodontidae									
genus indet.									
Stygimys									

Turonian			Coniacian		Santonian		Campanian			Maastrichtian	
E	**M**	**L**	**E**	**L**	**E**	**L**	**E**	**M**	**L**	**E**	**L**
									G		
									G		
									G		
										G	
										G	
											G
											G
						O	**O**				
						F	**F**				
						G	**G**				
O	O	**O**	O	O	**O**	**O**	**O**	**O**	**O**	**O**	**O**
F	F	F	F	F	F	F	F	F	F	F	F
G	G	**G**	G	G	**G**	**G**	**G**	**G**	**G**	G	**G**
G	G	**G**	G	G	**G**	G	G	G	**G**?		
						G	**G**	G	**G**	G	**G**
						G	**G**				
									G?	G	**G**
											G
F	F	**F**	F	F	**F**	**F**	**F**	**F**	**F**	F	**F**
G	G	**G**	G	G							
					G	**G**	**G**	**G**	**G**	G	**G**
					F?	**F**?	**F**	**F**	**F**	F	**F**
					G?	**G**?	**G**	**G**	**G**	G	**G**
					G	**G**	**G**	**G**	**G**	**G**?	**G**
						F	**F**	**F**	**F**	**F**	**F**
						G	**G**	**G**	**G**	**G**	**G**
											G
											G
									F?		
									G?		
									F?	F	**F**
									G?		
										G	**G**

	Barremian	Aptian		Albian			Cenomanian		
Taxon	**L**	**E**	**L**	**E**	**M**	**L**	**E**	**M**	**L**
Symmetrodonta			**O**	**O**	O	**O**	**O**	O	**O**
Spalacotheriidae			**F**	**F**	F	**F**	**F**	F	**F**
Spalacotheroides			**G**	**G**					
genus indet.					G				
Spalacotheridium						**G**	**G**	G	G
Symmetrodontoides									
Spalacolestes						**G**	**G**		
Tribotheria			**O**	**O**	O	**O**	**O**	O	O
Aegialodontidae			**F**	**F**					
Kermackia			**G**	**G**					
Tritinitherium			**G**	**G**					
Picopsidae			**F**	**F**	F	**F**	**F**	F	F
Comanchea			**G**	**G**					
genus indet.					G	G	G	G	G
Picopsis									
Pappotheriidae			**F**	**F**	F	**F**	**F**		
Pappotherium			**G**	**G**					
Slaughteria			**G**	**G**					
genus indet.					G	G	G		
Deltatheroidea									
Deltatheroides									
Holoclemensiidae			**F**	**F**					
Holoclemensia			**G**	**G**					
Potamotelsidae									
Potamotelses									
Family indet.			F	F					
Montanolestes			**G**	**G**					
Zygiocuspis									
genus indet.									
Falepetrus									
Paleomolops									
Marsupialia			**O**?	**O**?	O	**O**?	**O**?	**O**	**O**
family indet.			F	F	F	F	F	F	F
Kokopellia			**G**	**G**					
genus indet.					G	G	G	G	
Anchistodelphys									
Aenigmadelphys									
Iugomortiferum									
Dakotadens									**G**
Iqualadelphis									
Ectocentrocristus									

Turonian			Coniacian		Santonian		Campanian			Maastrichtian	
E	**M**	**L**	**E**	**L**	**E**	**L**	**E**	**M**	**L**	**E**	**L**
O	O	**O**	O	O	**O**	**O**	**O**	O	**O**		
F	F	**F**	F	F	**F**	**F**	**F**	F	**F**		
G	G	**G**									
		G	G	G	**G**	**G**	**G**	G	**G**?		
O	O	**O**	O	O	O	**O**	**O**	O	**O**	O	**O**?
F	F	**F**	F	F	**F**	**F**	**F**				
G	G										
		G	G	G	**G**?	**G**	**G**				
									F	F	**F**?
									G	G	**G**?
						F	**F**				
						G	**G**				
							F	F	F		
							G				
								G			
									G		
									G		
O	**O**	**O**	O	**O**	**O**	**O**	**O**	**O**	**O**	**O**	**O**
F	F	F				F	F		F		
							G				
									G		
							G				
G	G	**G**									
						G	**G**				
									G		

	Barremian	Aptian		Albian			Cenomanian		
Taxon	**L**	**E**	**L**	**E**	**M**	**L**	**E**	**M**	**L**
Deltatheriididae									**F**
Bistius									
Alphadon									**G**
Protalphadon									**G**
Albertetherium									
Turgidodon									
Varalphadon									
Peradectidae									
Peradectes									
Stagodontidae									**F**?
Pariadens									**G**
genus indet.									
Eodelphis									
Boreodon									
Didelphodon									
Pediomyidae									
genus indet									
Pediomys									
Aquiladelphis									
Glasbiidae									
Glasbius									
Eutheria									
Insectivora									
Nyctitheriidae									
Paranyctoides									
Leptictidae									
Gypsonictops									
Palaeoryctidae									
Cimolestes									
Batodon									
Family indet.									
Alostera									
Order indet.									
Family uncertain									
Avitotherium									
Gallolestes									

Turonian			Coniacian		Santonian		Campanian			Maastrichtian	
E	**M**	**L**	**E**	**L**	**E**	**L**	**E**	**M**	**L**	**E**	**L**
F	F	**F**	F	**F**	**F**	**F**	**F**	**F**	**F**	**F**	**F**
									G		
G	G	**G**	G	**G**	**G**	**G**	**G**	**G**	**G**	**G**	**G**
G	G	**G**	G	G	G	G	**G**				
						G	**G**				
									G	G	**G**
						G	**G**				
									F?	F	**F**
									G?	G	G
F	F	**F**?	F	F	**F**	**F**	**F**	**F**	**F**	**F**	**F**
G	G	**G**?	G	G	G						
						G	**G**	G	**G**	G	**G**
									G		
										G	**G**
					F	**F**	**F**	F	**F**	F	**F**
					G	**G**	**G**				
						G?	**G**	G	**G**	G	**G**
						G	**G**	G	**G**		
											F
											G
						O	**O**	O	**O**	O	**O**
						F?	**F**?	F	**F**?		
						G	**G**	G	**G**		
									F	F	**F**
									G	G	**G**
									F	F	**F**
									G	G	**G**
											G
											F
											G
									O		
									F		
									G		
									G		

Chapter 9

Use of Event Beds and Sedimentary Cycles in High-Resolution Stratigraphic Correlation of Lithologically Repetitive Successions

The Upper Ordovician Kope Formation of Northern Kentucky and Southern Ohio

CARLTON E. BRETT, THOMAS J. ALGEO, and PATRICK I. MCLAUGHLIN

CARLTON E. BRETT, THOMAS J. ALGEO, and PATRICK I. MCLAUGHLIN • Department of Geology, University of Cincinnati, Cincinnati, Ohio 45221-0013.

P.J. Harries (ed.), *High-Resolution Approaches in Stratigraphic Paleontology.*

1. INTRODUCTION

Thick, lithologically repetitive successions often present a challenge to the stratigrapher attempting correlation of such units at a regional scale. The recurrence of just a few rock types generally inhibits correlation solely on the basis of lithologic criteria, and gamma ray, stable isotope, or magnetic susceptibility patterns commonly provide inadequate resolution or insufficiently distinctive signals for high-resolution correlation work. Yet reliable fine-scale correlations are required in order to address many problems in paleoecology, taphonomy, and process sedimentology (e.g., community gradients, proximality trends in tempestites). Under such conditions, establishing a high-resolution stratigraphic framework requires cm-scale analysis of individual sections to identify local marker horizons of distinctive paleontologic, ichnologic, taphonomic, or sedimentologic characteristic from which regional correlations can be built up. Critical to the success of this approach is the increasing recognition of the highly episodic nature of sediment accumulation, such that single geologic events (e.g., storms, turbidity currents, sediment slumps, ashfalls, and earthquake shocks; Seilacher, 1982; 1991; Clifton, 1988) commonly yield an event layer of regional extent.

The Kope Formation (Upper Ordovician, Cincinnatian Series) of the Tristate (Ohio-Kentucky-Indiana) region comprises just such a lithologically repetitive succession, consisting of approximately 70-73 m of finely interbedded shales and limestones containing no lithologically unique marker horizons. Although these strata have been the subject of innumerable paleontologic investigations (see Davis and Cuffey, 1998, for references), they have only recently become the focus of high-resolution stratigraphic study (e.g., Dattilo, 1996, 1998; Diekmeyer, 1998; Holland et al., 2000). This is due in part to a widely prevalent view that the Cincinnatian Series displays complex lateral facies relationships, and the plethora of regional names (i.e., the differences in Ohio, Kentucky and Indiana) conveys the impression of a rather disorderly mosaic of facies. Although depositional sequences have been delineated regionally by Holland

(1993, 1998) and Holland and Patzkowsky (1996), it would appear from past literature that meter-scale correlation between outcrops more than a few hundred meters apart is impossible. But is this really the case? We tested this idea through high-resolution stratigraphic analysis of the Kope Formation in a series of closely spaced, relatively new roadcuts along the AA Highway (Alexandria-to-Ashland; KY Rte. 9) in northern Kentucky (Potter *et al.*, 1991; Brett and Algeo, 2001a, b; Fig. 1).

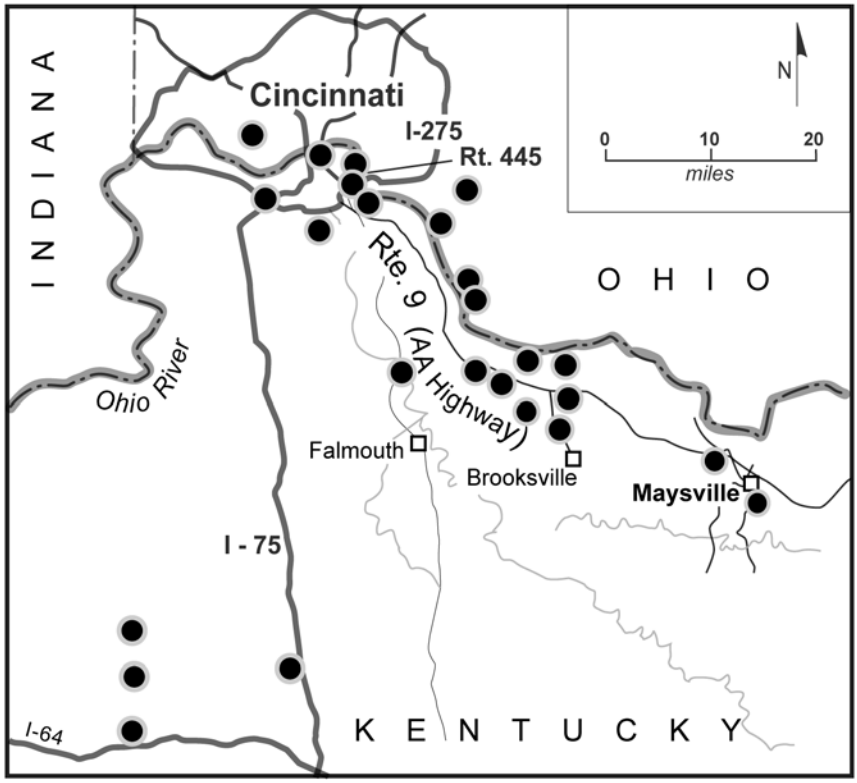

Figure 1. Location map of study locales in the Tristate area (Ohio-Kentucky-Indiana). Many good Kope Fm. exposures are found along the Ohio River and the AA Highway (KY Rte. 9) between Cincinnati and Maysville; somewhat sparser outcrops are present to the south in north-central Kentucky.

In this contribution, we will report on our studies of event beds and sedimentary cycles within the Kope Formation. We will: 1) describe types of event beds and meter- and decameter-scale cycles prevalent in the Kope; 2) demonstrate their utility for regional high-resolution stratigraphic correlation using the Fulton submember of the Kope as an example; 3) document our ability to establish a high-resolution (m-scale) correlation

framework for the entire Kope Formation along a ca. 80-km transect between Cincinnati, Ohio and Maysville, Kentucky (Fig. 1); and 4) propose a new subdivision of the Kope Formation into submembers based on this stratigraphic framework (see also Brett and Algeo, 2001b). While this contribution focuses on the methodology of high-resolution stratigraphic correlation, the broader aims of our work are to develop a process-based model for deposition of mixed carbonate-siliciclastic successions of the type represented by the Kope Formation.

2. REGIONAL GEOLOGIC SETTING

Upper Ordovician (Cincinnatian Series) strata in southern Ohio and northern Kentucky were deposited on the northern margin of the Lexington Platform, a carbonate-dominated feature of positive relief bounded by subsiding siliciclastic-dominated basins to the southeast (Taconic Foreland Basin) and northwest (Sebree Trough; Figs. 2-3; Rooney, 1966; Cressman, 1973; Keith, 1989; Mitchell and Bergström, 1991; Bergström and Mitchell, 1992). The Sebree Trough was a shallow depression that developed during the Shermanian (late Chatfieldian) Age and disappeared by Richmondian time, existing for only about 7-8 Ma (Wickstrom *et al.*, 1992; Kolata *et al.*, 2001). Its origin has been linked to subsidence associated with far-field stresses of the Taconic Orogen (Mitchell and Bergström, 1991; Ettensohn, 1992; Rast *et al.*, 1999; Ettensohn *et al.*, 2002), possibly compounded by upwelling of cool, corrosive deep waters along the trough axis (Cressman, 1973; Schwalb, 1980; Kolata *et al.*, 2001). On its eastern flank, an embayment known as the Point Pleasant Basin extended southeastward approximately along the line of the present Ohio River between Cincinnati, Ohio and Maysville, Kentucky (Fig. 3); formation of this embayment may have been controlled by subsidence along the Ironton-Vanceburg Fault (Ettensohn *et al.*, 2002). The boundary between the northern margin of the Lexington Platform and the Point Pleasant Basin (the area of this study) was a fairly uniform north-dipping ramp, as evidenced by a regionally consistent orientation of gutter casts in the Kope Formation (Jennette and Pryor, 1993, fig. 7).

The northern part of the Late Ordovician Lexington Platform was located in a subtropical climate zone, about 20-25º south of the paleoequator (Scotese, 1990; Ettensohn, 1992; Fig. 2). With an extensive area of warm tropical seas to the north, the region was frequently affected by tropical storms (Fig. 3), as reflected in the prevalence of carbonate tempestites in the Cincinnatian Series (Tobin and Pryor, 1981; Jennette and Pryor, 1993;

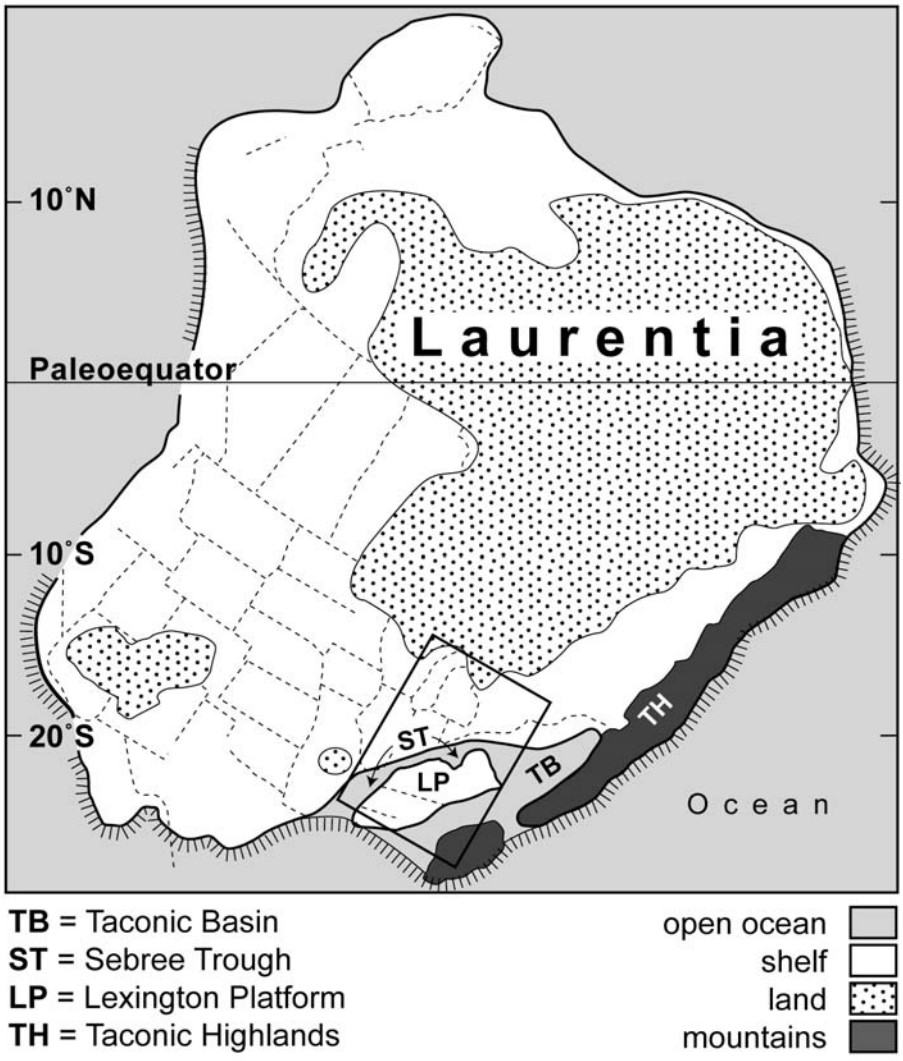

Figure 2. Paleogeography of Laurentia during the Late Ordovician. Note that the Lexington Platform is separated from cratonic shelf areas to the north and west by the Sebree Trough, and from the Taconic Highlands to the south and east by the Taconic Foreland Basin. Inset rectangle is area of Figure 3. Modified from Scotese (1990) and Blakey (2001).

Drummond and Sheets, 2001). At the same time, large quantities of siliciclastic sand, silt, and mud were derived from upland areas to the northeast and east as a consequence of the Taconic and Blountian orogenies (Dewey and Kidd, 1974; Shanmugam and Walker, 1980; 1984; Shanmugam and Lash, 1982; Rowley and Kidd, 1991; Lehmann *et al.*, 1994). During

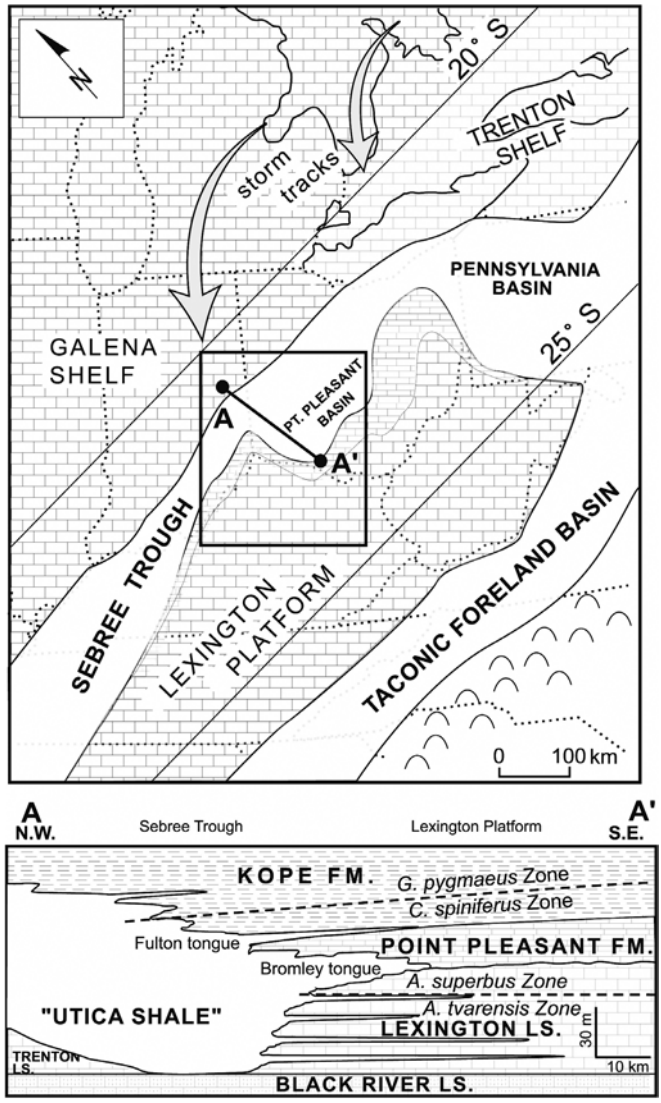

Figure 3. (top) Paleogeography of the greater Midwest region during the Late Ordovician. Note the Point Pleasant Basin, an embayment in the Lexington Platform, within the study area (inset rectangle, Figure 2). Tropical storms moved across the shallow Trenton/Galena shelves and intersected the northern margin of the Lexington Platform. Line A-A' gives location of cross-section (below). Regional cross-section, A-A', of Mohawkian- and Edenian-age strata from the Lexington Platform into the Sebree Trough. Approximate positions of graptolite (*C. spiniferus-G. pygmaeus*) and conodont (*A, tvarensis-A. superbus*) zonal boundaries are indicated. Note the change from platform carbonates into dark Utica-type shales in the trough; the Bromley and Fulton are dark-shale tongues that onlap the platform margin. Modified from Keith (1989), Mitchell and Bergström (1991), Ettensohn (1992), Jennette and Pryor (1993), and Ettensohn *et al.* (2002).

Chatfieldian and Rocklandian time, these sediments were trapped in the Taconic Foreland Basin as black shales (e.g., Utica and Antes shales) and turbiditic flysch (Martinsburg-Reedsville formations), but by late Mohawkian time sedimentation had outstripped subsidence, resulting in overfilling of the foreland basin and southwestward transport of siliciclastics along the axis of the Sebree Trough (Fig. 3).

3. STRATIGRAPHY

The Kope Formation in northern Kentucky is part of the stratotype of the North American Cincinnatian Provincial Series, which is subdivided into the Edenian, Maysvillian, and Richmondian stages (see Davis, 1992, and Davis and Cuffey, 1998, for earlier references). The Edenian-age Kope Formation is a thick (70-73 m) package of shale-dominated strata between the older (Shermanian-age) Point Pleasant and younger (Maysvillian-age) Fairview formations, both of which are limestone dominated (Fig. 4). The Kope consists predominantly of soft, pale to medium gray, readily weathering mudstones or shales interbedded with abundant thin (<5 cm) beds of light-gray laminated calcisiltite, and medium to thick (5 to 60 cm) beds of skeletal packstones and grainstones dominated by brachiopod, bryozoan, and crinoid debris. The formation was named by Weiss and Sweet (1964) for exposures at Kope Hollow, near Levanna in southern Ohio; the term was used in substitution for the biostratigraphically based Eden or Latonia Formation (see Diekmeyer, 1998, for review).

The Kope has been biostratigraphically subdivided to a limited degree. Bassler (1906) recognized three members in the "Eden Shales" based on bryozoan assemblages (Fig. 4): (a) the Economy Member, characterized by *Aspidopora newberryi* (ca. 16 m thick; originally reported as 28 m thick owing to inclusion of the upper beds of the underlying Point Pleasant Fm.); (b) the Southgate Member, typified by *Batostoma jamesi* (ca. 36-37 m thick); and (c) the McMicken Member, marked by *Dekayella ulrichi* (ca. 16-21 m thick). Mitchell and Bergström (1991) recognized two graptolite biozones within the Kope, a lower *Climacograptus spiniferus* zone and an upper *Geniculograptus typicalis-Geniculograptus pygmeaeus* zone (Fig. 3); the contact is within the Middle Kope, near the base of the Grand View submember of Brett and Algeo (2001b). Limited faunal turnover within the Kope has precluded development of finer biozonation schemes.

Lithostratigraphy, in some cases combined with biostratigraphic criteria, has provided the basis for a more detailed subdivision of the Kope. Early workers recognized several lithologically and faunally distinctive intervals:

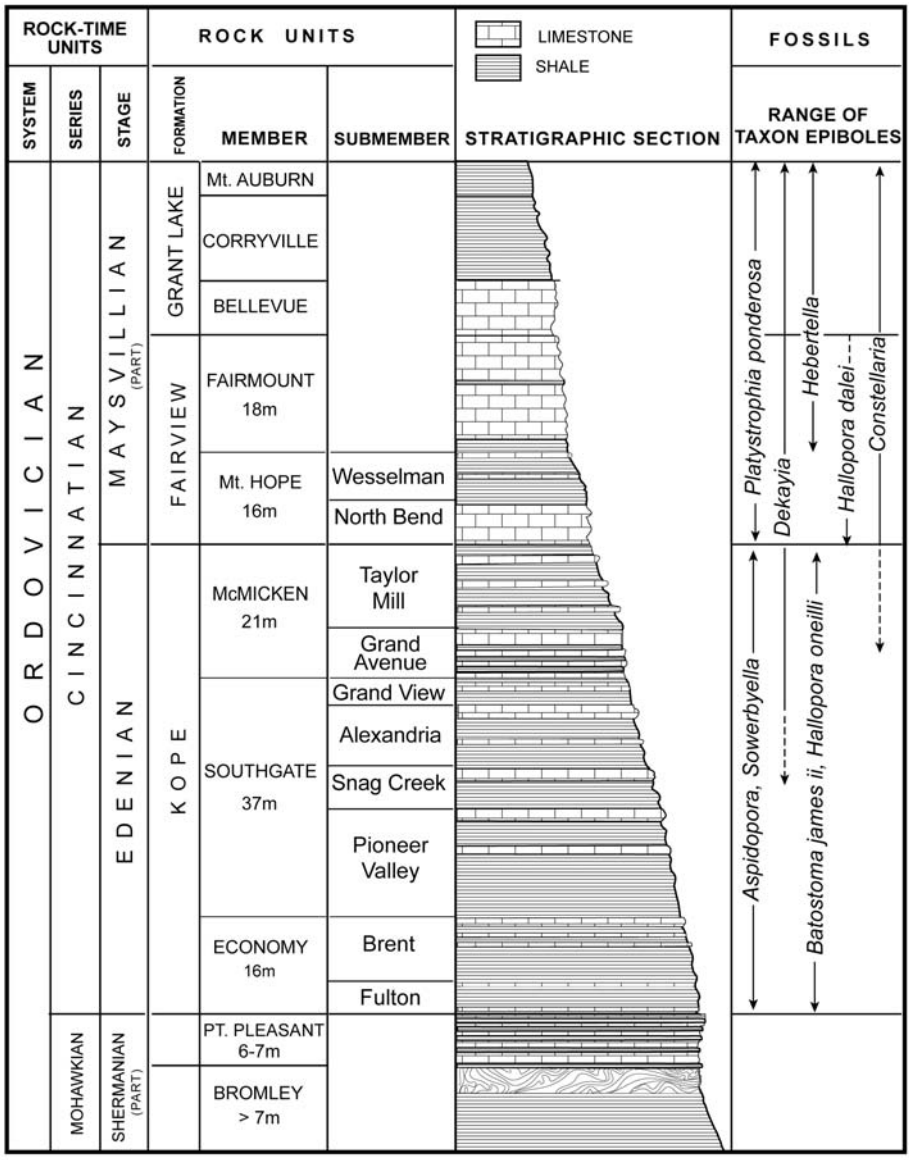

Figure 4. Stratigraphy of the Upper Ordovician in the Tristate area. Modified from Caster *et al.* (1955) with Kope Formation submembers introduced by Brett and Algeo (2001b). In this contribution, a high-resolution correlation framework will be established for the entire Kope Fm. in northern Kentucky, with a detailed example given for the Fulton submember.

(1) *Triarthrus*-bearing dark shale tongues in the basal 7 m of the Eden Shales (subsequently termed the lower Economy Member) were named the "Fulton beds" by Foerste (1905; Figs. 3-4); and (2) a 2.5- to 3-m-thick bundle of

limestones about 10 m below the top of the Kope Fm. was termed the "Grand Avenue Member" by Weiss and Sweet (1964; Fig. 4). More recently, Holland *et al.* (1997; 2001b) identified about 40 meter-scale cycles within a 60-m-thick composite section in northern Kentucky representing all but the lower 12 m of the Kope Formation. The most detailed subdivision of the Kope to date was proposed by Brett and Algeo (2001b), who combined Holland *et al.*'s section with the basal 12 m of the Kope from nearby Duck Creek to generate a complete reference section for the formation. Brett and Algeo retained the member names of Bassler (1906) and the cycle numbers of Holland *et al.* (1997) but proposed a further subdivision of the Kope into submembers (Fig. 4) based on thick, homogenous mudstone intervals ("Big Shales") that were shown to be traceable well beyond the Cincinnati area (see below).

4. EVENT-STRATIGRAPHIC MARKERS

Event beds, recording geologically instantaneous events usually at a local to regional scale, are extremely useful in establishing high-resolution correlations. In the Kope Formation, such stratigraphic marker horizons may be recognized on the basis of: (1) distinctive faunal assemblages, (2) taphonomic features, (3) trace fossils, (4) sedimentary structures, mostly associated with storm sedimentation, and (5) other characteristics. In this section, we describe some of the more important types of event beds that proved useful in high-resolution correlation of the Kope Formation.

4.1 Event Beds with Distinctive Faunal Assemblages

Limited faunal turnover in the Kope Formation does not allow much biostratigraphic zonation beyond the three members identified by Bassler (1906) on the basis of bryozoan assemblages. However, distinctive faunal assemblages are nonetheless useful for intraformational correlation of the Kope (Holland, 1997). These fall into two categories: (1) faunal epiboles marked by very high concentrations of otherwise rare fossil types, including both proliferation and incursion epiboles (*sensu* Brett and Baird, 1997), and (2) shell beds containing a ubiquitous fossil taxon that exhibits an unusual taphonomic characteristic or morphotype.

Among the most useful epiboles are *Triarthrus* beds, which are typically composed of dark brownish gray, laminated shale beds containing abundant intact or fragmental molts of the trilobite *T. becki* (Fig. 5A; Whiteley *et al.*, 2002). Owing to similarities to *Triarthrus* epiboles in the Mohawkian-age

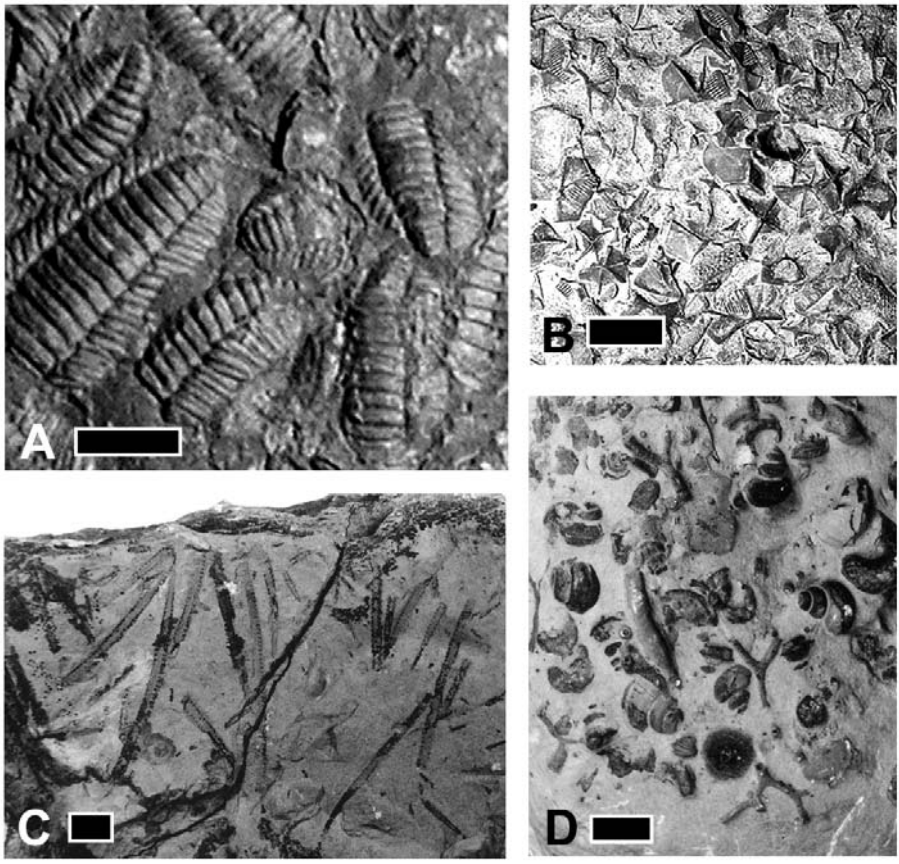

Figure 5. Faunal epibole event beds. (A) Cluster of articulated thoracopygidial molts of *Triarthrus becki*; from the Alexandria submember at Sycamore Creek, Cincinnati, Ohio. (B) Packstone containing large numbers of stellate plates of the rhombiferan *Cheirocystis fultonensis*; from Fulton submember, KY Rte. 8 roadcut, near Augusta, Kentucky. (C) Weakly aligned graptolites (*Geniculograptus* cf. *G. typicalis*) in calcareous shale; from Snag Creek submember, KY Rte. 17 ("White Castle site"), Covington, KY. (D) Gastropod-rich nodule in siliciclastic mudstone; from Alexandria submember, KY Rte. 9. All scale bars = 1 cm.

Bromley Shale of Ohio and Kentucky (Ulrich, 1888; Ulrich and Bassler, 1914) and to the Utica Shale of New York, these are thought to represent condensed beds formed during brief incursions of dysoxic water from the Sebree Trough onto the Lexington Platform. Some *Triarthrus* beds exhibit current-aligned columns of the cladid crinoid *Merocrinus curtus,* together with fully articulated *Triarthrus* exoskeletons; these appear to represent obrutionary deposits that terminated "incursion epiboles" (*sensu* Brett and Baird, 1997). In the Kope, *Triarthrus* beds are found in (1) cycles F2-F4 of

the Fulton submember, and (2) cycle H28 of the Alexandria submember.

There are several other types of epibole horizons of importance in the Kope Formation. First, an epibole of the rhombiferan cystoid *Cheirocystis fultonensis* (Fig. 5B) is found in cycle F1 of the Fulton submember, about 0.5 m above the base of the Kope; this bed has been found consistently over an area of ~500 km^2 in northern Kentucky and southern Ohio (Sumrall and Schumacher, 2002). Second, epiboles of current-aligned rhabdosomes of the graptolite *Geniculograptus typicalis* are found in calcareous siltstones in cycle H21 (Big Shale 3) of the Snag Creek submember (Fig. 5C). These beds may record incursions of graptolite swarms onto the Lexington Platform from the Sebree Trough, where graptolitic facies predominate, and represent "taphonomic epiboles" (*sensu* Brett and Baird, 1997). Third, concretionary siltstones with well-preserved molluscs, primarily gastropods, occur near the tops of major limestones at several levels in the Kope (Fig. 5D). Several of these are named beds, including the Newport Plaza hiatus bed (cycle H12, Pioneer Valley submember) and the Carrolton gastropod bed (cycle H25, Big Shale 4 of the Alexandria submember).

The second type of faunal event bed useful in correlation is that containing common taxa exhibiting distinctive morphotypes. An example is provided by the strophomenid brachiopod *Sowerbyella rugosa*. While fairly ubiquitous in the lower half of the Kope Fm, *S. rugosa* nearly disappears at the Pioneer Valley-Snag Creek submember contact (top of cycle H20), only to reappear in abundance in a few beds of cycles H25-H28, where it displays an unusually elongated hingeline (Fig. 6A). With this exception, higher beds in the Kope are nearly devoid of *S. rugosa*, despite little apparent change in facies; its abrupt disappearance thus also represents a bioevent of regional significance within the Kope Formation.

4.2 Taphonomic Event Bed

Certain stratigraphic intervals are characterized by unusual taphonomic features. One example involves perhaps the most ubiquitous fossil in the Kope, the orthid brachiopod *Onniella* (Fig. 6B). Most *Onniella* are preserved as white to yellowish shells, but two horizons within the Kope contain distinctively colored shells: 1) the "black *Onniella* beds" (cycle H25, Alexandria submember), and 2) the "red *Onniella* beds" (cycles H27-H30, Alexandria submember). These discolorations may have a diagenetic (i.e., burial) origin, but the horizons containing the distinctively colored shells are traceable for 80 km across the study area, making them useful for correlation purposes.

A second type of taphonomic event bed is obrutionary lagerstätten, which

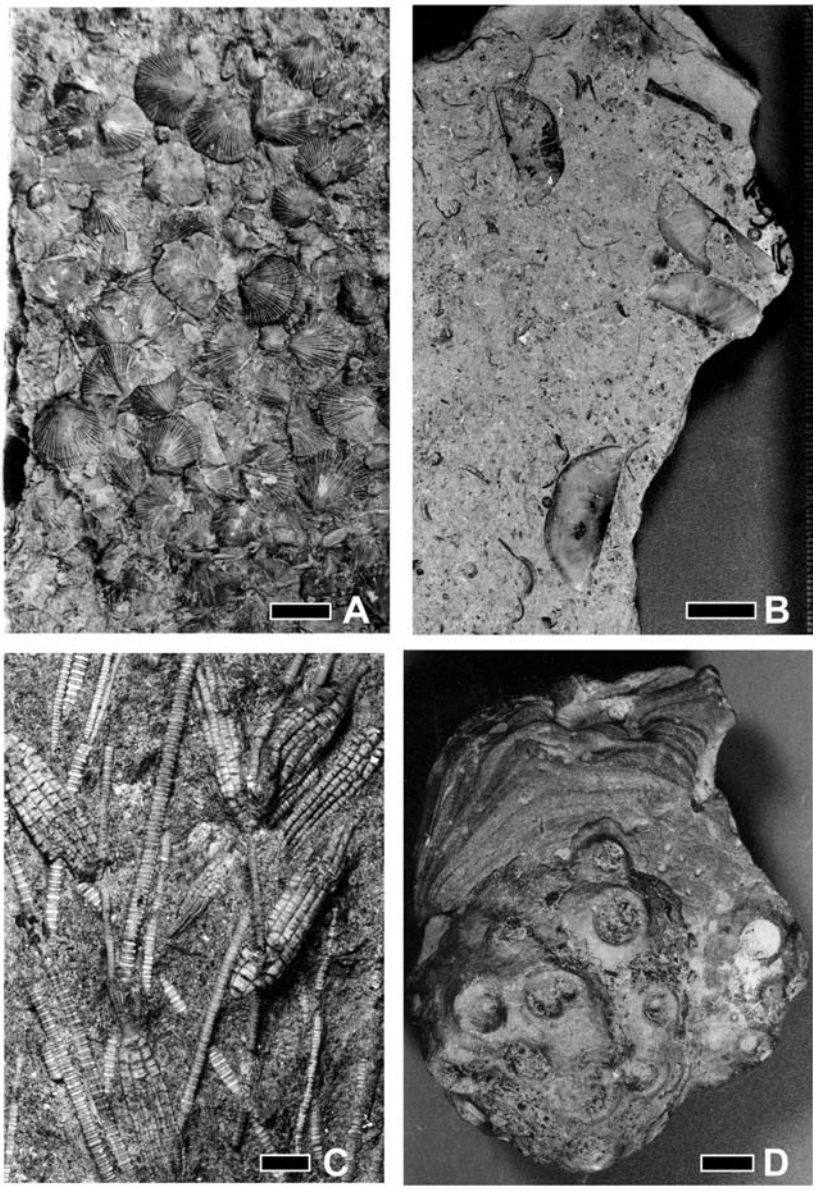

Figure 6. Other taphonomic event beds. (A) Wacke-packstone containing unusual *Sowerbyella rugosa* morphotype with an elongate hingeline, beds H23-H24 of Snag Creek submember; Rte. 6 roadcut northeast of Fosters, Kentucky. (B) Fossil grainstone with concentration of blackened *Onniella* forming an armored surface; from Alexandria submember, KY Rte. 9. (C) "Log jam" of oriented *Ectenocrinus* columns, note intact crowns; from Pioneer Valley submember, Alexandria, Kentucky). (D) Reworked siltstone concretion with encrusting bryozoans and crinoid holdfasts; from cycle H15 of Pioneer Valley submember, KY Rte. 17 ("White Castle site"), Covington, KY. All scale bars = 1 cm.

represent fossil assemblages that were rapidly buried, usually by smothering under a mud blanket. These deposits exhibit exceptional preservation of even fragile fossils (Brett and Seilacher, 1991; O'Brien *et al.*, 1994; Brett et al, 1997; Hughes and Cooper, 1999). The Kope contains several types of obrutionary deposit. "Butter shales" (any of several "Big Shales") are characterized by concentrations of enrolled or prone trilobites (Brandt, 1985; Schumacher and Shrake, 1997). Large numbers of articulated *Flexicalymene granulosa* are found in shales of cycle H16 of the Pioneer Valley submember (Hughes and Cooper, 1999), and this horizon has been traced for at least 10 km (Holland *et al.*, 2000). Abundant articulated specimens of the trilobites *Cryptolithus* and *Acidaspis* are found in cycle H25 (Big Shale 4) of the Alexandria submember, in a bed that has been traced approximately 20 km north-south through the Cincinnati area; at other levels in the Kope these trilobites are found only as disarticulated elements. Another type of lagerstätten is beds containing masses of parallel-oriented crinoid columns ("log jams"), probably formed through mass mortality associated with storm-generated currents. In some cases, crinoid columns at bed bases are oriented at approximately a right angle to those on the bed tops, indicating a change in current direction or a shift to wave-dominated flow. Some of these layers (e.g., an *Ectenocrinus* "log jam" in cycle H9, Big Shale 2 of the Pioneer Valley submember; Fig. 6C) have been found to persist over several outcrops (D. Schmidt, pers. comm.).

A third type of taphonomic marker horizon in the Kope is hardgrounds (Meyer, 1990). These commonly take the form of layers of nodules exhumed from underlying mudstones that were subsequently colonized by boring and encrusting organisms. Among the more commonly identifiable encrusters are crinoid holdfasts, edrioasterioids, and bryozoan protoecia (basal disks). For example, edrioasteroid holdfasts are prevalent in a bed of reworked and encrusted nodules in cycle H15 of the Pioneer Valley submember (Fig. 6D; Wilson, 1985). This bed is apparently traceable from near Big Bone Lick, Kentucky, northeast to the vicinity of Batavia, Ohio, a distance of about 50 km (S. Felton, pers. comm., 1999).

4.3 Trace-Fossil Event Bed

Certain beds contain an abundance of a characteristic, easily identifiable trace fossil that can be found at the same stratigraphic level in multiple, closely-spaced outcrops, reflecting occurrence of conditions particularly favorable to a certain behavior or its preservation. One such trace fossil is *Diplocraterion*, a distinctive U-shaped (or bell-shaped when larger) dwelling trace associated with hummocky cross-stratified siltstone beds (Fig. 7A). It

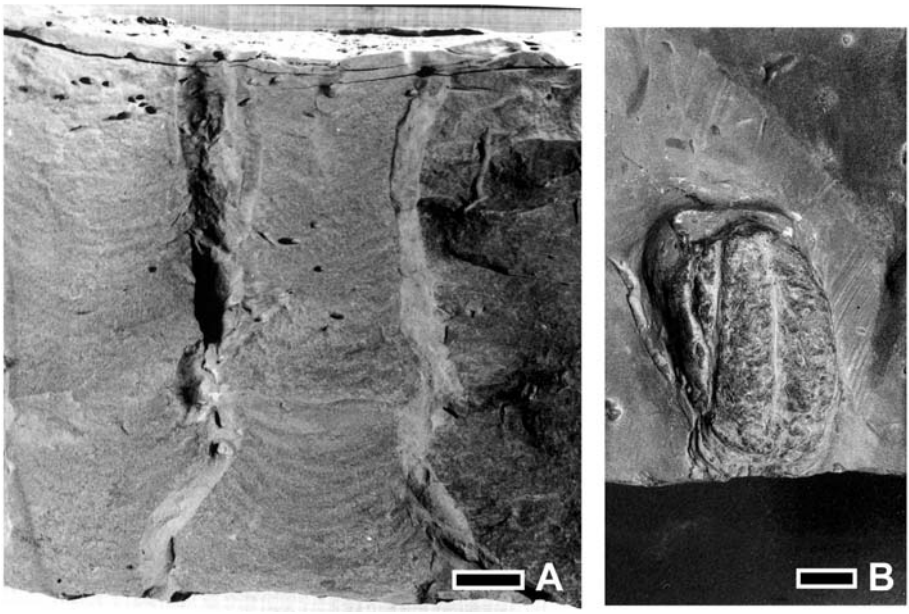

Figure 7. Ichnologic event beds. (A) Side view of laminated siltstone showing spreiten of the U-shaped burrow *Diplocraterion*; Taylor Mill submember, Mason/Reidlin Road, Taylor Mill, Kentucky. (B) The trilobite resting trace *Rusophycus*; from lower Kope Formation, KY Rte. 17 ("White Castle site"), Covington, KY. All scale bars = 1 cm.

is most common in cycles H38-H40 of the Taylor Mill submember but also occurs sporadically at other stratigraphic levels (e.g., H1, H24-H28). Evidently, the trace makers colonized storm silt layers in large numbers; thus, these beds represent a type of epibole or biotic event horizon (*sensu* Brett and Baird, 1997). A second trace fossil that occurs in locally correlatable horizons is *Rusophycus*, which is prevalent at several levels in the Kope (Fig. 7B). It was long considered to be a trilobite resting trace but has recently been reinterpreted on the basis of juxtaposition with other burrow types (e.g., *Planolites*) as a hunting trace (Brandt *et al.*, 1995). This suggests that concentrations of this trace represent enhanced opportunities for predation as, for example, after storm erosion has unroofed infaunal organisms such as worms in large numbers. Such behaviors are associated with specific events and, as such, commonly result in regionally correlatable marker horizons.

4.4 Storm-Event Beds

Beds containing unusual sedimentary structures have also proven to be useful in regional correlation. In the Kope Formation, storm sedimentation

processes are responsible for generating many of these features, including gutter casts, edgewise shell beds, megaripples, drag marks, among others (cf. Aigner, 1985; Nummedal, 1991; Brett, 1995). Other storm-related sedimentary structures have also proven to be traceable at a local to regional scale, including hummocky cross-stratification, graded bedding, intraformational scouring, and tool, flute, and prod marks, but as the general characteristics of these features are well known, they will not be discussed here.

Gutter casts are erosional features that form on the forward margin of storm-generated gradient currents, where fingers of sediment-laden water spiral downslope (Aigner, 1985); as a consequence, they form in parallel series at spacings of a few meters. Individual gutter casts are generally 5 to 10 cm in width and thickness, are asymmetric in cross-section, and have bases heavily ornamented by tool marks and flute casts parallel to the direction of current flow as well as by randomly oriented exhumed burrows (Fig. 8A). Jennette and Pryor (1993) documented a consistent orientation within a gutter cast bed in cycle H39 of the Taylor Mill submember (their cycle 20) at >20 localities across the greater Cincinnati area, demonstrating generation from a single flow down a north-northwesterly paleoslope. Gutter cast beds are found at more than a dozen horizons within the Kope, most abundantly within the Fulton, Brent, and Pioneer Valley submembers (see Algeo and Brett, 2001).

Distinctive coarse skeletal debris layers, such as beds of edgewise-oriented or shingled shells are also useful in correlation. In the Cincinnatian Series, beds of this type commonly contain edgewise *Rafinesquina* shells that, in some cases, are clustered at the bottoms of gutter casts (Fig. 8B). Three such horizons (called the "first, second, and third *Fracta* beds" by Des Jardins, 1933, and the "first, second, and third shingled beds" by Hyde, 1959) have been identified and traced regionally in the Maysvillian of the Tristate area (Dattilo, 1996). These particular event beds permitted identification of time lines cutting across facies contacts, as they are present in lithofacies mapped as Fairview Formation in Kentucky, while the second shingled *Rafinesquina* bed was used by Ford (1967) to define the base of his Miamitown Shale at the type locality in southwestern Ohio. The shingled brachiopod beds appear to represent major storms or, possibly, seismic events (A. Miller, pers. comm., 1998) that aggregated the flattish to gently concavo-convex brachiopod shells and oriented them in edgewise clusters over a large area of seafloor. In the Kope Formation, shingled shell beds are found mainly within coarse grainstone beds at the tops of decameter-scale cycles, for example in cycles H23-H24, H28, H35-H36, and H39.

Megaripples are generally found capping thick, fine- to medium-grained

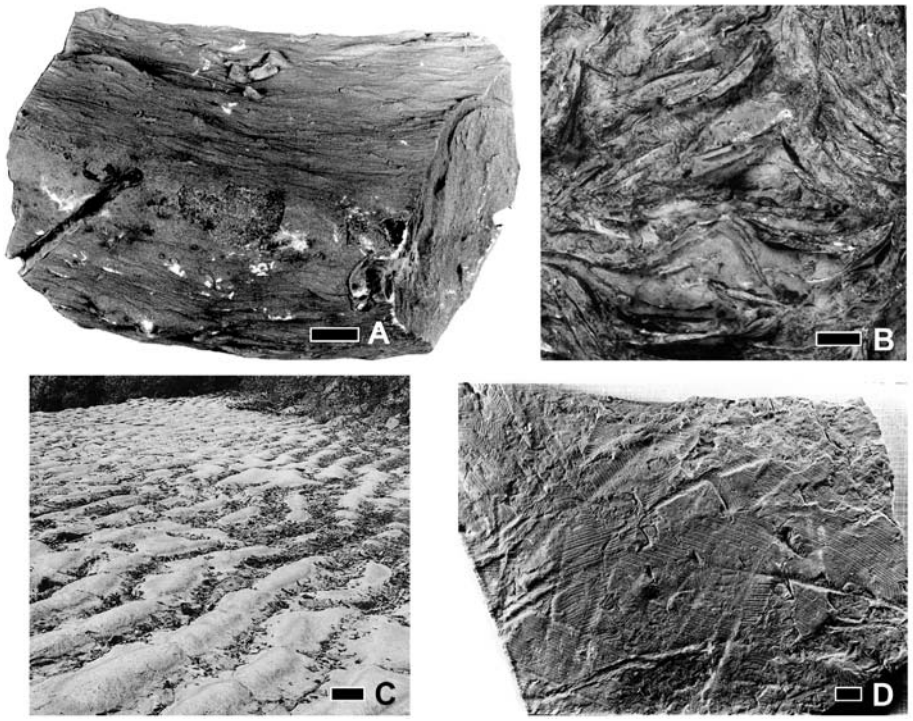

Figure 8. Tempestite event beds. (A) Bottom side of gutter; note nearly rectangular cross section to left and well-defined lineations formed as tool, prod, and flute marks; from base of Pioneer Valley submember, KY Rte. 445, Brent, Kentucky. (B) Top view of edgewise coquina of *Rafinesquina* shells; note multiple orientations of shell sets; from Grand Avenue submember, Mason/Reidlin Road, Taylor Mill, Kentucky. (C) Megaripples on top of medium-grained fossil grainstone; crest-to-crest wavelength ca. 1 m; from Taylor Mill submember, US Rte. 50 West, 4 mi east of North Bend, Ohio; photo from Jennette and Pryor (1993). (D) Cast of crinoid stem drag marks; note arcuate character of grooves, probably due to columnals being rotated around a pivot point on soft silt; Alexandria submember, KY Rte. 17 ("White Castle site"), Covington, Kentucky. Scale bars in A, B, D = 1 cm; bars in C = 25 cm.

grainstone beds at the tops of m-scale cycles. They are usually symmetrical with amplitudes from 2 to 10 cm and wavelengths from 40 to 100 cm (Fig.8C). Prominent examples are found at several dozen horizons within the Kope Formation, but they can sometimes be uniquely characterized on the basis of ripple amplitude, wavelength, and orientation. They are inferred to have formed during the final stage of storm sedimentation, as storm waves or combined flows molded the surface of grainstone deposits for the last time.

Crinoid drag or roll marks represent a special type of tool mark found at certain stratigraphic levels in the Kope. These occur as a series of parallel

scratches in an arcuate configuration (Fig. 8D), formed as oscillating currents dragged crinoid columns over the seafloor about a fixed pivot point. These crinoids may have been living or dead, attached to the seafloor by their holdfasts or detached and rotating about a calyx embedded in the sediment. These relatively rare features are generally developed on the tops of hummocky cross-stratified calcisiltite beds, suggesting that strong storm waves played a role in knocking over or detaching the columnals and in dragging them across the seafloor. The best-documented example is from cycle H29 of the Alexandria submember.

4.5 Other Event Beds

Finally, several enigmatic sedimentary structures are encountered in the Kope, which, despite uncertainty about their genesis, are nonetheless useful for correlation purposes. One such feature, millimeter "ripples," consists of sets of parallel, closely spaced ridges with flattened crests and troughs that are found mainly in calcisiltites (Fig. 9A). Jennette and Pryor (1993) observed that these "ripples" are penetrative, occurring in nested sets in all laminae of a given bed up to several centimeters in thickness, and that the

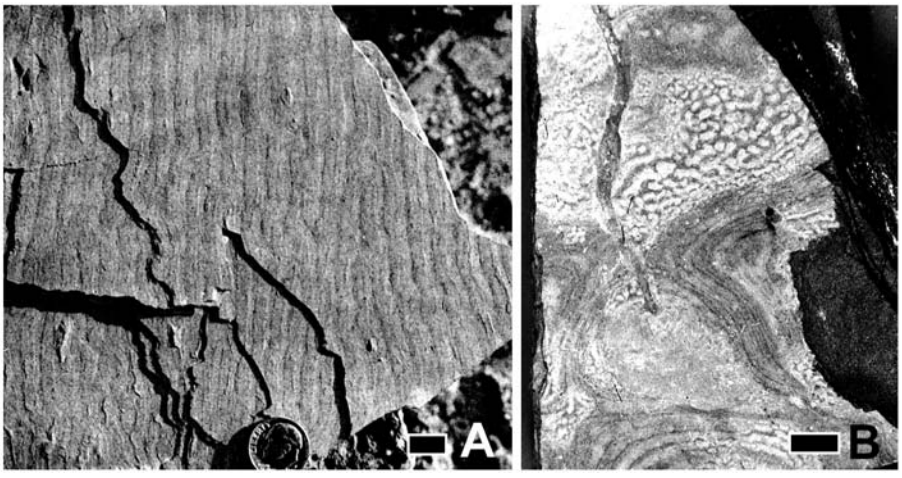

Figure 9. Other types of marker horizons. (A) Millimeter "ripples" in siltstone; note that the "ripples" occur in parallel, nested arrays on successive laminae of the siltstone (visible on broken edges); probably from Taylor Mill submember, Alexandria, Kentucky; photo from Jennette and Pryor (1993). (B) *Kinneyia*, an enigmatic feature that appears on the upper bedding surface of siltstones; note presence of *Kinneyia* only on crest of hummocky cross-strata and not in troughs; from Brent submember, KY Rte. 9 near Fosters, Kentucky. All scale bars = 1 cm.

"ripples" occasionally change spacing or amplitude upward within a bed in response to changes in grain size (Jennette and Pryor, 1993). Similar features have been attributed to wave rippling in very shallow water, but in the Cincinnatian Series these structures are found mainly in deeper-water facies, suggesting that another origin must be considered. Pflueger (1999) reviewed similar cases of "microripples" and concluded that they result from shearing within the sediment, i.e., below the sediment-water interface. Such shearing might, however, be induced by wave pounding of the seafloor or, perhaps, by seismic shocks. Millimeter "ripples" are found in a few beds (e.g., H40) and are commonly traceable over several outcrops.

A second enigmatic structure is runzel or wrinkle marks of a type known as *Kinneyia*, also found mainly in calcisiltites (Hughes and Hesselbo, 1997; Pflueger, 1999). Sometimes these consist of more-or-less regular patterns of shallow pits across the surface of a calcisiltite layer; in other cases, pitted areas abut areas of concentric but irregularly spaced laminae (e.g., Fig. 9B). Similar features have been interpreted as interference ripple marks, formed either subaqueously or subaerially (Klein, 1977; Allen, 1982; Seilacher, 1982; Hughes and Hesselbo, 1997). An alternative idea is formation in association with bacterial mats (Hagadorn and Bottjer, 1997). Pflueger (1999) presented experimental evidence that *Kinneyia* may form by the trapping of gas bubbles from organic decay, along the flattened upper surfaces of truncated ripples that were coated by microbial mats. Agitation of the sediment, again possibly seismically induced, may cause lateral migration of bubbles or vertical dewatering, creating the wrinkle marks. *Kinneyia* structures have been found in just a few beds of the Kope Formation (e.g., H1, H40).

5. CYCLE STRATIGRAPHY

The Kope Formation exhibits cyclicity at two readily apparent scales, a decameter (10-m) scale and a meter scale, both of which are useful in establishing a regional correlation framework (cf. Miller *et al.*, 1997; Holland *et al*., 2000). The 70 to 73 m thickness of the Kope Formation is divisible into eight decameter-scale cycles that are easily correlatable along the Cincinnati-Maysville axis of the present study. These decameter-scale cycles are equivalent to the eight informal submembers of the Kope recognized by Brett and Algeo (2001b). Each decameter-scale cycle consists of multiple smaller, "meter-scale" cycles that may be correlatable at a regional scale (Brett and Algeo, 2001a; Holland *et al.*, 2000, 2001b).

5.1 Meter-Scale Cycles

The Kope Formation is characterized by a large number (>40; Holland *et al.*, 1997) of small-scale (typically 0.5 m to 3.0 m thick) alternations of recessive weathering shales (mudstones) and ledge-forming, medium- to thick-bedded skeletal packstones and grainstones (Fig. 10). The mudstones vary from light to dark gray, may be massive, finely laminated, or micrograded, and contain fossil concentrations along some bedding planes (e.g., Fig. 5). This hemicycle may exhibit an upward increase in skeletal content and in the frequency of thin calcisiltite and shelly packstone interbeds (Jennette and Pryor, 1993; but see Webber, in press, for a discussion of more random patterns). The calcisiltite beds commonly exhibit hummocky cross stratification, laminated or burrow-mottled ichnofabric, and well-preserved trace fossils such as *Diplocraterion*, *Planolites*, and *Chondrites* (Fig. 7). The bases of these beds are sharp, preserve tool and prod marks as well as gutter casts, and, sometimes, have thin basal lags of fossil debris. The tops of calcisiltite beds are normally gradational into the overlying mudstones but occasionally preserve oscillation or interference ripple marks, or "runzel marks" (*Kinneyia*) of probable dewatering origin (Fig. 9B). Layers of small (5-10 cm) carbonate nodules commonly occur just below the bases of the overlying limestone hemicycle (Fig. 10). These appear to represent diagenetic underbeds, formed during periods of sediment starvation (see Aigner, 1985).

The limestone hemicycles consist of one or more sharp-based, subtabular skeletal packstone or grainstone beds, generally 5 to 30 cm in thickness and separated by thin shales or calcisiltites (Fig. 10). Internally, many of these beds are amalgamated, as shown by internal truncation surfaces, sharp changes in shell size, color, or taxonomic composition, or shaly partings (Barbour, 2001; Drummond and Sheets, 2001). Local relief on the bases of shell beds may be as much as 5 to 10 cm with irregular lumps or mounds of mudstone projecting upward into the overlying limestones. The bed bases may show gutter casts, tool marks, or other sole features indicative of scouring and loading (Fig. 8A), and small (mostly 1 to 5 cm) buff-colored clasts of reworked mudstone are commonly present as a basal lag. The skeletal debris tends to be dominated by brachiopod valves, bryozoan fragments, and crinoid ossicles, and these tend to be heavily broken and abraded and may exhibit a dark reddish to blackish discoloration (Fig. 6). The thickest beds tend to be grainstones, and these have a tendency to be dominated by crinoid ossicles and small twiggy bryozoans, whereas large ramose bryozoans are more abundant in thinner layers with a packstone texture. The tops of the limestone hemicycles may exhibit firm- or

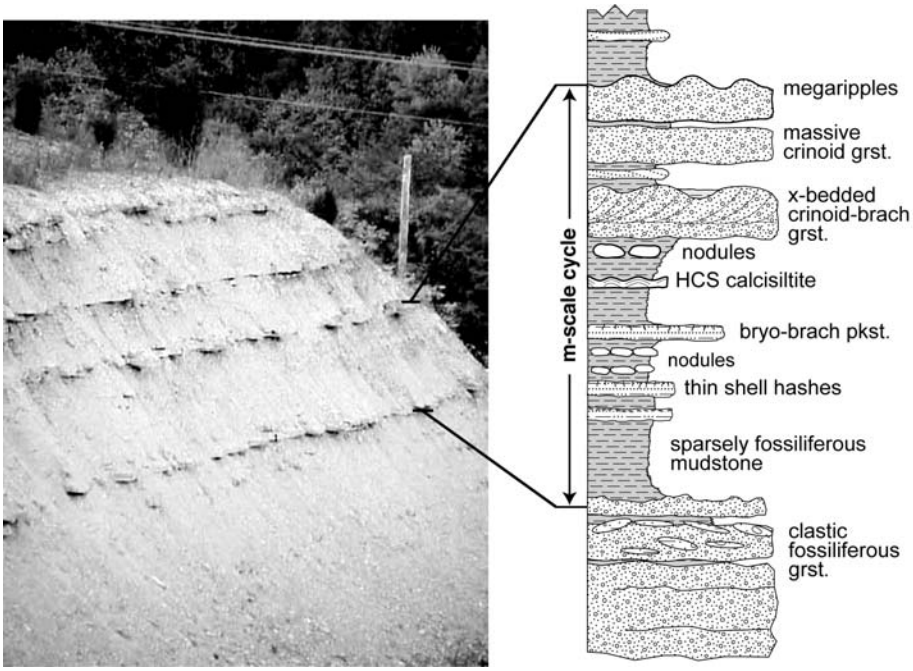

Figure 10. Meter-scale cycles; note sharp bases of limestone bed bundles, nodular underbeds, and rippled tops. Photo of Brent submember at KY Rte. 445 roadcut, Brent, Kentucky; approximately 9 m of section visible.

hardground development or molding into megaripples with a wavelength from 0.5 to 1.5 m (Fig. 8C).

The nature and interpretation of meter-scale cycles in the Kope Formation has long been debated (e.g., Tobin and Pryor, 1981), and current theory focuses on either eustatic fluctuations (Jennette and Pryor, 1993; Holland, 1997; Brett and Algeo, 2001a; Drummond and Sheets, 2001) or variable storm frequency or intensity (Holland *et al.*, 2001b). While it is not necessary to understand their genesis in order to use them for regional correlation purposes, their origin nevertheless has a bearing on lateral facies variation and degree of continuity. Relevant to the issue of their origin is that (1) Kope m-scale cycles are not simply random alternations of storm-influenced carbonate and background mud layers but, rather, represent an organized succession of lithologies, bedding patterns, and sedimentary structures and (2) shale hemicycles were deposited more rapidly than limestone hemicycles and, hence, are comparatively "time poor" (Brett and Algeo, 2001a). The mudstone intervals demonstrably do not represent gradual background accumulation but, rather, show evidence, such as micrograded beds and obrutionary (rapidly interred) fossil horizons, of accumulation as a series of episodic, rapid pulses. Conversely, most

limestone beds do not represent tempestites produced by single storm events but, rather, show evidence of long-term reworking of bioclasts and amalgamation of multiple storm-influenced layers (cf. Seilacher, 1985). Despite this, such beds frequently exhibit a signature (or "overprint") of the last event causing sediment mobilization. This includes basal lags of large, angular mudstone lithoclasts that would not withstand extensive reworking, as well as bedforms such as megaripples, hummocky cross-stratification, and millimeter ripples. Such beds are often laterally persistent and, in some cases, retain similar amalgamation patterns ("stratigraphic fingerprints") over distances of tens of kilometres. Such features suggest that m-scale cycles have an origin in extra-basinal mechanisms such as climate change or sea-level oscillation, rather than in intrinsic processes linked to the depositional system (Drummond and Sheets, 2001).

5.2 Decameter-Scale Cycles

Kope meter-scale cycles are organized into sets of thinning- and coarsening-upward units, yielding a readily apparent decameter-scale stacking pattern in outcrop (Fig. 11; Holland *et al.*, 1997). The mudstone hemicycles (termed "Big Shales" by Brett and Algeo, 2001a) are composed of medium to dark gray shale and range from 1 to 7 m in thickness, comprising about 1/3 to 1/2 of a decimeter-scale cycle. They generally contain a sparse, low-diversity fauna of diminutive brachiopods, bivalves, crinoids, and trilobites, well-preserved pelagic taxa (e.g., graptolites and nautiloids), pyritized burrows, and plastically deformed mollusc shells. These features are consistent with low-oxygen bottom-water conditions, representing stressed environmental conditions, and early sulfide formation and dissolution of aragonitic shells in the sulfate-reduction zone. Toward their tops, the mudstone-dominated intervals contain increasingly frequent, thinly laminated calcisiltites and fossil packstones, many of which are lenticular and laterally discontinuous ("precursor beds" of Brett, 1995, 1998). The greater abundance and diversity of fossil faunas in these beds suggests better-oxygenated bottom-water conditions. Just below the base of the overlying limestone hemicycle, a carbonate nodule layer is often encountered (Fig. 10).

The limestone hemicycle of a decameter-scale cycle consists of several m-scale cycles (typically four or five) and ranges from 2 to 10 m in thickness. Limestone beds typically comprise about 30-70% of this interval and are generally grouped in bundles, representing the amalgamated caps of individual m-scale cycles. The uppermost, capping limestone beds of decameter-scale cycles frequently exhibit irregularly hummocky, stained

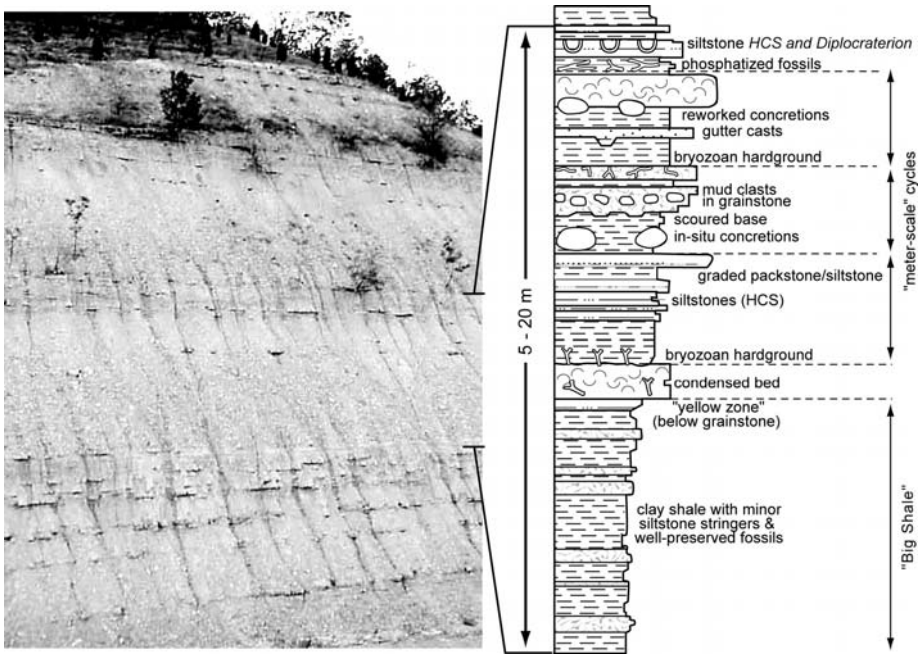

Figure 11. Decameter-scale cyclicity in Kope Formation. These larger stratal packages consist of a basal, 1- to 7-m-thick "Big Shale" overlain by a number of m-scale cycles; the latter tend to thin and become more amalgamated upward within each decameter-scale cycle. Seen here, from base to top, are the upper part of the Pioneer Valley submember, the complete Snag Creek and Alexandria submembers, and the lower part of the Grand View submember; from KY Rte. 445 roadcut, Brent, Kentucky. Diagram at right is an idealized decameter-scale cycle.

tops, darkened phosphatic- or pyrite-rich crusts as well as minor borings and encrusting organisms. Taphonomic features suggest that fossil debris in many beds has been subject to longer term reworking, marked by corroded fossil debris, hardgrounds, phosphatic staining, and other indications of an omission surface. The transition to an overlying "Big Shale" is typified by a thin bundle (0.1 to 0.5 m) of calcisiltites and/or packstones that shows excellent preservation of fossils, especially ramose bryozoans or, more rarely, a mollusc-dominated fauna.

As event beds are the building blocks of meter-scale cycles, the latter are the building blocks of decameter-scale cycles. Individual m-scale cycles tend to thin and become more carbonate-rich upward within decameter-scale cycles, so that the last few m-scale cycles may be represented by several closely stacked limestone bed bundles. The basal "Big Shales," ranging up to 7 m in thickness, may represent single, unusually thick and shaly m-scale cycles or, conversely, stacking of several thinner m-scale cycles lacking well-developed carbonate caps. In either case, the lower part of these "Big

Shales" clearly differs from the shale hemicycles of m-scale cycles toward the top of decameter-scale units in showing evidence of more dysoxic bottom-water conditions (e.g., impoverished biota, abundant pyrite) and containing fewer calcisiltite/packstone interbeds. These features suggest that the basal portions of "Big Shales" represent maximum highstand conditions. This is consistent with an analysis of Kope faunal patterns by Holland *et al.* (2001a), who inferred abrupt shifts toward deeper water biofacies and gradual transitions back toward shallower water facies within their "20 meter cycles."

6. EXAMPLE OF DETAILED CORRELATION: FULTON SUBMEMBER OF THE KOPE FORMATION

To better illustrate the lateral continuity of cycles and component event beds in the Kope Formation, we will elaborate on the internal stratigraphy of one decameter-scale cycle, the Fulton submember, representing the basal 6 to 7 m of the Kope. The Fulton is bounded below by the limestone-dominated Point Pleasant Formation and above by Big Shale #2 (base of Brent submember) of the Kope; for this reason, it is easily identifiable throughout the study area. The Fulton displays excellent development of meter-scale cyclicity (four cycles averaging 1.5 m in thickness) and contains a number of highly distinctive, widely traceable event beds, providing the basis for high-resolution correlation at a regional scale (Fig. 12). On the basis of its composition and internal structure, each Fulton cycle is readily correlatable along the 80-km-long Cincinnati-Maysville axis.

6.1 Cycle F1

The first Fulton cycle starts in the upper half meter of the Point Pleasant Fm with a stack of compact *Merocrinus*-bearing skeletal grainstones including the uppermost "Sugar Creek bed." This distinctive bed is identifiable across the study area as it contains large platters as well as having a heavily mineralized upper surface. Near Cincinnati, the "Sugar Creek bed" is overlain by approximately 40 to 50 cm of pale-gray-to-green, yellow weathering, sticky clay shale containing only thin lamina of the otherwise rare brachiopods *Onniella emacerata* and *Leptaena*. These basal shales of the Fulton submember are overlain by a 20-cm interval containing two or three pale-gray concretion layers capped by a two-part concretionary packstone to calcisiltite. This bed contains dalmanellid brachiopods and

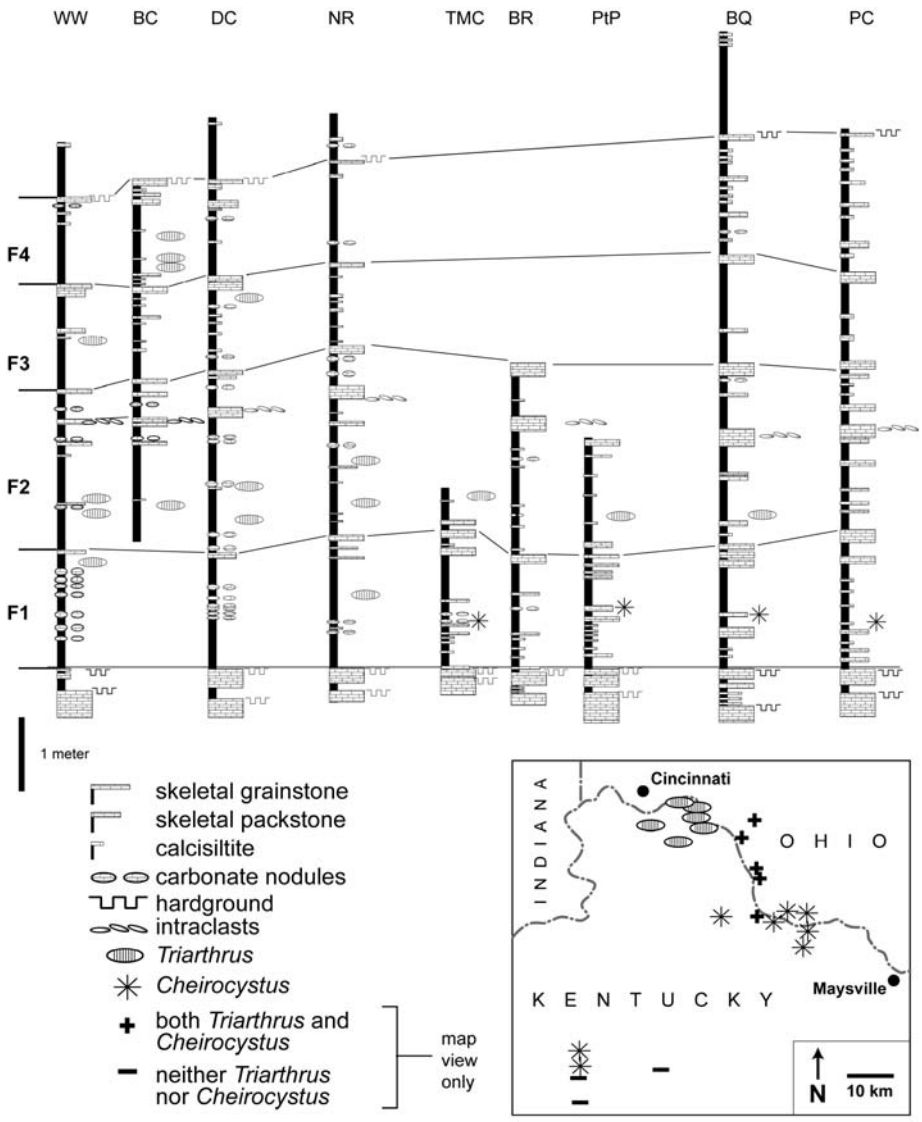

Figure 12. Detailed cross-section of the Fulton submember along the Cincinnati, Ohio-Maysville, Kentucky axis. The Fulton submember consists of four m-scale cycles, here numbered F1-F4 (the basal Kope is not exposed at KY Rte. 445 and, hence, was not numbered by Holland *et al.* (1997)). The distribution of *Triarthrus* and *Cheirocystis* beds in the Fulton submember is shown in the map inset at lower right.

crinoid fragments near Cincinnati, but passes laterally into a thin packstone containing abundant plates and columnals of the rhombiferan cystoid *Cheirocystis fultonensis* (Figure 5B), plus abundant brachiopods *Onniella,* and *Zygospira,* the trilobite *Flexicalymene*, and rare *Aspidopora* bryozoans.

This thin bed has a very distinctive taphonomic signature and can be traced over an area of at least 500 km in northern Kentucky (Fig. 12). It is consistently 50 to 60 cm above the base of the Kope.

6.2 Cycle F2

Packstones containing abundant fragmentary *Onniella*, *Cryptolithus*, and columnals of *Merocrinus* form the base of this cycle in the Cincinnati area. Southeastward, these muddy packstones grade into thicker (20-cm) *Merocrinus*-rich grainstones. Near Cincinnati, the upper grainstone is overlain by two concretionary, rusty weathering calcisiltites that mark the base of the overlying shaly interval. These are interbedded with pale olive gray to dark brownish gray shales, which contain lenses of packstone or fossiliferous mudstone with *Merocrinus* columns. Articulated specimens of the trilobite *Triarthrus* found within this interval are widespread and may be current aligned. Complete *Onniella* and a small number of articulated *Isotelus* and *Cryptolithus* also occur at this level. These are followed by over 1 m of nearly pure claystones that vary in color from pale olive gray to dark brownish gray. Particularly notable is a zone from 12 to 20 cm thick of dark brownish gray, slightly platy shale containing abundant cranidia of *Triarthrus* plus the small inarticulate brachiopod *Mesobolus*. A thin *Merocrinus*-bearing calcareous siltstone may occur within this band. This is the thickest dark brownish gray unit and *Triarthrus* have been found rarely in this interval as far to the southeast as Holst Creek (Fig. 12). Locally, at "Waterworks Creek," near Fort Thomas, Kentucky, the lower portion of the dark brownish gray shale fills a gutter-like scour cut some 10 cm into the underlying olive mudstone. Near Cincinnati the *Triarthrus* beds pass upward into about 50-80 cm of variegated olive to dark gray sparsely fossiliferous shales. However, tracing this interval to the south, thin calcisiltites give way to more prominent skeletal wackestones and packstones. This interval is capped by a weakly developed crinoidal pack- to grainstone, which breaks locally into several thin packstones and varies from 0 to 10 cm; locally it is represented by a series of starved ripples. A distinctive feature of this bed near Cincinnati is the presence of ellipsoidal concretions at its base; where the bed is missing in starved ripple troughs, the concretions are still present.

6.3 Cycle F3

The base of this cycle is a 60- to 80-cm-thick interval composed of two *Merocrinus*-bearing grainstones. The lower one is a thick, megarippled, fine-grained, crinoid-brachiopod grainstone and is typically the thickest and

most prominent grainstone in the Fulton. It contains abundant, 5- to 12-cm diameter nodules, some of which are bored and encrusted by crinoid holdfasts. Large columnals and articulated stems of *Merocrinus* are also abundant in this bed. At Cincinnati, this prominent bed is overlain by ca. 30 cm of gray shale containing one to two thin concretion horizons, which again give way to calcisiltites and thin skeletal packstones to the south. This shaly interval is in turn overlain by a prominent skeletal grainstone containing abundant nautiloids, *Cryptolithus* trilobites, and brachiopods. Approximately 1.0-1.5 m of olive gray shale, typically carrying two to three hummocky cross-stratified calcisiltites, forms the shaly interval of cycle F3. The middle calcisiltite, commonly 60-70 cm above the base, locally displays large gutter and pot casts. A thin seam of dark shale approximately 15 cm below the top of this interval contains rare *Triarthrus* remains. A cluster of articulated specimens of the normally very rare trilobite *Achatella* was found in this shale interval in Lawrence Creek near Maysville, Kentucky.

6.4 Cycle F4

This cycle begins with a sharp-based grainstone, which in some cases is an amalgam of at least two closely stacked beds up to 15 cm thick. The shale hemicycle contains gray shale with a few thin calcisiltite beds and rare *Triarthrus* near Cincinnati. To the south calcisiltite beds grade into thin skeletal packstones containing *Zygospira*, gastropod molds, an abundance of *Flexicalymene* fragments and rare *Achatella* trilobite fragments. In the area of Holst Creek to Brooksville, Kentucky, a spectacular gutter-cast-bearing, brownish siltstone bed occurs about 20 cm above the base of the shale hemicycle. Cycle F4 is overlain by a pyrite- and conodont-rich grainstone containing fine-sand-sized steinkerns, gastropod internal molds, and burrow tubes termed the Duck Creek bed. This bed exhibits a considerable abundance of conodonts (e.g., *Phragmodus undatus*, *Plectodina furcata*) at the Clays Ferry type section in central Kentucky (Sweet and Bergström, 1984) and has been used to define the contact between the Fulton and Brent submembers of the Kope.

7. REGIONAL HIGH-RESOLUTION CORRELATION OF THE KOPE FORMATION

7.1 Procedure

Using the same approach applied to the Fulton submember (see above),

we studied more than 60 sections in northern Kentucky representing all submembers of the Kope Formation (Algeo and Brett, 2001). Each section was measured and described at a centimeter scale, noting lithology, fossil content, taphonomic features, sedimentary structures, bedding characteristics, and other salient features. Certain event beds were collected and slabbed for detailed petrographic examination. Measured sections were then compared, and field sections revisited as needed, in order to verify correlations.

In general, we established regional correlations proceeding from larger-scale features (e.g., the "Big Shales" and decameter-scale cycles) to smaller-scale features (e.g., m-scale cycles and event beds; Figs. 13-14). Each decameter-scale cycle (or submember of the Kope) exhibits a highly distinctive succession of beds, based on lithology, bed thickness, and spacing, that provides a "bar code" unique to that stratigraphic interval. These characteristic bedding patterns were generally identifiable in a succession of outcrops, changing only gradually if at all across the 80-km-wide study area. Although individual beds are sometimes visibly discontinuous at an outcrop scale, we observed that these beds were commonly present at the same stratigraphic level in the next outcrop a few kilometers distant. From this, we concluded that such apparently discontinuous beds are generally persistent as a series of lenses over a broader area.

Other researchers have used different approaches for regional correlation of the Kope Formation. Correlations based on generalized stratigraphic trends in lithology are possible where stratigraphic sections are converted to running averages of percent shale. This procedure, which has a ca. 1-meter scale of resolution, was applied to the Fairview Formation and Miamitown Shale by Dattilo (1996, 1998) and to the Kope Formation by Webber (2001). Another approach is statistical cross-correlation of shale-limestone "bar codes" for pairs of stratigraphic sections to establish the best match. Holland *et al.* (2000) employed this approach to correlate the Kope in the White Castle section of Hughes and Cooper (1999) with the KY Rte. 445 reference section of Holland *et al.* (1997). Both of these approaches have yielded reasonable results, but we think that neither is superior to our method of comparing event beds and cycles in high-resolution (cm-scale) measured sections.

7.2 Implications

High-resolution regional correlation of the Southgate and McMicken members, representing the middle and upper Kope, respectively,

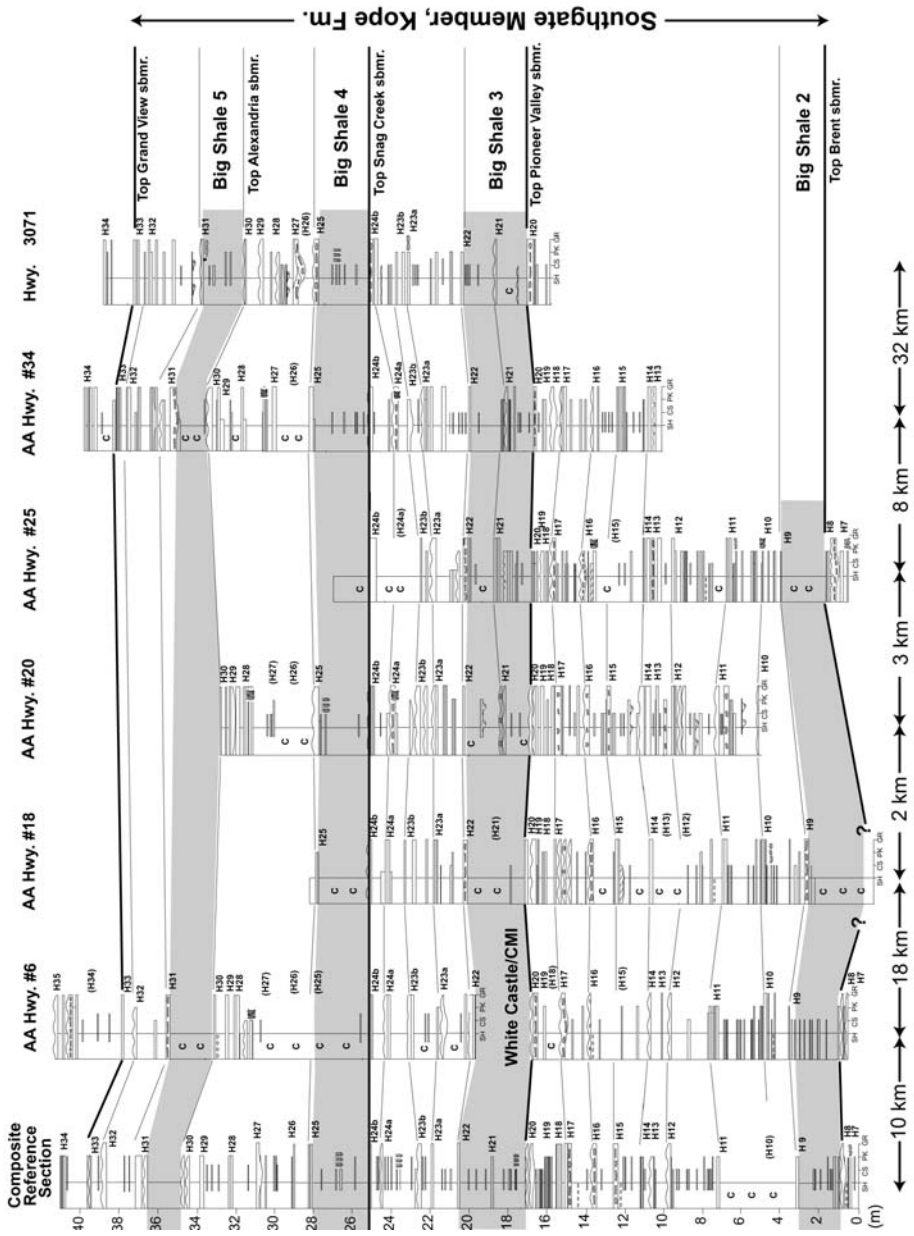

Figure 13. Generalized correlated cross-section of the Southgate Member (Pioneer Valley, Snag Creek, Alexandria, and Grand View submembers) of the Kope Fm. along the Cincinnati, Ohio-Maysville, Kentucky axis. Lithologic key: SH = shale, CS = calcisiltite, PK packstone, and GR = grainstone; C = covered. Big Shales 2-5 are shaded. Cycle numbers are those of Holland *et al.* (1997), prefixed with an "H" to distinguish them from cycles of the Fulton submember of the Kope and those of other Edenian-Maysvillian formations in the Tristate area.

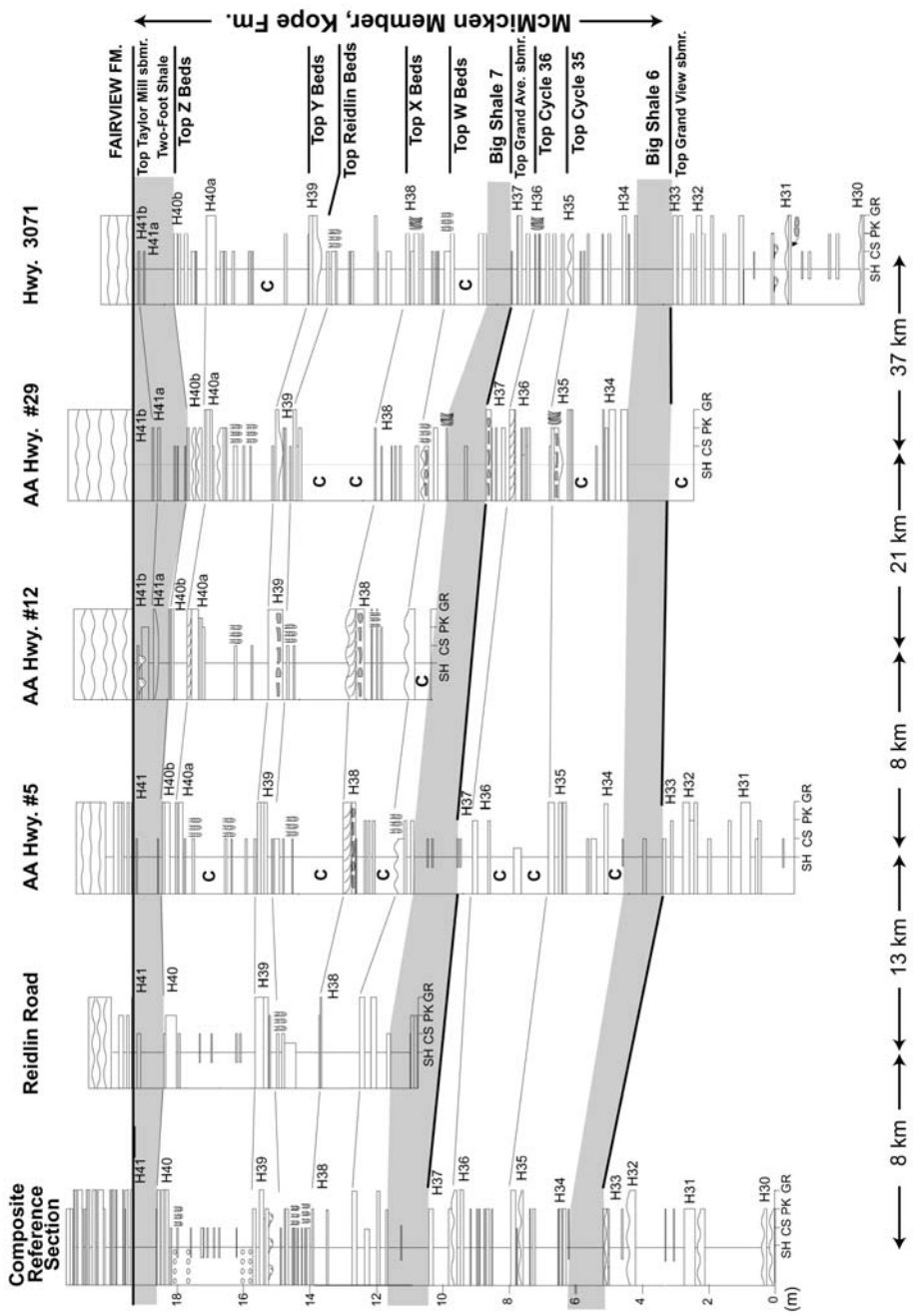

Figure 14. Generalized correlated cross-section of the McMicken Member (Grand Avenue and Taylor Mill submembers) of the Kope Fm. along the Cincinnati, Ohio-Maysville, Kentucky axis. See Figure 13 caption for more information.

demonstrates the regional continuity of all decameter-scale and most m-scale stratal packages (Figs. 13-14). Almost all cycle-capping limestone beds are continuous across the study area (possibly excepting H26), in many instances exhibiting similar thicknesses and sedimentary structures from Cincinnati to Maysville, a distance of 80 km. In some cases, even single event beds (e.g., distinctive calcisiltites containing gutter casts or *Diplocraterion* such as those in cycles H38-H40) can be traced over this distance. Furthermore, changes in thickness and lithofacies across the study area are small. The Kope Formation exhibits no discernible change in thickness regionally, a slight thinning of the middle Kope being compensated by a slight increase in thickness of the upper Kope at Maysville. Facies within any single cycle are also quite similar regionally, although capping limestones tend to be slightly thicker and calcisiltites slightly more numerous at Maysville than at Cincinnati (Figs. 13-14). Thus, the empirical evidence suggests that the internal stratigraphy of the Cincinnatian Series hews more closely to a "layer-cake" model than to the local facies mosaic that has been depicted in recent publications (e.g., Davis and Cuffey, 1998).

The strong lateral correlatability of meter-scale and finer stratal packages and the uniformity of thicknesses and lithofacies over the 80-km-long Cincinnati-Maysville transect are somewhat surprising in as much as preliminary work on a north-south Cincinnati-Lexington transect has revealed more pronounced lateral variation within the Kope. These observations strongly suggest that the former transect is nearly parallel to regional depositional strike, possibly with a slight increase in proximality in the direction of Maysville. Other evidence for an increase in depositional proximality toward Maysville includes a faunal gradient analysis (Webber, in press) as well as lateral facies relations in the overlying Fairview and Grant Lake formations (Schumacher, 1992, 1998). These observations provide empirical support for Wickstrom *et al.*'s (1992) reconstruction of an east-southeast-oriented embayment in the Sebree Trough, running parallel to the axis of the Ohio River between Cincinnati and Maysville (Fig. 3).

A further implication of the regional fine-scale correlation of the Kope demonstrated here is that the processes responsible for producing decameter- and m-scale patterns of cyclicity operated over wide areas of the Lexington Platform, at least parallel to and, to some degree, across depositional strike. This result strongly supports the inference that patterns of stratigraphic accumulation in the Cincinnati Series were controlled by allocyclic processes (e.g., eustatic or climatic changes) as opposed to strictly local autogenic phenomena.

8. SUMMARY

A regional high-resolution correlation framework has been developed for the Upper Ordovician (Edenian) Kope Formation on the basis of event beds and sedimentary cyclicity. The correlation framework comprises eight decameter-scale and forty-one meter-scale cycles along a ca. 80-km transect from Cincinnati to Maysville, Kentucky. In addition, many individual event beds containing faunal epiboles or distinctive ichnofossils, taphonomic features, or sedimentary structures can be traced at a local to regional scale. Thus, the recent paradigm of the Cincinnatian Series as a complex facies mosaic is incorrect. Rather, the Kope Formation displays a very predictable, layer-cake-like stratigraphy, at least parallel to depositional strike. The wide correlatability of small-scale stratal packages suggests ultimate control of Kope sedimentation by allocyclic forcing mechanisms, possibly glacio-eustasy. This study demonstrates that accurate high-resolution regional correlation of thick, lithologically repetitive successions is possible given sufficiently detailed stratigraphic observations.

ACKNOWLEDGMENTS

We thank Peter Harries, Steve Holland, Mark Patzkowsky, and Colin Sumrall for reviews of an earlier draft of this paper. Arnie Miller, Dave Meyer and Steve Felton all provided important insights and discussion on Kope stratigraphy, paleoecology, and depositional environments. Evelyn Mohalski prepared the figures, and Paula Work and Rich Krause aided in photography of specimens. Carl Brett also gratefully acknowledges the Department of Geology, University of Cincinnati for providing support for fieldwork.

REFERENCES

Aigner, T., 1985, Storm Depositional Systems: Dynamic Stratigraphy in Modern and Ancient Shallow Marine Sequences, *Lect. Notes Earth Sci*. **3**:174 p.

Algeo, T. J., and Brett, C. E., 2001, Roadlog for Sequence, Cycle & Event Stratigraphy of Upper Ordovician & Silurian Strata of the Cincinnati Arch Region, in: *1999 Field Conf. Great Lakes Section SEPM-SSG and Kent. Soc. Prof. Geol.*, Kentucky Geological Survey, Lexington, pp. 1-33, 136-144.

Allen, J. R. L, 1982, *Sedimentary Structures: Their Character and Physical Basis*, Elsevier, Amsterdam, Devel. Sed. **30(A&B)**.

Barbour, S. L., 2001, Multi-scale anlysis of spatial faunal variability and microstratigraphy in the Fairview Formation (Upper Ordovician), northern Kentucky, in: *Sequence, Cycle & Event Stratigraphy of Upper Ordovician & Silurian Strata of the Cincinnati Arch Region*

(T. J. Algeo and C. E. Brett, eds.), Kentucky Geological Survey, Lexington, pp. 117-122.

Bassler, R. S., 1906, A study of the James types of Ordovician and Silurian Bryozoa, *Proc. U. S. Nat. Mus.* **30**:1-66.

Bergström, S. M. and Mitchell, C. E., 1992, The Ordovician Utica shale in the eastern mid-continental region: Age, lithofacies, and regional relationships, in: *Special Papers in Paleontology: A Special Tribute to Thomas W. Amsden* (J. R. Chaplin and J. E. Barrick, eds.), Okla. Geol. Surv. Bull. **145**:67-89.

Blakey, R. 2000. Ordovician paleogeographic reconstruction. Website: http://vishnu.glg.nau.edu/rcb.

Brandt, D. S., 1985, Ichnologic, taphonomic, and sedimentologic clues to the deposition of Cincinnatian shales (Upper Ordovician), Ohio, in: *Biogenic Structures: Their Use in Interpreting Depositional Environment* (H. A. Curran, ed.), SEPM Sp. Pub. **35**:299-307.

Brandt, D. S., Meyer, D. L., and Lask, P. B., 1995, *Isotelus* (Trilobita) "hunting burrow" from Upper Ordovician strata, Ohio, *J. Paleont.* **69**:1079-1083.

Brett, C. E., 1995, Sequence stratigraphy, biostratigraphy, and taphonomy in shallow marine environments, *Palaios* **10**:597-616.

Brett, C. E., 1998, Sequence stratigraphy, paleoecology, and evolution: Biotic clues and responses to sea-level fluctuations, *Palaios* **13**:241-262.

Brett, C. E., and Algeo, T .J., 2001a, Event beds and small-scale cycles in Edenian to lower Maysvillian strata (Upper Ordovician) of northern Kentucky: Identification, origin, and temporal constraints, in: *Sequence, Cycle & Event Stratigraphy of Upper Ordovician & Silurian Strata of the Cincinnati Arch Region* (T. J. Algeo and C. E. Brett, eds.), Kentucky Geological Survey, Lexington, pp. 65-86.

Brett, C.E., and Algeo, T.J., 2001b, Stratigraphy of the Upper Ordovician Kope Formation in its type area, northern Kentucky, including a revised nomenclature, in: *Sequence, Cycle & Event Stratigraphy of Upper Ordovician & Silurian Strata of the Cincinnati Arch Region* (T. J. Algeo and C. E. Brett, eds.), Kentucky Geological Survey, Lexington, pp. 47-64.

Brett, C. E., and Baird, G. C., 1997, Epiboles, outages, and ecological evolutionary bioevents: Taphonomic, ecological, and evolutionary factors, in: *Paleontological Events: Stratigraphic, Ecological, and Evolutionary Implications* (C. E. Brett and G. C. Baird, eds.), Columbia University Press, New York, pp. 249-285.

Brett, C. E., and Seilacher, A., 1991, Fossil lagerstätten: A taphonomic consequence of event sedimentation, in: Cycles and Events in Stratigraphy (G. Einsele, W. Ricken, and A. Seilacher, eds.), Springer, New York, pp. 283-297.

Brett, C. E., Moffat, H. A., and Taylor, W. L., 1997, Echinoderm taphonomy, taphofacies, and lagerstätten, in: *Geobiology of Echinoderms* (J. A:Waters and C. G. Maples, eds.), *Paleont. Soc. Pap.* **3**:147-190.

Caster, K. E., Dalve, E. A., and Pope, J. K., 1955, *Elementary Guide to the Fossils and Strata of the Ordovician in the Vicinity of Cincinnati, Ohio*, Cincinnati Museum of Natural History, Cincinnati.

Clifton, H. E., ed., 1988, *Sedimentologic Responses of Convulsive Geologic Events*, Geol. Soc. Am. Sp. Pap. **229**:157 p.

Cressman, E. R., 1973, Lithostratigraphy and depositional environments of the Lexington Limestone (Ordovician), U. S. Geol. Surv. Prof. Pap. **768**:61 p.

Dattilo, B.F., 1996, A quantitative paleoecological approach to high-resolution cyclic and event stratigraphy: The Upper Ordovician Miamitown Shale in the type Cincinnatian, *Lethaia* **29**:21-37.

Dattilo, B. F., 1998, The Miamitown Shale: Stratigraphic and historic context (Upper Ordovician, Cincinnati, Ohio, region), in: *Sampling the Layer Cake That Isn't: The Stratigraphy and Paleontology of the Type-Cincinnatian* (R. A. Davis and R. J. Cuffey,

eds.), Ohio Div. Geol. Surv. Guidebook **13**:49-59.

Davis, R. A., ed., 1992, *Cincinnati Fossils: An Elementary Guide to the Ordovician Rocks and Fossils of the Cincinnati, Ohio, Region*, Cincinnati Museum of Natural History, Cincinnati.

Davis, R. A., and Cuffey, R. J., eds., 1998, *Sampling the Layer Cake That Isn't: The Stratigraphy and Paleontology of the Type-Cincinnatian* (R. A. Davis and R. J. Cuffey, eds.), Ohio Div. Geol. Surv. Guidebook **13**.

Des Jardins, L. H., 1934, The preglacial physiography of the Cincinnati region, Unpubl. M .S. thesis, University of Cincinnati, Cincinnati.

Dewey, J. F. and Kidd, W. S. F., 1974, Continental collisions in the Appalachian-Caledonian belt: Variations related to complete and incomplete suturing, *Geology* **2**:543-546.

Diekmeyer, S. C., 1998, Kope to Bellevue formations: The Reidlin Road/Mason Road site (Upper Ordovician, Cincinnati, Ohio region), in: *Sampling the Layer Cake That Isn't: The Stratigraphy and Paleontology of the Type-Cincinnatian* (R. A. Davis and R. J. Cuffey, eds.), Ohio Div. Geol. Surv. Guidebook **13**:10-35.

Drummond, C., and Sheets, H., 2001, Taphonomic reworking and stratal organization of the tempestite deposition; Ordovician Kope Formation, northern Kentucky, U.S.A., *J. Sed. Res.***71**:621-627.

Ettensohn, F. R., 1992, Changing interpretations of Kentucky geology: Layer cake, facies, flexure, and eustasy, *Ohio Div. Geol. Surv. Misc. Rep.* **5**:184 p.

Ettensohn, F. R., Hohman, J. C., Kulp, M. A., and Rast, N., 2002, Evidence and implications of possible far-field responses to the Taconian Orogeny: Middle-Late Ordovician Lexington Platform and Sebree Trough, east-central United States: *Southeastern Geol*. **41**: 1-36.

Foerste, A.F., 1905, The classification of the Ordovician rocks of Ohio and Indiana, *Science*, **22(new ser.)**:149-152

Ford, J. P., 1967, Cincinnatian geology in southwest Hamilton County, Ohio: *AAPG Bull*. **51**:918-936.

Hagadorn, J. W., and Bottjer, D. J., 1997, Wrinkle structures: Microbially mediated sedimentary structures common in subtidal siliciclastic settings at the Proterozoic-Phanerozoic transition, *Geology* **11**:1047-1050.

Holland, S. M., 1993, Sequence stratigraphy of a carbonate-clastic ramp: The Cincinnatian Series (Upper Ordovician) in its type area, *Geol. Soc. Am. Bull*. **105**:306-322.

Holland, S. M., 1997, Using time/environment analysis to recognize faunal events in the Upper Ordovician of the Cincinnati Arch, in: *Paleontological Events: Stratigraphic, Ecological, and Evolutionary Implications* (C. E. Brett and G. C. Baird, eds.), Columbia University Press, New York, pp. 309-334.

Holland, S. M., 1998, Sequence stratigraphy of the Cincinnatian Series (Upper Ordovician, Cincinnati, Ohio, region), in: *Sampling the Layer Cake That Isn't: The Stratigraphy and Paleontology of the Type-Cincinnatian* (R. A. Davis and R. J. Cuffey, eds.), Ohio Div. Geol. Surv. Guidebook **13**:135-151.

Holland, S .M., and Patzkowski, M. E., 1996, Sequence stratigraphy and long-term lithologic change in the Middle and Upper Ordovician of the eastern United States, in: *Paleozoic Sequence Stratigraphy: Views from the North American Craton* (B. J. Witzke, G. A. Ludvigsen, and J. E. Day, eds.), *Geol. Soc. Am. Sp. Pap*. **306**:117-130.

Holland, S. M., Meyer, D. L., and Miller, A., 2000, High-resolution correlation in apparently monotonous rocks: Upper Ordovician Kope Formation, Cincinnati Arch, *Palaios* **15**:73-80.

Holland, S. M., Miller, A. I., Dattilo, B. F., Meyer, D. L., and Diekmeyer, S. L., 1997, Cycle anatomy and variability in the storm-dominated type Cincinnatian (Upper Ordovician):

Coming to grips with cycle delineation and genesis, *J. Geol*. **105**:135-152.

Holland, S. M., Miller, A. I., and Meyer, D. L., 2001a, Sequence stratigraphy of the Kope-Fairview interval (Upper Ordovician, Cincinnati, Ohio area), in: *Sequence, Cycle & Event Stratigraphy of Upper Ordovician & Silurian Strata of the Cincinnati Arch Region* (T. J. Algeo and C. E. Brett, eds.), Kentucky Geological Survey, Lexington, pp. 93-102.

Holland, S. M., Miller, A. I., Meyer, D. L., and Dattilo, B., 2001b, The detection and importance of subtle biofacies within a single lithofacies: The Upper Ordovician Kope formation of the Cincinnati, Ohio region, *Palaios* **16**:205-217.

Hughes, N. C., and Cooper, D. L., 1999, Paleobiologic and taphonomic aspects of the "*Granulosa*" trilobite cluster, Kope Formation (Upper Ordovician, Cincinnati region), *J. Paleont.* **73**:306-319.

Hughes, N. C., and Hesselbo, S. P., 1997, Stratigraphy and sedimentology of the St. Lawrence Formation, Upper Cambrian of the northern Mississippi Valley, *Mil. Pub. Mus. Contrib. Biol. Geol.* **91**:1-50.

Hyde, D. E., 1959, A structural and stratigraphic study of the Fairview-McMillan formational contact in the Cincinnati area, *Compass* **36**:161-171.

Jennette, D. C., and Pryor, W .A., 1993, Cyclic alternation of proximal and distal storm facies: Kope and Fairview formations (Upper Ordovician), Ohio and Kentucky, *J. Sed. Pet.* **63**:183-203.

Keith, B. D., 1989, Regional facies of the Upper Ordovician Series of eastern North America, in: *The Trenton Group (Upper Ordovician Series) of eastern North America: Deposition, Diagenesis, and Petroleum* (B. D. Keith, ed.), *AAPG Stud. Geol.* **39**:1-16.

Klein, G. de V., 1977, *Clastic Tidal Facies*, University of Illinois, Champaign, Cont. Ed. Pub.

Kolata, D. R., Huff, W. D., and Bergstrom, S. M., 2001, The Ordovician Sebree Trough: An oceanic passage to the Midcontinent United States, *Geol. Soc. Am. Bull*. **113**:1067-1078.

Lehmann, D. M., Brett, C. E., and Cole, R., 1994, Tectonic and eustatic influences upon the sedimentary environments of the Upper Ordovician strata of New York and Ontario, in: *Tectonic and Eustatic Controls on Sedimentary Cycles* (J. M. Dennison and F. M. Ettensohn, eds.), *SEPM Concepts Sed. Paleont*. **4**:181-201.

Meyer, D.L., 1990, Population paleoecology and comparative taphonomy of two edrioasteroid (Echinodermata) pavements: Upper Ordovician of Kentucky and Ohio, *Hist. Biol.* **4**:155-178.

Miller, A. I., Holland, S. M., Dattilo, B. F., and Meyer, D. L., 1997, Stratigraphic resolution and perceptions of cycle architecture: Variations in meter-scale cyclicity in the type Cincinnatian Series, *J. Geol*. **105**:737-743.

Mitchell, C. E., and Bergström, S. M., 1991, New graptolite and lithostratigraphic evidence from the Cincinnati region, U.S.A., for the definition and correlation of the base of the Cincinnatian Series (Upper Ordovician), in: *Advances in Ordovician Geology* (C. R. Barnes and S. H. Williams, eds.), *Geol. Surv. Can. Pap*. **90-9**:59-77.

Nummedal, D., 1991, Shallow marine storm sedimentation: The oceanographic perspective, in: *Cycles and Events in Stratigraphy* (G. Einsele, W. Ricken, and A. Seilacher, eds.), Springer, New York, pp. 227-248.

O'Brien, N. R., Brett, C. E., and Taylor, W .L., 1994, Microfabric and taphonomic analysis in determining sedimentary processes in marine mudstones: Example from the Silurian of New York, *J. Sed. Res*. **A64**:847-852.

Pflueger, F., 1999, Matground structures and redox facies, *Palaios* **14**:25-39.

Potter, P. E., Ausich, W. I., Klee, J., Krissek, L. A., Mason, C. E., Schumacher, G. A., Wilson, T. R. and Wright, E .M., 1991, *Geology of the Alexandria-Ashland Highway (Kentucky Highway 546), Maysville to Garrison*, Kentucky Geological Survey, Lexington.

Rast, N., Ettensohn, F. R., and Rast, D. E., 1999, Taconian seismogenic deformation in the

Appalachian Orogen and the North American craton, in: *Continental Tectonics* (C. MacNiocaill and P. D. Ryan, eds.), *Geol. Soc. Lond. Spec. Pub.* **164**:127-137.

Rooney, L.F., 1966, Evidence of unconformity at the top of the Trenton Limestone in Indiana and adjacent states, *AAPG Bull*. **50**:533-546.

Rowley, D.H., and Kidd, W.S.F., 1991, Stratigraphic relationships and detrital composition of the Middle Ordovician flysch of western New England: Implications for the evolution of the Taconic Orogeny, *J. Geol*. **89**:199-218.

Schumacher, G.A., 1992, Lithostratigraphy, cyclic sedimentation, and event stratigraphy of the Maysvill e, Kentucky area, in: *Changing Interpretations of Kentucky Geology: Layer Cake, Facies, Flexure, and Eustasy* (F. R. Ettensohn, ed.), *Ohio Div. Geol. Surv. Misc. Rep*. **5**:165-172.

Schumacher, G.A., 1998, A new look at the Cincinnatian Series from a mapping perspective, in: *Sampling the Layer Cake That Isn't: The Stratigraphy and Paleontology of the Type-Cincinnatian* (R. A. Davis and R. J. Cuffey, eds.), *Ohio Div. Geol. Surv. Guidebook* **13**:111-119.

Schumacher, G.A., and Shrake, D.L., 1997, Paleoecology and comparative taphonomy of an *Isotelus* (Trilobita) fossil Lagerstätten from the Waynesville Formation (Upper Ordovician, Cincinnatian Series) of southwestern Ohio, in: *Paleontological Events: Stratigraphic, Ecological, and Evolutionary Implications* (C. E. Brett and G. C. Baird, eds.), Columbia University Press, New York, pp. 131-161.

Schwalb, H., 1980, Hydrocarbon entrapment along a Middle Ordovician disconformity, *Kent. Geol. Surv. Series XI, Sp. Pub.* **2**:35-41.

Scotese, C. R., 1990, *Atlas of Phanerozoic Plate Tectonic Reconstructions: International Lithophase Program (IUU-IUGS)*, *Paleomap Proj. Tech. Rep*. **10-90-1**.

Seilacher, A., 1982, Distinctive features of sandy tempestites, in: *Cyclic and Event Stratification* (G. Einsele and A Seilacher, eds.), Springer Verlag, Berlin, pp. 371-385.

Seilacher, A., 1985, The Jeram model: Event condensation in a modern intertidal environment, in: *Sedimentary and Evolutionary Cycles* (U. Bayer and A. Seilacher, eds.), *Lect. Notes Earth Sci.* **1**:336-346.

Seilacher, A., 1991, Events and their signatures: An overview, in: *Cycles and Events in Stratigraphy* (G. Einsele, W. Ricken, and A. Seilacher, eds.), Springer, New York, pp. 222-226.

Shanmugam, G., and Lash, G. G., 1982, Analogous tectonic evolution of the Ordovician foredeeps, southern and central Appalachians, *Geology* **10**:562-566.

Shanmugam, G., and Walker, K. R., 1980, Sedimentation, subsidence, and evolution of a foredeep basin in the Middle Ordovician, southern Appalachians, *Am. J. Sci*. **280**:479-496.

Shanmugam, G., and Walker, K. R., 1984, Anatomy of the Middle Ordovician Sevier Shale Basin, eastern Tennessee, *Sediment*. **43**:315-337.

Sumrall, C.D., and Schumacher, G.A., 2002, *Cheirocystis fultonensis*, a new glyptocystitid rhombiferan from the Upper Ordovician of the Cincinnati Arch, *J. Paleont.* **76**: 843-851.

Sweet, W. C., and Bergström, S. M., 1984, Conodont provinces and biofacies of the Late Ordovician, *Geol. Soc. Am. Sp. Pap*. **196**:69-87.

Tobin, R. C., and Pryor, W. A., 1981, Sedimentological interpretation of an Upper Ordovician carbonate-shale vertical sequence in northern Kentucky, in: *Geological Society of America, 1981 Annual Meeting Field Trip Guidebooks, Vol. I: Stratigraphy and Sedimentology* (T. G. Roberts, ed.), American Geological Institute, Falls Church, pp. 1-10.

Ulrich, E. O., 1888, A correlation of the Lower Silurian horizons of Tennessee and of the Ohio and Mississippi valleys with those of New York and Canada (4 parts), *Am. Geol*. **1**:100-110, 179-190, 305-315, and **2**:39-44.

Ulrich, E. O., and Bassler, R .S., 1914, Report on the stratigraphy of the Cincinnati, Ohio

Quadrangle, *U. S. Geol. Surv. Open-File Rep.,* 122 p.

Webber, A. J., 2001, Use of high-resolution fossil data to assess the causes of meter-scale cyclicity in the type Cincinnatian Series (Upper Ordovician), *Geol. Soc. Am. Abstr. Prog.* **33**:??.

Webber, A. J., 2002, High-resolution faunal gradient analysis and an assessment of the causes of meter-scale cyclicity in the type Cincinnatian Series (Upper Ordovician), *Palaios* **17**:

Weiss, M. P., and Sweet, W. C., 1964, Kope Formation (Upper Ordovician): Ohio and Kentucky, *Science* **145**:1296-1302.

Whiteley, T. E., Kloc, G. J., and Brett, C. E., 2002, *Trilobites of New York*, Cornell University Press, Ithaca.

Wickstrom, L. A., Gra, J. D., and Steiglitz, R. D., 1992, Stratigraphy, structure, and production history of the Trenton Limestone (Ordovician) and adjacent strata in northwestern Ohio, *Ohio Div. Geol. Surv. Rep. Invest*. **0097-5680 143**:78 p.

Wilson, M. A., 1985, Disturbance and ecological succession in an Upper Ordovician cobble-dwelling hardground fauna, *Science* **228**:575-577.

Chapter 10

Late Devonian Sequence and Event Stratigraphy Across the Frasnian-Famennian (F-F) Boundary, Utah and Nevada

JARED R. MORROW and CHARLES A. SANDBERG

JARED R. MORROW • Department of Earth Sciences, University of Northern Colorado, Greeley, CO 80639. CHARLES A. SANDBERG • Geologist Emeritus, U.S. Geological Survey, Box 25046, MS 939, Federal Center, Denver, CO 80225-0046.

P.J. Harries (ed.), *High-Resolution Approaches in Stratigraphic Paleontology.*

1. INTRODUCTION

The biostratigraphy, sedimentology, sequence stratigraphy, and geochemistry of the late Frasnian (F-F) mass extinction, one of the five largest in the Phanerozoic record (Sepkoski, 1982, 1996), have been studied intensely during the past two decades. Short-term, step-wise extinction prior to and at the F-F boundary is associated with an abrupt reduction in global biomass and loss of up to 82% of marine tropical to subtropical species (Jablonski, 1991). The crisis simultaneously affected genetically and ecologically diverse groups of planktic, benthic, and nektic organisms representing virtually all trophic levels of the tropical marine biosphere.

These biologic changes were superimposed on a backdrop of rapid sea-level fluctuations, marked intervals of anoxic and dysoxic marine sedimentation, and significant increases in organic carbon burial and recycling accompanying major worldwide excursions or spikes in the geochemical record (e.g., Buggisch, 1972, 1991; Sandberg *et al.*, 1988; Goodfellow *et al.*, 1989a, 1989b; Joachimski and Buggisch, 1993, 2000, 2002; Wang *et al.*, 1996; Joachimski, 1997; Bratton *et al.*, 1999; Joachimski *et al.*, 2002).

Correlation of F-F boundary strata and contained event units is aided by detailed conodont biostratigraphy, which currently provides the highest resolution tool for regional to intercontinental correlations (e.g., Sandberg *et al.*, 1988; Ziegler and Sandberg, 1990, 1994; Sandberg and Ziegler, 1996). Individual Late Devonian conodont zones range from approximately 300 to 700 kyr in duration, averaging 500 kyr (Fig. 1; Ziegler and Sandberg, 1994; Sandberg and Ziegler, 1996). Even finer local to regional time resolution is

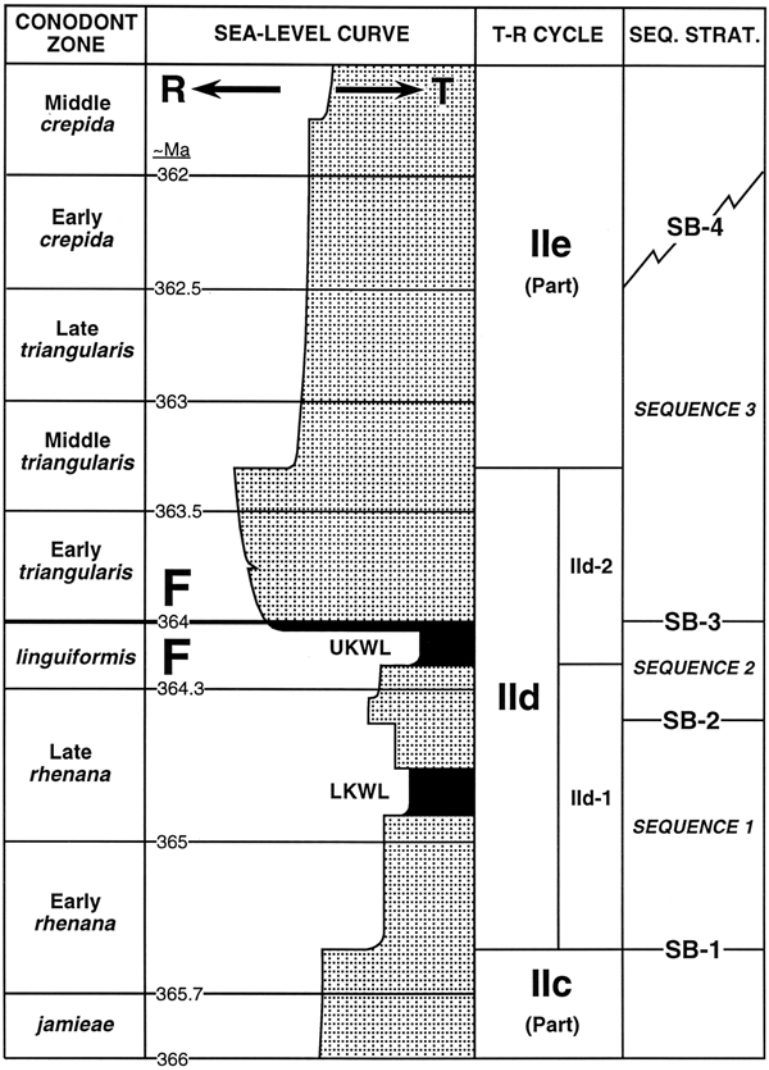

Figure 1. Standard Late Devonian conodont biozonation (Sandberg *et al.*, 1988; Ziegler and Sandberg, 1990; Sandberg and Ziegler, 1996), mid-Late Devonian eustatic sea-level curve (Johnson *et al.*, 1985, 1991; Johnson and Sandberg, 1989; Sandberg *et al.*, 2002), transgressive-regressive (T-R) cycles (modified from Johnson and Sandberg, 1989; scaled to conodont biozonation), and sequence stratigraphic units (discussed herein) across the F-F boundary interval. Absolute age calculations (**~Ma**) from Sandberg and Ziegler (1996). **F-F** = Frasnian-Famennian boundary; **R** and **T** = regression and transgression, respectively; **Seq. Strat.** = sequence stratigraphic units and sequence boundaries; and **UKWL** and **LKWL** = corresponding interval of Upper and Lower Kellwasser Limestones, respectively, at the type area.

attainable (e.g., Sandberg *et al.*, 1988; Schülke, 1995, 1999; Morrow and Sandberg, 1996). Detailed and integrated analyses of other fossil groups such as trilobites (e.g., Feist and Schindler, 1994; Feist, 2002), brachiopods (e.g., Sartenaer, 1985; McGhee, 1989; Day, 1990; Balinski, 2002; Sokiran, 2002), ostracodes (e.g., Groos-Uffenorde and Schindler, 1990; Casier *et al.*, 1996; Casier and Lethiers, 1998; Casier *et al.*, 2002) and cricoconarids (e.g., Schindler, 1993) provide additional high-resolution biostratigraphic correlation tools.

As demonstrated by this and previous work, a high-resolution approach (c.f., Kauffman, 1986, 1988; Sandberg *et al.*, 1988) integrating detailed, intercontinental stratigraphic, sedimentologic, and paleontologic data has permitted greater refinement of the F-F boundary geologic history when compared to studies based on a single data type or a limited geographic area. Integrated, high-resolution data are especially crucial when studying geologic intervals of rapid global and biological change, such as occurred during the Late Devonian. Furthermore, these data provide an extremely valuable tool for accurately interpreting tectonically and stratigraphically complex regions, such as the Great Basin.

2. F-F BOUNDARY FACIES AND SEA LEVEL

Of great importance to discussion of F-F boundary sequence stratigraphy, event stratigraphy, and mass extinction are rock types correlative with the upper Frasnian Kellwasser Limestone, named from its type area in the Kellwasser Valley, Harz Mountains, Germany (Roemer, 1850). In and adjacent to the type area, the Kellwasser Limestone consists of two distinct intervals of dark-gray to black, dysoxic to anoxic, organic-rich nodular limestone and shale that contain a diverse pelagic fauna (e.g., Ziegler, 1958, 1971; Buggisch, 1972; Becker, 1986, 1993; Lottmann *et al.*, 1986; Sandberg *et al.*, 1988; Walliser *et al.*, 1989; Schindler, 1990a, 1990b, 1993; Becker and House, 1994). The higher of these two intervals records the step-wise extinction and final F-F mass extinction episodes that occurred just before the end of Kellwasser sedimentation (Sandberg *et al.*, 1988; Becker *et al.*, 1989; Walliser *et al.*, 1989; Schindler, 1990a, 1990b, 1993; Schindler and Königshof, 1997).

Deep-water, basinal and submarine-rise Kellwasser-like facies are widespread throughout western and central Europe and North Africa and have also been reported from eastern and central North America (Over, 1997; Over and Rhodes, 2000), Iran, and southern China (Bai *et al.*, 1994; Muchez *et al.*, 1996; Walliser, 1996a). Also of importance are the regions where latest Frasnian deposition occurred in different paleotectonic settings

as, for example, in Australia (Becker *et al.*, 1991), Canada (Geldsetzer *et al.*, 1987; Wang *et al.*, 1996; George and Chow, 2002), and western North America (Sandberg *et al.*, 1988, 1989). In these regions, Kellwasser strata *sensu stricto* were not deposited, and the facies patterns typically reflect more local to interregional controls.

Changing sedimentation patterns that characterize the F-F boundary interval were strongly influenced by third- and higher-order, local and eustatic sea-level fluctuations. Based on multiple sections from Euramerica, Johnson *et al.* (1985, 1986a, 1991), Sandberg *et al.* (1988; 2002), and Johnson and Sandberg (1989) have presented an integrated third-order Late Devonian sea-level curve that is widely used for the F-F boundary interval (Fig. 1). This interval corresponds to the IId T-R (transgressive-regressive) cycle of Johnson *et al.* (1985, 1991), which encompasses the maximum transgression of Devonian global sea level. To aid in the discussion of the sea-level history and associated sequence and event stratigraphy across the F-F boundary, T-R cycle IId is herein further subdivided into earlier (IId-1) and later (IId-2) fourth-order subcycles (Fig. 1).

Other local to regional relative sea-level curves have been published, including F-F boundary data from Australia (Playford *et al.*, 1989; Southgate *et al.*, 1993; Becker and House, 1997), Belgium (Sandberg *et al.*, 1992; Muchez *et al.*, 1996), China (Ji, 1989; Muchez *et al.*, 1996), Morocco (Buggisch, 1991; Wendt and Belka, 1991), and Poland (Narkiewicz, 1989; Narkiewicz and Hoffman, 1989). Hallam and Wignall (1999) presented an alternative eustatic sea-level interpretation for the F-F boundary, based on a compilation of selected, previously published sea-level curves. Their study places the Frasnian-Famennian Stage boundary within the early transgressive phase of a major sea-level rise (Hallam and Wignall, 1999, p. 239), instead of within a major sea-level fall as interpreted by most other researchers. The detailed data from our study confirm lowering sea level through this interval, contradicting the Hallam and Wignall (1999) interpretation of a significant sea-level rise at or across the F-F boundary.

As documented by numerous workers including Sandberg *et al.* (1988, 1992, 2002), Schindler (1990a), and Buggisch (1991), major short-term eustatic sea-level rise and fall in the latest Frasnian *linguiformis* conodont Zone (Fig. 1) is associated with the final demise or drowning of stromatoporoid/coral-dominated mudmound ecosystems, onlapping of deeper-water lithofacies onto shelf margins, stratification of marine basins, onset of oceanic anoxia, and initiation of Upper Kellwasser Limestone deposition in Western Europe. Late in the *linguiformis* Zone, an abrupt sea-level fall is documented by lithofacies and conodont biofacies changes that peaked at the time of the terminal F-F boundary extinction. This latest Frasnian shallowing trend continued uninterrupted across the F-F boundary

into the early Famennian (Early *triangularis* Zone and early part of the Middle *triangularis* Zone), before sea level rose again in the middle part of the Middle *triangularis* Zone.

Characteristic facies responses to the F-F boundary shallowing include increased ventilation and oxygenation in formerly anoxic to dysoxic basins (corresponding to the end of Kellwasser sedimentation in Europe); increased shelf-to-basin siliciclastic transport, commonly via bypassing of relict late Frasnian reefs and mudmounds; concentration of microbiotic laminite, oncolite, or storm beds near the boundary; localized condensation and omission of stratigraphic section; and earliest Famennian collapse of late Frasnian shelf margins, resulting in catastrophic carbonate debris-flow deposition within deeper-water slope and basin settings. As documented in this report, catastrophic carbonate debris-flow deposition continued in parts of the Great Basin into the Late *triangularis* Zone, which follows the Middle *triangularis* Zone global sea-level rise at the beginning of T-R cycle IIe.

Deeper-water, post-extinction marine facies of the Middle and Late *triangularis* Zones, which onlapped and transgressed over the F-F boundary facies, contain a relatively diverse fossil assemblage reflecting the early stages of biotic recovery following the mass extinction. These distinctive facies changes and boundaries, together with associated biological and geochemical changes, provide a basis for an event-stratigraphic framework across the F-F boundary interval (e.g., Sandberg *et al.*, 1983, 1986, 1988, 1989, 1997, 2002; Walliser, 1984, 1996a, 1996b; Schindler, 1990a, 1990b, 1993; Schülke, 1995; Racki *et al.*, 2002).

3. LATE DEVONIAN PALEOGEOGRAPHY

Late Devonian paleogeographic reconstructions of the western U.S. (Sandberg and Poole, 1977; Sandberg *et al.*, 1989; Scotese and McKerrow, 1990) show that eastern Nevada and western Utah occupied the central part of a low-latitude, north-south trending, shallow-water, carbonate-dominated continental shelf that extended northward from Mexico into Alberta and western British Columbia (Fig. 2). An important Late Devonian structural feature that interrupted the middle to outer shelf in western North America was the Pilot Basin. This intra-shelf basin formed as a precursor to the extensive Mississippian foreland basin that resulted from the Antler orogeny, a Late Devonian to Early Mississippian accretionary event that thrust lower and middle Paleozoic deep-water, oceanic strata over and against coeval shallow-water rocks of the continental shelf and shelf margin (Poole *et al.*, 1992).

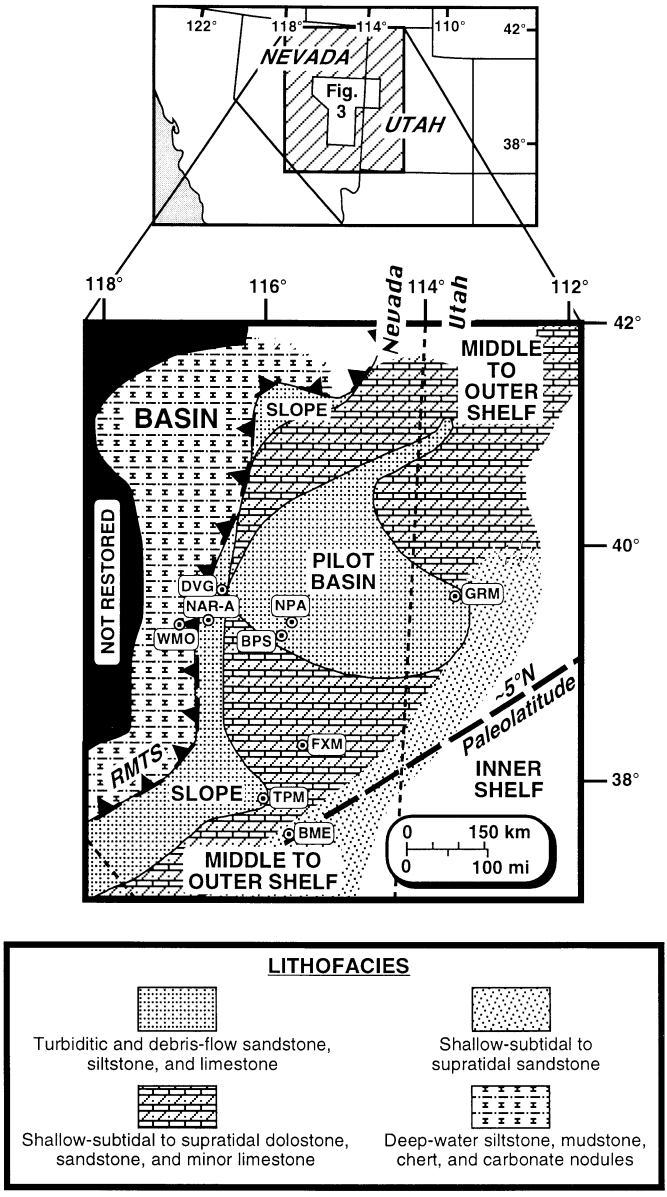

Figure 2. Generalized, partly restored earliest Famennian (Early *triangularis* Zone) lithofacies and paleogeography of east-central Nevada and west-central Utah, showing location of stratigraphic sections discussed in this paper (modified from Sandberg *et al.*, 1989). **RMTS** = approximate trace of Roberts Mountains thrust system; sawteeth indicate the hanging wall.

During the F-F boundary interval, the Pilot Basin was a rapidly subsiding,

deep-water depocenter that received sediments dominated by calcareous, siliceous, and carbonaceous silt, micrite, and thin, sandy turbidites and debris flows (Sandberg and Poole, 1977; Sandberg *et al.*, 1989). Beginning in the mid-Frasnian, the Pilot Basin was bounded to the west by a linear, eastward-migrating proto-Antler forebulge that separated the Pilot Basin on the east from the offshore Woodruff Basin to the west (Sandberg *et al.*, 2002, *in press*). At the time of the F-F boundary transition, this forebulge served as a relatively shallow-water source area for allochthonous material that was shed both westward and eastward into the adjacent deep-water slope settings.

In contrast to the predominately deep-water rocks of central Nevada, the surrounding carbonate-shelf rocks of eastern Nevada and western Utah consist predominantly of shallow-water carbonates that become increasingly sandy and dolomitic eastward towards the inner shelf (Fig. 2). In the late Frasnian, middle- to outer-shelf deposits commonly consisted of thick-bedded, massive biostromal carbonates dominated by stromatoporoid, coral, and stromatolite framework builders. Earliest Famennian shelf lithologies are characterized by shallow-subtidal to peritidal, thin-bedded, sandy, peloidal lime mudstone and dolostone that lack the dominant framework organisms characteristic of the pre-mass-extinction setting.

Compression associated with the Antler Orogeny thrust oceanic basin rocks 75 to 200 km eastward onto the slope and outer shelf, resulting in a complex tectonic interfingering of shallow- and deep-water facies along the zone of the north-south trending Roberts Mountains Thrust System (RMTS, Fig. 2). Both within the RMTS and farther to the west in central Nevada, F-F boundary basinal oceanic rocks are often poorly exposed, with internally faulted, folded, and structurally truncated outcrops. West of central Nevada, post-Paleozoic volcanism, sedimentation, and erosion have covered or removed most or all Devonian strata (Poole *et al.*, 1992).

4. STRATIGRAPHIC SECTIONS

Our data are based on nine well-exposed, shelf-to-basin F-F boundary stratigraphic sections from the central Great Basin region of east-central Nevada and west-central Utah (Fig. 3). Fig. 4 summarizes lithologic symbols and abbreviations used in the stratigraphic columns. Because the conodont biostratigraphy and paleoecology of these sections were treated by Morrow (1997, 2000), only the position of conodont collections is shown on the columnar sections herein.

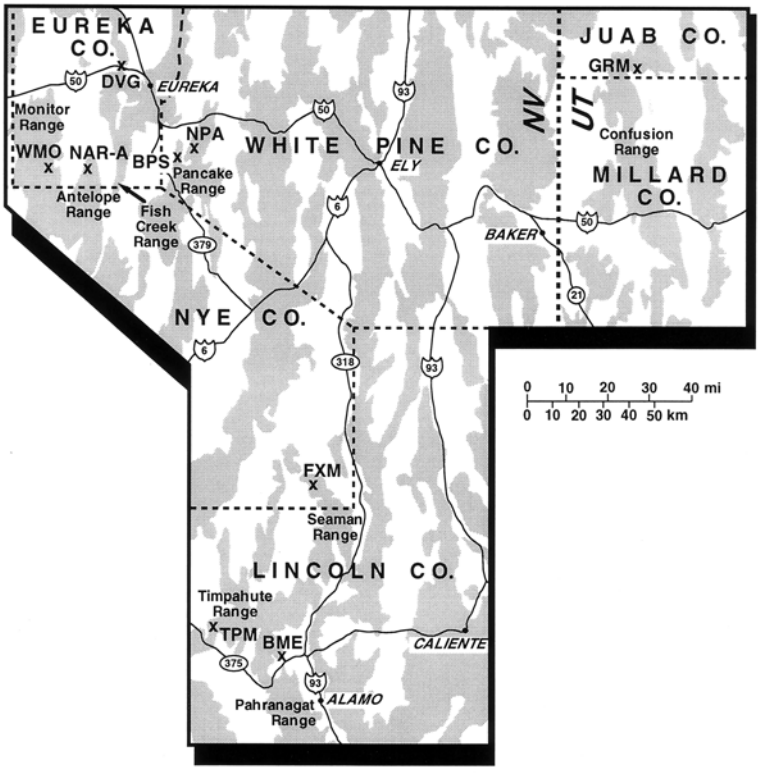

Figure 3. Stratigraphic section locality map, east-central Nevada and western Utah. Abbreviations used: **BME** = Bactrian Mountain East; **BPS** = Black Point South; **DVG** = Devils Gate; **FXM** = Fox Mountain; **GRM** = Granite Mountain; **NAR-A** = Northern Antelope Range; **NPA** = Northern Pancake Range; **TPM** = Tempiute Mountain; and **WMO** = Whiterock Canyon. Shaded pattern on figure shows extent of mountain ranges. See Morrow (1997) for detailed locality descriptions. See Figure 2 for area of coverage.

Interest in sequence stratigraphic analysis of Upper Devonian Great Basin strata including the F-F boundary has increased in the past decade (e.g., Estes, 1992; Giles, 1994; LaMaskin, 1995; Chamberlain and Warme, 1996; LaMaskin and Elrick, 1997; Morrow, 1997; Morrow and Sandberg, 1997). Although many individual exposures of F-F boundary rocks are excellent, structural complication, abrupt lateral facies changes, lack of regionally continuous outcrop, scarcity of constrained well-log data, and poor seismic stratigraphic resolution have hampered the recognition of stratal geometries and the lateral extent and nature of systems tracts. Lack of detailed biostratigraphic data has increased difficulties in placing these strata within a sequence stratigraphic framework, especially in dating and correctly

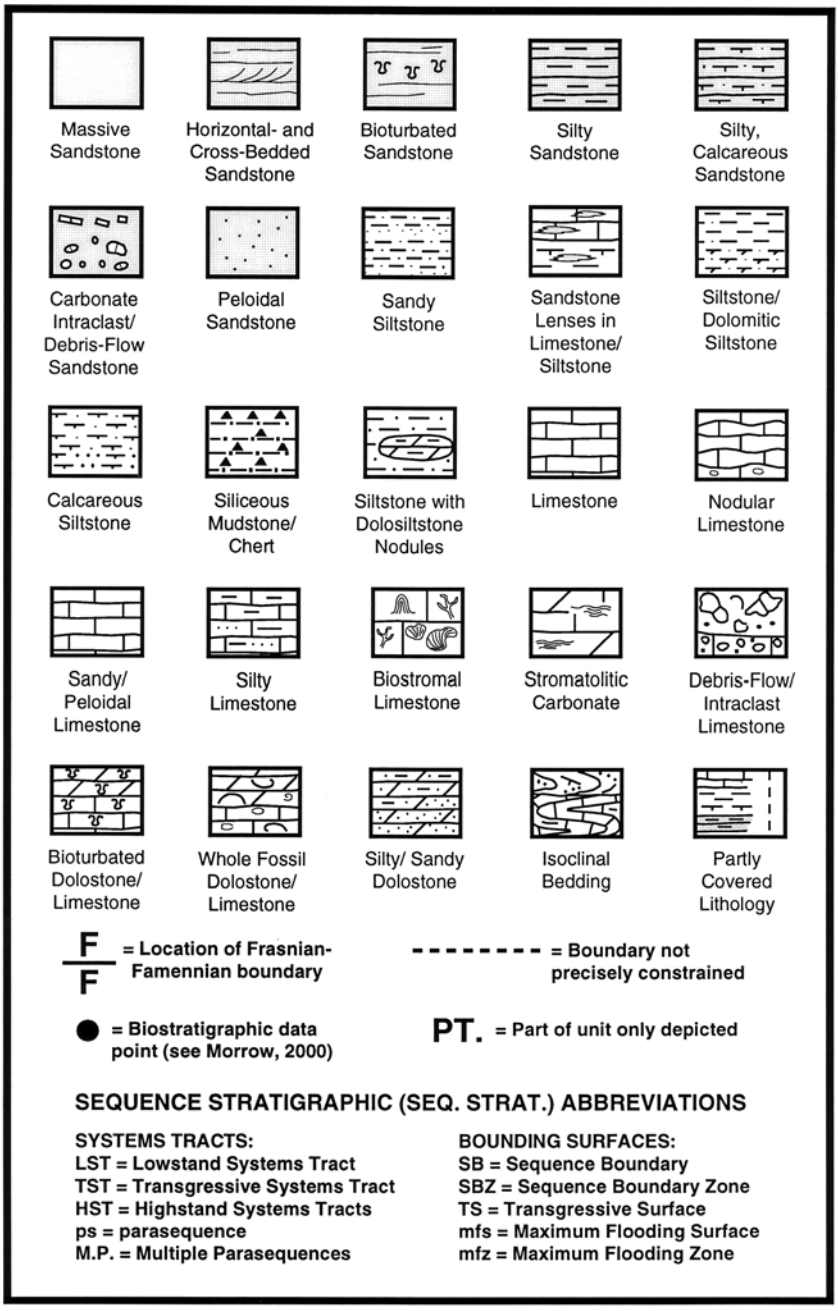

Figure 4. Key to lithologic symbols and abbreviations used in stratigraphic sections.

correlating regionally significant surfaces and boundaries. The Late

Devonian in western North America was a time of transition from a passive to active continental margin, and the early tectonic effects of this compression, which included development of an uplifted proto-Antler forebulge and subsiding backbulge (Pilot) basin, cannot be ignored when examining and correlating systems tract boundaries or relative sea-level history (Sandberg *et al.*, in press).

As shown by Johnson *et al.* (1985, 1991), large-scale, regionally extensive Late Devonian third- and fourth-order flooding surfaces can be correlated from the Great Basin region on an intra- and intercontinental scale, demonstrating that local to regional tectonic and sedimentation effects do not prohibit the recognition of important, laterally continuous bounding surfaces for sequence stratigraphic analysis. Johnson *et al.* (1996) discussed the correspondence between T-R cycles and sequence stratigraphic units, which are defined and bounded by different surfaces. T-R cycle boundaries are defined by marine transgression surfaces and are therefore placed at the top of the shallowest water facies interval. Because of this, where lowstand systems tracts are present they would be included in the uppermost part of the T-R cycle, instead of at the base of the succeeding cycle (i.e., as within a systems-tract approach).

Where possible, T-R cycles are equated herein to depositional sequences. The sequence stratigraphic concepts and terminology of Vail (1987), Van Wagoner *et al.* (1987), and Sarg (1988) are used (Fig. 4). Following the usage of Montañez and Osleger (1993) and Elrick (1996), the terms "sequence boundary zone (SBZ)" and "maximum flooding zone (mfz)" are applied where these features are represented by transitional changes within and between systems tracts, parasequences, or bundled cycles, as opposed to relatively sharp, recognizable surfaces that are described using the traditional "sequence boundary (SB)" and "maximum flooding surface (mfs)" concepts.

Where carbonate sequence stratigraphy is applied across a mass extinction interval such as the F-F boundary, pre- and post-extinction systems tracts may be vastly different due to the loss of entire carbonate-producing ecosystems and major fluctuations in carbonate productivity. These changes could greatly suppress the sediment production and export potential of carbonate platforms, affecting both "keep-up" and "catch-up" modes of sedimentation, and leading to temporarily attenuated or carbonate-depleted systems tracts even where the site of the former "carbonate factory" was adequately covered and accommodation space was available. Overall shelf-to-basin characteristics of the systems tracts and associated bounding surfaces or zones identified in the study are summarized in Fig. 5.

FEATURE	PALEOGEOGRAPHIC SETTING		
	BASIN	SLOPE	OUTER SHELF
LST	Rarely developed; where recognized, consisting of distal, condensed debris-flow sandstone stringers/ microturbidites containing reworked faunas; in most distal setting, marked by increased silt to very fine sand content	Often thin and condensed; with sharp, erosive basal contacts; consisting of shelf- to slope-derived carbonate-clast debris-flows within shelf-derived quartz sand or silt matrix; reworked faunas common	Not clearly recognized in this study; typically, sequence boundary zone marked by peritidal to supratidal rocks reflecting little or no available accomodation space; evidence of extensive subaerial erosion lacking
TST	Thin, retrogradational and aggradational parasequences and parasequence sets composed of facies indicating high organic productivity (>carbonate and/or silica); often condensed	Thin, retrogradational and aggradational parasequences and parasequence sets reflecting high organic productivity (>carbonate and/or rare silica) or reduced average grain size; soft sediment deformation common	Thick, retrogradational or aggradational parasequences and parasequence bundles dominated by carbonate framework-rich organisms[1] or bioclastic peloidal carbonate[2] with abundant lime mud
HST	Dominated by aggradational, thin, siliceous and calcareous siltstone parasequences with rare limestone or dolostone concretionary nodules; rarely, slight increase in siliclastic grain size late in highstand	Silty and sandy, thin-bedded, aggradational or progradational carbonate turbidites with common soft sediment deformation; increasing siliciclastic and carbonate allochem grain-size with upper slope sandstones in late highstand	Thick, progradational, framework organism-dominated carbonate parasequences[1] or progradational, carbonate-siliciclastic parasequences[1+2] with increasing siliciclastic component in late highstand interval
Para-seq.	Thin, poorly delineated; dominated by pelagic/ hemipelagic sediments, with thicknesses of individual beds/sets controlled by productivity and/or climate; punctuated by relatively rare event beds	Thin, poorly delineated; dominated by periodic influx of upslope-derived turbidites and/or debris-flow sediments; soft sediment deformation and event beds very common	Thick, well delineated; defined by changes in carbonate lithology which demonstrate progradational, aggradational, or retrogradational stacking patterns; mixed siliciclastic and carbonate parasequences and parasequence sets common
SB	Often difficult to recognize where convergent with conformable surfaces in distal setting; based on prominent allodapic beds, fine-grained siliciclastic maxima, or abrupt facies changes with intervening transgressive surface	Recognized by marked increase in quartz sand or allodapic carbonate grains, sharp contact with LST above (if developed), or presence of transgressive surfaces and/or condensed sedimentation intervals with deeper water facies above	Gradational boundary zones of very condensed, extremely shallow-water peritidal/supratidal interval overlying shallowing-upward parasequence packages; evidence of extensive channels/subaerial erosion not noted in study interval
TS	Typically identified by abrupt upward shift from light to dark sediments (redox boundary shift), increased Corg burial, and sedimentary condensation with concentrated phosphatic material and minor and trace elements	Undulatory condensation surfaces with abundant quartz sand, diagenetic silica, hematite, limonite, phosphatic skeletal debris, and small intraclasts; bracketed by shallower, siliciclastic facies below and deeper, carbonate facies above	Sharp, oxidized surfaces, rarely with bioclastic lags; recognized primarily as horizon between shallower, peritidal to supratidal facies below and deeper, subtidal carbonate facies above
mfs	Consist primarily of diffuse zones marked by highest percentage of pelagic biogenic material or increase in carbonate nodules within fine siliciclastic sequences	Diffuse zones of deepest water facies including very fine-grained siliciclastics, pelagic carbonates, and distal turbidites with common soft sediment deformation; or as sharp, oxidized condensation surfaces with abundant silica and phosphate	Diffuse zones of deepest water facies such as subtidal, silty, nodular bioclastic carbonates[1+2] or beneath thick, biostromal carbonates[1] reflecting maximum available accomodation space

[1]= pre-mass extinction; [2]= post-mass extinction

Figure 5. Generalized summary of characteristics of sequence stratigraphic components (systems tracts and bounding surfaces) recognized within the study.

4.1 Bactrian Mountain East (BME)

Section BME (Fig. 6) is a downward continuation of the well-documented Famennian Bactrian Mountain section described by Johnson *et al.* (1969), Sandberg and Poole (1970, 1977), and Sandberg and Ziegler (1973, 1993). At a similar, inner-shelf locality near White Horse Pass, Elko County, Nevada, shallow-water F-F boundary sections generally yield relatively few conodonts and often lack the pelagic species necessary for direct correlation with standard conodont biozonations (Sandberg *et al.*, 1988). As at the White Horse Pass section, conodont faunas at BME are dominated by shallow-water conodont species of *Polygnathus* and *Icriodus* (Morrow, 2000). Nevertheless, correlation with an alternate Late Devonian nearshore conodont zonation (Sandberg and Dreesen, 1984) provides a biostratigraphic framework that can be correlated approximately with the pelagic zonation.

As a characteristic example of F-F boundary shelf facies, the upper Frasnian part of section BME is composed of highstand peloidal wackestones/packstones and stratiform amphiporid/stromatoporoid/coral biostromes (units 3-4), which are overlain by peritidal rocks containing a condensed, incomplete record of the F-F boundary transition. The highest biostromes are tentatively placed within the older, Late *rhenana* Zone part of the IId T-R cycle (IId-1, Fig. 1), although definitive age control is lacking. This assumption is consistent with the growth and extinction histories of correlative biostromes, reefs, and mudmounds in Europe that are more tightly constrained biostratigraphically (e.g., in Germany, Gischler, 1992, and references therein; and in Belgium, Sandberg *et al.*, 1992), as well as the minimum age estimate of inner-shelf amphiporid banks at White Horse Pass (Sandberg *et al.*, 1988).

A 5-m-thick interval of dolomitic sandstones, silty to sandy dolostones, and microbiotic laminites (unit 5) overlies the highest biostrome and includes the F-F boundary. This interval contains the major shallowing at both the termination of T-R cycle IId-2 and a widely recognized, global-scale, third-order sequence boundary, here termed "SBZ-3" (after Johnson *et al.*, 1985, 1991; Sandberg *et al.*, 1988). At BME, clear evidence for significant subaerial erosion (e.g., solution breccia, karsting, ravinement, channeling) at this sequence boundary is lacking. The regressive to early transgressive deposits within SBZ-3 are peritidal to supratidal sandstones and stromatolitic dolostones with sand-filled desiccation cracks and rare, cm-scale teepee structures.

In unit 6, conodonts indicate a Famennian (Middle or Late *triangularis*

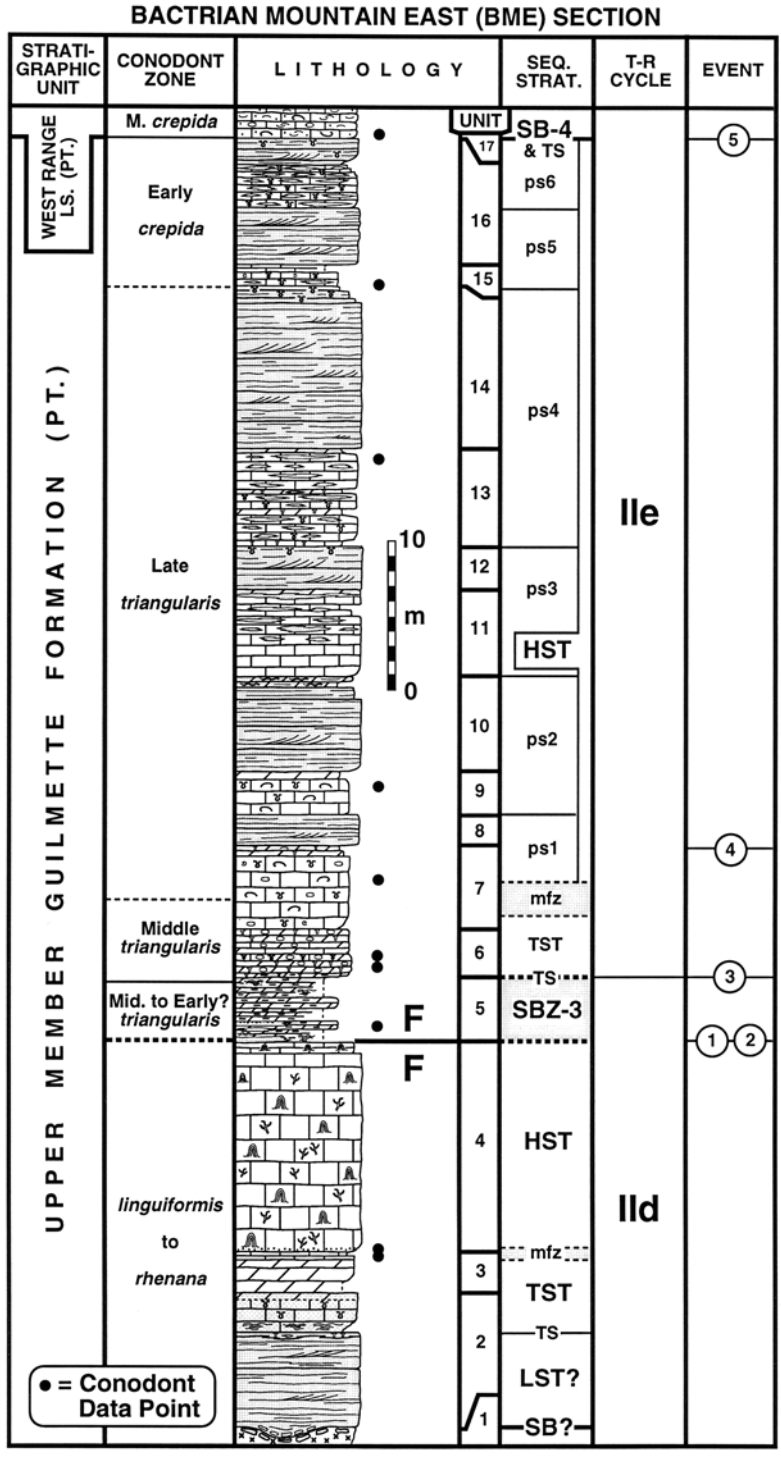
BACTRIAN MOUNTAIN EAST (BME) SECTION
STRATI-GRAPHIC UNIT
CONODONT ZONE
LITHOLOGY
SEQ. STRAT.
T-R CYCLE
EVENT
WEST RANGE LS. (PT.)
UPPER MEMBER GUILMETTE FORMATION (PT.)
M. crepida
Early crepida
Late triangularis
Middle triangularis
Mid. to Early? triangularis
linguiformis to rhenana
UNIT
SB-4
& TS
ps6
ps5
ps4
ps3
HST
ps2
ps1
mfz
TST
TS
SBZ-3
HST
mfz
TST
TS
LST?
SB?
10
m
0
F
F
IIe
IId
1
2
3
4
5
● = Conodont Data Point

Zone) age, and the overall increase in biodiversity (including conodonts, brachiopods, molluscs, and multi-tiered burrow assemblages) reflects the relative deepening and improved environmental conditions associated with post-extinction recovery. With continued relative high sea level in the Late *triangularis* Zone (early T-R cycle IIe), progradational parasequences of sparsely bioclastic to peloidal wackestones and plane-bedded, cross-bedded,and ripple-laminated fine- to coarse-grained quartz arenites dominate. Cross-bed sets within quartz arenites dip NW and NNW, indicating an offshore to oblique offshore-longshore transport direction. This general observation is supported by Estes (1992), who recorded craton-to-basin paleocurrent directions in correlative upper Guilmette Formation quartz arenites exposed in the Pahranagat Range, 8 km west of section BME.

Further deepening in the Middle *crepida* Zone is evidenced by the nodular, bioclastic West Range Limestone of unit 17 that overlies a sharp transgressive surface (Fig. 7a) at the top of sandstone and carbonate strata of the uppermost Guilmette Formation. The West Range Limestone represents a subtidal, relatively low-energy open-marine carbonate unit that onlaps middle-shelf facies and is transitional to the overlying/laterally equivalent, deep-water lower member of the Pilot Shale, as demonstrated by Sandberg *et al.* (1989). The Guilmette-West Range contact is interpreted to mark a forced sequence boundary (SB-4) that is diachronous across the basin, reflecting the tectonically driven expansion of the Pilot Basin across the middle-shelf, outer-shelf, and slope settings (Sandberg *et al.*, 1989).

In summary, important events recognized at section BME include: (1) breakdown of stromatoporoid/coral ecosystems and end of biostromal growth; (2) abrupt shallowing (SBZ-3) at the F-F boundary; (3) marked transgression, increased accommodation space, and biologic diversification in the early post-extinction interval associated with the beginning of T-R cycle IIe; (4) initiation of major siliciclastic influx into prograding highstand parasequences; and (5) abrupt deepening and forced SB-4 at the Guilmette Formation-West Range Limestone contact.

4.2 Fox Mountain (FXM)

Section FXM (Fig. 8) is stratigraphically and paleogeographically similar to section BME, although the F-F boundary interval at FXM is represented by thinner, more condensed, and slightly deeper-water strata. As at BME,

Figure 6. Stratigraphy, conodont biostratigraphy, sequence stratigraphy, and event stratigraphy of Bactrian Mountain East (BME) section in NE1/4 sec. 11 (unsurveyed), T. 5 S., R. 59 E., lat 37.53° N., long 115.33° W., Lincoln County, Nevada (Mount Irish SE 7.5-minute quadrangle).

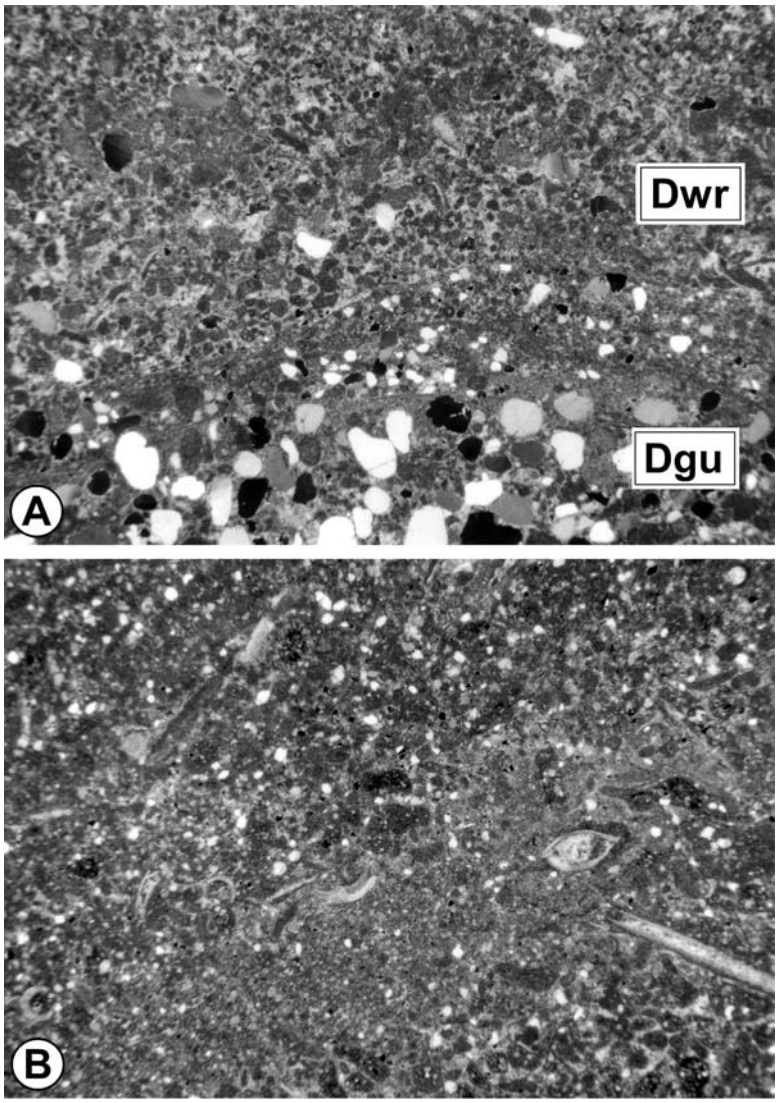

Figure 7. A. Photomicrograph of relatively sharp, undulatory contact between unit 16, upper member of the Guilmette Formation (**Dgu**), and unit 17, basal West Range Limestone (**Dwr**), Bactrian Mountain East (BME) section. Uppermost Guilmette facies consist of sandy peloidal packstone containing ≤40% medium- to coarse-grained quartz sand, overlain by West Range facies of skeletal peloidal wackestone characterized by a diverse fossil allochem assemblage. This contact marks SB-4, which is interpreted to be a forced sequence boundary driven by the lateral expansion of the Pilot Basin. Field of view is 1 cm across; crossed nicols. B. Photomicrograph of Middle to Late *triangularis* Zone, silty, peloidal lime wackestone containing relatively diverse fossil allochem assemblage including molluscs, brachiopods, echinoderm ossicles, and ostracods, top of unit 7, upper member Guilmette Formation, Fox Mountain (FXM) section. Field of view is 6 mm across; crossed nicols.

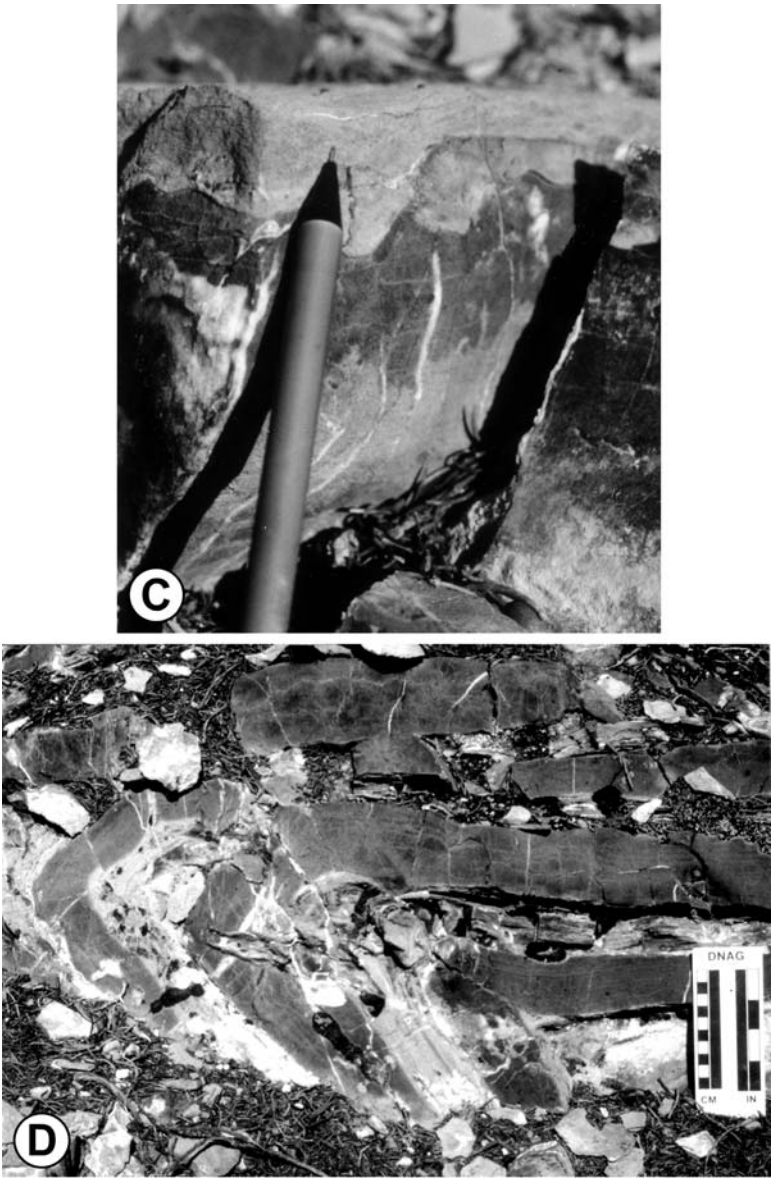

Figure 7. Continued.. C. Outcrop photograph of Early *rhenana* Zone condensed interval (at pencil tip) containing abundant chert, fine- to medium-grained quartz sand, phosphatic peloids, phosphatized ostracods, cricoconarids, and conodonts, top of unit 6, Devils Gate Limestone, Tempiute Mountain (TPM) section. Pencil for scale. D. Outcrop photograph of *linguiformis* Zone isoclinal synsedimentary folding in upper-slope turbidite beds composed of dark-gray to black, silty lime mudstone and laminated, pink calcareous siltstone couplets, middle of unit 11, Devils Gate Limestone, Tempiute Mountain (TPM) section. Scale is 10 cm long. This interval is bounded above and below by undeformed planar beds of similar lithology.

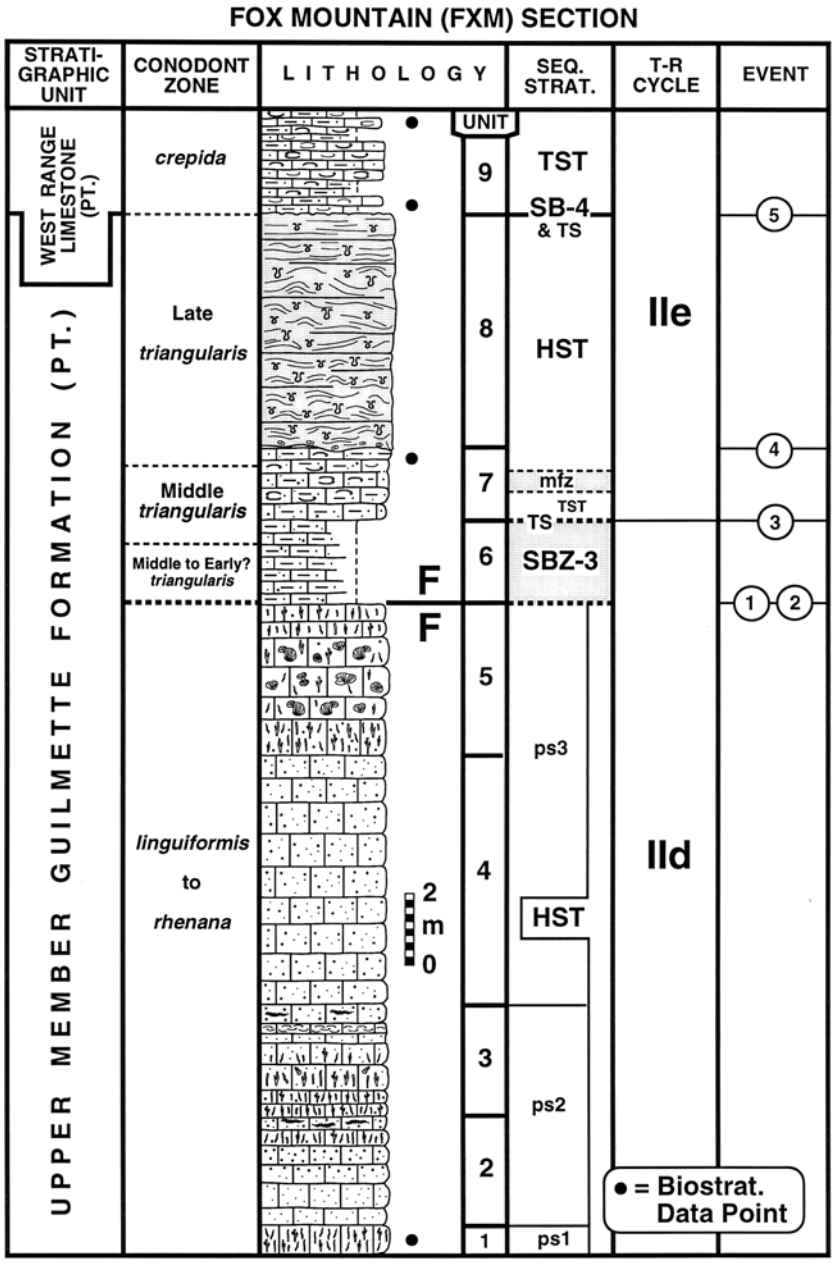

Figure 8. Stratigraphy, conodont biostratigraphy, sequence stratigraphy, and event stratigraphy of Fox Mountain (FXM) section in NW1/4 sec. 13, T. 4 N., R. 61 E., and SW1/4 sec. 12, T. 4 N., R. 61 E., lat 38.21° N., long 115.08° W., Nye County, Nevada (Timber Mtn. Pass NE 7.5-minute quadrangle).

the uppermost Frasnian part of section FXM consists of shallowing-upward parasequences of oncoidal/peloidal wackestone to packstone and stratiform stromatoporoid/coral bafflestone to wackestone biostromes. The stratigraphy and structure of Fox Mountain and the adjacent Seaman Range area were most recently described by Hurtubise and Du Bray (1992) and Du Bray and Hurtubise (1994). Brachiopod data were given by Mayer (1994).

The F-F boundary and associated SBZ-3 occur at the base of a 2-m-thick, peritidal to shallow-subtidal peloidal wackestone interval (unit 6), which is overlain by a transgressive, deeper-water, thin-bedded, sandy, bioclastic wackestone and packstone interval (unit 7; Fig. 7b) containing Famennian (Middle to Late *triangularis* Zone) shallow-water conodonts (Morrow, 2000) and athyrid and productid brachiopod species (J. Day, in Morrow, 2000). A major siliciclastic influx within the Late *triangularis* Zone marks unit 8, although the interval appears more condensed, clastic-rich, and amalgamated by bioturbation than correlative strata at section BME. Consequently, the interval is not readily divisible into discrete parasequence packages.

Transgressive, thin-bedded, silty bioclastic limestones of the West Range Limestone (unit 9) sharply overlie the medium-grained quartz arenite of unit 8, and mark the same forced SB-4 as at BME. Famennian brachiopods from this interval include a relatively diverse assemblage containing at least four species of athyrids, rhynchonellids, and spiriferids (J. Day, in Morrow, 2000). In summary, important events recorded at section FXM correspond closely to those recognized at section BME (Fig. 6).

4.3 Tempiute Mountain (TPM)

In contrast to sections BME and FXM, section TPM (Fig. 9) represents a deeper-water, upper-slope facies of the Devils Gate Limestone (Sandberg *et al.*, 1997). Previous studies of Tempiute Mountain include Chamberlain and Gillespie (1993), Morrow (1993, 1997, 2000), Chamberlain and Warme (1996), Kuehner (1997), Sandberg *et al.* (1997), and Chamberlain (2000). Section TPM is characterized both by deeper-water facies containing pelagic conodont faunas that allow detailed biocorrelation and by interbeds of shelf-derived sediments that allow correlation with sequence stratigraphic units and event markers recognized in the shallower-water setting to the east.

At this locality, the base of the F-F boundary transition interval is marked by the Alamo Breccia, an impact-related carbonate megabreccia unit that occupies more than 15,000 km^2 of southern Nevada and forms an important event marker for regional correlation of Upper Devonian strata across middle- and outer-shelf settings (Warme and Sandberg, 1995, 1996; Chamberlain and Warme, 1996; Kuehner, 1997; Warme and Kuehner, 1998; Chamberlain, 2000). The Alamo Breccia was proposed as a formal member

of both the Guilmette Formation and Devils Gate Limestone by Sandberg *et al.* (1997).

The base of section TPM is at the top of the highest normally graded carbonate turbidite (Unit A) that caps the Alamo Breccia (Fig. 9). Overlying the Alamo Breccia is a 7-m-thick interval of thin-bedded, cherty, cricoconarid-bearing limestone (unit 1) marked by an oxidation zone resulting from diagenetic alteration, possibly related to a fault. The interpretation of a relatively deep-water, maximum flooding setting for this post-breccia interval is consistent with sedimentologic and conodont biofacies data presented by Sandberg and Warme (1993) and Warme and Sandberg (1995). Our finding of deep-water entomozoan ostracodes in this interval, just south of our measured section, contradicts the interpretation of Chamberlain and Warme (1996), who considered the alteration zone to represent a sequence-boundary paleosol.

The next higher interval (units 2-3) includes silty, sandy, and peloidal turbiditic limestone marked at the top by a possible sequence boundary. Thin transgressive and highstand parasequences of overlying units 4-5 are dominated by multiple-sourced turbidites, generally ≤20 cm thick, which are characterized by black, micrograded, very fine- to fine-grained, lithic quartz sandstone and quartzite that are overlain by dark-gray, irregularly cross-laminated, peloidal lime wackestone and very fine-grained sandstone capped by pink, laminated siltstone. Overlying this interval is unit 6, which contains a condensed, cherty, sandy, and phosphatic lag bed containing abundant conodonts, phosphatized entomozoan and other ostracodes, cricoconarids, and peloids (Fig. 7c). Unit 6 is interpreted to record Early *rhenana* Zone SB-1 and associated transgressive surface marking the base of overlying T-R cycle IId-1.

Above is unit 7, which consists of transgressive, thin-bedded limestones, sandstones, and calcareous siltstones. Unit 7 is sharply overlain by unit 8, which consists of a 5-m-thick, massive, poorly sorted, intraclast- and peloid-rich quartz sandstone and sandy limestone interval with reworked atrypid brachiopods and thamnoporid corals. Unit 8 is interpreted to contain multiple event beds recording the transport and deposition of shallow-water-derived sediments into the slope setting, possibly due to localized shelf-margin collapse during transgression. Beds overlying unit 8 include maximum flooding zone and highstand siliceous siltstones, calcareous siltstones, silty limestones, and quartz sandstones (units 9-10). Unlike unit

Figure 9. Stratigraphy, conodont biostratigraphy, sequence stratigraphy, and event stratigraphy of Tempiute Mountain (TPM) section in SW1/4 sec. 1 (unsurveyed), T. 4 S., R. 56 E., lat 37.62° N., long 115.64° W., Lincoln County, Nevada (Tempiute Mountain North and Tempiute Mountain South 7.5-minute quadrangles).

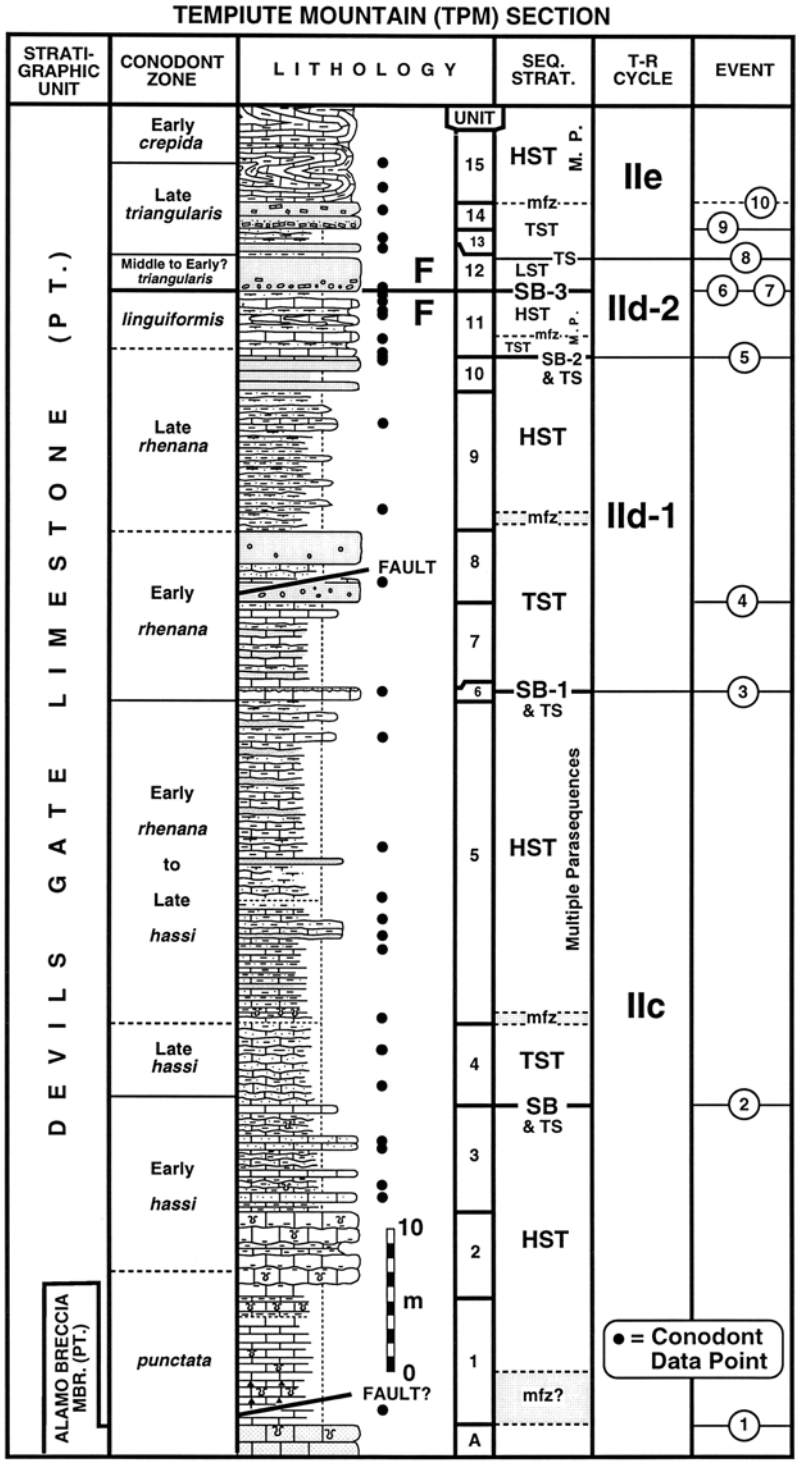
TEMPIUTE MOUNTAIN (TPM) SECTION
STRATI-GRAPHIC UNIT
CONODONT ZONE
LITHOLOGY
SEQ. STRAT.
T-R CYCLE
EVENT
UNIT
DEVILS GATE LIMESTONE (PT.)
ALAMO BRECCIA MBR. (PT.)
Early crepida
Late triangularis
Middle to Early? triangularis
linguiformis
Late rhenana
Early rhenana
Early rhenana to Late hassi
Late hassi
Early hassi
punctata
F
F
FAULT
FAULT?
10
m
0
15
14
13
12
11
10
9
8
7
6
5
4
3
2
1
A
HST
M. P.
mfz
TST
TS
LST
SB-3
HST
mfz
M. P.
TST
SB-2 & TS
HST
mfz
TST
SB-1 & TS
HST
Multiple Parasequences
mfz
TST
SB & TS
HST
mfz?
IIe
IId-2
IId-1
IIc
10
9
8
6
7
5
4
3
2
1
● = Conodont Data Point

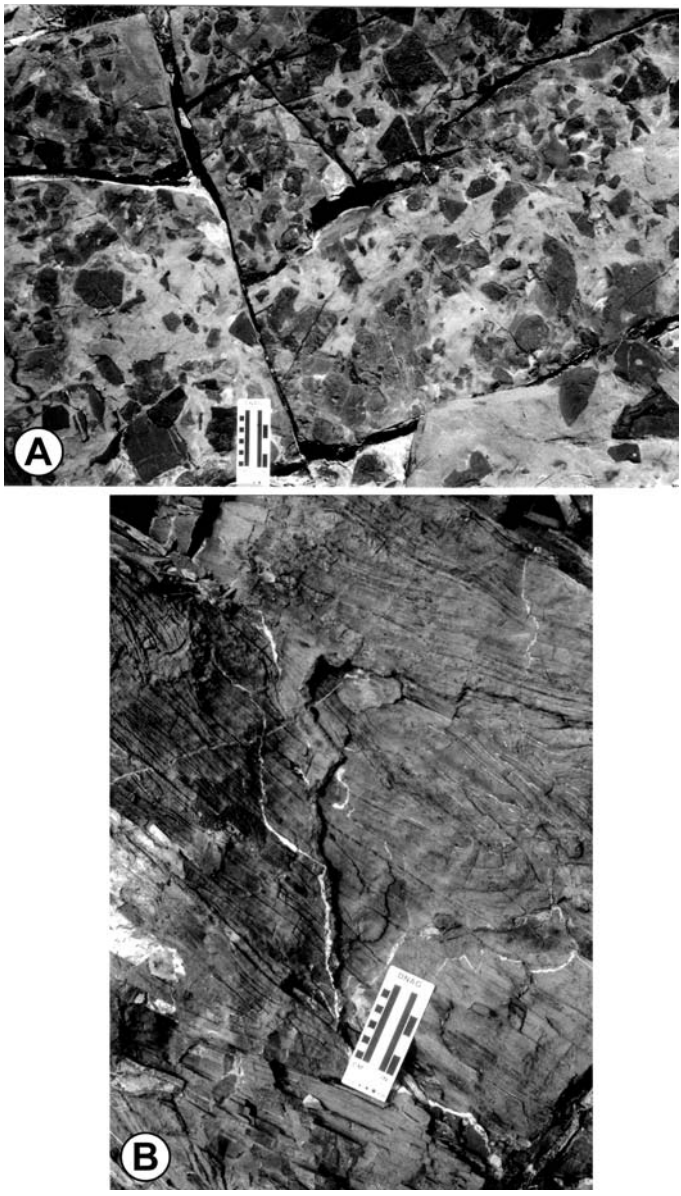

Figure 10. A. Outcrop photograph of spectacular, Early to Middle *triangularis* Zone carbonate-clast debris-flow breccia containing a light-colored, poorly sorted, silty to coarse-grained sandstone matrix, equivalent to unit 12 of Tempiute Mountain (TPM) section, exposed 3.5 km south of section TPM, Devils Gate Limestone; view of upper bedding plane surface. Scale is 10 cm long. B. Outcrop photograph of isoclinal, synsedimentary folding in thin-bedded slope turbidites composed of dark-gray to black, silty, spiculiferous lime mudstone/wackestone and laminated, pink calcareous siltstone couplets, unit 15, Devils Gate Limestone, Tempiute Mountain (TPM) section. Scale is 10 cm long.

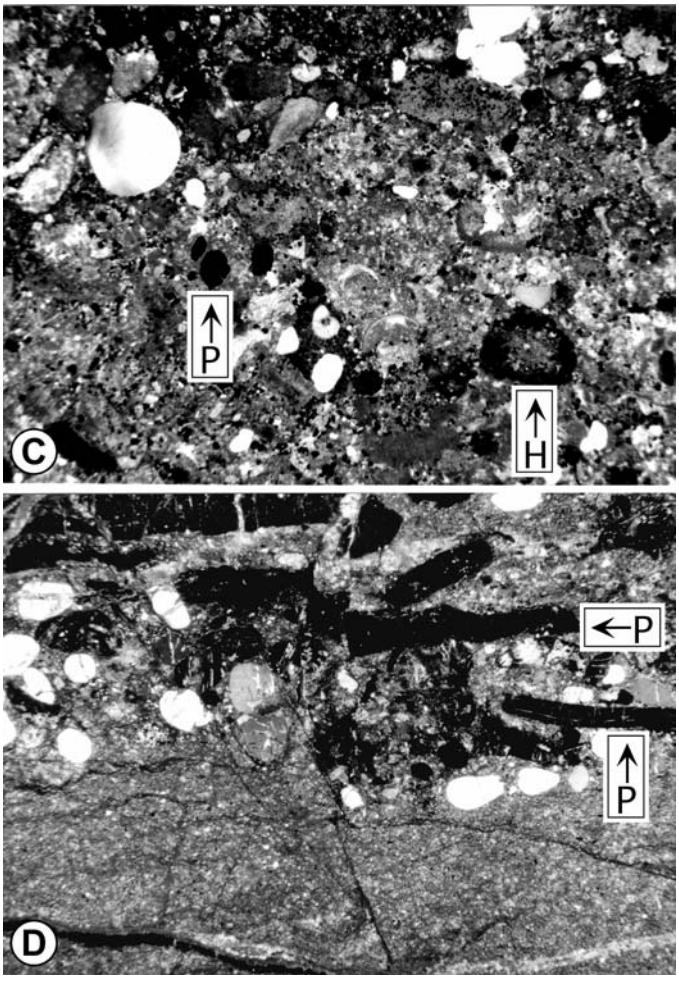

Figure 10. Continued. C. Photomicrograph showing latest *linguiformis* Zone sandy, peloidal bioclastic grainstone containing phosphatic peloids (**P**), disseminated hematite, and hematite-replaced allochems (**H**), top of unit 7, lower member Pilot Shale, Granite Mountain (GRM) section. Field of view is 6 mm across; crossed nicols. This layer directly underlies the F-F boundary and corresponding SB-3. D. Photomicrograph of early *linguiformis*? Zone lime mudstone sharply overlain by sandy, phosphatic packstone containing abundant silt to medium-grained quartz sand, phosphatic peloids, and phosphatic skeletal debris (**P**) at the top of unit 5, lower member Pilot Shale, Black Point South (BPS) section. This contact is interpreted to mark one of multiple, closely spaced condensed intervals formed by the transgression at the base of T-R cycle IId-2. Field of view is 6 mm across; crossed nicols.

8, the unit 10 sandstone lacks clear evidence of abundant redeposited clasts or basal submarine erosion and is considered to be of probable late highstand origin.

The sequence boundary marking the top of this interval (SB-2) is sharply

transgressed by uppermost Frasnian *linguiformis* Zone strata that mark the base of T-R cycle IId-2, and consist of turbidites of dysoxic, irregularly laminated, dark-blue-gray to black, silty lime mudstone and pink, laminated calcareous siltstone (unit 11) that locally show synsedimentary deformation such as isoclinal folding (Fig. 7d). Laminations within the black lime mudstone are defined by variations in quartz silt concentration, and rarely are disrupted and cross-cut by silt-filled burrows.

The F-F boundary is placed directly above unit 11 at SB-3, which is marked by a sharp, erosive contact with the overlying limestone intraclast-bearing, peloidal quartz sandstone (unit 12) containing reworked latest Frasnian (Late *rhenana* or *linguiformis* Zone) conodonts at its base. At the end of Tempiute Mountain 3.5 km southward, this unit tapers to approximately 1 m in thickness but forms a spectacular limestone debris-flow breccia (Fig. 10a) containing ≤50 cm-wide clasts of slope to outer-shelf, dark peloidal limestone, silty and sandy limestone, quartzite, and scarce pebbles of black radiolarian chert in a poorly sorted, silty to coarse-grained sandstone matrix. Roughly imbricated clasts within this bed dip SE, indicating a NW, probable shelf-to-basin, current direction. This paleocurrent orientation is confirmed at section TPM, where cross-bedding within unit 12 dips NW and NNW, also indicating an offshore to oblique offshore-longshore transport direction. The top of this sandstone unit is Late *triangularis* Zone in age, showing that the Early to Middle *triangularis* Zone interval is condensed within the approximately ≤3 m thickness of unit 12.

Deeper-water, Late *triangularis* Zone siltstone and sandy siltstone (unit 13) of the lower part of T-R cycle IIe are punctuated by a 2 m interval of massive, tan to pink, poorly sorted, intraclast-rich, silty to coarse-grained quartz sandstone and sandy limestone debris-flow breccia (unit 14) containing abundant clasts ≤20 cm-across of dark peloidal lime mudstone and silty to sandy limestone. In the middle of unit 14, a sharp, oxidized surface separates the debris-flow interval into upper and lower parts and may indicate a depositional break. Like unit 12, this bed is laterally continuous but thinner at the south end of Tempiute Mountain, where it forms a 1-m-thick bed similar in composition and texture to that at section TPM. Early Famennian debris-flow-event deposits are a widespread and characteristic feature of slope-to-basin F-F boundary sections in the region, and are discussed in more detail below.

Overlying unit 14 are deeper-water, retrogradational parasequence couplets of isoclinally folded, turbiditic, dysoxic, dark blue-gray to black, spicule-rich wackestone and pink, laminated calcareous siltstone that evidence localized slope failure (unit 15; Fig. 10b). At section TPM, the forced SB-4 associated with onlapping of the West Range Limestone at sections BME and FXM would lie above the study interval (see Chamberlain

and Warme, 1996).

Important events recorded at section TPM include: (1) the Alamo Event; (2) an Early *hassi* Zone sequence boundary; (3) SB-1, sharp transgressive surface, and condensed interval marking the base of T-R cycle IId-1; (4) deposition of shallow-water-derived, sandy debris-flow event beds; (5) SB-2 and subsequent transgression leading to the start of dark, dysoxic sedimentation within the *linguiformis* Zone (start of T-R cycle IId-2); (6) sea-level fall, SB-3, and turnover in conodont faunas at the F-F boundary; (7) erosive deposition of debris-flow breccia within subsequent lowstand deposits; (8) deepening at the start of T-R cycle IIe; (9) deposition of a second, Late *triangularis* debris-flow breccia event unit; and (10) further deepening that continued at least into the Early *crepida* Zone, with abundant soft-sediment deformation in upper-slope deposits.

4.4 Granite Mountain (GRM)

At section GRM (Fig. 11), the F-F boundary interval is in the lower part of the lower member of the Pilot Shale, a sequence of deep-water, protoflysch turbiditic calcareous and siliceous siltstone, sandstone, and debris-flow limestone deposited in the eastward-expanding intrashelf Pilot Basin (e.g., Sandberg *et al.*, 1980, 1989; Fig. 2 this report). The regional Upper Devonian stratigraphy and biostratigraphy of the Pilot Shale in the Confusion Range/Granite Mountain area has been documented by Sandberg and Poole (1977), Gutschick and Rodriguez (1979), and Sandberg *et al.* (1980, 1989, 1997). F-F boundary sedimentology, conodont biostratigraphy, and event stratigraphy have been analyzed in detail at two localities near Granite Mountain—the Little Mile-and-a-Half Canyon section (Sandberg *et al.*, 1980, 1989, 1997) and the Coyote Knolls section (Sandberg *et al.*, 1988, 1997). Major, minor, and trace element concentrations in F-F boundary strata at these two localities have been geochemically analyzed (Goodfellow *et al.*, 1989b; Bratton *et al.*, 1999). In the upper Frasnian interval, section GRM contains a higher ratio of limestone than the Coyote Knolls section; this has aided in the recovery and documentation of *linguiformis* Zone conodont faunas.

Section GRM begins with a series of retrogradational parasequences of bioturbated, fine-grained quartz sandstone and calcareous siltstone to silty limestone (units 2-3) that contain increasing amounts of lamination and oxidized condensation surfaces between parasequences upward through the interval. The overlying highstand deposits at the top of T-R cycle IId-1 (unit 4) consist of dark-gray, bioturbated silty limestones locally showing

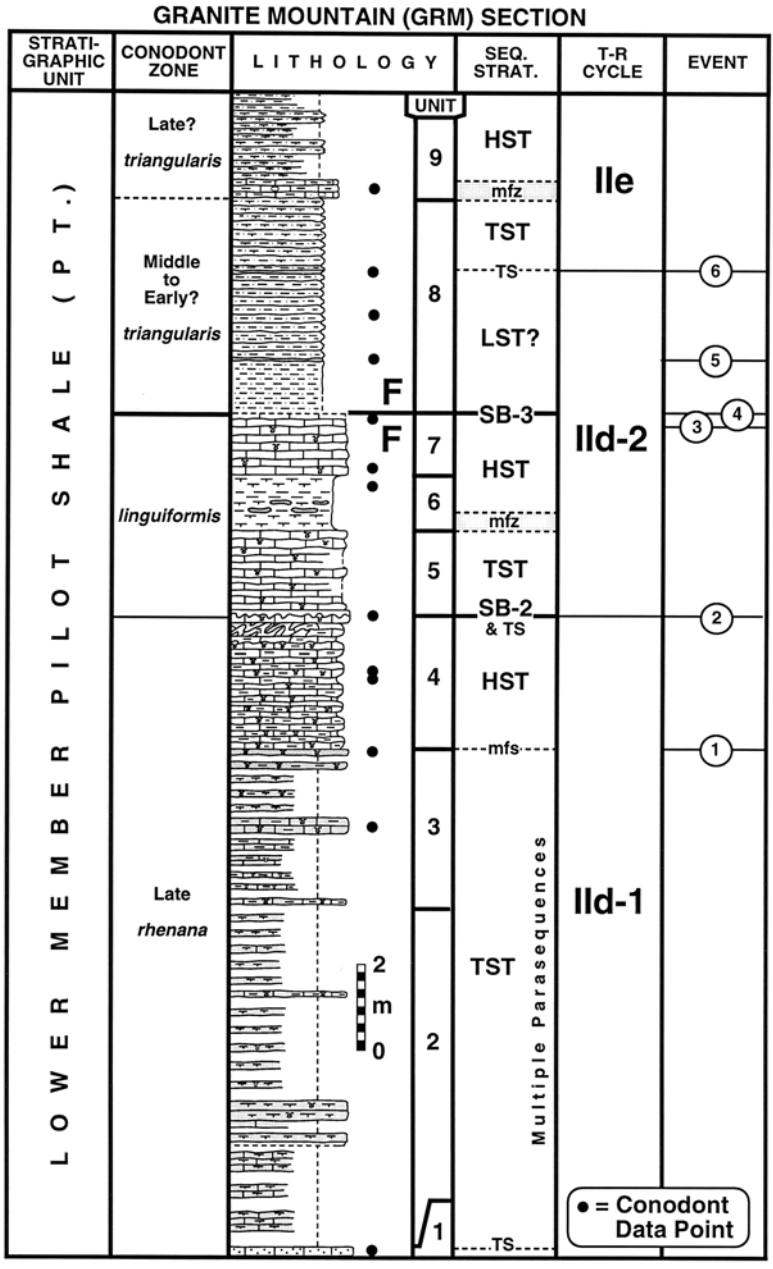

Figure 11. Stratigraphy, conodont biostratigraphy, sequence stratigraphy, and event stratigraphy of Granite Mountain (GRM) section in SW1/4 and SE1/4 sec. 17 (unsurveyed), T. 14 S., R. 16 W., lat 39.60° N., long 113.67° W., Juab County, Utah (Granite Mountain 7.5-minute quadrangle).

synsedimentary deformation. These are capped by a thin, bioclastic sandstone bed (basal unit 5) containing abundant quartz sand, bioclasts, phosphatic peloids, ichthyoliths, and *linguiformis* Zone conodonts. This sandstone bed is interpreted to represent a sequence boundary (SB-2) and subsequent transgressive surface with associated condensed interval marking the start of T-R cycle IId-2.

The overlying latest Frasnian interval (units 5-7) contains dark-brown, organic-rich calcareous siltstone and dark-gray to brown, sandy, bioclastic peloidal limestone that record the abrupt deepening and shallowing of T-R cycle IId-2 within the *linguiformis* Zone. The F-F boundary lies at the top of unit 7, which is capped by a thin, highly oxidized, sandy bioclastic grainstone bed containing abundant disseminated hematite crystals and partly hematite-replaced bioclasts (Fig. 10c).

Overlying this sequence boundary (SB-3), are Early? to Middle *triangularis* Zone lowstand and transgressive deposits (unit 8) consisting of medium-brown, organic-rich laminated shales and siltstones containing very thin, medium- to coarse-grained quartz sand debris-flow beds that are overlain by Late *triangularis* Zone, deeper-water, sparsely fossiliferous calcareous siltstones and silty lime mudstones (unit 9) marking the maximum flooding zone interval.

Events recognized at section GRM include: (1) relative deepening associated with the transition from oxidized, fine-grained siliciclastic to dark, organic-rich limestone deposition within T-R cycle IId-1; (2) SB-2, transgressive surface, and condensation at the base of T-R cycle IId-2; (3) late *linguiformis* Zone shallowing just prior to the F-F boundary; (4) F-F boundary mass extinction and SB-3; (5) deposition of earliest Famennian lowstand to early transgressive, very thin-bedded, coarse-grained siliciclastic event beds correlative with other coeval high-energy-event marker beds present at other localities; and (6) transgressive surface, deepening, and increased carbonate content marking the base of T-R cycle IIe.

4.5 Northern Pancake Range (NPA)

At section NPA (Fig. 12), the F-F boundary transition lies within a series of mixed turbiditic sandstones, limestones, and siltstones of the lower member of the Pilot Shale. At this locality, the Pilot Shale overlies the upper member of the Devils Gate Limestone. The approximate stratigraphic thickness between the top of the Devils Gate Limestone and the base of unit 4 in section NPA (Fig. 12) is 190 m. However, covered intervals in the strike valley between exposures of the two formations probably mask several faults and folds.

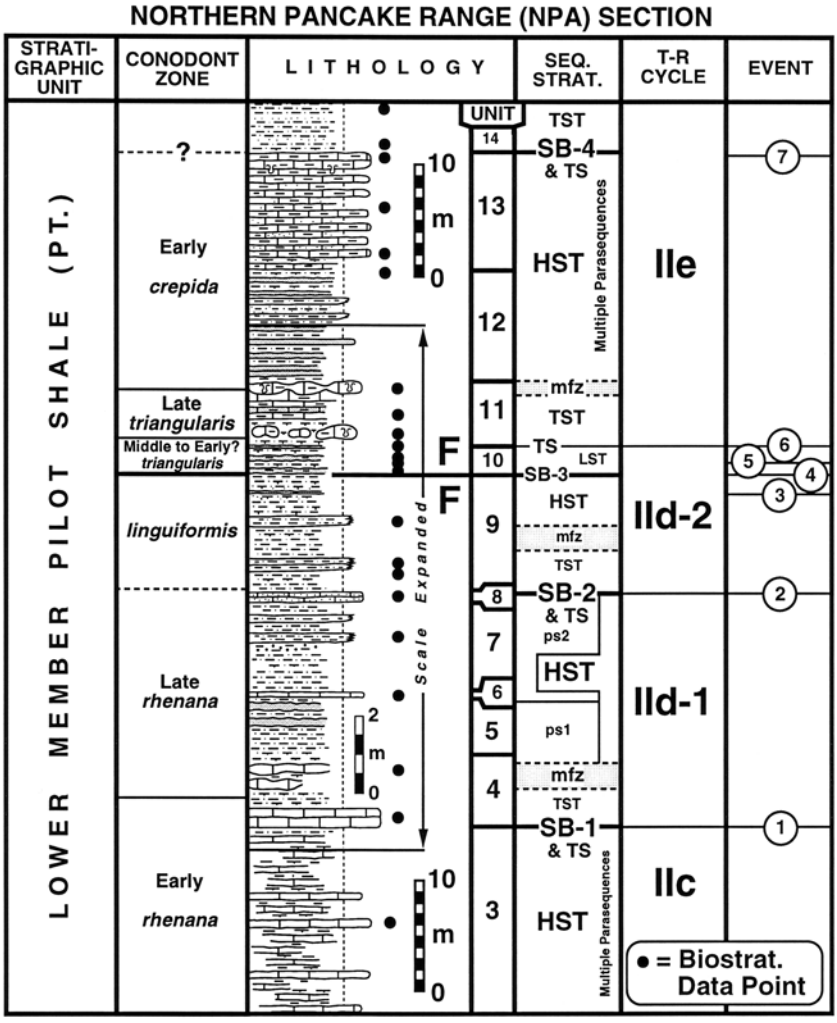

Figure 12. Stratigraphy, conodont biostratigraphy, sequence stratigraphy, and event stratigraphy of Northern Pancake Range (NPA) section. Note scale change across the F-F boundary. Section is located in NE1/4 sec. 35 and SE1/4 sec. 26, T. 17 N., R. 55 E., lat 39.30° N., long 115.74° W., White Pine County, Nevada (Pancake Summit SW 7.5-minute quadrangle).

The base of section NPA is within Early *rhenana* Zone highstand parasequences of thin- to medium-bedded, laminated turbidites. These turbidites consist of bioclastic, peloidal wackestone and dark-brown, calcareous and siliceous siltstone (unit 3) containing bioclastic-rich horizons of spicules, cricoconarids, and small brachiopods. Strata above the overlying SB-1 and transgressive surface that marks the beginning of T-R

cycle IId-1 consist of laterally persistent, transgressive and maximum flooding zone units of dark-blue-gray to black, silty, cricoconarid-bearing lime mudstones and wackestones that characteristically weather a light blue gray (unit 4). The overlying Late *rhenana* Zone highstand parasequences of interbedded dark-gray to black siltstone, sandstone, and limestone (units 5-7) are capped by a distinctive silty-sandy bioclastic grainstone bed (unit 8) that is interpreted to mark SB-2 and a transgressive surface at the base of T-R cycle IId-2. This bed contains abundant phosphatic inarticulate brachiopods, ichthyoliths, and conodonts (>7,000 platform conodont elements per kg of dissolved sample) that indicate the late part of the Late *rhenana* Zone (Morrow, 2000).

The deeper-water sequence within T-R cycle IId-2 consists of medium- to dark-brown, laminated, calcareous and siliceous siltstone containing abundant disseminated organic material and hematite (unit 9). Late highstand influx of red to orange, hematitic, very fine-grained quartz sand records increasing oxygenation of the basin and the beginning of shallowing in the latter part of the *linguiformis* Zone that culminated at the F-F boundary (SB-3). The Early? to Middle *triangularis* Zone (unit 10) consists of thin-bedded, silty to very fine-grained, oxidized? debris-flow quartz sandstones and siltstones (unit 10) that contain scattered organic material, rare conodonts, and rare, unidentifiable lingulid brachiopods (J. Day, in Morrow, 2000). These are interpreted as lowstand sediments that underlie transgressive, condensed, silty, nodular lime mudstone and calcareous siltstone (Late *triangularis* and Early *crepida* Zones, unit 11) at the base of T-R cycle IIe.

Debris-flow sandstones within unit 10 are probably correlative with lower Famennian high-energy units recorded in other sections, most notably the well-developed Early *triangularis* Zone limestone debris-flow breccia present at Devils Gate (Sandberg *et al.*, 1988; also see below). Overlying highstand parasequences of siltstone and sandstone (unit 12) are capped by late highstand deposits of turbiditic, silty and sandy bioclastic wackestone and packstone (unit 13). Abrupt deepening above, as indicated by siliceous siltstone (unit 14), is interpreted to mark the forced SB-4 associated with the tectonic expansion of the Pilot Basin.

Significant events at section NPA (Fig. 22) include: (1) SB-1 and transgression marking the base of T-R cycle IId-1; (2) SB-2, transgressive surface, and condensed interval at the base of T-R cycle IId-2, which preceded the deposition of dark, laminated, organic-rich sediments during the *linguiformis* Zone; (3) shallowing and increased basin oxygenation in the latter part of the *linguiformis* Zone; (4) continued shallowing and SB-3 at the F-F boundary; (5) earliest Famennian debris-flow quartz sandstone event stringers; (6) relative increase in carbonate content associated with abrupt

transgression and condensation at the base of T-R cycle IIe; and (7) retrogradational, deeper-water facies of the expanded Pilot Basin (SB-4).

4.6 Black Point South (BPS)

Section BPS (Fig. 13) begins 37 m above the top of the Devils Gate Limestone. The F-F boundary facies, which lie in the lower member of the Pilot Shale, are quite different from that of section NPA. The lower part of section BPS comprises Early(?) to Late *rhenana* Zone transgressive parasequences of turbiditic, medium-brown, very fine-grained calcareous sandstone and sandy siltstone (units 1-2) that contain abundant bedding-parallel feeding traces filled with coarser peloidal and bioclastic (fecal) material. An oxidized, limonite- and peloid-rich horizon capping unit 3 is interpreted as a maximum flooding surface that is overlain by highstand parasequences of sandy siltstone and very fine-grained sandstone (unit 4) similar to the underlying transgressive beds.

The top of T-R cycle IId-1 is delimited by SB-2 situated beneath unit 5, which is a bioclastic wackestone to lime mudstone containing at least two distinct surfaces of sandy, oxidized, phosphatic-grain-rich packstone (Fig. 10d). These surfaces are interpreted to be condensed intervals marking transgressive surfaces (start of T-R cycle IId-2) within the earliest phase of the subsequent transgressive systems tract deepening. The overlying unit 6 *linguiformis* Zone consists of parasequences of dysoxic, medium-olive-gray to dark-brown, laminated, organic-rich, sandy calcareous siltstone. Unit 6 is capped by the F-F boundary and SB-3, which are overlain by lowstand or transgressive?, oxidized, silty peloidal packstone and very fine-grained quartz sandstone of unit 7.

Overlying Famennian strata are truncated or removed by a prominent, laterally variable, 11-m-thick carbonate debris-flow event bed (unit 8) containing abundant, ≤15 cm-diameter clasts of dark-gray to blue-gray, silty, peloidal lime mudstone, bioclastic wackestone, and bioclastic packstone with common articulated brachiopods. The diverse megafauna sampled from this interval includes at least eight species of early Famennian athyrid, spiriferid, rhynchonellid, orthid, and productid brachiopods (J. Day, in Morrow, 2000). Late *triangularis* Zone conodont faunas recovered from this debris-flow bed contain common reworked late Frasnian (*linguiformis* Zone) elements that increase in relative abundance upward through unit 8, comprising as much as 45% of the total conodont fauna recovered near the top of the bed (Morrow, 2000). This upward-increase in reworked Frasnian elements suggests that erosion, eastward-transport, and redeposition of

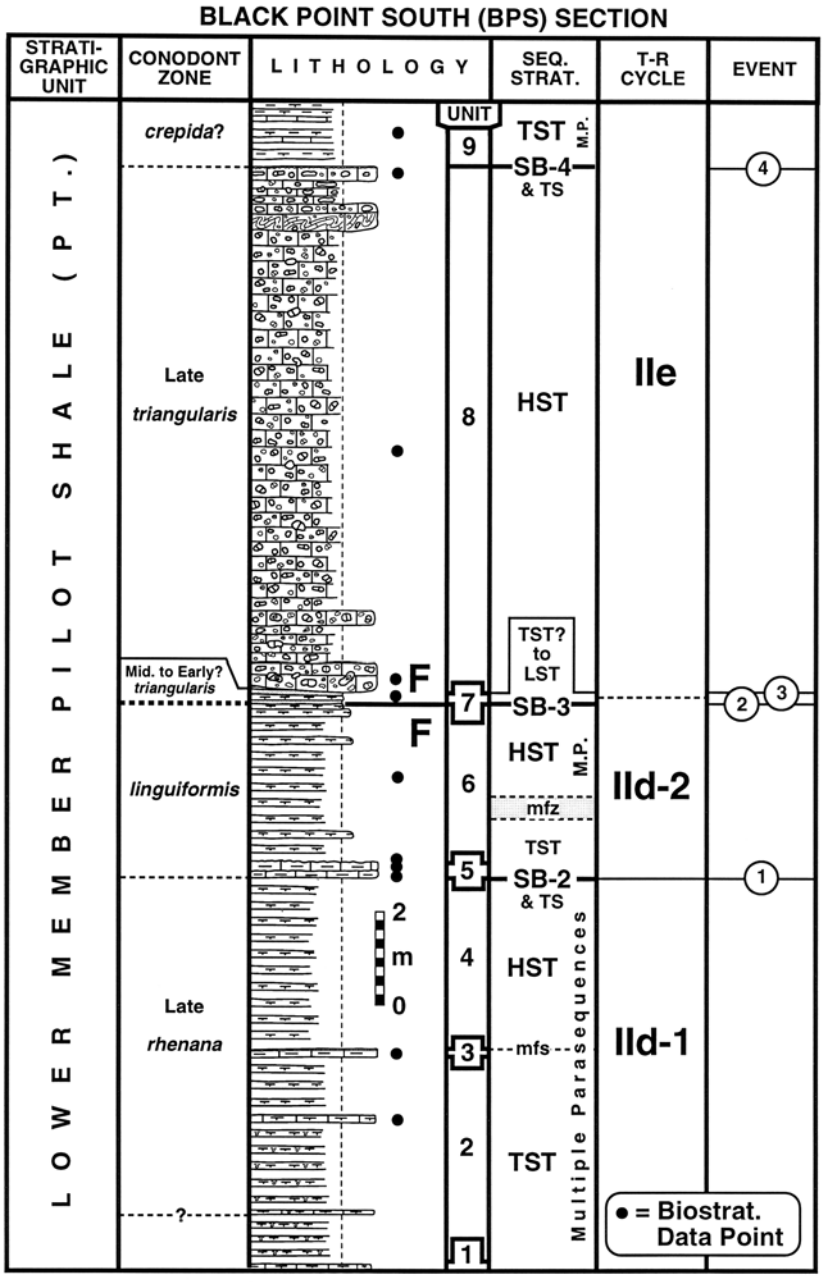

Figure 13. Stratigraphy, conodont biostratigraphy, sequence stratigraphy, and event stratigraphy of Black Point South (BPS) section in NW1/4 sec. 13 (unsurveyed), T. 16 N., R. 54 E., lat 39.26° N., long 115.85° W., White Pine County, Nevada (Black Point 7.5-minute quadrangle).

progressively older carbonate slope or shelf-edge material continued throughout the episode of debris-flow sedimentation.

Traced laterally north and south along strike, this debris-flow unit shows marked variation in thickness. In laterally continuous exposures 150 m north of section BPS, the unit 8 debris-flow bed thickens to more than 16 m, and downcuts as much as 1.5 m into underlying Frasnian strata, removing unit 7 and the top of unit 6 present at BPS. This debris flow can be correlated at least 15 km to the south near Nevada Governors Spring (C. A. Sandberg and F. G. Poole, unpub. data, 1995), although there it appears to consist of multiple, thinner beds intercalated within the Pilot Shale.

The top of unit 8 is an irregular, oxidized, burrowed or bored surface capped by abundant siltstone intraclasts, limonite, hematite, phosphatic debris, and quartz sand that are interpreted to mark SB-4 and a transgressive surface. This thin, ≤3 cm-thick transgressive lag is sharply overlain by *crepida*? Zone parasequences of silty and sandy peloidal lime mudstone and dark-brown, laminated, sandy siltstone that continue upward to the top of the section.

The summary of events present at section BPS include: (1) formation of SB-2 and multiple transgressive surfaces associated with deepening at the base of T-R cycle IId-1, followed by deposition of dark, dysoxic sediments within the *linguiformis* Zone; (2) shallowing and formation of SB-3 at the F-F boundary, with the subsequent start of T-R cycle IId-2 placed approximately just above this event marker; (3) deposition of carbonate debris-flow event bed (unit 8) within the Late *triangularis* Zone, with localized reworking and removal of latest Frasnian and earliest Famennian strata; and (4) relative deepening and development of forced SB-4 associated with expansion of the Pilot Basin.

4.7 Devils Gate (DVG)

The well-exposed Devils Gate section (Fig. 14), located 13 km west of Eureka at the type locality of the Devils Gate Limestone (Fig. 3), has received intense study over the past quarter-century (Sandberg and Poole, 1977; Sandberg *et al.*, 1988, 1989, 2001, *in press*; Ziegler and Sandberg, 1990) and is an important regional North American reference section for the Early *hassi* to Early *crepida* Zones of the Late Devonian standard conodont

Figure 14. Stratigraphy, conodont biostratigraphy, sequence stratigraphy, and event stratigraphy of Devils Gate (DVG) section. Stratigraphy, biostratigraphy, and events shown are after Sandberg and Poole (1977), Sandberg *et al.* (1988, 1989), and Ziegler and Sandberg (1990). Note scale change across the F-F boundary. Section is located in SE1/4 sec. 23, SW1/4 sec. 24, NW1/4 sec. 25, and NE1/4 sec. 26, T. 20 N., R. 52 E., lat 39.57° N, long 116.07° W, Eureka County, Nevada (Devon Peak 7.5-minute quadrangle).

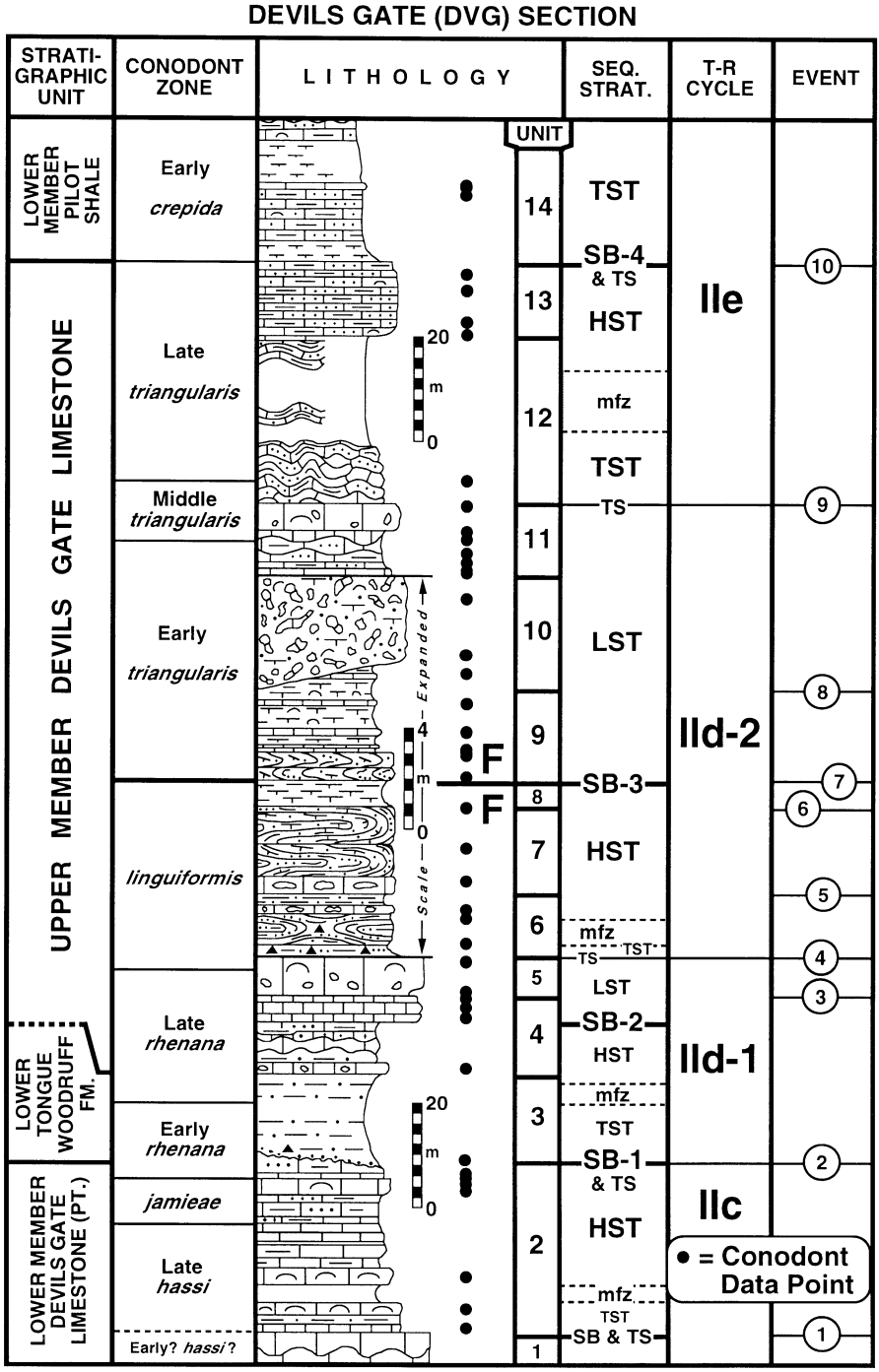

zonation (Ziegler and Sandberg, 1990). In addition to high-resolution

stratigraphy, sedimentology, and conodont biostratigraphy, the F-F boundary interval at DVG has also received detailed study for its regional to global event stratigraphy (Sandberg *et al.*, 1983, 1986, 1988, 1989, 1997, 2001, in press), brachiopod faunas (Sartenaer, 1985, 1988), ostracode faunas (Casier *et al.*, 1996; Casier and Lethiers, 1998), trace and rare earth element and organic-carbon content (Goodfellow *et al.*, 1989b), stable isotope content (Joachimski and Buggisch, 2000), and magnetostratigraphy (R. Reynolds and C.A. Sandberg, unpub. data, 1989).

Because of the importance of section DVG as an interregional F-F boundary reference locality, its event and sequence stratigraphy are discussed herein. For consistency with our other measured sections in this report and for convenience in tying systems tracts and important bounding surfaces to the F-F boundary and event stratigraphy described by Sandberg and others (references above), generalized unit numbers are assigned to the previously published DVG measured section (Fig. 14). In addition, the specific events shown in Fig. 14, which were previously documented by Sandberg and others, are re-numbered for consistency with the other columnar sections herein.

The base of our DVG section is near the top of an interval of shallow-water subnodular limestone (unit 1). This interval is bracketed below and above by Early *hassi* and Late *hassi* Zone faunas, respectively, but cannot be more precisely dated because its conodont faunas are dominated by non-diagnostic, shallow-water species of *Polygnathus* and *Icriodus* (Ziegler and Sandberg, 1990). Unit 1 represents a highstand systems tract that is capped by a sequence boundary and transgressive surface overlain by a Late *hassi*, *jamieae*, and early Early *rhenana* Zone interval of moderately deep-water lime and siliceous mudstone with bioclastic wackestone (unit 2). This interval is terminated by SB-1, which is directly overlain by a distinctive transgressive surface and condensed interval that contains extremely abundant Early *rhenana* Zone conodonts (>300,000 platform conodont elements per kg of dissolved sample), including the important, short-lived index species *Palmatolepis semichatovae*. Because of the global distribution of this species and associated eustatic deepening, this event is termed the '*semichatovae* transgression' or '*semichatovae* rise' (Sandberg *et al.*, 2001, 2002, *in press*). The *semichatovae* rise marks the base of T-R cycle IId-1 and the upper contact of the lower member of the Devils Gate Limestone.

Deposits of the overlying transgressive systems tract and maximum flooding zone (unit 3) comprise Early and Late *rhenana* Zone, deep-water siliceous siltstone and chert of the lower tongue of the Woodruff Formation (Sandberg *et al.*, *in press*). This interval is capped by Late *rhenana* Zone highstand deposits of thin-bedded, subnodular, silty limestone and SB-2 (lower part of unit 4). Above, medium-bedded (upper part of unit 4) and

thick-bedded, massive, debris-flow limestone (unit 5) containing common transported spherical stromatoporoids, atrypid brachiopods, and horn corals (Sandberg *et al.*, 1988) comprise probable lowstand deposits of the overlying sequence. This debris-flow bed is capped by a sharp transgressive surface marking the base of T-R cycle IId-2.

Overlying unit 5 is a thin transgressive systems tract composed of dark, anoxic, cherty siltstone (base of unit 6). This interval is directly beneath a maximum flooding zone (center of unit 6) marked by cherty, syndepositionally deformed, isoclinally folded slope limestones. Earliest highstand deposits consist of dark, nodular limestone and siltstone (top of unit 6), with the subtle turnaround from transgressive to highstand sedimentation evidenced within conodont faunas that show a corresponding reduction from 63% to 35% in abundance of the deep-water genus *Palmatolepis* (Sandberg *et al.*, 1988). As documented by Sandberg *et al.* (1988, 1997, 2002), marked sea-level fall beginning in the latest part of the *linguiformis* Zone is evidenced by changes in lithofacies (unit 7) and the concurrent increase in the relative abundance of the generally shallow-water conodont genus *Icriodus* from 0% to 31%. This late highstand interval is capped by an unfossiliferous, 1-m-thick, dark-yellow-brown calcareous mudstone (unit 8) that marks the highest, final extinction step directly beneath the F-F boundary (Fig. 15a).

SB-3 at the F-F boundary is overlain by an Early *triangularis* Zone lowstand systems tract consisting of isoclinally folded calcareous siltstone, calcareous mudstone, and thin-bedded limestone (unit 9) that is truncated above by a spectacular, massive debris-flow bed (unit 10; Fig. 15b). This debris flow is interpreted as a high-energy event unit resulting from sudden collapse of the adjacent carbonate shelf margin and ensuing tsunami (Sandberg *et al.*, 1988, 1997, 2002).

Compared to other F-F boundary sections both regionally and globally, this earliest Famennian lowstand systems tract is unusually thick, has a relatively high carbonate content, and contains an excellent record of Early *triangularis* Zone faunas. The Devils Gate area maintained adequate accommodation space during the maximum extent of the eustatic fall across the F-F boundary, yet was proximal to a relatively shallow-water carbonate sediment source that filled this space and preserved a record of the interval.

Subsequent late Early and early Middle *triangularis* Zone deposits of subnodular, silty, and debris-flow limestones (unit 11) are capped by a transgressive surface marking the base of T-R cycle IIe. The overlying transgressive and highstand interval at the top of the Devils Gate Limestone (units 12-13) consists of thin-bedded, silty limestone showing abundant

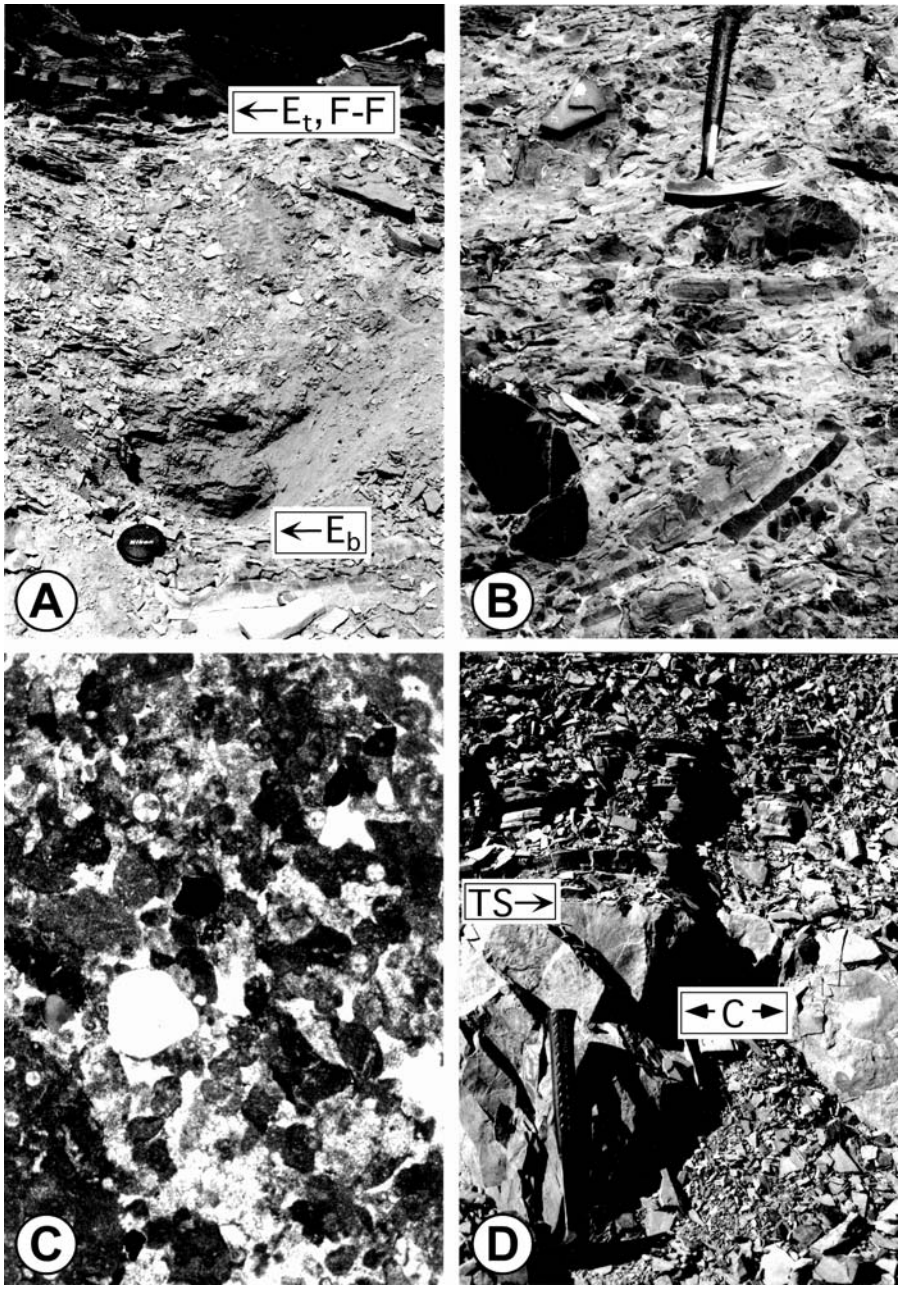

Figure 15. A. Outcrop photograph of Devils Gate (DVG) section, showing 1 m thick latest *linguiformis* Zone, dark-yellowish-brown, calcareous mudstone marking the largest, and final, step in the F-F boundary mass extinction; units 7-9, Upper Member Devils Gate Limestone. Base of extinction interval (**E_b**) overlies isoclinally folded, silty slope limestones; top of

synsedimentary deformation. SB-4 and an onlap surface are placed at the top of unit 13, which underlies Early *crepida* Zone transgressive deposits of calcareous siltstone and silty, debris-flow limestone of the lower Pilot Shale (unit 14). Unit 14 evidences tectonic deepening and westward expansion of the Pilot Basin, which established a short-term connection between the Pilot and Woodruff basins (Sandberg *et al.*, 2001, *in press*).

The likely paleogeographic setting of the upper Devils Gate Limestone was on a slope adjacent to the eastern margin of a developing, north-south trending, submarine forebulge, which is predicted by regional tectonic models (e.g., Carpenter *et al.*, 1994; Giles, 1994; Giles and Dickinson, 1995) and documented by correlations between Devils Gate and the northern Antelope Range (Sandberg *et al.*, 2001, *in press*). This forebulge, which was an eastward-migrating structure related to the developing Antler Orogeny, separated the deep-water basins of the Pilot Shale to the east and the Woodruff Formation to the west. As evidenced at DVG, two short-term connections between these basins developed – one associated with the *semichatovae* rise at the start of T-R cycle IId-1, which caused expansion of the Woodruff Basin eastward to Devils Gate; and a second associated with westward expansion of the Pilot Basin during the Early *crepida* Zone. Applying the forebulge model, allochthonous sediments present at Devils Gate were shed and transported from a relatively shallow-water submarine ridge on the west and redeposited to the east as slope debris flows transitional to, and intercalated with, lower Pilot Basin sediments. Redeposited shallow-water, possibly forebulge-derived, sediments are also documented within the previously discussed sections NPA and BPS, and at section NAR-A, discussed below.

---

extinction interval (**E_t**) corresponds with F-F boundary, and is interpreted to mark SB-3. Core holes from paleomagnetic analysis are visible directly above F-F boundary. See Sandberg *et al.* (1988) for detailed discussion of this interval. Lens cap is 6 cm across. B. Outcrop photograph of Devils Gate (DVG) section, showing Early *triangularis* Zone carbonate debris-flow breccia containing poorly sorted, redeposited intraclasts of shelf- to slope-derived carbonates and transported whole fossils and skeletal debris including corals and brachiopods, within the middle of unit 10, Upper Member Devils Gate Limestone. This unit is interpreted to be a catastrophic event bed resulting from a possible tsunami caused by sudden collapse of the adjacent tectonic forebulge. See Sandberg *et al.* (1988) for detailed discussion of this interval. Hammer for scale. C. Photomicrograph of *linguiformis* Zone sandy, coated-grain peloidal packstone/grainstone containing abundant micrite-coated calcispheres and rare allochems including other calcareous algae and ostracods, upper part of unit 6, Fenstermaker Wash Formation, Northern Antelope Range (NAR-A) section. This lithology is a characteristic example of upper Frasnian sediments at this locality. Field of view is 4 mm across; crossed nicols. D. Outcrop photograph of Late *rhenana* Zone dolosiltstone concretion interval (**C**) at the top of unit 3, overlain by transgressive surface (**TS**) and *linguiformis*? Zone black, laminated siliceous radiolarian mudstone and shale at the base of unit 4, Woodruff Formation, Whiterock Canyon (WMO) section. Hammer for scale.

Following Sandberg *et al.* (1988, 1997, 2001, 2002, *in press*), important events at section DVG include: (1) Early or Late *hassi* Zone sequence boundary and transgressive surface that cap a shallow-water shelf carbonate interval (unit 1); (2) SB-1 and subsequent *semichatovae* rise at the onset of T-R cycle IId-1, which is marked by a sharp transgressive surface and condensed sedimentation interval (base of unit 3) and initiated a short-term connection with the Woodruff Basin, as evidenced by deep-water, highstand sediments of the lower tongue of the Woodruff Formation; (3) late highstand debris-flow sedimentation events (unit 5) across the Late *rhenana* Zone-*linguiformis* Zone boundary, which record the end of T-R cycle IId-1; (4) transgression, start of T-R cycle IId-2, and onset of basinal anoxia within the *linguiformis* Zone (base of unit 6); (5) beginning of abrupt sea-level fall late in the *linguiformis* Zone and concurrent change in conodont biofacies (base of unit 7); (6) deposition of extinction layer (unit 8) and final step in the mass extinction; (7) turnover in conodont faunas and SB-3 formation at the F-F boundary; (8) catastrophic deposition of thick, Early *triangularis* Zone carbonate debris-flow bed (unit 10); (9) deepening event and transgressive surface marking base of T-R cycle IIe; and (10) forced SB-4 and further deepening associated with westward expansion of the Pilot Basin, which established a second, short-term link with the Woodruff Basin to the west.

4.8 Northern Antelope Range (NAR-A)

Compared to other F-F boundary sections in the region, facies development at section NAR-A (Fig. 16) is atypical, reflecting a paleogeographic setting strongly influenced by the developing proto-Antler forebulge. The F-F boundary at NAR-A lies within a relatively homogenous interval of allodapic, quartz-sand-rich, coated-grain peloidal and debris-flow limestones. This interval was previously assigned to various lithostratigraphic units, including "quartzose limestone" within the uppermost Denay Limestone (Johnson *et al.*, 1986b), unnamed Devonian [Frasnian] sandstone (Johnson *et al.*, 1980, 1996), the upper part of the Fenstermaker Wash Formation (Hose *et al.*, 1982), and the Fenstermaker Limestone (Waldman, 1990). These and other rocks in the northern Antelope Range area are also discussed by Merriam (1963), Trojan (1978), and Poole and Sandberg (1993).

As originally defined, the lower part of the Fenstermaker Wash Formation incorporates strata of varied lithology and origin that are more accurately assigned to the upper Denay Limestone (Johnson *et al.*, 1989, p. 178). Waldman (1990) informally proposed a restricted "Fenstermaker Limestone" to encompass only the upper, cliff-forming part of the

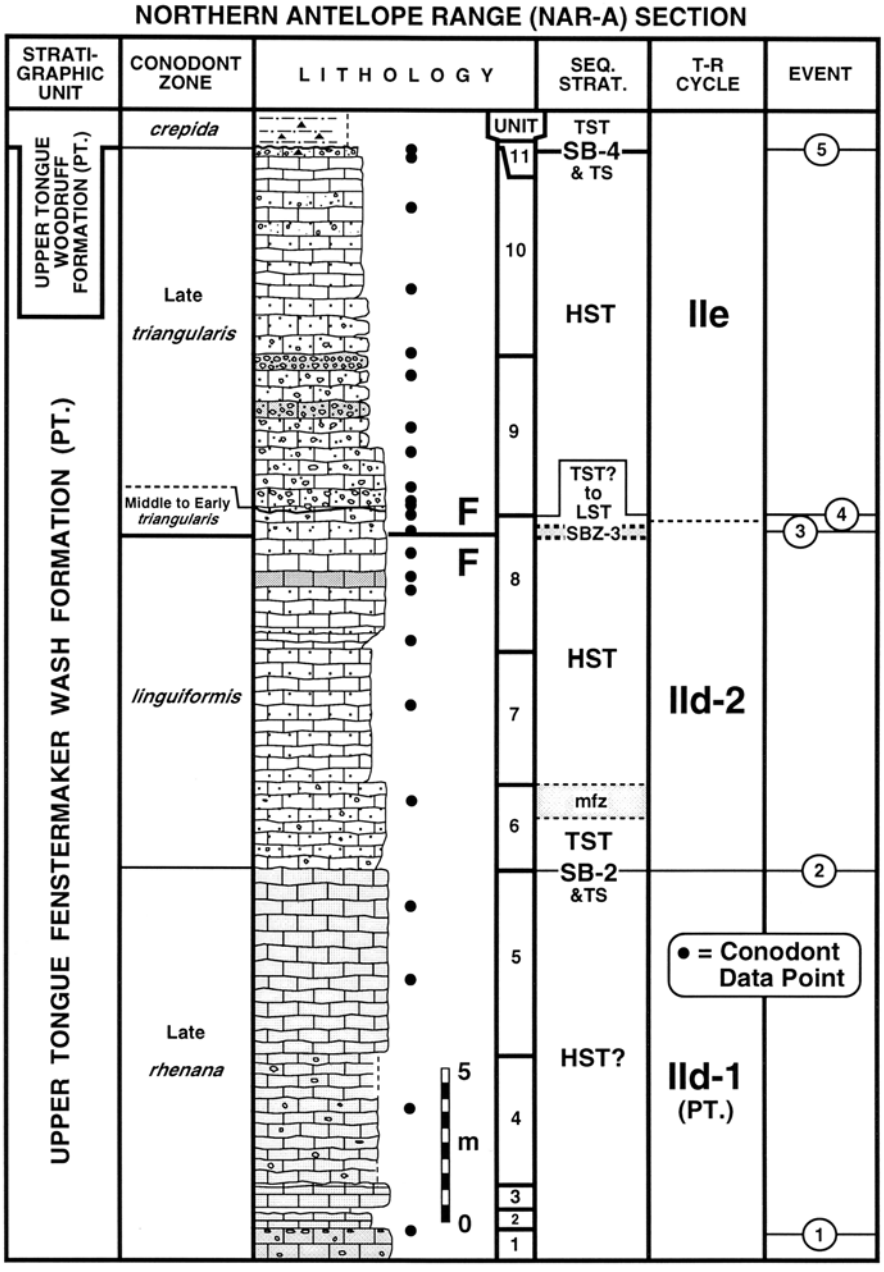

Figure 16. Stratigraphy, conodont biostratigraphy, sequence stratigraphy, and event stratigraphy of Northern Antelope Range (NAR-A) section in NE1/4 sec. 20, T. 16 N., R. 51 E., lat 39.24° N., long 116.24° W., Eureka County, Nevada (Cockalorum Spring 7.5-minute quadrangle).

Fenstermaker Wash Formation, including the sandy and debris-flow limestones of latest Frasnian and earliest Famennian age. However, the Fenstermaker Limestone is now recognized to be the highest of several similar, forebulge-related units intercalated between tongues of deep-water, lower-slope Woodruff Formation. Based on this, Sandberg *et al.* (*in press*) have redesignated the Fenstermaker Limestone as the upper tongue of the Fenstermaker Wash Formation.

Tongues of the Fenstermaker Wash Formation, as defined by Sandberg *et al.*, are currently recognized in the northern Antelope Range and in isolated outcrops intercalated within the Woodruff Formation in the southern Fish Creek Range (Poole *et al.*, 1983; Sans, 1985; Waldman, 1990; C.A. Sandberg and F.G. Poole, unpub. data, 1994-2001). In addition, thin tongues of this unit are probably also present in the northern Pancake Range (Fig. 3), just east of the Fish Creek Range.

In the northern Antelope Range, the upper tongue of the Fenstermaker Wash Formation, including the F-F boundary, is most commonly exposed on dip slopes, making detailed measurement and sampling of this interval difficult (e.g., Waldman, 1990). However, our section NAR-A, which was measured upward across a triangular, laterally fault-bounded block located approximately 600 m south of section III of Johnson *et al.* (1980), contains an F-F boundary interval (late Late *rhenana* through Late *triangularis* Zones) that is complete and well exposed on ledges and cliff faces.

The F-F boundary transition is dominated by reworked and resedimented peloidal carbonate and quartz sand grains of relative shallow-water origin incorporated into allodapic-sediment gravity and debris flows. The quartz sand is commonly admixed with carbonate grains, and discrete quartz sandstone lenses or beds are rare. An unusual feature of section NAR-A is the relative homogeneity of the outcrop expression. Recognition of medium- to large-scale features such as bedding, bed contacts, or other sedimentary structures is difficult due to the relatively monotonous color, texture, and massive outcrop profile of the section.

Waldman (1990) favored a relatively shallow-water depositional setting for this interval based on its uniform medium- to dark-olive-gray color, abundance of peloids and coated carbonate grains, and scarcity of preserved bedding, which is probably due to the combined effects of episodic, rapid deposition and common bioturbation. However, his interpretation of a shallow-water depositional site for the upper tongue of the Fenstermaker Wash Formation is contradicted by its consistent content of pelagic conodonts representative of the deeper-water, offshore palmatolepid-polygnathid biofacies and by its enclosure within tongues of the deep-water Woodruff Formation (Morrow, 2000; Sandberg *et al.*, in press).

We now consider that the depositional site of the upper tongue of the

Fenstermaker Wash Formation was on the western, outboard slope of the developing, proto-Antler submarine forebulge, which also influenced sedimentation at Devils Gate (Sandberg *et al.*, 2001). By our interpretation, carbonate, clastic, and lithic grains comprising this interval at NAR-A were derived from a relatively shallow-water setting to the east and redeposited to the west on a deeper-water slope transitional to, and intercalated with, tongues of the lower-slope to basin Woodruff Formation.

Section NAR-A (Fig. 16) begins within a Late *rhenana* Zone interval of massive, medium-olive-gray, sandy, coated-grain peloidal packstone and grainstone containing as much as 40% fine- to medium-grained subangular to subrounded quartz sand, common limestone intraclasts, and rare calcispheres (units 1-3). Interestingly, rare quartz sand grains in this interval contain abundant microscopic planar fractures and subhedral to euhedral hematite inclusions, which tie the provenance of these grains to the mid-Frasnian Alamo Impact Event (Warme and Sandberg, 1995; Sandberg *et al.*, *in press*). The presence of these unique marker grains gives evidence of late Frasnian reworking and redeposition of Alamo Breccia sediments, probably from the adjacent rising forebulge to the east.

The unit 1-3 interval, which is tentatively placed within a highstand systems tract, is overlain by 10 m of possible late highstand deposits composed of massive, medium-olive-gray, sandy, coated-grain peloidal limestone characterized by an increase in peloidal limestone intraclasts (unit 4) and a relative decrease in quartz sand to ≤20% (unit 5). At the start of, or within the early part of, the *linguiformis* Zone, an overlying sequence boundary (SB-2) and transgressive surface, which corresponds to the base of T-R cycle IId-2, is placed at a laterally persistent bedding plane break that marks a sharp upward decrease of quartz sand to ≤5% and a concurrent increase of poorly sorted peloids and peloidal limestone intraclasts (unit 6; Fig. 15c). The subsequent transgressive and highstand sediments (units 6-8) consist of massively bedded, medium- to dark-olive-gray and black, sandy, coated-grain peloidal packstones and grainstones.

The F-F boundary and inferred sequence boundary zone (SBZ-3) lie near the top of unit 8, coinciding with an increase in small (≤2 mm), silty, peloid-bioclast wackestone intraclasts. Above the F-F boundary at the top of unit 8 is a thin, 0.7-m-thick interval yielding earliest Famennian (Early or Middle *triangularis* Zone) conodonts. No obvious bedding surfaces or sedimentologic breaks were noted in this homogeneous interval, and the included conodont faunas contain up to 20% reworked late Frasnian elements (Morrow, 2000). The 0.7-m-thick interval is interpreted to include thin lowstand to possible transgressive sediments marking the F-F boundary sea-level fall and start of the post-extinction rise at the base of T-R cycle IIe.

The development of the post-SBZ-3 systems tract is interrupted by a Late

triangularis Zone carbonate debris-flow interval (unit 9). This interval consists of massive to thick-bedded, medium-olive-gray, sandy bioclast-intraclast packstone containing matrix-supported clasts, generally ≤15 cm across, composed of silicified whole fossil and bioclastic packstones and wackestones, laminated lime mudstones, and massive lime mudstones. Reworked late Frasnian megafossils in this interval include atrypid brachiopods, unidentified solitary rugosan corals, and favositid tabulate corals. The lower contact of this debris-flow unit is sharp and erosive, displaying ≤15 cm of relief. Within the upper part of unit 9 at least two additional distinct debris-flow event beds have relatively sharp lower contacts and show clast-supported fabric and internal grading. The upper boundary of the debris-flow interval is gradational and indistinct, and overlying strata (unit 10) contain both coarse-grained, sandy debris-flow lenses and characteristic Fenstermaker Wash Formation coated-grain peloidal packstone and grainstone.

Overall, intraclast size decreases upward through and above unit 9, and clasts in unit 10 are generally ≤5 cm across. At the top of the upper tongue of the Fenstermaker Wash Formation (top of unit 10) is a Late *triangularis* Zone, 40-cm-thick debris-flow bed containing lime mudstone, peloidal bioclast wackestone and packstone, and pink siltstone intraclasts up to 4 cm across in a sandy, clast-supported matrix. Chert nodules ≤10 cm across and reworked silicified brachiopods and horn corals are also present. Unit 10 is capped by a ≤5-cm-thick, irregular, oxidized hardground surface marking SB-4, which is overlain by *crepida* Zone, deep-water, light-brown siliceous and dolomitic siltstone and dark, bedded chert of the upper tongue of the Woodruff Formation (Sandberg *et al.*, *in press*).

Important events recorded at section NAR-A include: (1) reworking and redeposition of Alamo Impact-derived quartz sand grains, probably from the developing proto-Antler forebulge to the east; (2) pronounced decrease in quartz sand and abrupt deepening across SB-2, forming the transgressive surface that marks the base of T-R cycle IId-2; (3) F-F boundary extinction and faunal turnover at SBZ-3, overlain by thin lowstand to transgressive deposits marking the start of T-R cycle IIe; (4) deposition of Late *triangularis* Zone debris-flow event bed that truncates and downcuts into older sediments; and (5) sharp transgressive surface, abrupt deepening, and tectonically-forced SB-4 associated with onlapping facies of the upper tongue of the Woodruff Formation.

4.9 Whiterock Canyon (WMO)

Devonian rocks in the area of Whiterock Canyon, northern Monitor Range, have been discussed by Merriam (1963) and Poole and Sandberg (1993).

The WMO section (Fig. 17) preserves a relatively complete record of the F-F boundary within a deep-water interval of dark-brown, laminated calcareous, dolomitic, and siliceous siltstone and black, laminated siliceous mudstone, chert, and shale of the lower Woodruff Formation. The F-F boundary interval has been analyzed for selected major, minor, and trace element geochemistry (Morrow, 1997; Bratton *et al.*, 1999).

The basal exposures of section WMO are within a sequence of interbedded laminated, dark-brown to black siliceous siltstone, mudstone, shale, and chert and laminated, turbiditic, dark gray to black silty lime mudstone (unit 1) that is dated as early Frasnian *transitans* Zone (Sandberg, unpub. data, 1995; Morrow, 2000). A sequence boundary is tentatively placed at a turbiditic, silty limestone bed that is overlain by a 16-m-thick transgressive to highstand interval (unit 2) dominated by multiple thin parasequence couplets (10-13 cm-thick) of laminated, dark-gray to black siliceous mudstone/bedded radiolarian chert and laminated, dark-gray to black shale that are *jamieae* to *rhenana* Zone in age, and hence correlative with the upper part of T-R cycle IIc. At the top of unit 2, late highstand shallowing and a sequence boundary zone (SBZ-1 equivalent?) are inferred by an increase in organic-rich, dark-brown siltstone, which is overlain by a transgressive to highstand interval of laminated, organic-rich, dark-brown calcareous siltstone with rare dolomudstone nodules (unit 3) that is dated as Late *rhenana* Zone age at its top (Sandberg, unpub. data, 1995; Morrow, 2000). This interval therefore corresponds to at least part of T-R cycle IId-1, although the age of the base is poorly constrained.

Overlying a probable sequence boundary (SB-2) and transgressive surface at the top of unit 3 is a 3.5-m-thick interval of *linguiformis*? Zone pyrite-rich, interbedded laminated black siliceous mudstone/bedded radiolarian chert and laminated dark-brown shale placed within T-R cycle IId-2 (Fig. 15d). This interval shows a marked increase in laminated, organic- and hematite-rich siltstone in the upper 0.5 m (unit 4). The siliciclastic increase in the upper part of the unit is considered to record the rapid, latest *linguiformis* Zone shallowing that is documented in nearshore sections, such as at Devils Gate. The F-F boundary and concurrent SB-3 are placed at the contact between the highest black siliceous mudstone/chert and medium- and dark-brown, organic-rich dolosiltstone (unit 5). This unit is assigned to earliest Famennian (Early to Middle *triangularis* Zone) lowstand deposits based on bedding-plane occurrences of the zonal indicator conodont *Palmatolepis triangularis*. Above unit 5, flooding and deepening is inferred (start of T-R cycle IIe) by deposits of light- to dark-brown, laminated/banded siliceous siltstone, mudstone, and minor shale that contain Late *triangularis* Zone dolomudstone nodules $\leq$80 cm across in the middle of the interval (unit 6).

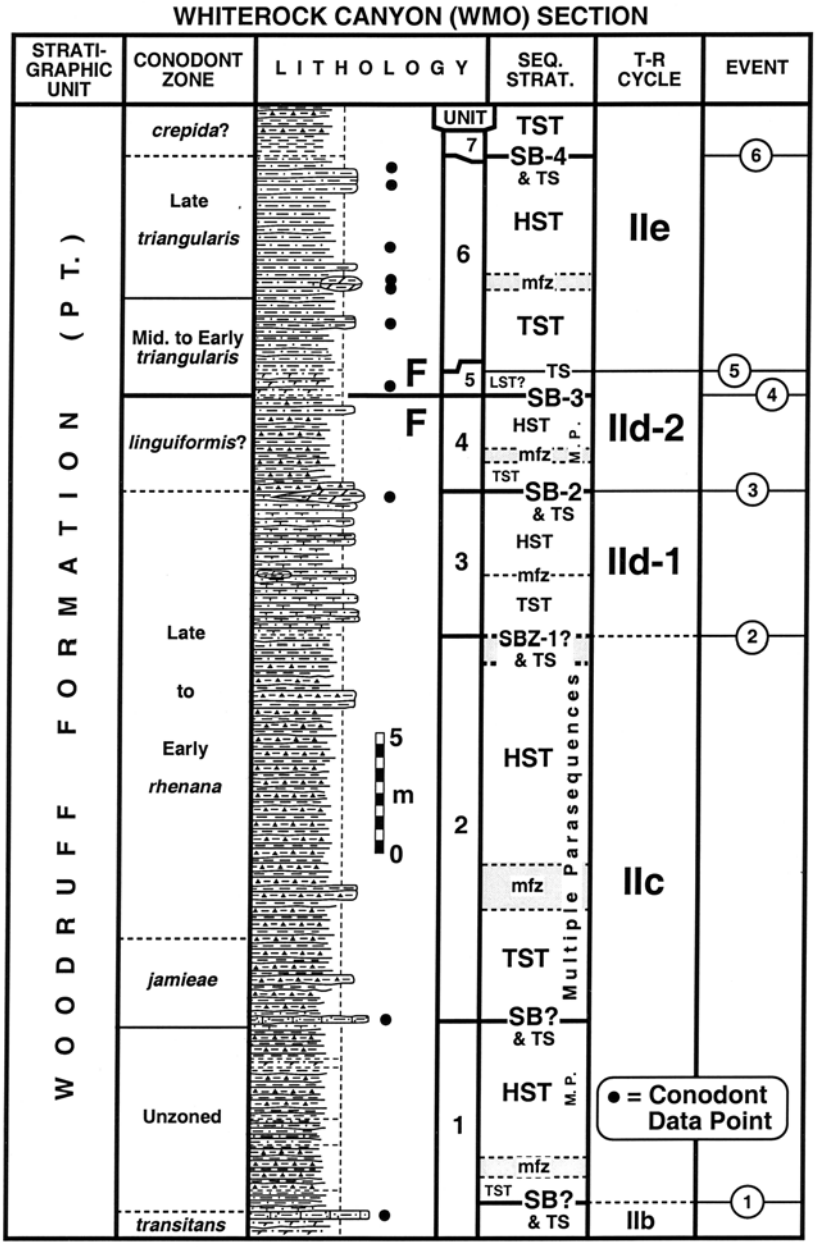

Figure 17. Stratigraphy, conodont biostratigraphy, sequence stratigraphy, and event stratigraphy of Whiterock Canyon (WMO) section. Selected elemental geochemistry of section WMO is discussed in Bratton *et al.* (1999). Section is located in NW1/4 sec. 3 (unsurveyed), T. 15 N., R. 49 E., lat 39.20° N., long 116.44° W., Eureka County, Nevada (Horse Heaven Mountain 7.5-minute quadrangle).

Overlying a possible SB-4-equivalent horizon at the top of unit 6, an interval of interbedded, dark-brown to black fissile shale and black, bedded radiolarian chert (unit 7) records a transgression and deepening eventtentatively dated as *crepida* Zone. This widespread deepening event, which is associated with structural expansion of the Pilot Basin (Fig. 2) as recorded at more landward sections, is also recorded within the deep-water, transitional facies Woodruff Formation at section NAR-A.

The overall series of events recognized at section WMO include: (1) probable sequence boundary and subsequent deepening that correlates with the start of T-R cycle IIc; (2) SBZ-1, deepening, and increase in carbonate content concurrent with the lower part of T-R cycle IId-1; (3) SB-2, overlying transgressive surface, and deepening at the start of T-R cycle IId-2; (4) SB-3 and faunal turnover at the F-F boundary; (5) deepening marking the base of T-R cycle IIe; and (6) tectonically-driven? sequence boundary and abrupt deepening evidenced by black, laminated shale and chert deposition in the early Famennian (*crepida*? Zone).

5. INTERPRETATION OF F-F BOUNDARY STRATIGRAPHY

Black, organic- and cephalopod-rich limestones and shales of the typical upper Frasnian Kellwasser facies have been recognized on several continents. They are tied to major concurrent changes in ocean geochemistry (redox boundary level fluctuations, higher elemental and organic carbon concentrations within sediments, etc.), sea-level fluctuations, and step-wise mass extinction (termed the "Kellwasser Event" by Walliser, 1980, 1984, 1996a). In the western U.S., Sandberg *et al.* (1983, 1986, 1988, 1989, 1997) have shown that slope-to-basin strata coeval with the Lower and Upper Kellwasser Limestones in Europe (i.e., those deposited during the middle Late *rhenana* and *linguiformis* Zones, see Fig. 1) contain a record of geologic and biologic events across the F-F boundary that can be readily correlated with those on other continents, thus reinforcing the global magnitude and synchroneity of events within the mass extinction.

Late Frasnian sedimentation in the western U.S., however, is characterized by the lack of development of Kellwasser Limestone *sensu stricto* facies. Lower and Upper Kellwasser-equivalent rocks in offshore sections of the study area are often dark-colored, organic-rich, and laminated, but lack the extremely high concentrations of shell material (goniatites, nautiloid cephalopods, buchiolid bivalves, entomozoan ostracodes, etc.) found in Kellwasser strata within and adjacent to the type region (e.g., Schindler, 1990a, 1993). Although most of these taxa are

sporadically represented within coeval deeper-water upper Frasnian strata in the western U.S., they generally do not occur in sufficient quantity to form whole-fossil packstones, grainstones, and rudstones such as those characteristic of the well-developed Kellwasser facies.

A probable key to explaining this difference is the comparison of rock-accumulation rates of stratigraphic sections containing the Kellwasser Limestone with rates calculated for coeval Great Basin strata (Fig. 18). Although representative of a variety of paleodepositional settings, the Great Basin sections consistently show significantly higher latest Frasnian rock-accumulation rates reflecting greater carbonate and/or clastic sediment production, transport, and accumulation. These higher accumulation rates were clearly enhanced by the region's close proximity to the emergent North American craton and the impinging Antler orogenic belt, which could have simultaneously provided both more sediment and greater accommodation space via tectonic subsidence. A similar trend is seen to the north in Alberta, Canada, where the average estimated sedimentation rate across the F-F boundary (*linguiformis* and Early *triangularis* Zones) is 46 m/m.y. (Wang *et al.*, 1996), a value consistent with accumulation rates in the Great Basin.

In contrast to North America, the passive to extensional, offshore platform or submarine-rise paleogeographic settings of the European and North African sections were relatively far removed from significant clastic sources at this time, and pelagic- or nektic-bioclast fallout constituted the main sediment source. As a result, sedimentation and resulting rock-accumulation rates in these settings were significantly lower (Sandberg *et al.*, 1988). This is shown in Fig. 18, where the average Late *rhenana* through Late *triangularis* rock-accumulation rate at representative western European and North African sections is approximately 3 m/m.y., a value only about 15% of coeval average accumulation rates in the Great Basin.

6. INTERPRETATION OF SEQUENCE STRATIGRAPHY

The approximate timing of major sequence boundaries and depositional sequences interpreted from our measured sections are shown on Fig. 1. The most marked vertical changes associated with the late Frasnian (F-F) mass extinction are recorded in shelf settings. Here, pre-extinction, late Frasnian biostrome-dominated facies are succeeded by post-extinction, early Famennian peritidal and shallow-subtidal mud-rich bioclastic carbonates and coarse siliciclastics. The general trend of increased early Famennian offshore transport of shelf-derived fine- to coarse-grained siliciclastics is

STRATIGRAPHIC SECTION	ROCK ACCUMULATION RATE (m/m.y.)		Fa/Fr PERCENT
	Late *rhenana* and *linguiformis* Zones	Early and Middle *triangularis* Zones	
Kellwasser-Tal (G)*	0.5	0.4	80
La Serre 'C' (F)*	2.2	2.9	132
Aeke-Tal (G)*	2.4	0.9	38
Steinbruch Schmidt (G)*	4.2	1.9	45
El Atrous I (M)*	4.2	0.4	9.5
Achguig X (M)*	4.4	2.2	50
TPM	8.0	2.5	31
WMO	8.8	4.2	48
GRM	18	5.3	29
NPA	28	3.3	12
DVG	30	21	70
BME	60 (est.)	9.4 (est.)	16

* = Kellwasser Limestone Developed

Figure 18. Compared F-F boundary rock-accumulation rates (uncorrected for compaction) from Germany (**G**), France (**F**), Morocco (**M**), and selected sections in this study. Approximate numerical Frasnian (Late *rhenana* and *linguiformis* Zones) and Famennian (Early and Middle *triangularis* Zones) time values used in these calculations are based on the conodont biochronology of Sandberg and Ziegler (1996). Stratigraphic data for Kellwasser-Tal and Aeke-Tal sections, Harz Mountains, Germany, for La Serre 'C' section, Montagne Noire, France, and for El Atrous I and Achguig X sections, Morocco, are from Schindler (1990a); data for Steinbruch Schmidt section, Rheinisches Schiefergebirge, Germany, are from Sandberg *et al.* (1988), Schindler (1990a), and Ziegler and Sandberg (1990). **Fr:Fa PERCENT** column shows the rate of Frasnian to Famennian accumulation rates for each section.

also reflected in continental slope and Pilot Basin sections, where sandstone and sandstone-dominated turbidites and debris-flow beds are abundant.

Increased onshore-to-offshore siliciclastic delivery was clearly tied to the major eustatic sea-level drop beginning just below the F-F boundary (SB-3), which provided a means of transporting shallow shelf sands across the outer shelf to the shelf margin and adjacent slope settings (Sandberg *et al.*, 1988). Moreover, overall lowered carbonate productivity on the shelf and lack of organized biogenic build-up communities in the immediate post-extinction

interval promoted more siliciclastic transport via increased accommodation space and a lack of actively growing organic shelf-margin barriers. A third consideration involves the sedimentary record of catastrophic events such as widespread platform-margin collapse, which has been proposed for the earliest post-extinction interval (Sandberg *et al.*, 1988). Such an extremely high-energy event, resulting in tsunami, could have also contributed significantly to the erosion, transport, and redeposition of shelf-derived siliciclastics and shelf-margin carbonate intraclasts observed in deeper-water sections.

Three regionally widespread third-order sequence boundaries (SB-1, SB-3, and SB-4) and one fourth-order sequence boundary (SB-2), which together define and bound two fourth-order (Sequences 1 and 2) and one third-order (Sequence 3) depositional sequence across the F-F boundary interval, are recognized. These are interpreted on the basis of characteristics summarized in Fig. 5. Our sequence boundaries and systems tracts are correlated to eustatic sea-level fluctuations within the Johnson *et al.* (1985, 1991) T-R cycles IIc, IId (IId-1 and IId-2 herein), and IIe (Fig. 1). Based on the calculated time-span of corresponding Late Devonian conodont zones (Sandberg *et al.*, 1988, 1989; Ziegler and Sandberg, 1994; Sandberg and Ziegler, 1996), the duration of Sequences 1 and 2 are approximately 1.0 m.y. and 0.4 m.y., respectively. When combined, these sequences constitute a third-order composite sequence package. Sequence 3, bounded below by SB-3 and the F-F boundary and bounded above by the diachronous SB-4, has an overall duration range of about 1.5 to 2 m.y.

Above SB-1, evidence for transgression and its associated stratigraphic condensation is best displayed at sections TPM and DVG, where a sharp, undulatory surface is overlain by deeper-water facies containing abundant phosphatic peloids, biogenic chert, and conodonts. T-R cycle IId is divided into T-R cycles IId-1 and IId-2 based on a rapid fourth-order regressive-transgressive pulse that occurred within the approximately 0.3-m.y.-long *linguiformis* Zone (Sandberg *et al.*, 1988) and resulted in formation of SB-2 within the intervening interval. Similar to that above SB-1, the interval directly overlying SB-2 in slope-to-basin settings is characterized by condensed sedimentation, with well-developed oxidized and mineralized omission surfaces concentrating trace elements, phosphatic peloids, ichthyoliths, coarse-grained quartz sand, and phosphatic fossil debris. These condensed intervals are generally overlain by dark-colored, laminated organic-rich sediments equivalent in age to the Upper Kellwasser Limestone (e.g., sections TPM, GRM, NPA, DVG, and WMO).

As documented in the individual stratigraphic columns, lowstand systems tracts are poorly developed above SB-1 and SB-2. This may be related to the nature of the sea-level fluctuations that formed the sequence boundaries.

As shown by Johnson *et al.* (1985, 1991), these fluctuations consisted of rapid transgressive pulses after the preceding highstand interval, with relatively short periods of intervening low sea level. Shorter periods of lowered sea level could have prevented well-developed lowstand systems tracts from forming. In the case of SB-3, which was formed by a prolonged interval of lowered sea level, the lateral development of lowstand deposits reflects both the increased delivery of coarser clastics to the slope and basin settings and a lack of accommodation space on the shelf. As a result, lowstand systems tracts were best developed in the upper slope position (e.g., sections TPM and DVG), which retained adequate accommodation space and was proximal to sediment supply.

SB-4 is interpreted as a highly diachronous, forced sequence boundary characterized by the apparent lack of an unconformity and no lowstand sedimentation but showing an abrupt deepening associated with the tectonic expansion of the Pilot and Woodruff basins, which in the study area is dated within the Early and Middle *crepida* Zones. The age of strata directly underlying this sequence boundary appears to become significantly younger in a basin-to-shelf direction. This relationship contrasts with that expected in a "normal", eustatically driven sequence boundary in which all strata below the boundary are older than those above, and the age of the sequence boundary base becomes progressively older in a shoreward direction. SB-4 may have resulted from accelerated subsidence rates related to foreland and back-bulge basin formation, which was driven by prolonged eastward-verging flexure and compression of the Antler orogeny. In this part of Nevada, the orogeny culminated during the latest Devonian to Early Carboniferous (Poole *et al.*, 1992).

Of the four primary sequence boundaries recognized, SB-3 at the F-F boundary is marked by the greatest eustatic drop, the widest paleogeographic distribution, and most pronounced shifts in sedimentation and biofacies patterns (Sandberg *et al.*, 1988; Morrow, 2000). During maximum extent of sea-level fall in the earliest Famennian (Early to early Middle *triangularis* Zone), the Late Devonian shoreline shifted offshore to the west by several hundred kilometers at the latitude of Lincoln County, Nevada (Sandberg *et al.*, 1989). Across SB-3, evidence of some submarine slope-front erosion (c.f., Sarg, 1988) is present at section TPM, together with localized dolomitization, desiccation cracks, rip-up clasts, and teepee structures at shelf section BME. However, a lack of other widespread features such as high-relief channels, thick evaporites, solution breccia, or other large-scale karst features beneath SB-3 in shelf sections BME and FXM may indicate that this paleotectonic setting did not experience extensive subaerial or vadose erosion during maximum sea-level fall. This suggests that SB-3 is a small-scale type 1 sequence boundary in the usage of Sarg (1988) after Vail

and Todd (1981). However, as illustrated by the carbonate sequence stratigraphic studies of Goldhammer *et al.* (1993), Montañez and Osleger (1993), and Elrick (1996), where sea-level fluctuations affect relatively low-angle carbonate ramp margins, it is often difficult to identify the resulting sequence boundaries specifically as either type 1 or type 2. The sequence boundaries themselves may be recognized only as transitional zones between progradational facies packages below and retrogradational packages above (e.g., SBZ-3 in sections BME and FXM).

Stratigraphic condensation above sequence boundary SB-3 (or within SBZ-3) appears to be relatively severe at most sections, and the approximately 800 k.y. interval between the start of the latest *linguiformis* Zone eustatic drop and beginning of the subsequent mid-Middle *triangularis* Zone transgression is generally represented by ≤5 m of section in most paleogeographic settings (with the exception of section DVG). This indicates an average rock-accumulation rate of ≤7 m/m.y. across this interval, a value that is ~25% of the average rock-accumulation rate for subsequent transgressive and highstand deposits in the Late *triangularis* Zone. In addition, slope deposits recording this interval are dominated by lowstand turbidite or debris-flow event beds that give further evidence of only episodic sedimentation.

7. INTERPRETATION OF EVENT STRATIGRAPHY

7.1 Events

We recognize ten significant eustatic, depositional, or biological events or episodes across the F-F boundary interval (numbered I through X, Fig. 19, Table 1). These ten events, which are recognized in two or more of our sections, are correlated on the basis of conodont biostratigraphy, relative superposition, and/or distinguishing sedimentologic character. With the future discovery of additional F-F boundary sections and more extensive analyses, the number of laterally persistent, correlative event markers will undoubtedly increase.

The composite event-stratigraphic column is in turn correlated to several other previously established event-stratigraphic chronologies (Fig. 19, Table 1), including the F-F boundary event stratigraphy of Sandberg *et al.* (1988, 2002), the Nevada/western U.S. latest Middle Devonian to earliest Mississippian event framework of Sandberg *et al.* (1997; after Sandberg *et al.*, 1983, 1986, 1989), the Late Devonian event stratigraphy of the southern

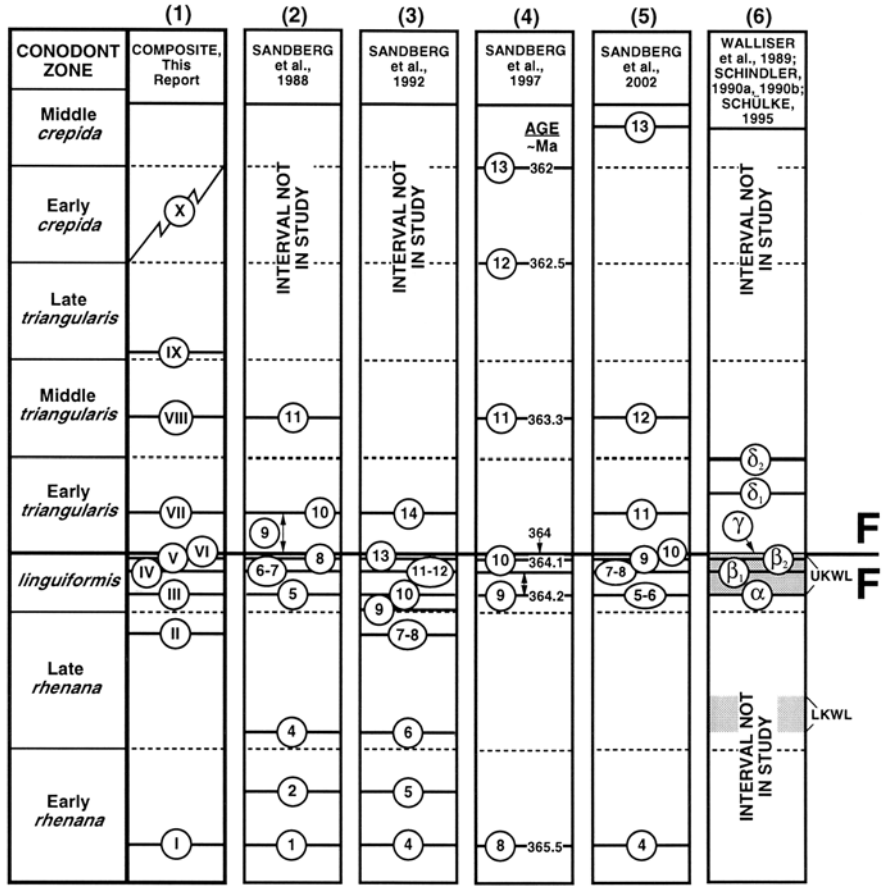

Figure 19. Graphic comparison of F-F boundary conodont biozonation and composite event stratigraphy from this study **(1)** with other published chronologies including the: **(2)** global F-F boundary events of Sandberg *et al.* (1988); **(3)** Late Devonian event stratigraphy of the southern Belgium shelf (Sandberg *et al.*, 1992); **(4)** latest Middle Devonian to earliest Mississippian eustatic and epeirogenic events in Nevada and western U.S. (event numbers from Sandberg *et al.*, 1997; events after Sandberg *et al.*, 1983, 1986, 1989; approximate numerical age calculations from Sandberg and Ziegler, 1996; and Sandberg *et al.*, 1997); **(5)** Euramerican Late Devonian event stratigraphy of Sandberg *et al.* (2002); and **(6)** F-F boundary event stratigraphy of Western Europe and Morocco (compiled from Walliser *et al.*, 1989; Schindler, 1990a, 1990b; and Schülke, 1995).

Belgium shelf (Sandberg *et al.*, 1992), and the Kellwasser Limestone F-F boundary event stratigraphy of Walliser *et al.* (1989), Schindler (1990a, 1990b), and Schülke (1995). The individual event steps in the composite column and their associated geologic history are summarized below.

Table 1. Summary comparing the F-F boundary conodont biozonation and composite event stratigraphic framework of this report with other published event chronologies. Numbers along top row correspond to columns shown graphically in Fig. 19. Events shown in bold designate important, global-scale events recognized wherever the interval has been studied. **Not in study** = events identified in this report that were not recognized elsewhere because these stratigraphic intervals were beyond the scope of the respective study; **Not recognized** = events identified in this report that were not recognized as discrete events in other published chronologies, although the stratigraphic interval was encompassed by the respective study.

(1)	(2)	(3)	(4)	(5)	(6)-part	(6)-part
This report	**Sandberg *et al.*, 1988**	**Sandberg *et al.*, 1992**	**Sandberg *et al.*, 1997**	**Sandberg *et al.*, 2002**	**Walliser *et al.*, 1989; Schindler, 1990a/b**	**Schülke, 1995**
Early *crepida* Zone:						
Event X	Not in study	Not in study	Events 12-13	Not recognized	Not in study	Not in study
Late *triangularis* Zone:						
Event IX	Not in study	Not in study	Not recognized	Not recognized	Not in study	Not in study
Middle *triangularis* Zone:						
Event VIII	**Event 11**	Not in study	**Event 11**	**Event 12**	Not in study	Not in study
Early *triangularis* Zone:						
Event VII	Event 10, Event 9_{end}	Event 14	Not recognized	Event 11	Not recognized	Not recognized
F-F Boundary:						
Event VI	Event 9_{start}	Event 13_{end}	Not recognized	Event 10	Event γ	Event γ
***linguiformis* Zone:**						
Event V	**Event 8**	**Event 13_{start}**	**Event 10**	**Event 9**	**Event β_2**	**Event β**
Event IV	**Events 6-7**	**Event 12**	**Event 9_{end}**	**Events 7-8**	**Event β_1**	**Event β**
Event III	**Event 5**	**Event 10**	**Event 9_{start}**	**Events 5-6**	**Event α**	**Event α**
Late *rhenana* Zone:						
Event II	Not recognized	Events 7-8	Not recognized	Not recognized	Not in study	Not in study
Early *rhenana* Zone:						
Event I	**Event 1**	**Event 4**	**Event 8**	**Event 4**	Not in study	Not in study

7.1.1 Event I, T-R Cycle IId-1 Major Deepening, Early *rhenana* Zone

This marks a eustatic sea-level rise defining the base of T-R cycle IId-1 that is associated with the worldwide drowning of carbonate platforms and reefs (including F2h reef facies in Belgium) and the introduction of the short-lived, opportunistic conodont *Palmatolepis semichatovae* onto shelf areas (Sandberg *et al.*, 2002). This event has been previously recognized on a global scale (Sandberg *et al.*, 1983, 1986, 1988, 1992, 1997, 1998) and forms an important stratigraphic datum within the study area. The amount of stratigraphic condensation at the base of this flooding event may be quite high, reflecting the rate and magnitude of sea-level rise, sediment starvation, and onlapping of deeper-water facies onto the shelf.

In the latter half of the Early *rhenana* Zone, a regression in Western Europe is evidenced by the bloom or abundance acme of the shallower-water conodont *Ancyrognathus triangularis* (e.g., events 2 and 5 of Sandberg *et al.*, 1988 and 1992, respectively), which usually occurs adjacent to reef and mudmound facies. Although present in low relative abundance within the study area at the correlative stratigraphic interval (e.g., within unit 3, section DVG; see conodont data in Ziegler and Sandberg, 1990), this species does not show the marked acme noted in the European sections and, lacking other criteria for recognition, this biofacies-related event is not well developed in the western U.S. In Belgium, the *Ag. triangularis* regression preceded an early Late *rhenana* Zone transgression (events 4 and 6, respectively, of Sandberg *et al.*, 1988 and 1992), which provided accommodation space for growth of F2j mudmounds in Belgium and equivalent carbonate mudmounds elsewhere. A return to deeper-water conditions in the early Late *rhenana* Zone is also associated with black, anoxic sediments of the Lower Kellwasser Limestone in Europe and North Africa, and with dark-colored, laminated, organic-rich siltstones within the study area (e.g., unit 9, section TPM; units 5-7, section NPA; and the upper part of unit 3, section DVG).

7.1.2 Event II, Shallowing, Late *rhenana* Zone

This regressive event formed fourth-order SB-2. In slope and basin settings, lowstand sediments are rarely present above this interval; rather, SB-2 is directly overlain by condensed transgressive deposits of the succeeding transgressive systems tract (event III). This response is similar to that observed at the older, underlying SB-1.

A regression correlative with event II is also recorded on the Belgium platform by a sharp facies change and karst formation on the underlying F2j mudmounds (events 7 and 8, respectively, of Sandberg *et al.*, 1992). An

additional, younger regional event near the Late *rhenana-linguiformis* Zone boundary in Belgium consists of hematite staining associated with a relatively widespread volcanic episode (event 9 of Sandberg *et al.*, 1992).

7.1.3 Event III, T-R Cycle IId-2 Major Deepening, *linguiformis* Zone

This event is the first of several closely timed sedimentologic, biologic, and geochemical events marking accelerated environmental deterioration and step-wise mass extinction that culminated at the F-F boundary. The rapid eustatic sea-level rise at the base of T-R cycle IId-2 is a global-scale event associated with widespread expansion of marine anoxia, increased organic carbon burial, a major extinction step within trilobite taxa (Feist and Schindler, 1994), and the initiation of Upper Kellwasser Limestone deposition in the type area. As evident within the study area, the rapid transgression marked by event III resulted in extensive stratigraphic condensation; deposition of dark-gray to black, fine-grained, organic-rich, laminated, anoxic to dysoxic, siliciclastic sediments; and associated geochemical fluctuations (e.g., Bratton *et al.*, 1999).

7.1.4 Event IV, Major Shallowing, *linguiformis* Zone

Latest Frasnian stratigraphic, sedimentologic, and biofacies patterns record a significant eustatic sea-level fall beginning just prior (~0.1 m.y., Sandberg *et al.*, 1997) to the F-F boundary, which continued unbroken across the boundary into the early part of the Famennian (event 9 of Sandberg *et al.*, 1988). Within the study area, this shallowing is best preserved within deeper-water slope-to-basin settings (e.g., sections GRM, NPA, DVG, and WMO), where accommodation space remained adequate, deposition was potentially continuous, and earliest Famennian catastrophic, high-energy sedimentation events did not rework or obliterate the underlying latest Frasnian record (e.g., sections TPM and BPS). Facies changes associated with this shallowing and regression include increased fine-grained siliciclastic delivery into previously carbonate- or chert-dominated settings (e.g., sections DVG and WMO, respectively) and an increase in coarse-grained, quartz-sand microturbidites within previously fine-grained clastic environments (e.g., section NPA). This facies shift is accompanied by an increase in shallow-water icriodid conodont taxa within pelagic faunas (e.g., section DVG), and a change from anoxic to dysoxic/oxygenated redox conditions (Bratton *et al.*, 1999).

7.1.5 Event V, Final Mass Extinction Step, Latest *linguiformis* Zone

In the most stratigraphically complete and well-developed F-F boundary sections, the top of the Frasnian is marked by a thin, generally featureless extinction layer of altered, carbonate-depleted mudstone containing few or no fossils. The base of this layer marks the final, and most severe, extinction step within the late Frasnian mass extinction episode, wherein most previously dominant taxa were lost in an interval that ranged from 20 kyr to as little as a few days (Sandberg *et al.*, 1988). This includes the extinction of gephuroceratid goniatites, ancyrodellid conodonts, and ozarkodinid conodonts, as well as major diversity or abundance reductions within entomozoan ostracodes, homoctenid cricoconarids, palmatolepid conodonts, polygnathid conodonts, and ancyrognathid conodonts. Concurrent with these biotic losses were short-term abundance blooms within opportunistic disaster taxa including a large, thin-shelled bivalve species and several species of conodonts.

In most sections of this study, a discrete extinction layer is not present at the F-F boundary. Instead, depositional hiatuses characterized by stratigraphic condensation and hardgrounds have superimposed earliest Famennian strata above *linguiformis* Zone rocks containing conodont faunas indicative of late, but not latest Frasnian age (e.g., section GRM). This situation is further complicated where earliest Famennian events such as turbidites, debris flows, or synsedimentary deformation have reworked or admixed *linguiformis* and *triangularis* Zone faunas (e.g., sections TPM, BPS, DVG, and NAR-A). This mixing can occur at the cm- or less scale, thus care must be taken when applying data from this transition interval to high-resolution phylogenetic studies or evaluations of F-F boundary biotic survivorship.

7.1.6 Event VI, F-F Boundary

Recognized in all previous event chronologies, event VI marks the F-F boundary and the associated abrupt facies changes that were used to identify SB-3. Because the terminal Frasnian mass extinction layer (event V) may not always be developed or preserved, this change is recognized here as a separate event marked by the abrupt facies shift from deep- to shallow-water or event strata characteristic of the F-F boundary transition. It must be emphasized that the actual amount of geologic time comprised by this event on the outcrop will vary. As a result, event VI may overlap or cross-cut one or more of the other earlier, unpreserved latest Frasnian events, depending on the degree of condensation, omission, or submarine erosion across the interval.

7.1.7 Event VII, Catastrophic Debris Flow Deposition, Early *triangularis* Zone

Within a post-extinction period of continued regression accompanied by telescoping of shallow- and deep-water conodont biofacies (event 9 of Sandberg *et al.*, 1988), Early *triangularis* Zone lithofacies development is interrupted by event VII, which consists of spectacular debris-flow breccias and sandy limestone-intraclast turbidite beds. These beds were probably deposited from high-energy waves or tsunami generated by shelf-margin collapse (event 10 of Sandberg *et al.*, 1988; event 14 of Sandberg *et al.*, 1992; event 11 of Sandberg *et al.*, 2002). Within the study area, the catastrophic breccia deposits are best developed in the upper-slope setting (e.g., sections TPM and DVG), where accommodation space and proximity to shallower-water carbonate and siliciclastic source material were optimum. In the more distal slope setting, event VII is developed as thin-bedded limestone-intraclast and sandstone turbidites containing abundant redeposited shelf- and slope-derived conodont elements, megafossils, and clasts that record the more offshore effects of the high-energy episode (e.g., sections GRM and NPA). At sections BPS and NAR-A, Early *triangularis* Zone deposits are extremely thin or lacking, and it is possible that event VII is recorded by erosion at these localities.

The Early *triangularis* Zone interval also contains the maximum development of the *Icriodus* conodont biofacies shift and the beginning of early post-extinction diversification within the important conodont genus *Palmatolepis*. These biotic changes have been recognized by numerous workers (e.g., Sandberg *et al.*, 1988), and are further distinguished as a distinct event (δ_1) in the western European sections studied by Schülke (1995). Within the study area, the high relative abundance of *Icriodus* is time-transgressive and persists into strata as young as Late *triangularis* Zone (Morrow, 2000). In well-documented western European and Moroccan sections, the end of the Early *triangularis* Zone also marks the extinction of the last homoctenid cricoconarids, a bioevent recognized by Walliser *et al.* (1989) and Schindler (1990a, 1990b) as event δ, and by Schülke (1995) as event δ_2.

7.1.8 Event VIII, T-R Cycle IIe Major Deepening, Middle *triangularis* Zone

This event is a global-scale, third-order eustatic sea-level rise marking the base of T-R cycle IIe. In several slope and Pilot Basin sections (e.g., sections TPM, GRM, and NPA), the eustatic deepening is characterized by an upward shift from clastic-dominated lowstand sedimentation to

carbonate-dominated transgressive strata consisting of abundant turbidites and carbonate concretions. In the middle shelf, the concurrent facies shift is from extremely shallow-water, sand- and dolostone-dominated peritidal rocks to peloidal limestones that are interbedded above with shelf-derived quartz sandstones deposited later in the highstand interval (e.g., sections BME and FXM).

The body and trace fossil record directly above event VIII is relatively diverse, including several newly evolved conodont and brachiopod species indicating that the post-mass-extinction recovery was well underway. With the exception of section DVG, the evolutionary record of the earliest phases of the post-extinction recovery interval remains largely cryptic within the study area, due to both stratigraphic condensation/omission and an incomplete record preserved in the shallower-water shelf settings.

7.1.9 Event IX, Catastrophic Debris Flow Deposition, Late *triangularis* Zone

A second major interval of debris-flow sedimentation is recorded in several slope and Pilot Basin sections (e.g., sections TPM, BPS, and NAR-A). Event IX is evidenced by thick carbonate and mixed carbonate-siliciclastic breccias and conglomerates that generally show marked lateral variations in thickness and degree of downcutting into underlying lowest Famennian and uppermost Frasnian strata. These highstand debris-flow deposits appear to correlate with the initiation of quartz sandstone-dominated parasequence deposition on the middle shelf (e.g., section BME), and may in part represent shallower-water-derived slope or base-of-slope apron deposits associated with progradational sedimentation packages (e.g., Cook, 1983; Sarg, 1988). Unlike typical highstand slope sediments, however, these debris-flow beds are locally very coarse grained and erosive (see unit 8, section BPS) and evidence an unusual, higher energy depositional mechanism similar to that inferred for the older event VII debris-flow episode.

7.1.10 Event X, Tectonically-Driven Expansion of Pilot Basin, Early to Middle *crepida* Zones

Event X is the diachronous deepening episode associated with the tectonically driven expansion of the Pilot Basin and associated settings. This event is correlative with events 12 and 13 of Sandberg *et al.* (1997), who recognized two discrete events within this same interval. This deepening occurred during an approximately 0.7 m.y.-long interval encompassing the Early *crepida* and early Middle *crepida* Zones. Within the study area, event

X correlates to SB-4, and is marked by either (1) abrupt onlap of deeper-water facies (including the West Range Limestone, lower member of the Pilot Shale, or the upper Woodruff Formation), or (2) relative deepening within units that span the interval, such as the Pilot Shale and Woodruff Formation.

As demonstrated by Sandberg and Poole (1977) and Sandberg *et al.* (1989, 2001), the overall age span of the early Pilot Basin (i.e., depositional site of the lower member of the Pilot Shale) ranges from the Early *hassi* to Late *marginifera* Zones, a time interval of about 8.5 m.y. Event X marks an episode of accelerated, widespread subsidence and relative deepening that is superimposed onto this overall long-term trend of Pilot Basin expansion. The event is recorded in all settings, including the offshore Woodruff slope, Pilot Basin, and shelf. This provides evidence that subsidence was not restricted solely to the intrashelf area but instead affected the entire continental margin.

8. SUMMARY AND CONCLUSIONS

(1) Across the F-F boundary, a total of three widely distributed depositional sequences are identified. These depositional units include two fourth-order sequences, Sequence 1 (early Early *rhenana* Zone to late Late *rhenana* Zone, ~1-m.y.-duration) and Sequence 2 (late Late *rhenana* Zone to Early *triangularis* Zone, ~0.4-m.y.-duration), and one third-order sequence, Sequence 3 (Early *triangularis* Zone to Early and Middle *crepida* Zones, ~1.5- to 2-m.y.-duration).

The lithology and thickness of these sequences change drastically when traced in a shelf-to-basin direction. Stratigraphic units attain a maximum thickness in outer-shelf and upper-slope settings, where accommodation space and sediment supply were both optimal. Shoreward of this setting, the sequences become thinner as a result of shallower water, lower subsidence rates, and longer breaks in sediment accumulation. Basinward, sequences are thinner and condensed due to lowered sediment supply, except where gravity-flow events transported material from the shallower-water setting or where slope bedding is locally thickened and repeated through slumping and synsedimentary folding.

Slope depositional sites on the eastern margin of the Antler foreland basin and western margin of the Pilot back-bulge basin contain abundant allochthonous turbiditic and debris-flow sediments that document an intervening shallow-water source area. A north-south trending structural forebulge was the most likely shallow-water source area, which is consistent with regional mid-Late Devonian tectonic models.

In all paleotectonic settings, rock-accumulation rates of Frasnian sequences are higher than Famennian rates within the same setting. The higher Frasnian rates are probably due to both higher eustatic sea level forming greater accommodation space and to higher carbonate productivity in shallow-water settings. During the earliest Famennian, eustatic sea level was significantly lower, marine coverage of middle- to outer-shelf areas was reduced, and shallow-water carbonate export potential was temporarily curtailed by the effects of the late Frasnian mass extinction on the organic sediment producers.

(2) Sequences 1, 2, and 3 are defined and bracketed by four laterally persistent, correlatable sequence boundaries or sequence boundary zones. The oldest of these, SB-1 (early Early *rhenana* Zone), is a third-order sequence boundary that is generally characterized by a sharp contact that separates relatively shallow-water sediments below from deeper-water, condensed deposits above. Because little or no eustatic sea-level fall preceded the deepening episode, recognizable late highstand and lowstand sediment packages are not developed across the boundary.

The next younger sequence boundary, SB-2 (late Late *rhenana* Zone), is a fourth-order boundary formed by short-term sea-level fall and rise within the overall transgressive phase of the late Frasnian. Lowstand sediments are only rarely developed, and highstand sediments beneath the boundary are generally overlain directly by transgressive sediments of the succeeding depositional sequence.

SB-3 (*linguiformis* Zone-Early *triangularis* Zone boundary) is a global-scale, third-order boundary formed by major, protracted eustatic sea-level fall that began ~0.1 m.y. prior to the F-F boundary and continued ~0.75 m.y. into the early Famennian. The marked facies changes across this sequence boundary, which include the loss of biostromal carbonates on the shelf, resulted from the effects of sea-level fall, mass extinction, and collapse of carbonate-shelf margins. Earliest Famennian lowstand sediments above this sequence boundary are locally thick and well developed in the slope setting, where catastrophically emplaced debris-flow event beds are common. In other slope localities, lowstand deposits are thin or lacking as a result of stratigraphic condensation or submarine erosion produced by the high-energy events documented in other sections.

The youngest third-order sequence boundary, SB-4 (Early *crepida* Zone to Middle *crepida* Zone), formed by tectonic downwarping and expansion of the intracratonic Pilot Basin and offshore Woodruff slope settings. Significant sea-level fall is not apparent prior to SB-4, and the sequence boundary is characterized by a sharp contact separating shallower-water facies below from much deeper-water, transgressive facies above. No lowstand sediments are associated with this boundary. Where constrained

by conodont biostratigraphy, the age of SB-4 is significantly diachronous, becoming younger in an onshore direction.

(3) Devonian transgressive-regressive (T-R) cycles IIc, IId, and IIe are documented within the study area, and T-R cycle IId, which spans the F-F boundary, is further subdivided into subcycles IId-1 and IId-2. Where lowstand systems tracts are absent, sequence boundaries and overlying transgressive surfaces marking T-R cycle boundaries are in contact. Where lowstand sediments are present, which is common only in the upper-slope setting, a significant stratigraphic interval may separate sequence boundaries and T-R cycle boundaries.

(4) For the approximately 3.5-m.y. interval encompassed by our composite event stratigraphy (Fig. 19; early Early *rhenana* Zone to start of Middle *crepida* Zone), ten laterally persistent, correlatable physical, biological, geochemical, or tectonic events are recognized. Combined with evolutionary episodes that define seven conodont biozone boundaries spanning the F-F boundary, a total of 17 widespread events are recognized. This total results in an average temporal resolution across the F-F boundary of less than 210 k.y. per event. Considering only the approximately 800-k.y. interval encompassed by the *linguiformis* and Early *triangularis* Zones, average temporal resolution is much finer and approaches 100 k.y. per event. As documented by Sandberg *et al.* (1988), however, the timing of individual events during the culmination of the mass extinction episode at the end of the Frasnian was probably much less. It is clear that with ongoing detailed, global-scale study of F-F boundary stratigraphy, biostratigraphy, and geochemistry, the abundance and temporal resolution of correlatable events will continue to increase (e.g., Sandberg *et al.*, 2002).

(5) Sequence stratigraphy and T-R cycles provide a valuable stratigraphic framework within which other short-duration but potentially widespread physical, biological, and geochemical events can be ordered and correlated. Upper Devonian strata of the central Great Basin are characterized by structural complexity, limited extent of continuous exposure, and common vertical and lateral facies changes. If the sequence stratigraphy paradigm is to be successfully applied in a geologically complex area like the Great Basin, it is crucial that sequence, systems tract, and bounding surface correlations are verified by an independent dating method such as provided by conodont biostratigraphy. When tested and calibrated against a refined high-resolution template, integrated sequence and event stratigraphy is a comprehensive tool not only for shelf-to-basin correlation and basin analysis but also for unraveling the history of biotic crisis intervals.

ACKNOWLEDGMENTS

Great appreciation is expressed to Erle G. Kauffman, whose pioneering work on the development of Cretaceous high-resolution stratigraphic analysis set a new standard for the detailed study of sedimentary rocks of all ages. Special thanks are given to Willi Ziegler, Forschungsinstitut Senckenberg, for his support of global-scale Devonian research and his tremendous contribution to our understanding of Late Devonian events and geology. He also helped study several of the measured sections of this report during his many visits to the Great Basin. Forrest G. (Barney) Poole is also gratefully acknowledged for his collaboration with us during the past quarter-century, including measuring and describing many Great Basin stratigraphic sections and sharing numerous ideas on the geologic history of the region. Thanks are also given to the following individuals, who provided helpful suggestions and/or field support: John F. Bratton, Alan K. Chamberlain, Peter J. Harries, Stephen T. Hasiotis, Marilyn S. Miller, Wallace G. Morrow, Eberhard Schindler, Otto H. Walliser, and John E. Warme. Finally, Peter J. Harries, Eberhard Schindler, and a third anonymous reviewer are thanked for their critical and beneficial comments regarding the manuscript.

This study was supported by grants and/or facilities to Morrow from the American Association of Petroleum Geologists, the Fulbright Foundation, the Geological Society of America, the Paleontological Society, Sigma Xi, the U.S. Geological Survey, the Universität Göttingen, and the University of Colorado-Boulder, who are all gratefully acknowledged. We thank the Bradley Scholarship fund, U.S. Geological Survey, which provided primary research support for Sandberg and supplemental field funds for Morrow.

REFERENCES

Bai, S. L., Bai, Z. Q., Ma, X. P., Wang, D. R., and Sun, Y. L., 1994, Famennian and the Frasnian-Famennian (F-F) boundary, in: *Devonian Events and Biostratigraphy of South China*, Peking University Press, Beijing, pp. 62-101.

Balinski, A., 2002, Frasnian-Famennian brachiopod extinction and recovery in southern Poland, in: *Biotic Responses to the Late Devonian Global Events* (A. Balinski, E. Olempska, and G. Racki, eds.), *Acta Pal. Pol.* **47**:289-305.

Becker, R. T., 1986, Ammonoid evolution before, during, and after the "Kellwasser Event"—review and preliminary new results, in: *Global Bio-Events* (O. H. Walliser, ed.), Spring Verlag, Berlin*, Lect. Notes Ear. Sci.* **8**:181-188.

Becker, R. T., 1993, Anoxia, eustatic changes, and Upper Devonian to lowermost Carboniferous global ammonoid diversity, in: *The Ammonoidea: Environment, Ecology and Evolutionary Change* (M. R. House, ed.), *Syst. Ass. Sp. Pub.* **47**:115-163.

Becker, R. T., Feist, R., Flajs, G., House, M. R., and Klapper, G., 1989, Frasnian-Famennian

extinction events in the Devonian at Coumiac, southern France, *Comp. Rend. Acad. Sci., Paris*, **309(Série II)**:259-266.

Becker, R. T., and House, M. R., 1994, Kellwasser events and goniatite successions in the Montagne Noire with comments on possible causations, *Cour. Forsch. Senck.* **169**:45-77.

Becker, R. T., and House, M. R., 1997, Sea-level changes in the Upper Devonian of the Canning Basin, Australia, *Cour. Forsch. Senck*. **199**:129-146.

Becker, R. T., House, M. R., Kirchgasser, W. T., and Playford, P. E., 1991, Sedimentary and faunal changes across the Frasnian/Famennian boundary in the Canning Basin of Western Australia, *Hist. Biol.* **5**:183-196.

Bratton, J. F., Berry, W. B. N., and Morrow, J. R., 1999, Anoxia pre-dates Frasnian-Famennian boundary mass extinction horizon in the Great Basin, USA*, Palaeogeo., Palaeoclim., Palaeoeco*. **154**:275-292.

Buggisch, W., 1972, Zur Geologie und Geochemie der Kellwasserkalke und ihrer begleitenden Sedimente (Unteres Oberdevon), *Abh. Hess. Land. Bodenforsch*. **62**:1-68.

Buggisch, W., 1991, The global Frasnian-Famennian >>Kellwasser Event<<, *Geol. Rund.* **80**:49-72.

Carpenter, J. A., Carpenter, D. G., and Dobbs, S. W., 1994, Antler orogeny: Paleostructural analysis and constraints on plate tectonic models with a global analogue in southeast Asia, in: *Structural and Stratigraphic Investigations and Petroleum Potential of Nevada, with Special Emphasis South of the Railroad Valley Producing Trend*, (S. W. Dobbs and W. J. Taylor, eds.), Nevada Petroleum Society, Reno, 1994 Conference Volume II, pp. 187-240.

Casier, J.-G., Devleeschouwer, X., Lethiers, F., Préat, A., and Racki, G., 2002, Ostracods and fore-reef sedimentology of the Frasnian-Famennian boundary beds in Kielce (Holy Cross Mountains, Poland), in: *Biotic Responses to the Late Devonian Global Events* (A. Balinski, E. Olempska, and G. Racki, eds.), *Acta Pal. Pol*. **47**:227-246.

Casier, J.-G., Lethiers, F., and Claeys, P., 1996, Ostracod evidence for an abrupt mass extinction at the Frasnian/Famennian boundary (Devils Gate, Nevada, USA), *Comp. Rend. Acad. Sci., Paris* **322(Série Iia)**:415-422.

Chamberlain, A. K., 2000, Structure and Devonian stratigraphy of the Timpahute Range, Nevada, Unpubl. Ph.D. dissertation, Colorado School of Mines, Golden.

Chamberlain, A. K., and Gillespie, C. W., 1993, Evidence of late Mesozoic thrusting, Timpahute Range, south-central Nevada, in: *Structural and Stratigraphic Investigations and Petroleum Potential of Nevada, with Special Emphasis South of the Railroad Valley Producing Trend*(C. W. Gillespie, ed.), Nevada Petroleum Society, Reno, 1994 Conference Volume II, pp. 139-155.

Chamberlain, A. K., and Warme, J. E., 1996, Devonian sequences and sequence boundaries, Timpahute Range, Nevada, in: *Paleozoic Systems of the Rocky Mountain Region* (M. W. Longman and M. D. Sonnenfeld, eds.), SEPM Rocky Mountain Section, pp. 63-84.

Cook, H. E., 1983, Ancient carbonate platform margins, slopes, and basins, in: *Platform Margin and Deep Water Carbonates* (H. E. Cook, A. C. Hine, and H. T. Mullins, eds.), *SEPM Short Course Notes* **12**: 5.1-5.189.

Day, J., 1990, The Upper Devonian (Frasnian) conodont sequence of the Lime Creek Formation of north-central Iowa in comparison with Lime Creek ammonoid, brachiopod, foraminifer and gastropod sequences, *J. Paleont*. **64**:614-628.

Du Bray, E. A. and Hurtubise, D. O., 1994, Geologic map of the Seaman Range, Lincoln and Nye Counties, Nevada, *U. S. Geol. Surv. Misc. Geol. Invest.* Map I-2282, 1:50,000.

Elrick, M., 1996, Sequence stratigraphy and platform evolution of Lower-Middle Devonian carbonates, eastern Great Basin, *Geol. Soc. Am. Bull.* **108**:392-416.

Estes, J. E., 1992, Stratigraphy of the Devonian Guilmette Formation, Pahranagat Range, Lincoln County, Nevada, Unpubl. M.S. thesis, Colorado School of Mines, Golden.

Feist, R., 2002, Trilobites from the latest Frasnian Kellwasser Crisis in North Africa (Mrirt, central Moroccan Meseta), in: *Biotic Responses to the Late Devonian Global Events* (A. Balinski, E. Olempska, and G. Racki, eds.), *Acta Pal. Pol*. **47**:203-210.

Feist, R., and Schindler, E., 1994, Trilobites during the Frasnian Kellwasser crisis in European Late Devonian cephalopod limestones, *Cour. Forsch. Senck*. **169**:195-223.

Geldsetzer, H. H. J., Goodfellow, W. D., McLaren, D. J., and Orchard, M. J., 1987, Sulfur-isotope anomaly associated with the Frasnian-Famennian extinction, Medicine Lake, Alberta, Canada, *Geol*. **15**:393-396.

George, A.D., and Chow, N., 2002, The depositional record of the Frasnian/Famennian boundary interval in a fore-reef succession, Canning Basin, Western Australia, in: Late Devonian Biotic Crisis: Ecological, Depositional and Geochemical Records (G. Racki and M. R. House, eds.), Palaeogeo. Palaeoclim. Palaeoeco. 181:347-374.

Giles, K., 1994, Stratigraphic and tectonic framework of the Upper Devonian to lowermost Mississippian Pilot Basin in east-central Nevada and western Utah, in: *Structural and Stratigraphic Investigations and Petroleum Potential of Nevada, with Special Emphasis South of the Railroad Valley Producing Trend* (S. W. Dobbs and W. J. Taylor, eds.), Nevada Petroleum Society, Reno, 1994 Conference Volume II, pp. 165-186.

Giles, K., and Dickinson, W. R., 1995, The interplay of eustacy and lithospheric flexure in forming stratigraphic sequences in foreland settings: An example from the Antler foreland, Nevada and Utah, in: *Stratigraphic Evolution of Foreland Basins* (S. L. Dorobek and G. M. Ross, eds.), *SEPM Sp. Pub.* **52**:187-211.

Gischler, E., 1992, Das devonische Atoll von Iberg und Winterberg im Harz nach Ende des Riffwachstums, *Geol. Jahrb. Reihe A* **129**:5-193.

Goldhammer, R. K., Lehmann, P. J., and Dunn, P. A., 1993, The origin of high-frequency platform carbonate cycles and third-order sequences (Lower Ordovician El Paso Gp., West Texas): Constraints from outcrop data and stratigraphic modeling, *J. Sed. Pet.* **63**:318-359.

Goodfellow, W. D., Geldsetzer, H. H. J., McLaren, D. J., Orchard, M. J., and Klapper, G., 1989a, The Frasnian-Famennian extinction: Current results and possible causes, *in:* N. J. McMillan, A. F. Embry, and D. J. Glass, eds., *Devonian of the World*, *Can. Soc. Petrol. Geol. Mem.* **14(III)**:9-21.

Goodfellow, W. D., Geldsetzer, H. H. J., McLaren, D. J., Orchard, M. J., and Klapper, G., 1989b, Geochemical and isotopic anomalies associated with the Frasnian-Famennian extinction, *Hist. Biol.* **2**:51-72.

Groos-Uffenorde, H., and Schindler, E., 1990, The effect of global events on entomozoacean Ostracoda, in: *Ostracoda and Global Events* (R. Whatley and C. Maybury, eds.), Chapman and Hall, London, pp. 101-112.

Gutschick, R. C., and Rodriguez, J., 1979, Biostratigraphy of the Pilot Shale (Devonian-Mississippian) and contemporaneous strata in Utah, Nevada, and Montana, *Brig. Young Univ. Geol. Stud.* **26**:37-62.

Hallam, A., and Wignall, P. B., 1999, Mass extinctions and sea-level changes, *Ear. Sci. Rev.* **48**:217-250.

Hose, R. K., Armstrong, A. K., Harris, A. G., and Mamet, B. L., 1982, Devonian and Mississippian rocks of the northern Antelope Range, Eureka County, Nevada, *U. S. Geol. Surv. Prof. Pap*. **1182**:1-19.

Hurtubise, D. O., and DuBray, E. A., 1992, Stratigraphy and structure of the Seaman Range and Fox Mountain, Lincoln and Nye Counties, Nevada, *U. S. Geol. Surv. Bull*. **1988-B**:1-31.

Jablonski, D., 1991, Extinctions: A paleontological perspective, *Science* **253**:754-757.

Ji, Q., 1989, On the Frasnian-Famennian mass extinction event in South China, *Cour. Forsch. Senck*. **117**:275-301.

Joachimski, M. M., 1997, Comparison of organic and inorganic carbon isotope patterns across the Frasnian-Famennian boundary. **132**:133-145.

Joachimski, M. M., and Buggisch, W., 1993, Anoxic events in the late Frasnian—Causes of the Frasnian-Famennian faunal crisis?, *Geol*. **21**:675-678.

Joachimski, M. M., and Buggisch, W., 2000, The Late Devonian mass extinction—Impact or Earth-bound event?, *in Catastrophic Events and Mass Extinctions: Impacts and Beyond*, *LPI Contribution* **1053**:83-84.

Joachimski, M.M., and Buggisch, W., 2002, Conodont apatite $\delta^{18}O$ signatures indicate climatic cooling as a trigger of the Late Devonian mass extinction, *Geology* **30**:711-714.

Joachimski, M.M., Pancost, R.D., Freeman, K.H., Ostertag-Henning, C., and Buggisch, W., 2002, Carbon isotope geochemistry of the Frasnian-Famennian transition, in: *Late Devonian Biotic Crisis: Ecological, Depositional and Geochemical Records* (G. Racki and M. R. House, eds.), *Palaeogeo. Palaeoclim. Palaeoeco*. **181**:91-109.

Johnson, J. G., Klapper, G., and Elrick, M., 1996, Devonian transgressive-regressive cycles and biostratigraphy, northern Antelope Range, Nevada: Establishment of reference horizons for global cycles, *Palaios* **11**:3-14.

Johnson, J. G., Klapper, G., Murphy, M. A., and Trojan, W. R., 1986b, Devonian series boundaries in central Nevada and neighboring regions, western North America, in: *Devonian Series Boundaries; Results of World-Wide Studies* (W. Ziegler and W. Rolf, eds.), *Cour. Forsch. Senck*. **75**:177-196.

Johnson, J. G., Klapper, G., and Sandberg, C. A., 1985, Devonian eustatic fluctuations in Euramerica, *Geol. Soc. Am. Bull*. **96**:567-587.

Johnson, J. G., Klapper, G., and Sandberg, C. A., 1986a, Late Devonian eustatic cycles around margin of Old Red continent, in: *Late Devonian Events Around the Old Red Continent* (M. J. M. Bless and M. Streel, eds.), *Soc. Géol. Belg. Ann*. **109**:141-147.

Johnson, J. G., Klapper, G., and Trojan, W. R., 1980, Brachiopod and conodont successions in the Devonian of the northern Antelope Range, central Nevada, *Geol. Palaeont.* **14**:77-116.

Johnson, J. G., Reso, A., and Stephens, M., 1969, Late Upper Devonian brachiopods from the West Range Limestone of Nevada, *J. Paleont*. **43**:1351-1368.

Johnson, J. G., and Sandberg, C. A., 1989, Devonian eustatic events in the western United States and their biostratigraphic responses, in: *Devonian of the World* (N. J. McMillan, A. F. Embry, and D. J. Glass, eds.), *Can. Soc. Petrol. Geol. Mem.* **14(III)**:171-178.

Johnson, J. G., Sandberg, C. A., and Poole, F. G., 1989, Early and Middle Devonian paleogeography of western United States, in: *Devonian of the World* (N. J. McMillan, A. F. Embry, and D. J. Glass, eds.), *Can. Soc. Petrol. Geol. Mem.* **14(III)**:161-182.

Johnson, J. G., Sandberg, C. A., and Poole, F. G., 1991, Devonian lithofacies of western United States, in: *Paleozoic Paleogeography of the Western United States-II* (J. D. Cooper and C. H. Stevens, eds.), Pac. Sec. SEPM, Field Trip Guidebook **67**:83-105.

Kauffman, E. G., 1986, High-resolution event stratigraphy: Regional and global bio-events, *in:* O. H. Walliser, ed., *Global Bio-Events*, Springer Verlag, Berlin, *Lect. Notes Ear. Sci.* **8**:279-335.

Kauffman, E. G., 1988, Concepts and methods of high-resolution event stratigraphy, *Ann. Rev. Ear. Planet. Sci*. **16**:605-654.

Kuehner, H.-C., 1997, The Late Devonian Alamo impact breccia, southeastern Nevada, Unpubl. Ph.D. dissertation, Colorado School of Mines, Golden.

LaMaskin, T. A., 1995, Cyclostratigraphy and sequence stratigraphy of the Middle-Upper Devonian Guilmette Formation, southern Egan and Schell Creek Ranges, Nevada, Unpubl. M.S. thesis, University of New Mexico, Albuquerque.

LaMaskin, T. A., and Elrick, M., 1997, Sequence stratigraphy of the Middle to Upper

Devonian Guilmette Formation, southern Egan and Schell Creek ranges, Nevada: *Geol. Soc. Am. Sp. Pap*. **321**:89-112.

Lottmann, J., Sandberg, C. A., Schindler, E., Walliser, O. H., and Ziegler, W., 1986, Devonian events at the Ense area (Excursion to the Rheinisches Schiefergebirge), in: *Global Bio-Events* (O. H. Walliser, ed.), Springer Verlag, Berlin*, Lect. Notes Ear. Sci.* **8**:17-21.

Mayer, P. S., 1994, Late Devonian (Famennian) brachiopods of the West Range Limestone and the Pilot Shale of eastern Nevada, Unpubl. M.S. thesis, Oregon State University Corvallis.

McGhee, G. R., Jr., 1989, Evolutionary dynamics of the Frasnian-Famennian extinction event, in: *Devonian of the World* (N. J. McMillan, A. F. Embry, and D. J. Glass, eds.), *Can. Soc. Petrol. Geol. Mem.* **14(III)**:23-28.

Merriam, C. W., 1963, Paleozoic rocks of Antelope Valley, Eureka and Nye Counties, Nevada: *U. S. Geol. Surv. Prof. Paper* **423**:1-67.

Montañez, I. P., and Osleger, D. A., 1993, Parasequence stacking patterns, third-order accommodation events, and sequence stratigraphy of Middle and Upper Cambrian platform carbonates, Bonanza King Formation, southern Great Basin, in: *Carbonate Sequence Stratigraphy, Recent Developments and Applications* (B. Loucks and J. F. Sarg, eds.), *AAPG Mem.* **57**:305-326.

Morrow, J. R., 1993, Preliminary report on lithofacies, conodont biofacies, and depositional history at the Frasnian/Famennian (mid-Upper Devonian) boundary, Tempiute Mountain, Nevada, U.S.A., *in: Abstracts, IGCP Global Boundary Events Conference, Kielce, Poland, September 27-29, 1993*, Polish Geological Institute, Warsaw, pp. 37.

Morrow, J. R., 1997, Shelf-to-basin event stratigraphy, conodont paleoecology, and geologic history across the Frasnian-Famennian (F-F, mid-Late Devonian) boundary mass extinction, central Great Basin, western U. S., Unpubl. Ph.D. dissertation, University of Colorado, Boulder.

Morrow, J. R., 2000, Shelf-to-basin lithofacies and conodont paleoecology across Frasnian-Famennian (F-F, mid-Late Devonian) boundary, central Great Basin (western U.S.A.): *Cour. Forsch. Senck.* **219**:1-57.

Morrow, J. R., and Sandberg, C. A., 1996, Conodont faunal turnover and diversity changes through the Frasnian-Famennian (F/F) mass extinction and recovery episodes, in: *Sixth North American Paleontological Convention Abstracts of Papers* (J. E. Repetski, ed.), *Paleont. Soc. Sp. Pub.* **8**:284.

Morrow, J. R., and Sandberg, C. A., 1997, Sequence stratigraphy across the F-F (mid-Late Devonian) boundary, central Great Basin: A conodont-based 'reality check', *Geol. Soc. Am. Abs. Prog*. **29**:41.

Muchez, P., Boulvain, F., Dreesen, R., and Hon, H., 1996, Sequence stratigraphy of the Frasnian-Famennian transitional strata: a comparison between South China and southern Belgium, *Palaeogeo. Palaeoclim. Palaeoeco. I***23**:289-296.

Narkiewicz, M., 1989, Turning points in sedimentary development in the Late Devonian in southern Poland, in: *Devonian of the World* (N. J. McMillan, A. F. Embry, and D. J. Glass, eds.), *Can. Soc. Petrol. Geol. Mem.* **14(II)**:619-635.

Narkiewicz, M., and Hoffman, A., 1989, The Frasnian/Famennian transition: The sequence of events in southern Poland and its implications, *Acta Geol. Pol*. **39**:13-28.

Over, D. J., 1997, Conodont biostratigraphy of the Java Formation (Upper Devonian) and the Frasnian-Famennian boundary in western New York State, *Geol. Soc. Am. Sp. Pap.* **321**:161-177.

Over, D. J., and Rhodes, M. K., 2000, Conodonts from the upper Olentangy Shale (Upper Devonian, central Ohio) and stratigraphy across the Frasnian-Famennian boundary, *J.*

Paleont. **74**:101-112.

Playford, P. E., Hurley, N. F., Kerans, C., and Middleton, M. F., 1989, Reefal platform development, Devonian of the Canning Basin, Western Australia, in: *Controls on Carbonate Platform and Basin Development*, *SEPM Sp. Pub*. **44**:187-201.

Poole, F. G., and Sandberg, C. A., 1993, Relation of transitional-facies Woodruff Formation to Late Devonian continental margin in Nevada, *AAPG Bull*. **77**:1458.

Poole, F. G., Sandberg, C. A., and Green, G. N., 1983, Allochthonous Devonian eugeosynclinal rocks in southern Fish Creek Range of central Nevada*, Geol. Soc. Am. Abs. Prog*. **15**:304.

Poole, F. G., Stewart, J. H., Palmer, A. R., Sandberg, C. A., Madrid, R. J., Ross, Jr., R. J., Hintze, L. F., Miller, M. M., and Wrucke, C. T., 1992, Latest Precambrian to latest Devonian time; Development of a continental margin, in: *The Cordilleran Orogen: Coterminous U. S.* (B. C. Burchfiel, P. W. Lipman, and M. L. Zoback, eds.), Geological Society of America, Boulder, pp. 9-56.

Racki, G., Racka, M., Matyja, H., and Devleeschouwer, X., 2002, The Frasnian/Famennian boundary interval in the South Polish-Moravian shelf basins: integrated event-stratigraphical approach, in: *Late Devonian Biotic Crisis: Ecological, Depositional and Geochemical Records* (G. Racki and M. R. House, eds.), *Palaeogeo. Palaeoclim. Palaeoeco*. **181**:251-297.

Roemer, F. A., 1850, Beiträge zur geologischen Kenntnis des nordwestlichen Harzgebirges, III: *Palaeontographica* **5**:1-46.

Sandberg, C. A., and Dreesen, R., 1984, Late Devonian icriodontid biofacies models and alternate shallow-water conodont zonation, in: *Conodont Biofacies and Provincialism* (D. L. Clark, ed.)*, Geol. Soc. Am. Sp. Pap*. **196**:143-178.

Sandberg, C. A., Gutschick, R. C., Johnson, J. G., Poole F. G., and Sando, W. J., 1983, Middle Devonian to Late Mississippian geologic history of the Overthrust belt region, western United States, in: *Geologic Studies of the Cordilleran Thrust Belt 2*, Rocky Mountain Association of Geologists Denver, pp. 691-719.

Sandberg, C. A., Gutschick, R. C., Johnson, J. G., Poole F. G., and Sando, W. J., 1986, Middle Devonian to Late Mississippian geologic history of Overthrust Belt region, western United States, in: *Late Devonian Events Around the Old Red Continent* (M. J. M. Bless and M. Streel, eds.), *Soc. Géol. Belg. Ann*. **109**:205-207.

Sandberg, C. A., Morrow, J. R., and Warme, J. E., 1997, Late Devonian Alamo impact event, global Kellwasser Events, and major eustatic events, eastern Great Basin, Nevada and Utah, *Brig. Young Univ. Geol. Stud*. **42**:129-160.

Sandberg, C. A., Morrow, J. R., and Ziegler, W., 2002, Late Devonian sea-level changes, catastrophic events, and mass extinctions, in: *Catastrophic Events and Mass Extinctions: Impacts and Beyond* (C. Koeberl and K. G. MacLeod, eds.), *Geol. Soc. Am. Sp. Pap*. **356**:473-487.

Sandberg, C. A., and Poole, F. G., 1970, Conodont biostratigraphy and age of West Range Limestone and Pilot Shale at Bactrian Mountain, Pahranagat Range, Nevada*, Geol. Soc. Am. Abs. Prog*. **2**:139.

Sandberg, C. A., and Poole, F. G., 1977, Conodont biostratigraphy and depositional complexes of Upper Devonian cratonic-platform and continental-shelf rocks in the western United States, in: *Devonian of North America* (M. A. Murphy, W. B. N. Berry, and C. A. Sandberg, eds.), *Camp. Mus. Contrib*. **4**:144-182.

Sandberg, C. A., Poole, F. G., and Gutschick, R .C., 1980, Devonian and Mississippian stratigraphy and conodont zonation of Pilot and Chainman Shales, Confusion Range, Utah, in: *Paleozoic Paleogeography of the West-Central United States, Rocky Mountain Paleogeography Symposium I* (T. D. Fouch and E. R. Magathan, eds.), SEPM Rocky

Mountain Section, Denver, p. 71-79.
Sandberg, C. A., Poole, F. G., and Johnson, J .G., 1989, Upper Devonian of Western United States, in: *Devonian of the World* (N. J. McMillan, A. F. Embry, and D. J. Glass, eds.), *Can. Soc. Petrol. Geol. Mem.* **14(III)**:183-220.
Sandberg, C. A., and Warme, J. E., 1993, Conodont dating, biofacies, and catastrophic origin of Late Devonian Alamo Breccia, southern Nevada, in: *Structural and Stratigraphic Relationships of Devonian Reservoir Rocks, East Central Nevada* (C. W. Gillespie, ed.), Nevada Petroleum Society, Reno, 1993 Field Conf. Guidebook, pp. 171-172.
Sandberg, C. A., and Ziegler, W., 1973, Refinement of standard Upper Devonian conodont zonation based on sections in Nevada and West Germany, *Geol. Palaeont*. **7**:97-110.
Sandberg, C. A., and Ziegler, W., 1993, Refinement of standard Late Devonian conodont zonation based on sections in Nevada and Germany, in: *Structural and Stratigraphic Relationships of Devonian Reservoir Rocks, East Central Nevada* (C. W. Gillespie, ed.): Nevada Petroleum Society, Reno, Nevada, 1993 Field Conference Guidebook, p. 173-182.
Sandberg, C. A., and Ziegler, W., 1996, Devonian conodont biochronology in geologic time calibration, *Senck. Lethaia* **76**:259-265.
Sandberg, C. A., Ziegler, W., Dreesen, R., and Butler, J. L., 1988, Late Frasnian mass extinction: Conodont event stratigraphy, global changes, and possible causes, *Cour. Forsch. Senck*. **102**:263-307.
Sandberg, C. A., Ziegler, W., Dreesen, R., and Butler, J. L., 1992, Conodont biochronology, biofacies, taxonomy, and event stratigraphy around middle Frasnian Lion Mudmound (F2h), Frasnes, Belgium, *Cour. Forsch. Senck*. **150**:87 p.
Sans, R. S., 1985, Origin of Devonian rock units in the southern Fish Creek Range, Nye County, Nevada, Unpubl. M.S. thesis, Oregon, Oregon State University, Corvallis.
Sarg, J. F., 1988, Carbonate sequence stratigraphy, in: *Sea-Level Changes—An Integrated Approach*: *SEPM Sp. Pub*. **42**:155-181.
Sartenaer, P., 1985, The stratigraphic significance of rhynchonellid genera at the Frasnian-Famennian boundary, *Cour. Forsch. Senck* **75**:319-330.
Sartenaer, P., 1988, A second North American representative of the middle Frasnian rhynchonellid genus *Caryorhynchus* Crickmay, C.H., 1932, J. Paleont. **62**:539-546.
Schindler, E., 1990a, Die Kellwasser-Krise (hohe Frasne-Stufe, Ober-Devon), *Gött. Arb. Geol. Paläont*. **46**:115 p.
Schindler, E., 1990b, The late Frasnian (Upper Devonian) Kellwasser Crisis, in: *Extinction Events in Earth History* (E. G. Kauffman and O. H. Walliser, eds.), Springer Verlag, Berlin, *Lect. Notes Ear. Sci.* **30**:151-159.
Schindler, E., 1993, Event-stratigraphic markers within the Kellwasser Crisis near the Frasnian/Famennian boundary (Upper Devonian) in Germany, *Palaeogeo. Palaeoclim. Palaeoeco*. **104**:115-125.
Schindler, E., and Königshof, P., 1997, Sedimentology and microfacies of Late Devonian Kellwasser Limestones in relation to paleobathymetry (Upper Kellwasser Horizon, late Frasnian), *Zent. Geol. Paläont., Teil I* **5/6**:597-607.
Schülke, I., 1995, Evolution Prozesse bei *Palmatolepis* in der frühen Famenne-Stufe (Conodonta, Ober-Devon), *Gött. Arb. Geol. Paläont* **67**:108 p.
Schülke, I., 1999, Conodont multielement reconstructions from the early Famennian (Late Devonian) of the Montagne Noire (southern France), *Geol. Palaeont., Sonderb.* **3**:123 p.
Scotese, C. R., and McKerrow, W. S., 1990, Revised world maps and introduction, in: *Palaeozoic Palaeogeography and Biogeography* (W. S. McKerrow and C. R. Scotese, eds.)*, Geol. Soc. Lond. Mem.* **12**:1-24.
Sepkoski, J. J., Jr., 1982, A compendium of fossil marine families*, Milw. Pub. Mus. Contrib. Biol. Geol*. **51**:125 p.

Sepkoski, J. J., Jr., 1996, Patterns of Phanerozoic extinction: A perspective from global data bases, in: *Global Events and Event Stratigraphy in the Phanerozoic* (O. H. Walliser, ed.), Springer Verlag, Berlin, pp. 35-52.

Sokiran, E.V., 2002, Frasnian-Famennian extinction and recovery of rhynchonellid brachiopods from the East European Platform in: *Biotic Responses to the Late Devonian Global Events* (A. Balinski, E. Olempska, and G. Racki, eds.), *Acta Pal. Pol*. **47**:339-354.

Southgate, P. N., Kennard, J. M., Jackson, M. J., O'Brien, P. E., and Sexton, M. J., 1993, Reciprocal lowstand clastic and highstand carbonate sedimentation, subsurface Devonian reef complex, Canning Basin, Western Australia, in: *Carbonate Sequence Stratigraphy, Recent Developments and Applications* (R. G. Loucks and J. F. Sarg, eds.), *AAPG Mem*. **57**:157-179.

Trojan, W. R., 1978, Devonian stratigraphy and depositional environments of the northern Antelope Range, Eureka County, Nevada, Unpubl. M.S. thesis, Oregon State University, Corvallis.

Vail, P. R., 1987, Seismic stratigraphy interpretation using sequences stratigraphy, part 1: Seismic stratigraphy interpretation procedure, in: *Atlas of Seismic Stratigraphy* (A. W. Bally, ed.)*, AAPG Stud. Geol*. **27**:1-10.

Vail, P. R., and Todd, R. G., 1981, North Sea Jurassic unconformities, chronostratigraphy and sea-level changes from seismic stratigraphy, in: *Proceedings, Petroleum Geology of the Continental Shelf, Northwest Europe Conference* (L. V. Illing and G. D. Hobson, eds.)*,* Heydon and Sons, London, pp. 216-235.

Van Wagoner, J. C., Mitchum, R. M., Jr., Posamentier, H. W., and Vail, P. R., 1987, Key definitions of sequence stratigraphy, part 2: Seismic stratigraphy interpretation procedure, in: *Atlas of Seismic Stratigraphy* (A. W. Bally, ed.)*, AAPG Stud. Geol*. **27**:11-14.

Waldman, J. L., 1990, Stratigraphy and depositional environments of the Upper Devonian Fenstermaker Limestone, Eureka County, Nevada, Unpubl. M.S. thesis, Oregon State University, Corvallis.

Walliser, O. H., 1980, The geosynclinal development of the Variscides with special regard to the Rheno-hercynian Zone, in: *Mobile Earth International Geodynamics Project, Final Report* (H. Closs, K. von Gehlen, H. Illies, E. Kuntz, J. Neumann, and E. Seibold, eds.), Boppard, pp. 185-195.

Walliser, O. H., 1984, Geologic processes and global events, *Terra Cog.* **4**:17-20.

Walliser, O. H., 1996a, Global events in the Devonian and Carboniferous, in: *Global Events and Event Stratigraphy in the Phanerozoic* (O. H. Walliser, ed.), Springer Verlag, Berlin, pp. 225-250.

Walliser, O. H., 1996b, Patterns and causes of global events, in: *Global Events and Event Stratigraphy in the Phanerozoic* (O. H. Walliser, ed.), Springer Verlag, Berlin, pp. 7-19.

Walliser, O. H., Groos-Uffenorde, H., Schindler, E., and Ziegler, W., 1989, On the Upper Kellwasser Horizon (boundary Frasnian/Famennian), in: *Contributions to Devonian Palaeontology and Stratigraphy, Part II: Various Devonian Topics* (O. H. Walliser and W. Ziegler, eds.), *Cour. Forsch. Senck*. **110**:247-255.

Wang, K., Geldsetzer, H. H. J., Goodfellow, W. D., and Krouse, H. R., 1996, Carbon and sulfur isotope anomalies across the Frasnian-Famennian extinction boundary, Alberta, Canada, *Geol*. **24**:187-191.

Warme, J. E., and Kuehner, H.-C., 1998, Anatomy of an anomaly: The Devonian catastrophic Alamo impact breccia of southern Nevada, *Int. Geol. Rev*. **40**:189-216.

Warme, J. E., and Sandberg, C. A., 1995, The catastrophic Alamo Breccia of southern Nevada: Record of a Late Devonian extraterrestrial impact, *Cour. Forsch. Senck*. **188**:31-57.

Warme, J. E., and Sandberg, C. A., 1996, Alamo megabreccia: Record of a Late Devonian

impact in southern Nevada, *GSA Today* **6**:1-7.

Wendt, J., and Belka, Z., 1991, Age and depositional environment of Upper Devonian (Early Frasnian to Early Famennian) black shales and limestones (Kellwasser Facies) in the eastern Anti-Atlas, Morocco, *Facies* **25**:51-90.

Ziegler, W., 1958, Conodontenfeinstratigraphische Untersuchungen an der Grenze Mitteldevon/Oberdevon und in der Adorfstufe, *Notizbl. Hess. Landesamt. Bodenfor. Wiesb*. **87**:7-77.

Ziegler, W., 1971, Conodont stratigraphy of the European Devonian, in: *Symposium on Conodont Biostratigraphy* (W. C. Sweet and S. M. Bergström, eds.), *Geol. Soc. Am. Mem.* **127**:227-284.

Ziegler, W., and Sandberg, C. A., 1990, The Late Devonian standard conodont zonation, *Cour. Forsch. Senck*. **121**:1-115.

Ziegler, W., and Sandberg, C. A., 1994, Conodont phylogenetic-zone concept, *Newslet. Strat*. **30**:105-123.

Chapter 11

Vertebrate Biostratigraphy of the Smoky Hill Chalk (Niobrara Formation) and the Sharon Springs Member (Pierre Shale)

KENNETH CARPENTER

1. INTRODUCTION

Throughout much of the Western Interior of North America there is a

KENNETH CARPENTER • Department of Earth and Space Sciences, Denver Museum of Natural History, 2001 Colorado Blvd., Denver, CO 80205.

P.J. Harries (ed.), *High-Resolution Approaches in Stratigraphic Paleontology.*

thick sequence of Upper Cretaceous marine rocks, which in places exceeds 6000 m (Weimer 1983). These sediments record a meridional seaway that connected the Gulf of Mexico to the Arctic Ocean during the Late Cretaceous. Marine vertebrate fossils are extremely common in some of these beds, especially in the Smoky Hill Chalk Member of the Niobrara Formation and in the overlying Sharon Springs Member of the Pierre Shale. Most specimen collecting has concentrated on the Smoky Hill Chalk because of the exquisite quality of the fossils. As a result, there is a large volume of literature that spans over 100 years (e.g., Cope 1875; Williston 1906; Goody 1970). Unfortunately, however, most collections have treated the Smoky Hill as a single fauna, despite early evidence to the contrary (e.g., Williston 1897). Recently, attempts have been undertaken to determine the biostratigraphic distribution of the various vertebrate taxa (Stewart 1988, 1990a; Bennett 1990, 2000; Sheldon 1996; Everhart 2001) and this has provided insights into the faunal changes that have occurred (Carpenter 1990, 1996a, also below; Sheldon 1996).

The Smoky Hill Chalk has been extensively studied by Hattin (1982) in western Kansas, where it ranges from Upper Coniacian to Lower Campanian (~87.3-80.64 Mya; Kauffman *et al.*, 1993), and the studies of Bennett (2000), Sheldon (1996) as well as Everhart (2001) rely on the marker units identified by Hattin (1982). He discovered 23 marker units (mostly bentonite seams or beds of distinctive lithology) in a 181.8 m composite section of the Smoky Hill Chalk. The Sharon Springs Member has been studied by Gill and Cobban (1966) in eastern Wyoming and by Gill *et al.* (1972) in western Kansas. The Sharon Springs Member is both older and younger in Kansas (~80.64-77 Mya based on ammonites, Kauffman *et al.*, 1993) than in Wyoming (80.57-78.25 Mya based on ammonites, Kauffman *et al.*, 1993). This age difference is due to the Sharon Springs deposition environment developing first and terminating last in what is now the Kansas region (Gill *et al.*, 1972). The Sharon Springs Member is thinner than the chalk, being 38.7 m thick in Wyoming and 68.6 m thick in Kansas. Although the Sharon Springs has many bentonitic marker units (Gill *et al.*, 1972), deposition was of such short duration that little change occurs in the vertebrate fauna (Carpenter, 1990, 1996a, and below). The contact between the Smoky Hill Chalk and the Sharon Springs Member is best seen in western Kansas, where it is gradational (Gill *et al.*, 1972; Hattin 1982). In eastern Wyoming, the Sharon Springs is separated from the Smoky Hill Chalk by the Gammon Ferruginous Member. This member is chronostratigraphically equivalent to the top of the Smoky Hill Chalk and basal Sharon Springs of Kansas (Gill *et al.*, 1972, fig. 3).

2. HISTORY OF COLLECTING FOSSIL VERTEBRATES

It is not known when the first fossil vertebrates were collected from the Smoky Hill Chalk or the Sharon Springs Member. Considering that bone often erodes out of the exposures, it seems probable that Native Americans were the first collectors. One of the first specimens collected for scientific study was an upper jaw fragment of a fish that was collected in 1803 by the Lewis and Clark Expedition. The jaw is believed to have been found in Smoky Hill Chalk exposures in what is now northeastern Nebraska. It was named *Saurocephalus lanciformis* by Richard Harlan in 1824, who compared it to an ichthyosaur, a marine reptile. In 1868, E. D. Cope, of The Academy of Natural Science of Philadelphia, received a fragmentary reptile skeleton from Captain Theophilus Turner, a U. S. Army surgeon stationed at Fort Wallace in western Kansas (see Almy, 1987, for a history of the discovery). Cope described the specimen as the long-necked plesiosaur, *Elasmosaurus platyurus* (Cope 1869, 1871). Much of the specimen was articulated in marked contrast to most of the Cretaceous vertebrate fossils that were being described from southern New Jersey. Thus alerted to the presence of articulated material in the West, Cope and O. C. Marsh of Yale University led expeditions to Kansas beginning in 1870. Numerous specimens of fish, reptiles and aquatic birds were collected and named, albeit most of the specimens were fragmentary because collecting techniques had not reached the level of sophistication developed only a decade later. Most of the specimens came from the Smoky Hill Chalk where preservation is better than the selenite encrusted bones of the Sharon Springs Member. For a variety of reasons, both men later hired others to continue to collect on their behalf: Benjamin Mudge and Samuel Williston for Marsh, and Charles Sternberg for Cope.

Based in part on the scientific papers generated by Marsh and Cope during the 1870s and 1880s on the specimens, other museums and universities expressed an interest in acquiring specimens. Williston began collecting in 1890 for the University of Kansas many years after he left Marsh's employment. The University has continued to collect from both the Smoky Hill Chalk and Sharon Springs Member sporadically since that time. In the 1880s, Cope financial difficulties forced Sternberg to become a freelance collector for other museums, mostly in Europe and Canada. Barnum Brown led American Museum of Natural History expeditions in 1903 and 1904 to Kansas, Wyoming and South Dakota where they collected in the Smoky Hill Chalk and the Sharon Springs Member (Carpenter, 1996a). Fredrick Loomis from Amherst College also collected from the Sharon Springs Member in Wyoming in 1903 (Loomis, 1915).

In 1948, David Dunkle, from the National Museum of Natural History, made a collection from the Sharon Springs Member in eastern Wyoming (Gill and Cobban, 1966). He returned in 1973 for the Cleveland Museum of Natural History and made another small collection. Yet another large collection of vertebrates from the area was made by amateur paleontologists Asa Maxson and James Mellinger. These collections were transferred to the University of Colorado Museum in 1973. The University of Nebraska State Museum collected from the Sharon Springs Member in northwestern Nebraska beginning in 1966 (Martin and Tate, 1967). Further collecting from the area continued during the 1970s by the University of Kansas under the leadership of Larry Martin (S. C. Bennett, pers. comm., 1990). In 1967, the Field Museum of Natural History collected from the Sharon Springs Member near Fairburn, South Dakota. The South Dakota School of Mines has also collected sporadically for many years from near Fairburn, Buffalo Gap and several other localities in western South Dakota (Welles and Bump 1949). More recently, J. Martin (pers. comm., 1989) has begun more systematic collecting in South Dakota.

The specimens collected from the Smoky Hill Chalk and Sharon Springs Member have been described in an enormous body of literature, the most notable of which are fishes by Stewart (1899, 1900), Bardack (1965, 1976), Bardack and Sprinkle (1969), Goody (1970, 1976), Stewart (1988); mosasaurs by Cope (1871) Williston (1898), Russell (1967); sea turtles by Cope (1873), Hay (1905), Zangerl (1953a, b), pterosaurs by Eaton (1910), Miller (1972), Bennett (1994), plesiosaurs by Williston (1903), Welles (1952, 1962), Welles and Bump (1949), Carpenter (1996b, 1997, 1999), and birds by Marsh (1880) and Martin and Tate (1976).

3. VERTEBRATE BIOSTRATIGRAPHY OF THE SMOKY HILL CHALK AND SHARON SPRINGS MEMBER

The number of vertebrate specimens seen per square kilometer of outcrop in the Sharon Springs Member equals or exceeded that for the Smoky Hill Chalk in western Kansas (Carpenter 1996a). However, these specimens have not attracted as much attention because of encrustation and damage by selenite crystals. Only bones recovered from concretions are undamaged by selenite growth. Deep excavations into the Sharon Springs Member have demonstrated that selenite growth is a weathering phenomenon (Gill and Cobban, 1966; Carpenter 1996a) resulting in the dissolution of pyrite and the recombination of the liberated sulfur with carbonate in the weathered zone.

Stewart (1990a) identified six biostratigraphic zones within the Smoky Hill Chalk Member, to which a new one, the *Dolichorhynchops* zone may be added for the Sharon Springs Member. The zones of Stewart (1990a) were created because many of the standard macrofossils used in zonation of the Western Interior are poorly preserved in the Chalk. This problem is especially true for ammonite shells as noted by Hattin (1982), but not for their aptychi (J. D. Stewart, pers. comm.). The *Dolichorhynchops* zone is used for convenience because ammonite preservation in the Sharon Springs Member is generally very poor due to selenite growth. Concretions, in which well-preserved ammonites occur, are generally spotty or restricted to specific horizons.

The distribution of vertebrate taxa within the zones of the Smoky Hill Chalk and Sharon Springs Member is shown in Table 1 and graphically in Figure 1. The dinosaurs *Niobrarasaurus colei* and *Claosaurus agilis* are also included in Table 1 for completeness, but were not included in Figure 1 because these erratics are carcasses that had drifted to sea and are not part of the normal marine community. *Pteranodon* and several bird taxa are included because they were apparently all piscivores and lived hundreds of miles from land. For some taxa, the various zones represent their first appearance datum (FAD) or last appearance datum (LAD). In addition, some taxa are limited to a single zone, which may indicate endemism. The age of zones is based on cross-correlating the zones of Stewart (1990a) with Hattin (1982), and Hattin (1982) with Kauffman *et al.* (1993). As a result, the lower part of the Smoky Hill Chalk is now considered older than reported by Stewart (1990a) or Hattin (1982), and the Sharon Springs younger.

Vertebrate fossils are not well known from the Fort Hays Limestone Member underlying the Smoky Hill Chalk Member. A few taxa are mentioned by Stewart (1990a): *Ptychodus mortoni*, *Squalicorx*, *Cretoxyrhina*, and *Cretolamna*, and these also occur higher in the Smoky Hill Chalk. Several partial fish skeletons have been collected from a quarry near Lyons, Colorado, and are housed at the Denver Museum of Natural History. They have yet to be studied, however.

3.1 *Protosphyraena pernicosa* Zone

This zone is named for a fish whose remains are moderately abundant and distinctive. Of the 34 vertebrate taxa in this zone, seven fish and one reptile taxa do not occur higher than the top of the *P. pernicosa* zone. An additional 20 fish, five reptiles and a bird extend into younger zones in the

Table 1. Biostratigraphic distribution of vertebrates in the Smoky Hill Chalk, Niobrara Formation, and Sharon Springs Member, Pierre Shale.

standard Kansas biostratigraphic zones (Hattin 1982)	*Inoceramus* (*Volviceramus*) *grandis*		*Inoceramus* (*Cladoceramus*) *undulatoplicatus*	*Clioscaphites vermiformis*	*Clioscaphites choteauensis*	*Inoceramus* (*Endocostea*) *balticus*	Inoceramus (Endocostea) balticus	*Baculites obtusus* - *Baculites asperiformis*
biostratigraphic zones of Stewart (1990) modified	*Protosphyraena pernicosa*	*Spinaptychus* n.sp.	*Cladoceramus undulatoplicatus*	*Clioscaphites vermiformis* - *Clioscaphites choteauensis*		*Spinaptychus sternbergi*	*Hesperornis*	*Dolichorhynchops*
marker units of Hattin (1982)	1-3	4-5	6-7	8-10		11-20	21-23	
Scapanorhynchus rhaphiodon	X							
Ptychodus martini	X							
Belonostomus sp.	X	X						
Micropycnodon kansasensis	X							
Lepisosteus sp.	X							
Protosphyraena pernicosa	X							
Bananogmius zitteli	X							
Chelosphargis advena	X							
Pseudocorax laevis	X	X						
Ptychodus anonymous	X	X						
Martinichthyes ziphoides	X	X						
Protosphyraena nitida	X	X						
cf. "*Macropoma*" sp.		X						
Ichthyornis cf. *I. anceps*		X						
Enchodus dirus		X	X					
Paraliodesmus guadagnii	X		X	X				
Squalicorx falcatus	X	X	X	X				

Pychodus mortoni	X	X	X	X			
Pteranodon sternbergi	X	X	X	X			
Niobrarasaurus colei		X		X			
Ichthyornis sp.	X		X	X			
"Pachyrhizodus" leptopsis			X	X			
Pseudocorax falcatus				X			
Urenchelys abditus				X			
Caproberyx sp.				X			
Trachichthyoides sp.				X			
Laminospondylus transversus	X	X		X	X		
Clidastes liodontus	X	X	X	X	X		
Tylosaurus nepaeolicus	X	X	X	X	X		
Kansius sternbergi				X	X		
Pteranodon longiceps				X	X		
Bananogmius evolutus					X		
Bananogmius favirostris					X		
Leptecodon rectus					X		
Osmosoma garretti					X		
Bothremys barberi					X		
Ectenosaurus clidastoides					X		
Claosaurus agilis					X		
Nyctosaurus gracilis					X		
Parahesperornis alexi					X		
Ichthyornis victor					X		
Cretoxyrhina mantelli	X	X	X	X		X	
Apsopelix anglicus	X			X	X	X	
Platecarpus planifrons	X	X	X			X	
Protosphyraena tenuis		X	X	X	X	X	
Apteodus sp.				X	X	X	
Enchodus shumardi						X	
Rhinobatus incertus						X	
Hadrodus marshi						X	
Protostega gigas						X	
?*Lophochelys natatrix*						?	
?*Ctenochelys stenopora*						?	
Polycotylus latipinnis						X	
Baptornis advenus						X	
Apatornis celer						X	
Ichthyornis dispar						X	
Cretolamna appendiculata	X	X	X	X		X	X
Xiphactinus audax	X	X	X	X	X	X	X

Ichthyodectes ctenodon	X	X	X	X	X	X	X
Gillicus arctuatus	X	X	X	X	X	X	X
Saurodon leanus	X	X	X	X	X	X	X
Pachyrhizodus minimus	X	X	X	X	X	X	X
Cimolichthyes nepaholica	X	X	X	X	X	X	X
Pachyrhizodus caninus	X	X	X		X		X
Enchodus petrosus	X	X					X
Enchodus gladiolus	X		X	X	X		X
Toxochelys latiremis	X			X		X	X
Protosphyranea gladius		X		X		X	X
Stratodus apicalis		X		X	X	X	X
Clidastes propython				X	X	X	X
Platecarpus tympanicus				X	X	X	X
Tylosaurus proriger				X	X	X	X
"*Saurodon*" *pygmaeus*					X	X	X
Styxosaurus snowii					X	X	X
Squalicorax cf. aff. *S. kaupi*						X	X
Saurocephalus lanciformis						X	X
Dolichorhynchops osborni						X	X
Hydralmosaurus serpentinus						X	X
Hesperornis regalis						X	X
cf. *Sphenocephalus* sp.							X
Globidens dakotensis							X
Plioplatecarpus cf. *P. primaevus*							X
Elasmosaurus platyurus							X
Pteranodon n. sp.							X

Smoky Hill Chalk. *Lepisosteus* is primarily a freshwater fish and its presence in marine strata is at odds with its normal lifestyle. The age of the *P. pernicosa* zone is lower Upper Coniacian.

LAD: *Scapanorhynchus rhaphiodon*, *Ptychodus martini*, *Micropycnodon kansasensis*.

FAD: *Protosphyraena nitida, Belonostomus* sp., *Paraliodesmus guadagnii, Martinichthys ziphoides, Toxochelys latiremis*.

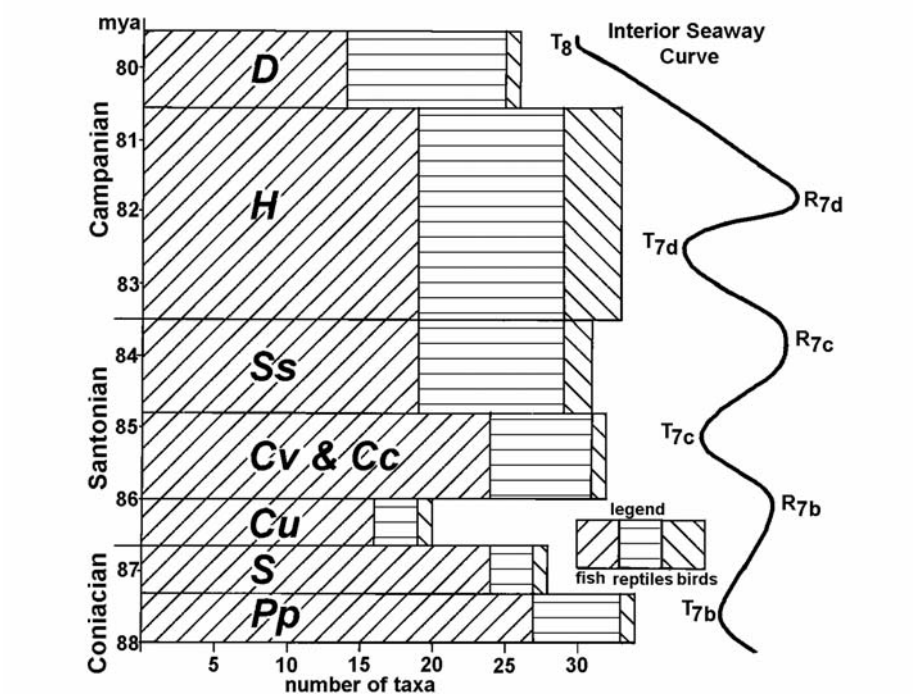

Figure 1. Diversity of vertebrate taxa by biostratigraphic zone. Abbreviations: Pp = *Protosphyraena pernicosa*; S = *Spinaptychus* n.sp.; Cu = *Cladoceramus undulatoplicatus*; Cv & Cc = *Clioscaphites vermiformis-Clioscaphites choteauensis*; Ss = *Spinaptychus sternbergi*; H = *Hesperornis*; D = *Dolichorhynchops*. Seaway curve for the Interior Seaway showing fourth-order transgression and regressions of Kauffman (1984).

Endemics: *Protosphyraena pernicosa*, *Bananogmius zitteli*, and the turtle *Chelosphargis advena*.

3.2 *Spinaptychus* n. sp. Zone

This zone is based on the distinctive aptychi of an ammonite, but the species has not yet been named. Twenty-nine taxa are known, of which two are endemic. The zone also marks the LADs for six fish species and the FAD for four fish species. Seventeen other taxa are also known in both older and younger zones. A possibly new genus of coelacanth is present that may be closely related to *Macropoma* (Stewart *et al.*, 1991). This zone is upper Upper Coniacian.

LAD: *Belonostomus* sp., *Pseudocorax laevis*, *Ptychodus anonymous*, *Martinichthyes ziphoides*, *Protosphyraena nitida.*

FAD: *Enchodus dirus*, *Protosphyraena tenuis*, *P. gladius*, *Stratodus apicalis*.

Endemics: cf. "*Macropoma*", *Ichthyornis* cf. *I. anceps*.

3.3 *Cladoceramus undulatoplicatus* Zone

Inoceramids are one of the few invertebrates that are well preserved in the Smoky Hill Chalk. One of these, *Cladoceramus undulatoplicatus*, is the most distinctive and dominant in this zone (Hattin 1982). Twenty-one vertebrate taxa have been identified. However, none are endemic, and only one FAD and LAD occur. This zone marks the lowest number of vertebrate taxa in the Smoky Hill Chalk for reasons discussed below. Kauffman *et al.* (1993) have determined the *C. undulatoplicatus* zone to be upper Lower Santonian. Obradovich (1993) reports a radiometric date of 84.88 $\pm$ 0.28 Ma from the top of this zone.

LAD: *Enchodus dirus*

FAD: *"Pachyrhizodus" leptopsis*

3.4 *Clioscaphites vermiformis and Clioscaphites choteauensis* Zone

Clioscaphites vermiformis and *C. choteauensis* are typically recognized as two separate macrofossil zones in the Western Interior (Kaufmann *et al.*, 1993). However, because preservation of ammonites in the Smoky Chalk is so poor, Stewart (1990a) combined these two zones for convenience. The combined zone has 32 vertebrate taxa, of which four are endemic fish. The zone also marks the LAD for four fish and one reptile, and the FAD for two fish and four reptiles. The age of the zone is Middle Santonian.

LAD: *Paraliodesmus guadagnii*, *Squalicorx falcatus*, *Pychodus mortoni*, *Pteranodon sternbergi*, *"Pachyrhizodus" leptopsis*.

FAD: *Kansius sternbergi*, *Apteodus* sp., *Clidastes propython*, *Platecarpus tympanicus, Tylosaurus proriger*.

Endemics: *Pseudocorax falcatus*, *Urenchelys abditus*, *Caproberyx* sp., *Trachichthyoides* sp.

3.5 *Spinaptychus sternbergi* Zone

This zone is based on the distinctive aptychi of an ammonite. The zone is rich in vertebrate remains, in part because of the abundance of exposures (see Bennett 2000). Thirty-one taxa of vertebrates are known in the zone. The LAD of two fish and two reptiles occur, as do the FAD of one fish and one reptile. It also has nine endemic species. This zone is Upper Santonian.

LAD: *Laminospondylus transversus*, *Kansius sternbergi*, *Clidastes liodontus, Tylosaurus nepaeolicus*.

FAD: *"Saurodon" pygmaeus, Styxosaurus snowii*.

Endemics: *Bananogmius evolutus*, *Bananogmius favirostris*, *Leptecodon rectus, Osmosoma garretti*, *Bothremys barberi*, *Ectenosaurus clidastoides*, *Pteranodon longiceps*, *Nyctosaurus gracilis*, *Parahesperornis alexi*, *Ichthyornis victor.*

3.6 *Hesperornis* Zone

Williston (1897) introduced the name "*Hesperornis* beds" because so many of Marsh's specimens of this flightless bird were recovered from these strata. The *Hesperornis* zone occupies the western-most beds of the Smoky Hill Chalk. Of the 33 vertebrate taxa, nine are endemic, including three birds. The identity of two turtles, *Lophochelys natatrix* and *Ctenochelys stenopora*, has not been established with confidence and are not included in the taxa count of Figure 1. The zone also marks the LAD for four fish and one reptile, and the FAD for one fish, two reptiles and one bird. The age for the zone is Lower Campanian.

LAD: *Cretoxyrhina mantelli*, *Apsopelix anglicus*, *Protosphyraena tenuis*, *Apteodus* sp., *Platecarpus planifrons.*

FAD: *Saurocephalus lanciformis*, *Dolichorhynchops osborni*, *Hydralmosaurus serpentinus*, *Hesperornis regalis*.

Endemics: *Enchodus shumardi*, *Squalicorax* cf. aff. *S. kaupi, Rhinobatus incertus, Hadrodus marshi*, *Protostega gigas*, ?*Lophochelys natatrix*, ?*Ctenochelys stenopora*, *Polycotylus latipinnis*, *Baptornis advenus*, *Apatornis celer, Ichthyornis dispar*.

3.7 *Dolichorhynchops* Zone

Although the polycotylid plesiosaur *Dolichorhynchops* appears in the Smoky Hill Chalk, it is more common in the Sharon Springs Member (Carpenter 1996b). Its remains are easily diagnosed in the field making it a useful tool for identifying this zone. Twenty-six taxa are known, but it is not known which are endemic,and which mark LADs because, although vertebrate fossils are known in the overlying members of the Pierre Shale, they remain mostly unstudied. Nevertheless, based on fishes from the Bearpaw Shale (Stewart and Carpenter, in prep.), as well as the marine reptile record, a major turnover of the vertebrate fauna occurs during the five million years separating Sharon Springs "time" and Bearpaw "time." The *Dolichorhynchops* zone is Middle Campanian based on its ammonite fauna.

FAD: *Globidens dakotensis*, *Plioplatecarpus* cf. *P. primaevus*, *Elasmosaurus platyurus.*

4. DISCUSSION

A total of 82 vertebrate taxa are known from the Smoky Hill Chalk and Sharon Springs Member (two turtle taxa whose presence is questionable are not included). This diversity includes 50 fish, 24 reptile (including dinosaurs), and 8 bird taxa. Fish therefore comprise 61% of the taxa, reptiles 29%, and birds 10%. Interestingly, the three small fishes (<20 cm), *Kansius sternbergi*, *Leptocodon rectus,* and *Omosoma garretti,* were apparently commensal, living within the shell of the inoceramid *Platyceramus platinus* (Stewart 1990b). Why these fishes have not been found in beds younger than *Spinaptychus sternbergi* is not known, nor has this been discussed by Stewart (1990b).

Few taxa extend through all zones, and those that do are fishes: *Xiphactinus audax*, *Ichthyodectes ctenodon*, *Gillicus arctuatus, Saurodon leanus*, *Pachyrhizodus minimus*, and *Cimolichthyes nepaholica*. The ichthyodectids first appear in strata older than the Smoky Hill Chalk, with *Gillicus* known from the Dakota Formation of Colorado (Stewart and Carpenter, in prep.). *Saurodon* and *Cimolichthyes* have no record before the Smoky Hill Chalk, whereas *Pachyrhizodus minimus* does (Stewart, 1990a). More significant is that most taxa have limited ranges. Several taxa have pre-Smoky Hill Chalk records, but have LADs within the Chalk (e.g., the sharks *Ptychodus* and *Scapanorhynchus*), whereas most other taxa have both FADs and LADs within the Chalk.

In considering the vertebrate faunas for the Smoky Hill Chalk and Sharon Springs Member (Fig. 1), the fewest taxa are present in the *Cladoceramus undulatoplicatus* zone. Stewart (1990a) and Everhart (pers. comm.) believe that the low numbers reflect inadequate sampling of this zone. Although this may be true in part, I suspect that this zone will prove to have less diversity because this zone was preceded by a gradual decrease from the *Protosphyraena pernicosa* zone. This trend is seen in both the diversity of fishes and reptiles. Considering how more resistant fossilized reptile bone is to erosion and how easily it is seen in the field, the reduction by half of the reptiles in the *Cladoceramus undulatoplicatus* zone as compared to the *Spinaptychus* n. sp. zone may be real. The vertebrate fauna rebounds by the Middle Santonian and continues with periodic fluctuations marking extinction and/or immigration (Fig. 1).

The various fluctuations in diversity correlate loosely with the transgressive-regressive pulses in the Interior Seaway as documented by Kauffman (1984). These correlation couplets of diversity decreases-regression and diversity increases-transgression include: *Spinaptychus* n. sp. and *Cladoceramus undulatoplicatus* - R_{7b}, *Spinaptychus sternbergi* - R_{7c}, top of *Clioscaphites vermiformis-Clioscaphites choteauensis* - T_{7c}, and

Hesperornis - T_{7d} (in part). There is, however, no increase in diversity during the Claggett Transgression (T_8) as would be expected. For example, the drop in avian diversity between the *Hesperornis* and *Dolichorhynchops* zones is real based on exhaustive collecting efforts made in the Sharon Springs Member in eastern Wyoming where every bone fragment was documented (Carpenter 1996a). What is not known at this time, however, is if the faunal decrease occurred between the *Hesperornis* and *Dolichorhynchops* zones, or between the lower and upper halves of the *Hesperornis* zone. As can be seen in Figure 1, the *Hesperornis* zone encompasses a considerably greater amount of time than any of the other zones and the effects of the R_{7d} regression cannot be seen in the vertebrate record. I predict that reassessment of the biostratigraphy of this zone will demonstrate a decrease in taxa diversity coincident with the R_{7d} event, in which case the apparent diversity decrease between the *Hesperornis* and *Dolichorhynchops* zones will be much less.

Several taxa seem not to occur in intervening zones where they would be expected (e.g., absence of *Platecarpus planifrons* from the *Clioscpahites vermiformes-C, chotaeuensis* and *Spinaptychus sternbergi* zones) Although some of these absences may be due to insufficient sampling, the absence of others from well-sampled zones may be real and indicate an emigration away from the area. For example, the tuna-like *Pachyrhizodus caninus* is absent from well collected *Hesperornis* zone, although it is present in zones above and below it. *Pachyrhizodus* is also known from the Mooreville Chalk of the Gulf Coast suggesting that it left the Seaway in western Kansas during a cooler water incursion (Kauffman 1984). Whether similar explanations can account for other gaps in taxa ranges have yet to be examined.

Kauffman (1984) has noted that water temperature and/or salinity changes of the Interior Seaway coincide with many of the transgression-regression cycles. Some of these cycles also correspond to extinction and/or immigration of the microbiota (Kauffman 1984; Watkins *et al.*, 1993). Surprisingly, though, the effects on the microbiota did not impact some of the planktonivore fishes, such as *Gillicus*, suggesting that these fishes were more generalist plankton feeders. Environmental changes apparently lead to the extinction of the mollusc-feeding shark *Ptychodus* in the *Clioscaphites vermiformes-C. choteauensis* zone and its ecological replacement by the molluscivore mosasaur *Globidens* in the *Dolichorhynchops* zone.

5. CONCLUSIONS

Vertebrates of the Smoky Hill Chalk and Sharon Spring Member can be divided into seven biostratigraphic zones. Except for the exceptionally long *Hesperornis* zone, the zones average approximately 0.93 Ma. Many taxa are long ranging, extending through several zones. However, the FAD and LAD of other taxa define narrow time intervals, and some appear to be confined to a single zone. Far from resolving issues for the Niobrara-basal Pierre Seaway, several areas for future research were identified:

- Causes for the turnover in the vertebrate faunas between zones.
- Ecological replacements for taxa that become extinct.
- Refinement of the biostratigraphy for the *Hesperornis* zone to determine if there is a decrease at the R_{7d}.
- Enhanced sampling of the *Cladoceramus undulatoplicatus* zone to determine if the low diversity of vertebrates is real.
- Determination of changes in the relative abundance of various taxa from zone to zone.

ACKNOWLEDGMENTS

This paper is dedicated to Erle G. Kaufmann, whom I first met when I was a freshman in 1974. Erle was a guest lecturer at the University of Colorado at that time, and it was his lecture on the taphonomy of the Holzmaden Shales that convinced me to work on the vertebrate taphonomy of the Sharon Springs Member. In later years, I would take various undergraduate and graduate classes from him after he left the Smithsonian Institution for the Geology Department at the University of Colorado.

Over the years I have profited greatly from discussions with J. D. Stewart and Mike Everhart on the marine vertebrates of the Smoky Hill Chalk and Sharon Springs Member. J. D. taught me how to identify fossil fish from the Chalk and Sharon Springs Member when he lived one summer in Boulder, Colorado, in the mid-1970s. Review comments on earlier versions of this manuscript by Chris Bennett, Mike Everhart, Judith Harris, Jim Martin, Larry Martin, Peter Robinson, and J. D. Stewart are acknowledged and appreciated. Special thanks to the late Asa Maxson and James Mellinger for their enthusiastic collecting from the Sharon Springs Member at Red Bird, Wyoming. It was their specimens in the University of Colorado that prompted my early interest in the vertebrate fauna of the Sharon Springs Member. Finally, a special thanks to Peter Harries for allowing me to submit a contribution to this volume.

REFERENCES

Almy, K., 1987, Thof's dragon and the letters of Capt. Theophilus H. Turner, M.D., U.S. Army, *Kansas Hist*. **10**:170-200.

Bardack, D., 1965, Anatomy and evolution of chirocentrid fishes*, Univ. Kansas Paleont. Contrib.* **10**:1-88.

Bardack, D., and Sprinkle, G., 1969, Morphology and relationships of saurocephalid fishes, *Fieldiana* **16**:297-339.

Bennett, C., 1990, Inferring stratigraphic position of fossil vertebrates from the Smoky Hill Chalk Member from locality data: in *Niobrara Chalk Excursion Guidebook* (S. C. Bennett, ed.), University of Kansas Museum of Natural History and Kansas Geological Survey, Lawrence, pp. 43-72

Bennett, C., 1994, Taxonomy and systematics of the Late Cretaceous *Pteranodon* (Pterosauria: Pterodactyloidea), *Occ. Papers Nat. Hist. Mus. Univ. Kansas* **169**:1-70.

Bennett, C., 2000, Inferring stratigraphic position of fossil vertebrates from the Niobrara Chalk of western Kansas, *Kansas Geol. Surv., Curr. Res. Earth Sci. Bull*. **244**:1-8.

Carpenter, K., 1990, Upward continuity of Niobrara fauna with Pierre Shale fauna, in: *Niobrara Chalk Excursion Guidebook* (S. C. Bennett, ed.), University of Kansas Museum of Natural History and Kansas Geological Survey, Lawrence, pp 73-81

Carpenter, K., 1996a, *Sharon Springs Member, Pierre Shale (Lower Campanian): Depositional Environment and Origin of Its Vertebrate Fauna, with a Review of North American Cretaceous Plesiosaurs*. Ph.D. Thesis, University of Colorado, Boulder.

Carpenter, K., 1996b, A revision of short-necked plesiosaurs from the Cretaceous of the Western Interior, North America. *N. Jhrb. Geol. Paläont. Abh*. **201**:259-287.

Carpenter, K., 1997, Comparative cranial anatomy of two North American Cretaceous plesiosaurs, in: *Ancient Marine Reptiles* (J. M. Calloway and E. L. Nicholls, eds.), Academic Press, San Diego, pp. 191-216.

Carpenter, K., 1999, Revision of North American elasmosaurs from the Cretaceous of the Western Interior. *Paludicola* **2**:148-173.

Cope, E., 1868, Note on the fossil reptiles near Fort Wallace, in: *Notes on the Geology of the Survey for the Extension of the Union Pacific Railway, Eastern Division, from the Smoky Hill River, Kansas, to the Rio Grande* (J. Leconte, ed.), Review Printing House, Philadelphia, pp. p. 68

Cope, E., 1871, On the fossil reptiles and fishes of the Cretaceous rocks of Kansas*. U. S. Geological Survey of Wyoming and Contiguous Territories, Fourth Annual Report,* F. V. Hayden, U.S. Geologist, Washington, D.C.

Cope, E., 1873, *Toxochelys latiremis*, *Acad. Nat. Sci. Phila., Proc.* 1-10.

Cope, E., 1875, The Vertebrata of the Cretaceous formations of the West*, U. S. Geol. Surv. Terr., Hayden Survey* **2**:1-303.

Eaton, G.F., 1910, Osteology of *Pteranodon*, *Mem. Conn. Acad. Arts and Sci.* **2**:1-38.

Everhart, M.J., 2001, Revisions to the biostratigraphy of the Mosasauridae (Squamata) in the Smoky Hill Chalk Member of the Niobrara Chalk (Late Cretaceous) of Kansas, *Kansas Acad. Sci. Trans.* **104**:56-75.

Gill, J., and Cobban, W., 1966, The Red Bird section of the Upper Cretaceous Pierre Shale in Wyoming, *U. S. Geol. Surv. Prof. Pap*. **393-A**:1-73.

Gill, J., Cobban, W., and Schultz, L., 1972, Stratigraphy and composition of the Sharon Springs Member of the Pierre Shale in western Kansas, *U. S. Geol. Surv. Prof. Pap.* **728**:1-50.

Goody, P., 1970, The Cretaceous teleostean fish *Cimolichthys* from the Niobrara Formation of Kansas and the Pierre Shale of Wyoming, *Am. Mus. Novitates* **2434**:1-29.

Goody, P., 1976, *Enchodus* (Teleostei: Enchodontidae) from the Upper Cretaceous Pierre Shale of Wyoming and South Dakota with an evaluation of the North American enchodontid species, *Palaeontolographica Abt. A* **152**:91-112.

Harlan, R., 1824, On a new fossil of genus of the order Enalio Sauri (of Contbeare*), Acad. Nat. Sci. Phila. Jour.* **3**:225-232.

Hattin, D., 1982, Stratigraphy and depositional environment of Smoky Hill Chalk Member, Niobrara Chalk (Upper Cretaceous) of the type area, western Kansas, *Kansas Geol. Surv. Bull*. **225**:1-108.

Hay, O., 1905, A revision of the species of the family of the fossil turtles called Toxochelyidae with descriptions of two new species of *Toxochelys* and a new species of *Porthochelys*), *Am. Mus. Nat. Hist. Bull.* **21**:177-185.

Kauffman, E., 1984, Paleobiogeography and evolutionary response dynamic in the Cretaceous Western Interior Seaway of North America, in: *Jurassic-Cretaceous Biochronology and Paleogeography of North America* (G. E. G. Westermann, ed.), *Geol. Assoc. Can. Sp. Pap.* **27**:273-306.

Kauffman, E., Sageman, B.B., Kirkland, J.I., Elder, W.P., Harries, P., and Villamil, T., 1993, Molluscan biostratigraphy of the Cretaceous Western Interior Basin, North Amerca, in: *Evolution of the Western Interior Basin* (W. G. E. Caldwell and E. G. Kauffman, eds.), *Geol. Assoc. Can. Sp. Pap.* **39**:397-434.

Loomis, F., 1915, A new mosasaur from the Ft. Pierre, *Am. Jour. Sci. 4th series* **39**:555-566.

Marsh, O. C, 1880,. Odontorinthes, *U. S. Geol. Surv. Mono*. **7**:1-201

Martin, L, and Tate, J., 1972, A *Hesperornis* from the Pierre Shale, *Nebr. Acad. Sci. Affil. Soc. Proc.* **77**: 49-50.

Miller, H.W. The taxonomy of the *Pteranodon* species from Kansas. *Trans. Kansas Acas. Sci*. **74**:1-19.

Obradovich, J. D., 1993, A Cretaceous time scale, in *Evolution of the Western Interior Basin* (W. G. E. Caldwell and E. G. Kauffman, eds.), *Geol. Assoc. Can. Sp. Pap.* **39**:379-396.

Russell, D., 1967, Systematics and morphology of American mosasaurs, *Peabody Mus. Nat. Hist., Yale Univ., Bull.* **23**:1-237.

Sheldon, M. A., 1996, Stratigraphic distribution of mosasaurs in the Niobrara Formation of Kansas, *Paludicola* **1**:21-31.

Stewart, A., 1899, Notice of three new Cretaceous fishes, with remarks on the Saurodontidae Cope, *Kansas Univ. Quart.* **8**:107-112.

Stewart, A., 1900, Teleosts of the Upper Cretaceous, *Univ. Geol. Surv. Kansas Bull.* **6**:257-403.

Stewart, J. D., 1988, The stratigraphic distribution of Late Cretaceous *Protosphyraena* in Kansas and Alabama*, Ft. Hays Studies* **10**:.80-94.

Stewart, J. D., 1990a, Niobrara Formation vertebrate stratigraphy, in: *Niobrara Chalk Excursion Guidebook* (S. C. Bennett, ed.), *Univ. Kansas Mus. Nat. Hist. Kansas Geol. Surv.*, Lawrence, pp. 19-30.

Stewart, J. D., 1990b, Niobrara Formation symbiotic fish in inoceramid bivalves, in: *Niobrara Chalk Excursion Guidebook* (S. C. Bennett, ed.), *Univ. Kansas Mus. Nat. Hist. Kansas Geol. Surv.*, Lawrence, pp. 31-41.

Stewart, J. D., Everhart, P. A., and Everhart, M.J., 1991, Small coelacanths from Upper Cretaceous rocks of Kansas. *J. Vert. Paleont.* **11(suppl. 3)**:56A.

Watkins, D. K, Bralower, T. J., Covington, J. M., and Fisher, C. G., 1993, Stratigraphy and paleoecology of the Upper Cretaceous calcareous nannofossils in the Western Interior Basin, North America, in: *Evolution of the Western Interior Basin* (W. G. E. Caldwell and E. G. Kauffman, eds.), *Geol. Assoc. Can. Sp. Pap*. **39**:521-537.

Weimer, R., 1983, Relation of unconformities, tectonics, and sea level changes, Cretaceous of the Denver Basin and adjacent areas, in *Mesozoic Paleogeography of West-central United States* (M. Reynolds, and, E. Dolly, eds*), SEPM Rocky Mtn. Sect. Rocky Mountain Paleogeography Symposium* **2**:359-376.

Welles, S., 1952, A review of the North American Cretaceous plesiosaurs, *Univ. Calif. Publ. Geol. Sci.* **29**:47-143.

Welles, S., 1962, A new species of elasmosaur from the Aptian of Columbia, and a review of the Cretaceous plesiosaurs, *Univ. Calif. Publ. Geol. Sci.* **46**:1-96.

Welles, S., and Bump, J., 1949, *Alzadasaurus pembertoni,* A new elasmosaur from the Upper Cretaceous of South Dakota, *J. Paleont*. **23**:521-535.

Williston, S., 1897, The Kansas Niobrara Cretaceous, *Kansas Geol. Surv.* **2**:235-246.

Williston, S., 1898, Mosasaur, *Univ. Geol. Surv. Kansas Mono*. **4**:83-221.

Williston, S., 1903, North American plesiosaurs, Part 1, *Field Columb. Mus. Publ., Geol. Ser* **73**:1-77.

Williston, S. 1906, North American plesiosaurs, *Elasmosaurus*, *Cimoliasaurus*, and *Polycotylus.* Am. J. Sci. **21**:221-236.

Zangerl, R., 1953a, The vertebrate fauna of the Selma Formation of Alabama. Part 3. The turtles of the family Protostegidae, *Fieldiana, Geol. Mem*. **3**:1-133.

Zangerl, R., 1953b, The vertebrate fauna of the Selma Formation of Alabama. Part 4. The turtles of the family Toxochelyidae: *Fieldiana, Geol. Mem*. **3**:137-277.

Chapter 12

Limestone Concretions as Near-Isochronous Surfaces

A Cretaceous Example from the Western Interior of North America

ERLE G. KAUFFMAN

1. INTRODUCTION

Regionally, concretions are debated as to whether they are essentially isochronous and approximate real time lines or whether they are randomly

ERLE G. KAUFFMAN • Department of Geological Sciences, Indiana University, 1001 East Tenth Street, Bloomington, IN 47405.

P.J. Harries (ed.), *High-Resolution Approaches in Stratigraphic Paleontology.*

distributed through the various sequences. Kauffman (1965, 1985), Hudson, (1978), Kauffman *et al*. (1985), Astin (1986), Curtis and Coleman (1986), Svarda and Bottjer (1988), Coleman (1993) Tsujita (1995), Graber (1996), and Mozely (1996) are but a few of the papers of interest on concretions which relate to the study area and or modern day examples. Here, a Cretaceous example is presented because there are independent means for establishing temporal control; abundant volcanic bentonites/ashes are excellent datums so long as they can be differentiated (Fig 1-1 and 1-2). Very active volcanism characterizes the Western Interior United States and Canada during the Cretaceous. The Cretaceous of the Gulf Coast has fewer ash deposits and they are, in general, smaller, but they are still much thicker and more prevalent than contemporary ashes. Establishing a high-resolution chronostratigraphic framework is becoming increasingly viable as more detailed stratigraphic sections are measured and described, a process well underway within the Cretaceous deposits of the Western Interior.

Up to 700 – 800 volcanic events, most of them larger to much larger than today's events, characterize the Cretaceous of the Western Interior. For example, multiple centimeter to rare meters-thick volcanic ashes are known in the Cretaceous. In the Albian, bentonites (altered volcanic ashes) 1 to 3 m thick have been identified (pers. obs.),, and this after a compaction ratio of 2 to 3 for unconsolidated ash versus bentonite. Bentonites approaching 1 m thick are even more numerous. Imagine a widespread single event, 1.5 m-thick bentonite 100's to potentially 1000s of kilometers from the volcanic source, subject to 3:1 compaction (4.5 m of ash originally), and one can get a sense of the magnitude of Cretaceous volcanic events as compared with today's explosive volcanic events.

This mid-Cretaceous volcanism was forced by substantial activity along two North American convergent margins: that between the northern Kula Plate and the Farallon Plate with the western edge of the North American Plate and the Caribbean Plate wedging its way, along east-west transforn zones, between North America and South America, and subducting below the western edge of the North American Plate along a north-south trending convergence zone represented today by the Lesser Antilles. These convergent margins produced an exceptional amount of ash, acting in unison (Pindell and Barrett, 1990).

Various concretion zones can be temporally bracketed by precisely dating these bentonites. With one to several bentonites lying between known concretion horizons, it is relatively easy to constrain the ages of individual concretion zones with an extrapolated "absolute age". And by examining the stratigraphic context of bentonites and concretion biozones, to determine the synchroneity or diachroneity of each concretion horizon.

Figure 1. (1) A cone-in-cone limestone concretions, with a solid core of limestone, middle Graneros Shale (Cenomanian), on north side of Arkansas River, Pueblo State Recreation Area, Colorado. Note thin bentonites, three above the concretion, a thick one laterally persistent to it, and three just below it. (2) A somewhat higher interval [zone of *Mytiloides labiatus* (Schlotheim)] off the coast of Venezuela, Isla Borracha, with eight zones of persistent limestone concretions.

Abundant exposures throughout the Western Interior Basin make this possible in this over 7.5 x 10^6 km^2 outcrop belt. There is more or less continuous outcrop made possible by the emplacement of the Rocky Mountain belt, which extends from Northern Mexico, across all of west-central North America to Alaska. The uplift and subsequent erosion

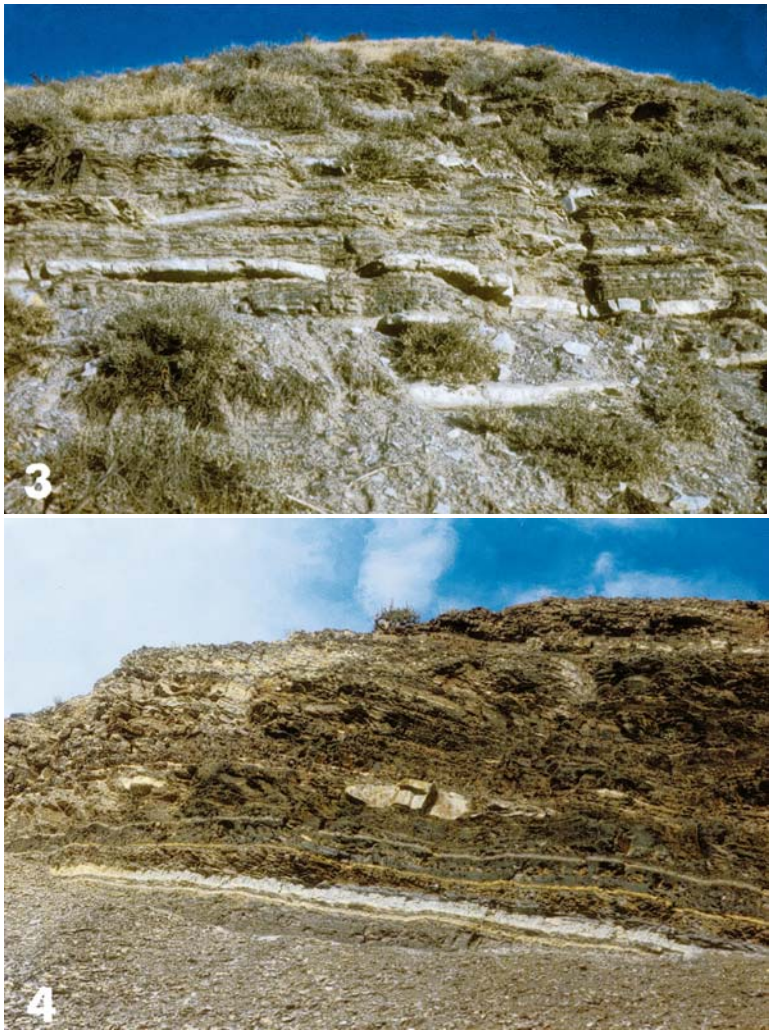

Figure 1. Continued. (3) Bridge Creek Limestone Member with a zone of incipient concretions about half way down, and a zone of lenticular concretions two limestones up from the base of the exposed section, 0.5 mi southeast of Lyons, Co. (4) Two zones of lenticular concretions, one very large, a second directly above it, very small. Note correlatable ash swarm just below one with a big white weathering ash (bentonite), others in the swarm are yellow and six ashes above it, the big one being white again; south-central Wyoming, Mowry Shale.

associated with these orogenically active areas has revealed numerous Cretaceous concretion-bearing outcrops in the region.

Evolutionary rates for biostratigraphically important ammonites and bivalves yield average values of 0.2-0.5 Ma per-assemblage (Kauffman *et al*., 1993); to correlate an ash and a concretion zone precisely with an ammonite-bivalve biozone gives a refined time scale. In the Albian through

the Maastrichtian, the association of numerous concretions with abundant volcanic ashes/bentonites gives an ideal situation for dating limited only by the analytical error associated with the dating techniques, which currently range from 0.20 to 0.35 Ma. The abundance of bentonties allows for an unprecedented chronology of the biostratigraphic system. Evolutionary rates in certain groups match the average resolution error calculated for the ashes or bentonites. The result is the ability to delimit relative biostratigraphic time with a radiometric chronology, and to use this dual dating value to evaluate the potential isochroneity of selective concretionary horizons. As numerical refinement on the ashes or bentonites improves, and more ashes or bentonites are dated, so will the biostratigraphic temporal precision improve. This depends on new technology and greater refinement in dating of minerals. This will allow tighter age constraints to be put on bentonites and ashes, and thus on biozones and concretions.

2. A REGIONAL VIEW OF LIMESTONE CONCRETIONS

Most limestone concretionary horizons of any size in the Western Interior Basin have at least a 1,600 km range, sometimes much more. The lateral extent of these concretion zones and their thickness, far surpasses Pleistocene and modern examples. This reflects that: (1) the Late Cretaceous was a prominent greenhouse interval, with climate zones so broadly distributed to the extent that there were no permanent ice masses at either pole, and the biogeographic spread of cool temperate fauna and flora reached the poles. Polar climate zones, i.e., Arctic and Antarctic, as well as Subarctic and Subantarctic zones, did not exist at this time. (2) Sea level was elevated 200-300 m higher than today. These features, in combination with relatively reduced elevation of large portions of continental areas (i. e., the site of the Western Interior Seaway), allowed for widespread flooding of the continents. A seaway connected the cold temperate, in Alaska and northernmost Canada, with the tropics across North America (the Western Interior Seaway). In eastern Asia and Europe, a similar situation existed; they were transected by substantial north-south seaways that connected cool North Temperate waters with the eastern arm of Tethys. (3) Tethys was a circum-global ocean, and Tethyan flow was uninterrupted though the Proto-Caribbean and Eastern Tethys. India was only half way to its point of intersection with the East Asian block, and the Caribbean Plate was essentially open, characterized initially by the first wave of island arcs, and,

toward the end of the Cretaceous, by three waves of arcs but no epicontinental land masses. Waters could flow around the islands, especially in the deep channels. The result was a seaway, which flowed across southern Europe, the Near and Far East, and the Caribbean, establishing a circum-global Tethyan flow. This allowed circum-global distribution of larvae belonging to biostratigraphally significant taxa (Kauffman, 1973).

The result of this widespread flooding of the continents was warm seaways, protected from prevailing winds, sometimes oxygen poor, and sometimes of hyper- or subnormal salinity. These protected conditions were apparently perfect for the preservation of abundant bentonites, especially where the seaways were relatively proximal to volcanically active margins. We ideally want concretions to form along bedding planes that have been characterized by: (1) pods of carbonate-rich sediment or zones of dense shell accumulations in a sediment that bears very few shells except locally (e.g., 1-2 and 1-3); (2) hollows that collected shells from the immediately surrounding area; (3) random shell distribution with concretions triggered by the breakdown of organic material (as is apparent from Baird, et al.'s (1986) study of the Mazon Creek Member, Middle Pennsylvanian); (4) concretions needing another catalyst to trigger formation of a nucleus around which the precipitation of $CaCO_3$ is triggered; (5) or random formation of non-nucleated concretions.

Once a limestone concretion is nucleated, it can grow to its ultimate size, either *in situ*, or, on a small scale, it will extend to the most calcareous part of the sediment - shell beds (but see Mozeley (1996) for an alternative view of concretion formation). It may form a firmground in the vicinity of the nucleus, or if there is no obvious nucleus, near the center of the concretion; "growth" lines delineating different phases of concretion growth indicate this. It is difficult to determine the nucleus in some cases where it lacks a shell or bone near the center of the potential concretionary mass. Many concretions contain so many fossils that a nucleus is difficult to determine, unless it contains "growth lines". Once the concretion has a nucleus or nuclei, it can grow to its ultimate size rapidly prior to compaction. This relatively early diagenetic formation of concretions is supported by the lack of flattening of skeletal material within the concretion. Regardless of whether the concretion is fossiliferous, those formed near or at the surface, stand out as circular to ovate objects because of the beds around the concretion are themselves compacted by 3:1 to 5:1. The compaction takes after the concretion/limestone or zoned concretion has formed a few meters below the sediment-water interface. This process, as documented by Elder *et al*. (1994), is widespread and individual limestone and chalk beds grade into concretionary horizons as the shoreline is approached.

3. FORMATION OF LIMESTONE CONCRETIONS

Limestone concretions have a large range of size and shape (Figs. 1 and 2), but most are round, ovate to flattened-ovate, and sometimes irregular. They presumably form around a nucleus; this could be a shell, bone, or leaf from a carbonate producing plant (Kauffman, 1965; Hudson, 1978; Svarda and Bottcher, 1988; Desrochers and Al-Asam, 1993; Ludvigson, et al., 1994; Tsujita, 1995; among others). But in a few cases there is no apparent nucleus, at least so far as can be determined. The bulk of the evidence suggests that most concretions an early diagenetic features or at least from prior pronounced diagenetic modification of the sedimentary environment surrounding them. The evidence favoring their early formation includes: 1) the uncompacted nature of the fossils within them in contrast to highly compacted nature of the fossils in the adjacent generally fine-grained lithologies, such as shale or marlstones; 2) the later warping of beds around them as burial and dewatering proceed; and 3) the preservation of structures, such as primary bedding, which no other facies preserves.

Evidence for concretions forming early in diagenesis is also suggested by flattened concretionary masses or by the pathways for carbonate-charged waters being long and lenticular. These are probably along weakened zones in uncompacted sediment, possibly due to incipient fractures, due to differences in composition, or due to differences in the alignment of clays. Concretions also preserve bedding that is uncompressed. How does this happen? Very early diagenetic cementation of concretions seems to be the answer, usually around shells and bone in a bedding plane, local depression, or burrow filling. Sideritic limestone concretions form a little deeper in burial, and the shells or bones are not quite as well preserved. Some show incipient fracture patterns but there are, by and large, whole shells that show only slight to moderate signs of compaction.

One of the most critical elements of concretion formation is nucleation. Because concretions, by and large, are early diagenetic phenomena, their formation is generally initiated in the center and growth procedes outward. This is also supported by the banding (Fig. 1-1), when it can be seen, that shows inward starting points and subsequent outward migration of successive layers. The entire process occurs in a relatively short time. Based on studies of modern concretionary masses, the earliest phases are represented by gelatinous masses or a localized firmground, followed by a

Figure 2. (1) Bridge Creek Limestone Member, 0.5 mi east-southeast of Lyons, Co, showing two zones of lenticular limestone concretions, one near the base of the section, one nearly half way up. Note boundary between horizontal Bridge Creek Limestone Member (Maximum flodding surface), and gently dipping downlap surface in Fairport Shale (downlap surface). (2) A section through the Bridge Creek Limestone Member dipping 40º, showing basal bed as a series of lenticular limestone concretions.

phase when the cement precipitation is just forming. Based on the analysis of concretions and the fossils they contain, it is during this initial phase that the near perfect preservation of shells and bones occurs. I still accept the arguments of Mozely (1996) that some concretions (e.g., septarian concretions) initiate from the outside and the inside structure forms later, but this process does not hold for the vast majority of concretions.

Septarian limestone concretions form at moderate depths in the sediment, are broken and slightly compressed, but never as much as in the surrounding shale, which shows large-scale compaction of whole to large fragments of specimens. It is unknown whether these concretions go through a near sediment surface alteration or not. This seems logical, if before they get buried deeper the fossils are ‘frozen’ in the concretionary matrix. They become secondarily broken as the concretion, under deeper burial, begins to dessicate, crack open, with cracks becoming thinner as you go to the perimeter of the concretion. These cracks are always filled with far coarser

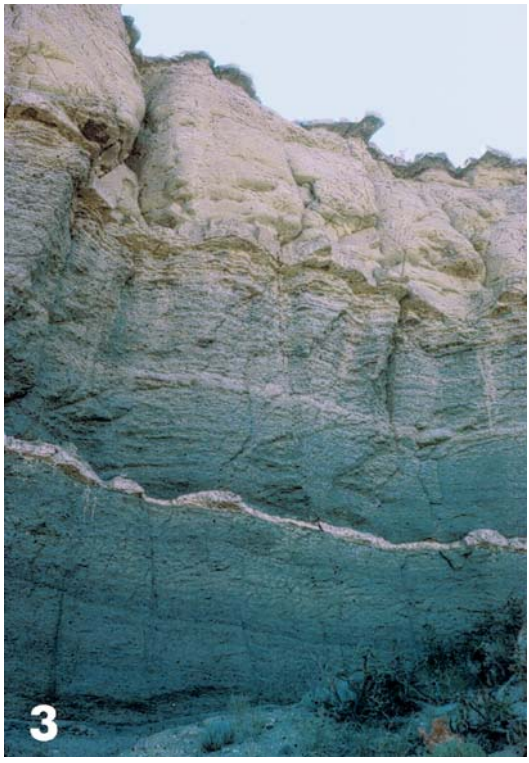

Figure 2. Continued. (3) Upper Blue Hill Shale Member (Middle Turonian) showing closely spaced lenticular concretions about one-third of the way up from the base, and another zone of subovate concretions about midway through the sections. North side of Pueblo Reservoir, west of Pueblo, Co. (4) Concretion in the Graneros Shale. Note that they maintain a constant position below a triplet of closely spaced bentonites. Northeast of dam to Pueblo Reservoir, west of Pueblo, Co.

material then background matrices. The usual cement is large, bladed calcite crystals, in some cases alternating in position with from a different direction towards the outer concretion.

Cone-in-cone concretions (Fig. 1-1) are apparently formed early in diagensis judging from the manner in which beds of shale are wrapped around them. They are nearly always barren of fossils, and those that occur are concentrated on the outside of the concretion. Astin (1986) and Pratt (2001) give an insight into the formation of these atypical concretions.

Potentially you could go from a limestone concretion just below the sediment-water interface, to a layered limestone concretion a little deeper below the surface, to a banded limestone and siderite mixed concretion at slightly greater depth. Siderite is always on the outside, showing it was a later addition to the concretion. With deeper burial, septarian limestone concretion forms with the shells dislocated and the fragments flattened even more. This is a working hypothesis.

4. PALEOECOLOGY OF LIMESTONE CONCRETIONS

Ideally, limestone concretions should contain a fauna characteristic of the setting in which they were formed. For example, increasingly brackish environments should experience a diminution of fully marine elements an increase in the number of brackish elements, followed by a reduction in brackish elements and a decrease in size of the fossils, and increase in the number of fresh water taxa, followed finally by communities made up only of freshwater elements. There is a decrease in diversity as one goes from estuarine mouth to fresh water (Kauffman, based on personal observation in the Potomac River and Chesapeake Bay, and equivalent taxa in the Cretaceous of the Western Interior Basin).

In a transect extending from shoreface environments, as indicated by sandstone (conglomerate to fine-grained), to furthest offshore settings, as determined by the development of bedded limestone (the most distal facies in the Cretaceous of the Western Interior of North America and Mexico; e.g., Kauffman and Caldwell, 1993), there are 34 paleocommunities, most of them nearshore as might be expected from comparison with modern distribution patterns and influenced by the increased degree of environmental variability in the shallower habits. There is a slight decline in overall diversity offshore, although this reduction is not mirrored in abundance. This represents a diversity trend that has several reversals in it,

representing local accumulation of taxa around preferred habitats and/or local accumulation of largely whole shells from the "neighborhood" ("disturbed neighborhood communities" of Fagerstrom, 1988).

The molluscan fauna, excepting ammonites and inoceramids that became extinct near the very end of the Cretaceous, is largely generically continuous from the Upper Cretaceous to the present. Paleoecology deals with reconstructing the lifestyles of taxa. In the case of the dominantly molluscan faunas, which continued to evolve across the Cretaceous–Tertiary boundary to the Recent, it is a matter of knowing what regulates the distribution of modern communities, and tracing the same conditions to the Cretaceous, with few exceptions. This makes the idea of comparative control on the distribution of communities versus paleocommunities a reality, especially when they occur in similar facies.

Paleoecology means reconstructing the life habits of biotas (in this case mollusks, burrowing arthropods, and worms, predominantly reflected in the concretions), their range of chemical and physical tolerance (measured through geochemistry of pristine shell material and sedimentology in concretions and their temperature range (measured through inferences based on observation of paleoecological and modern ecological temperature ranges)

A composite example is drawn from the Late Albian–basal Cenomanian Glencairn–Skull Creek Cycle, the best fresh- to brackish-water sequence, and from the Greenhorn Cycle (Cenomanian to Middle Turonian) of the Western Interior Basin, United States of America, which goes from onshore to offshore, including fresh and brackish facies. This is the time of unprecedented maximum flooding. This was the second highest sealevel stand, following the Ordovician.

5. PALEOCOMMUNITIES RECORDED IN CONCRETIONS

There are 34 freshwater to slightly brackish water through lower brackish and finally to fully marine communities (*sensu* Kauffman, 1967), all of them found partially in concretions, as follows.

5.1 Freshwater Paleocommunities

There are five freshwater communities some of which contain taxa, such as *Mesoneritina,* that can survive slight brackish water. Each association has

seven to 14 taxa, in some cases in nodules, rarely in concretions. (A) *Lioplacoides stachi* assemblages is the most abundant mollusk (85%). Collectively, all of the other eight taxa make up 15% total. (B) *Lioplacoides stachi*/*Parateinostoma occultum* assemblage (74%); all of the other six species of mollusks only 26% of the total. (C) *Lioplacoides stachi*/*Pachychiloides macilentus* assemblage (81%), including 11 other species (19%). (D) *Mesoneritina naticiformis*/*Lioplacoides stachei* assemblage (89%), the nine other species make up only 11%. (E) *Pachychiloides chrysalis* assemblage (53.5%); all of the five others make up 46.5 of the total. (F) *Mesoneritina naticiformis* (50% of the total) and *Pachychiloides cleburni* (43% of the total) make up collectively 93% of the total. This leaves 7% to be distributed among three other taxa. *Mesoneritina* and *Lioplacoides* can withstand slightly brackish conditions, others are of small size *(Brachidontes, Ursirivus*), colonizing only in the fall and winter seasons when rain input is at a minimum (Fursich and Kauffman, 1984). Although most are in matrix, incipient concretions are present at all levels.

5.2 Brackish Paleocommunities

Brackish facies, in concretions and nodules, bear the following communities (listed from least saline to most saline order): (G) A freshwater assemblage mixed with a few, small brackish-water elements, usually small *Brachidontes*, *Ursirivus* and rarely others; (H) An equally mixed brackish water and fresh water components in the spring, and brackish components in the fall. Freshwater components are *Lioplacoides*, *Parateinostoma*, *Pachychiloides*, and *Mesoneritina*; brackish-water components in concretions, nodules, and loose in the sediment are typically large *Brachidontes*, *Neritina*, *Protodonax*, in low to moderate numbers without ammonites or inoceramids. They may live through the duration of brackish water, but only in marginal populations.

(I) Brackish taxa characterize this assemblage, without freshwater taxa. *Ursirivus pyriformis* predominates; there are three subsets. Subset 1: the corbulid *U. pyriformis* and the persistent oyster *Crassostrea soleniscus* association, with *Veloritina durkeii* and *Pyrgulifera humerosa*. *C. soleniscus* represents only 3% of the fauna, but is present in all samples taken. Large *Brachidontes* occurs in only two out of 19 samples, and is large. Subset 2: dominated by *U. pyriformis*, whereas *P. humerosa* and *V. durkeii* are subdominant. The *U. pyriformis* is by far the most common species in any sample. The rare species include the gastropods *Zaptychius haldemani* and *V. durkeii*, or the occasional mytilid *Brachidontes multilinigera*. (J) *C. soleniscus* alone, or with very rare associates appears to represent a true recurring association. It is spread throughout the Bear River Formation

(Fursich and Kauffman, 1984), usually in monotypic or near-monotypic layers. Bioherms with up to 10 cm of relief represent of *in situ* growth. The shells are not bored, a sign of their estuarine origin (pers. obs.). The shells are thin (compared to those at fully marine forms) and small. They appear to have lived under subnormal salinity.

The lower estuarine today contains diverse taxa. The lower estuarine fauna was more widespread during the Cretaceous, and characterized a greater range and number of concretions, including normal limestone concretions in both non-calcareous and slightly calcareous shales, without ammonites, inoceramids, or fully marine bivalves and gastropods. The lower estuary is divisible into six zones, labeled K through P.

K. This represents thick-shelled oyster beds, primarily *Crassostrea*, but also *Cubitostrea* both of which are secondarily preserved in incipient concretions, or constitute actual concretions. The source of the limestone is clearly from the shell bed itself.

L. This assemblage is composed of *Callianassa*, *Crassostrea*, Cardiidae, Mactridae, Mytilidae especially *Brachidontes*, and indicates a shallow, slowly circulating estuary (lower part), estuarine pond, to fully marine, shallow water on a protected coast. The diversity increases as you go from lower brackish to fully marine. This assemblage occurs in concretions, silty concretions, siltstone, and silty claystone or shale.

M. This biofacies consist of *Corbula* and *Callistina* assemblage, with secondary molluscan elements such as *Tellina*, various Ostreidae, Mactridae, Cardiidae, *Brachidontes*, and *Callianassa* burrows. Environmental indicators point to very shallow water, mobile to firm substrate, and strong to moderate current activity at depths under 20 m, in estuarine mouth brackish to normal nearshore marine waters. These assemblages occur in sandy concretions, siltstone, and sandstone substrates.

N. This is a *Corbula*-dominated, composing 90-95% of the fauna, assemblage, which also contains large oysters, Mactridae, Cardiidae, and Mytilidae. Environmental implications are estuarine mouth to normal marine, inner shelf, firm coarse clastic substrate, under moderate current activity, at depths rarely exceeding 30 m. They occur in sandy concretions, incipient concretions, siltstone, and very fine-grained sandstone.

O. Diverse, middle brackish bay fauna including *Crassostrea*, *Brachidontes*, *Modiolus*, and secondarily, *Anomia*, *Barbatia*, and *Anatimya* characterize this assemblage. Environmental implications are mid-estuarine brackish bays of modestly depleted salinity, in shallow, well-circulated platforms on stable, moderately firm substrates, especially those including wood or aquatic vegetation. Substrates are concretions, silty claystone, or siltstone habitats.

P. This comprises an estuarine-mouth assemblage including

Brachidontes, *Corbula* (dominant), *Geltena*, *Idonearca*, *Tellina*, *Callistina*, and Pteriidae. Secondary elements are *Anomia*, *Crassostrea* (large), Mactridae, aporrhaid gastropods, and *Callianassa* burrows. Environmental implications are lower estuary to normal marine, waters less then 30 m, on moderately firm to soft substrate such as wood or shell banks. Incipient concretions in silty clay or plain calcareous substrates are the preferred facies.

5.3 Fully-Marine Paleocommunities

There are 18 fully marine communities that occur in incipient concretions, concretions, zoned limestone and siderite concretions, and septarian limestone concretions, listed below.

Q. *Lopha*-dominated assemblage, that is associated with Inoceramidae, Cardiidae, gastropods such as *Pugnellus*, *Turritella*, and *Rostellana*. It occurs as incipient concretions and lenses, or only in matrix, usually sand, silt, or silty shale. The calcium carbonate surrounds big oyster beds forming nodules and concretions. All carbonate cement is probably locally derived, commonly from the same bed as contains the fossils.

R. *Cubitostrea* assemblage, commonly associated with one or more of the following taxa: *Lopha*, *Exogyra*, small inequivalve Inoceramidae, Cardiidae, Mactridae, *Turritella*, *Rostellana*, *Xenophora*, *Pyropsis* and other diverse shallow-water genera of lesser importance. Environmental implications are firm substrate, normal to slightly subnormal salinity, active but not strong currents, and normally above wave base. These occur at inner sublittoral depths, primarily between 3 and 34 m. Some may range to the outer edge of the brackish-normal marine front, commonly ranging up into the lower estuary. They occur in true and incipient concretions, or less densely in silty shale all the way shoreward to fine-grained sandstone.

S. Large *Exogyra*, with the addition of *Pinna*, Cardiidae, Mactridae, *Cubitostrea*, small inequivalve, byssate Inoceramidae, *Turritella*, are dominant; this may also contain small, uncommonly encountered other taxa. Environmental implications are normal marine salinity, firm substrate, high energy environment with water depths normally not exceeding 5-20 m, but some elements of the fauna can extend into deeper water. Incipient concretions yield this fauna, as does the surrounding sediment that ranges from clay to fine-grained sandstone.

T. Small *Exogyra*, Inoceramidae (large and small), *Cubitostrea* and/or *Ostrea*, *Pycnodonte*, and less commonly Mactridae and *Turritella*. Environments are commonly firm bottom, relatively slow sedimentation, active but not strong currents, normal salinity, inner shelf depths at 25-70 m. Small nodules and small concretions, calcareous shale with incipient

concretions, and both calcareous and non-calcareous shale to siltstone are primary sites. Environments are firm to moderately firm, relatively slow sedimentation (although I've seen the same thing in relatively active sedimentation in Germany), active but not strong currents, normal salinity, inner shelf environments at a depth of 30-200 m.

U. *Pycnodonte* assemblage is characterized by this oyster. It is associated with different types of Inoceramidae, small *Exogyra* or *Ostrea*, barnacles (gooseneck and boring), diverse ammonites, and serpulid worms. Ecological implications are normal salinity, firm to moderately firm substrates, weak currents, with intervals of non-circulating water, at 70-350 m water depth. These occur as normal and incipient concretions, partially cemented, and normal shale to calcareous shales.

V. Small "*Ostrea*" assemblage are common; secondary associates are large to giant Inoceramidae, and "*Ostrea*" encrusting on ammonites. Ecological inferences are either encrusting large cepholopods, or lying free on the calcareous or non-calcareous substrate. Ecological implications are semi-firm substrates, low energy active currents, normal salinity, in water depths of 200-1000 feet, maybe more. Occurs as concretions, incipient concretions, or in calcareous shale.

W. Small *Pycnodonte* assemblage is the last of the oysters. It is commonly associated with large, flat, non-byssate Inoceramidae, barnacles (gooseneck and boring), small lucinids, diverse assemblages of ammonites, and serpulid worms. Ecological implications are normal salinity, normal to moderately reduced oxygen, quiet water to gently circulating currents, and soft substrate (where attached to inoceramids) to firm (where attached by themselves). Small to large concentrations are associated with incipient and normal concretions, pyritiferous shale, normal calcareous shale, and black to dark grey shale are preferred substrates. The latter indicate much organic carbon.

X. Small, inequivalve, robust to moderately robust, byssate Inoceramidae (examples *Cremnoceramus dimidius*, *Inoceramus pictus*, *Inoceramus howelli*, etc.) are the primary taxa, associated with firm to moderately firm substrate, strong to moderately elevated currents, and normal salinity. These generally occur with facies indicative of inner shelf water depths, from a few to as much as 100 meters. *Pseudoperna*, *Ostrea*, *Pycnodonte*, and Lucinidae are typical associates. These occur in limestone beds, concretions, incipient concretions, shell beds, or scattered on the substrate, usually in carbonate sediments.

Y. Large, flat, thin-shelled, non-byssate Inoceramidae (i.e., *Platyceramus*, *Inoceramus*, etc.) dominate this assemblage. Umbos are either swollen or flat. *Inoceramus flaccidus* and *Platyceramus platinus* are examples. They are associated with *Pseudoperna*, *Ostrea*, and rarer

Pycnodonte are among Ostreidae, and Lucinidae and barnacles (gooseneck and boring), among other common taxa. They generally occur as limestone pods, concretions, incipient concretions, aggregated along cracks and seeps (the Inoceramidae probably had chemosymbionts), and just scattered along the substrate. They indicate moderate to deep water, 50 m to as much as 1000 m.

Z. This is made up of an assemblage of very large, moderately to highly inequivalve Inoceramidae (e.g., *Volviceramus*) with their inflated inflated valve mostly buried in the substrate (determined by the lack of borings on all but the upper rim of the lower valve, but they are spread over the top of the cap valve). Common associates are ostreids (*Pseudoperna*, *Pycnodonte*, etc.), boring barnacles, and scattered ammonites. These occur in the limestone beds, concretions, incipient concretions, or scattered in calcareous shale. They are distributed between 50 m possibly shallower, to 1000 m.

5.4 Multi-Taxic Assemblages

Most multi-taxic assemblages do not occur as concretions or incipient concretions. Nodules occur sparingly. Those that occur as concretions, incipient or true, are mentioned below.

(AA). *Pinna* or *Atrina* assemblages dominate this community, with sparse to common associates. *Exogyra*, *Cubitostrea*, some *Crassostrea*, Cardiidae, small robust Inoceramidae, *Turritella*, *Idonearca* or *Trigonarca*, aporrhaid gastropods and tubes of *Callianassa* sp. are moderately common. Primarily they occur under a few m, but occasionally as much as 100 m. They occur in incipient concretions, but they thrive in fine-grained sandstone, siltstone, or even silty shale.

(BB). Delicate pectinoid assemblage containing *Syncyclonema*, *Delectopecten*, and/or *Amussium* are moderately common in calcareous facies. Common associates are thin shelled, subequivalve, non-byssate inoceramids, small Ostreidae, and diverse ammonites, including heteromorphs. Environmental implications are soft to firm substrates, normally calcareous, in middle to outer shelf depths of 100 m to 200 m or deeper. These occur as concretions, incipient concretions, limestone beds, calcareous and chalky shale.

5.5 Complex Multi-Taxic Communities

Complex multi-taxic communities associated with concretions, incipient concretions, nodules, as well as normal marine sedimentary facies are as follows:

(CC). Estuarine mouth to marine nearshore assemblage including

Brachidontes, *Corbula*, *Geltena*, Tellinidae, *Idonearca*, *Callistina*, and important secondary elements such as *Anomia*, *Crassostrea*, Mactridae, apporhaid gastropods, and *Callianassa* are all or mostly present. The range is 10 to 100 m or deeper. Rare concretions, incipient concretions, shell beds with partial cementation, and scattered around the substrate, all are common modes of preservation.

(DD). This is made up of diverse, inner- to middle-shelf assemblages containing the bivalves *Exogyra*, small *Ostrea*, *Callistina*, *Nuculana*, small subequivalve and large flat species of Inoceramidae; *Astarte* and *Crassatella* are locally associated. Dominant gastropods are *Lispodesthes*, and dominant ammonites are Scaphitidae and Baculitidae. Ahermatypic corals occur locally in numbers, primarily on patch reefs (Coates and Kauffman, 1973). Environmental implications are soft to moderately hard shale substrates in quiet water or with gentle current action, normal marine conditions, or those characterized by oxygen deficiency, the most probably depths are in the mid-shelf range of 10 to 50. Pods scattered in calcareous and clay shale are the preferred habitats.

(EE). Diverse, outer- to middle-shelf assemblage composed of the bivalves *Crassatella*, small *Plicatula*, small *Ostrea*, *Exogyra*, *Corbula*, *Callistina*, and the gastropods *Turritella* and aporrhaids are common. They are dominated by large, flat inoceramids, small subeqivalve inoceramids, and a diverse assemblage of ammonites including large ornate forms (e.g., Acanthoceratids, *Prionocyclus*, etc.), small, smooth involute forms (e.g., *Borissiakoceras*), *Scaphites*, and aberrant heteromorphs, such as *Allocrioceras*. Environmental implications are firm to moderately soft shale substrate, quite possibly cool waters, normal salinity, and midshelf depths of 70-140 m although certain elements such as *Plicatula* and the ostreids suggest even shallower depths. Concretions, incipient concretions, and carbonate clay shale are the preferred facies.

(FF). Diverse outer shelf, mid-basin assemblage are composed of large, flat, inoceramids without swollen umbos (i.e., those lacking geniculation), small thin-shelled subequivalve inoceramids, delicate *Ostrea* and ostreiform *Pycnodonte* encrusting the Inoceramidae, *Lucina*, *Nucula*, *Nuculana*, *Pteria*, *Tellina*, and delicate small pectinids such as *Syncyclonema*. Commonly associated gastropods include *Cerithiella* and similar genera, acmaeids, aporrhaids such as *Lispodesthes*, and more rarely *Bellifusus* and *Euspira*. Diverse, associated ammonites include large, coarsely ornate forms such as *Metoicoceras*, small ornate forms such as *Kanabiceras*, aberrant heteromorphs, small baculitids and *Scaphites*. Implied environments are quiet waters of normal salinity, soft to very soft calcareous mud substrate with local hard surfaces (mainly Inoceramidae shells), and depths of 10 to 200 m. The bedded limestones occasionally contain rudistid bivalves in

growth position (*Durania* spp. primarily). Dense boring and calcareous algae are locally characteristic. Substrates are concretions, incipient concretions, local hardgrounds, and primarily in calcareous claystone or clay shales.

(GG). Inner- and middle-shelf ammonite assemblage are composed of *Scaphites*, small *Baculites*, large ornate forms (e.g., *Prionocyclus*), and smooth, involute, narrow ventered forms such as *Borrisiakoceras*. Bottom environmental implications are derived from the scaphitids that were nektobenthic (Landman and Waage, 1993); this is the only assemblage found associated with high energy, nearshore, shallow water deposits. Silty concretions, calcarenite, and clay shale to silty clay shale are the preferred substrate.

(HH). Middle- and outer-shelf diverse ammonite assemblage is composed of two to three genera of large ornate forms (e.g., *Acanthoceras*), small ornate forms such as *Eucalycoceras*, small *Baculites*, smooth involute forms such as *Borrisiakoceras*, and aberrant heteromorphs (e. g., *Allocrioceras*). Common secondary benthic associates are inoceramids (small robust or delicate subequivalve forms), small pectinids, encrusting oysters, *Pteria*, and the gastropods *Cerithiella*, *Lispodesthes* or other aporrhaiids, and acmaeids. Environmental implications are offshore, open-water marine habitats over midshelf depths. Concretions, incipient concretions, and calcareous clay are commonly associated.

(II). The composition of the restricted ammonite assemblage is of *Baculites*, and/or *Sciponoceras*, aberrant small heteromorphs, and large robust ornate forms, *Allocrioceras* and related forms, and large genera such as *Metoicoceras*, *Dunveganoceras*, and *Acanthoceras*. Associated taxa include thin-shelled inoceramids (large, flat and small, subequivalve types), small Ostreidae, and delicate pectinids and pteriids. This assemblage implies open-marine conditions overlying quiet bottoms of midshelf or outer shelf depths (50-270 m). Substrates are primarily carbonate-rich to shaley that are shallowly buried when they, through early diagenetic cementation, turn into concretions and incipient concretions.

Through the examination of the fossils in each nodule, incipient concretion, and well-developed concretion, and pairing that to the lithotype as determined by thin-section analyses, a series of facies appears that demonstrate an onshore-offshore gradient. Fossils and lithology seem to match environments of deposition as one goes from sandstone, through sandy shale, through silty shale, through non-calcareous clay shale, through calcareous shale of different grades, into limestone interbedded with chalky shale, into limestone and chalk as exposed in the Western Interior Seaway of North America. Accompanying this sedimentologic gradient, the fauna changes from a diverse nearshore assemblage, recognized by large ornate

species, to a delicately ornate to smooth, smaller to much smaller assemblage of lower diversity. These are reflected in early diagenetic nodules, concretions, and septarian concretions spread throughout the Cretaceous sequence.

6. SUMMARY

Limestone concretions may be chalky, pure limestone, zoned siderite (usually outside) and limestone, silty or sandy limestone, cone-in-cone limestone, and septarian limestone. All but the zoned concretions and septaria appear to form almost at the sediment-water interface, buried only a few meters below the surface, judging from the minimal compaction of the shells they commonly bear. Zoned concretions commonly show incipient fracturing of the shells along compressive lines, but they are not flattened as they are in surrounding shale.

Concretions may be nearly synchronous over extensive areas, "synchronous" within a biozone (average 0.2-0.8 Myr), or scattered with respect to time lines. This can be tested in the Western Interior Basin because there are common to very common altered volcanic ashes which serve as time lines. Given a single ash or bentonite layer for reference, one can match the position of the concretions zone with those ash falls and determine the synchroneity or lack thereof in concretion horizons. Surprisingly, most concretion zones fall into the synchronous to nearly-synchronous range (Kauffman, 1965).

Limestone concretions normally form around fossils or some other biotic material. Hypotheses for their formation range from the concentration of fossils prior to the development of concretions, as opposed to the random formation of concretions with or without fossil shell and bone. Both hypotheses have evidence supporting them. But the favored one is the concentration of shells prior to concretion formation, even in a shelly bed where shells extend beyond the concretion. Limestone concretions preserve things in the original state, not flattened as preserved in shale, where the true dimensions of a fossil are masked by the deformation history. Septarian and cone-in-cone concretions have undergone post-burial diagenesis which leaves the fossils fragmented the pieces separated. Limestone concretions are very important in evolutionary studies because they present evidence of undeformed fossil taxa.

Concretions commonly preserve faunas indicative of the paleoenvironment in which the form. Examples are taken from the Cretaceous Western Interior Basin of North America. There are 34 faunal

assemblages spread across the basin, from very slightly brackish to fully marine, deep water. Brackish water paleocommunities comprise 16 distinct assemblages, and they record conditions ranging from freshwater dominated with scattered brackish-water taxa (community A) to a much more diverse and abundant fauna comprised of a mixture of marine and a few brackish water taxa (community P). The 14 marine paleocommunites range from the most nearhsore (community Q) to the most marine in chalks and limestone (community II). The facies and the paleocommunities correlate to the paleoenvironmens from which they came in every case.

By integrating concretion growth (early in diagenesis, as evidenced by the undeformed nature of the fossils), with absolute age volcanic ash or bentonite, as well as biostratigraphy (0.2 to 0.5 My per ammonite and bivalve zone in the Western Interior), an unprecedented opportunity to integrate these diverse sciences of sedimentation, paleontology, and radiometry is gained and realized.

REFERENCES

Astin, T. R., 1986, Septarian crack formation in carbonate concretions from shales and mudstones, in: *Features of Mineral Diagenesis in Hydrocarbon Reservoirs* (R. K. Harrison, and D. J. Morgan, eds.), *Clay Min.* **21**:617-631.

Baird, G. C., Sroka, S. D., Shabica, C. W., and Kuecher, G. J., 1986, Taphonomy of Middle Pennsylvanian Mazon Creek area fossil localities, northeast Illinois: Significance of exceptional fossil preservation in syngenetic concretions, *Palaios* **1**:271-285.

Coates, A. G., and Kauffman, E. G., 1973, Stratigraphy, paleontology, and paleoenvironment of a Cretaceous coral thicket, Lamy, New Mexico, *J. Paleont*. **47**:953-968.

Curtis, C. D., and Coleman, M. L., 1986, Controls on the precipitation of early diagenetic calcite, dolomite and siderite concretions in complex depositional sequences, in: *Roles of Organic Matter in Sediment Diagenesis* (D. L. Gautier, ed.), *SEPM Sp. Pub*. **38**:23-33.

Elder, W. P., Gustason, E. R., and Sageman, B. B., 1994, Correlation of basinal carbonate cycles to nearshore parasequences in the Late Cretaceous Greenhorn Seaway, Western Interior U.S.A., *Geol. Soc. Am. Bull*. **106**:892-902,

Fagerstrom, J. A., 1988, A structural model for reef communities, *Palaios* **3**:217-220.

Fursich, F., and Kauffman, E. G., 1984, Paleoecology of marginal marine sedimentary cycles in the Albian Bear River Formation of south-western Wyoming, *Palaeont*. **27**:501-536.

Graber, E. R., 1996, Isotopic composition of diagenetic carbonate concretions at the Cretaceous-Tertiary boundary in south-central Texas, USA; Implications for their growth, *Carb. Evap*. **11**:59-69.

Hudson, J. D., 1978, Concretions, isotopes, and the diagenetic history of the Oxford Clay (Jurassic) of central England, *Sediment*. **25**:339-367.

Kauffman, E. G., 1965, Collecting in concretions, nodules, and septaria, in: *Handbook of Paleontologic Techniques* (D. L. Raup and B. Kummel, eds.), W. H. Freeman Co., San Francisco, pp. 175-194.

Kauffman, E. G., 1967, Coloradoan macroinvertebrate assemblages, central Western Interior United States, in: *Paleoenvironments of the Cretaceous Seaway in the Western Interior: A Symposium* (E. G. Kauffman and H. E. Kent, eds.), *Colo. Sch. Mines Sp. Pub*.:67-143.

Kauffman, E. G., 1974, Cretaceous Bivalvia, *in*: *Atlas of Paleobiology* (A. Hallam, ed.), Elsevier, New York, pp. 351-383.

Kauffman, E. G., 1985, Dynamics of Cretaceous epicontinental seas, *Earth Sci. Bull*. **18**:52.

Kauffman, E. G, Pratt, L. M, Barlow, L. K., Elder, W. P., Fisher, C. G. Glenister, L. M., Gustason, E. R., Johnson, C. C., Kirkland, J. I., McManamen, D., and Sageman, B. B., 1985, A field guide to the stratigraphy, geochemistry, and depositional environments of the Kiowa-Skull Creek, Greenhorn, and Niobrara marine cycles in the Pueblo-Canon City area, Colorado, in: *Fine-Grained Deposits and Biofacies of the Cretaceous Western Interior Seaway; Evidence of Cyclic Sedimentary Processes* (Pratt, L. M., E. G. Kauffman, and F. B. Zelt, eds.), *SEPM Guidebook* **4**:FRS-1-FRS-26.

Kauffman, E. G., and Caldwell, W. G. E., 1993, The Western Interior Basin in space and time, in: Evolution of the Western Interior Basin (W. G. E. Caldwell and E. G. Kauffman, eds.), *Geol. Assoc. Can. Sp. Pap.* **39**:1-39.

Landman, N. H., and Waage, K. M., 1993, Scaphitid ammonites of the Upper Cretaceous (Maastrichtian) Fox Hills Formation in South Dakota and Wyoming, *Bull. Am. Mus. Nat. Hist.* **215**:1-257.

Ludvigson, G. A., Witzke, B. J., Gonzalez, L. A., Hammond, R. H., and Plocher, O. W., 1994, Sedimentology and carbonate geochemistry of concretions from the Greenhorn marine cycle (Cenomanian-Turonian), eastern margin of the Western Interior Seaway, in: Perspectives on the Eastern Margin of the Cretaceous Western Interior Basin (G. W. Shurr, G. A. Ludvigson, and R. H. Hammond, eds.), *Geol. Soc. Am. Sp. Pap*. **287**:145-173.

Mozley, P. S., 1996, The internal structure of carbonate concretions in mudrocks: A critical evaluation of the conventional concentric model of concretion growth, *Sed. Geol*. **103**:85-91.

Pindell, J. L., and Barrett, S. F., 1990, Caribbean plate tectonic history, in*: The Caribbean Region* (G. Dengo and J. E. Case, ed.), Geological Society of America Boulder, 1 sheet.

Pratt, B. R., 2001, Septarian concretions; internal cracking caused by synsedimentary earthquakes, *Sediment*. **48**:216-218.

Svarda, C. E., and Bottjer, D. J., 1988, Limestone concretion growth documented by trace-fossil relations, *Geology* **16**:908-911.

Tsujita, C. J., 1995, Origin of concretion-hosted shell clusters in the Late Cretaceous Bearpaw Formation, southern Alberta, Canada, *Palaios* **10**:408-423.

Chapter 13

CONOP9 Programs for Solving the Stratigraphic Correlation and Seriation Problems as Constrained Optimization

PETER M. SADLER, WILLIAM G. KEMPLE, and MARILYN A. KOOSER

1. THE CONOP9 PROGRAMS

A 'zipped' version of the program CONOP9 2007 along with read-me files, sample files, and other documentation can be viewed at the below mentioned URL link. An earlier version of CONOP9 was initially supplied with 'High-Resolution Approaches in Stratigraphic Paleontology' (PJ Harries, editor) and described in Chapter 13 of that volume. This is an updated version of the program, and the documentation supplied with this version supersedes the information supplied in that chapter.

To view the 'zipped' version of the CONOP9 Programs, please visit:
http://geology.usf.edu/faculty/data/harries/resources.htm

PETER M. SADLER • Department of Earth Sciences, University of California, Riverside, California 92521. WILLIAM G. KEMPLE • Naval Postgraduate School, Monterey, California, 93943. MARILYN A. KOOSER • Department of Earth Sciences, University of California, Riverside, California 92521.

P.J. Harries (ed.), *High-Resolution Approaches in Stratigraphic Paleontology.*

2. DISCLAIMER

The developer writes these programs for his own research needs and intellectual development. They are made available "as-is" as a professional courtesy to fellow researchers who wish to examine his solutions or try new applications. The programs are distributed free of charge, but without any legal implication that they will be accurate, correct, or suitable to any particular instance of the stratigraphic correlation and seriation problems. Neither the developer, nor the authors, nor the publisher assume any legal responsibility or liability for the consequences of decisions that are based upon the output of the programs, whether these result from the internal algorithms or the settings of parameters that must be adjusted by the user to suit each application.

The Users' Guide and Reference Manual are updated, as time permits, but always lag somewhat behind experiences that emerge from the continually on-going augmentation, testing, and correcting of the programs. The author makes no representation that any component of the program has been subject to systematic beta-testing on a par with commercial software. While users should not expect anything approaching full technical support, the developer will attempt to respond to requests for help and welcomes both suggestions for improvement and notification of errors. Where results are found suitable for scientific publication, the author requests the courtesy of citation in those publications.

Index